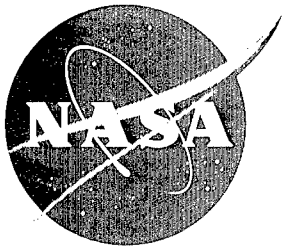

NASA Conference Publication 3325

The 1995 NASA Aerospace Battery Workshop

Compiled by
J.C. Brewer

Proceedings of a workshop sponsored by the
NASA Aerospace Flight Battery Systems Program,
and held in Huntsville, Alabama
November 28–30, 1995

February 1996

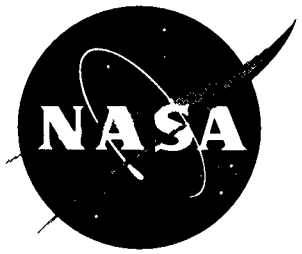

NASA Conference Publication 3325

The 1995 NASA Aerospace Battery Workshop

Compiled by
J.C. Brewer
Marshall Space Flight Center • MSFC, Alabama

Proceedings of a workshop sponsored by the
NASA Aerospace Flight Battery Systems Program,
and held in Huntsville, Alabama
November 28–30, 1995

National Aeronautics and Space Administration
Marshall Space Flight Center • MSFC, Alabama 35812

February 1996

Preface

This document contains the proceedings of the 28th annual NASA Aerospace Battery Workshop, hosted by the Marshall Space Flight Center on November 28-30, 1995. The workshop was attended by scientists and engineers from various agencies of the U.S. Government, aerospace contractors, and battery manufacturers, as well as international participation in like kind from a number of countries around the world.

The subjects covered included nickel-cadmium, nickel-hydrogen, nickel-metal hydride, and lithium-based technologies.

Introduction

The NASA Aerospace Battery Workshop is an annual event hosted by the Marshall Space Flight Center. The workshop is sponsored by the NASA Aerospace Flight Battery Systems Program which is managed out of NASA Lewis Research Center and receives support in the form of overall objectives, guidelines, and funding from Code AE, NASA Headquarters.

The 1995 Workshop was held on three consecutive days and was divided into five sessions. The first day consisted of a General Session and a Management and Problem Resolution of On-orbit Spacecraft Batteries Focused Session. The second day consisted of a Nickel-Hydrogen Session and a Battery and Electrode Impregnation Modeling Focused Session. The third and final day was devoted to a Nickel-Cadmium Session.

On a personal note, I would like to take this opportunity to thank all of the many people that contributed to the organization and production of this workshop:

> **The NASA Aerospace Flight Battery Systems Program**, for their financial support as well as their input during the initial planning stages of the workshop.
>
> **John Bush** and **Eric Lowery**, NASA Marshall Space Flight Center; **Mark Toft**, NASA Goddard Space Flight Center; and **Joe Stockel**, Office of Research and Development, for serving as Session Organizers, which involved soliciting presentations, organizing the session agenda, and orchestrating the session during the workshop;
>
> **Huntsville Hilton**, for doing an outstanding job in providing an ideal setting for this workshop and for the hospitality that was shown to all who attended;
>
> **Marshall Space Flight Center employees**, for their help in stuffing envelopes, registering attendees, handling the audience microphones, and flipping transparancies during the workshop.

Finally, I want to thank all of you that attended and/or prepared and delivered presentations for this workshop. You were the key to the success of this workshop.

Jeff Brewer
NASA Marshall Space Flight Center

Table of Contents

Preface iii

Introduction v

General Session 1

Space Power Requirements for Future NASA Missions
Dr. Daniel R. Mulville, NASA Headquarters 3

Basic Setup of Battery Testing System
John Zhang, Arbin Instruments 13

Prismatic-Cased Li/$(CF_x)_n$ P-40 Cell Performance Under Resistive Loads
L.M. King and N. Margalit, Tracor Battery Technology Center 21

Lithium-Thionyl Chloride Batteries for the Mars Pathfinder Microrover
Frank Deligiannis and Harvey Frank, Jet Propulsion Laboratory; Dr. R.J. Staniewicz and John Willson, SAFT America Inc. 41

Mars Pathfinder Battery Program Status
S. Surampudi, S. Dawson, D. Perrone, B. Otzinger, and M. Shirbacheh, Jet Propulsion Laboratory 59

Lithium-Ion Battery Program Status
S. Surampudi, C-K. Huang, M. Smart, E. Davies, D. Perrone, S. Di Stefano, and G. Halpert, Jet Propulsion Laboratory 87

Bipolar and Monopolar Lithium-Ion Battery Technology at Yardney
P. Russell, J. Flynn, and T. Reddy, Yardney Technical Products Inc. 111

The USAF Phillips Laboratory Sodium-Sulfur Battery Technology Program -- Results & Status
Capt. Marc Rainbow, USAF; and Andrew Somerville, The Aerospace Corporation 149

Management and Problem Resolution of On-orbit Spacecraft Batteries Focused Session 173

Battery Performance of the Skynet 4A Spacecraft During the First Six Years of On Station Operation
P.J. Johnson and N.R. Francis, Matra Marconi Space UK Ltd. 175

60% DOD Event on the NiCd Batteries of the Upper Atmosphere Research Satellite, After 3.5 Years in LEO Orbit
Mark R. Toft, NASA Goddard Space Flight Center; and Richard E. Calvin, Lockheed-Martin 199

Soft-Short Management and Remediation in 10-Year-Old NiCds in GEO Orbit
Nicanor A. Flordeliza, GE American Communications Satellites, Inc.; and Ronald W. Bounds, Aerospace Consulting Group, Inc. 211

NOAA-9 Power Management
Ron Boyce, Lockheed-Martin 227

Nickel-Hydrogen Session 247

High Energy Density Micro-Fiber Based Nickel Electrode for Aerospace Batteries
Jennifer Francisco, Dennis Chiappetti, and Dwaine Coates, Eagle-Picher Industries, Inc. 249

Mars Global Surveyor
D. Ginder, D. Coates, J. Francisco, C. Graskemper, and C. Fox, Eagle-Picher Industries 255

Air Force Ni-H_2 IPV Storage Testing
Capt Shawn Smellie, USAF Phillips Lab; and Carole A. Hill, The Aerospace Corporation 281

Hubble Space Telescope Onboard Battery Performance
Gopalakrishna M. Rao and Harry Wajsgras, NASA Goddard Space Flight Center; Hari Vaidyanathan, COMSAT Laboratories; and Jon D. Armantrout, Lockheed-Martin 307

Single Battery Power Subsystems: On-Line Reconditioning
R.F. Tobias, TRW Space and Electronics Group 335

Nickel-Hydrogen Battery State of Charge During Low Rate Trickle Charging
C. Lurie and S. Foroozan, TRW Space and Electronics Group; J. Brewer and L. Jackson, NASA Marshall Space Flight Center 359

Performance Features of 22-Cell, 19 Ah Single Pressure Vessel Nickel Hydrogen Battery
Gopalakrishna M. Rao, NASA Goddard Space Flight Center; and Hari Vaidyanathan, COMSAT Laboratories 375

Battery and Nickel Electrode Modeling Focused Session 395

First Principles Nickel-Cadmium and Nickel-Hydrogen Spacecraft Battery Models
P. Timmerman, B. V. Ratnakumar, S. DiStefano, Jet Propulsion Laboratory 397

Mathematical Models for Electrochemical Impregnation of Nickel Electrodes
Chien-Hsien Ho, Gowri S. Nagarajan, Mahesh Murthy, J. W. Van Zee, University of South Carolina 407

Nickel-Hydrogen and Silver-Zinc Battery Cell Modeling at The Aerospace Corporation
Albert H. Zimmerman, The Aerospace Corporation 439

Mathematical Modeling of a Nickel-Hydrogen Cell
Pauline De Vidts, Javier Delgado, and Ralph E. White, University of South Carolina 447

Ni-H_2 Battery Model Requirements
D.P. Hafen and J.D. Armantrout, Lockheed-Martin Missiles and Space 489

Requirements for a Nickel Electrode Impregnation Model
Rolan C. Farmer, Darren Scoles, and David F. Pickett, Eagle-Picher Power Systems Department
..... 493

Nickel-Cadmium Session 501

Good and Bad Features of Ni-Cd Cell Designs
Sidney Gross, Northwest Engineering Consultants 503

Selecting Ni-Cd Flight Cells for the NOAA/TIROS Program
Mark R. Toft, NASA Goddard Space Flight Center 539

NASA Battery Testbed: A Designed Experiment for the Optimization of LEO Battery Operational Parameters
F. Deligiannis, D. Perrone, S. DiStefano, Jet Propulsion Laboratory 579

Ni-Cd and Ni-H_2 Battery Performance on Engineering Test Satellite-VI
S. Kuwajima and H. Kusawake, National Space Development Agency of Japan 597

1995 NASA Aerospace Battery Workshop Attendance List 631

General Session

National Aeronautics and
Space Administration

SPACE POWER REQUIREMENTS FOR FUTURE NASA MISSIONS

by

DR. DANIEL R. MULVILLE
NASA HEADQUARTERS
WASHINGTON, D.C.

presented at

NASA BATTERY WORKSHOP
HUNTSVILLE, AL

NOVEMBER 28, 1995

National Aeronautics and Space Administration

"CUSTOMERS"

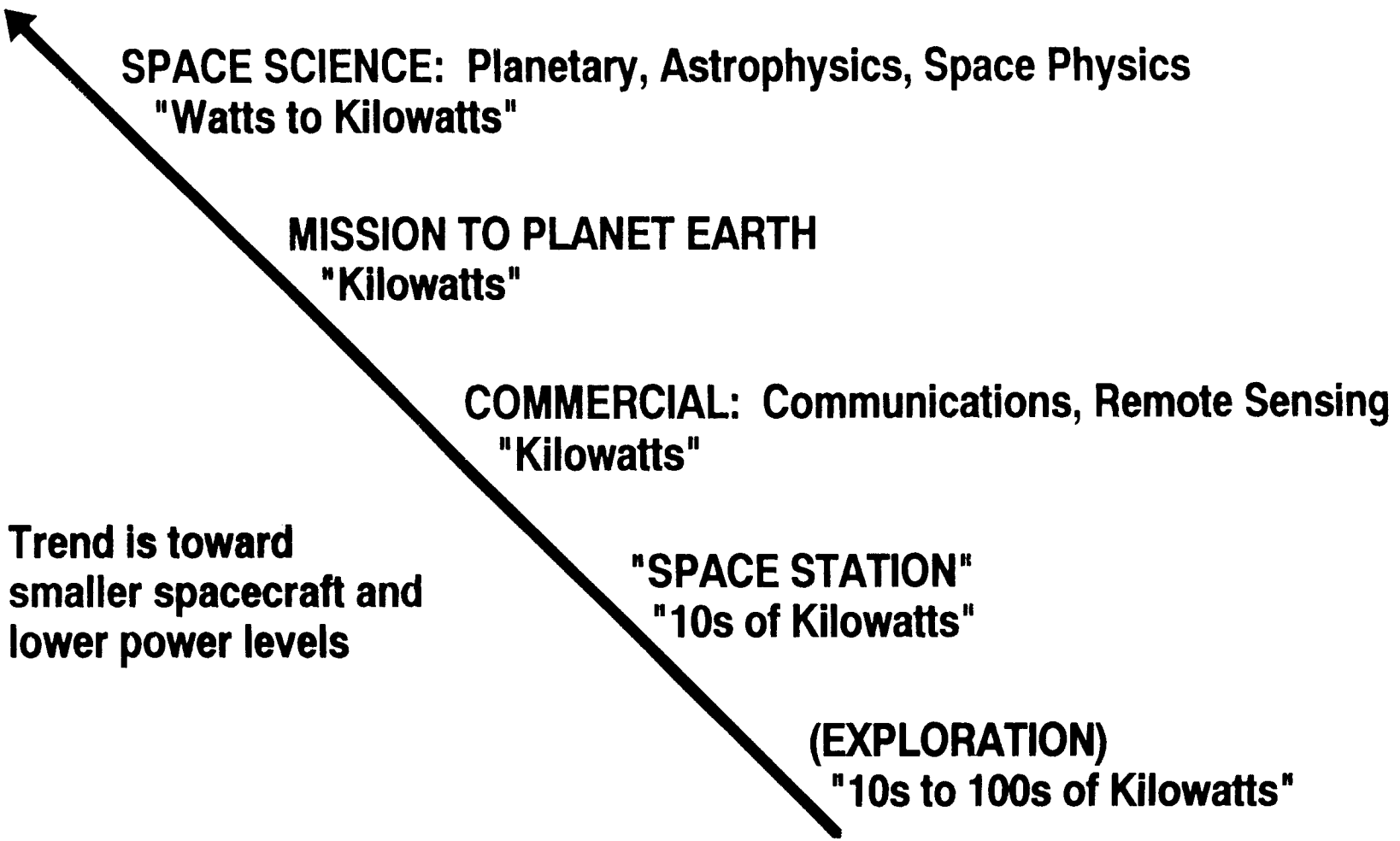

National Aeronautics and Space Administration

PROGRAMMATIC CHANGES

LAST YEAR	THIS YEAR
• Technologies for NASA User	• NASA and Commercial Use
• Users Consulted in Planning and Prioritization	• Users are "Customers"
• Industry Consulted in Planning and Prioritization	• Industry a "Partner/Customer"
• NASA Lead Technology Development	• Industry Lead Technology Development
• Non-Aerospace Applications Secondary	• Non-Aerospace Applications Important
• Performance over Cost	• Performance to Cost
• Reliance on NASA Technology	• Leverage External Capability

TECHNICAL PRIORITIES

LAST YEAR	THIS YEAR
• Large Spacecraft	• Small Spacecraft
• Initial Cost	• Life Cycle Cost
• "High Power" Systems	• "Low Power" Systems
• Maximum Data Generation	• Maximum Information Content
• Erectable Spacecraft	• Deployable Spacecraft
• Robust Systems	• Smart/Adaptive Systems
• "Astronaut Operated"	• Automation and Robotics

National Aeronautics and Space Administration

TECHNOLOGY STRATEGY

Traditional Mission Approach	"New" Mission Approach
Large Spacecraft	Small Spacecraft
Long Development Time (5-10 years)	Rapid Development (~3 years)
Multi-Disciplinary (many instruments)	Focused Objectives (fewer Instruments)
Expensive ($B)	Low-cost (~$ 100 M)
Infrequent (few/decade)	(Frequent (~ yearly)
Conservative: Little New Technology	Aggressive: New Technology

Key Technology Issues:

- Reduce mass to enable smaller launch vehicles, faster trip time and lower cost
- Simpler, more autonomous operations to reduce life cycle cost
- Reduce design, development and qualification time to enable frequent low-cost missions
- Increase payload fraction and science return
- Enable next generation missions
- Stimulate U.S. industry to promote strong world leadership capability
- Incorporate dual-use strategy into technology development

National Aeronautics and Space Administration

SPACECRAFT SYSTEMS

Mission	95	96	97	98	99	01	05
	COMMERCIAL (COMMUNICATIONS =>				EOS-AM =>PM	=>	CHEM
			REMOTE SENSING =>	MARS SURVEYOR =>		SIRTF	ASEP => TOPS
			SSTI =>		"DISCOVERY SERIES" =>		
			NEW MILLENNIUM =>				

Power Systems

- Chemical Storage
- Adv. Photovoltaic
- Power Mgt. and Distribution
- Dynamic Systems
- Radioisotope

High Cycle Life Batteries for LEO (2X Whr/kg)

Compact Batteries for GEO and Small S/C (1/2 Current Volume)

Li Batteries for Small S/C and Planetary Applications

Hi-Efficiency, Low Cost PV Arrays (1/2 Area, 1/2 Wt, 1/3 Cost)

Wide Temp. Solid State Power Electronic (-10°K to ~500°K)

Hi-Temp for Compact Power Systems **Lo-Temp. for Deep Space Ops**

(10X Increase in W/cm^3)

Adv. Low Vibration Refrigerator/ Freezer

Hi-Efficiency (~20%) Radioisotope

Integrated Power & Electric Propulsion

1/3 Weight
1/3 Size
1/3 Cost
3X Life

On-Board Propulsion

- Chemical Propulsion
- Electric Propulsion

Adv. Hi Isp Chemical Prop. for Large Delta V (Novel Storable Fuels, Lt. Wt. Components)

Low Cost, "Clean" Monoprop for Small S/C Orbit Insertion & Control

Electric Propulsion for Small Size, Lt. Wt.

Low Power Micro-elec., <.001 lbf for Vernier Control

Long-life Primary Electric (1/3 Wt. of Chemical Prop.)

National Aeronautics and Space Administration

NEW MILLENNIUM PROGRAM

Office of Space Science | Office of Space Access and Technology | Office of Mission to Planet Earth

- REVOLUTION IN SPACECRAFT TECHNOLOGY - SMALLER, CHEAPER, MORE FREQUENT MISSIONS
  - INCREASED AUTONOMY FOR LOWER OPERATIONS COST
  - REDUCED SIZE AND MASS FOR LOWER LAUNCH COSTS
  - GREATER CAPABILITY
- DIRECTED AT 21st CENTURY MISSIONS IN EARTH AND SPACE SCIENCE
  - ENHANCING CURRENT MISSIONS BY REDUCING TOTAL LIFE CYCLE COST
  - ENABLING NEW MISSIONS THROUGH TOTALLY NEW TECHNOLOGY
- VALIDATED THROUGH TECHNOLOGY DRIVEN SPACE MISSIONS
  - 2 YEAR DEVELOPMENT CYCLE FROM SELECTION TO FLIGHT
  - ACHIEVES RAPID INFUSION INTO MAINSTREAM SCIENCE MISSIONS
  - VALUABLE SCIENCE RETURNED AS PART OF MISSION OBJECTIVES
- FULL PARTNERSHIP AMONG NASA SCIENCE AND TECHNOLOGY OFFICES, INDUSTRY, UNIVERSITIES AND OTHER GOVERNMENT AGENCIES

MFP-95 3 pm-1

National Aeronautics and Space Administration

NASA AEROSPACE FLIGHT BATTERY SYSTEMS
PROGRAM FOCUS

PROGRAM HAS BEEN REFOCUSED TO ADDRESS "NEW" MISSION APPROACH

- **RESPONSIVE TO PROGRAM NEEDS**
- **NEW MILLENNIUM INITIATIVE**
  - DIRECTED AT REDUCING RISK ASSOCIATED WITH NEW Li-ION TECHNOLOGY
- **INTERACTIONS WITH OTHER GOVERNMENT AGENCIES**
  - JOINT PROGRAM WITH THE AIR FORCE
- **INTERACTIONS WITH INDUSTRY**

National Aeronautics and Space Administration

NASA AEROSPACE FLIGHT BATTERY SYSTEMS TECHNOLOGY FOCUS

SECONDARY BATTERIES

- Li-ION
- $Ni-H_2$ - IPV, CPV, SPV
- Ni-MH
- Ni-CD, ADVANCED Ni-CD

PRIMARY BATTERIES

- $LiSOCl_2$
- LiBCX

National Aeronautics and Space Administration

CONCLUSION

- **CHANGES IN TRADITIONAL APPROACH TO TECHNOLOGY DEVELOPMENT ARE REAL**
- **EMPHASIS ON SMALLER SPACECRAFT / DEDICATED MISSIONS**
  - LOWER COST / MORE FREQUENT MISSIONS
  - LOWER POWER / AUTONOMOUS SYSTEMS
  - INTEGRATED SPACECRAFT SUBSYSTEMS
- **FUTURE MISSIONS REQUIRE NEW TECHNOLOGY**
  - BATTERY PROGRAM REFOCUSED TO MITIGATE INHERENT RISK
- **FLIGHT VALIDATION OF NEW TECHNOLOGIES IS ESSENTIAL**

BASIC SETUP OF BATTERY TESTING SYSTEM

JOHN ZHANG

ARBIN INSTRUMENTS

3206 LONGMIRE DR

COLLEGE STATION, TX. 77845

PHONE: 409/693-0260 FAX: 409/693-0344

BASIC CONTROL MODE, BASIC BLOCK DIAGRAM AND CIRCUITRY

1. CONSTANT CURRENT CHARGE

CURRENT SOURCE

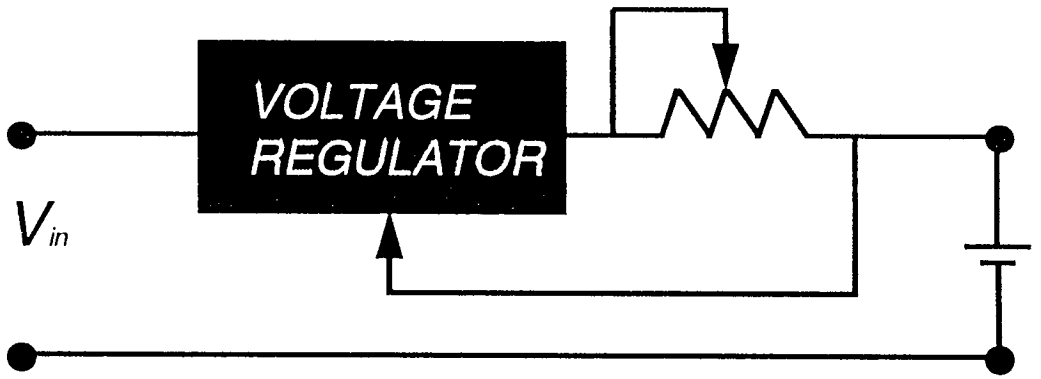

2. CONSTANT VOLTAGE CHARGE

VOLTAGE SOURCE (ANALOG FEEDBACK) OR
DIGITAL FEEDBACK TO ADJUST CURRENT SOURCE

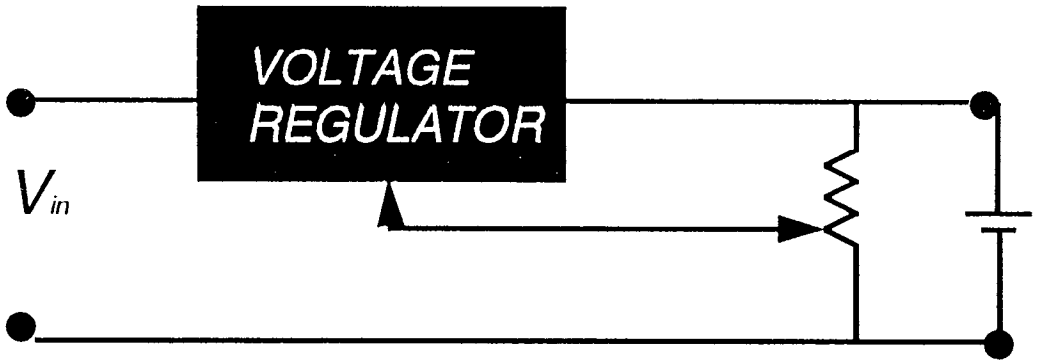

3. CONSTANT CURRENT DISCHARGE

DC ELECTRONIC LOAD

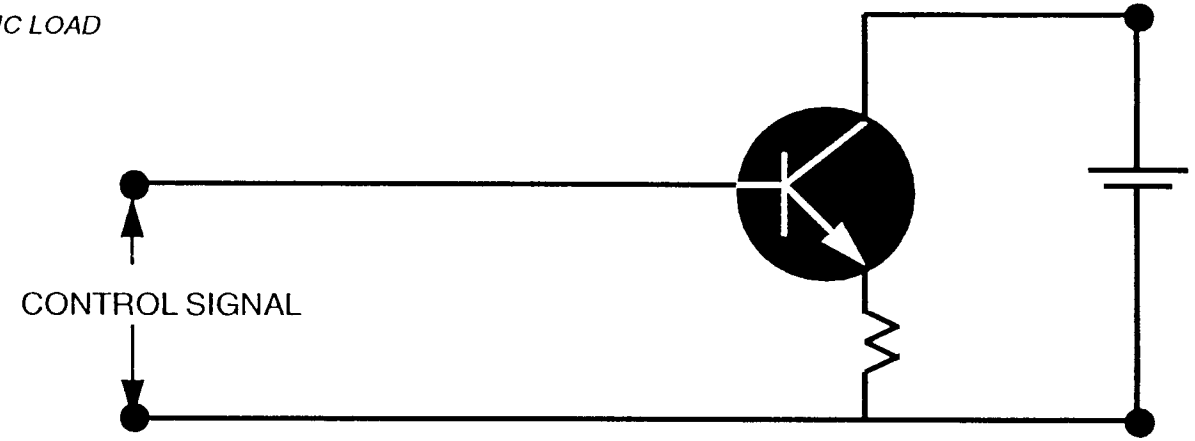

4. CONSTANT LOAD DISCHARGE

RESISTANCE BANK (AS SHOWN IN THE FIGURE)
OR DIGITAL FEEDBACK TO ADJUST
CURRENT SOURCE: R= V/I

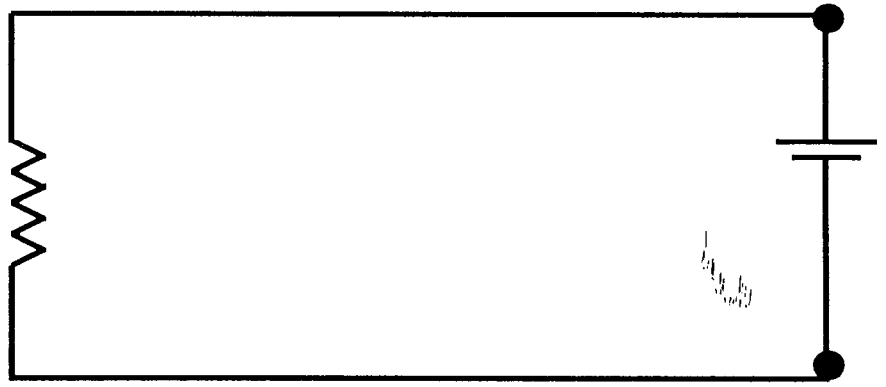

5. CONSTANT POWER DISCHARGE

DIGITAL FEEDBACK TO ADJUST CURRENT
SOURCE: P=V*I

6. REST

OPEN CIRCUIT OR I=O

CONSTRUCTION OF A BATTERY SYSTEM:

1. ADD-UP SYSTEM

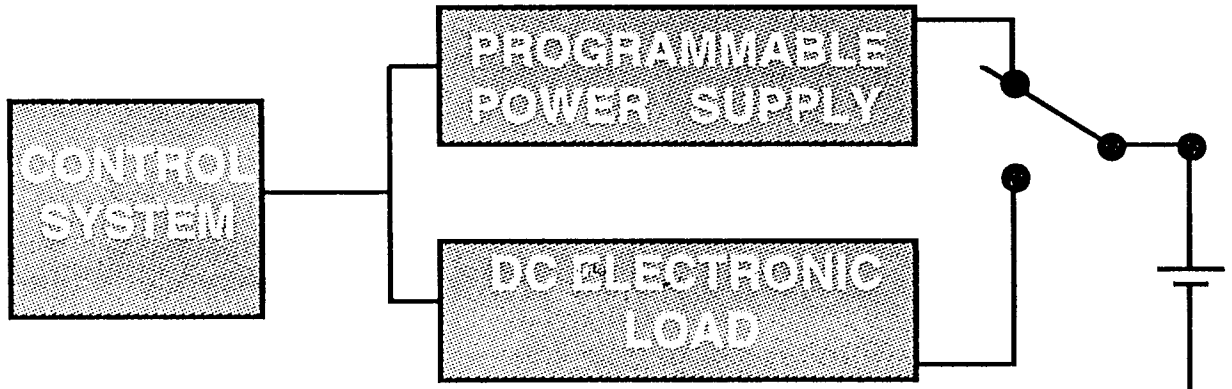

2. INTEGRATED SYSTEM

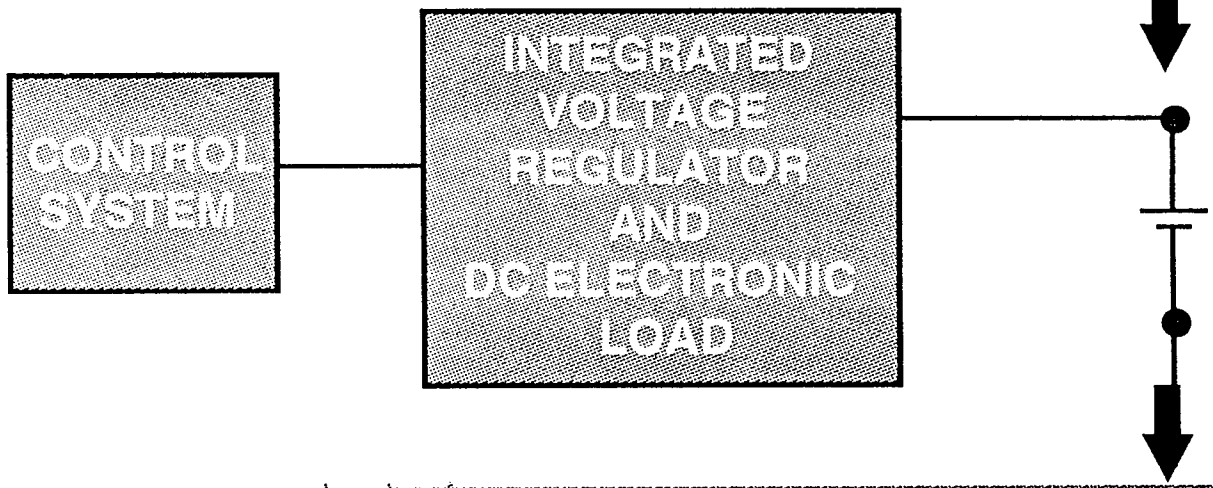

MULTICHANNEL BATTERY TESTING SYSTEM

ADD-UP MULTICHANNEL SYSTEM

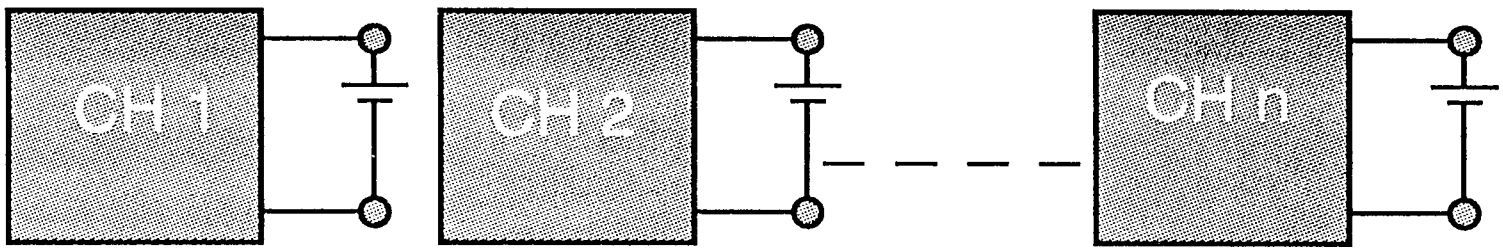

INTEGRATED MULTICHANNEL SYSTEM (IMS)

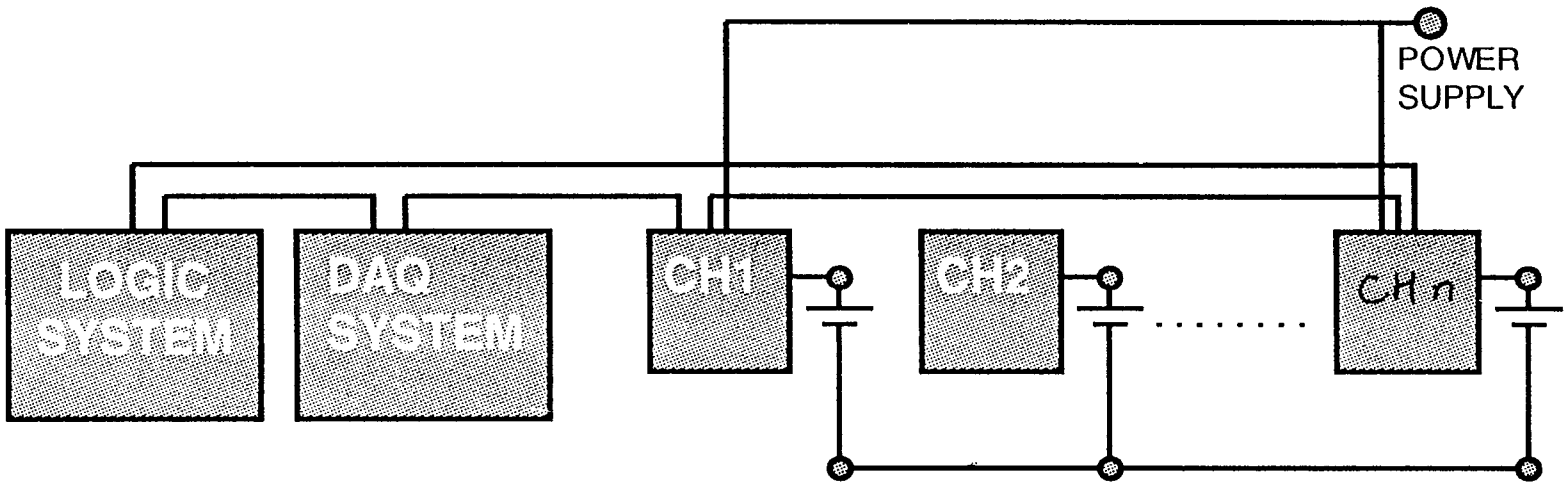

COMPUTER AUTOMATED BATTERY TESTING SYSTEM

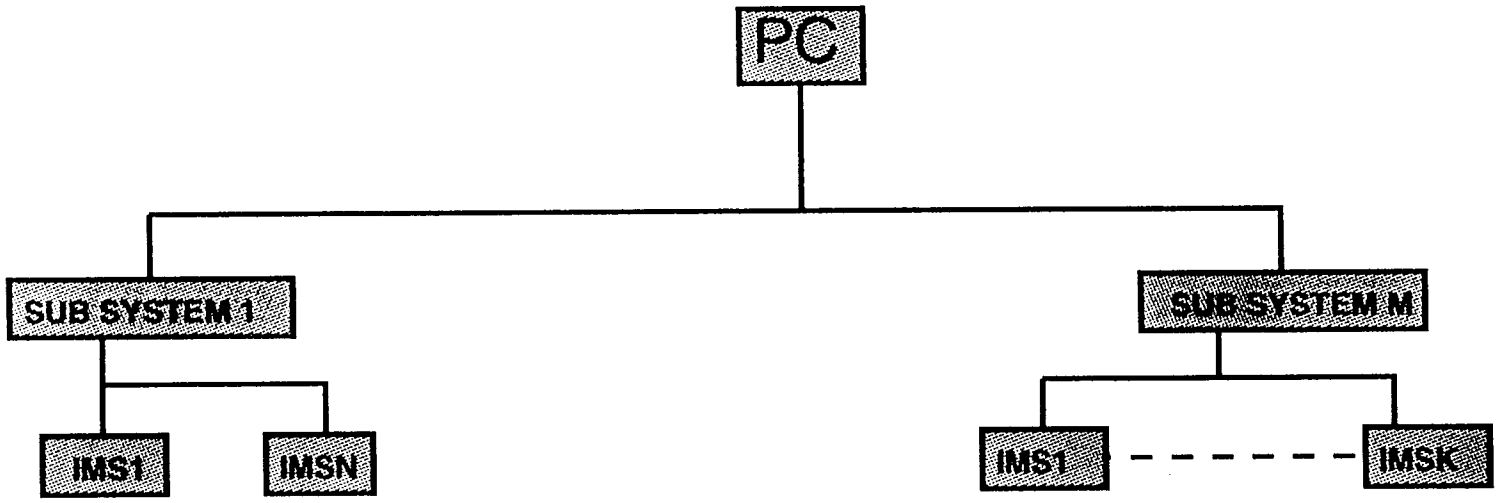

TERMINATION OF A CONTROL STEP:

- *TIME*
- *VOLTAGE*
- *CAPACITY*
- *CURRENT*
- *VOLTAGE CHANGE RATE dV/dt*
- *- DELTA V*
- *TEMPERATURE*
- *TEMPERATURE CHANGE RATE dT/dt*
- *ETC.*

NEW TECHNOLOGY IN BATTERY TESTING

REVERSE PULSE CHARGE: BIPOLAR CIRCUITRY

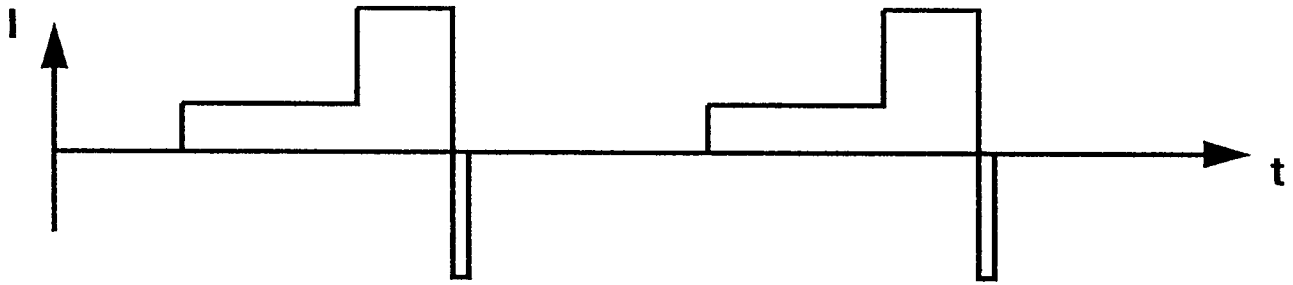

HIGH SPEED PULSE DISCHARGE IN TELECOMMUNICATION:

HIGH SPEED PULSE GENERATION
SYNCHRONIZED, FAST DAQ AND TREATMENT
FAST RESPOND CIRCUITRY

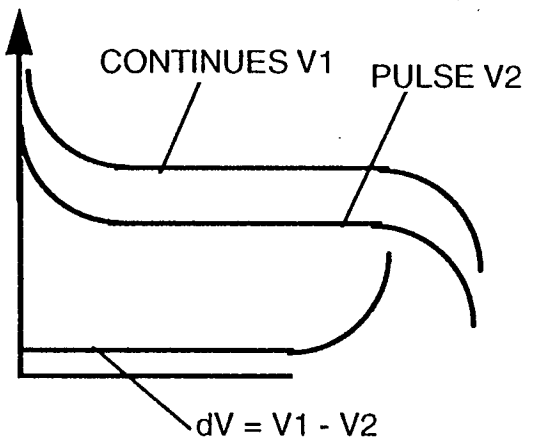

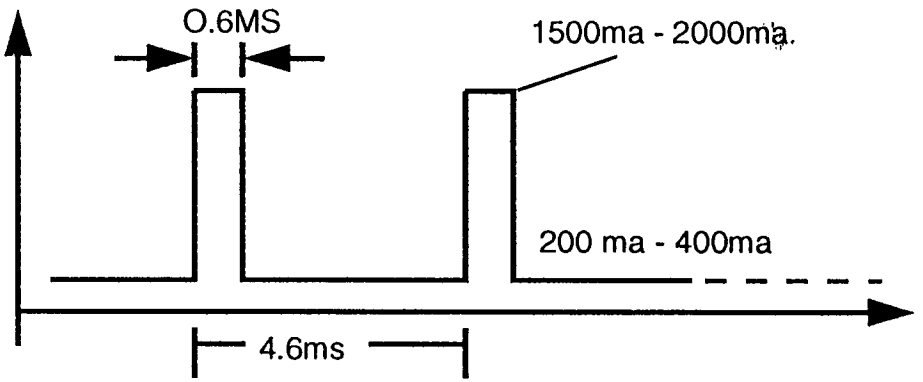

GSM STANDARD

Prismatic-Cased Li/$(CF_x)_n$ P-40 Cell Performance Under Resistive Loads

L. M. King and N. Margalit
Tracor Battery Technology Center
Rockville, MD

Presented at The 1995 NASA
Aerospace Battery Workshop
November 28, 1995

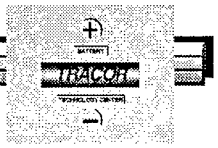

Manufacturer's Specifications

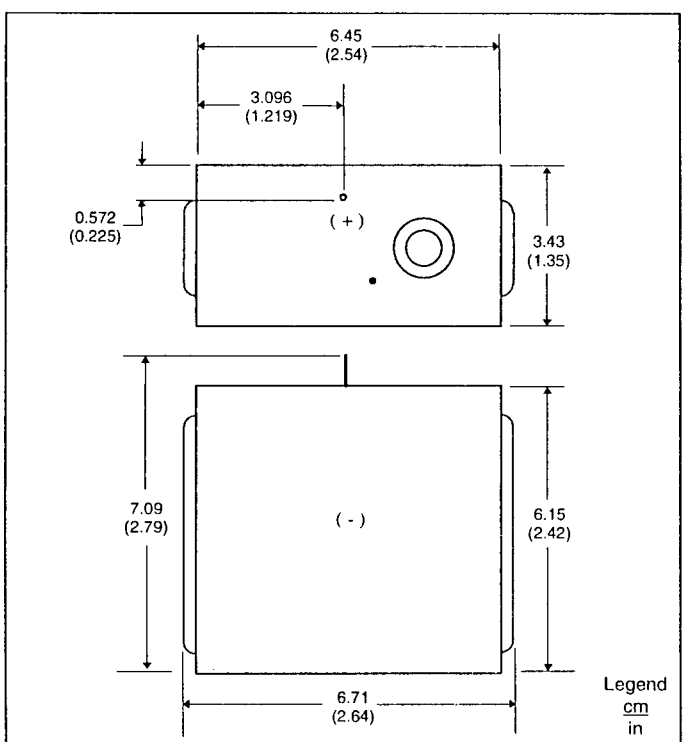

Manufacturer: Eagle-Picher Industries, Inc.
Mfg. Part Number: LCF-313
Cell Name: P-40
System: Li/CF_x with 1.0M $LiAsF_6$ in DMSI
Construction: Spiral Wrap
Terminal: McHenry-Ziegler Seal
(0.035" DIA pin)
Weight: 230 g (8.11 oz)
Volume: 141 cm^3 (8.6 in^3)
Open Circuit Voltage (OCV): 3.00 V
Rated Capacity: 43.5 Ah
(20°C, 175 mA, 2.0 V cutoff)
Maximum Current: 1 A
(0°C, 2.3 Ω, 2.3 V)
Nominal Storage Loss: 3% per year
Energy Density: 763 Wh/l (12.5 Wh/in^3)
Specific Energy: 462.6 Wh/kg (210 Wh/lb)

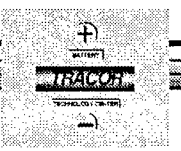

Comparison to Cells of Other Lithium Systems

CHEMISTRY	MANUFACTURER	SIZE	OCV (V)	SPECIFIC ENERGY (Wh/kg)	CAPACITY (Ah)	MAXIMUM CURRENT (A)
Li/CF_x	Eagle-Picher	P-40	3.00	463	43.5	1.0
Li/CF_x	Eagle-Picher	DD	3.00	610	39.0	1.0
Li/SO_2	Saft	2 x D	3.00	275	15.0	4.0
Li/SO_2Cl_2	Wilson-Greatbatch	DD	3.92	480	30.0	4.0
$Li/SOCl_2$	BEI	DD	3.65	440	28.0	0.5

Qualification Test

- Performance of the P-40 lithium-carbon monofluoride cell qualified using continuous and pulse resistive loads based on 40Ah nominal capacity.
- Screening Cells
- Constant Resistive Discharge Tests
- Storage with subsequent Constant Resistive Discharge Tests
- Pulse Discharge Tests

Screening Cells

- Screening performed on all cells tested at TBTC to ensure that the cells are in good working order prior to any discharge testing.
- The screening of 200 P-40 cells consisted of:
  - ⇨ a visual inspection for leakage and/or other physical deformities
  - ⇨ an open circuit voltage (OCV) measurement (passing criteria: $\geq$ 2.950 volts)
  - ⇨ an end-of-pulse closed circuit voltage (CCV) measurement (5 Ω pulse for 5 seconds, passing criteria: $\geq$ 2.500 volts).

Constant Resistive Discharge

- Matrix is a *selected* combination of 12 discharge rates and 6 temperatures.

- Cells with low H_2O/CH_3OH DMSI were tested at the higher temperatures and lower rates due to the possible contribution that proton donating material could make toward cell deterioration.

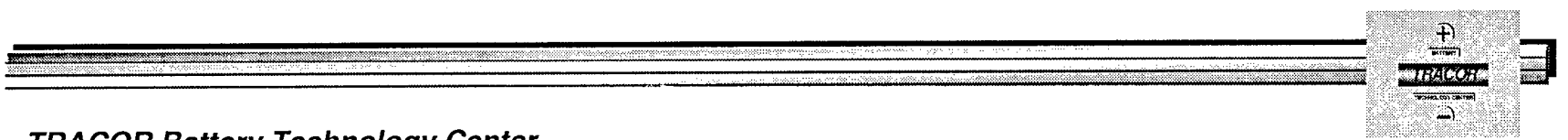

Constant Resistive Discharge Test Matrix

RESISTIVE DISCHARGE			QUANTITY OF CELLS TESTED AT TEMPERATURE:					
NOMINAL								
time (hr)	current (mA)	resistor (Ω)	-40°C (-40°F)	-23.5°C (-10°F)	0°C (32°F)	24°C (75°F)	49°C (120°F)	71°C (160°F)
20.0	2000	1.35			6	6	6	
31.6	1260	2.14		9	9	12*	9	9
50.0	800	3.38				9		
100	400	6.75		9	15	15	15	9
200	200	13.5				9		
316	126	21.4	9	9	15	15	15*	9*
500	80.0	33.8				6		
1000	40.0	67.5	9	9	9	15*	9*	9*
2000	20.0	135				6		
3160	12.6	214	6	6	9*	9*	9*	9*
5000	8.00	338				6		
10000	4.00	675			9*	9*	9*	

* Cells in these tests contain low H_2O (10 ppm) and low CH_3OH (12 ppm) DMSI. The remaining cells contain DMSI with 52 ppm H_2O and 307 ppm CH_3OH.

Storage with subsequent Constant Resistive Discharge

- Accelerated storage: cells were stored at elevated temperatures (49°C and 71°C) for periods of 1 to 3 months
- Room temperature storage for periods up to 2 years has been completed
- Cells to remain in storage up to 16 years
- After storage, cells were discharged at room temperature with either a 2.14Ω load ("31.6 hr" rate) or a 67.5Ω load ("1000 hr" rate).

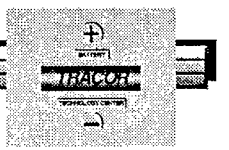

Storage with subsequent Constant Resistive Discharge Test Matrix

STORAGE		RESISTIVE DISCHARGE			QUANTITY OF CELLS TESTED AT TEMPERATURE:					
		NOMINAL								
temp (°C)	time	time (hr)	current (mA)	resistor (Ω)	-40°C (-40°F)	-23.5°C (-10°F)	0°C (32°F)	24°C (75°F)	49°C (120°F)	71°C (160°F)
24	1 yr	31.6	1260	2.14				12		
24	1 yr	1000	40	67.5				15		
24	2 yr	31.6	1260	2.14				12		
24	2 yr	1000	40	67.5				15		
24	4 yr	31.6	1260	2.14				12		
24	4 yr	1000	40	67.5				15		
24	8 yr	31.6	1260	2.14				12		
24	8 yr	1000	40	67.5				15		
24	16 yr	31.6	1260	2.14				5		
24	16 yr	1000	40	67.5				6		
49	1 mo	31.6	1260	2.14				12		
49	1 mo	1000	40	67.5				15		
49	3 mo	31.6	1260	2.14				12		
49	3 mo	1000	40	67.5				15		
71	1 mo	31.6	1260	2.14				12		
71	1 mo	1000	40	67.5				15		

Shaded areas are tests still in progress

Pulse Discharge Matrix

- Cells placed on a background load of 214Ω
- Two (2) second pulses of 3Ω (Tues.), 2Ω (Wed.) and 1Ω (Thurs.) are superimposed over the background twice per scheduled day, biweekly.

PULSE TEST	RESISTIVE DISCHARGE			QUANTITY OF CELLS TESTED AT TEMPERATURE:					
	NOMINAL								
3Ω/2Ω/1Ω x 2 S T,W,R AM&PM BI-WK	time (hr)	current (mA)	resistor (Ω)	-40°C (-40°F)	-23.5°C (-10°F)	0°C (32°F)	24°C (75°F)	49°C (120°F)	71°C (160°F)
	3160	12.6	214			6	6	6	
24°C / 2 yr storage	3160	12.6	214			6	6		
24°C / 4 yr storage	3160	12.6	214			6	6		

Shaded areas are tests still in progress

Constant Resistive Discharge Results

- In general:
  - ☞ expected voltage delay at high rates and low temperatures
  - ☞ operating voltage proportional to resistor value and temperature
  - ☞ 2nd plateau at 2.1V is additional capacity of Li / DMSI
- Room Temperature (24°C) Discharge at Various Rates
  - ☞ cells perform well over entire resistor range (1.35Ω to 675Ω)
  - ☞ 1.35Ω is half the manufacturer's spec (twice the current)
- 67.5Ω ("1000 hr" rate) Discharge at Various Temperatures
  - ☞ low operating voltage at -40°C (-40°F)
  - ☞ cells perform well between -23.5°C (-20°F) and 71°C (160°F)
  - ☞ cells not qualified above 71°C (160°F)

Room Temperature (24°C) Discharge at Various Rates

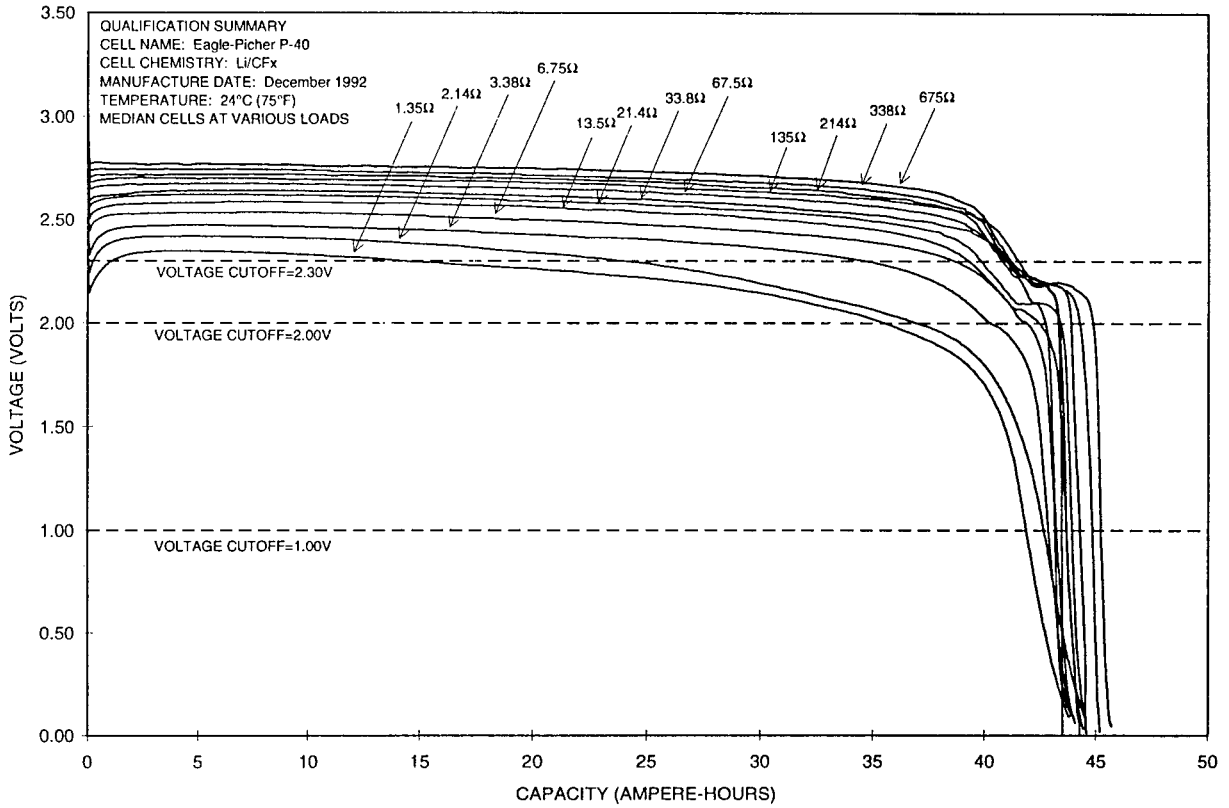

67.5Ω (1000 hr, 40 mA nominal) Discharge at Various Temperatures

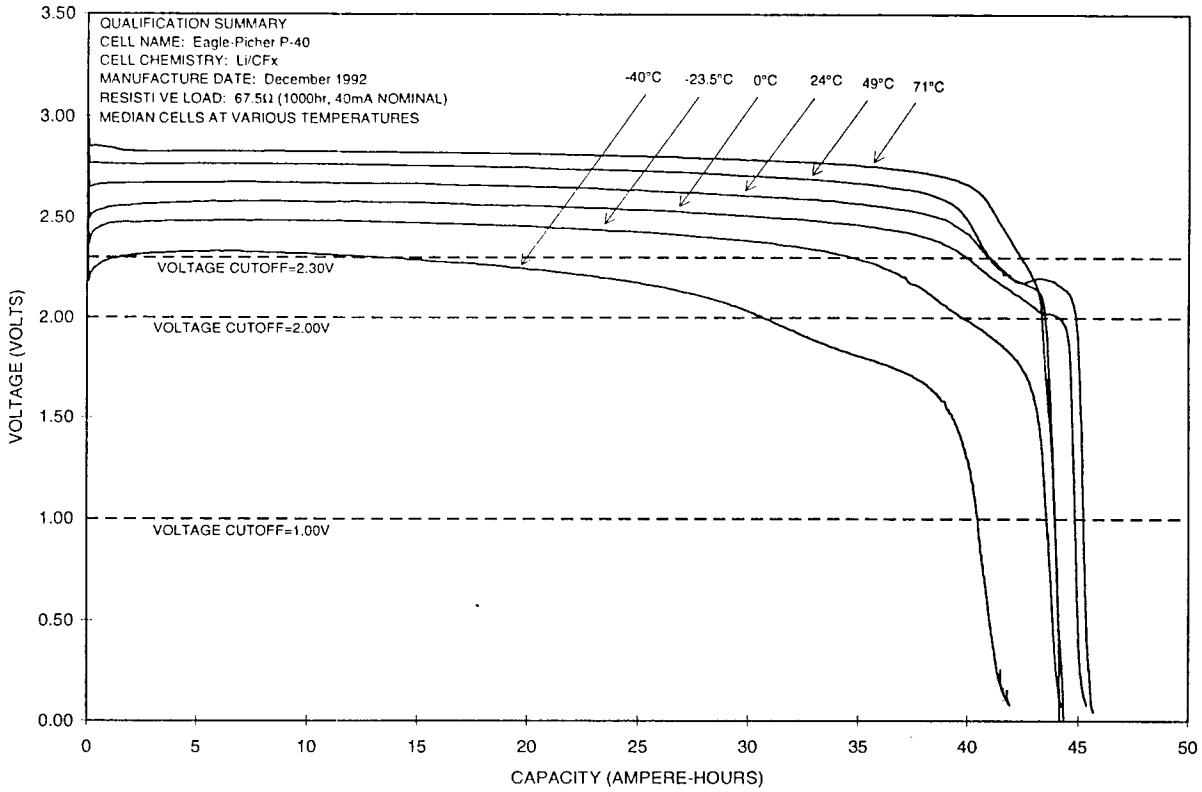

Capacity Delivered to 1.00V

RESISTIVE DISCHARGE			CAPACITY (Ah) TO VOLTAGE CUTOFF=1.00V:						
NOMINAL									
time (hr)	current (mA)	resistor (Ω)	-40°C (-40°F)	-23.5°C (-10°F)	0°C (32°F)	24°C (75°F)	49°C (120°F)	71°C (160°F)	88°C (190°F)
20.0	2000	1.35			42.63 **42.38** 41.51	42.10 **41.85** 41.58	42.18 **41.65** 41.65		
31.6	1260	2.14		40.43 **39.94** 38.93	42.34 **41.32** 39.82	43.66 **42.66** 42.59	42.36 **42.01** 41.56	42.49 **42.15** 41.48	
50.0	800	3.38				43.39 **42.86** 42.64			
100	400	6.75		42.24 **41.11** 39.72	44.07 **43.38** 42.23	43.92 **43.22** 42.19	43.92 **42.96** 42.59	42.84 **41.91** 17.28	
200	200	13.5				44.36 **43.68** 42.51			
316	126	21.4	36.89 **36.23** 35.69	42.81 **42.25** 41.97	44.70 **44.03** 42.69	44.25 **43.91** 43.19	44.02 **43.76** 43.38	44.13 **43.93** 43.47	43.26 **42.98** 42.81
500	80.0	33.8				44.55 **43.15** 43.13			
1000	40.0	67.5	40.54 **40.44** 39.48	44.08 **43.53** 42.64	45.05 **44.83** 43.63	45.31 **44.91** 44.56	44.45 **43.91** 43.55	44.26 **43.91** 43.69	42.65 **42.36** 41.89
2000	20.0	135				44.85 **43.68** 43.65			
3160	12.6	214	43.16 **42.63** 41.95	44.83 **44.18** 44.10	45.61 **44.89** 44.60	45.18 **44.82** 44.10	44.29 **43.78** 43.41	44.02 **43.67** 43.31	34.27 **13.11** 12.75
5000	8.00	338				44.02 **43.56** 43.27			
10000	4.00	675			45.57 **45.26** 44.85	44.39 **44.24** 43.82	43.68 **43.57** 43.04		

Middle (bold) number: test median

Top & bottom smaller numbers: test 95% confidence limits on the median

Storage with subsequent Constant Resistive Discharge Results

- Despite the storage conditions:
  - ☞ those cells discharged with 67.5Ω delivered capacities within error of each other
    - ↳ maximum capacity delivered: cells stored at 49°C for 3 months
  - ☞ those cells discharged with 2.14Ω delivered capacities within error of each other
    - ↳ maximum for the cells stored at 24°C for 1 year

Pulse Discharge Test Results

- Typical Pulse Profile
- End-of-Pulse Voltage
  - ⇨Room Temperature (24°C) Pulses
  - ⇨2Ω Pulses at Various Temperatures
- Background capacity delivered to 1.00V

PULSE TEST	RESISTIVE DISCHARGE			CAPACITY (Ah) TO VOLTAGE CUTOFF=1.00V:					
	NOMINAL								
3Ω/2Ω/1Ω x 2 S T,W,R AM&PM BI-WK	time (hr)	current (mA)	resistor (Ω)	-40°C (-40°F)	-23.5°C (-10°F)	0°C (32°F)	24°C (75°F)	49°C (120°F)	71°C (160°F)
	3160	12.6	214			45.65 **45.29** 45.21	44.60 **44.44** 44.07	44.03 **43.94** 43.92	

Room Temperature (24°C) Pulses

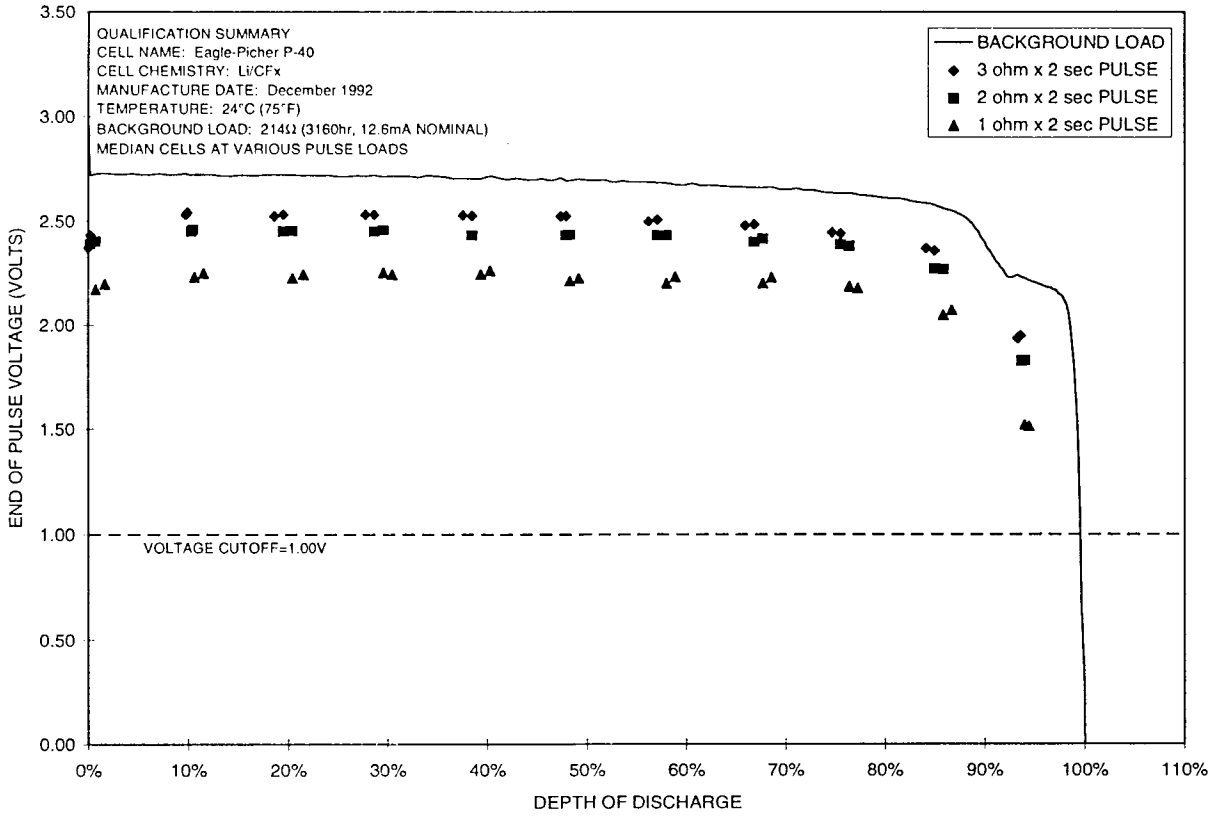

2Ω Pulses at Various Temperatures

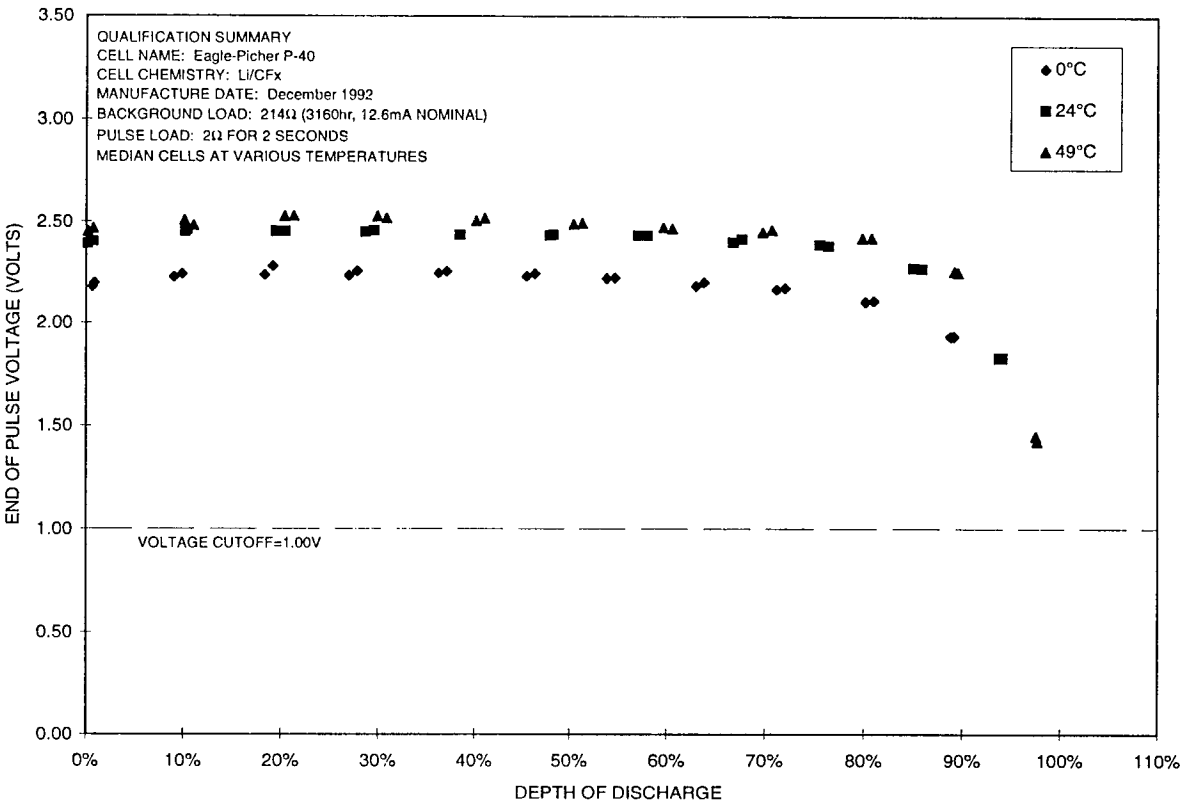

Safety Considerations

- No internal fuse: do not abuse or short circuit
- Do not operate above 71°C: not qualified
- Vented cells release DMSI ($(CH_3)_2SO_3$), a strong irritant

Conclusions

- The P-40 cell performs well in the -23.5°C to 71°C range with resistive loads ranging from 1.35Ω to 675Ω
- Storage w/ subsequent discharge: tests performed to date show little self-discharge up to 2 years
- Good pulse capability with 3Ω, 2Ω and 1Ω loads at 0°C, 24°C and 49°C

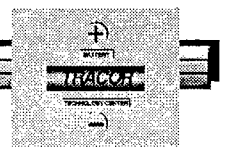

LITHIUM-THIONYL CHLORIDE BATTERIES FOR THE MARS PATHFINDER MICROROVER

FRANK DELIGIANNIS AND HARVEY FRANK
ELECTROCHEMICAL TECHNOLOGIES GROUP
JET PROPULSION LABORATORY

&

Dr. R.J. STANIEWICZ AND JOHN WILLSON
SAFT AMERICA INC.
RESEARCH & DEVELOPMENT CENTER

1995 NASA Aerospace Battery Workshop
November 28-30, 1995
Huntsville Hilton
Huntsville, AL

AGENDA

- BACKGROUND - MISSION DESCRIPTION
- BATTERY REQUIREMENTS
- CELL DESIGN
- BATTERY DESIGN
- TEST DESCRIPTIONS & RESULTS
- SUMMARY

BACKGROUND

- MARS PATHFINDER MISSION CONSISTS OF THE LANDER AND THE MICROROVER - ONE OF THE FIRST *FASTER-BETTER-CHEAPER* NASA/JPL MISSIONS
- MICROROVER IS CONSIDERED THE EXPERIMENT ON THE MARS PATHFINDER MISSION
- MAIN POWER PROVIDED TO MICROROVER BY SOLAR ARRAY
- LITHIUM PRIMARY BATTERIES SUPPORT
  - KEEP ALIVE CIRCUITS DURING THE NIGHT
  - DURING DUST STORMS
  - LOAD LEVELING WHEN WHEEL IS STUCK
- BATTERIES ARE ENCLOSED IN THE *Warm Electronic Box* (WEB)
  - BATTERY TEMPERATURE IS PROJECTED BETWEEN -30° C & +30° C

BATTERY REQUIREMENTS

- CLASS 'D' MISSION
- LITHIUM THIONYL CHLORIDE CHEMISTRY
- SIZE/CONFIGURATION = 'D' SIZE / SPIRAL WOUND
- THREE CELLS IN SERIES / THREE BATTERIES IN PARALLEL
- WEIGHT ALLOCATION:
  - CELLS = 1080g
  - WIRE & DIODES = 45g
  - CASES = 54g
- MAX DISCHARGE RATE = 750 mA
- OPERATING TEMPERATURE = -30° to +30° C

BATTERY REQUIREMENTS con't

- MINIMUM CAPACITY @ -30° C = 6 Ah
- MINIMUM OPERATING CELL VOLTAGE @ -30° C & 750 mA = 2.5 V
- SAFE
- STORAGE MODE TEMPERATURES
  - GROUND STORAGE @ 5° C for 21 MONTHS
  - INTEGRATION @ 40° C for 3 MONTHS
  - CRUISE @ 30° C for 8 MONTHS
- SURVIVE LAUNCH-CRUISE-LANDING ENVIRONMENTS

CELL DESIGN

- LITHIUM ANODE
  - WEIGHT = 4.11 g (INCLUDING 0.48g FOLDBACK Li)
  - CAPACITY = 14 Ah
  - EXCESS CAPACITY (FOLDBACK) = 1.85 Ah
- CARBON CATHODE
  - CARBON MIX = 61% SHAWINIGAN ACETYLENE BLACK
    20% EC 300J ACETYLENE BLACK
    19% PTFE
- ELECTROLYTE
  - CAPACITY = 20 Ah
  - COMPOSITION = 1.35 M $LiCl_4Al$ + 0.55 M SO_2 IN $SOCl_2$ & 3 ADDITIVES
- SEPARATOR = HESGON WOVEN GLASS ('M' WEAVE HEAT CLEANED)
- VENT = FUSITE 325 $\pm$50 psi

BATTERY DESIGN

- THREE 'D' SIZE CELLS IN SERIES (BATTERY)
- THREE BATTERIES IN PARALLEL (TOTAL NINE CELLS)
- ALUMINUM BATTERY CASE w/VENT HOLES
- CELLS WRAPPED IN KAPTON TAPE
- NON-CONDUCTIVE SPACERS BETWEEN CELLS
- ADHESIVE USED TO BOND CELLS TO ALUMINUM CASE
- EACH BATTERY HAS ONE DIODE AND ONE FUSE
- TWO HEATERS & ONE THERMISTOR PER BATTERY

BATTERY WEIGHT DISTRIBUTION

CELLS	9 x 118 g = 1062.0 g	85.4 %
BATTERY CASES	3 x 32.35g = 97.1 g	7.8 %
CELL SPACERS	4 x 4.35 g = 17.4 g	1.4 %
OTHER		
BONDING MATERIAL		
DIODES, FUSES		
HEATERS, PRTs		
CABLE, CONNECTOR		
KAPTON TAPE	66.3 g	5.4 %
	TOTAL 1242.8 g	

CELL/BATTERY LOT DESCRIPTION

- **SAFT WILL SUPPLY TWENTY-ONE 3-CELL BATTERIES & 25 CELLS**
  - **10 CELLS TESTED @ SAFT (5 @ R.Temp. & 5 @ -30° C)**
  - **15 CELLS TESTED @ JPL FOR ELECTRONIC COMPONENT CHECK**
  - **SIX 3-CELL 'TEST' BATTERIES (TESTED @ SAFT)**
  - **SIX 3-CELL 'SIM' (System Integration Model) BATTERIES TESTED ON 'SIM' MICROROVER @ JPL**
  - **THREE 3-CELL 'TEST & INTEGRATION' BATTERIES FOR TESTING & INTEGRATING FLIGHT UNIT @ JPL**
  - **THREE 3-CELL 'FLIGHT' BATTERIES**
  - **THREE 3-CELL 'FLIGHT SPARE' BATTERIES**

'TEST' BATTERY TEST PLAN

- SIX 3-CELL 'TEST' BATTERIES (TESTED @ SAFT)
  - QUASI-STATIC ACCELERATION @ 66g for 1 MINUTE IN BOTH DIRECTIONS (AXIAL & RADIAL) ON A CENTRIFUGE *(6 BATT.)*
  - RANDOM VIBRATION IN BOTH DIRECTIONS *(6 BATT.)*
  - PYRO-SHOCK PULSE IN BOTH DIRECTIONS *(6 BATT.)*
  - 35 THERMAL CYCLES BETWEEN -55° C & +60° C WITH 1 HOUR DWELL AT BOTH TEMPERATURES & 1 HOUR TRANSITION *(6 BATT.)*
  - 2 BATTERIES DISCHARGED @ 750 mA & -30° C
  - 1 BATTERY DISCHARGED @ 750 mA & 25° C
  - 2 BATTERIES SIMULATE MARTIAN SURFACE OPERATIONS
  - 1 BATTERY SHORT WITH FUSE REMOVED

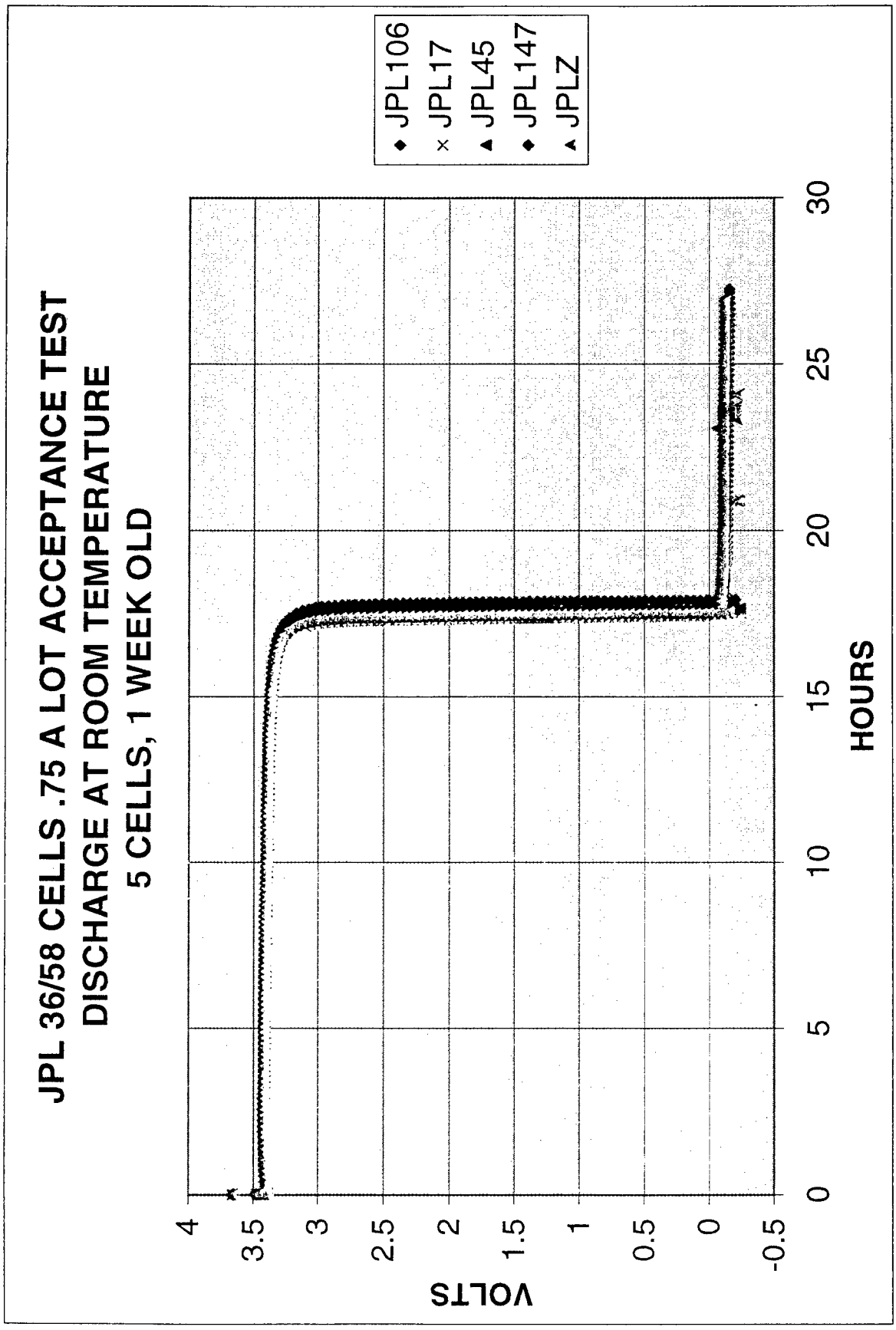
JPL 36/58 CELLS .75 A LOT ACCEPTANCE TEST
DISCHARGE AT ROOM TEMPERATURE
5 CELLS, 1 WEEK OLD
JPL106
JPL17
JPL45
JPL147
JPLZ
VOLTS
4
3.5
3
2.5
2
1.5
1
0.5
0
-0.5
HOURS
0
5
10
15
20
25
30

JPL147.XLS

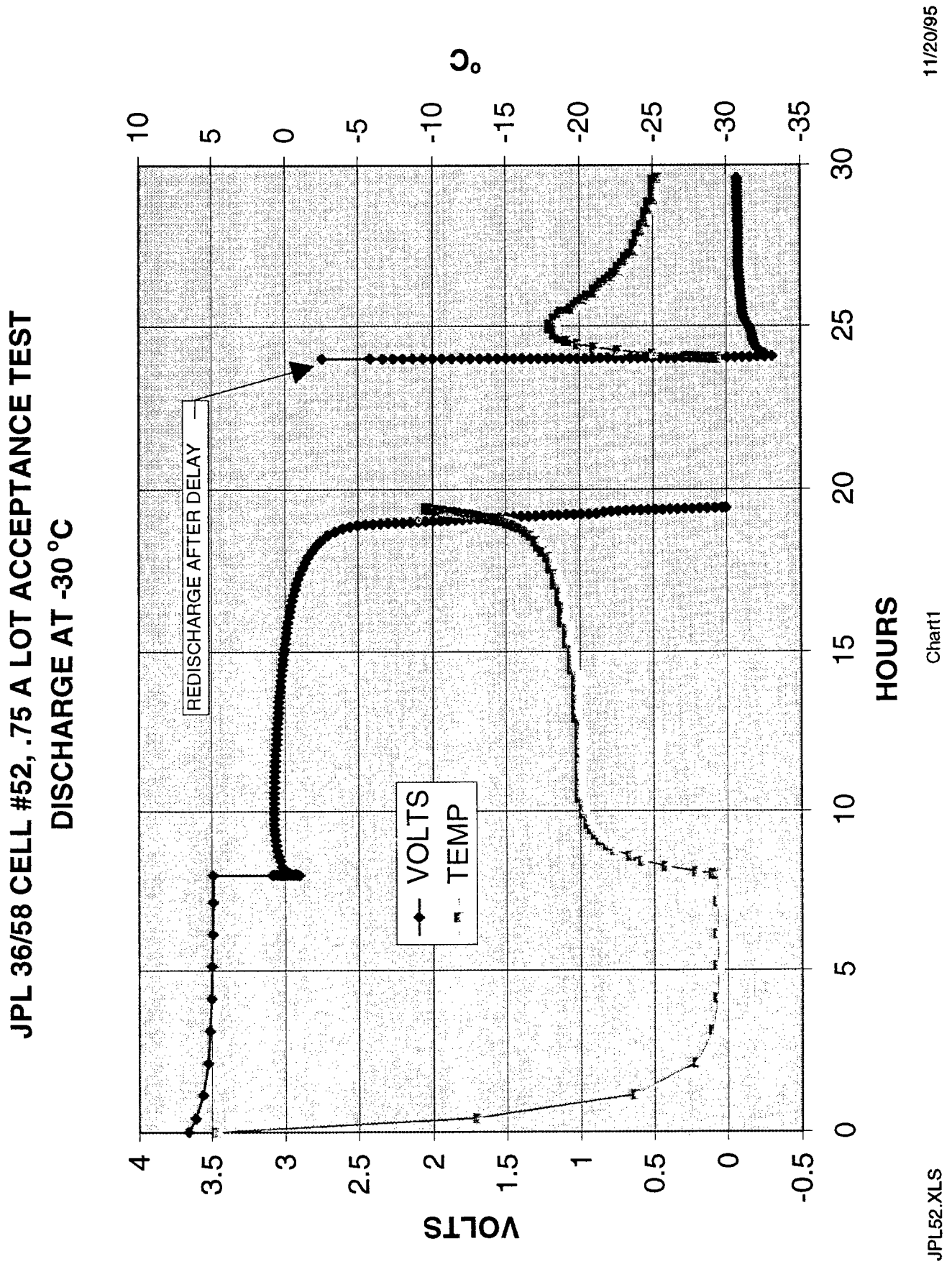
JPL 36/58 CELL #52, .75 A LOT ACCEPTANCE TEST
DISCHARGE AT -30 °C
REDISCHARGE AFTER DELAY
VOLTS
TEMP
VOLTS
°C
HOURS
11/20/95
Chart1
JPL52.XLS

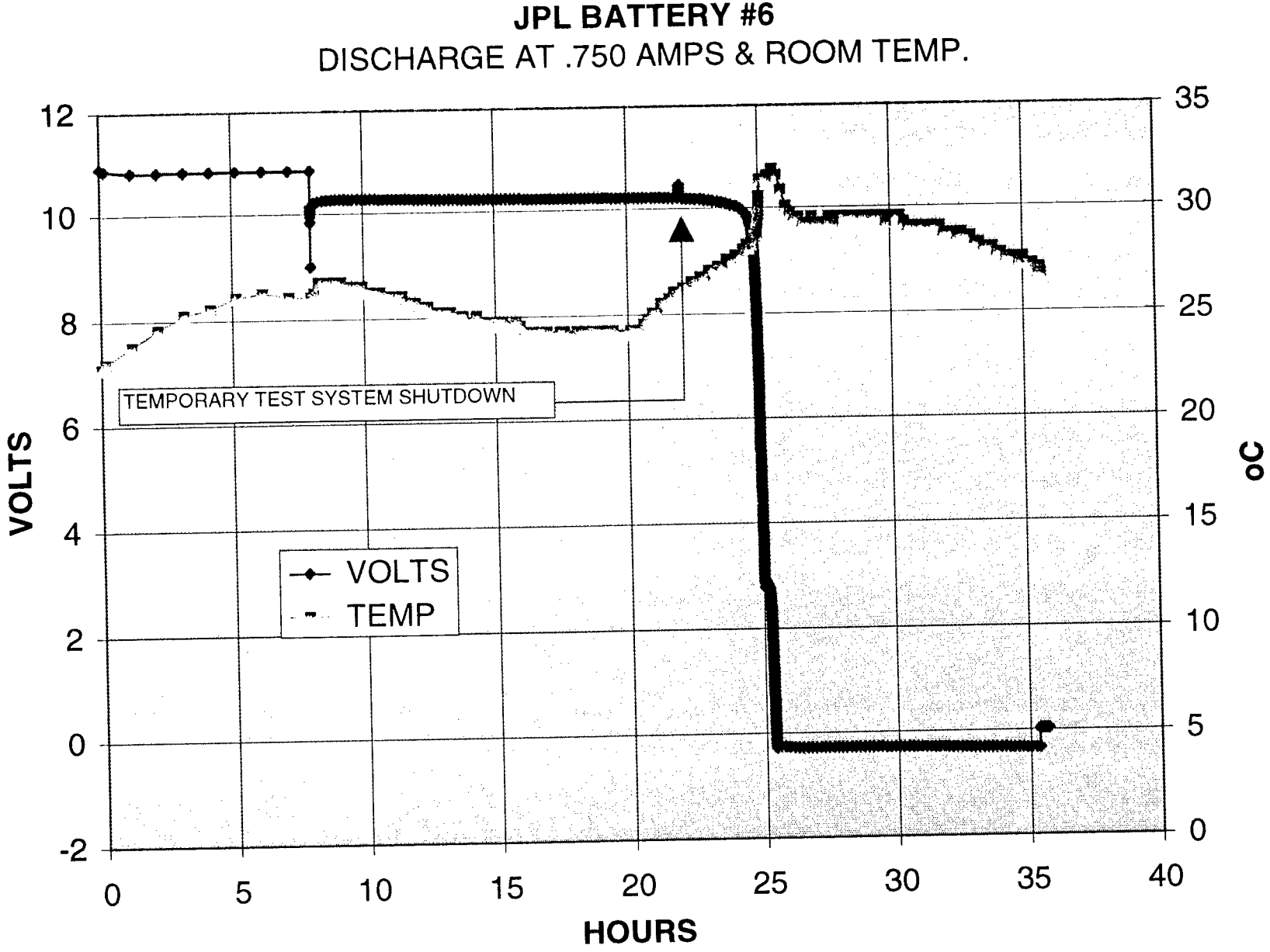

JPLBATT.XLS

11/20/95

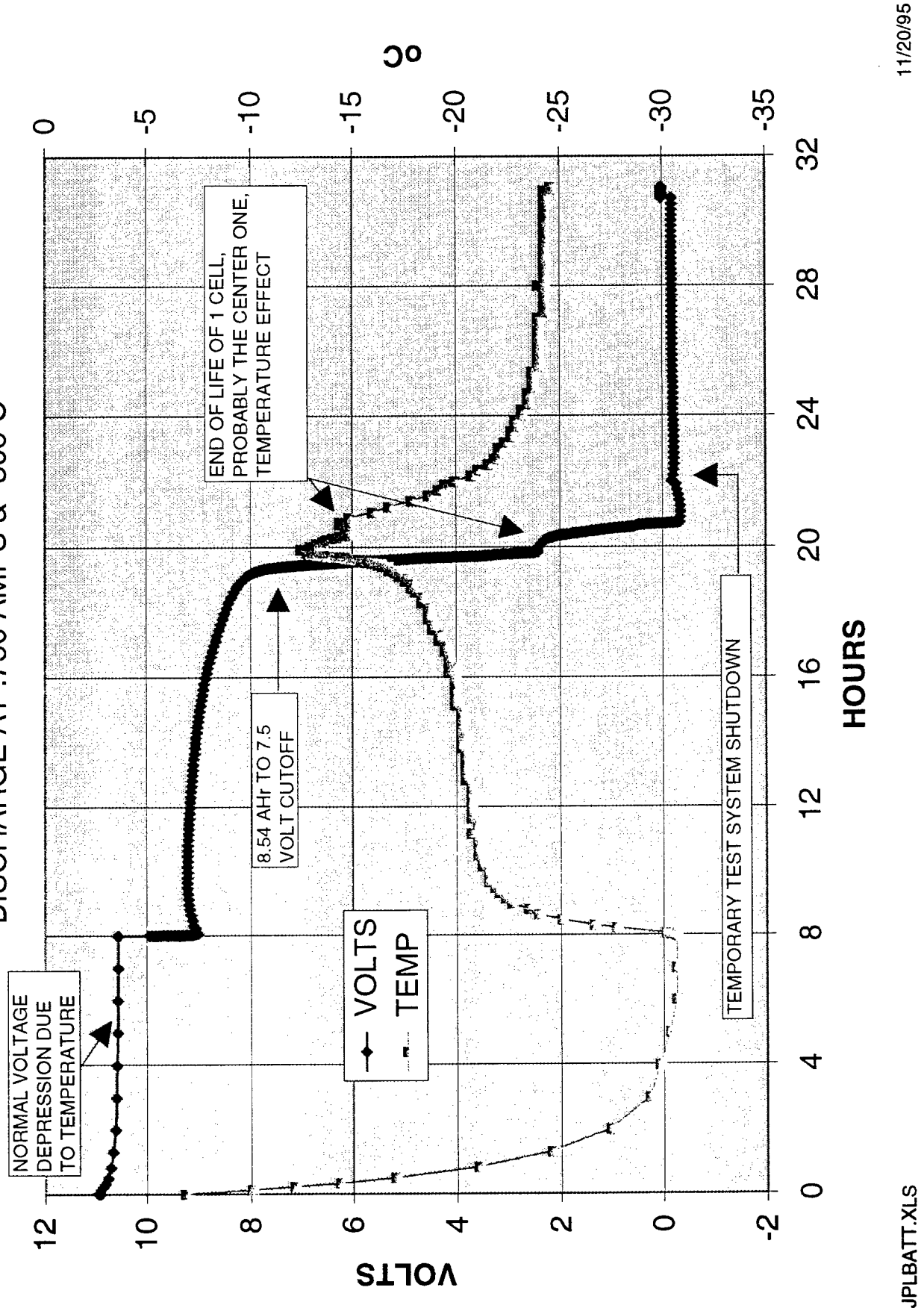
JPL BATTERY #5
DISCHARGE AT .750 AMPS & -30o C
NORMAL VOLTAGE DEPRESSION DUE TO TEMPERATURE
8.54 AHr TO 7.5 VOLT CUTOFF
END OF LIFE OF 1 CELL, PROBABLY THE CENTER ONE, TEMPERATURE EFFECT
TEMPORARY TEST SYSTEM SHUTDOWN
VOLTS
TEMP
VOLTS
oC
HOURS
12
10
8
6
4
2
0
-2
0
-5
-10
-15
-20
-25
-30
-35
0
4
8
12
16
20
24
28
32
JPLBATT.XLS
11/20/95

MARTIAN SURFACE BATTERY OPERATION

- **50 mA DISCHARGE FOR 10 HOURS (0.5 Ah)**
- **2 mA DISCHARGE FOR 6 HOURS (0.012 Ah)**
- **750 mA DISCHARGE FOR 15 MINUTES (0.1875 Ah)**
- **400 mA DISCHARGE FOR 30 MINUTES (0.2 Ah)**
- **750 mA DISCHARGE FOR 30 MINUTES (0.375 Ah)**
- **2 mA DISCHARGE FOR 45 MINUTES (0.0015 Ah)**
- **OPEN CIRCUIT FOR 6.5 HOURS (0.0 Ah)**

TOTAL / DAY (1.276 Ah)

REPEAT UNTIL BATTERY IS DEPLETED

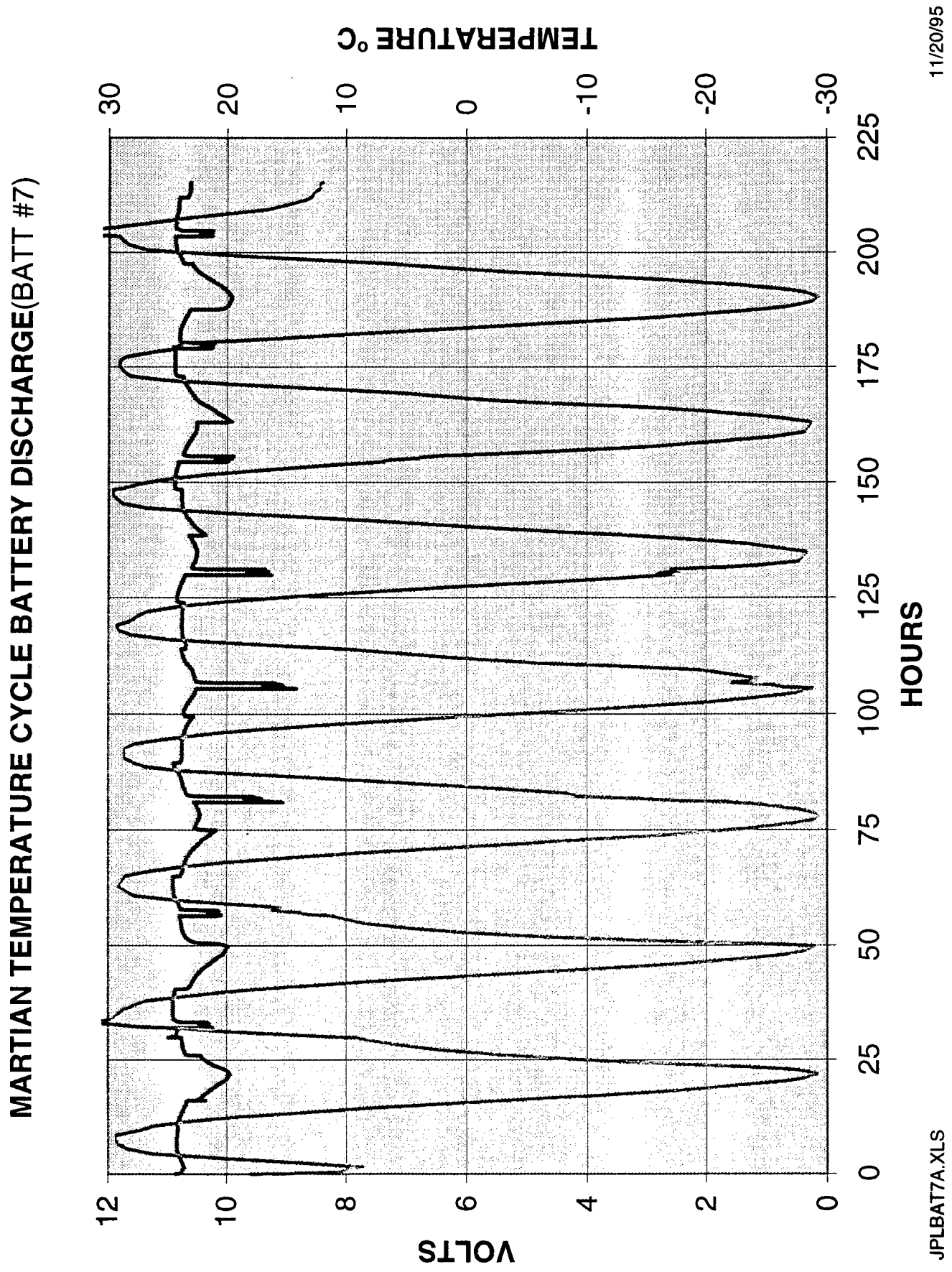
MARTIAN TEMPERATURE CYCLE BATTERY DISCHARGE(BATT #7)
TEMPERATURE °C
30
20
10
0
-10
-20
-30
VOLTS
12
10
8
6
4
2
0
HOURS
0
25
50
75
100
125
150
175
200
225
11/20/95
JPLBAT7A.XLS

SUMMARY

- Li-$SOCl_2$ PRIMARY BATTERY SELECTED FOR THE MARS PATHFINDER MICROROVER
- TEST BATTERIES & SIM BATTERIES DELIVERED & TESTED
- SPECIFIC ENERGY PENALTY
  - FROM CELL TO BATTERY LEVEL WAS 15%
  - FROM ROOM TEMPERATURE TO -30° C WAS 45%
- BATTERIES DELIVERED FROM SAFT AMERICA TO-DATE HAVE MET MARS PATHFINDER MICROROVER REQUIREMENTS
- CAN PROCEED WITH THE MANUFACTURING OF FLIGHT & FLIGHT SPARE UNITS

MARS PATHFINDER BATTERY PROGRAM STATUS

S. SURAMPUDI, S. DAWSON, D. PERRONE,
B. OTZINGER, and M. SHIRBACHEH

JET PROPULSION LABORATORY
PASADENA, CA 91109

NASA BATTERY WORKSHOP
HUNTSEVILLE, AL.
NOVEMBER 28-30, 1995

OUTLINE

- MISSION OVERVIEW
- BATTERY REQUIREMENTS
- Ag-Zn TECHNOLOGY ASSESSMENT
- EM BATTERY PERFORMANCE
- SUMMARY AND CONCLUSIONS

Mars Pathfinder Project

Mission Objectives

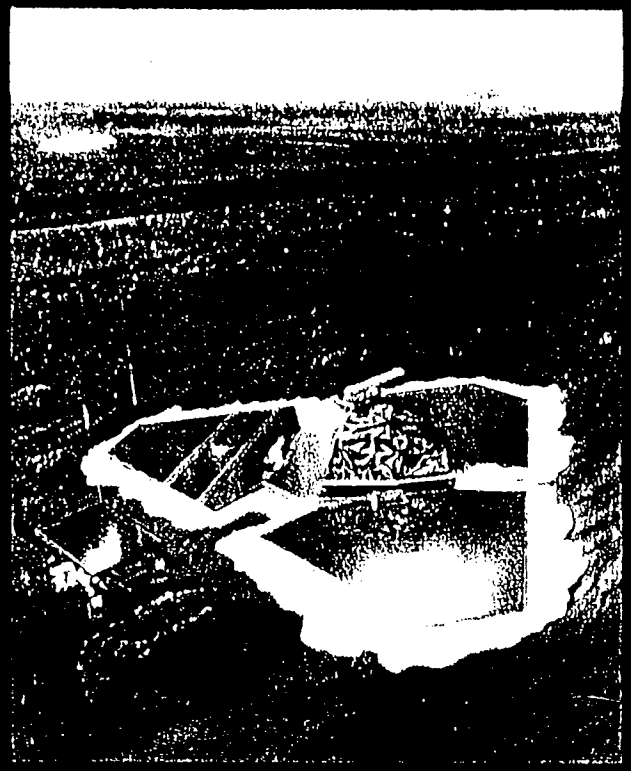

- Demonstrate a simple, reliable, and low cost system for placing science payloads on the surface of Mars
- Demonstrate NASA's commitment to low cost planetary exploration by completing the mission for a total cost of $271M including the launch vehicle and mission operations.
- Demonstrate the mobility and usefulness of a microrover vehicle on the surface of Mars.
- Science objectives:
  - Assess the structure of the Martian atmosphere during entry
  - Determine the elemental composition of Martian rocks and soil near the landing site
  - Investigate the surface geology and mineralogy of rocks near the landing site
  - Acquire data on the surface meteorological conditions at the landing site

Mars Pathfinder Project

Launch Phase

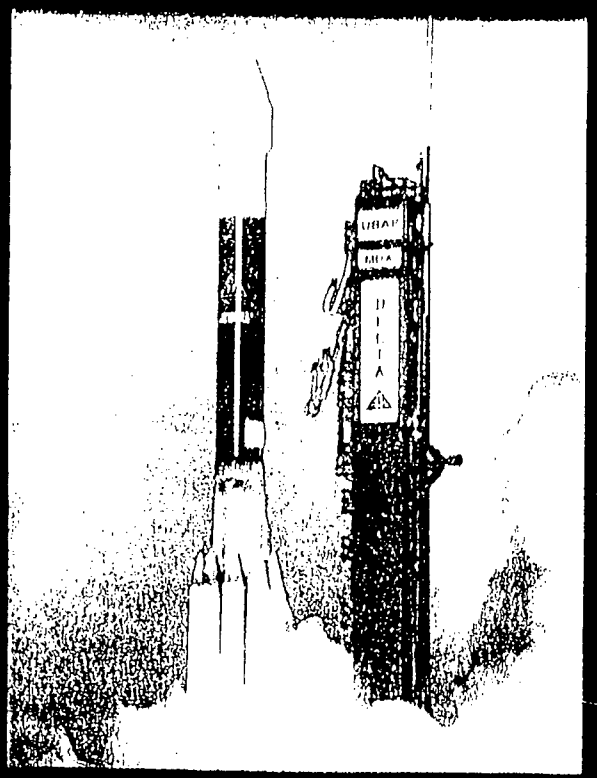

- Launch Vehicle: McDonnell Douglas Delta II (three stages)
- Launch From: Cape Canaveral
- Launch Period: December 2-25, 1996
- Launch Time: varies from 9:00 pm to 11:30 pm (PST)
- Launch Mass: 905 kg (includes 85 kg propellant)

Mars Pathfinder Project

Cruise Configuration

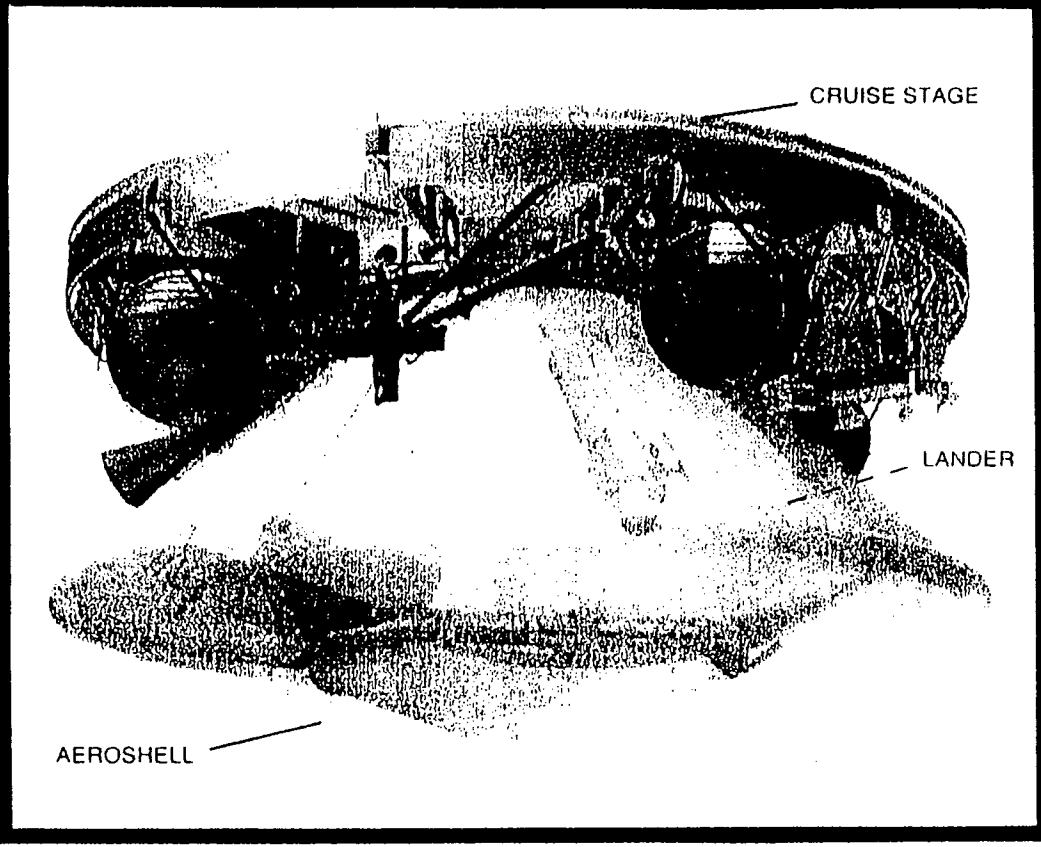

MPF BATTERY REQUIREMENTS

VOLTAGE	27 V
CAPACITY	40AH
RATE CAPABILITY	1-5 A
PULSE CAPABILITY	50 A FOR 40 MSEC
OPE./STORAGE TEMP	0-25° C
CYCLE LIFE	40
WET LIFE	14 MONTHS
WEIGHT	14.5 KG
DIMENSIONS	24.8 X 18.7 X 18.7 CM
	9.76 X 7.36 X 7.37 IN
VOLUME	8.7 L

BATTERY OPERATIONAL OVERVIEW

- PRE LAUNCH — 4 MONTH ACTIVE STORAGE
- LAUNCH — INVERTED BATTERY LAUNCH
- CRUISE — 7 MONTHS ACTIVE STORAGE
- EDL — 30 AH
- MARS OPT. OPERATIONS — 30 CYCLES (8 HOUR CHARGE 16 HOUR DISCHARGE)

TECHNICAL ISSUES

- CELLS/BATTERIES
  - 14 MONTH WET LIFE
  - 75% CAPACITY, AFTER 12M STORAGE
  - 30 CYCLES AFTER 12 M STORAGE
  - ELECTROLYTE LEAKAGE
- OPERATIONAL
  - OCV OR FLOAT STAND DURING CRUISE
  - STORAGE TEMPERATURE
  - CHARGE CONTROL

Ag-Zn TECHNOLOGY ASSESSMENT

TEST PROGRAM OBJECTIVES

OVERALL OBJECTIVE

- VERIFY Ag-Zn BATTERY TECHNOLOGY CAN MEET MISSION REQUIREMENTS

SPECIFIC OBJECTIVES

- DETERMINE THE EFFECT OF KEY DESIGN PARAMETERS (SEPARATOR SYSTEM) ON CELL WET AND CYCLE LIFE PERFORMANCE.

- DETERMINE THE INFLUENCE OF KEY OPERATING PARAMETERS (STORAGE TEMP. AND OCV/FLOAT STAND) ON CELL WET AND CYCLE LIFE PERFORMANCE.

TEST ARTICLES

- 40 AH CELLS WITH 5 LAYERS OF CELLOPHANE
- 40 AH CELLS WITH 6 LAYERS OF CELLOPHANE
- 40 AH CELLS WITH 5 LAYERS OF CELLOPHANE AND TWO LAYERS RAI POLY ETHYLENE

TEST PLAN OVERVIEW

1) CELL ACTIVATION/FORMATION
2) CAPACITY CHECK
3) FOUR MONTH ACTIVE STORAGE AT 25 C (PRE LAUNCH)
4) CAPACITY CHECK
5) SEVEN MONTH ACTIVE STORAGE AT SELECTED TEMPERATURES AND TYPE OF STAND (CRUISE STORAGE)
6) CAPACITY TEST (EDL)
7) CYCLE LIFE TEST(6-8 HOUR MCP CHARGE AND 3-5 A CONSTANT CURRENT DISCHARGE-20 AH)

CRUISE STORAGE TEST MATRIX

CELL PACK	SEPARATOR	TYPE OF STAND	STORAGE COND.
A	5 LAYERS OF CP	1.86 V FLOAT	30 ° C, 7 MONTHS
B	5 LAYERS OF CP	0CV	30 ° C , 7 MONTHS
C	5 LAYERS OF CP	1.86 V FLOAT	15 ° C, 7 MONTHS
D	6 LAYERS OF CP	0CV	15 ° C, 7 MONTHS
E	6 EPARATOR	1.86 V FLOAT	30 ° C, 7 MONTHS
F	6 LAYERS OF CP	0CV	30 ° C, 7 MONTHS
G	6 LAYERS OF CP	1.86 V FLOAT	15 ° C, 7 MONTHS
H	6 LAYERS OF CP	0CV	15 ° C, 7 MONTHS
I	5 LAYERS OF CP	NONE	NONE
S	5 LAYERS OF CP & 2 LAYERS RAI	NONE	NONE

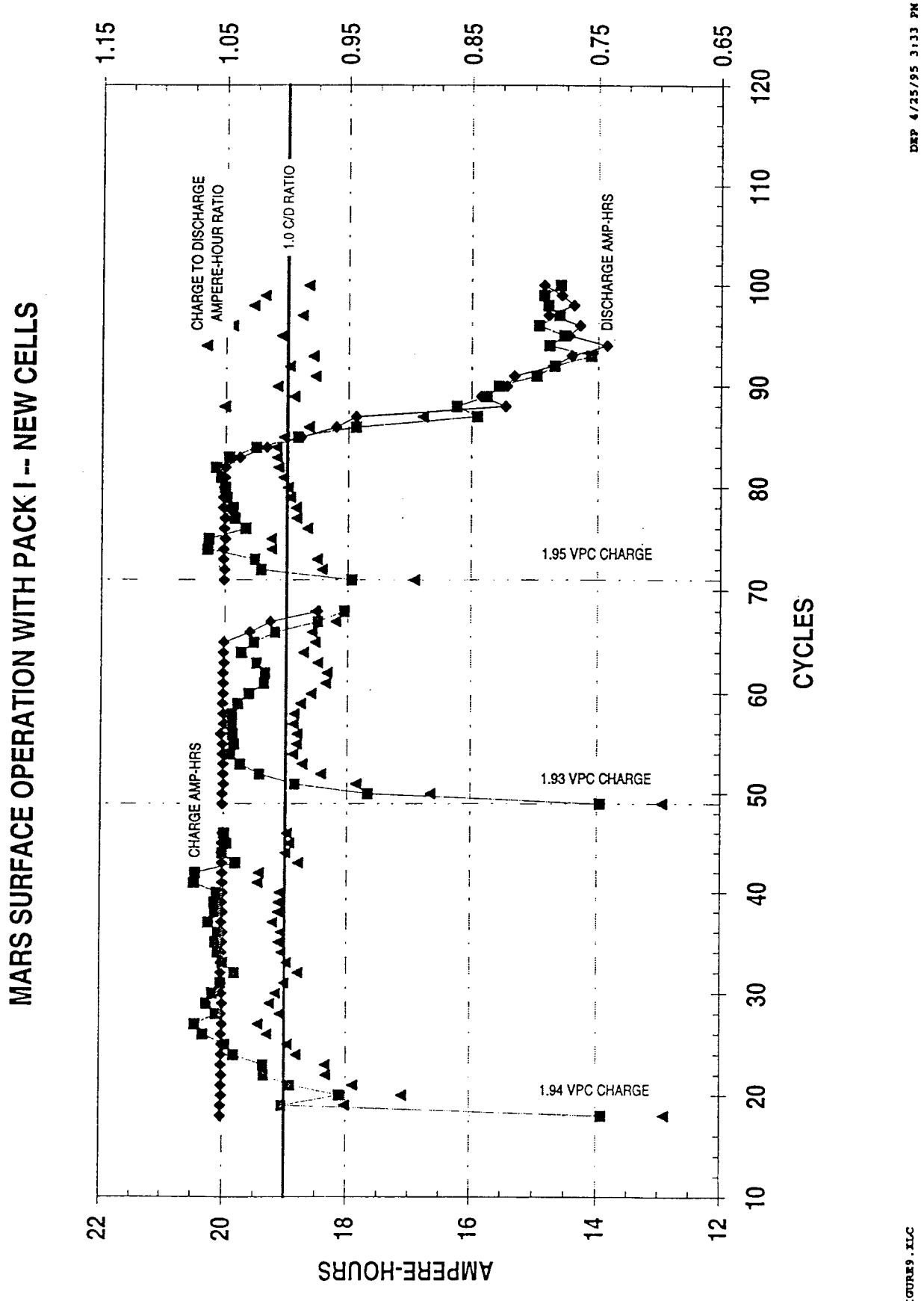
MARS SURFACE OPERATION WITH PACK I -- NEW CELLS
AMPERE-HOURS
CYCLES
CHARGE AMP-HRS
DISCHARGE AMP-HRS
CHARGE TO DISCHARGE AMPERE-HOUR RATIO
1.0 C/D RATIO
1.95 VPC CHARGE
1.93 VPC CHARGE
1.94 VPC CHARGE
DEP 4/25/95 3:33 PM
FIGURE9.XLC

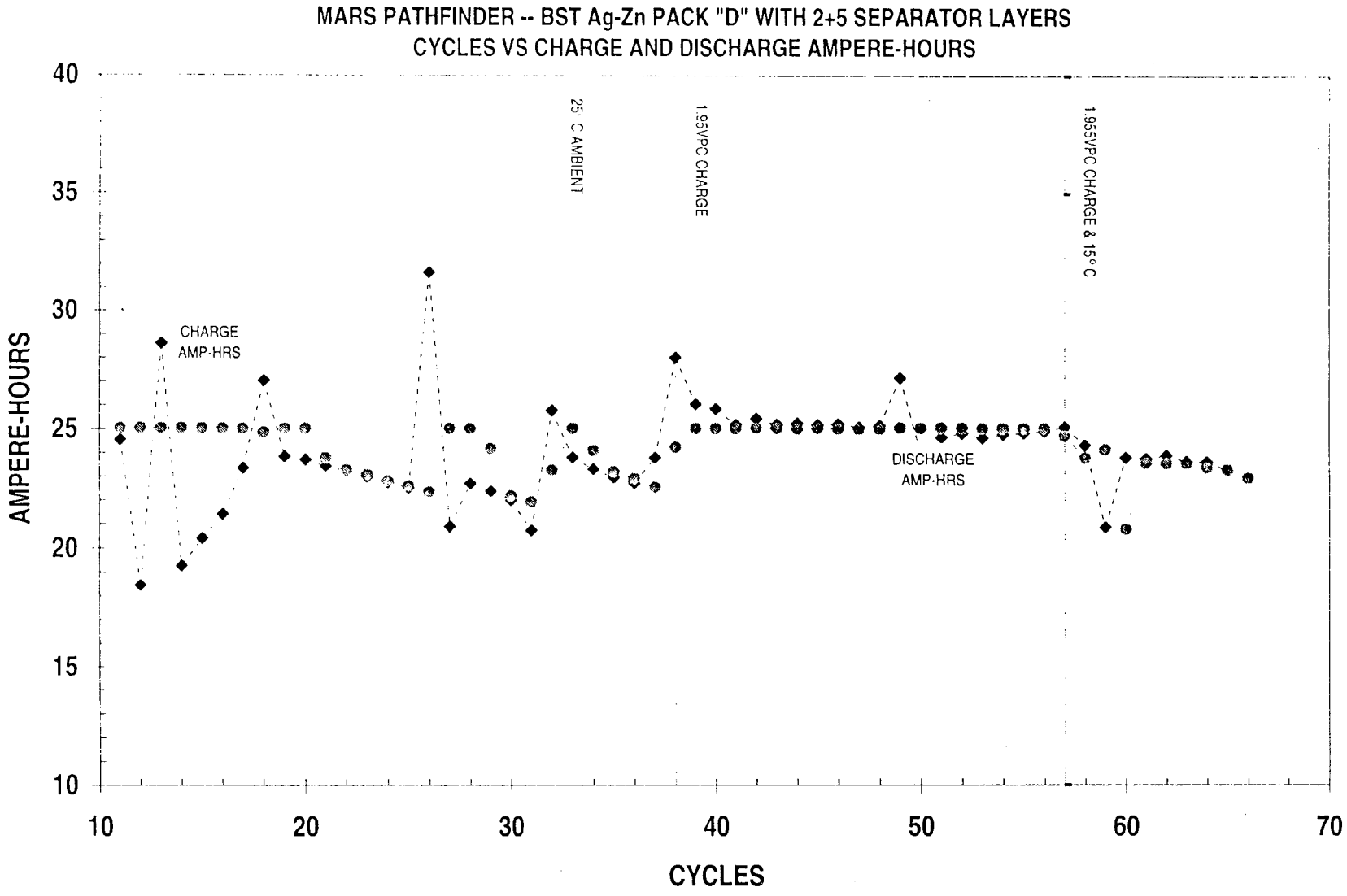

CDR0695.XLS H

D. PERRONE 11/22/95 10:04 AM

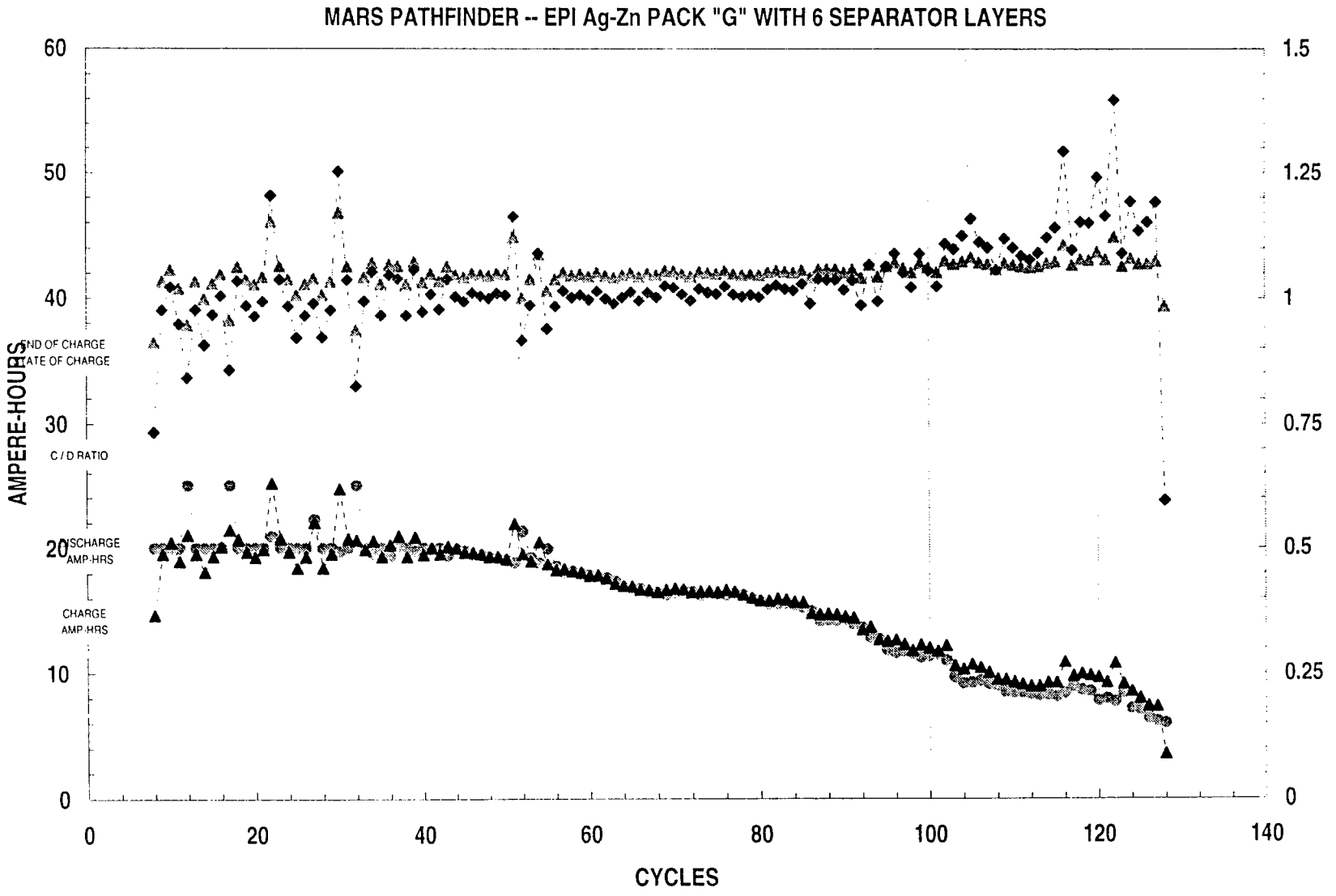

95014-0.XLS Chart1

D. PERRONE 11/22/95 10:19 AM

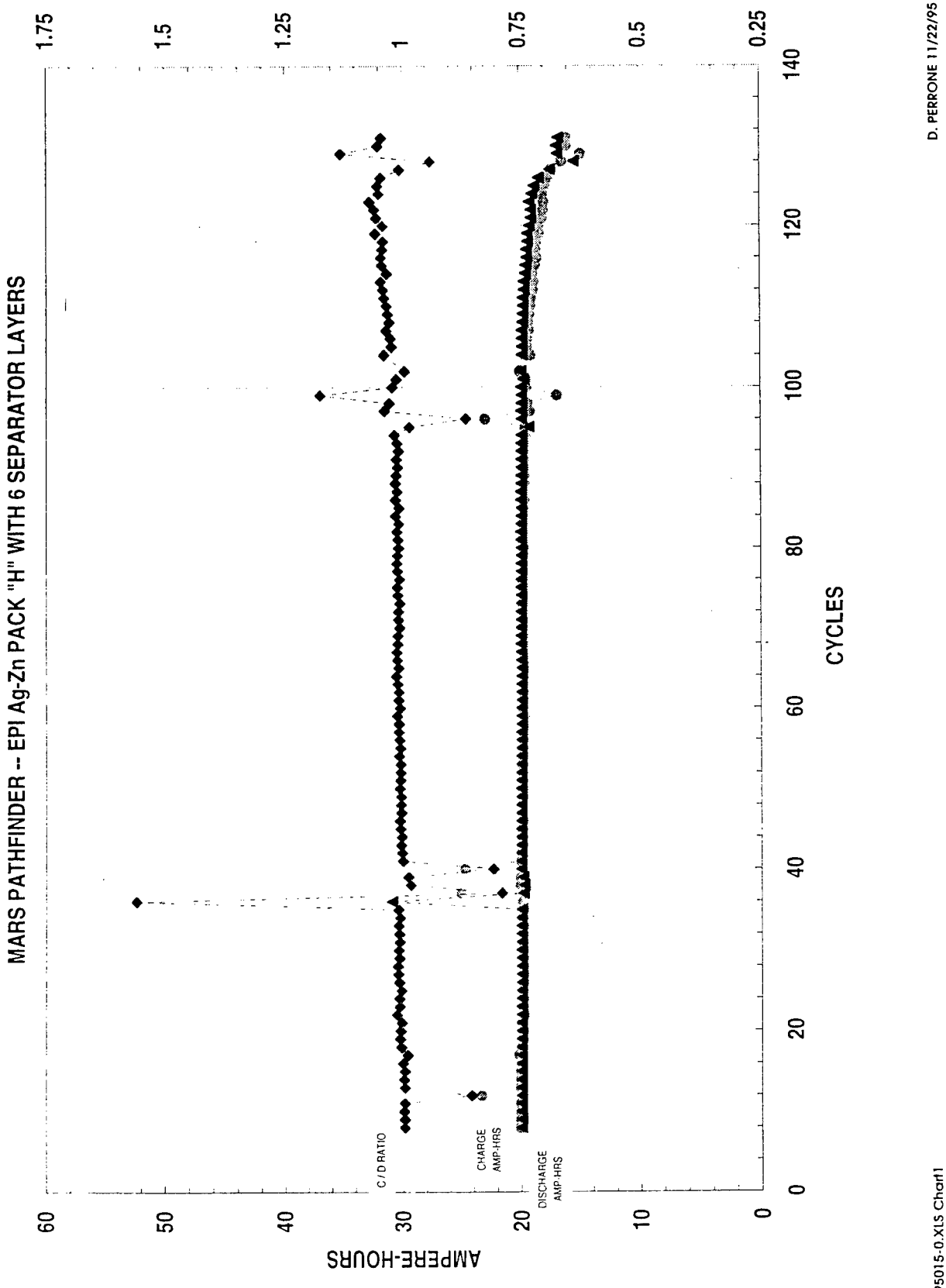
MARS PATHFINDER -- EPI Ag-Zn PACK "H" WITH 6 SEPARATOR LAYERS
AMPERE-HOURS
CYCLES
C / D RATIO
CHARGE AMP-HRS
DISCHARGE AMP-HRS
60
50
40
30
20
10
0
1.75
1.5
1.25
1
0.75
0.5
0.25
0
20
40
60
80
100
120
140
D. PERRONE 11/22/95 10:19 AM
95015-0.XLS Chart1

BATTERY INITIAL PERFORMANCE CHARACTERISTICS

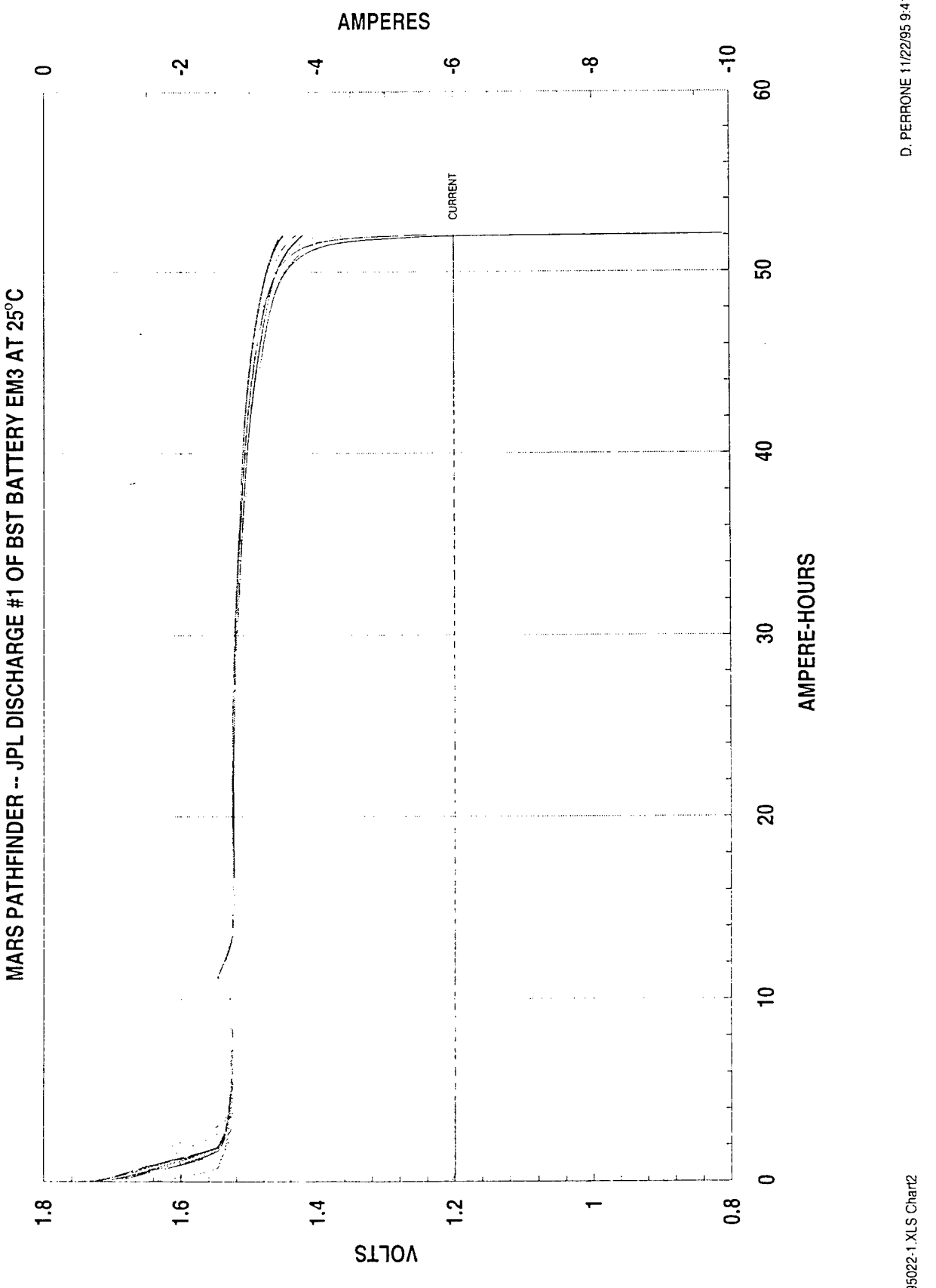
MARS PATHFINDER -- JPL DISCHARGE #1 OF BST BATTERY EM3 AT 25°C
AMPERES
0
-2
-4
-6
-8
-10
CURRENT
VOLTS
1.8
1.6
1.4
1.2
1
0.8
AMPERE-HOURS
0
10
20
30
40
50
60
D. PERRONE 11/22/95 9:41 AM
95022-1.XLS Chart2

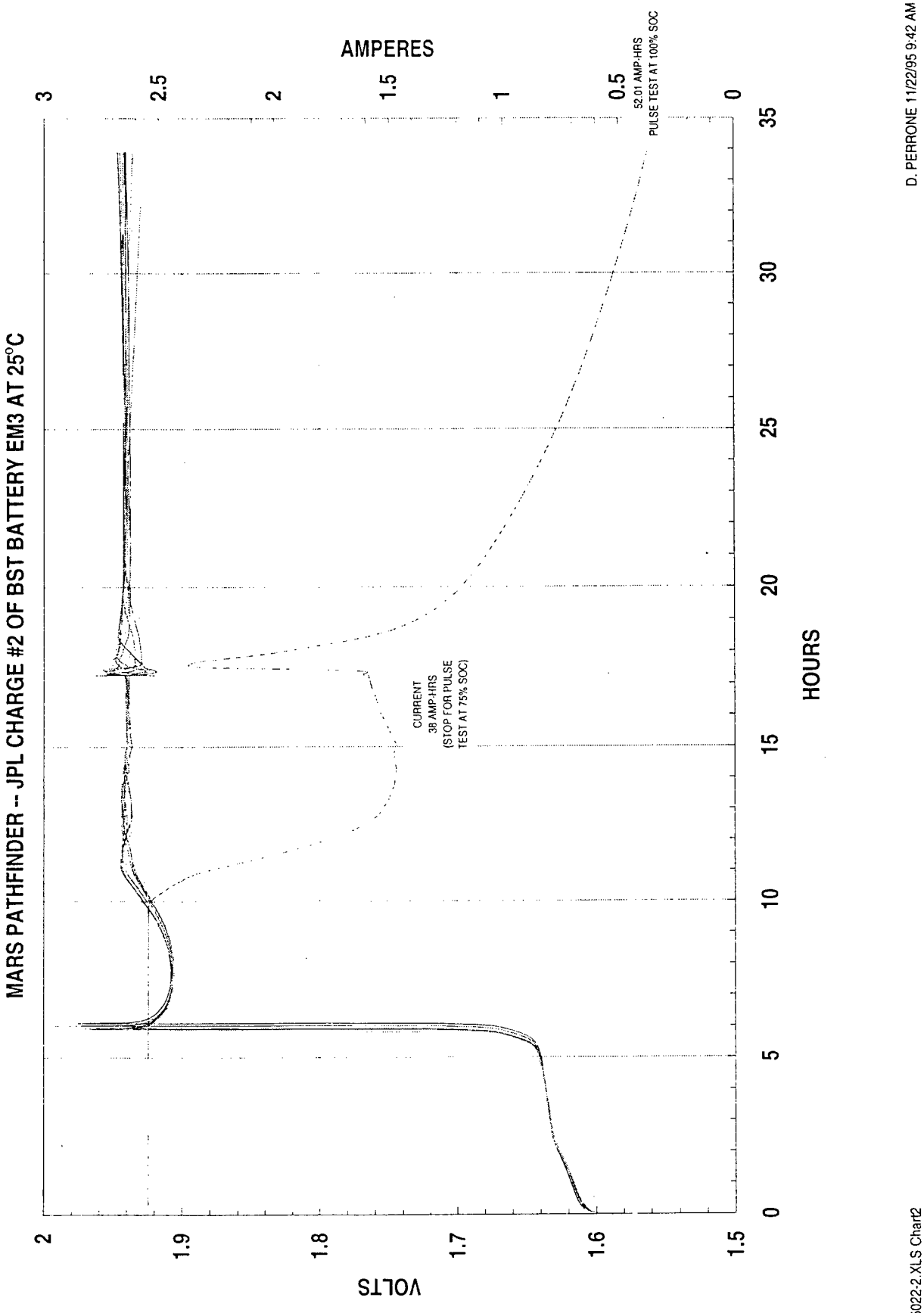
MARS PATHFINDER -- JPL CHARGE #2 OF BST BATTERY EM3 AT 25°C
AMPERES
VOLTS
HOURS
CURRENT
38 AMP-HRS
(STOP FOR PULSE
TEST AT 75% SOC)
52.01 AMP-HRS
PULSE TEST AT 100% SOC
D. PERRONE 11/22/95 9:42 AM
95022-2.XLS Chart2

MARS PATHFINDER -- 18 CELL Ag-Zn BATTERY (EM1)

JPL DISCHARGE #3-6 AT 5.0A WITH 6 HOUR CHARGESAT 4.5 AMPERES TO 1.94 VOLTS PER CELL AT 25°C

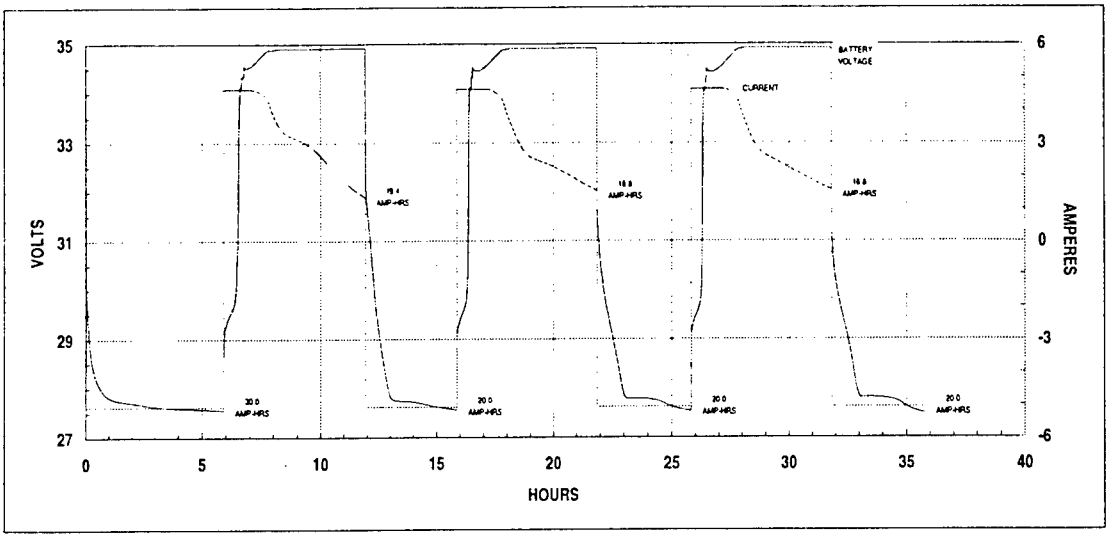

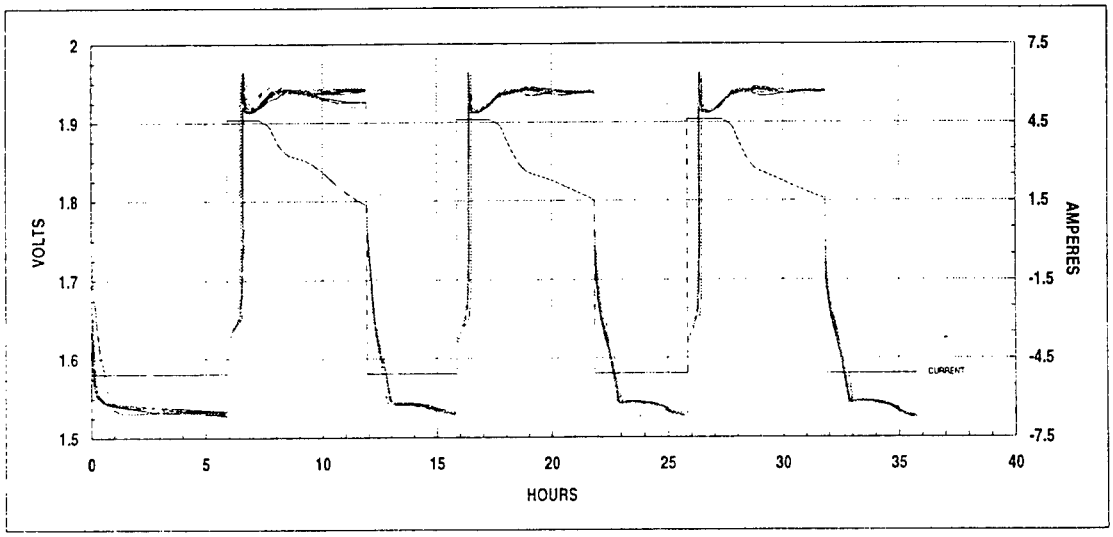

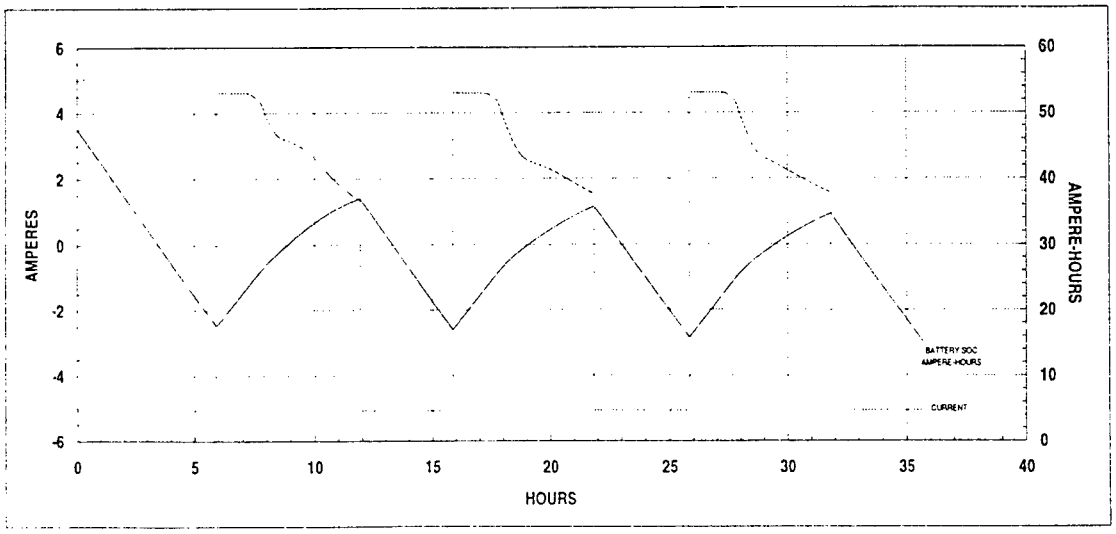

EM1-V.XLS Sheet2

D. PERRONE 11/22/95 9:51 AM

SUMMARY AND CONCLUSIONS

- Ag-Zn BATTERIES CAN MEET MPF MISSION REQUIREMENTS
  - WET LIFE
  - CYCLE LIFE

- Ag-ZN BATTERIES CAN PROVIDE > 100 CYCLES AFTER 14 MONTHS STORAGE UNDER THE FOLLOWING CONDITIONS
  - 6 LAYERS OF CELLOPHANE
  - STORAGE AT 15 C
  - OCV STAND
  - 50% DOD
  - MCP CHARGE

- EM BATTERY INITIAL PERFORMANCE LOOKS PROMMISSING

MARS PATHFINDER – EPI Ag-Zn PACK "A" WITH 5 SEPARATOR LAYERS
CYCLES VS CHARGE AND DISCHARGE AMPERE-HOURS AT 15° CELSIUS

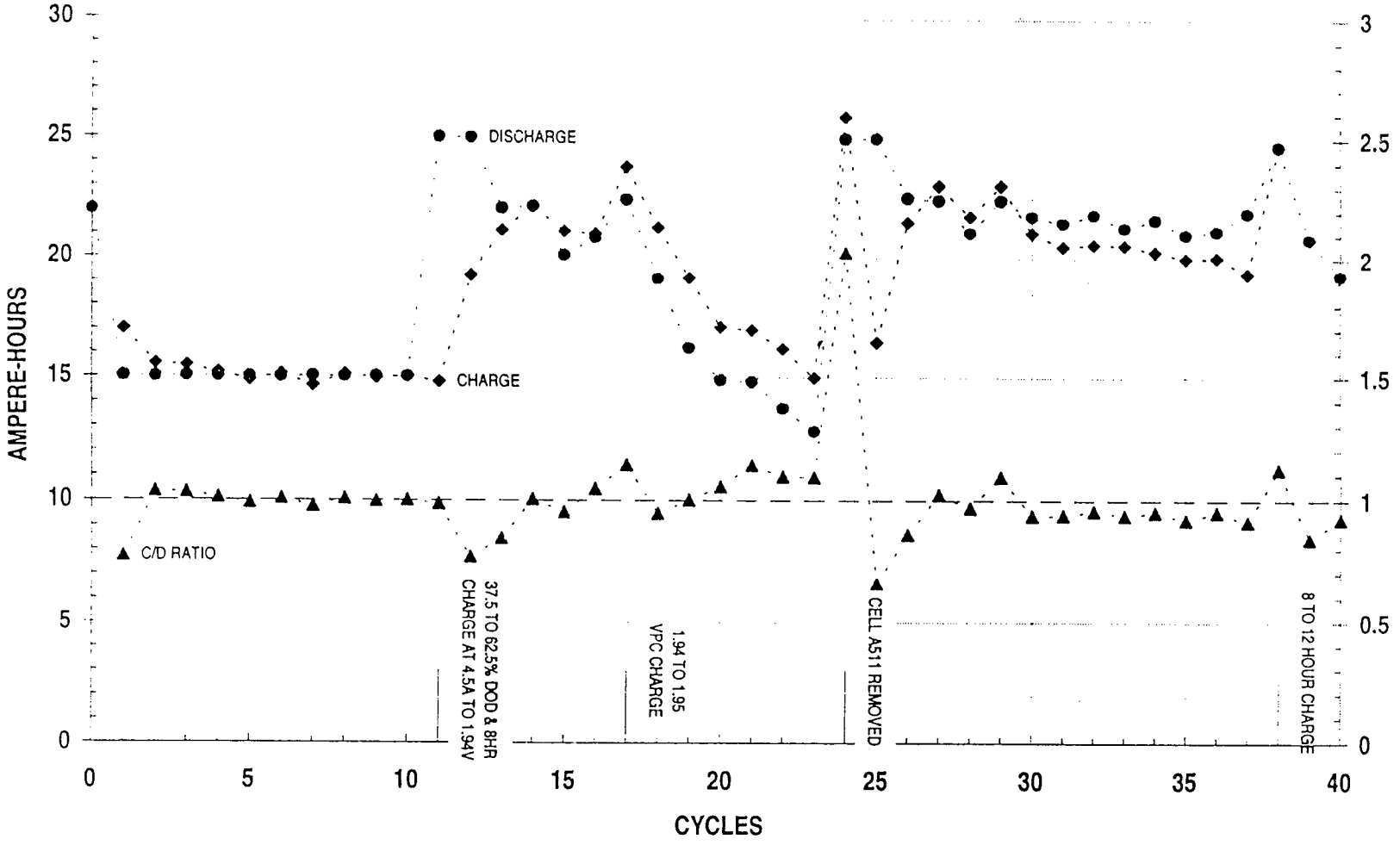

95003-0.XLS Chart1

D. PERRONE 4/25/95 3:07 PM

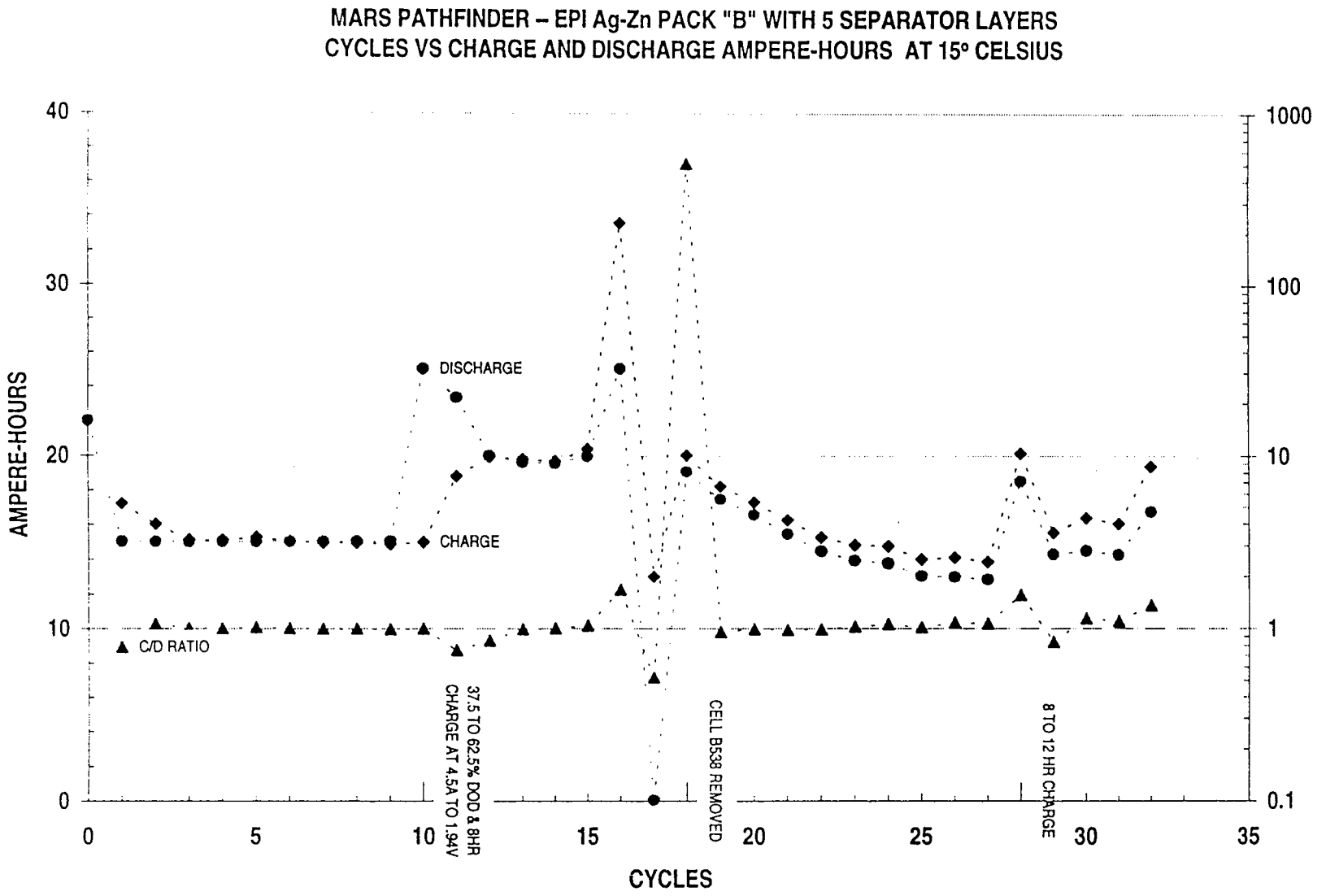

95004-0.XLS Chart1

D. PERRONE 4/25/95 3:08 PM

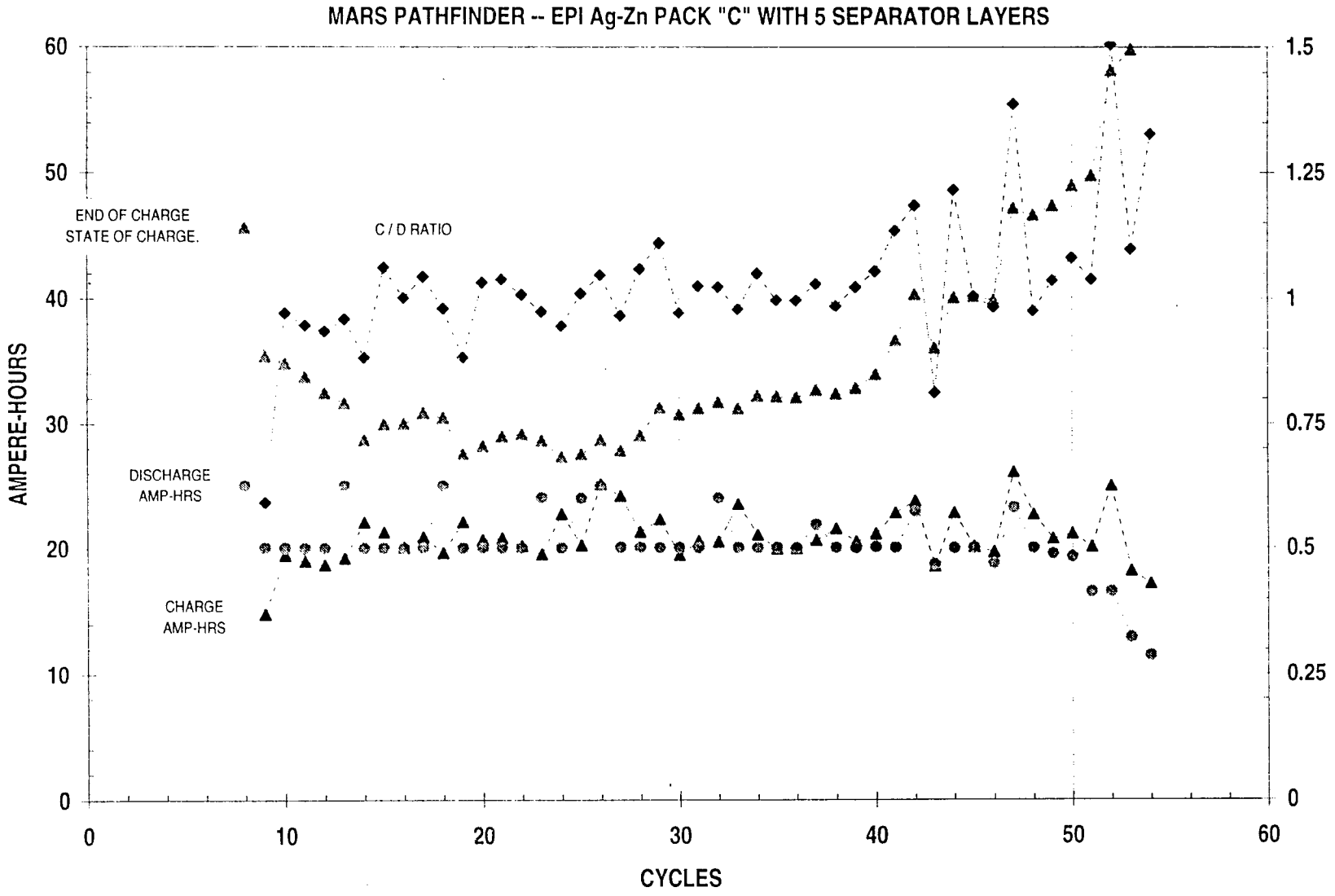

95011-0.XLS Chart1

D. PERRONE 11/22/95 10:20 AM

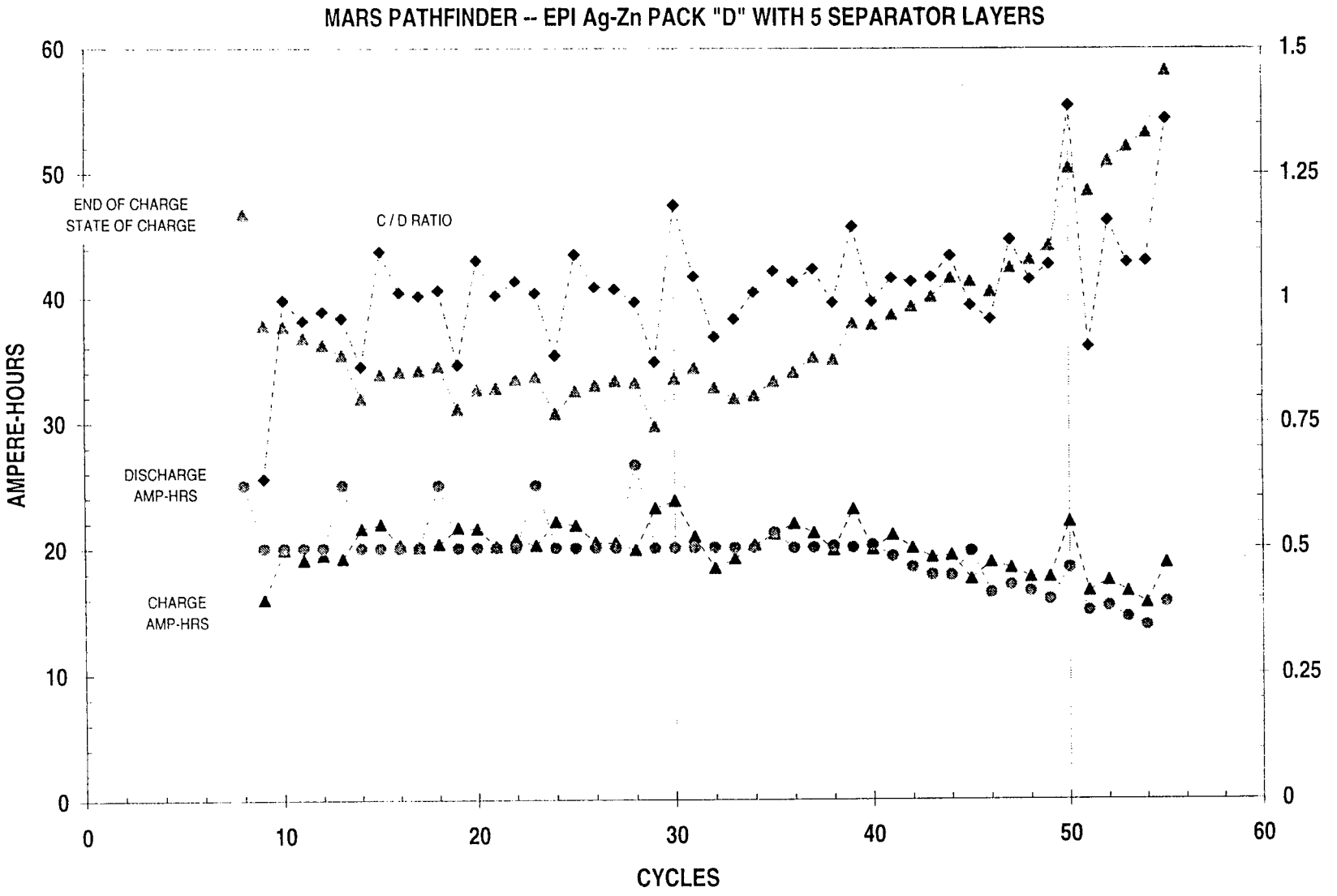

95012-0.XLS Chart1

D. PERRONE 11/22/95 10:21 AM

MARS PATHFINDER -- EPI Ag-ZN PACK "E" WITH 6 SEPARATOR LAYERS

CYCLE LIFE PERFORMANCE OF AGED CELLS AT 15° CELSIUS

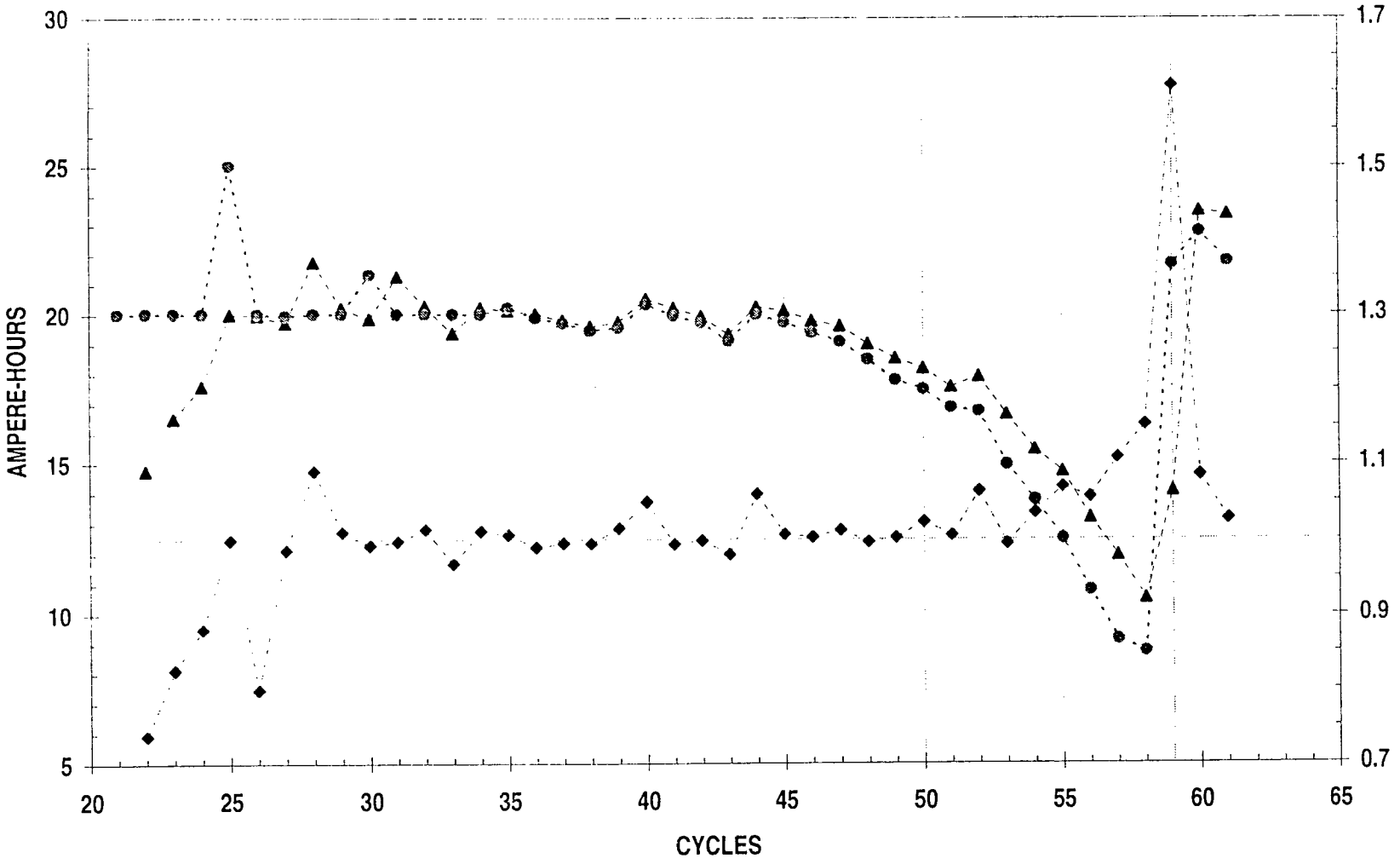

95008-0.XLS Chart1

D. PERRONE 11/22/95 3:36 PM

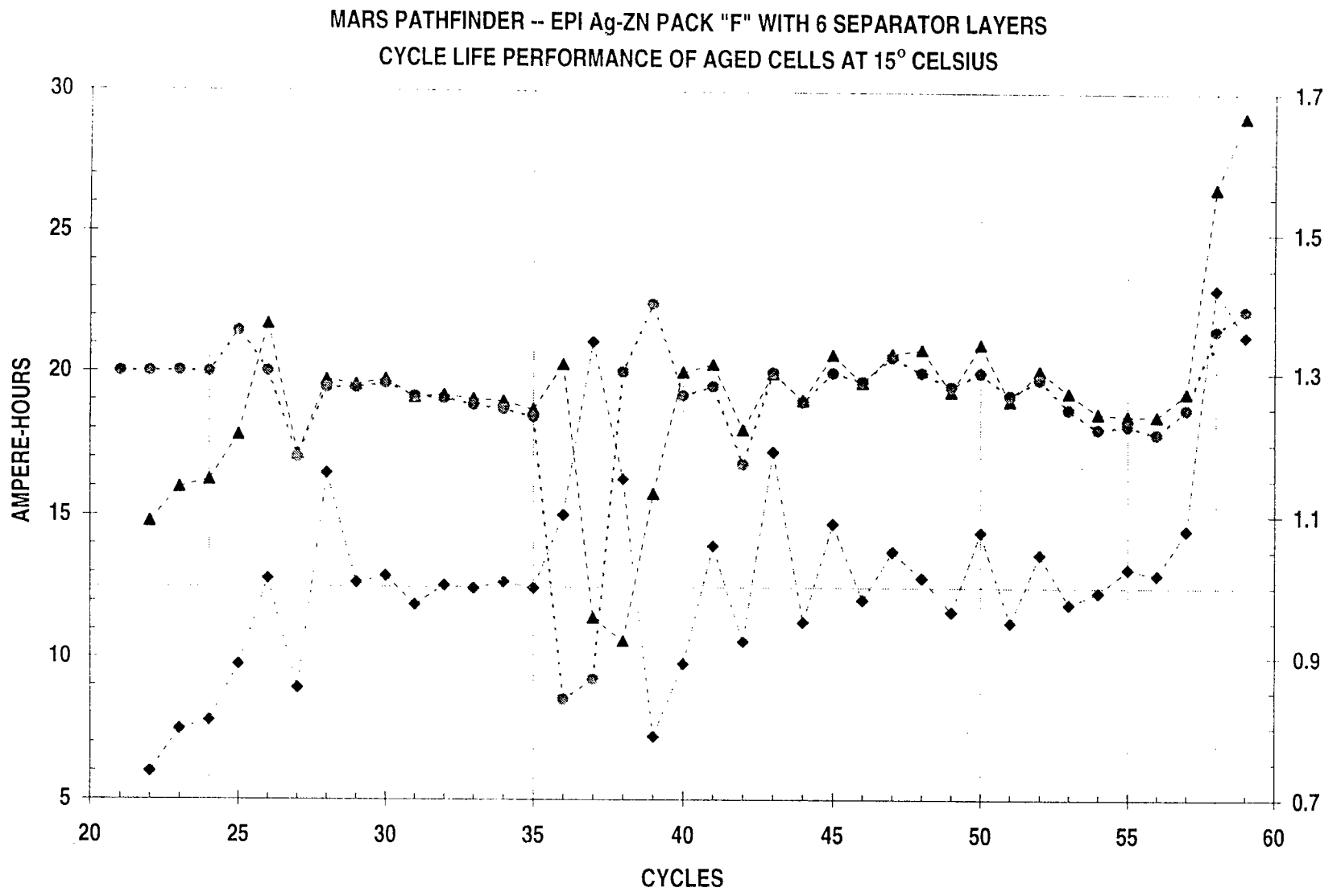
MARS PATHFINDER -- EPI Ag-ZN PACK "F" WITH 6 SEPARATOR LAYERS
CYCLE LIFE PERFORMANCE OF AGED CELLS AT 15° CELSIUS
AMPERE-HOURS
CYCLES
30
25
20
15
10
5
1.7
1.5
1.3
1.1
0.9
0.7
20
25
30
35
40
45
50
55
60
95009-0.XLS Chart1
D. PERRONE 11/22/95 3:37 PM

JPL

LITHIUM-ION BATTERY PROGRAM STATUS

S. SURAMPUDI, C-K. HUANG, M. SMART, E. DAVIES,
D. PERRONE, S. DISTEFANO, AND G. HALPERT

JET PROPULSION LABORATORY
PASADENA, CA 91109

NASA BATTERY WORKSHOP
HUNTSEVILLE, AL.
NOVEMBER 28-30, 1995

OUTLINE

- CODE-X Li-ION CELL R&D PROGRAM
- LOW TEMP SEC. Li R&D PROGRAM
- NM BATTERY PROGRAM OVERVIEW
- SUMMARY AND CONCLUSIONS

JPL

EVOLUTION OF FLIGHT BATTERIES

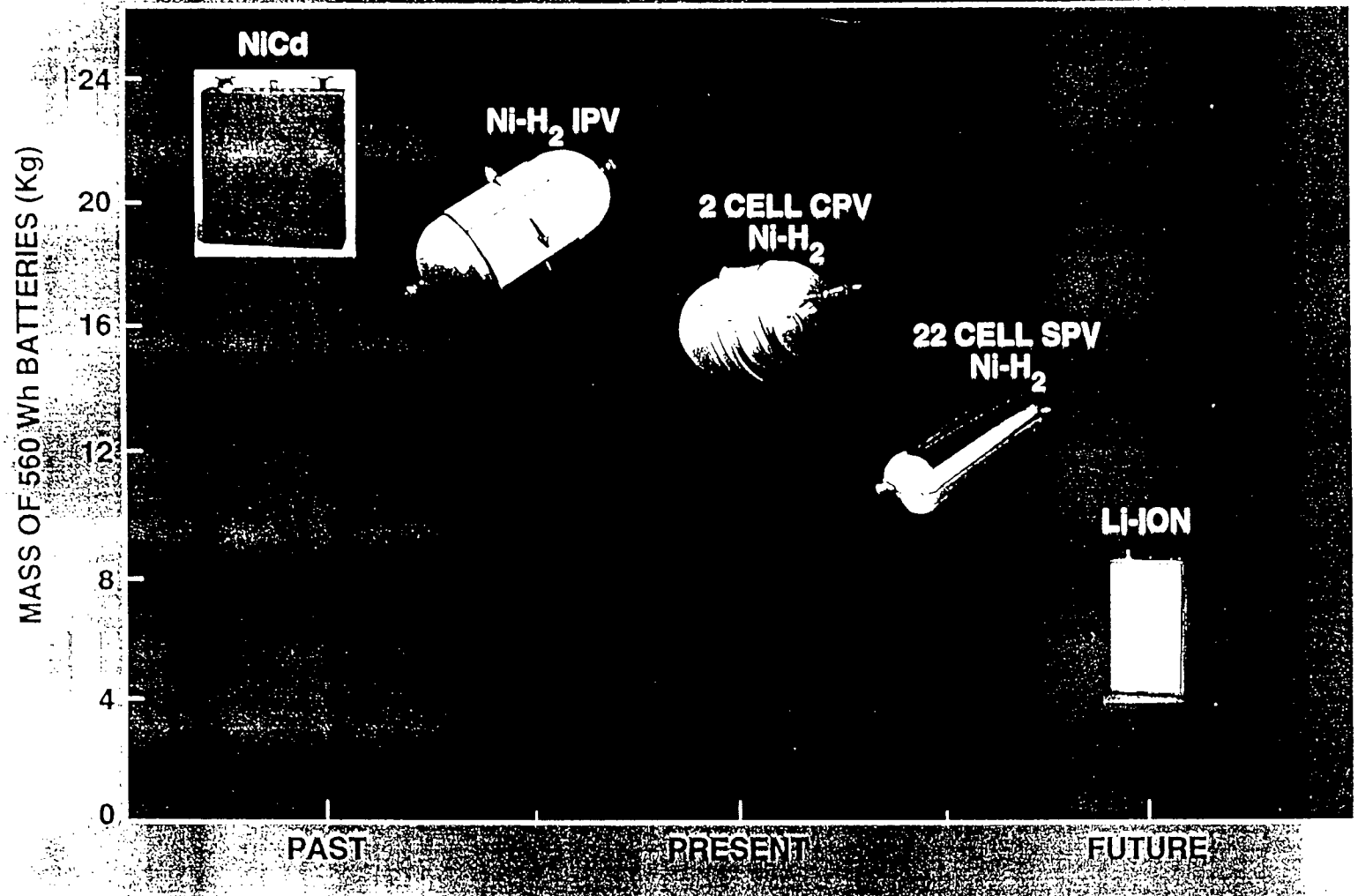

JPL

Overview of Code X Rechargeable Lithium- Ion Cell Development Task

Objective

- Develop rechargeable Li-ion cells for New Millenium and future NASA missions.

Benefits

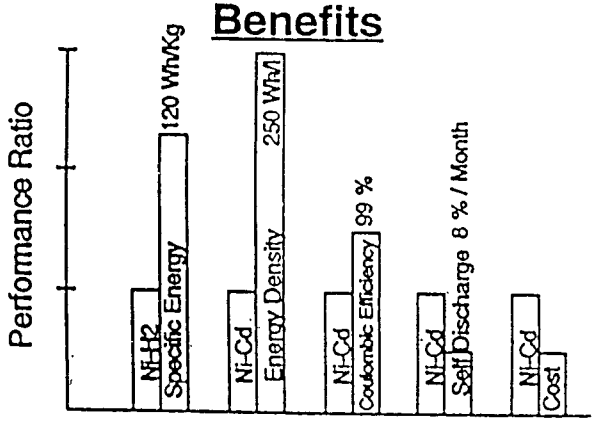

Applications

- New Millenium Spacecraft
- Rovers
- Landers
- Astronaut equipment
- Planetary Orbiters

Approach

- Select electrode materials and electrolytes - FY 1995
- Identify failure modes and mechanisms and enhance cycle life - FY 1996
- Demonstate Li-Ion cell technology with liquid electrolyte (120 Wh/kg , 1000 cycles) - FY 1997
- Select candidate polymer electrolytes for Li-Ion polymer cells - FY 1998
- Develop Li-Ion polymer cell technology (200 Wh/kg and 2000 cycles) - FY 2000

SCHEMATIC DIAGRAM OF A Li-ION CELL

JPL

(SPECIFIC ENERGY = 85 - 120 Wh/Kg)
(ENERGY DENSITY = 240 - 300 Wh/L)

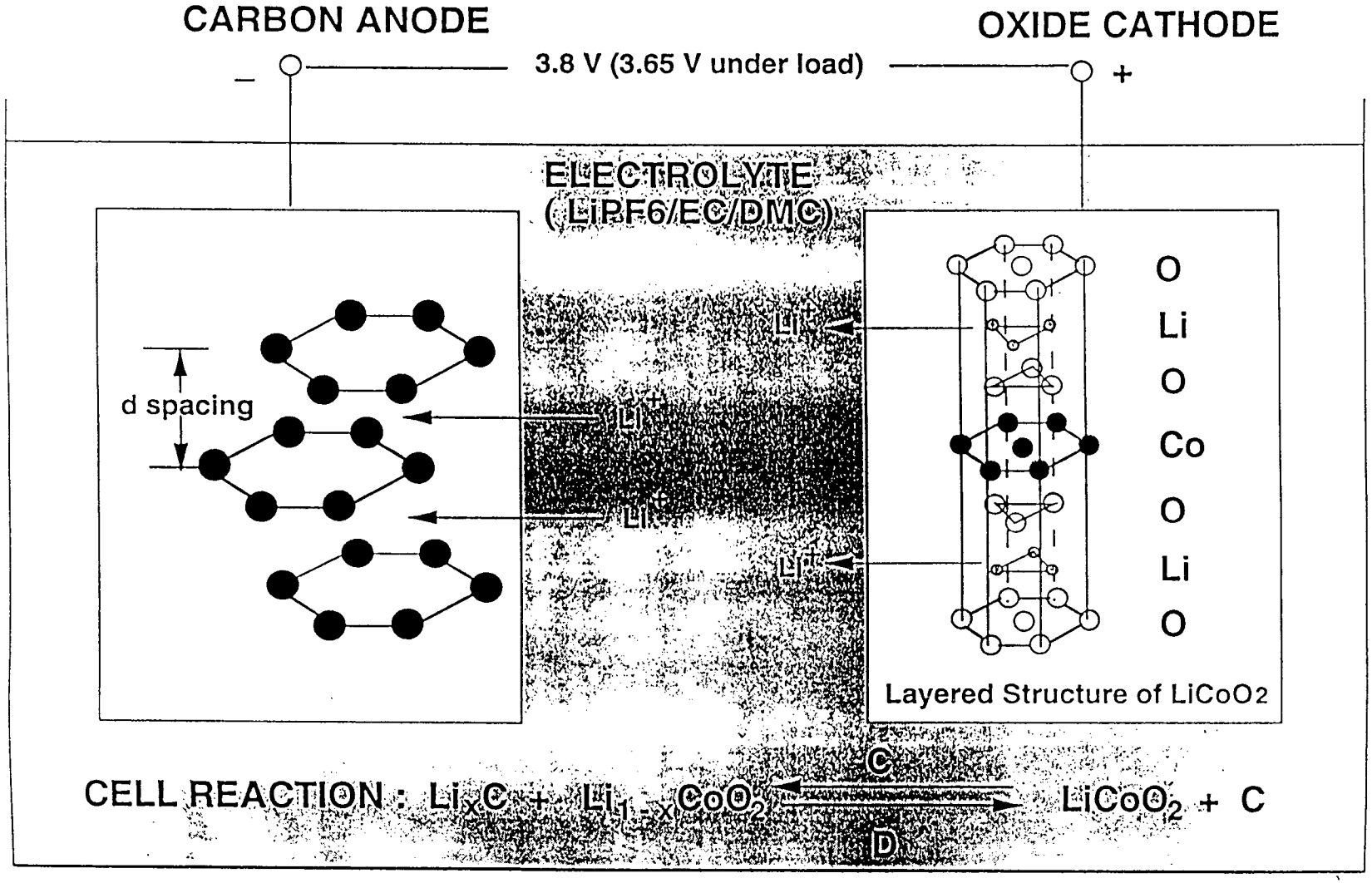

JPL

FY' 1995 Accomplishments

FY 1995 Objective

- Select electrode materials and electrolytes for 1st generation New Millennium Li-ion cells.

Electrolyte Studies

Electrolyte	Reversible Capacity (mAh/g)	Irreversible Capacity (mAh/g)
30 / 70 EC-DMC	250	60
50 / 50 EC-DMC	148	113
33 / 33 / 34 EC-DEC-DMC	253	58
30 / 70 EC-DEC	240	58

Anode Material Studies

	Reversible Capacity (mAh/g)	Irreversible Capacity (mAh/g)
Conoco Coke	150	153
Mitsubishi Coke	170	139
Osaka Carbon	250	70
Alfa Graphite	250	60
KS-15 Graphite	252	62
KS-44 Graphite	252	92
Mg_2Si Compound	200	90

Cycle Life Performance of JPL Experimental Li-ion Cell (350 mAh)

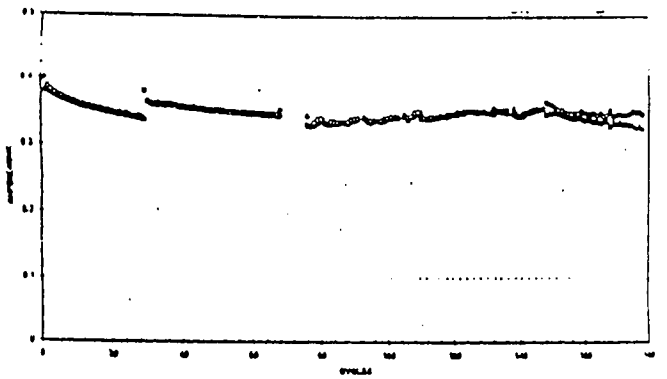

ELECTROCHEMICAL TECHNOLOGIES GROUP

JPL

Mg_2Si / $LiCoO_2$ Cell Development

Crystal Structure of Mg_2Si

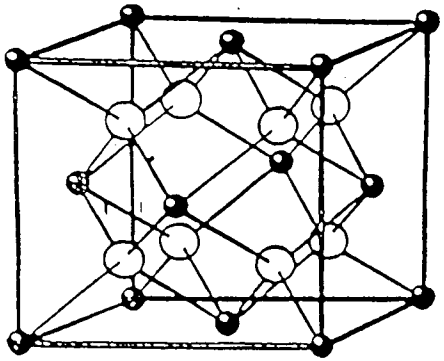

● Si ○ Mg

Si: (1/8)x8 + (1/2)x6 = 4

Mg: 8

LI (octa.) : (1/4)x12 + 1 = 4

LI: Mg: SI = 4: 8: 4 = 1: 2: 1

$LIMg_2SI$

(2) ELECTROCHEMICAL INTERCALATION OF LI INTO Mg_2SI

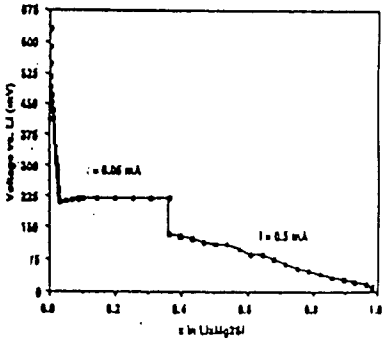

Charge & Discharge Profiles of Mg2Si / PEDMC / LiCoO2 Cell

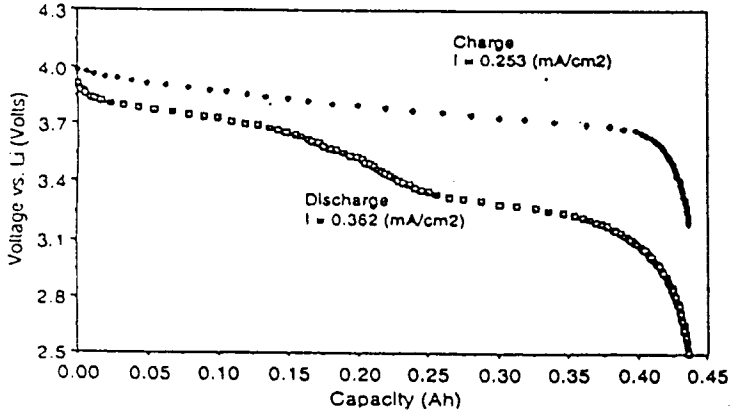

Cycle Life Performance of Mg_2Si / $LiCoO_2$

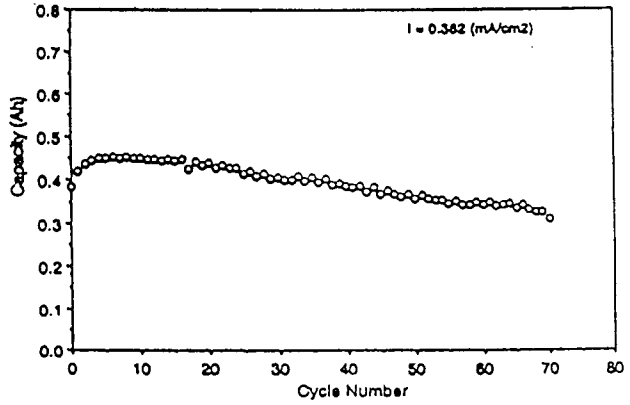

ELECTROCHEMICAL TECHNOLOGIES GROUP

JPL

EFFECT OF DESIGN PARAMETERS ON CELL PERFORMANCE (TAGUCHI STUDY)

OBJECTIVE

INVESTIGATE THE INFLUENCE OF DESIGN PARAMETERS ON CELL PERFORMANCE USING TAGUCHI METHOD

VARIABLES

(1) TYPE OF CARBON
(2) SOURCE OF LiCoO2
(3) ELECTRODE POROSITY
(4) INTERELECTRODE SPACING
(5) ELECTROLYTE SALT TYPE
(6) ELECTROLYTE SOLVENT TYPE
(7) CELL BALANCE

DESIGN MATRIX

	Type of Carbon	Source of LiCoO2	Electrode Porosity	Interelectrode Spacing	Electrode Salt Type	Cell Balance	Electrolyte Solvent type
1	pet coke	A	high	normal	LIAsF6	1.7	PC/DME
2	pet coke	A	high	tight	LIPF6	2.1	EC/DMC
3	pet coke	B	low	normal	LIAsF6	2.1	EC/DMC
4	pet coke	B	low	tight	LIPF6	1.7	PC/DME
5	nongraphitic	A	high	normal	LIPF6	1.7	EC/DMC
6	nongraphitic	A	high	tight	LIAsF6	2.1	PC/DME
7	nongraphitic	B	low	normal	LIPF6	2.1	PC/DME
8	nongraphitic	B	low	tight	LIAsF6	1.7	EC/DMC

CONCLUSION

MAJOR FACTORS CONTROLLING CELL PERFORMANCE ARE:

- ELECTRODE WEIGHT RATIO
- ELECTROLYTE SALT TYPE
- ELECTROLYTE SOLVENT TYPE
- TYPE OF CARBON

JPL

Results from Taguchi Analysis

Solvent Mixture

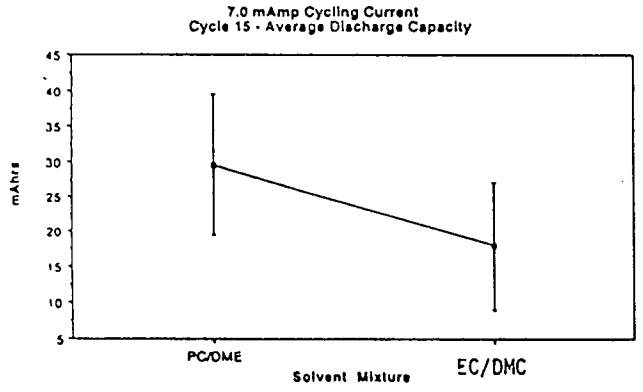

Salt Type

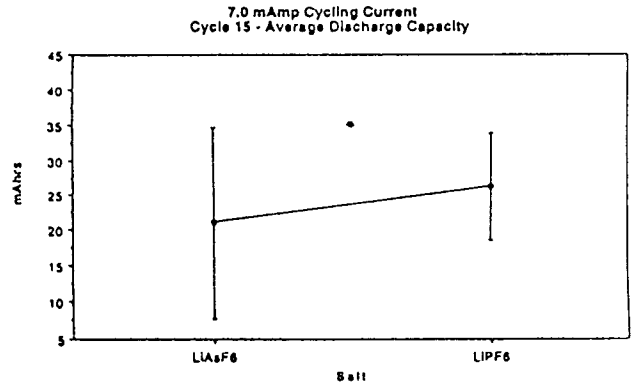

Cathode Porosity

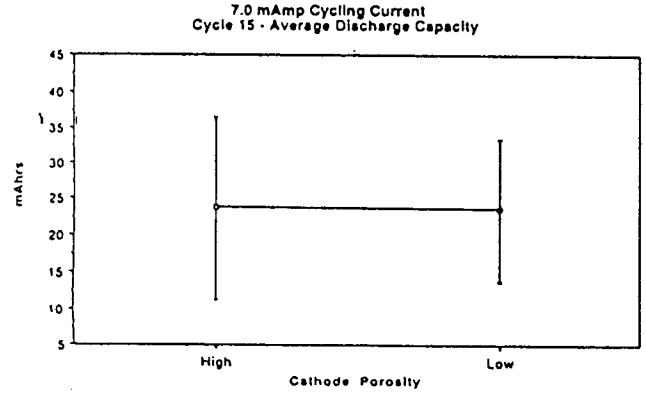

Cathode / Anode Ratio

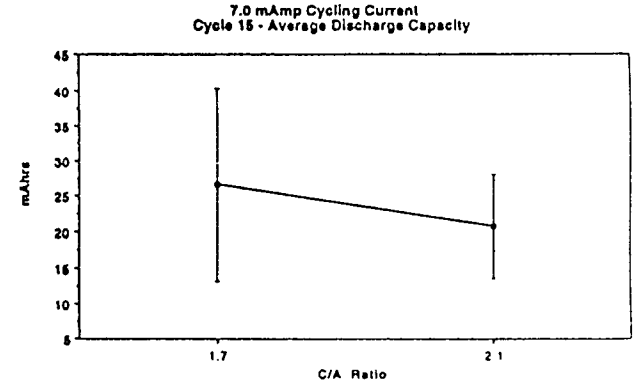

JPL

PERFORMANCE CHARACTERISTICS OF YARDNEY 5 Ah CELLS*

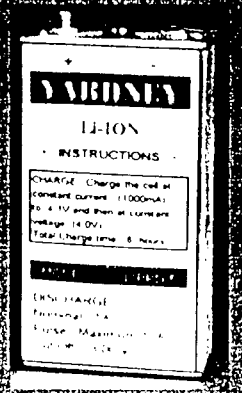

CYCLE LIFE PERFORMANCE

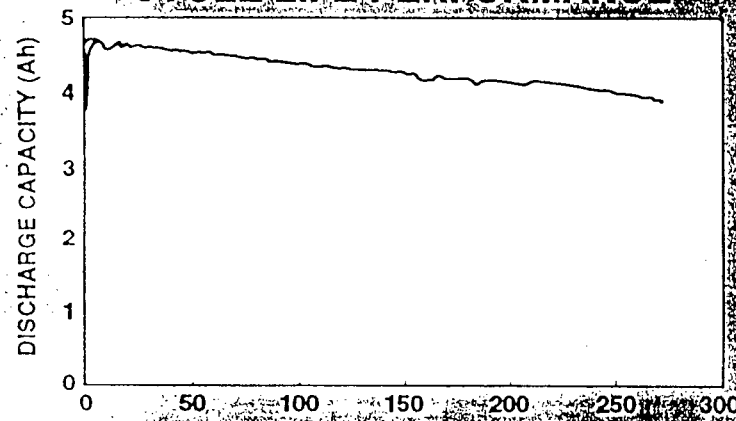

RATE CAPABILITY

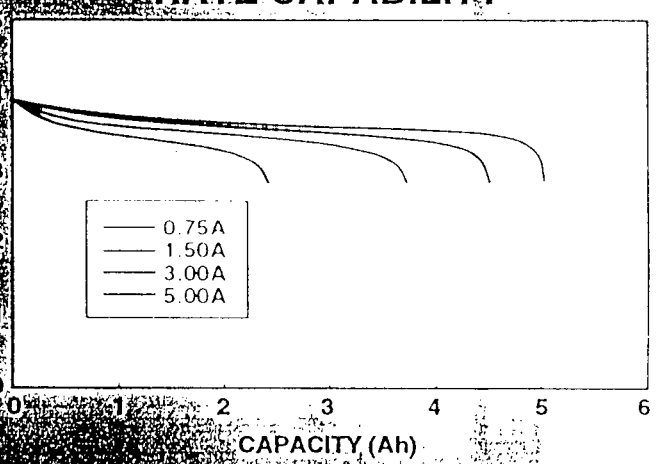

* DEVELOPED UNDER WL/WPAFB AND JPL SPONSORED PROGRAM

JPL

Cycle Life Performance of C / $LiCoO_2$ Cell

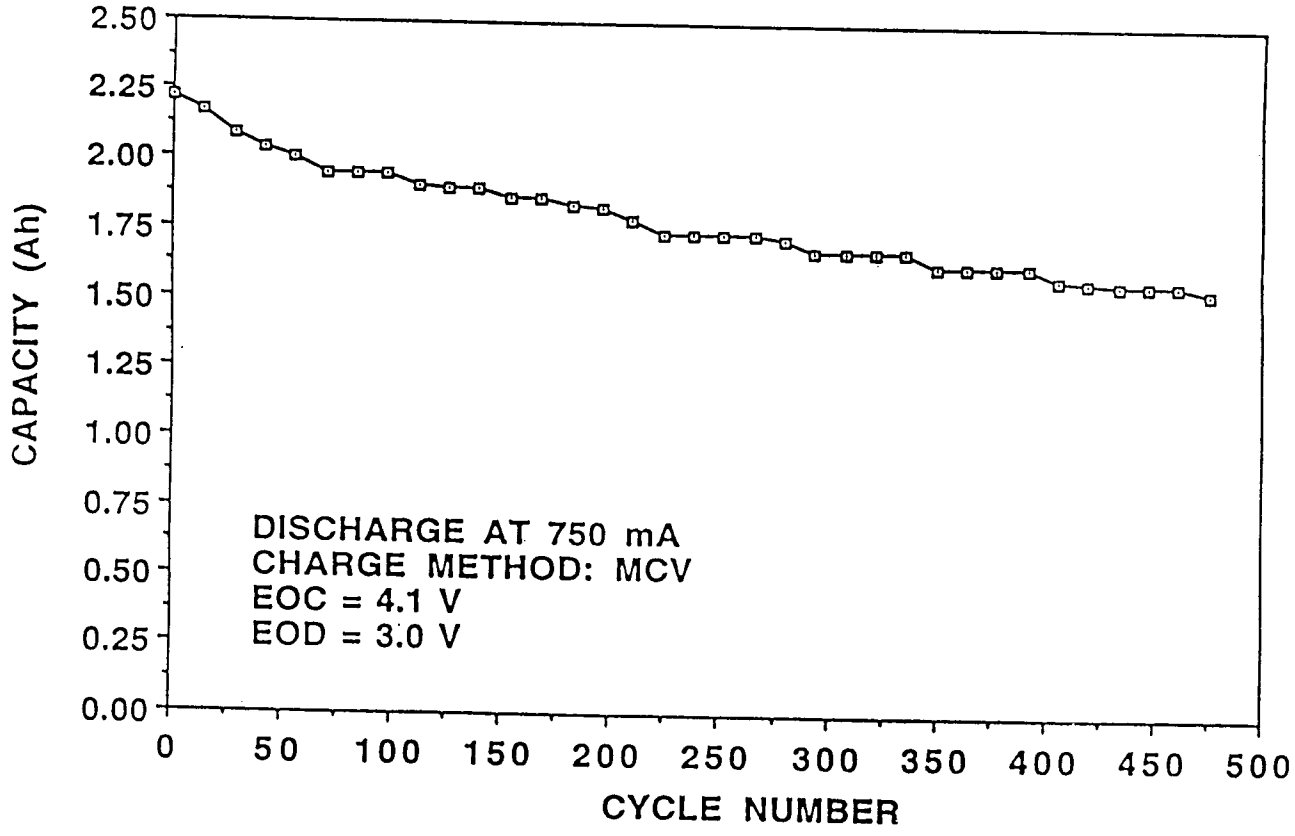

JPL

Technology Progression

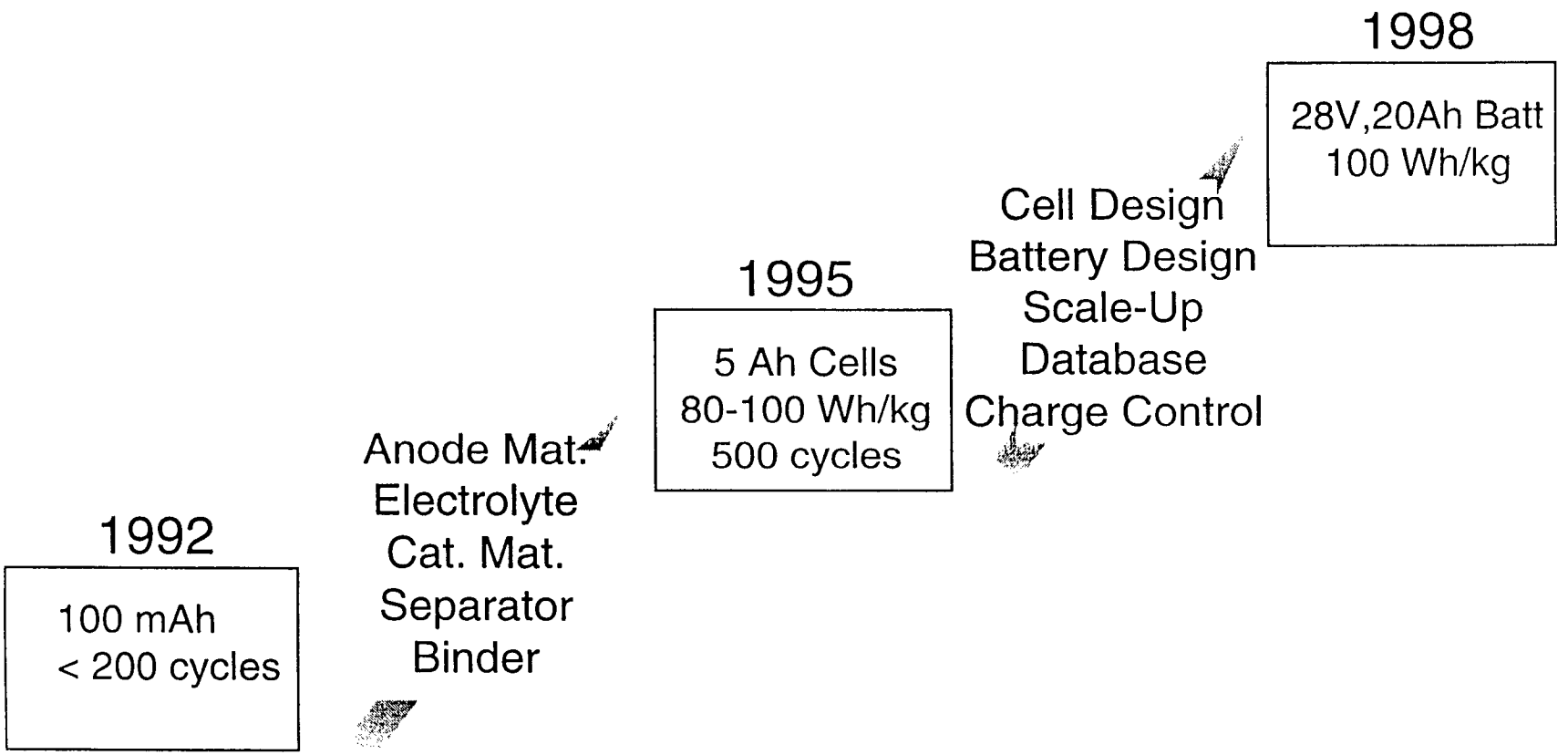

JPL

Low Temperature Rechargeable Lithium Cells

Objective

- Develop low temperature rechargeable lithium batteries for Mars Exploration programs.

CELL PERFORMANCE TARGETS

(1) CAPACITY (Ah)	5
(2) CYCLE LIFE	300
(3) OPERATIONAL TEMP. (C)	-60 ~ 20
(4) SPECIFIC ENERGY (Wh/Kg)	50
(5) ENERGY DENSITY (Wh/L)	100

Approach

- Identify electrolytes for low temperature Li - ion cells.
- Identify candidate electrode materials and cell components..
- Demonstrate technology at the 1 Ah cell level
  - -20 C 1996
  - -40 C 1998
- Scale up technology to the 5-20 Ah level.

Comparison of SOA Battery Technologies

SYSTEM	OPERATING TEMP. (°C)	SPECIFIC ENERGY(Wh/Kg) 0°C	-40°C
Ni-Cd	-20 - 50	30	5
Ni-H2(IPV)	-20 - 50	50	5
Ag-Zn	-20 - 50	100	5
NM Li	-20 - 50	70	10
CRYO Li	-60 - 20	85	50

Applications

- Mars Rover
- Mars Lander
- Mars Penetrator

Low Temperature Rechargeable Lithium Cells Electrolyte Studies

Objective

- Select promising electrolytes for low temperature Li- ion cells

Targets:

- Conductivity of 1 - 3 mS/cm at -40 C
- Favorable physical properties
- Voltage window : 1 - 4.5 V

Conductivity of EC-Based Electrolytes

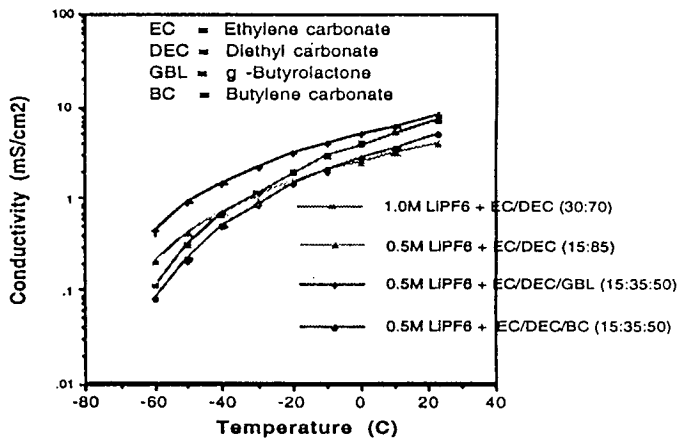

Conductivity of PC/DME Electrolyte Mixtures

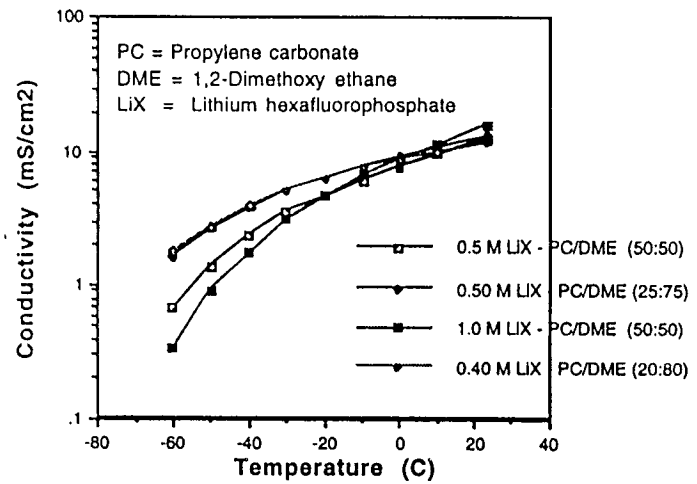

Conclusions and Accomplishments

- The conductivity of over 25 electrolyte systems have been evaluated.
- Propylene carbonate based systems display excellent low temperature performance
- Lower salt concentrations display better low temperature performance
- Low viscosity solvent additives have been shown to enhance conductivity
- Five promising electrolyte systems are being evaluated at the cell level.

ELECTROCHEMICAL TECHNOLOGIES GROUP

JPL

Low Temperature Rechargeable Lithium Cells Cell Studies

Experimental Cell (100 mAh @ RT)

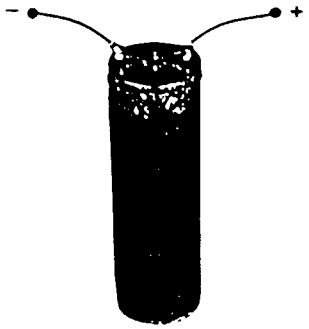

Cycle Life Performance at -40 C

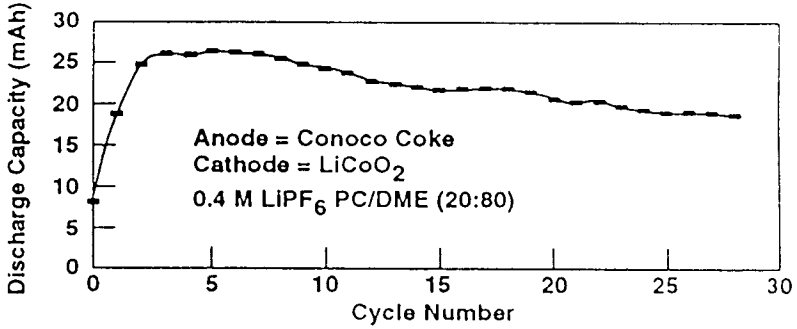

Summary of Cell Performance

ELECTROLYTE	ANODE / CATHODE	CAPACITY (mAh) 25 C	-20 C
0.5 M LIPF6 PC / DME (20:80)	COKE / LICoO2	100	25 (-40 C)
0.5 M LIPF6 PC / DME (20:80)	GRAPHITE / LICoO2	-	-
0.5 M LIPF6 PC / DME / DEC (25:25:50)	GRAPHITE / LICoO2	-	-
0.5 M LIPF6 EC / DEC (15:85)	GRAPHITE / LICoO2	330-340	145
0.5 M LIPF6 EC / DEC/DME (15:35:50)	GRAPHITE / LICoO2	50-60	60
1.0 M LIPF6 EC / DMC (30:70)	GRAPHITE / LICoO2	280-300	-
1.0M LIPF6 EC/DEC (30:70)	GRAPHITE / LICoO2	290-310	-

Conclusions

- PC/DME electrolyte has been successfully cycled at -40 C and displayed 25% of the capacity observed at room temperature.
- EC/DEC based electrolytes have been evaluated at the cell level at -20 C and shown to have 40 - 50 % of the capacity at room temperature.
- Cell level evaluation of the other promising electrolyte systems is in progress.

JPL

Performance Targets of NM Li-Ion Battery

• Voltage	28 - 30 volts
• Capacity	20 Ah
• Cycle Life	> 1000 cycles
• Operating Temperature	- 20 ~ 30°C
• Operational Life	> 10 yrs
• Specific Energy (Wh/kg)	> 100 (Battery Level)
	> 120 (Cell Level)
• Energy Density (Wh/L)	> 140 (Battery Level)
	> 240 (Cell Level)

JPL

SCHEMATIC OF A 28 V, 20 Ah Li-ION BATTERY

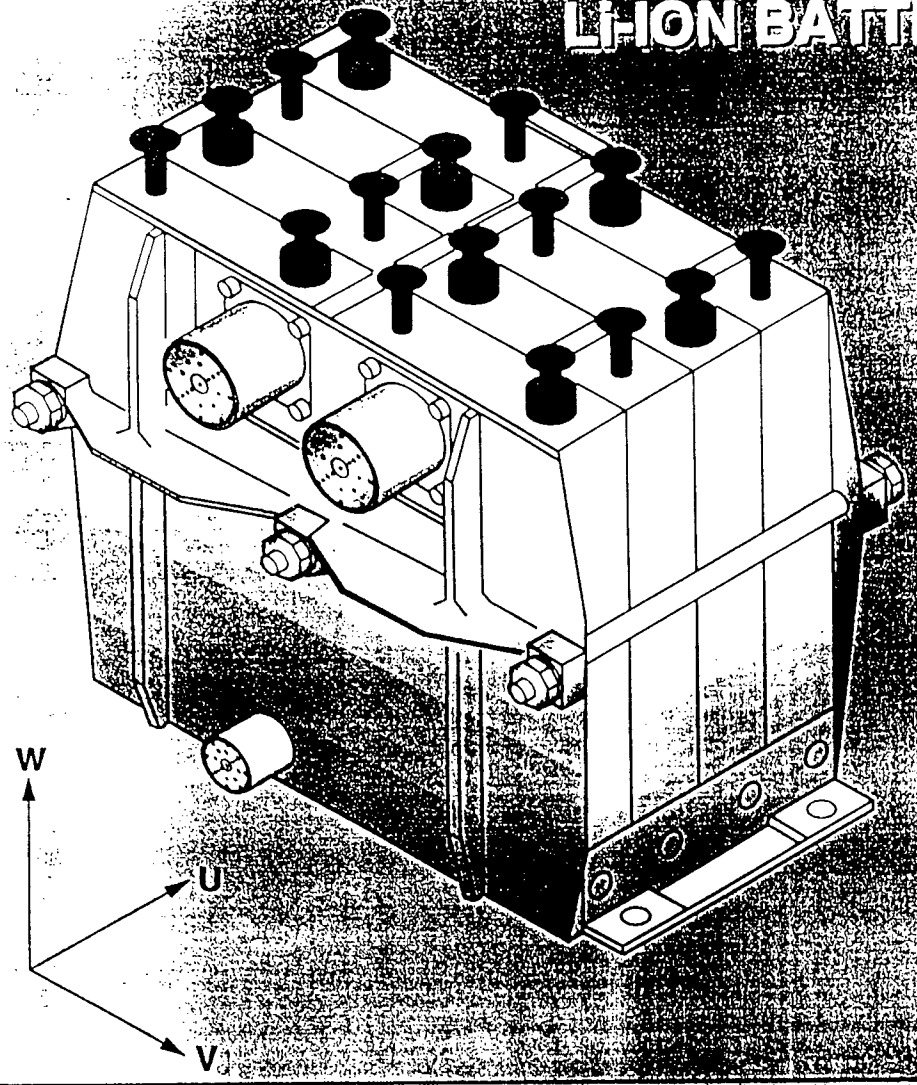

BATTERY INTERFACES

Electrical:	(1) Power Connector (J1) (2) Sensing Connector (J2) (3) Heater Connector (J3)
Mechanical:	4/8 Base Mounting Position
Thermal:	Surface mounting thermal Baseplate (0-30 C)

WIDTH (U): 12 cm
LENGTH (V): 18 cm
HEIGHT (W): 19 cm
WEIGHT: 6.24 (Kg)

JPL

Lithium-Ion Technology Status & NM Cell Performance Requirements

Property	U.S. Technology Status	NM Target
Capacity (Ahr)	1-5	20
Specific Energy (Whr/kg)	80	120
Energy Density (Whr/L)	< 220	> 250
Cycle Life	300-500	1000
Discharge Rate	< C/3	> C/2

Technical Approach

- Cell Level
  - Verify Materials Selection
  - Scale-up Processes
  - Optimize Cell Design
  - Fabricate 20 Ah Cells
  - Establish Performance Data Base
- Battery Level
  - Optimize Design (Electrical, Thermal, Mechanical)
  - Fabricate 28V, 20 AH Batteries (8 Cells Each)
  - Demonstrate Performance, Life, Environmental Capabilities
  - Intergrate Electronic Control Circuit in System to Produce "Smart Battery"

LITHIUM-ION BATTERY DEVELOPMENT SCHEDULE

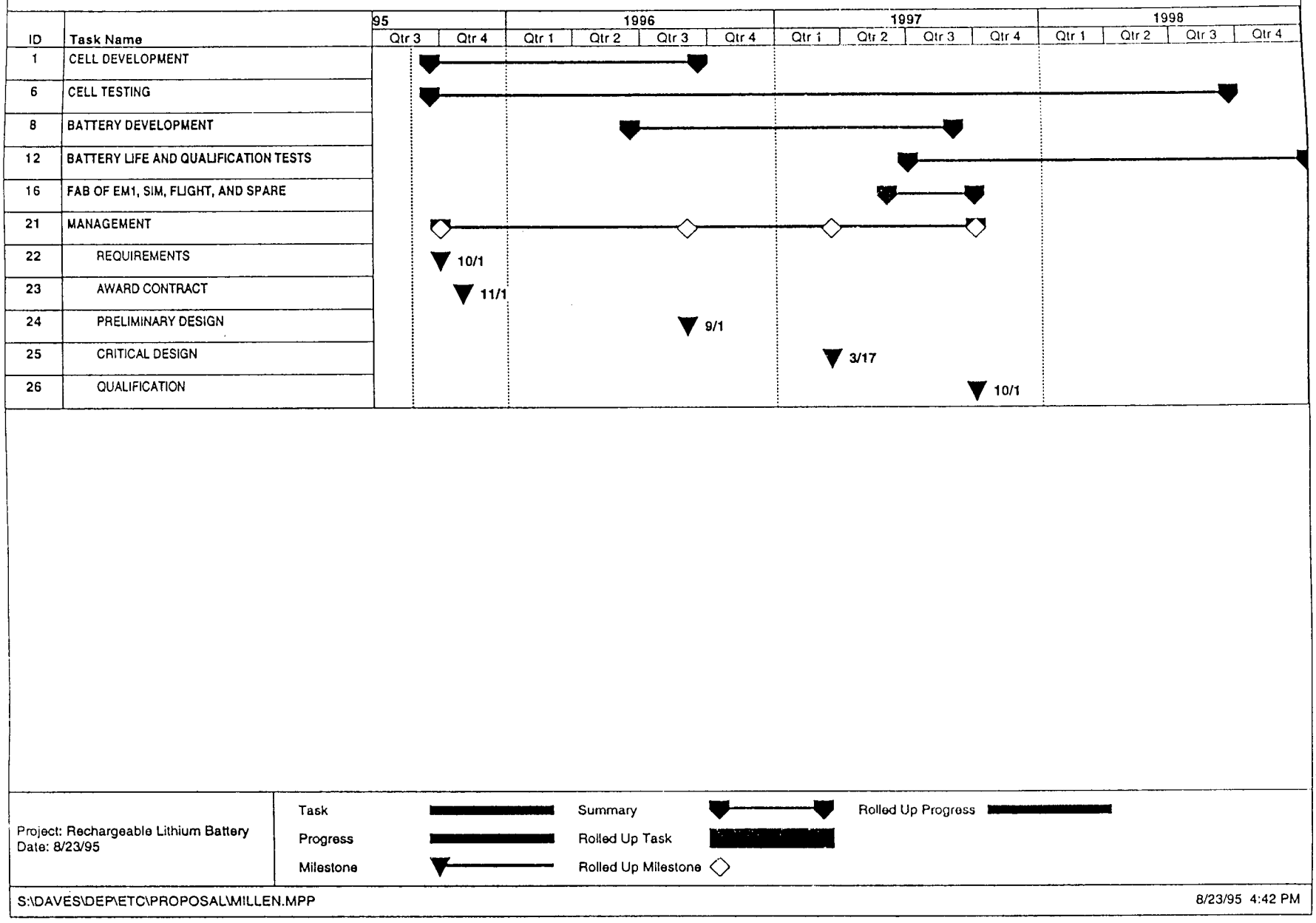

LITHIUM-ION BATTERY DEVELOPMENT SCHEDULE

ID	Task Name
1	CELL DEVELOPMENT
2	REVISIT MATERIAL SELECTION
3	SCALE-UP OF ELECTRODE FAB METHODS
4	CELL DESIGN OPTIMIZATION STUDIES
5	FABRICATION OF BREADBOARD CELLS
6	CELL TESTING
7	PERFORMANCE, LIFE, AND SAFETY
8	BATTERY DEVELOPMENT
9	BATTERY DESIGN STUDIES
10	FABRICATION OF CELLS
11	BATTERY FABRICATION FOR T AND Q
12	BATTERY LIFE AND QUALIFICATION TESTS
13	PERFORMANCE TESTING
14	ENVIRONMENTAL TESTS
15	LIFE TEST
16	FAB OF EM1, SIM, FLIGHT, AND SPARE
17	BATTERY FABRICATION
18	ACCEPTANCE TESTS
19	DELIVERY OF EM1
20	DELIVERY OF FLIGHT, SPARE & SIM
21	MANAGEMENT
22	REQUIREMENTS
23	AWARD CONTRACT
24	PRELIMINARY DESIGN
25	CRITICAL DESIGN
26	QUALIFICATION

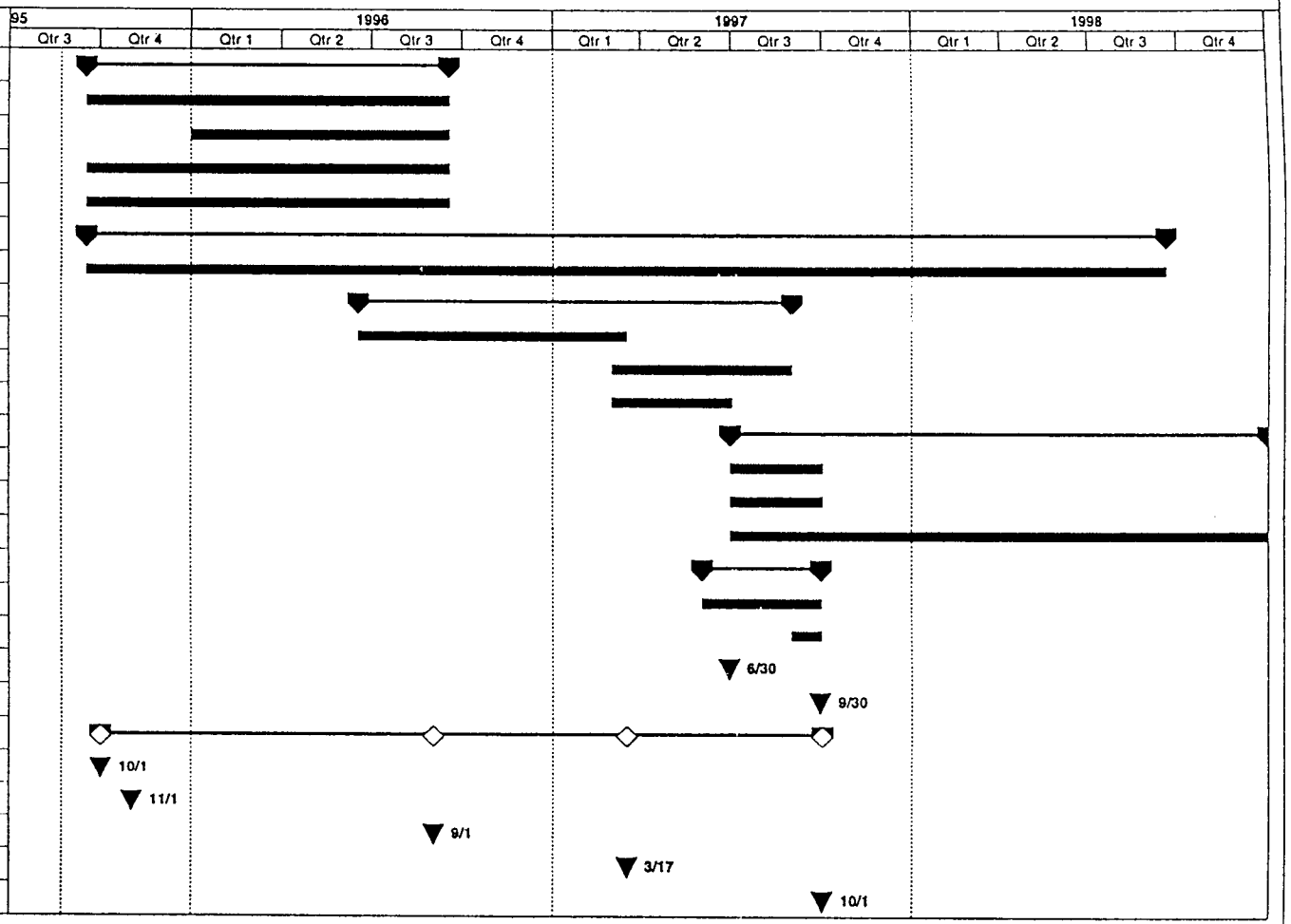

Project: Rechargeable Lithium Battery
Date: 8/23/95

Task
Progress
Milestone
Summary
Rolled Up Task
Rolled Up Milestone
Rolled Up Progress

S:\DAVES\DEP\ETC\PROPOSAL\MILLEN.MPP

8/23/95 4:41 PM

JPL

Summary of Accomplishments

(1) Identified promising materials for New Millenium Li-ion cells
- Graphite, $LiCoO_2$, 1M $LiPF_6$ in EC + DMC, and Celgard 2500

(2) Identified a new Li-ion cell chemistry based on Mg_2Si anodes.

(3) Yardney developed 3 and 5 Ah Li-ion cells under JPL and Airforce sponsored program.
- 100 Wh/Kg and 500 cycles @ 100 % DOD

(4) WGL (under contract from JPL) examined the effect of design parameters using Taguchi method.
- Cell performance is highly dependent on pack tightness and electrode capacity ratio.

(5) NM program is considering Li-ion cell technology for mission-1 (scheduled for launch in 1998).

(6) JPL in association with WL/WPAFB is proposing to develop Li-ion technology for NM applications by 1997/98

JPL

ACKNOWLEDGEMENT

THE WORK DESCRIBED HERE WAS CARRIED OUT AT JET PROPULSION LABORATORY, CALIFORNIA INSTITUTE OF TECHNOLOGY, UNDER CONTRACT WITH THE NATIONAL AERONAUTICS AND SPACE ADMINISTRATION (CODE X).

1995 NASA AEROSPACE BATTERY WORKSHOP

HUNTSVILLE HILTON
HUNTSVILLE, ALABANA
NOVEMBER 28-30, 1995

BIPOLAR AND MONOPOLAR LITHIUM-ION BATTERY TECHNOLOGY AT YARDNEY

P. RUSSELL, J. FLYNN, T. REDDY

YARDNEY TECHNICAL PRODUCTS, INC.
82 MECHANIC STREET • PAWCATUCK, CT 06379

G:\FILES\PRESENT\LI-ION\NASA.WPD

Lithium-ion Cells

Lithium-ion Battery Systems offer several advantages:

- Intrinsically safe
- Long cycle life
- Environmentally friendly
- High energy density
- Wide operating temperature range
- Good discharge rate capability
- Low self-discharge
- No memory effect

LI-ION BATTERIES

Anode or Negative Electrode:	Carbon, e.g., Coke, Graphite
Cathode or Positive Electrode:	Lithiated transition metal oxides, e.g., $LiMn_2O_4$, $LiNiO_2$, $LiCoO_2$
Electrolyte:	Organic Electrolytes, e.g., $LiPF_6$/EC-DMC, $LiClO_4$/PC-DEC
Average Operating Voltage:	3.6 - 3.7 V at C/3 rate
Mechanism:	$LiMO_2 \underset{\text{Discharge}}{\overset{\text{Charge}}{\rightleftharpoons}} Li_{1-x}MO_2 + xLi^+ + xe^-$
	$C + xLi^+ + xe^- \underset{\text{Discharge}}{\overset{\text{Charge}}{\rightleftharpoons}} Li_xC$

G:\FILES\PRESENT\LITHIUM\WLWC.WPD

LI-ION BATTERIES

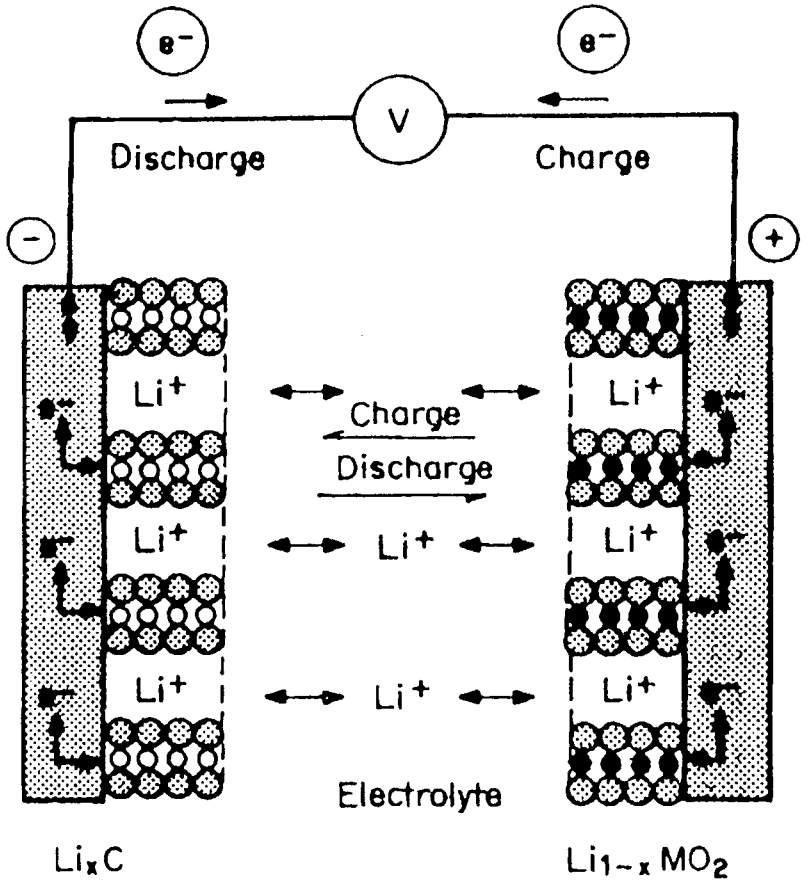

Scheme of the Electrochemical Process of a Lithium-ion Cell

G:\FILES\PRESENT\LITHIUM\NAVC.WPD

LI-ION BATTERIES

Comparison of Useable Specific Capacity (Ah/Kg) and Capacity Density (Ah/l) for Lithiated Carbon vs Lithium Metal

CHARACTERISTICS	Li-METAL	LiC_6
Theoretical Specific Capacity (Ah/Kg)	3,862	372
Theoretical Capacity Density (Ah/l)	2,047	837
Practical Specific Capacity (Ah/Kg)		
•Four-Fold Excess of Lithium	966	372
•90% Active Material in Carbon	966	335
Practical Capacity Density (Ah/l)		
•Four-Fold Excess of Lithium	516	837
•Porosity of Carbon Electrode (20%)	516	670

G:\FILES\PRESENT\LITHIUM\NUMC.WPD

Yardney TECHNICAL PRODUCTS INC

LI-ION BATTERIES

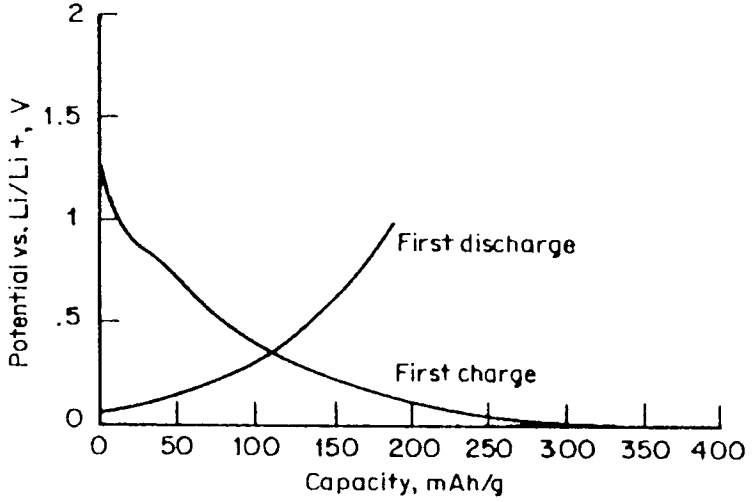

a

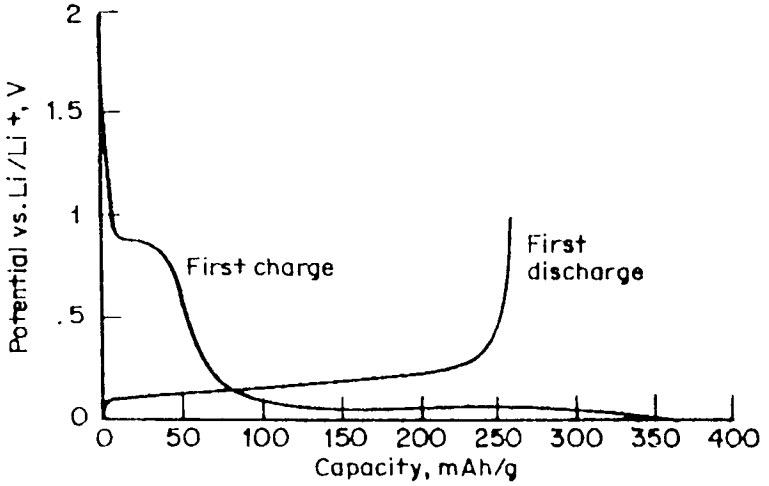

b

Representation of irreversible capacity associated with the first charge/discharge process (a) coke, (b) graphite

Yardney TECHNICAL PRODUCTS INC

LI-ION BATTERIES

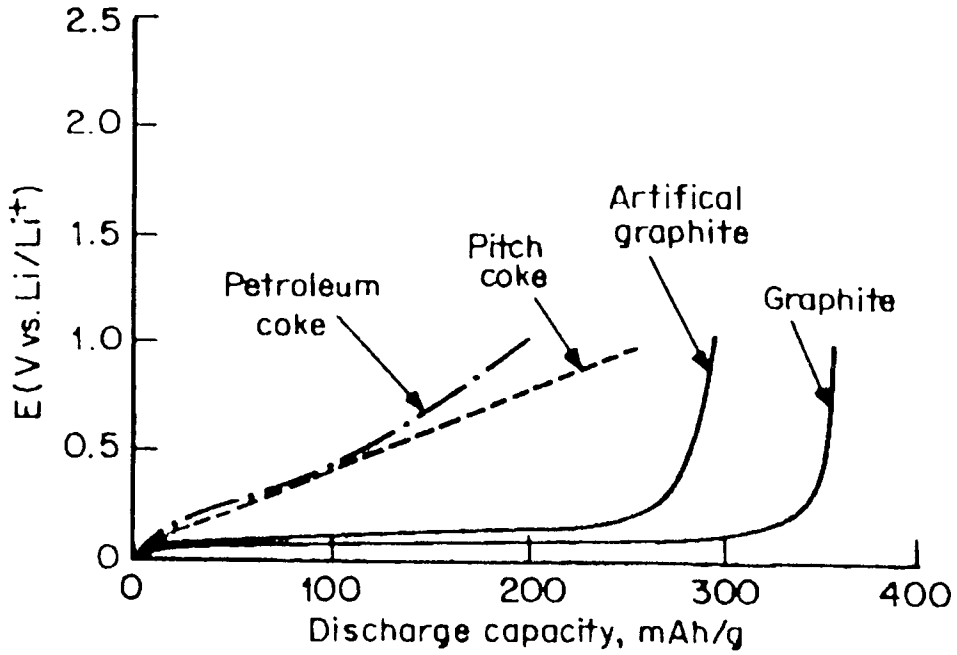

First discharge characteristics of carbon materials

G:\FILES\PRESENT\LITHIUM\MVC.WPD

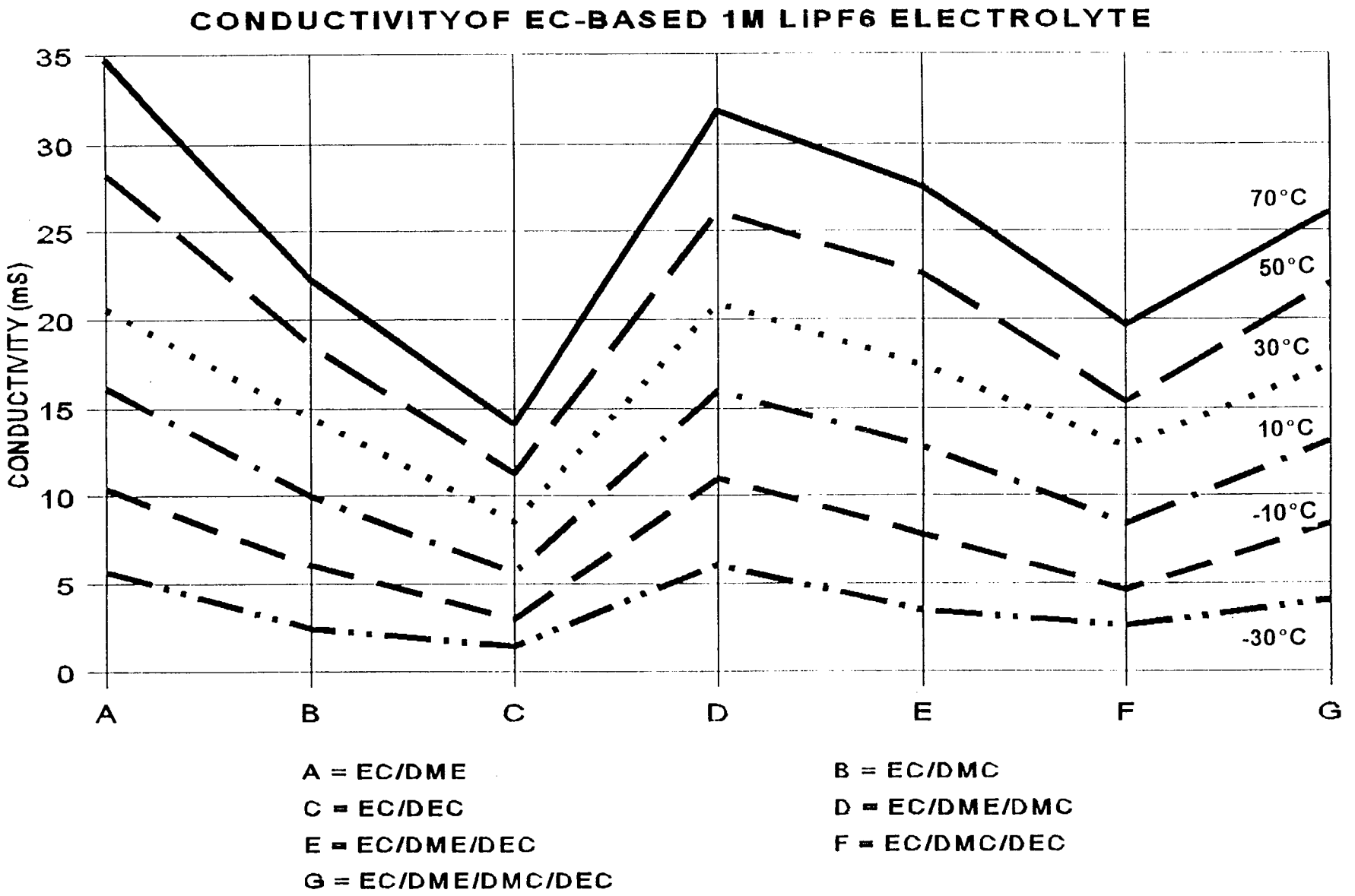
CONDUCTIVITYOF EC-BASED 1M LIPF6 ELECTROLYTE
CONDUCTIVITY (mS)
35
30
25
20
15
10
5
0
A
B
C
D
E
F
G
70°C
50°C
30°C
10°C
-10°C
-30°C
A = EC/DME
B = EC/DMC
C = EC/DEC
D = EC/DME/DMC
E = EC/DME/DEC
F = EC/DMC/DEC
G = EC/DME/DMC/DEC

CHEMICAL COMPATIBILITY OF $LiCoO_2$, $LiNiO_2$ AND $LiMn_2O_4$ IN EC-BASED 1.0M $LiPF_6$ ELECTROLYTES AFTER STORAGE FOR A WEEK AT DIFFERENT TEMPERATURES

Mixture		Room Temperature		40°C		60°C	
Oxide	Solvent (1)	Electrolyte Color	Analysis for Co, Ni, Mn	Electrolyte Color	Analysis for Co, Ni, Mn	Electrolyte Color	Analysis for Co, Ni, Mn
$LiCoO_2$	EC:DEC	Clear	.0027% Co	Purple	.1230% Co	Dark Purple	0.33% Co
	EC:DMC		.0010% Co	Light Purple	.0017% Co		0.41% Co
	EC:DME	Pale Yellow	.0013% Co	Dark Pink	.3215% Co	Dark Pink	0.66% Co
$LiNiO_2$	EC:DEC	Clear	.0005% Ni	Clear	.0008% Ni	Clear	No Ni
	EC:DMC		.0006% Ni		.0011% Ni		.0009%
	EC:DME	Pale Yellow	.0003% Ni		.0001% Ni		No Ni
$LiMn_2O_4$	EC:DEC	Pale Yellow	.0013% Mn	Grey	.0168% Mn	Grey	.053% Mn
	EC:DMC	Yellow	.0001% Mn		.0034% Mn		.13% Mn
	EC:DME		.0025% Mn	Pale Yellow	.0535% Mn	Dark Grey	.40% Mn

(1) 1M $LiPF_6$ electrolyte solvent mixture, 1:2 (V/V)

Voltammogram of Platinum Cathode

1M LiPF6 in EC:DMC, 1:2 Electrolyte

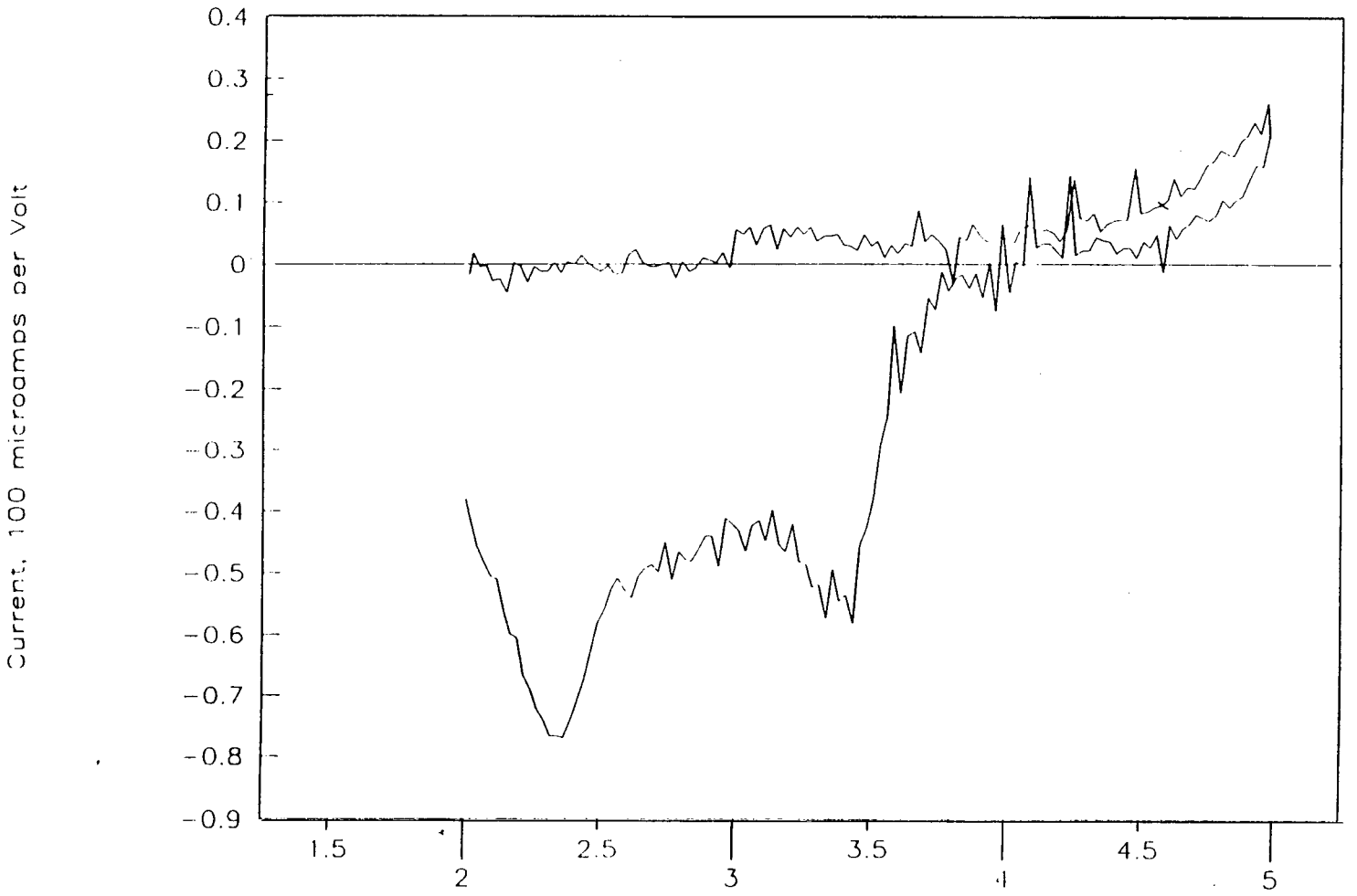

Yardney TECHNICAL PRODUCTS INC

Voltammogram of Platinum Cathode

1M LiPF6 in EC:DME, 1:2 Electrolyte

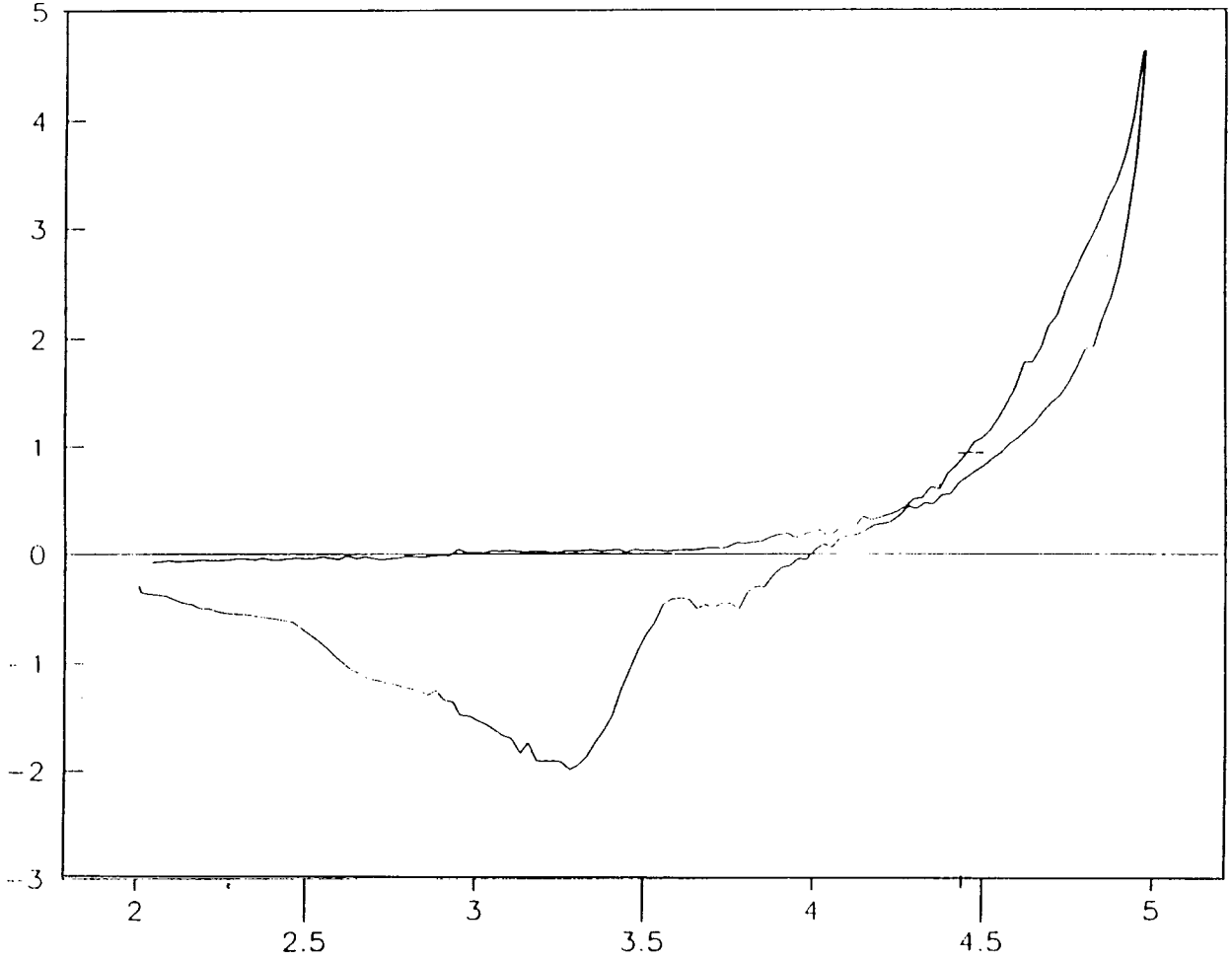

Vardney TECHNICAL PRODUCTS INC

YARDNEY'S PRISMATIC DESIGN EXPERIENCE

- Over 50 years experience on Prismatic Design Cells and Batteries with AgO-Zn and $LiSOCl_2$ chemistries
- Built 840V, 16,000 Ah AgO-Zn Battery (Albacore, 560 x LR 16,000)
- Built 500V, 4,000 Ah AgO-Zn Batteries (Dolphin, 330 x LR 4,000)
- Built 30V, 10,000 Ah $Li/SOCl_2$ Batteries (MESP)

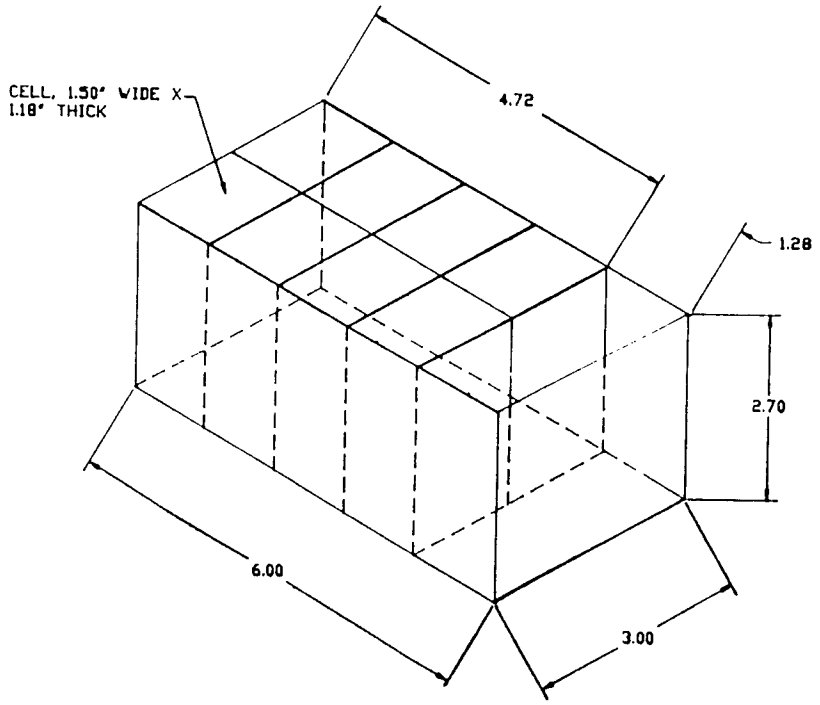

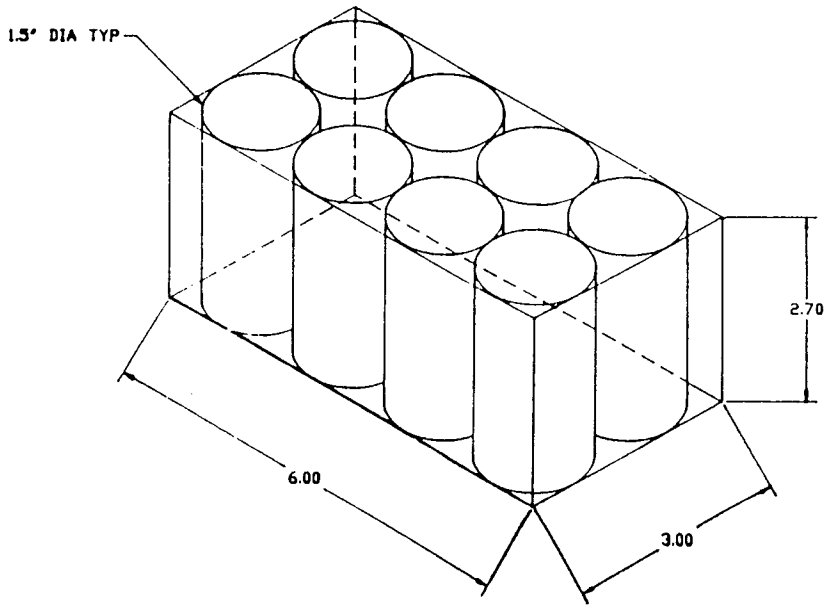

ABOUT 22% VOLUME ADVANTAGE OF PRISMATIC CELLS

Yardney TECHNICAL PRODUCTS INC

LI-ION BATTERIES

About 25% capacity loss after 500 cycles

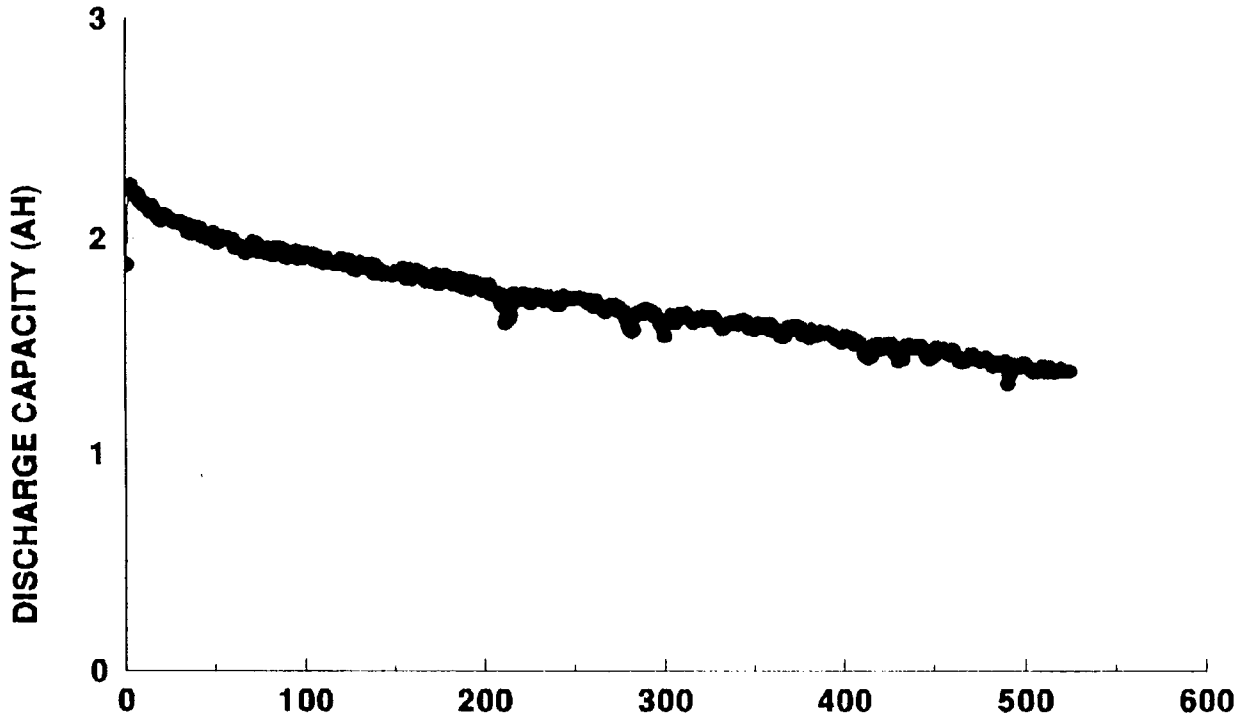

Discharge Capacity vs Cycle Number of a 2 Ah Prismatic Li-ion Cell.
Discharge Current: 750mA. Charge: 3 Hours. The Cell is Still Cycling.

G:\FILES\PRESENT\LITHIUM\LIMC.WPD

Yardney TECHNICAL PRODUCTS INC

LI-ION BATTERIES

Coulombic Efficiency of almost 1 shows excellent cycling efficiency

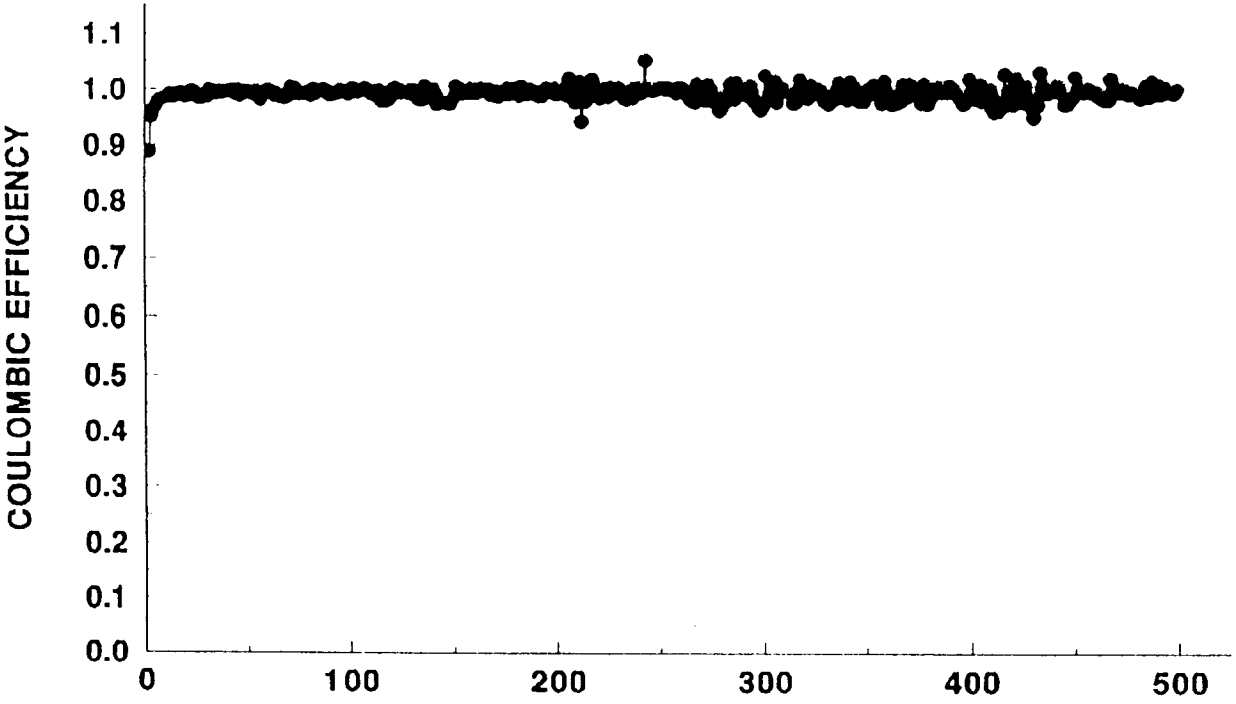

Coulombic Efficiency of a 2 Ah Prismatic Li-ion cell.
The cell is still cycling.

G:\FILES\PRESENT\LITHIUM\LMC.WPD

Vardney

LI-ION BATTERIES

Energy efficiency of 95% indicates insignificant polarization during charge/discharge cycles

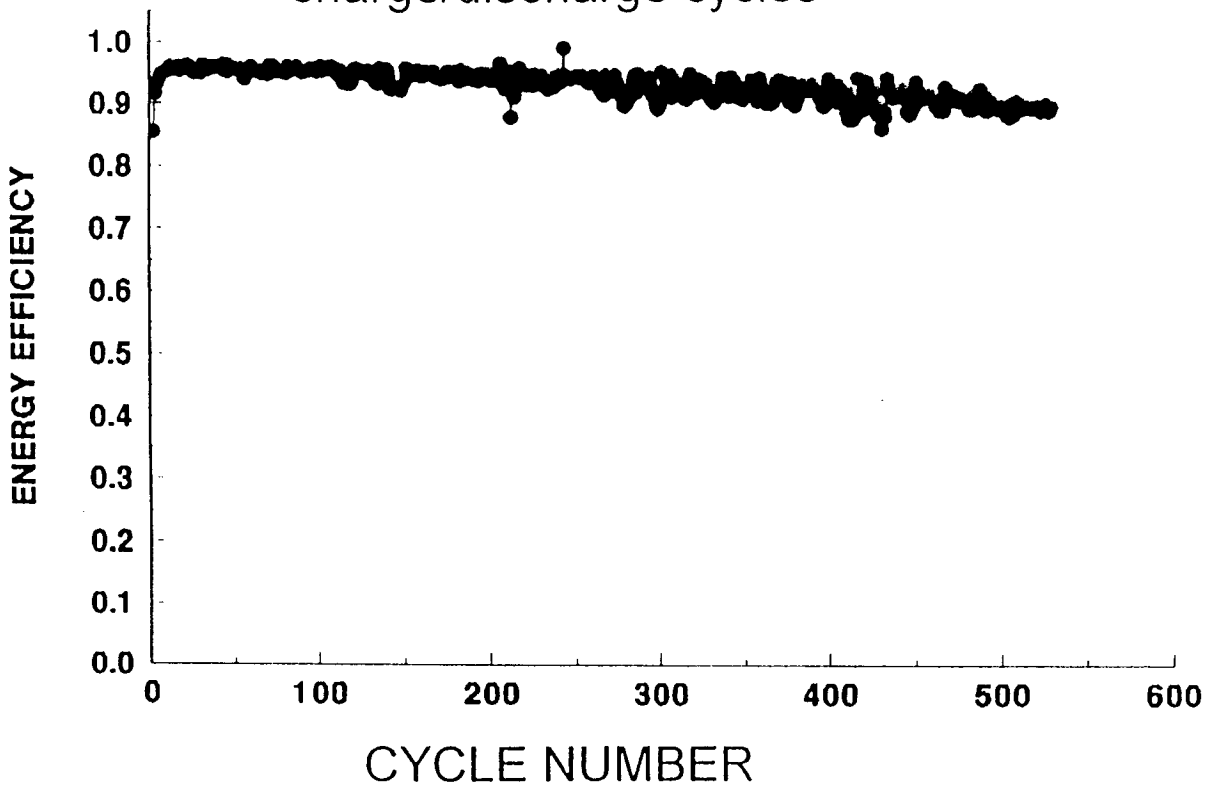

Energy efficiency of a 2Ah Prismatic Li-ion cell. The cell is still cycling.

G:\FILES\PRESENT\LITHIUM\WU.WMC WPD

Yardney

LI-ION BATTERIES

About 13% capacity loss after 270 cycles

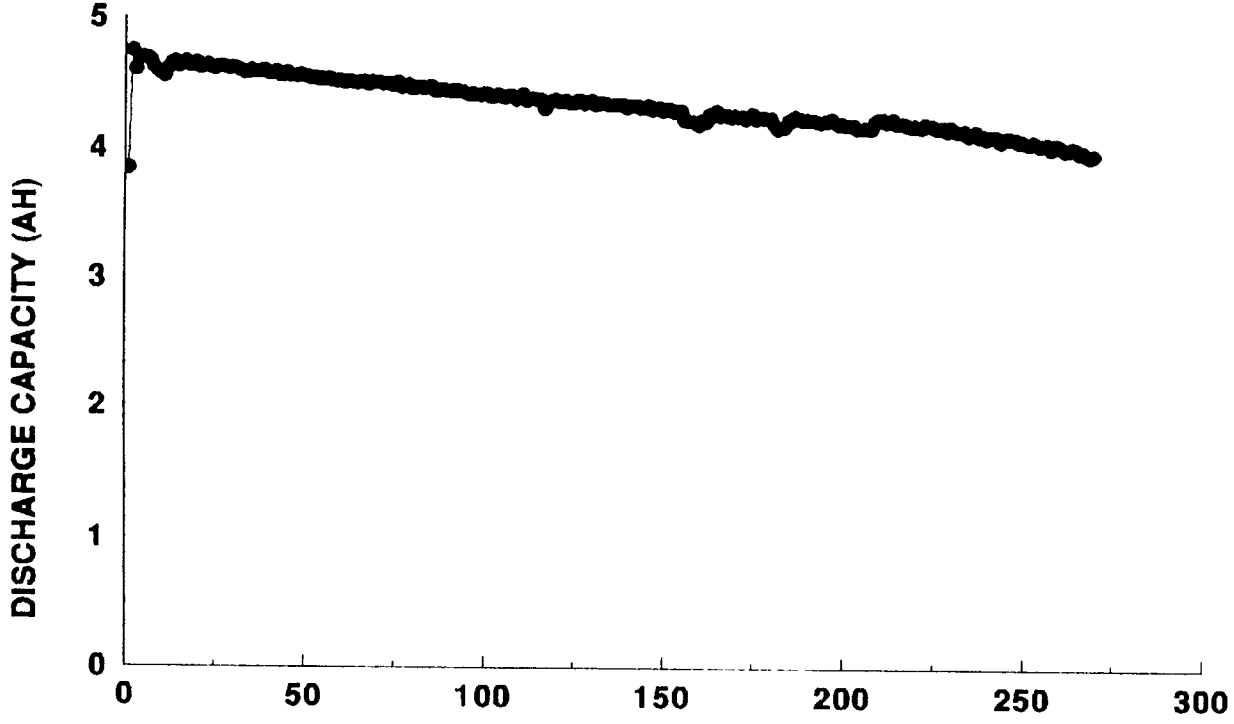

Discharge capacity vs cycle number of a Li-ion cell
at 1 Amp discharge rate. Charge: 3 Hours. The cell is still cycling.

G:\FILES\PRESENT\LITHIUM\NUMC.WPD

Yardney TECHNICAL PRODUCTS INC

Prismatic Li-ion Cell

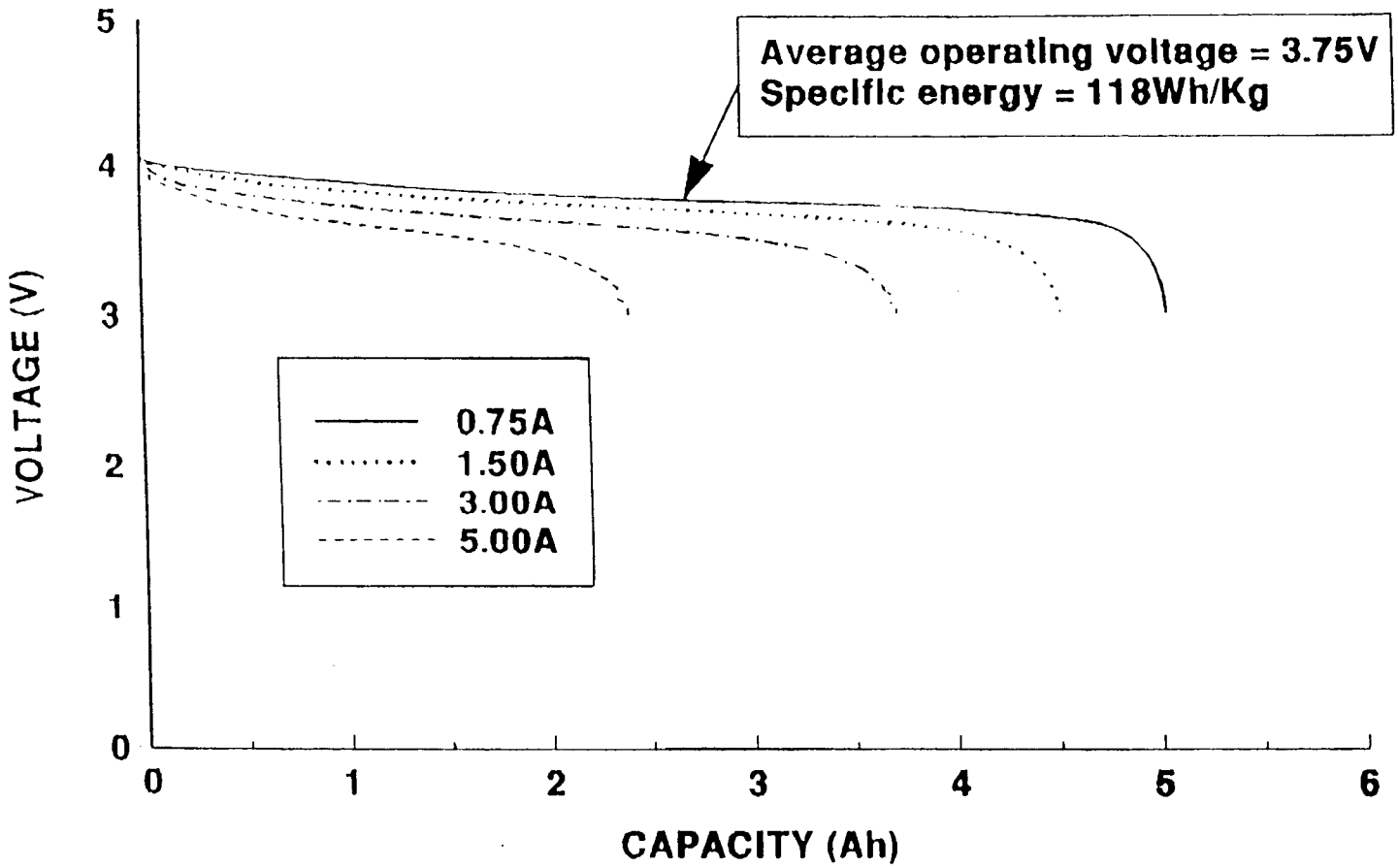

Discharge Behavior of a Prismatic Li-ion Cell in a Plastic Case at Various Current Drains.
Charge Rate: C/3

Yardney TECHNICAL PRODUCTS INC

Prismatic Li-ion Cell

Prismatic lithium-ion cell can deliver more than 1.2 kW/kg

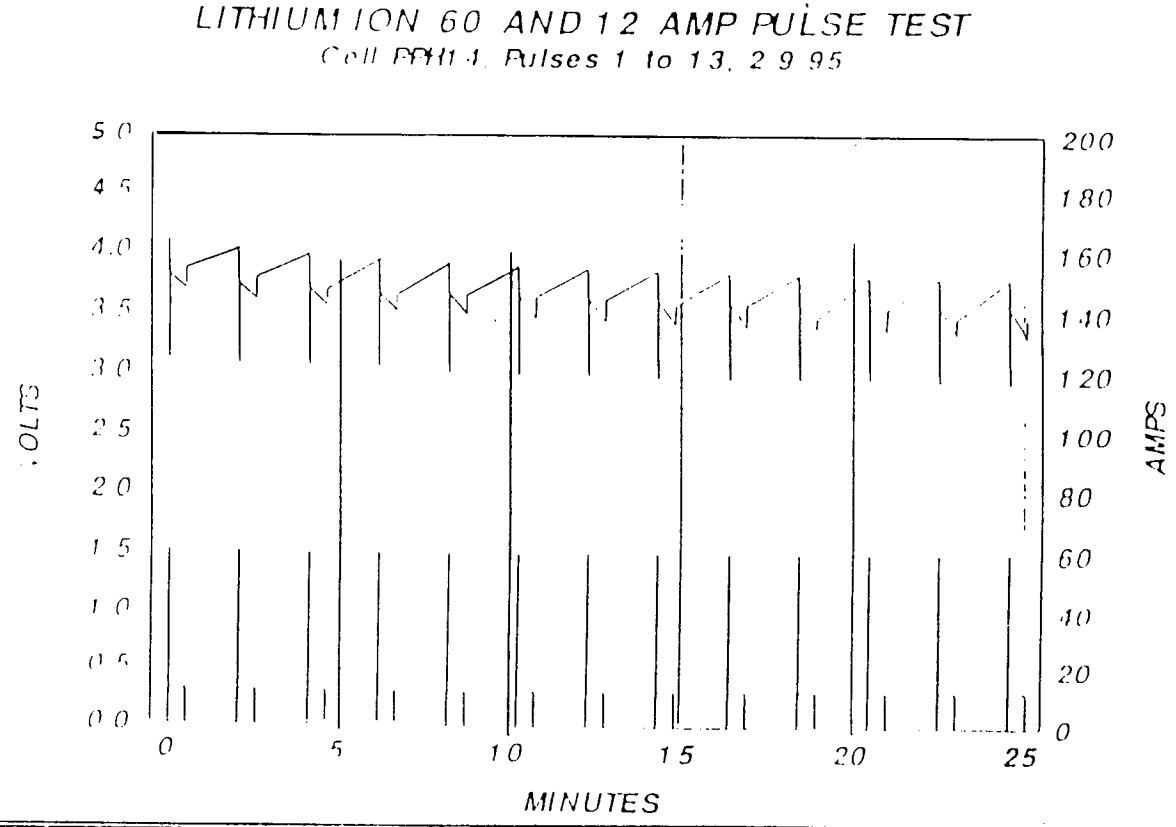

Pulse Discharge Characteristics of a Prismatic Lithium-ion Cell at 60 A for 1 sec, 12 A for 30 sec and then 90 sec Rest Period. Delivered Pulses = 25/Charge. Total Delivered Capacity - 2.92Ah.

(continued)

Yardney TECHNICAL PRODUCTS INC

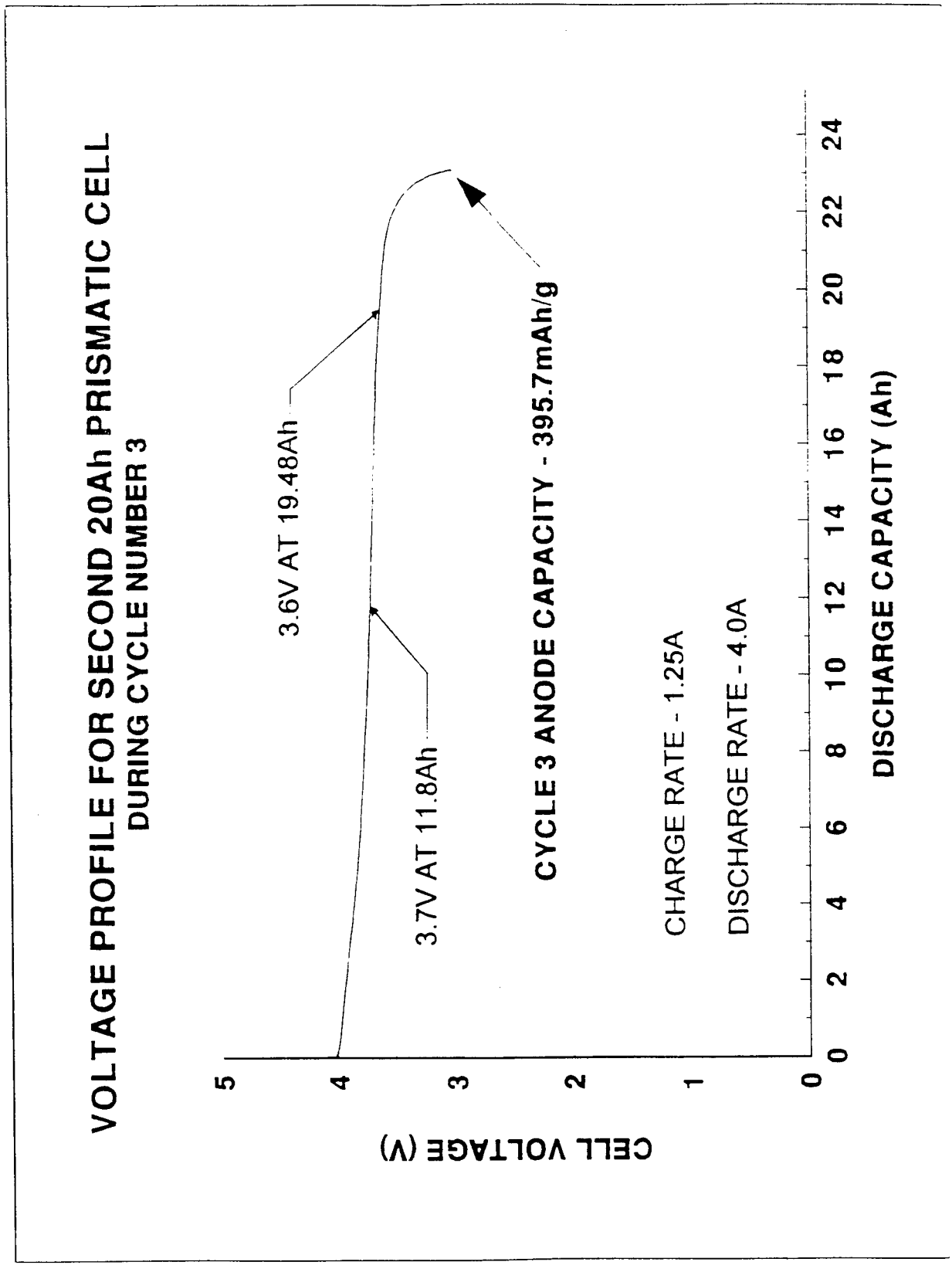
VOLTAGE PROFILE FOR SECOND 20Ah PRISMATIC CELL
DURING CYCLE NUMBER 3
3.6V AT 19.48Ah
3.7V AT 11.8Ah
CYCLE 3 ANODE CAPACITY - 395.7mAh/g
CHARGE RATE - 1.25A
DISCHARGE RATE - 4.0A
CELL VOLTAGE (V)
DISCHARGE CAPACITY (Ah)
0
1
2
3
4
5
0
2
4
6
8
10
12
14
16
18
20
22
24

DISCHARGE CAPACITY VS CYCLE NUMBER FOR 20Ah LI-ION CELL

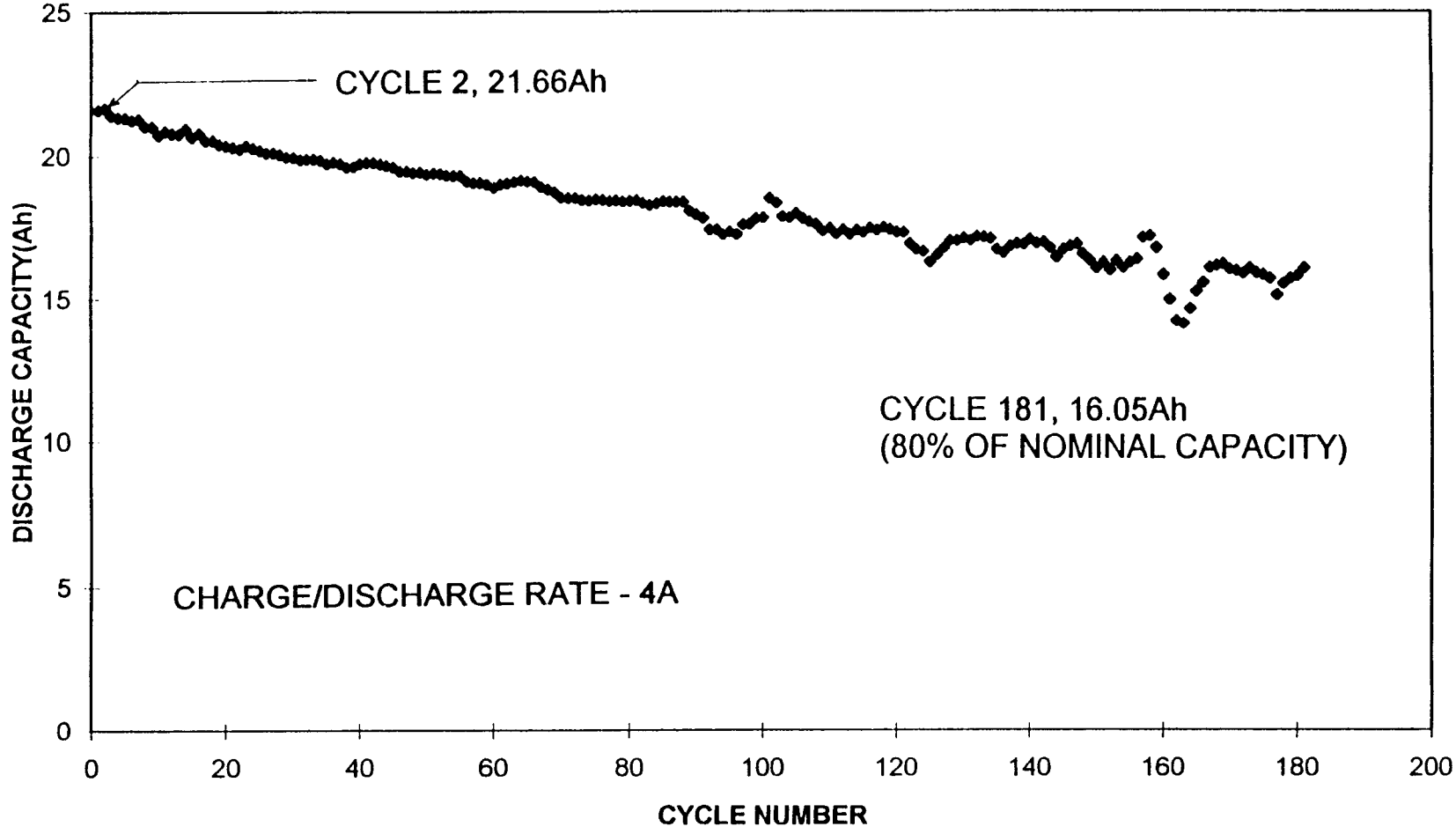

Yardney TECHNICAL PRODUCTS INC

LI-ION BATTERIES

CHARACTERISTICS OF YARDNEY'S PRISMATIC DESIGN LITHIUM-ION CELLS

PARAMETERS	METAL-CASE LI-ION CELL (3Ah)	PLASTIC-CASE LI-ION CELL (5Ah)	PLASTIC-CASE LI-ION CELL (20Ah)
AVERAGE OPERATING VOLTAGE AT C/5 (V)	3.7	3.7	3.7
RATED CAPACITY AT C/5 (Ah)	3.0	5.0	20.0
AVERAGE WEIGHT (gm)	135	157	600
SPECIFIC ENERGY (Wh/kg)	82	118	130
ENERGY DENSITY (Wh/l)	225	220	240
OPERATING TEMPERATURE RANGE CHARGE (°C) DISCHARGE (°C)	 0 TO 45 -20 TO +60	 0 TO 45 -20 TO +60	 0 TO 45 -20 TO +60

Yardney TECHNICAL PRODUCTS INC

PRISMATIC LI-ION CELL

SUMMARY:

- Developed 2, 3, 5 and 20Ah prismatic design lithium-ion cells. 5Ah and 20Ah cells provide specific energy of 118Wh/kg and 130Wh/kg and energy density of 220Wh/l and 240Wh/l, respectively.
- Lithium-ion cells show excellent safety characteristics.
- Lithium-ion cells can be operated over a wide temperature range.
- Prismatic cells can meet power tools requirements.
- The developed prismatic cells can provide more runtime of a laptop computer than the state-of-the-art technologies.
- Lithium-ion cells can meet the requirements of a wide variety of electronic applications including camcorders and cellular telephones.

Bipolar Lithium Batteries

YARDNEY'S BIPOLAR DESIGN EXPERIENCE

- Over 15 years experience with bipolar AgO-Zn and Li/$SOCl_2$ systems

- Developed high voltage bipolar Li/$SOCl_2$ battery for the DOD's applications

Yardney TECHNICAL PRODUCTS INC.

CHARACTERISTICS OF BIPOLAR DESIGN

- No bus bars or intercell connectors
- Insignificant resistance losses along or across electrode
- Minimal resistance losses in between cells
- Uniform current and potential distribution

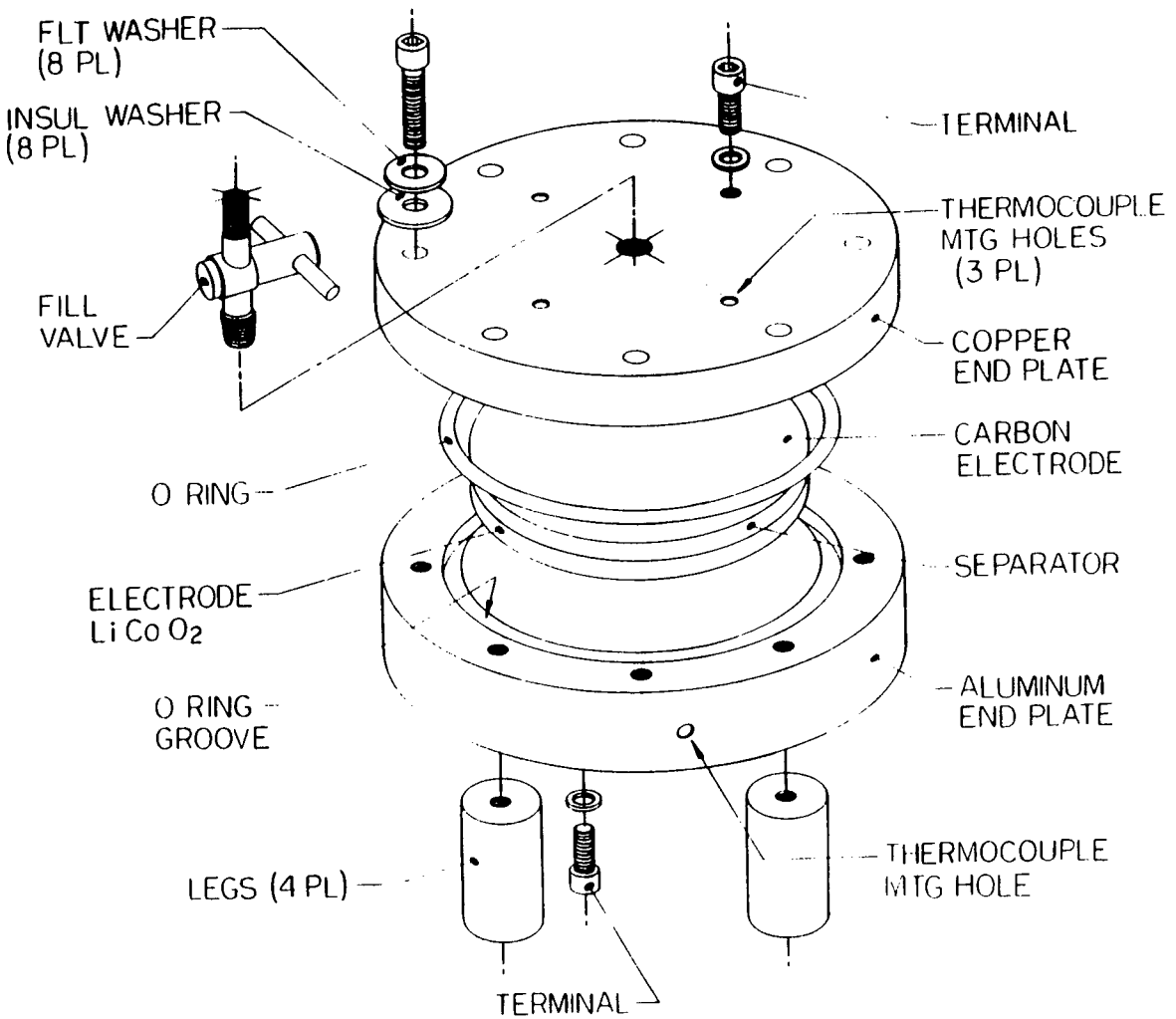

Single Cell Test Fixture

Yardney TECHNICAL PRODUCTS INC

High Rate Bipolar LI-ion Rechargeable Batteries

Commercially available graphitic carbon delivers 340 mAh/g capacity at C/3 rate

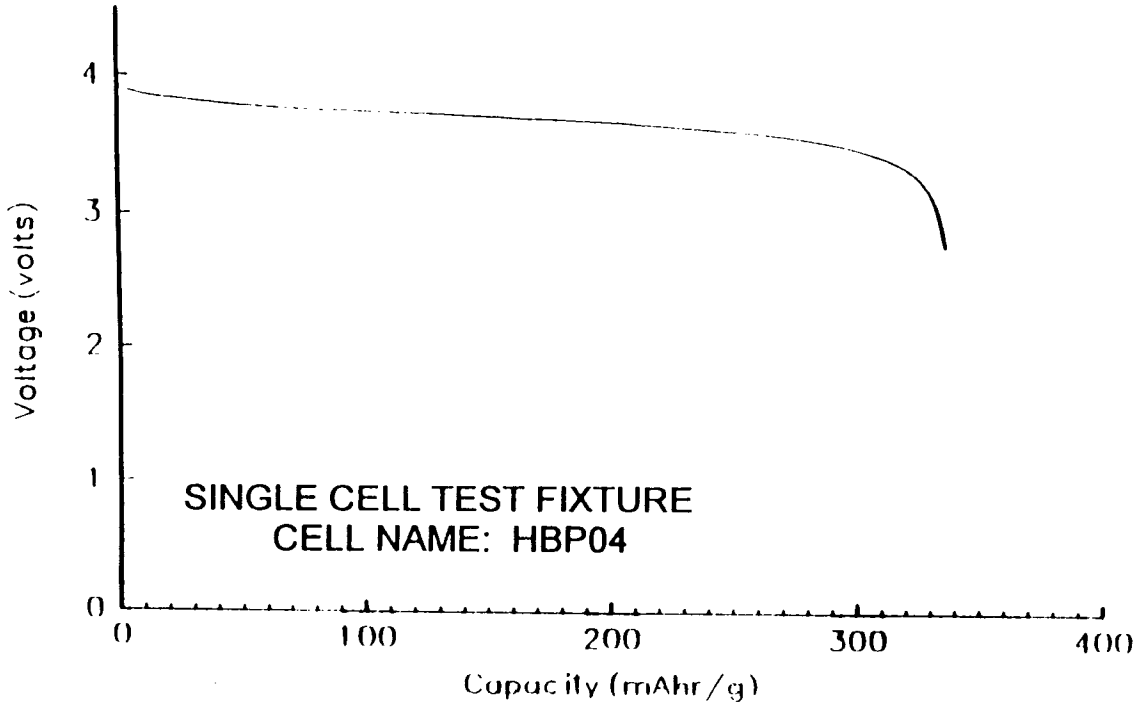

Discharge Behavior of a Li-ion Cell at 1.5 mA/cm^2

Yardney TECHNICAL PRODUCTS INC.

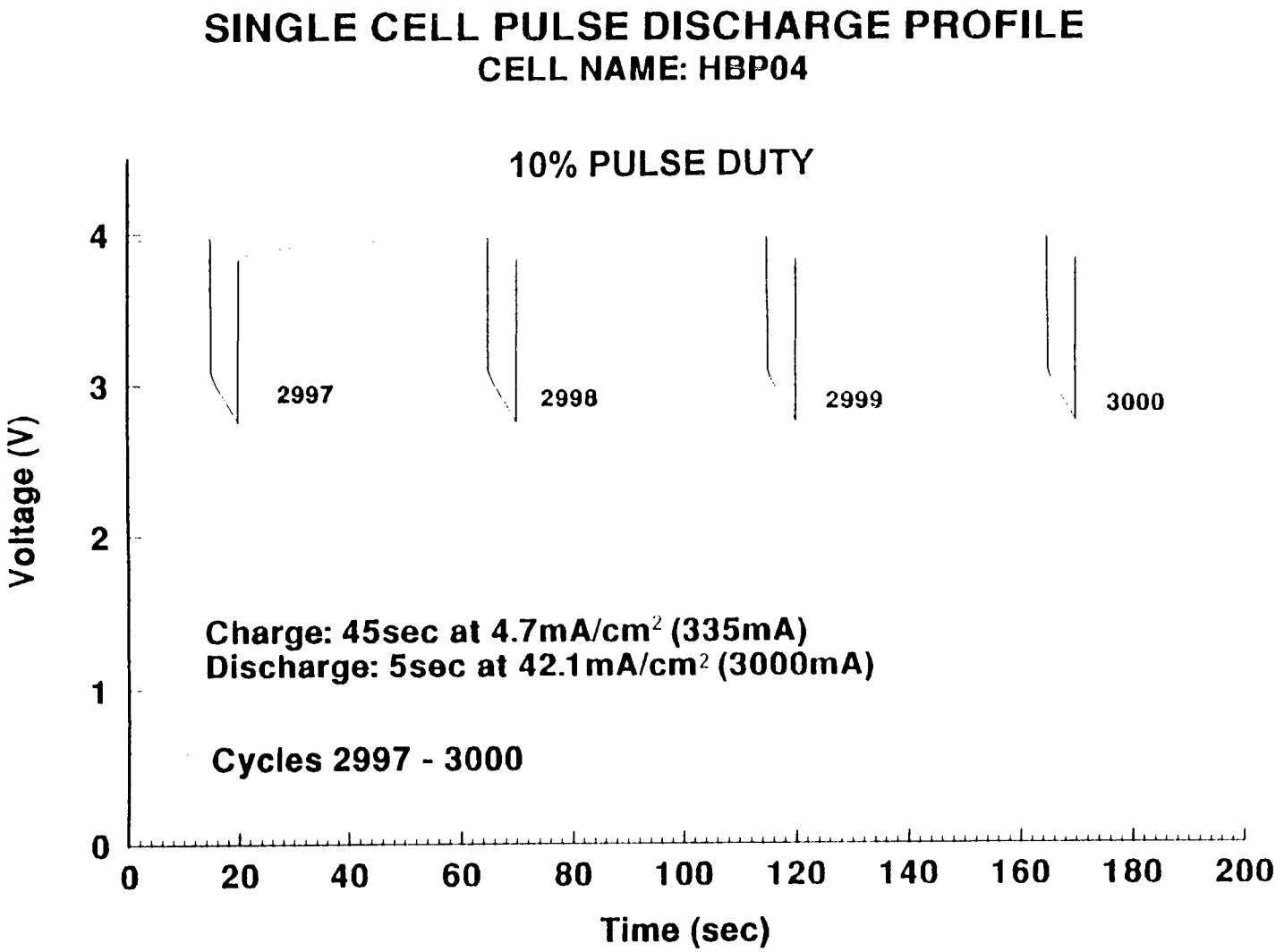

Yardney TECHNICAL PRODUCTS INC

High Rate Bipolar Li-ion Batteries

After 3000 pulse cycles, Li-ion cell shows insignificant polarization

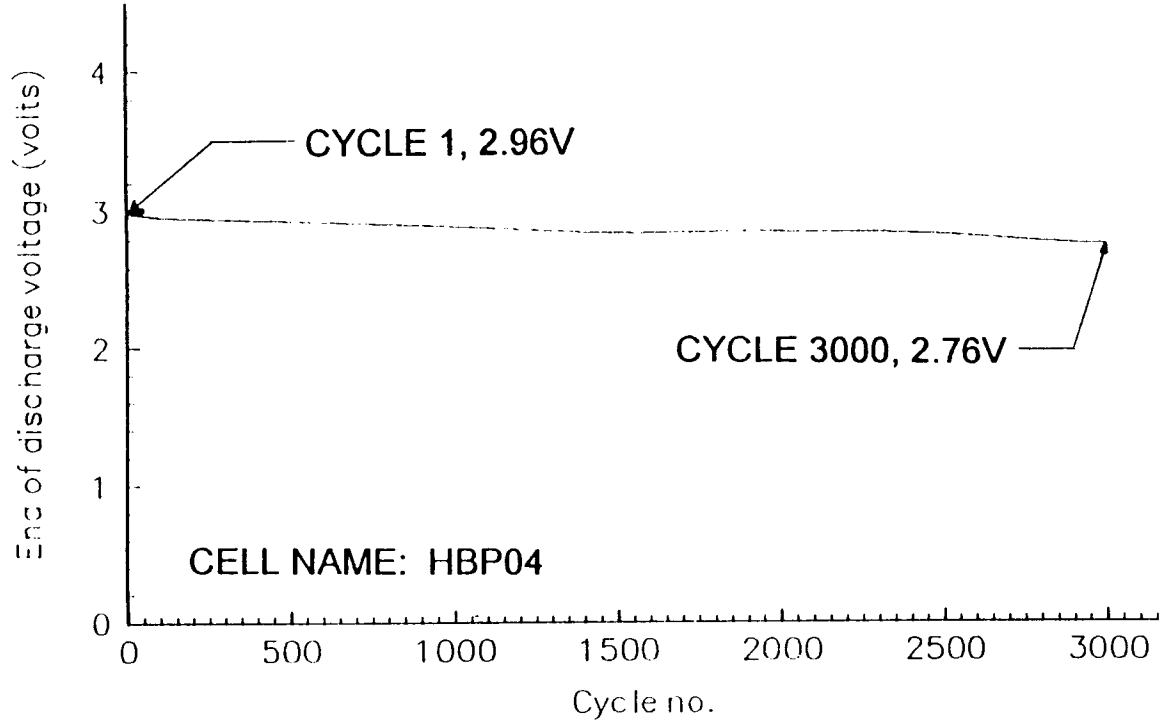

End of Discharge Voltage vs. Cycle Number of a Li-ion Cell Discharged at 42.1 mA/cm^2 for 5 seconds and charged at 5 mA/cm^2 for 45 seconds

Yardney TECHNICAL PRODUCTS INC

High Rate Bipolar Li-ion Batteries

After 3000 pulse cycles, continuous discharge behavior of Li-ion cell remains almost unchanged

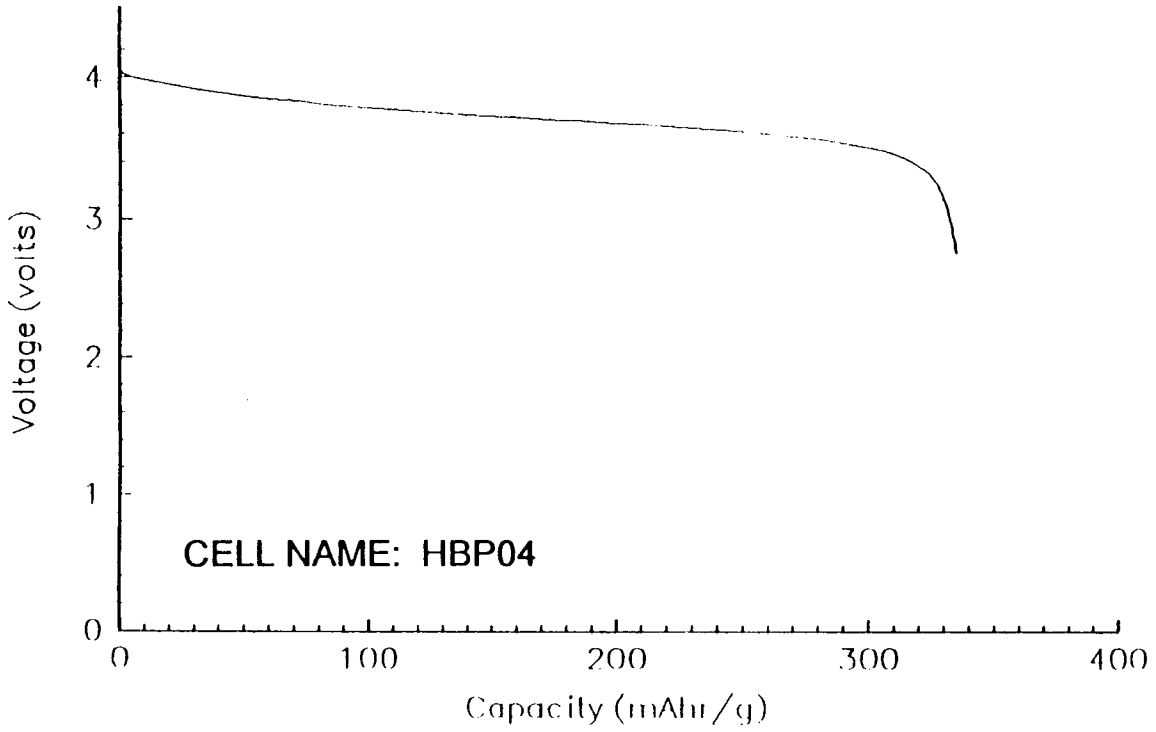

Discharge Behavior of a Li-ion Cell at 2 mA/cm^2
(after delivering 3000 pulse cycles)

Yardney TECHNICAL PRODUCTS INC

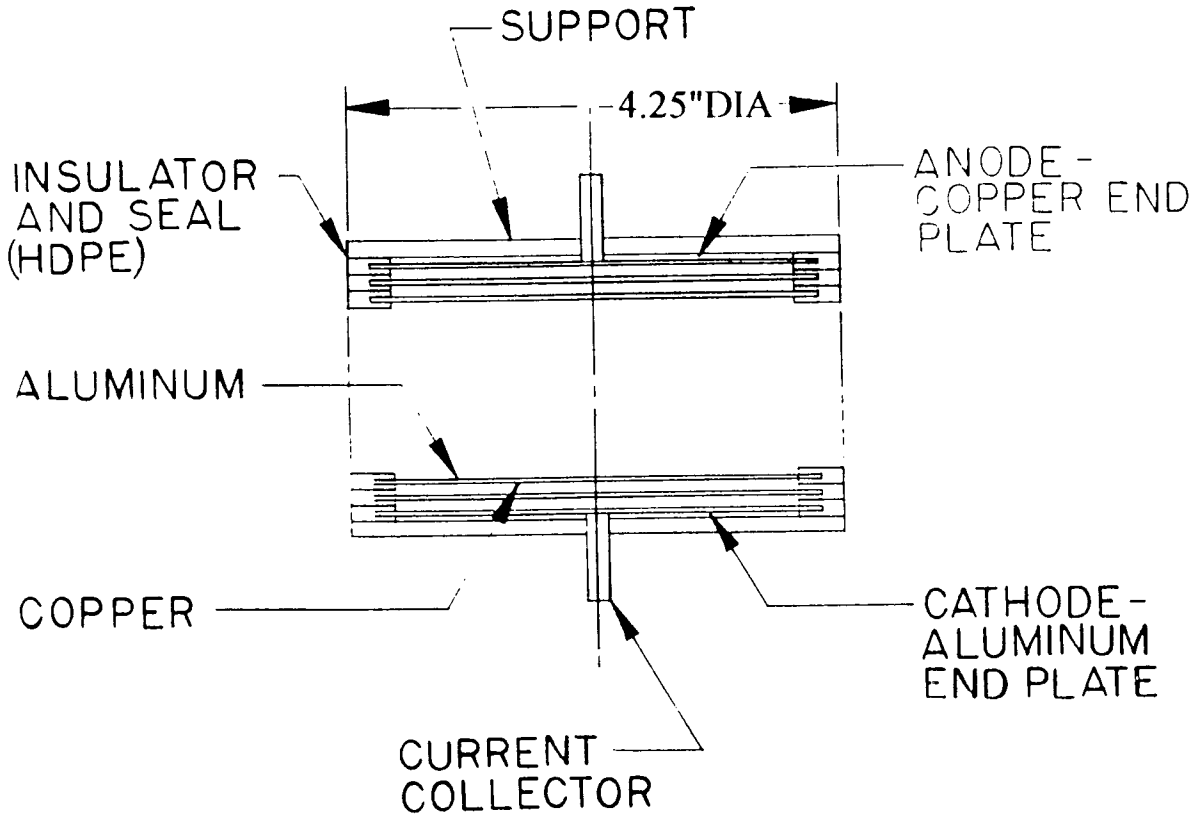

Multicell Assembly

Yardney TECHNICAL PRODUCTS INC.

High Rate Bipolar Li-ion Batteries

Li-ion Bipolar battery can deliver more than 3000 high pulse power cycles

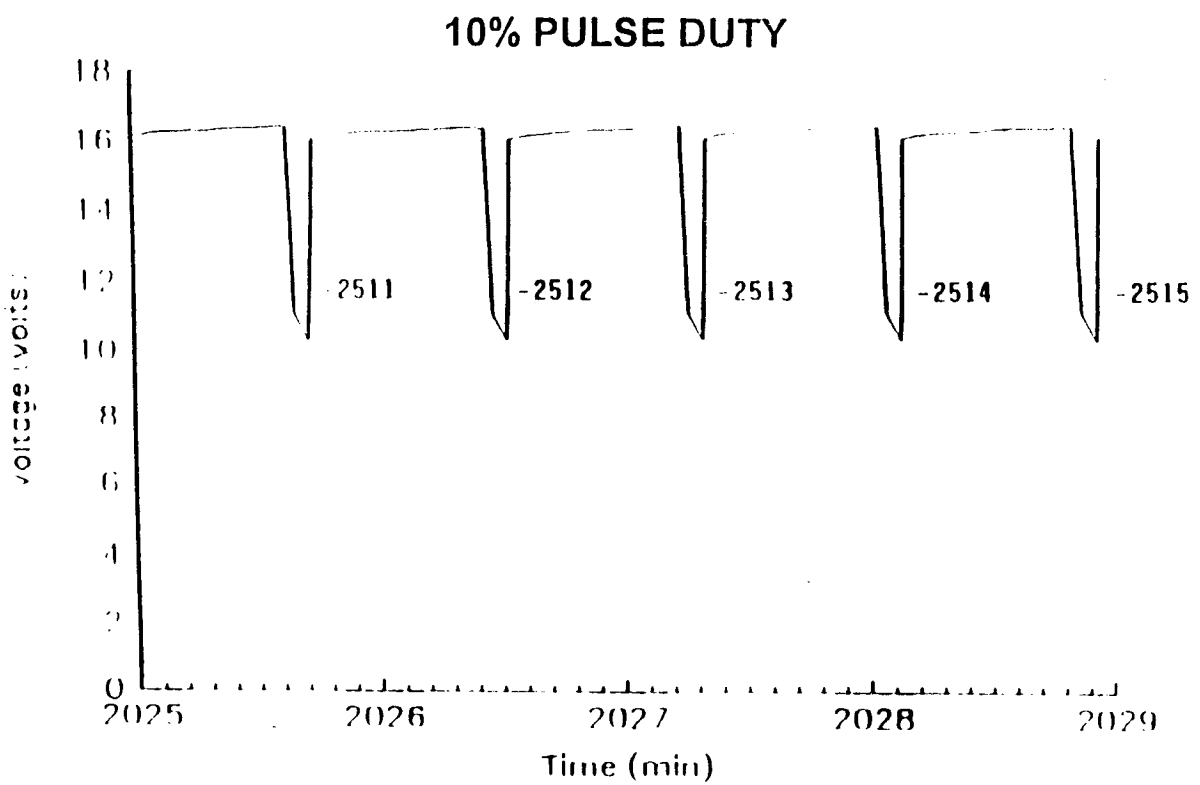

Charge/Discharge Behavior of a 4-Cell Stack Li-ion Battery at 5 mA/cm^2
Charge for 45 sec. and 45 mA/cm^2 Discharge for 5 sec.

Yardney TECHNICAL PRODUCTS INC

PULSE DISCHARGE DATA FOR FOUR-CELL STACK SBPNI4C1
10% PULSE DUTY

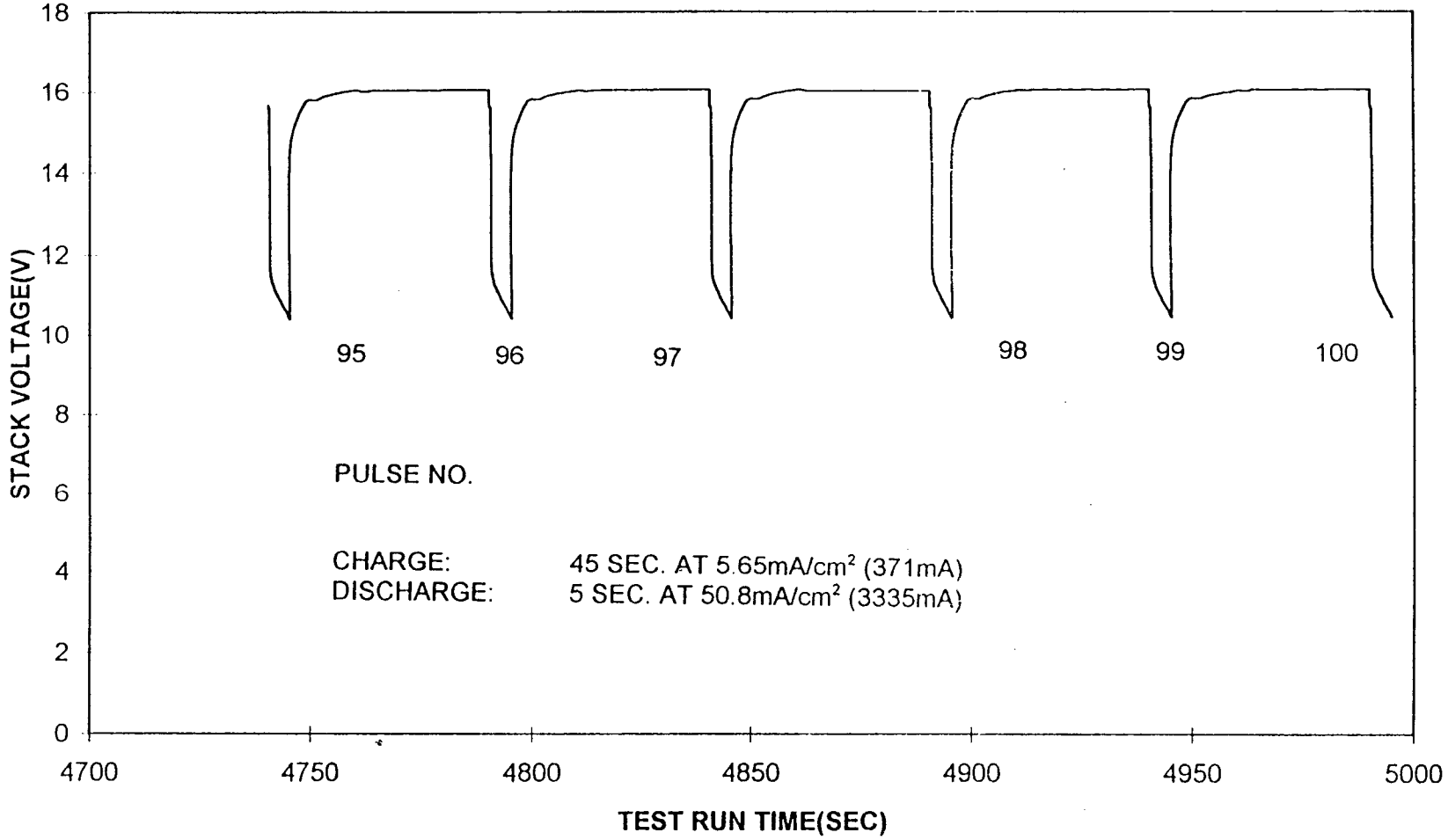

Yardney TECHNICAL PRODUCTS INC

END OF PULSE VOLTAGE VS CYCLE NUMBER FOR 5 SECOND PULSES AT 50.8mA/cm^2

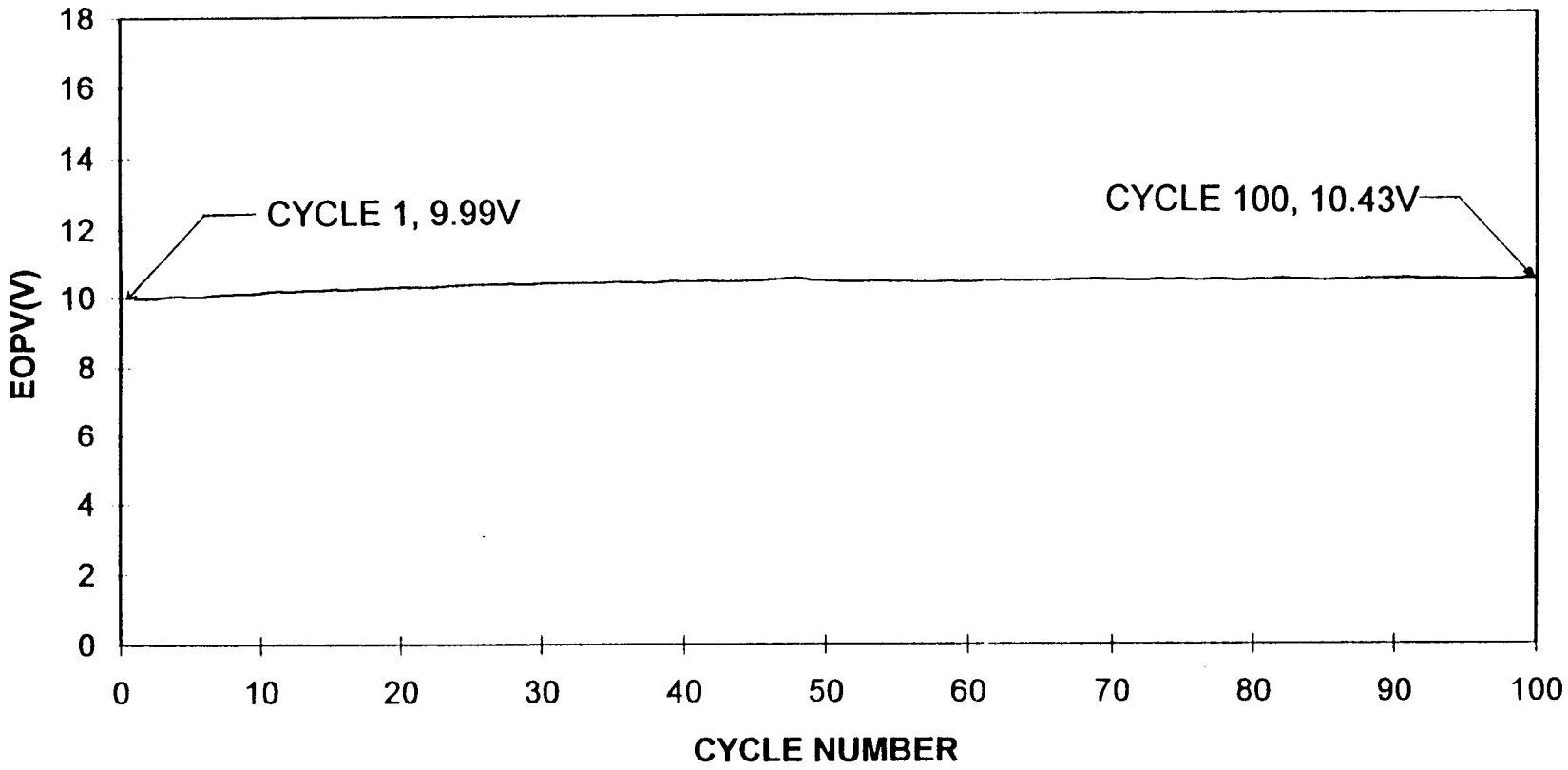

Yardney TECHNICAL PRODUCTS INC

PULSE DISCHARGE DATA FOR FOUR-CELL STACK SBPNI4C4
20% PULSE DUTY

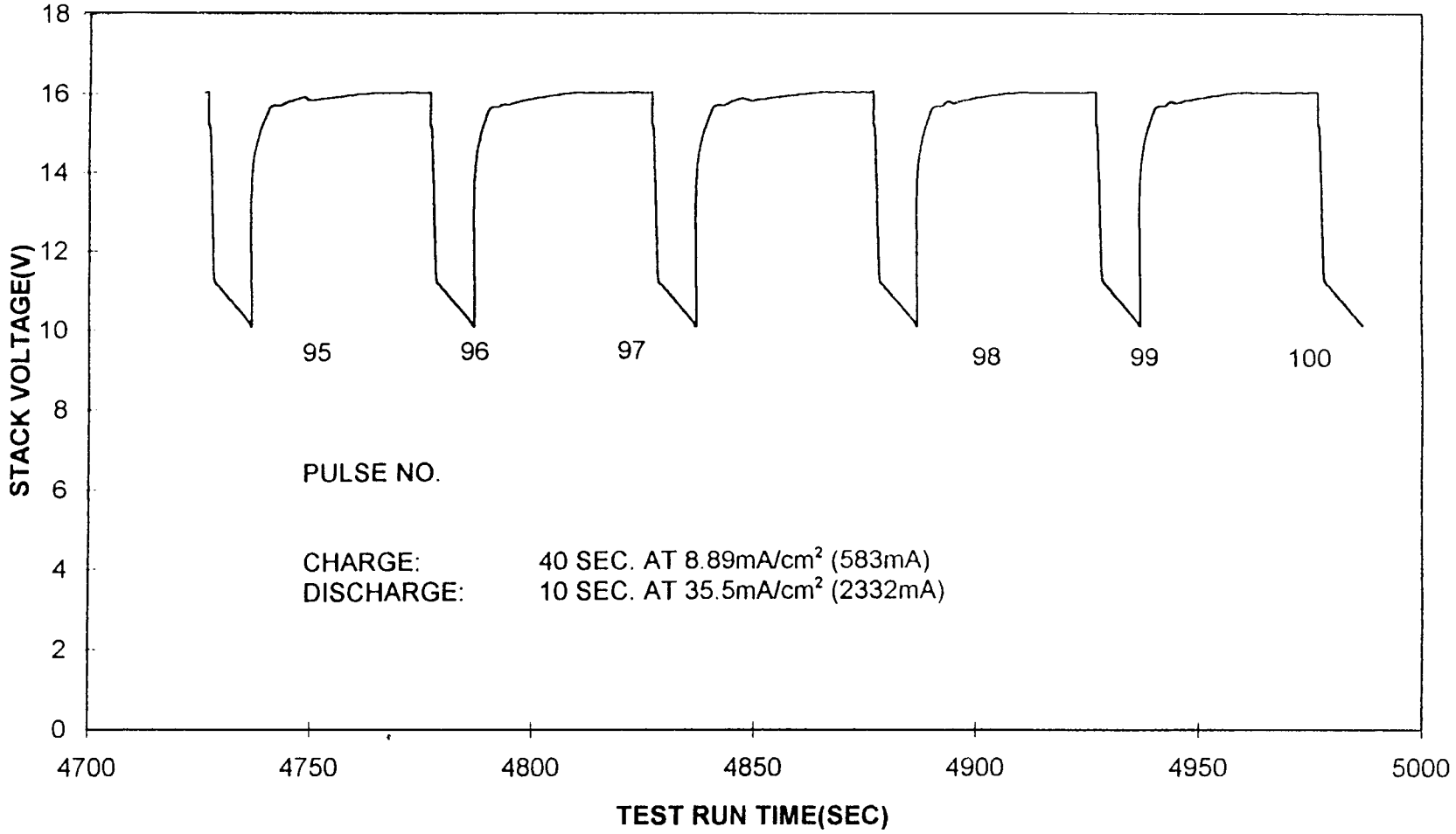

Yardney TECHNICAL PRODUCTS INC

SUMMARY:

Li-ion Systems in bipolar configuration

- Can deliver more than 3000 high rate pulse cycles
- Can provide continuous charge/discharge cycles even after delivering several thousands of high rate pulse cycles
- Shows low self-discharge rate (8% per month)
- Has little adverse effect on prolong float charge
- Can accept overload during charge and discharge for a short period of time

Yardney TECHNICAL PRODUCTS INC

Acknowledgment:

- Wright Laboratory, WPAFB, NASA-JPL and Phillips Laboratory for financial support

- William Clark, Paul Paterno, Sheila Danahey, and Hasmukh Patel for help in preparing cells and materials

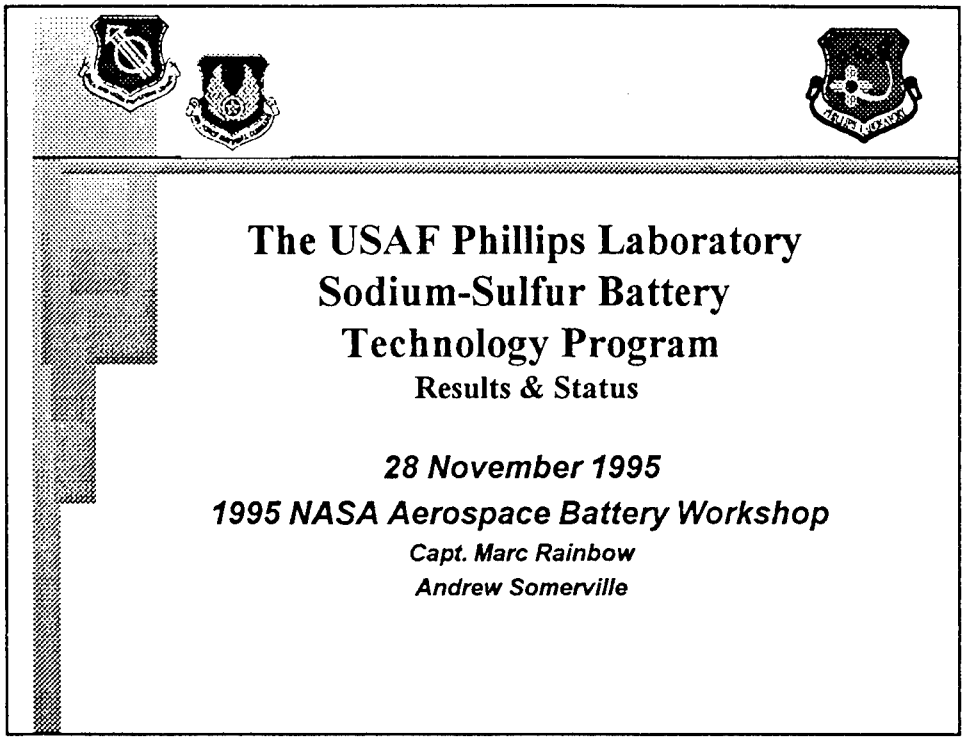
The USAF Phillips Laboratory
Sodium-Sulfur Battery
Technology Program
Results & Status
28 November 1995
1995 NASA Aerospace Battery Workshop
Capt. Marc Rainbow
Andrew Somerville

Outline

- *Background*
- *Safety and Abuse Test Results*
- *GEO and LEO Cycling Results*
- *Flight Test Status*
- *Summary*

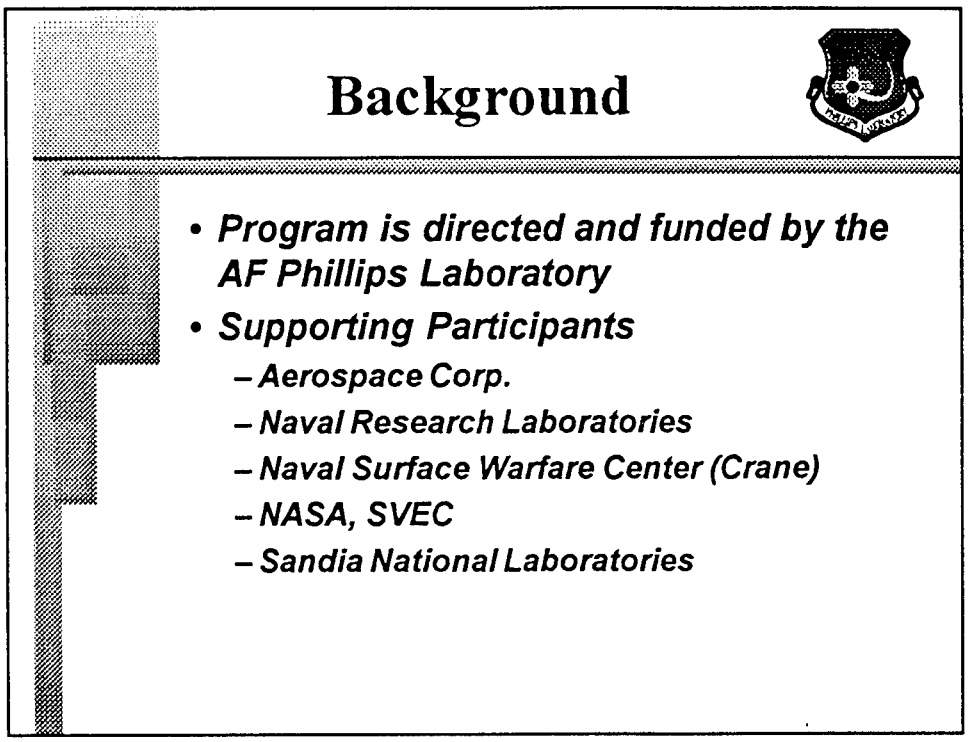

Funding for the Phillips Laboratory Sodium Sulfur Battery program has been provided solely from Air Force Funds. Technical assistance is provided by The Aerospace Corporation. The Naval Research Laboratory has been funded by Phillips Laboratory(PL) to design and fabricate hardware for the flight test portion of the program. PL has provided funding to the Naval Surface Warfare Center (NSWC) to carry out long term GEO and LEO cycling tests and to Sandia National Laboratories to carry out safety and abuse tests. NASA via the Space Vacuum Epitaxy Center (SVEC) at the University of Houston has provided assistance in scheduling and integrating the flight experiment aboard the Space Shuttle.

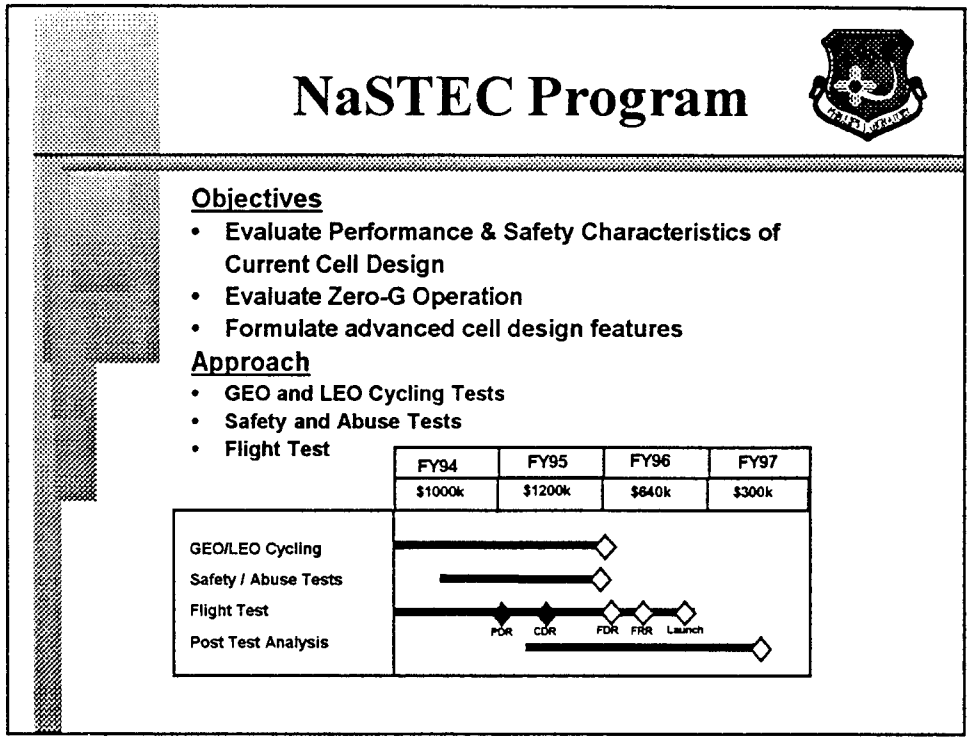

It is recognized by PL that in order to successfully develop Sodium Sulfur battery technology for use aboard military satellites that performance, reliability and safety of these cells must meet or exceed requirements for launch by military vehicles. The PL Sodium Sulfur Technology (NaSTEC) program was structured to demonstrate the capabilities and elucidate shortcomings in a.) the performance capability of NaS cells under GEO and LEO cycling regimes, b.) the safety characteristics and failure modes of cells when subjected to worst case environmental and abuse conditions and c.) to verify the capability of the cell to operate in a zero -g environment and to determine the effects of zero-g on cell performance. The PL program will evaluate the results of all tests to determine if cell design improvements are required in order to meet flight program requirements and, if so, will provide specific recommendations for a next generation cell design.

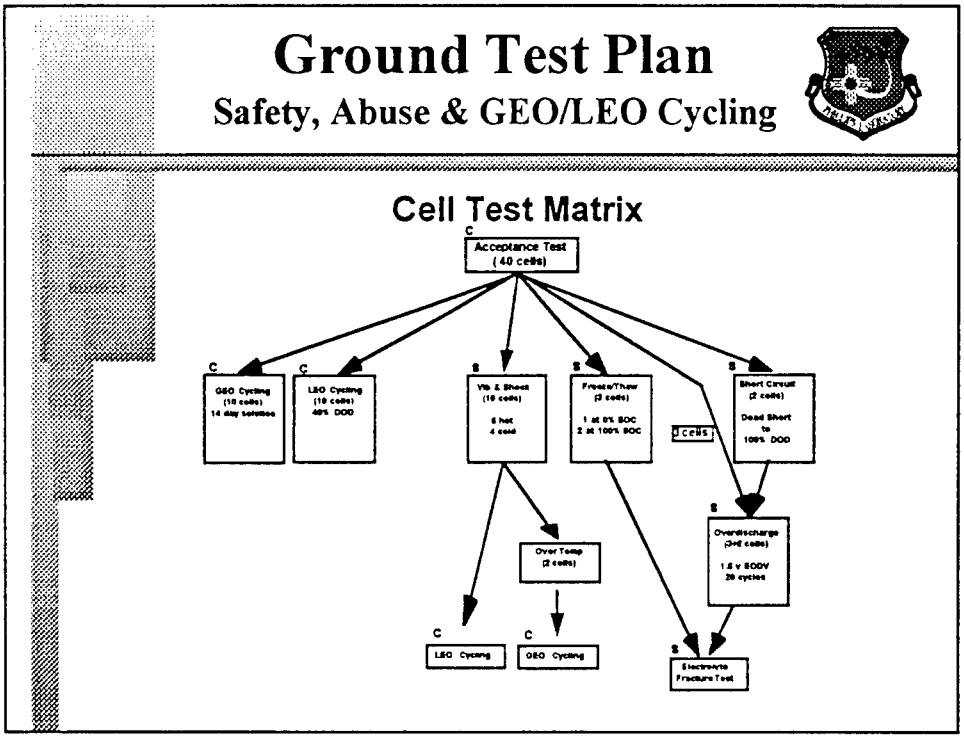

Due to the limited number of cells available for test and the large number of tests to be performed it was necessary to structure the program with cells being utilized in several tests. Careful consideration was given to the effects of multiple diverse tests on performance of the cells. Consequently, where it was believed that performance could be critically effected, as in the long term cycling tests at NSWC, new cells were used. In other tests where long term electrical performance was less critical, as in destructive tests, the test plan scheduled cells to undergo prior non - destructive tests. In this manner a relatively small number of cells were utilized to perform a large number of a tests.

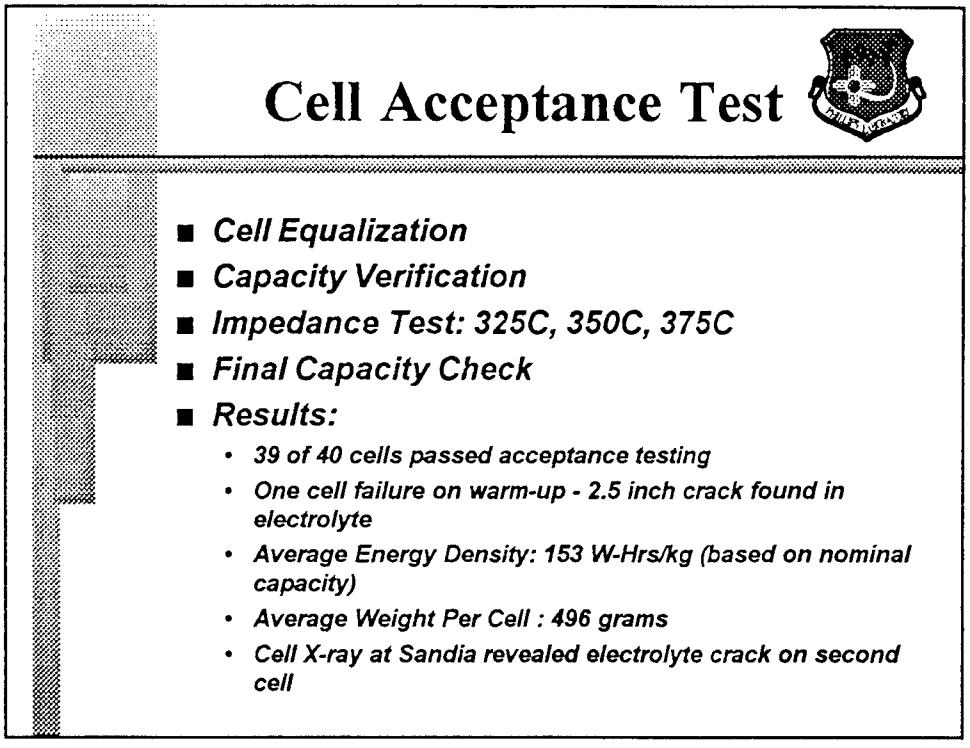

Each of the 40 cells delivered by the manufacturer (EPI) underwent acceptance testing at NSWC, Crane Ind. All cells were weighed, measured and leak tested. Each cell was discharged to a fixed voltage and then recharged at c/20 to a full state of charge. This was followed by three capacity verification cycles with a c/2 discharge and c/10 charge. Cell impedance was then measured through two cycles at temperatures of 325C, 350C and 375C and discharge rates of c/10, c/2 and charge rates of c/5. Three final capacity check cycles were then performed. The total number of cycles performed in acceptance testing was 23.

During acceptance testing cell #28 was removed from the test at cycle 14 (impedance test) due to anomalous performance. X-rays revealed that the cell had a 2.5 inch longitudinal crack in the cell electrolyte which had resulted in cell failure. All other cells successfully passed the acceptance test.

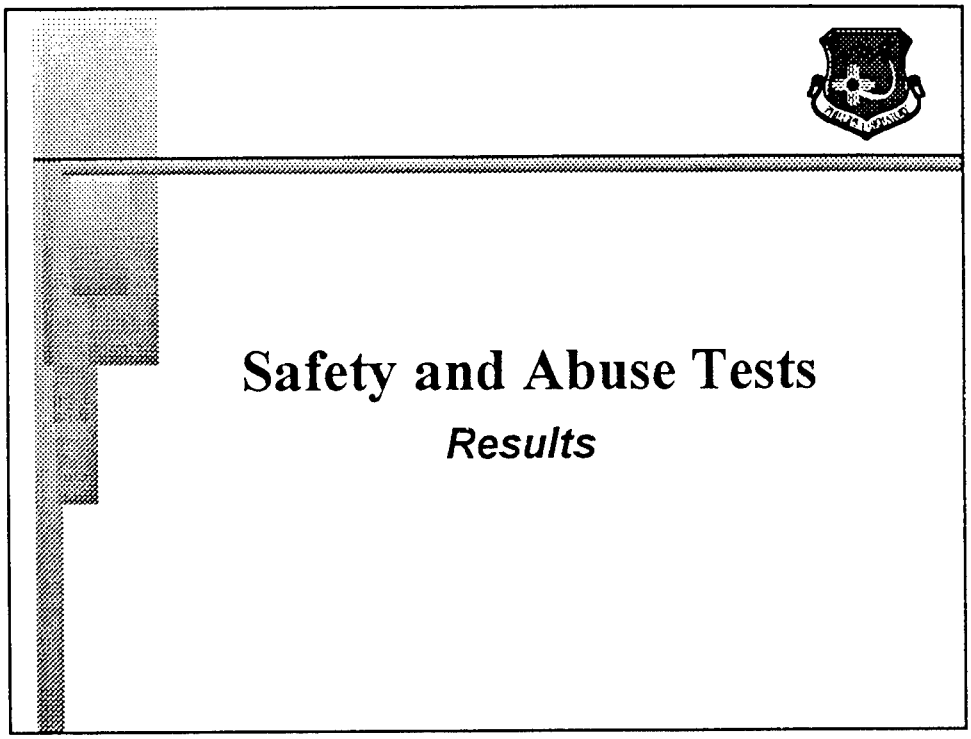
Safety and Abuse Tests
Results

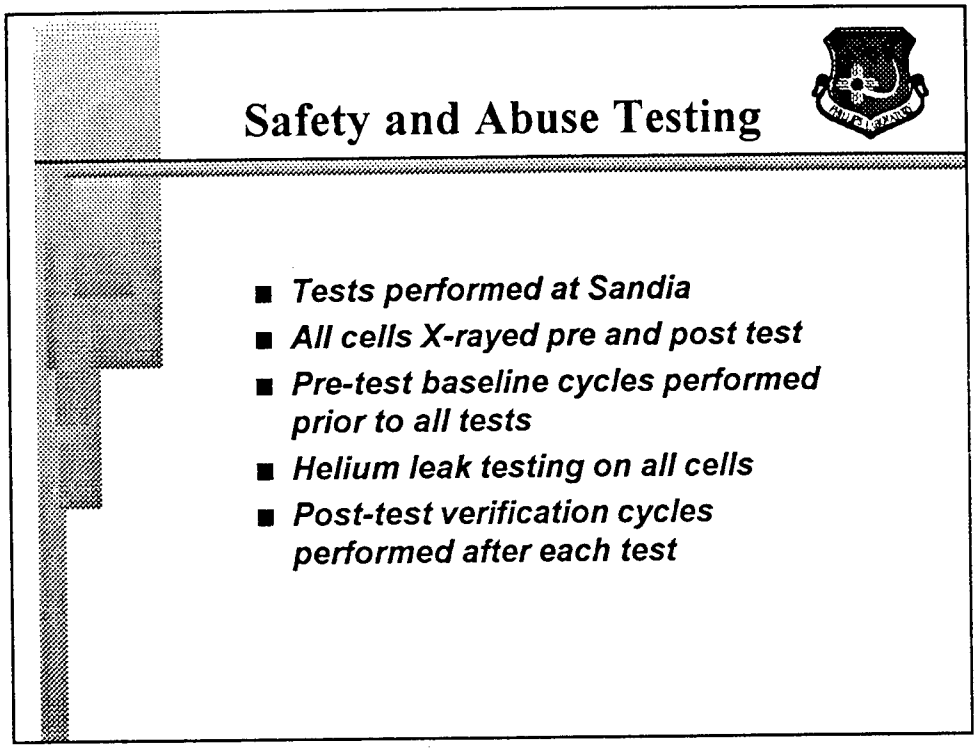

Following acceptance testing 19 cells were shipped to Sandia National laboratories for safety and abuse testing. Each cell underwent a visual inspection followed by X-ray examination. Helium leak checks were performed to verify cell case integrity.

In general, prior to the initiation of each test two performance verification cycles are performed and subsequent to each test three baseline cycles are performed to verify capacity

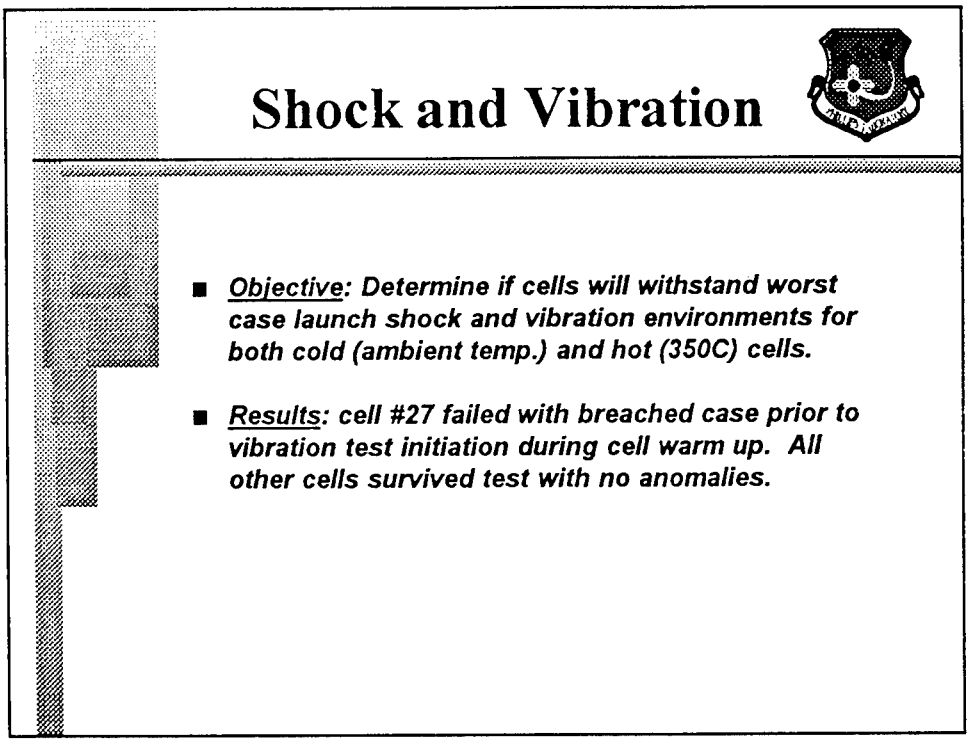

In order to enable operation of a sodium sulfur battery through launch a cell must be capable of surviving launch environments at operating temperature. Doing so will enable a NaS battery to provide power to the spacecraft through launch and orbit insertion and will avoid the cost and weight penalty which would be imposed by requiring battery warm-up on orbit.

The shock and vibration test provides a worst case simulation of launch vibration and shock environments. The test envelopes both Space Shuttle and Titan IV environments and was performed on cells in both a horizontal and vertical orientation at both ambient and operating temperature The hot test was performed on cells # 27, 18, 17, 19 and 21. Cell #27 failed during cell warm-up and prior to initiation of the test with a breached case. The remaining 5 cells survived the test with no adverse affects.

The cold test was performed on cell #'s 30, 33, 24 and 37. These four cells also survived the vibration and shock test at ambient temperature with no adverse effects.

This test verified the ruggedness of the NaS cell and confirms the launching an operating battery.

Shock and Vibration Test

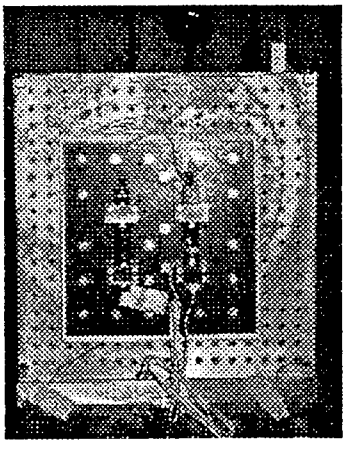

Vibration/Shock Mounting Fixture

Two cells are shown attached to the vibration/shock test fixture and mounted to the vibration table. For the hot test an oven enclosure was placed over the test fixture to heat the cells to operating temperature.

Cell Failure on Warm-up

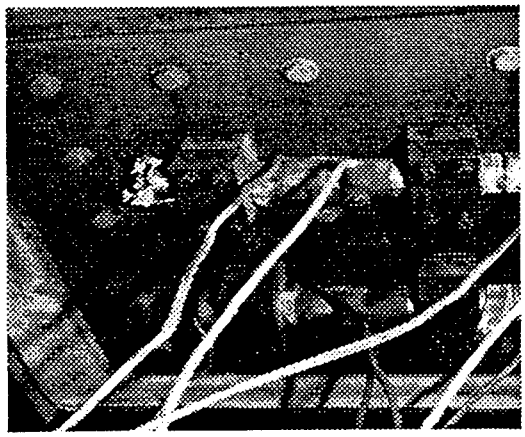

Shown is a photo of cell #27 which failed during the warm-up phase of a hot vibration/shock test. The cell breached at the cell base rupturing the cell case around the circumference of the base plate weld. Analysis of the cell to determine the cause of failure and cell breach is planned.

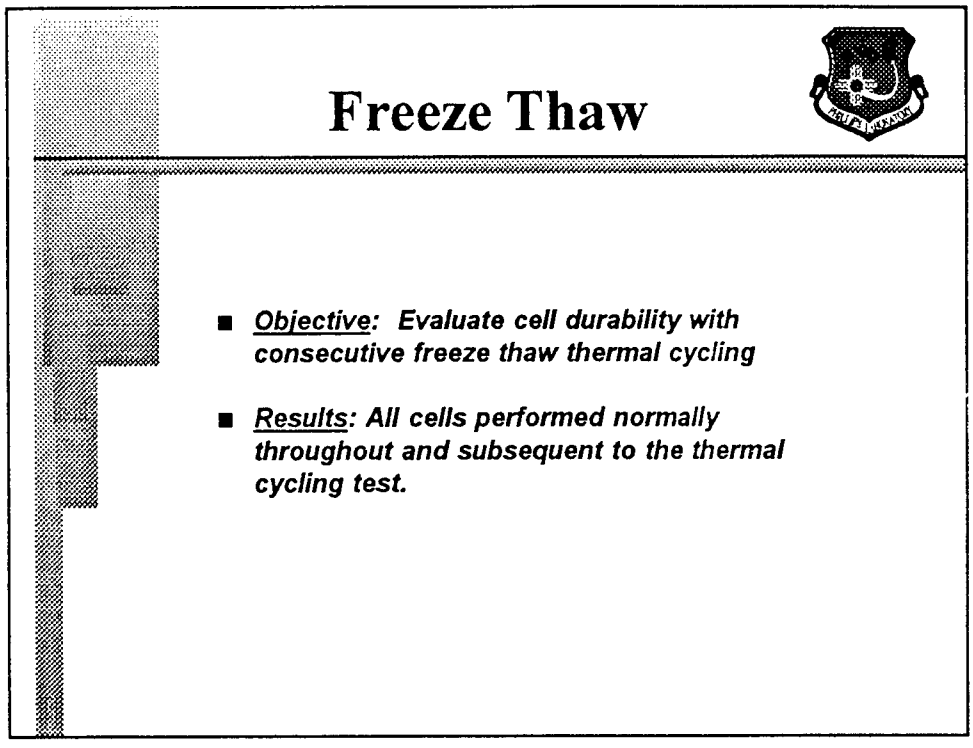

Cells tested included #12 and 20 at 100% SOC and #6 at 40% SOC. The cells were heated to an operating temperature of 350C by warming the cell from ambient to 85C at a rate of 25C per hour, then from 85C to 130C at a rate of 15C/hour and finally from 130C to 350C at a rate of 25C/hour. This warm-up procedure was followed for all cell tests.

Upon reaching operating temperature the two fully charged cells were subjected to a "GEO" electrical cycle consisting of a discharge at a C/4 rate to 40% state of charge followed by a five minute open circuit stand. The cells were then charged at a C/5 rate to a working voltage of 2.5V. Cooldown to ambient temperature was then done using the reverse of the warm-up procedure. This sequence was repeated a total of 10 times.

The 40% SOC cell was cycled five times using the preceding procedure with the addition of a C/4 discharge to 40% SOC at the end of the GEO cycle..

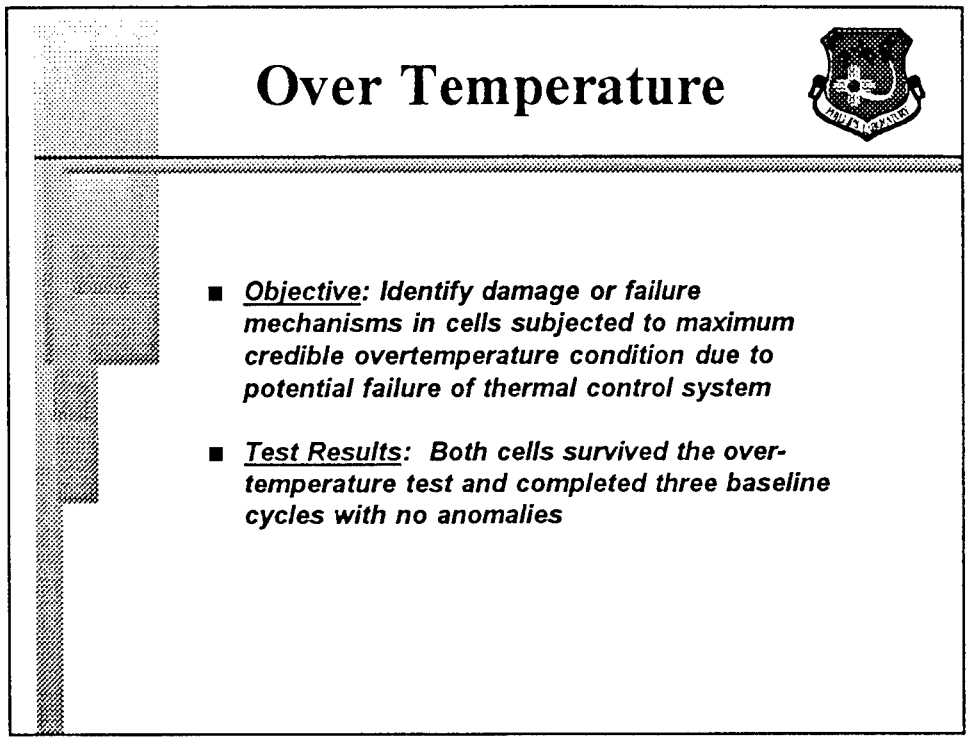

The selection of the maximum credible over temperature of 550C was based upon a thermal analysis indicating this to be the approximate maximum temperature a Sodium Sulfur battery could achieve given failure of the battery thermal control system with heaters on and radiator closed.

Two cells, #'s 17 and 21 were tested. After warming the cells to 350C three baseline capacity cycles were performed. This was followed by increasing the temperature to 550C followed by a two hour hold. The cell was then cooled to 350C. Three baseline capacity cycles were then performed. Each cell spent a total time of more than 8 hours at 500C or higher.

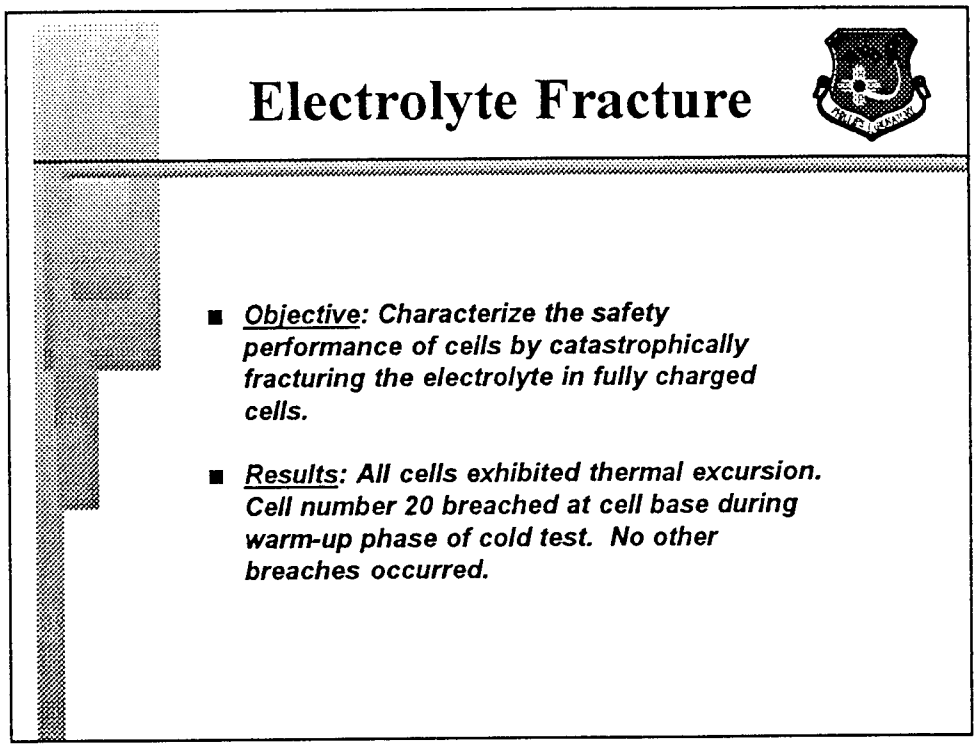

It is possible to catastrophically fail a fully charge Sodium Sulfur cell by subjecting to a high voltages which will fracture the Beta Alumina electrolyte. This method of fracturing the electrolyte was selected for the electrolyte fracture test in preference to mechanical techniques because it is more reproducible and avoids collateral damage to other cell components. It should be noted that in an operating battery it would not be possible to electrically fracture an electrolyte because the high voltages required could not be generated by the spacecraft electrical power system.

The electrolyte fracture test was performed on both cold and hot cells all fully charged. In the cold test cell #'s 15 and 20 were subjected to a constant current of 10A for 10 seconds. The cell temperature was then increased at 10C/Hr. Significant thermal excursion was noted but neither cell ruptured. Int he hot test cells #6, 8, 12, 22, 25, and 26 were brought to operating temperature then subjected to a 10A constant current for 30 seconds beyond cell failure. Cell #20 experienced a breach of the cell case at the base of the cell. No other breaches or ruptures occurred.

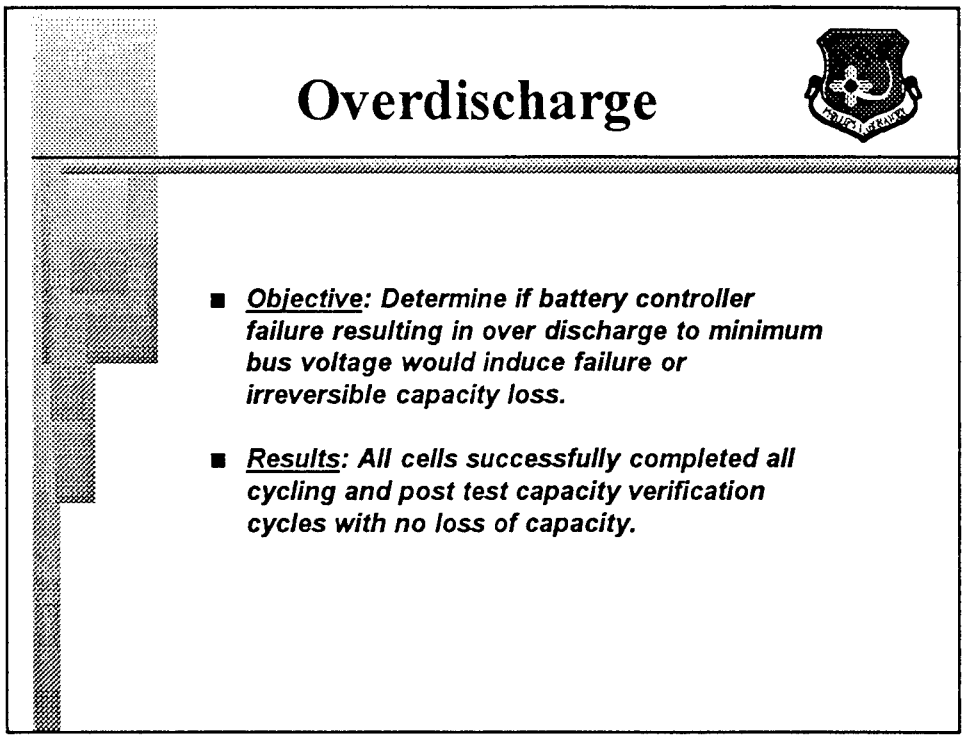

In the Over Discharge Test five cells, #'s 8, 15, 22, 25 and 26 were brought to operating temperature. Three baseline capacity cycles were performed. The cells were then discharged to a working voltage of 1.6 V in four sets of five cycles followed by two capacity verification cycles for a total of 20 discharge cycles and 8 capacity verification cycles. All cells successfully completed the test with no adverse affects.

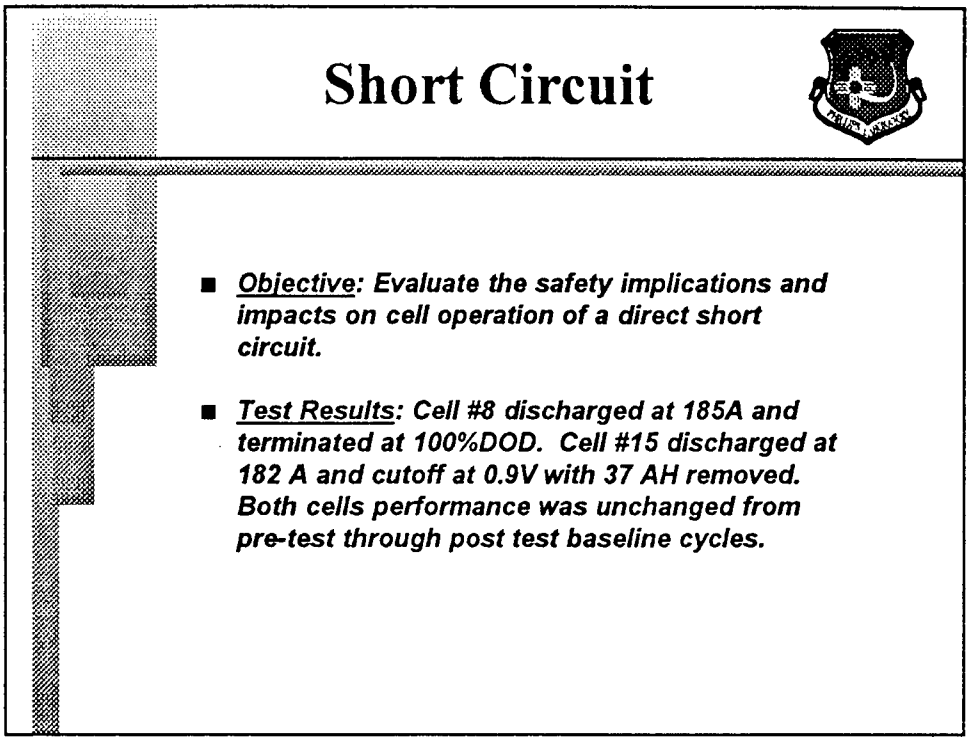

After warm-up to operating temperature and completion of 3 baseline capacity cycles the Short Circuit test was performed by discharging two cells (#'s 8 and 15) at maximum current (200 amp limit) to 100%DOD or until a working voltage of 0.9 V was attained. Cells were then left open circuit for 30 minutes followed by recharge at C/10 to 2.5V. This was followed with two baseline capacity cycles.

The test was designed to simulate the effects of a dead short on cell performance. Although a discharge limit of 200A was established for the experiment this limit was not achieved as internal cell impedance limited the maximum discharge rate for the two cells tested to 185 Amps and 182 Amps. Although a temperature rise was observed during the discharge there was no apparent adverse affect on these cells, each showing unchanged performance during the post test cycling.

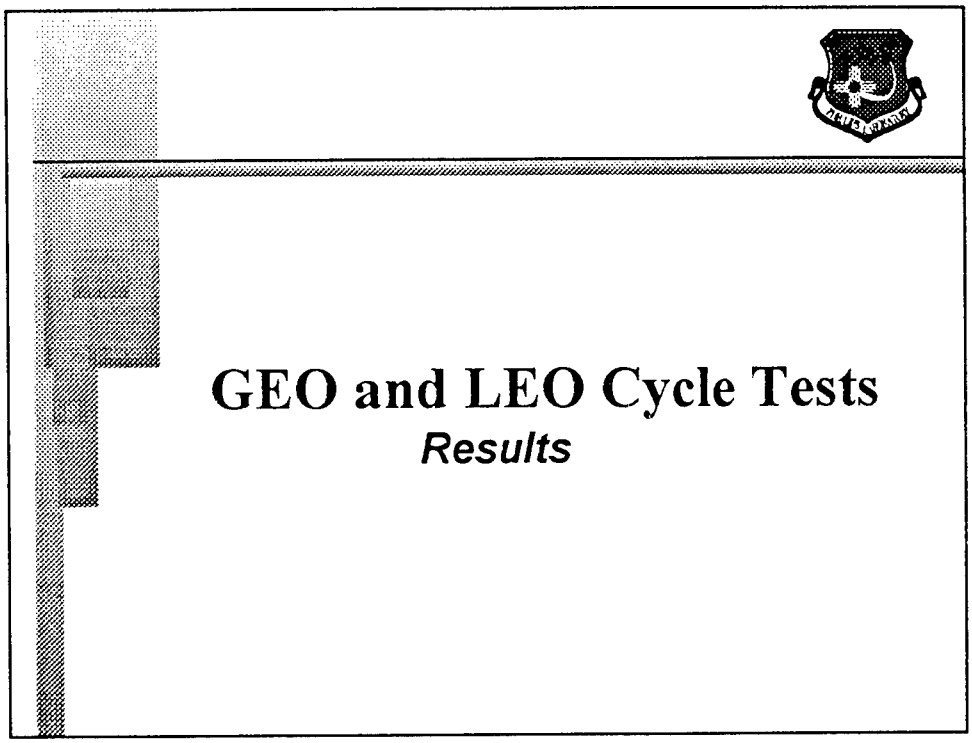
GEO and LEO Cycle Tests
Results

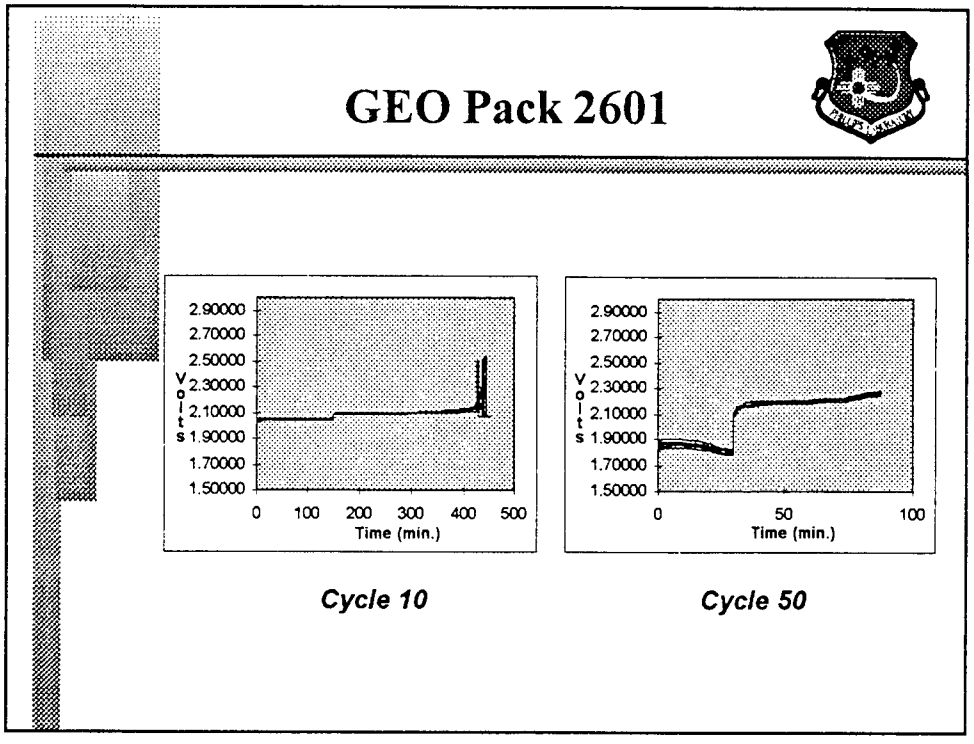

This slide shows cycle # 10 and Cycle #50 for the GEO cycling pack No. 2601. This test is a real-time GEO test. The variation in the charge discharge profile between cycle 10 and cycle 50 is due to the discharge occurring during a different point in the eclipse season (where the eclipse period is shorter than at cycle 10). As can be seen by the figures the voltage dispersion among cells is small and performance of all cells is excellent.

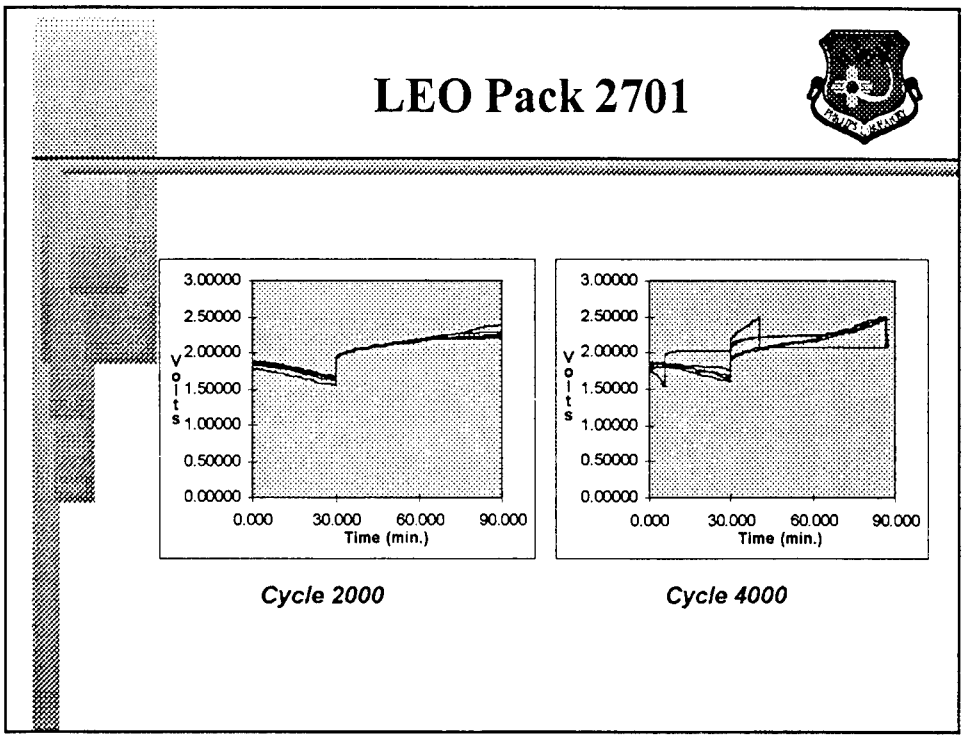

This slide shows a charge/discharge LEO cycle for each cell in pack 2701 at cycle 2000 and cycle 4201. At cycle 2000 charge and discharge control were being regulated using a pack average voltages. As illustrated in the cycle 4201 graph dispersion in cell voltages for both charge and discharge have increased and cell no. 9 reaches both charge and discharge cutoff voltages early in each portion of the cycle and is yielding and accepting less than 11 A-Hrs of charge. At cycle 3900 a decision was made to control charge and discharge for each cell individually rather than using pack average voltages. Prior to initiating this change in control three capacity verification cycles were performed beginning at cycle 3901. All cells yielded capacities greater than 40 A-Hrs with cell 9 having a capacity of 41 A-Hrs. This indicates the possible occurrence of recharge polarization in the test cells.

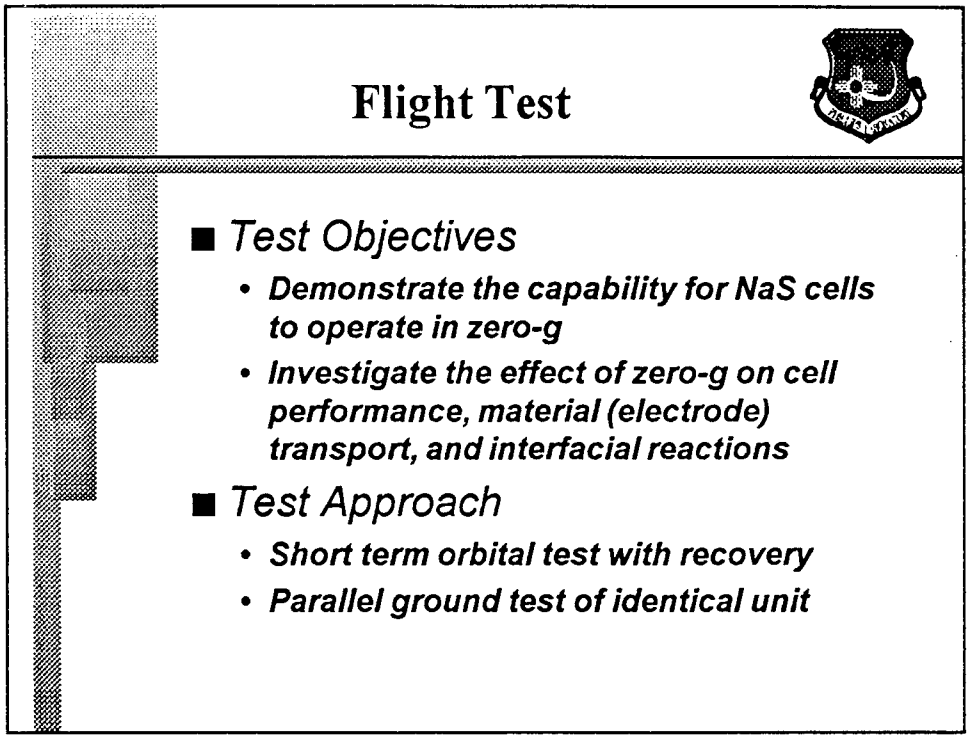

Since a sodium - sulfur battery uses liquid electrodes with a solid ceramic electrolyte the transport of electrode materials to the electrolyte surface is critical to performance. There is uncertainty as to how zero-g and the resulting absence of material convection may affect cell performance. The Sodium - Sulfur battery flight experiment will investigate the effects of zero - g on cell performance and increase understanding of material transport phenomena at the electrode - electrolyte interface.

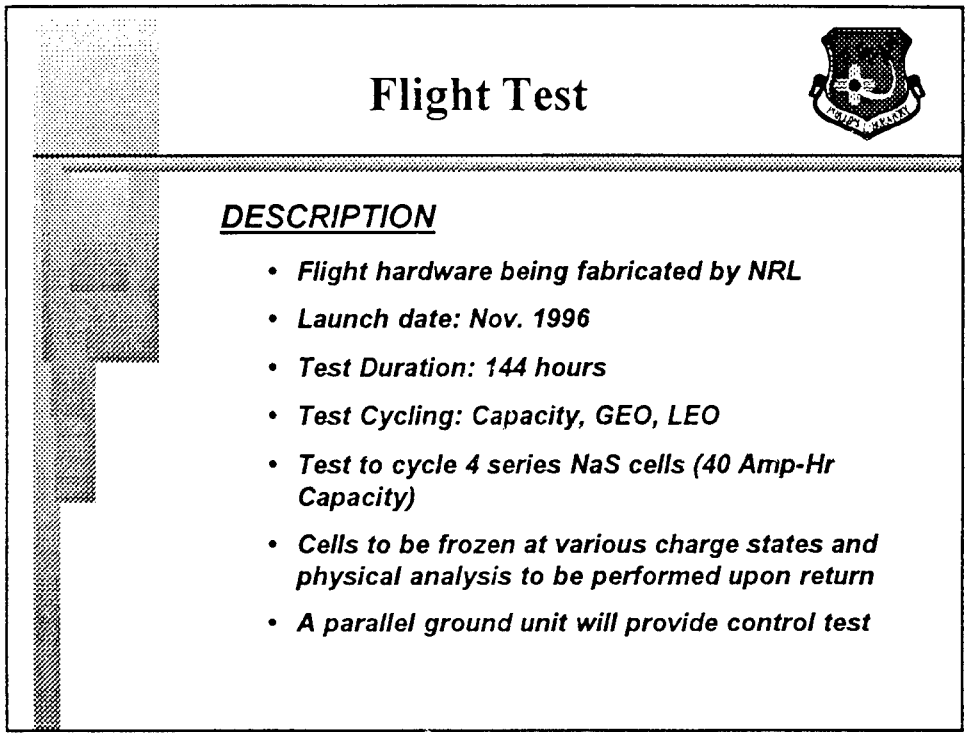

A parallel ground test using an identical setup will be operated by Phillips Laboratory in conjunction with the flight test. The ground test will duplicate conditions of the orbital test in every respect with the exception of the gravity environment and will serve as a control to assist in determining what, if any, effects zero-g has on cell operation.

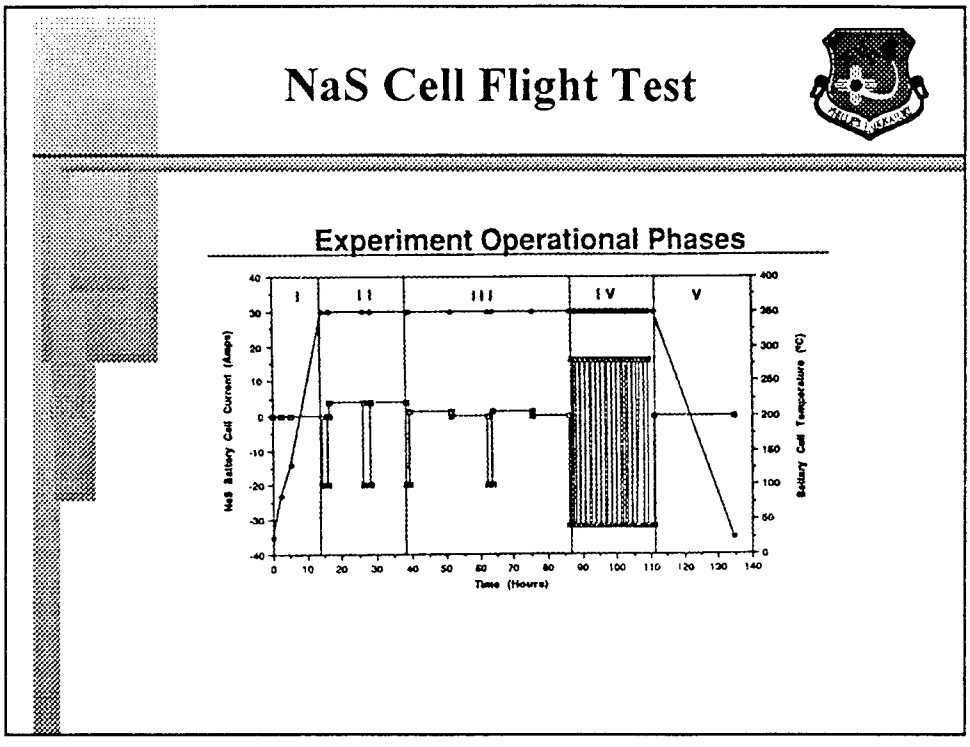

The flight experiment will fly in the Space Shuttle bay in a "Smart Can" provided by SII and attached to the Cross Bay Carrier for the Wake Shield Facility. Upon release of the Wake Shield the NaS experiment will be initiated with cell warm-up. After reaching operating temperature (350C) two conditioning cycles will be performed followed by 2 GEO cycles and 16 LEO cycles. After the final LEO cycle the four cells will be discharge to 100%, 80%, 60% and 40% SOC respectively and then cooled to ambient temperature for return.

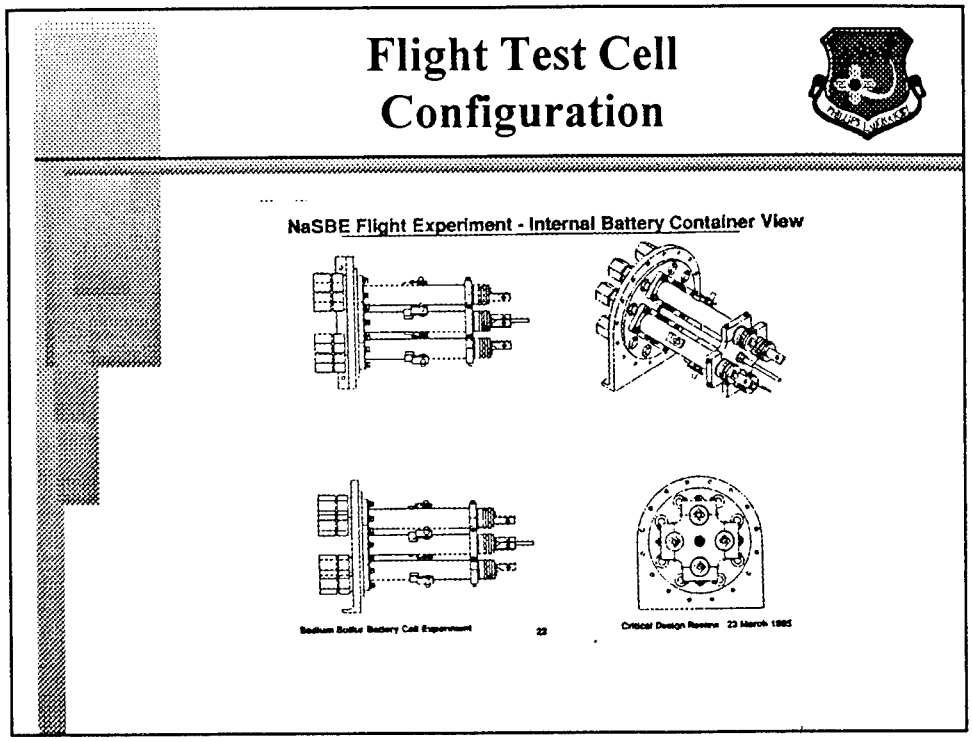

Flight hardware for the flight experiment is being designed and fabricated under the direction of the Phillips Laboratory by the Naval Research Laboratory. The experiment tests four 40A-Hr NaS cells wired in a series circuit and configured as shown in the illustration.

The experiment has been designed to fail safe. The flight container will hermetically contain all cell materials in the event of a worst case failure scenario wherein all four cells would simultaneously fail at full charge, breach and react all active materials.

Summary

- *The Phillips Laboratory has conducted and is continuing a test program to complete evaluation and development of NaS batteries and enable transition of the technology to users.*
- *Flight test of a NaS battery module is planned and is essential to verify zero-g operational capability.*
- *Results of Safety and Abuse Test to date confirm the capability of NaS to meet spacecraft operational and safety requirements and to launch with operating battery.*
- *Investigation of two breaches is underway to determine cause and to recommend, if necessary, design changes to prevent any worst case cell breaches.*
- *Causes of possible cell polarization in LEO cycling are being investigated.*

Management and Problem Resolution of On-orbit Spacecraft Batteries Focused Session

SKYNET 4A

BATTERY PERFORMANCE OF THE SKYNET 4A SPACECRAFT DURING THE FIRST SIX YEARS OF ON STATION OPERATION

P. J. JOHNSON and N. R. FRANCIS

MATRA MARCONI SPACE UK LTD.,
GUNNELS WOOD ROAD, STEVENAGE,
HERTFORDSHIRE, SG1 2AS.
ENGLAND.

MATRA MARCONI SPACE

Abstract.

The SKYNET 4A spacecraft is a three-axis stabilised geostationary earth-orbiting military communications satellite which was launched on 1st January 1990 aboard a Titan III launch vehicle. The power subsystem is a twin bus, twin battery semi-regulated system and is equipped with one 28-cell, 35 Ampère-hour battery per bus. The cells were manufactured by Gates Aerospace Batteries of Gainesville, FL., and the batteries were built, tested and integrated by British Aerospace Space Systems Ltd.

This paper presents a brief survey of the first six years of on-station operation and the operational battery management strategy that has been adopted. Thermal management constraints have led to an unconventional battery operational regime. However, no sign of degradation is evident and the observed spacecraft battery performance remains nominal.

SPACECRAFT IN ORBIT VIEW

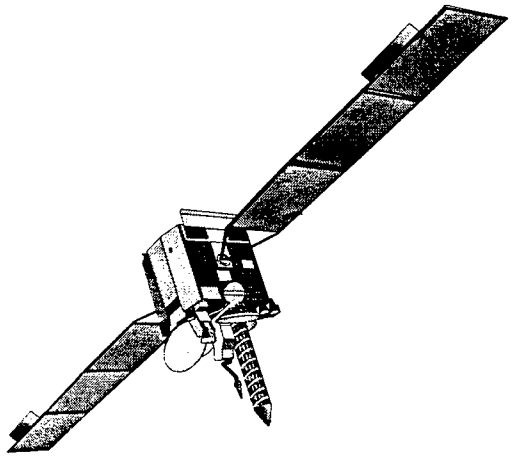

MATRA MARCONI SPACE

Introduction.

The SKYNET 4A spacecraft is one of a series of military satellites that provide flexible tactical communications for maritime and land forces and strategic communications. It was designed, built, integrated and tested by British Aerospace Space Systems Limited (now part of Matra Marconi Space UK Limited). It is a three-axis stabilised geostationary satellite which was launched on 1st January 1990 aboard a Titan III launch vehicle and is now positioned at longitude 34° W. A view of the spacecraft as it would appear in orbit is given above.

BLOCK DIAGRAM FOR THE POWER SUBSYSTEM

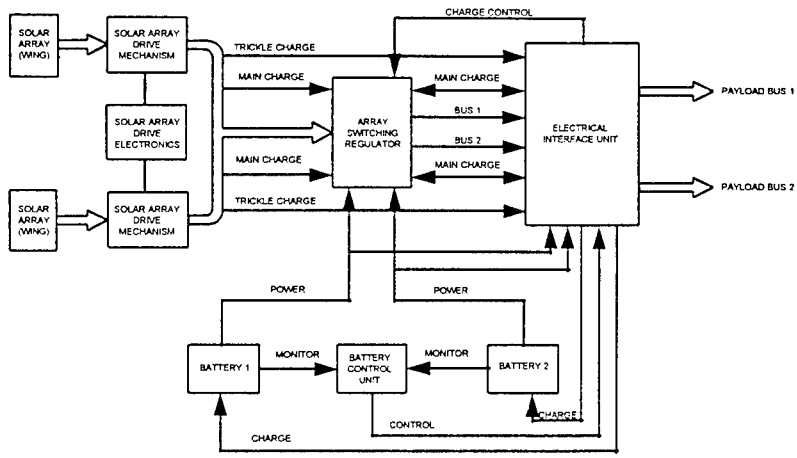

MATRA MARCONI SPACE

The power subsystem provides electrical power to the spacecraft subsystems and payload for all phases of the mission. The power supply is regulated in sunlight, unregulated in eclipse. A functional block diagram of the Power Subsystem (PSS) is shown above. The PSS may be described as a twin bus, twin battery, semi-regulated system. The power is generated from silicon n-on-p solar cells which are mounted on two solar array wings, each wing consisting of three panels. The solar array wings are independently steered about the pitch axis to stay pointing at the sun.

During periods when solar power is not available the satellite is powered from energy stored in the two nickel-cadmium batteries. The batteries are recharged in sunlight from dedicated solar array sections. Each battery consists of 28 cells to provide a supply voltage of nominally 29.6 V to 43 V at the PSS output interface.

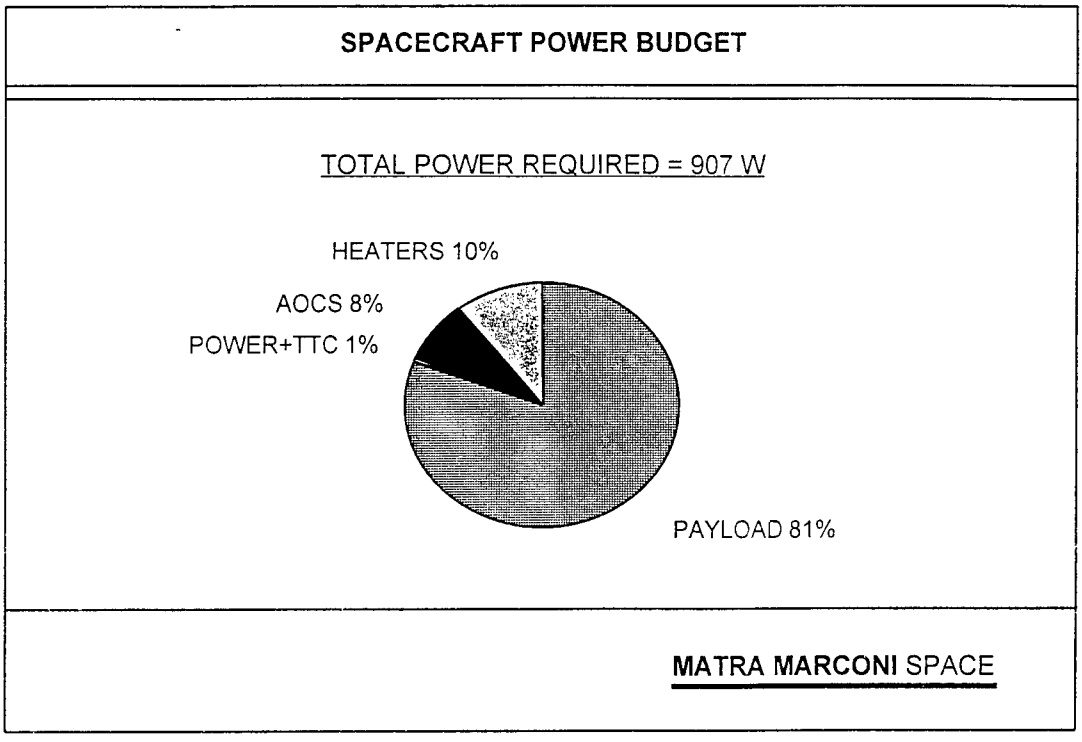

Battery Design.

From the manufacturers' estimates of their equipments' power requirements the total power budget, shown above, was derived. The total power requirement during the eclipse seasons for this mission is 907 W. At an average battery terminal voltage of 33.6 V (28 cells at 1.2 V per cell) and allowing for a one volt drop across the battery diodes and also for a possible maximum imbalance between the two buses of 5% then each battery may be required to deliver, during the peak eclipse period of 72 minutes:

$$907 \text{ W} \div 2 \times 1.05 \div (33.6 - 1) \text{ V} \times 1.2 \text{ h} = 17.5 \text{ Ah}$$

Setting the limit to depth of discharge at 50%, a battery of nameplate capacity 35 Ah was thus identified for this mission.

BASIC CELL PARAMETERS OF THE FLIGHT LOTS

	BATTERY 1 LOT 6	BATTERY 2 LOT 7
Negative Sinter Date	February 1985	March 1985
Positive Sinter Date	June 1985	June 1986
Electrolyte Fill Date	January 1987	January 1988
Electrolyte Quantity /cm^3	81.5	77. 0
Positive Plate Porosity	34.95 %	30.70 %
Negative Plate Porosity	31.10 %	28.90 %
Overcharge Protection / Ah	18.34	19.00
Separator	2536	2536

MATRA MARCONI SPACE

Cell Procurement.

Each battery consists of 28 nickel-cadmium cells of nameplate capacity 35 Ah manufactured by Gates Aerospace Batteries and having the designation 42B035AB03. Lot 6 of these cells was used for spacecraft battery number 1 and lot 7 cells was used for battery 2. Both lots used Pellon 2536 separator. The above table lists some of the fundamental statistics for these lots. The procurement specification for these cells was based on the NASA standard [1], except that the positive plaques were hot-gas passivated and the negative plates were silver treated. These plates were manufactured at a time when many of the manufacturer's customers were having extensive problems with these products. These events have been described in detail by Ford *et al.*[2].

Note that although the electrolyte fill quantity differs by 5%, a fill index of 0.78 was used on both lots. The difference in quantity was attributed to the differences in the porosities of the plates.

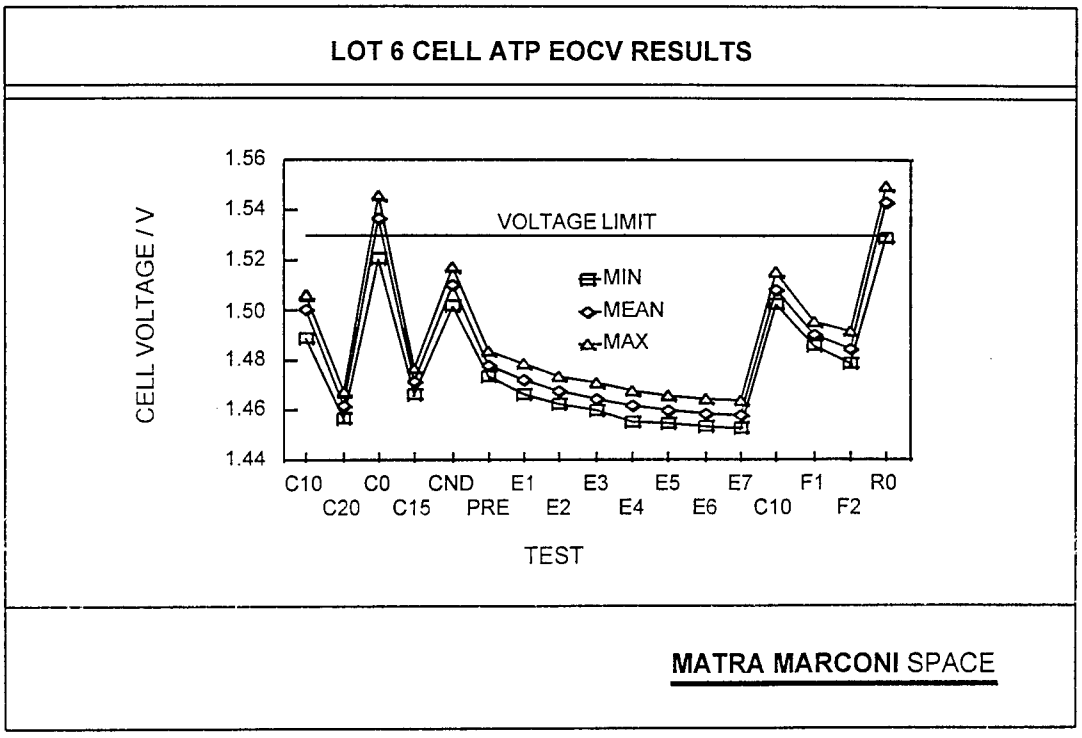

The cells were subjected to an Acceptance Test Procedure (ATP) which consisted of capacity tests at 20, 15, 10 and 0°C (C20, C15, C10, and C0), and a voltage rise test. The cells passed all these tests with the exception of lot 6 which went over voltage on the charge phase of the 0°C capacity test. The end of charge voltages (EOCV) throughout ATP testing are given in the above graph. Following the capacity tests, the cells were subjected to a conditioning cycle (CND) and then a sequence of seven exercise cycles (E1 to E7), a reference capacity test (C10) and two fade cycles (F1 and F2). The 0°C capacity test was then repeated (R0), and again the voltage limit was exceeded. Of the 68 cells tested, 63 cells exceeded the specification of 1.53 V and five cells were removed from test when their voltages reached 1.55 V. At the time, a gradual upward trend in end of charge voltages from this manufacturer's products had been observed, although no explanation was offered. Furthermore, the high thermal mass of the cell clamps and the excellent thermal path to the controlling cold plate of the thermal chamber held the cells close to the set temperature. During battery test and in orbit operations the cell temperatures were expected to rise towards the end of the charge phase, resulting in lower end of charge voltages than experienced in the cell level ATP. Thus lot 6 was considered "Acceptable as is".

BATTERY LEVEL ATP RESULTS

TEST	LOT 7 /Ah	LOT 6 /Ah	DIFFERENCE /Ah
Wake-up 1	39.02	38.93	-0.09
Wake-up 2	35.56	35.61	+0.05
-5°C Capacity	35.59	34.64	-0.95
0°C Capacity	34.80	34.97	+0.17
0°C Retest	36.80		
10°C Capacity (pre-environmental)	37.90	38.03	+0.13
10°C Capacity (post environmental)	38.29	37.48	-0.81
25°C Capacity	36.27	37.25	+0.98

MATRA MARCONI SPACE

Battery Build and Test.

Each battery consists of two series connected 14-cell half packs. The cells are stacked across their width to form a single line of cells. The cells are mounted on their sides with the terminals all along one side.

The results of the capacity tests performed during battery ATP are summarised in the table. Although lot 7 failed the 0°C capacity test it passed the subsequent retest. The lot 6 battery also failed the 0°C test but the margin of 0.03 Ah was within the measurement error and so no retest was considered necessary.

BATTERY POSITIONS WITHIN THE SPACECRAFT

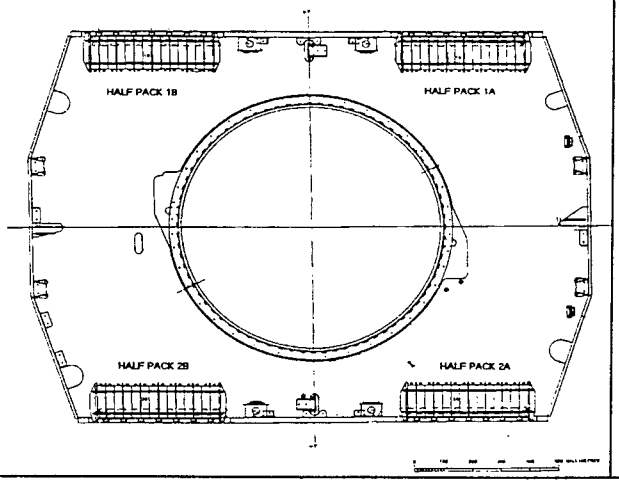

MATRA MARCONI SPACE

The battery half-packs were integrated into the spacecraft and the position of each battery is as follows:

Battery 1A	+Y (S)	-X (W)
Battery 1B	+Y (S)	+X (E)
Battery 2A	-Y (N)	-X (W)
Battery 2B	-Y (N)	+X (E)

Thus each battery is bolted to one of the Y-walls, and each half pack is located at either end of that wall as shown in the drawing above. This configuration means that battery 1 will be on the sun side (and therefore warmer) during winter and battery 2 will be on the sun side during the summer.

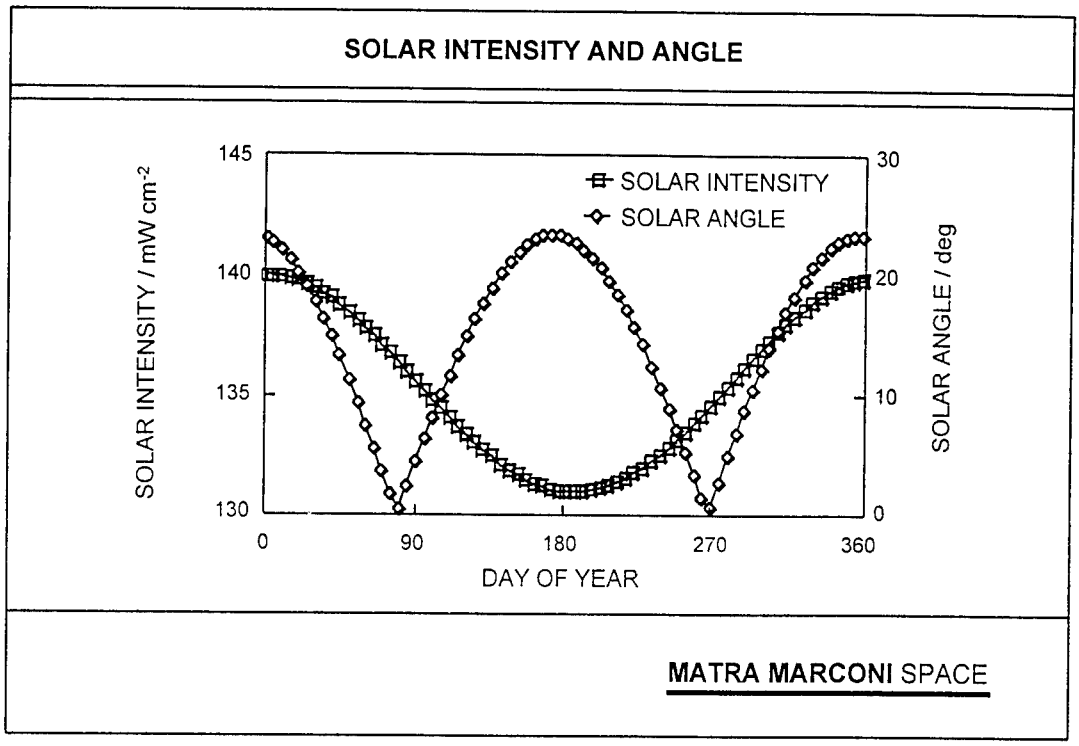

Solar Arrays.

Each solar array wing consists of three panels. It was a design goal that these panels should be identical and interchangeable. Only one size of solar cell was used. These cells were laid down as follows (per wing):

6 Sections of 7 strings for Main Power,
2 Trickle-Charge Sections of 1 string each,
1 Main Charge Section of 4 strings.

A string consists of 130 cells connected in series, giving a total of 12480 cells for the complete array. Selecting the cell size was a compromise between minimising the number of cells and keeping the trickle-charge current within acceptable limits.

With dedicated charge strings the charge and trickle-charge rates will vary throughout the year as functions of sun-earth distance and solar declination. The above figure shows the variation of solar intensity and the apparent declination angle throughout this year (this figure was compiled from the data contained in Reference [3]).

VARIATION OF SOLAR ARRAY POWER THROUGHOUT THE YEAR

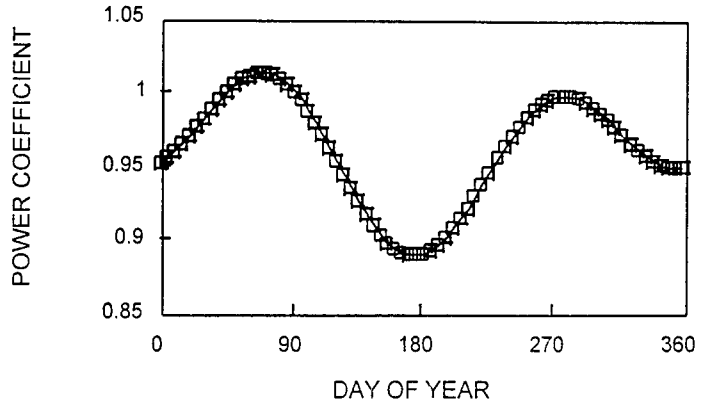

MATRA MARCONI SPACE

These two parameters combine to give the power coefficient for the solar arrays, shown above. The arrays also degrade with life. As an example, consider the trickle charge current. For a power coefficient of unity, the trickle charge current is estimated by the solar cell manufacturer to be 447 mA at beginning of life, degrading to 341 mA at the end of the seven year mission, giving a nominal value of 350 mA which corresponds to a rate of C/100. Accordingly, charge and trickle-charge currents, confirmed by telemetry, are predictable throughout the spacecraft lifetime.

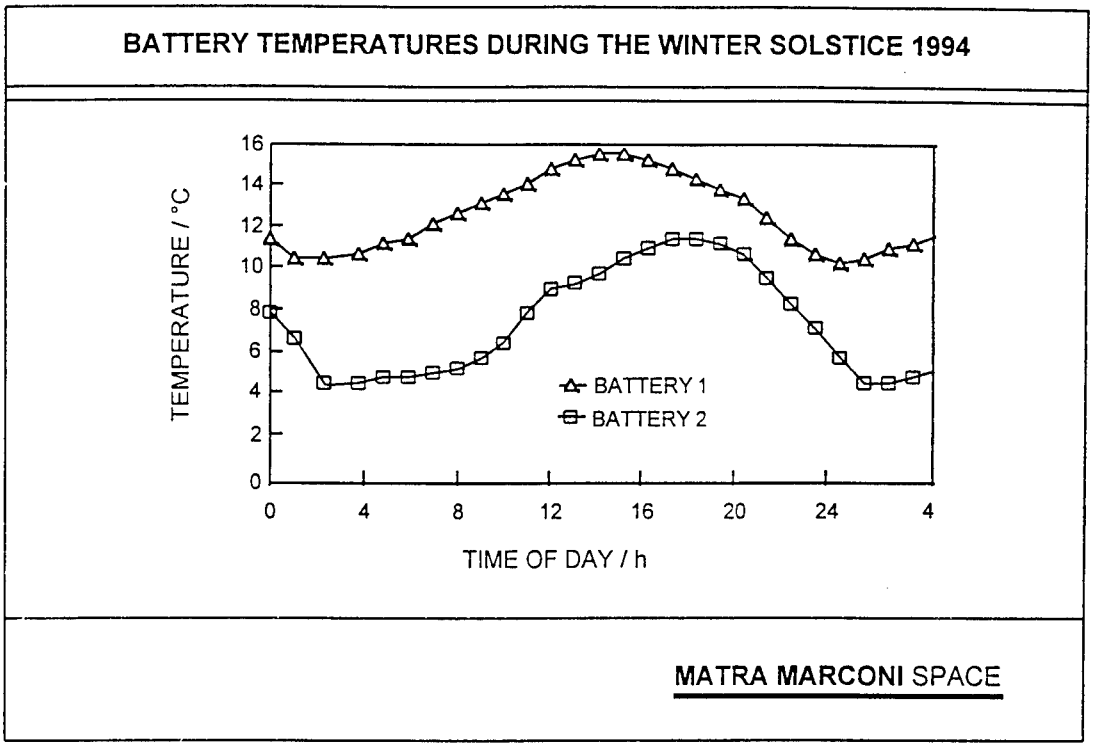

Battery Performance.

1. Solstice.

During the solstices, one battery is on the spacecraft wall facing the sun and the other battery is on the dark side of the satellite. Consider the winter solstice. The +Y wall of the spacecraft is facing the sun and so battery 1 will be expected to be the warmer of the two. Furthermore, from the graph of solar intensity it can be seen that the solar intensity is at a maximum at this time of the year. The above figure shows the thermal variation during the day for both batteries in the winter solstice. To maintain the batteries below the upper limit of 15°C trickle-charge for battery 1 was switched off by ground command from 13h00 to 23h15z. (At the position of 34° W spacecraft midday occurs at 14h16z). Trickle-charge is re-enabled at 23h15z providing that the average battery temperature is less than 15°C. If it is not, then trickle-charge is left disabled for a further 24 hours until 23h15z on the following day. The thermal behaviour of battery 2 during the same time frame is also shown in the figure. As this battery is on the cooler side of the spacecraft, interruption of the trickle-charge current is not necessary. However, this battery is still subject to daily thermal variations similar to those seen for battery 1.

BATTERY TEMPERATURES DURING THE SUMMER SOLSTICE 1995

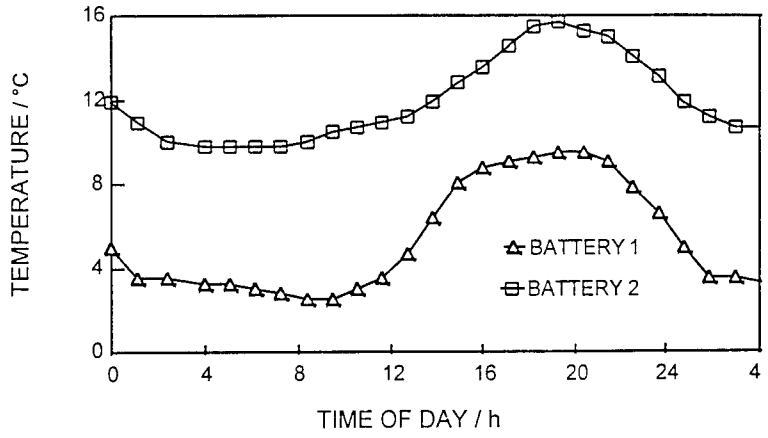

MATRA MARCONI SPACE

The pattern is repeated to a similar extent during the summer solstice, although the effect is less severe due to the lower solar intensity. Battery 1 is now on the cooler side of the spacecraft and it is no longer necessary to interrupt its trickle-charge. The temperatures of the two batteries during the day in summer solstice is shown above.

DURATION OF THE PERIODS WITH THE BATTERY OPEN-CIRCUIT

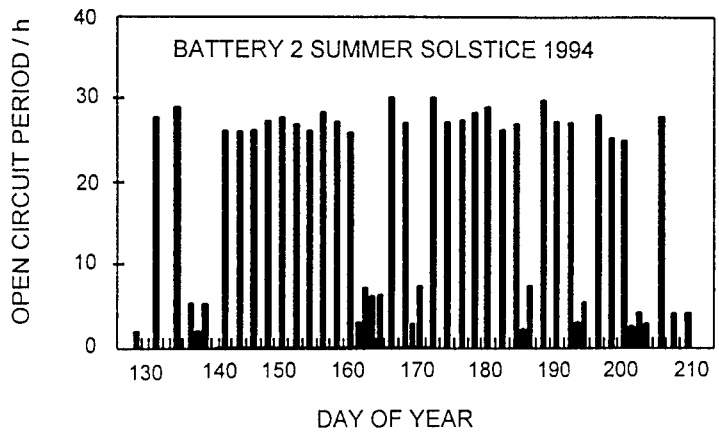

MATRA MARCONI SPACE

Interruption of trickle charge takes place over an eighty day period in summer solstice and a ninety day period in winter. The period of interruption for battery 2 during the 1994 Summer solstice is shown in the figure as an example. With the switching philosophy that has been adopted, the result is that trickle charge is disabled for approximately 24 hours in every 48 hour period for the battery which is on the sunny side of the spacecraft.

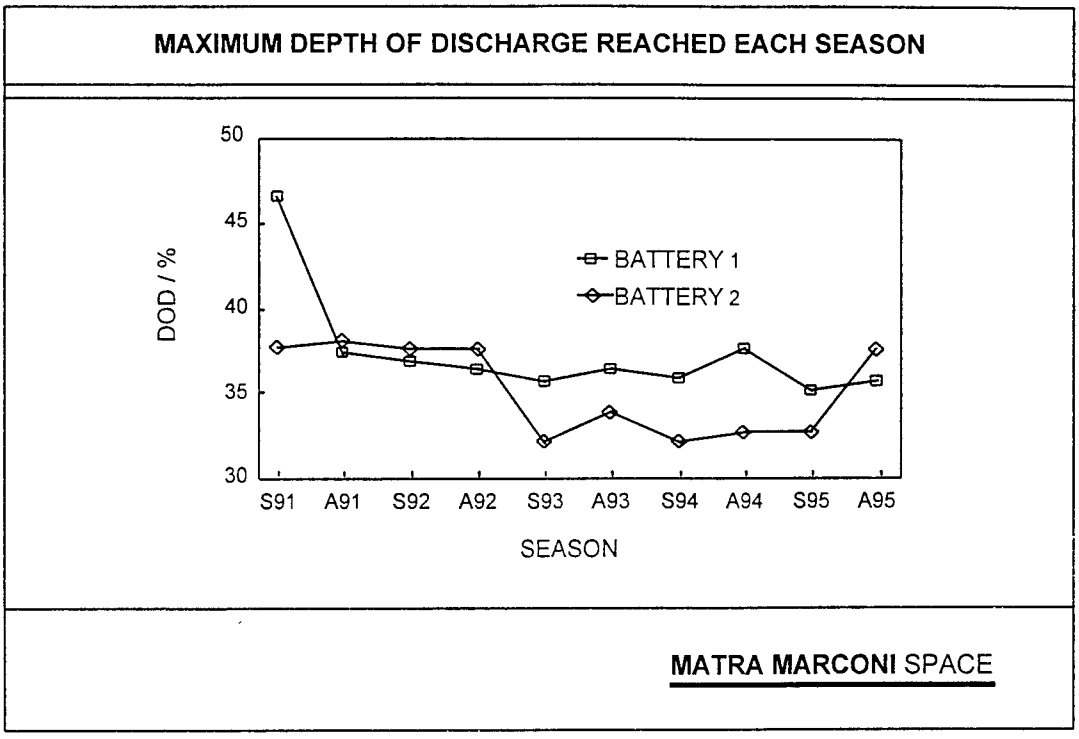

2. Eclipse.

The figure shows the maximum depth of discharge for each battery during the eclipse seasons. After the in-orbit test phase, the depth of discharge has stabilised at ~36% for battery 1 and was ~33% for battery 2, but following a payload reconfiguration it is now ~38%, still significantly lower than the design limit of 50%.

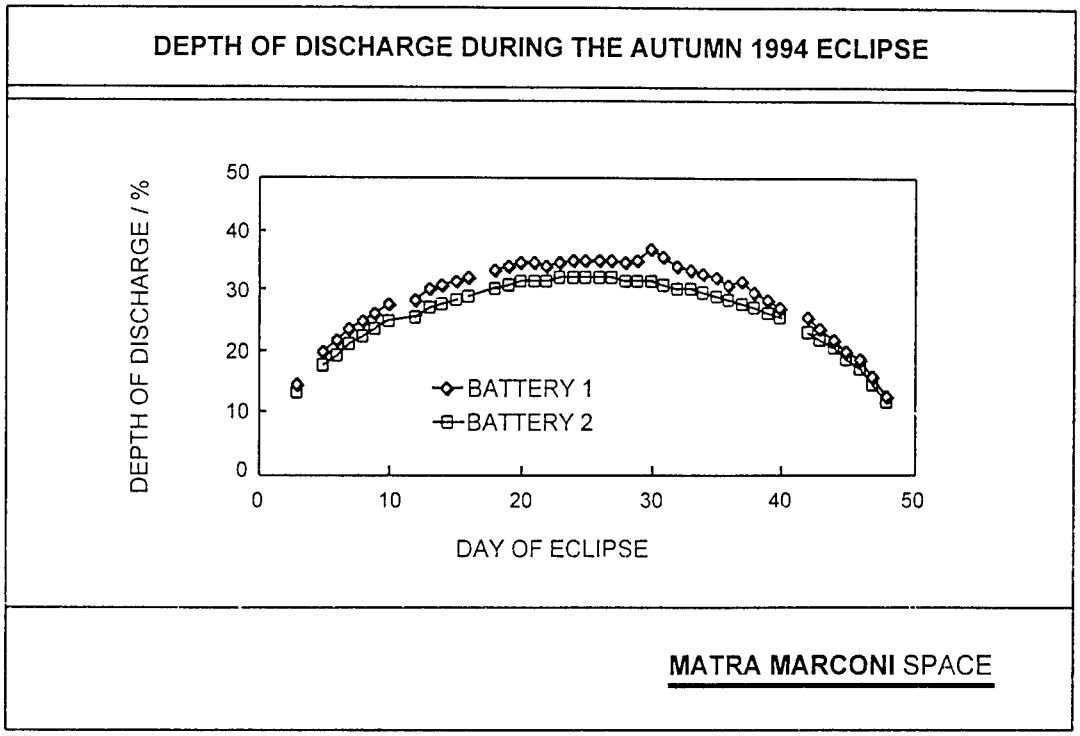

The figure shows the depth of discharge profile throughout the Autumn 1994 eclipse season. Peak depth of discharge for battery 1 was 37.6%, and on average the loading on battery 2 was 10.2% less than that for battery 1. Thus battery 2 will reach top of charge first and will terminate main charge both batteries, and battery 1 will continue charging on trickle-charge alone.

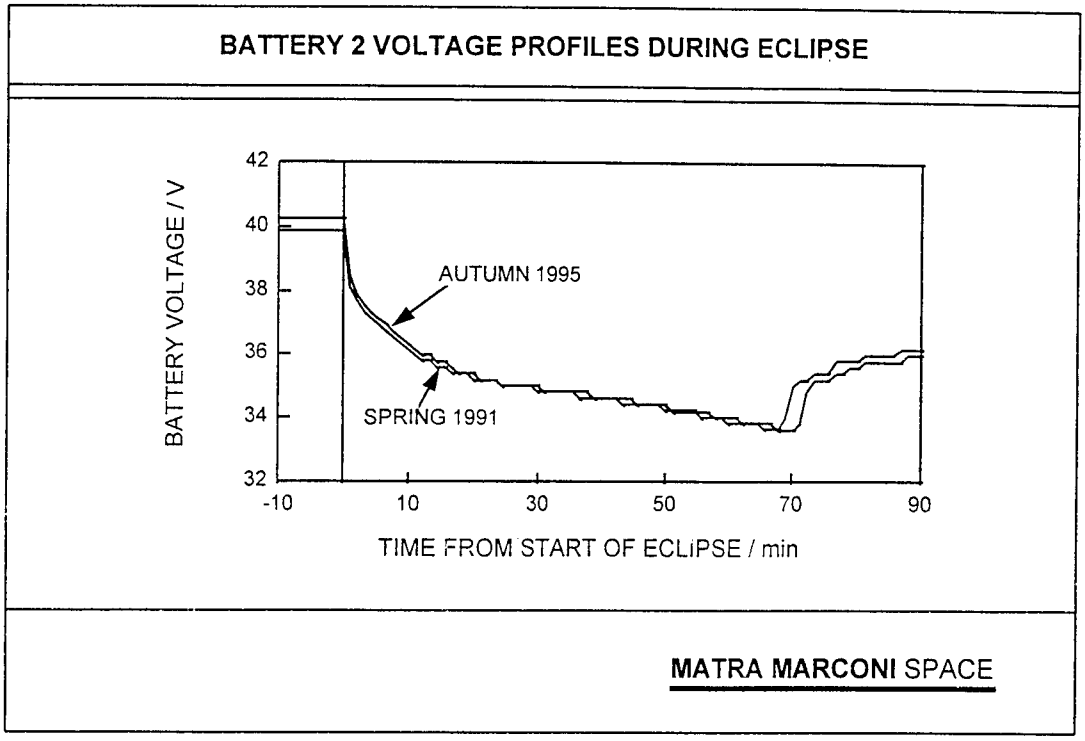

The above figure shows the discharge profile for the batteries during the longest day of the Autumn 1995 eclipse season. Also shown for comparison is the discharge profile from the Spring 1991 season. Apart from the small difference in eclipse duration, these discharge profiles are indistinguishable.

CHARGE TERMINATION CRITERIA

1. End of charge voltage trip level is reached,
2. Battery upper temperature limit is indicated by any thermistor, presently set at 21°C,
3. Average temperature of either battery reaches 15°C,
4. Rate of temperature rise exceeds 1°C in 15 minutes,
5. The charge input exceeds 1.05 times the charge withdrawn during the preceding eclipse.

MATRA MARCONI SPACE

Termination of main charge occurs when any one of the above criteria is met: Criteria 1 and 2, on either battery, lead to automatic charge termination for both batteries, while items 3, 4 and 5 require ground intervention. On Skynet 4A, the end of charge limit is set to 41.4V (equivalent to 1.48 volts per cell). This results in semi-autonomous charge termination throughout the eclipse season.

BATTERY RECHARGE FACTOR THROUGHOUT THE AUTUMN 1994 SEASON

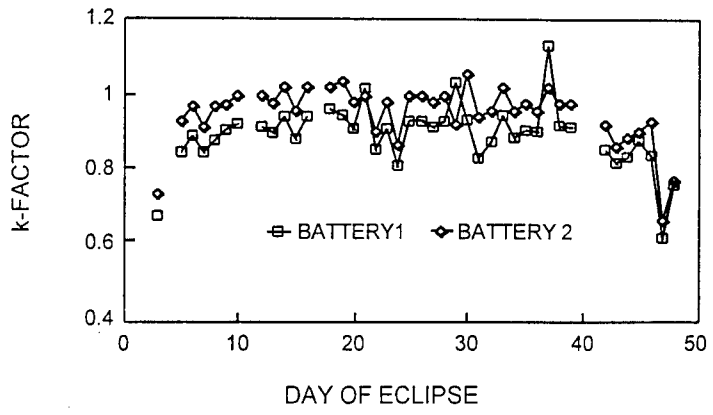

MATRA MARCONI SPACE

The ratio of charge returned to charge extracted, the k-factor, is shown above for the Autumn 1994 season. The average k-factor for battery 1 was 0.88 and for battery 2 it was 0.94. As bus 2 was less heavily loaded than bus 1 at that time, battery 2 reached the end of charge voltage limit first and terminated main charge for both batteries. The longest charge period with the available main charge current was ~8 hours, leaving in excess of 14 hours when the batteries are on trickle charge. Consequently, upwards of 5 Ah are available each day as "top-up" charge. Thus as long as the observed k-factor exceeds 0.8 no ground intervention is deemed necessary. Furthermore, for any eclipses less than 25 minutes' duration the batteries are recharged by trickle-charge alone. This occurred three times during the Autumn 1994 season, on 29th and 30th August and on 16th October.

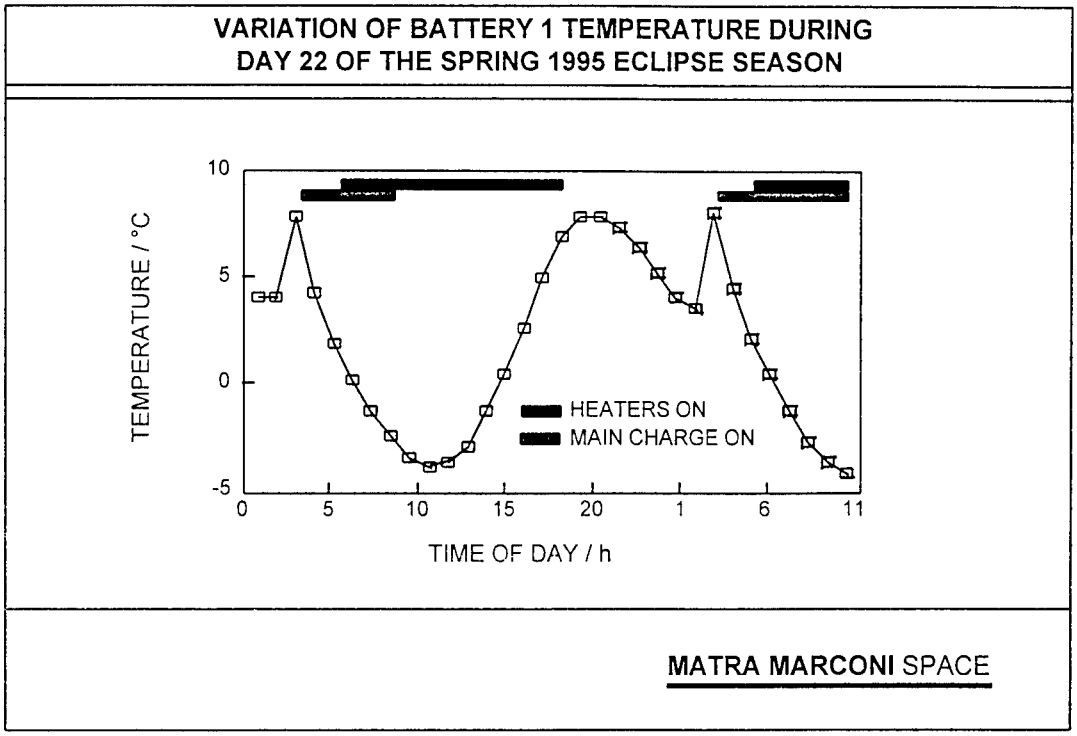

The figure shows the variation of the battery temperatures during a day in the eclipse season. At the end of the eclipse main charge is enabled and the battery begins to cool both by radiation and due to the endothermic effect of the recharge reaction. Note that the temperature at the end of the main charge phase is -0.8°C, and recall that the lot 6 cells failed the 0°C capacity test during cell ATP by exceeding the voltage limit on charge. This may explain the low k-factors observed as the voltage limit is being reached earlier than expected. The disposition of the ATP anomaly that the battery would not be close to 0°C at the end of the charge phase in orbit is clearly erroneous. Each battery half-pack has a main heater of 5.5 W and an adjustment heater of 3.2 W (the adjustment heater may be used to keep the temperatures of the two half-packs within 6°C of each other; however on this mission it has not been necessary to use this facility.) The main heater switches on when the battery temperature falls below 4°C. The temperature of the battery begins to rise as top of charge is approached. When full charge is reached (as indicated when any of the above criteria on either battery is satisfied) the battery is switched onto trickle-charge. The heater turns off when its temperature exceeds 8.5°C. The battery cools prior to the next eclipse when it will warm up again during the discharge phase, and then the sequence of events repeats itself.

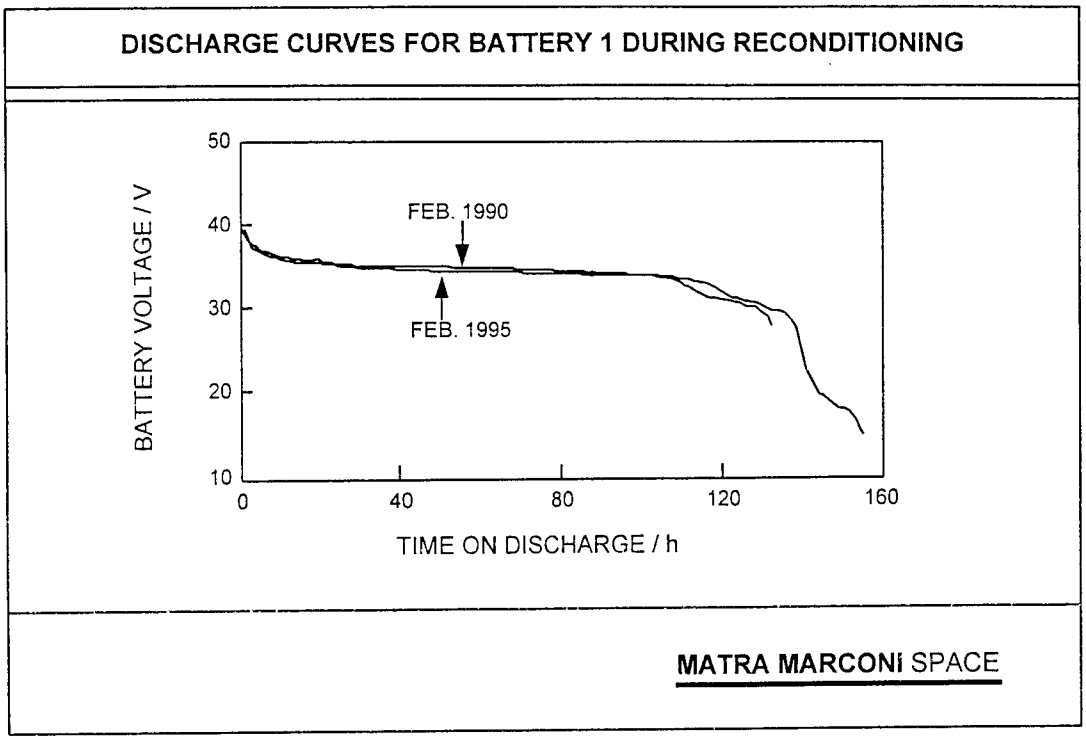

3. Reconditioning.

Both batteries are reconditioned consecutively prior to each eclipse season. The battery is discharged through a 102.5 Ω load resistor until the first cell reaches 400 mV or until all cells in the battery are less than 600 mV. Although it may be preferable to terminate the discharge when the first cell (for example) reaches 100 mV, ground station availability and "down-time" have to be taken into account when setting an end of discharge limit. Allowing for a maximum down-time of 30 minutes, 400 mV is considered a safe voltage level where a further 30 minutes of discharge would not lead to reversal.

The battery discharge profile during reconditioning is shown above. A second voltage plateau is just evident immediately before the termination of discharge, indicating that the battery cells are positive limited. Also shown for comparison is the discharge curve from the first reconditioning performed soon after the spacecraft was on station in February 1990. While the average battery discharge voltage has fallen by 100 mV, implying a rise in the internal resistance of the battery of the order of 7%, the capacity to 28V (equivalent to 1V per cell) has increased by 1.4 Ah over the five year period. Both these effects are attributed to normal electrolyte redistribution during lifetime.

BATTERY 1 TEMPERATURES DURING RECONDITIONING DISCHARGE

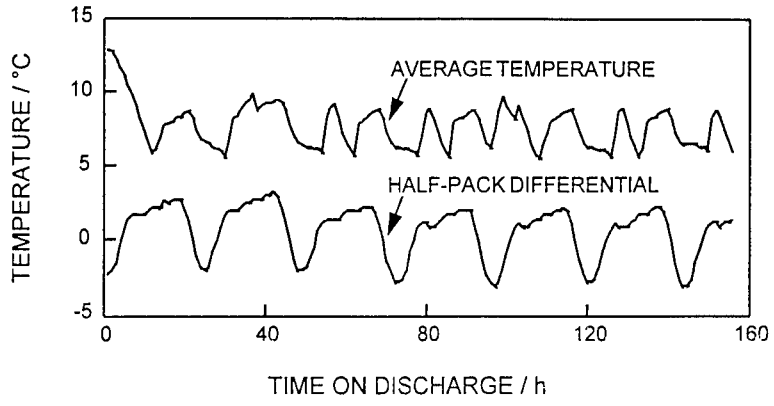

MATRA MARCONI SPACE

During the reconditioning process daily temperature cycling still occurs and this is illustrated above. With no trickle-charge to warm the battery the heaters come into use, adding to the cyclic thermal variation of the batteries. It can also be seen that the temperature between the two half-packs of the battery varies on a daily basis.

CAPACITY RETURNED DURING RECONDITIONING BEFORE EACH ECLIPSE SEASON.

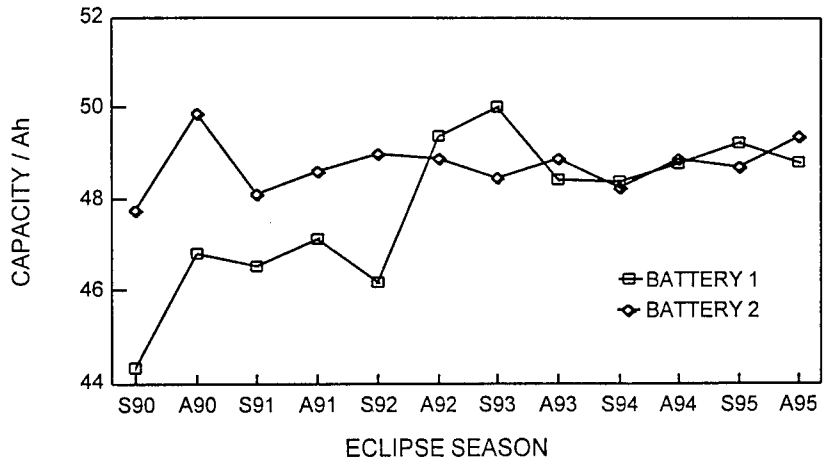

MATRA MARCONI SPACE

This figure shows the capacity delivered by the batteries during each reconditioning cycle so far performed. The 35AB03 cells used in these batteries had positive plates loaded with 12.65 ± 0.6 g dm^{-2} of active material. This leads to a theoretical capacity of 48.4 Ah (on average) for these batteries. The capacity returned during reconditioning therefore suggests that the positive plates are still fully electrochemically active.

BATTERY MANAGEMENT STRATEGY

1. The battery temperatures are strictly maintained below 15°C,
2. Overcharge is limited in eclipse by having a k-factor of less than unity,
3. Overcharge is limited in the hotter solstice by having trickle-charge enabled for only 50% of the time,
4. The depth of discharge is well within the design limit of 50%, only 33-38% has been seen since the completion of the in-orbit test programme.

MATRA MARCONI SPACE

Conclusions.

Limiting the upper operational battery temperature has been the overriding criterion in the battery management strategy. In order to achieve this it has been necessary to disable trickle-charge for periods of up to 30 hours in any given 48 hour period for the battery which is on the sun facing side of the spacecraft. This toggling of trickle-charge, along with the daily temperature variations appear to have no adverse effects on the in-orbit performance of the batteries. Indeed, the adopted battery management strategy, summarised above, may be beneficial as resistance rise has been less than expected and there is no evidence of capacity fading. There has therefore been no apparent negative effects of the open circuit stands or the thermal cycling on performance.

ACKNOWLEDGEMENTS

The authors are indebted to the following:

•The members of 1001 Space Unit, RAF Oakhanger, for their co-operation and provision of much of the data contained in this paper,

•Colleagues in the SKYNET Project Team, for many useful and informative discussions,

•The United Kingdom Ministry of Defence, for permission to publish this paper.

MATRA MARCONI SPACE

References.

1. NASA Specification NHB8073.1, "NASA Specification for Manufacturing and Performance Requirements of NASA Standard Aerospace Nickel-Cadmium Cells",(1988).

2. Ford, F. E., Rao, G. M., and Yi, T. Y., NASA Reference Publication 1326, "Handbook for Handling and Storage of Nickel-Cadmium Batteries: Lessons Learned," (1994).

3. Blumberg, R. E., and Boksenberg, A., "The Astronomical Almanac 1995.", HMSO, London,(1993).

60% DOD EVENT ON THE NICD BATTERIES OF THE UPPER ATMOSPHERE RESEARCH SATELLITE, AFTER 3.5 YEARS IN LEO ORBIT

Presented to
1995 NASA AEROSPACE BATTERY WORKSHOP

By
Mark R. Toft
Space Power Applications Branch
and
Richard E. Calvin
Lockheed-Martin, UARS FOT
NASA Goddard Space Flight Center

November 28 - 30, 1995

SPACECRAFT HISTORY

- The UPPER ATMOSPHERE RESEARCH SATELLITE (UARS) was deployed by Space Shuttle Discovery on September 12, 1991 for a nominal 36-month mission goal, which has been successfully completed
- 96-minute LEO orbit inclined 57 degrees to the equator (results in at least two full-sun periods per year)
- Spacecraft (S/C) built by General Electric (now Lockheed-Martin) and incorporates the Multimission Modular Spacecraft (MMS)
- On-board NASA Standard 50 AH batteries began exhibiting voltage and current-sharing divergence in January 1992, requiring monitoring and management on a continuous basis

DESCRIPTION OF DEEP-DISCHARGE EVENT

- Solar Array (S/A) Drive Assembly began exhibiting early degradation in June 1992, also requiring careful monitoring and management, and leading to a reduction in the permissible modes of operation
- One of two Earth Sensor Assemblies (ESA) failed in April 1993
- The second Earth Sensor failed on DOY 1995:082 at 02:14 UTC, or 9:14 PM EST. S/C commanded to Earth-Pointing Safehold and Solar Array driven to Index position

DESCRIPTION OF DEEP-DISCHARGE EVENT

- S/C subsequently commanded to Sun-Pointing Safehold, but thrusters did not fire:
  - Two command bits critical for proper thruster firing were disabled for shuttle launch, and were not properly reset after S/C deployment
  - S/A not properly illuminated, leaving S/C in negative energy balance
- Initial load shed upon battery voltage reaching 24.2 volts, followed almost immediately by a critical load shed at 23.8 volts

IMMEDIATE RESULTS OF DEEP-DISCHARGE EVENT

- Science instruments properly safed and unaffected
- Potential damage to part of Attitude Control System (thrusters)
- Batteries in almost-continuous discharge for approximately 3 hours, 45 minutes
  - Minimum load bus voltage of 23.0 volts, or ~1.045 volts/cell
  - Total depth-of-discharge was 57% for Battery 1, 60% for Battery 2 and 59% for Battery 3

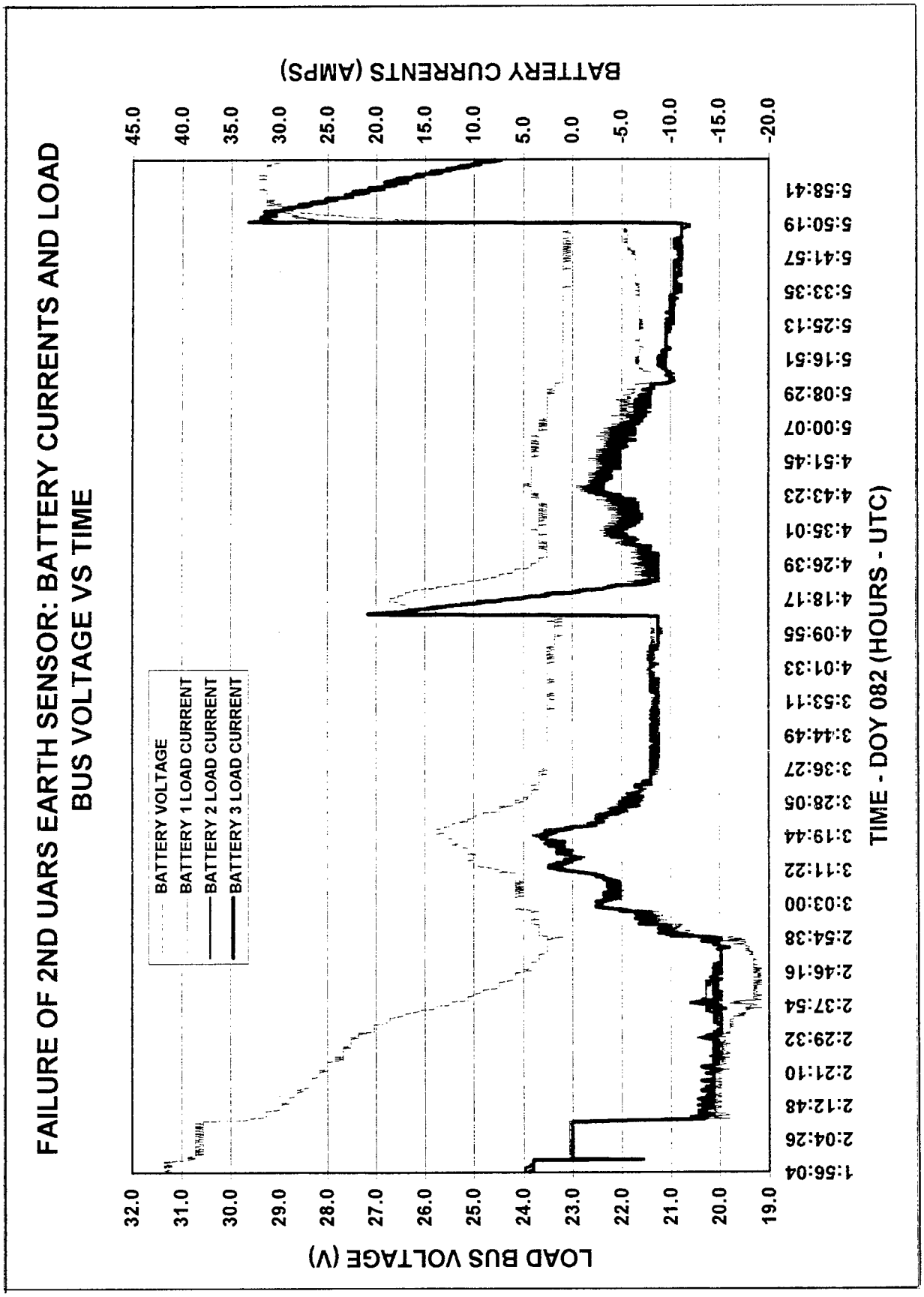
FAILURE OF 2ND UARS EARTH SENSOR: BATTERY CURRENTS AND LOAD BUS VOLTAGE VS TIME
BATTERY VOLTAGE
BATTERY 1 LOAD CURRENT
BATTERY 2 LOAD CURRENT
BATTERY 3 LOAD CURRENT
LOAD BUS VOLTAGE (V)
BATTERY CURRENTS (AMPS)
TIME - DOY 082 (HOURS - UTC)
32.0
31.0
30.0
29.0
28.0
27.0
26.0
25.0
24.0
23.0
22.0
21.0
20.0
19.0
45.0
40.0
35.0
30.0
25.0
20.0
15.0
10.0
5.0
0.0
-5.0
-10.0
-15.0
-20.0
1:56:04
2:04:26
2:12:48
2:21:10
2:29:32
2:37:54
2:46:16
2:54:38
3:03:00
3:11:22
3:19:44
3:28:05
3:36:27
3:44:49
3:53:11
4:01:33
4:09:55
4:18:17
4:26:39
4:35:01
4:43:23
4:51:45
5:00:07
5:08:29
5:16:51
5:25:13
5:33:35
5:41:57
5:50:19
5:58:41

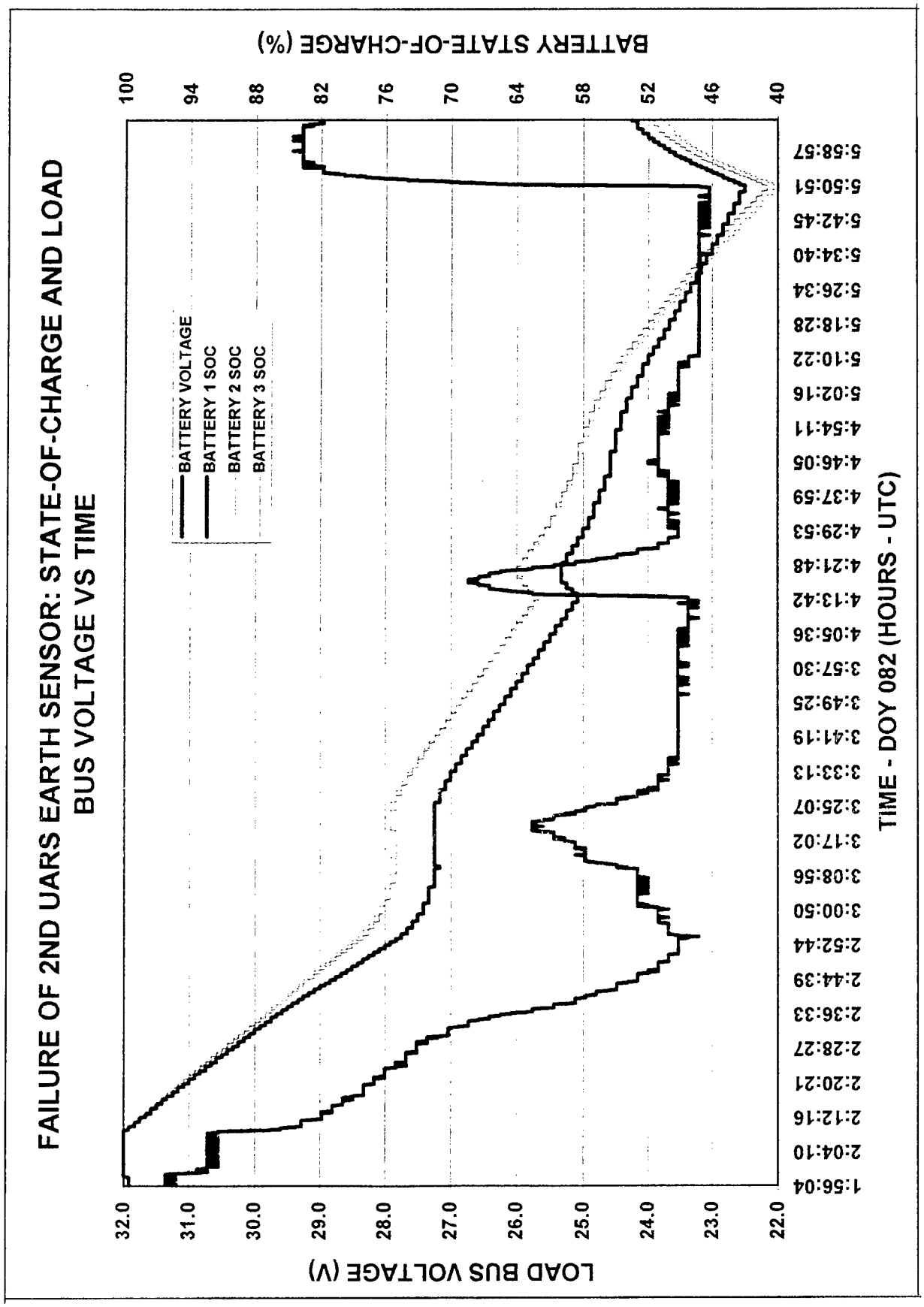
FAILURE OF 2ND UARS EARTH SENSOR: STATE-OF-CHARGE AND LOAD
BUS VOLTAGE VS TIME
LOAD BUS VOLTAGE (V)
BATTERY STATE-OF-CHARGE (%)
TIME - DOY 082 (HOURS - UTC)
BATTERY VOLTAGE
BATTERY 1 SOC
BATTERY 2 SOC
BATTERY 3 SOC
32.0
31.0
30.0
29.0
28.0
27.0
26.0
25.0
24.0
23.0
22.0
100
94
88
82
76
70
64
58
52
46
40
1:56:04
2:04:10
2:12:16
2:20:21
2:28:27
2:36:33
2:44:39
2:52:44
3:00:50
3:08:56
3:17:02
3:25:07
3:33:13
3:41:19
3:49:25
3:57:30
4:05:36
4:13:42
4:21:48
4:29:53
4:37:59
4:46:05
4:54:11
5:02:16
5:10:22
5:18:28
5:26:34
5:34:40
5:42:45
5:50:51
5:58:57

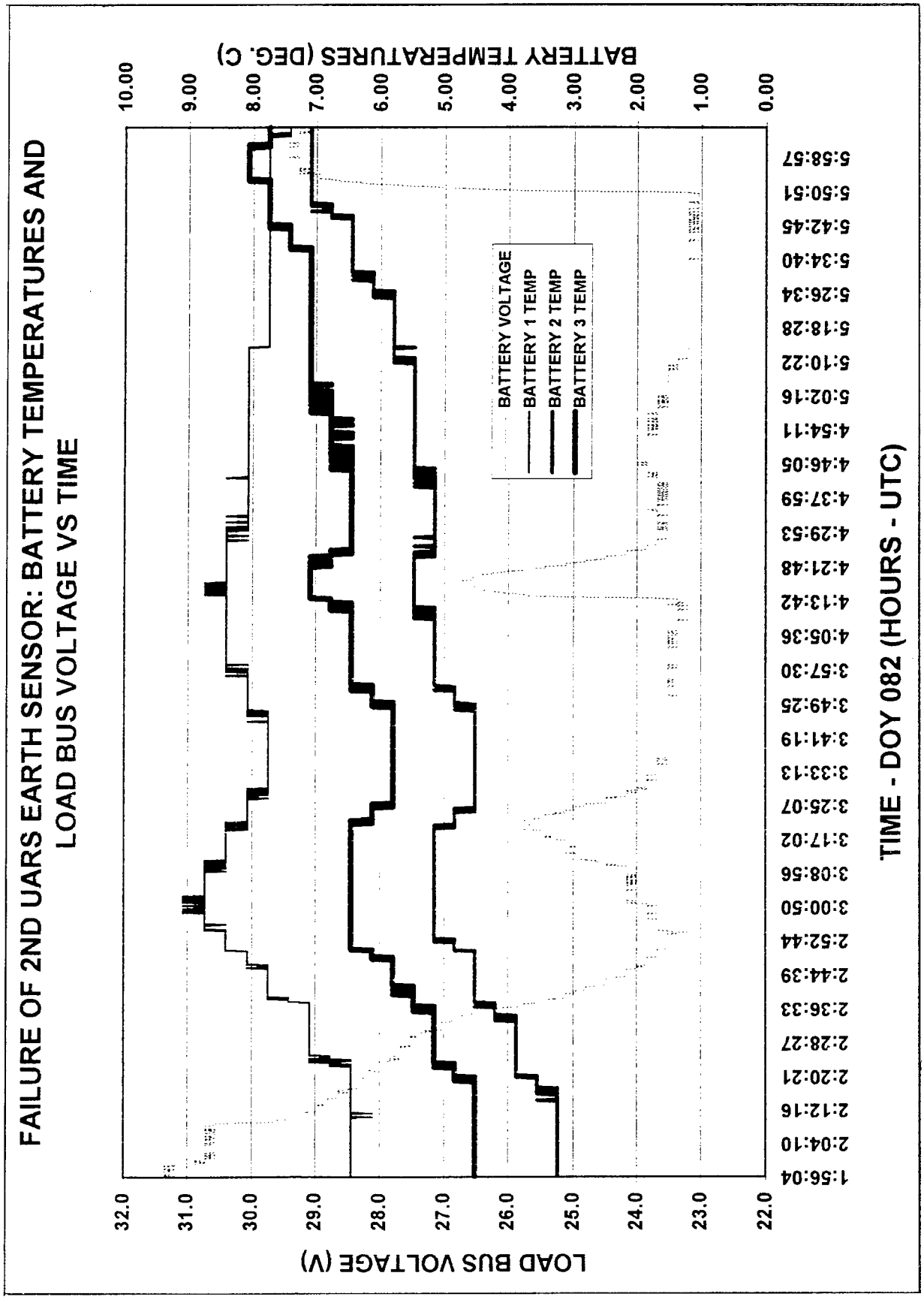
FAILURE OF 2ND UARS EARTH SENSOR: BATTERY TEMPERATURES AND LOAD BUS VOLTAGE VS TIME
LOAD BUS VOLTAGE (V)
BATTERY TEMPERATURES (DEG. C)
TIME - DOY 082 (HOURS - UTC)
BATTERY VOLTAGE
BATTERY 1 TEMP
BATTERY 2 TEMP
BATTERY 3 TEMP
32.0
31.0
30.0
29.0
28.0
27.0
26.0
25.0
24.0
23.0
22.0
10.00
9.00
8.00
7.00
6.00
5.00
4.00
3.00
2.00
1.00
0.00
1:56:04
2:04:10
2:12:16
2:20:21
2:28:27
2:36:33
2:44:39
2:52:44
3:00:50
3:08:56
3:17:02
3:25:07
3:33:13
3:41:19
3:49:25
3:57:30
4:05:36
4:13:42
4:21:48
4:29:53
4:37:59
4:46:05
4:54:11
5:02:16
5:10:22
5:18:28
5:26:34
5:34:40
5:42:45
5:50:51
5:58:57

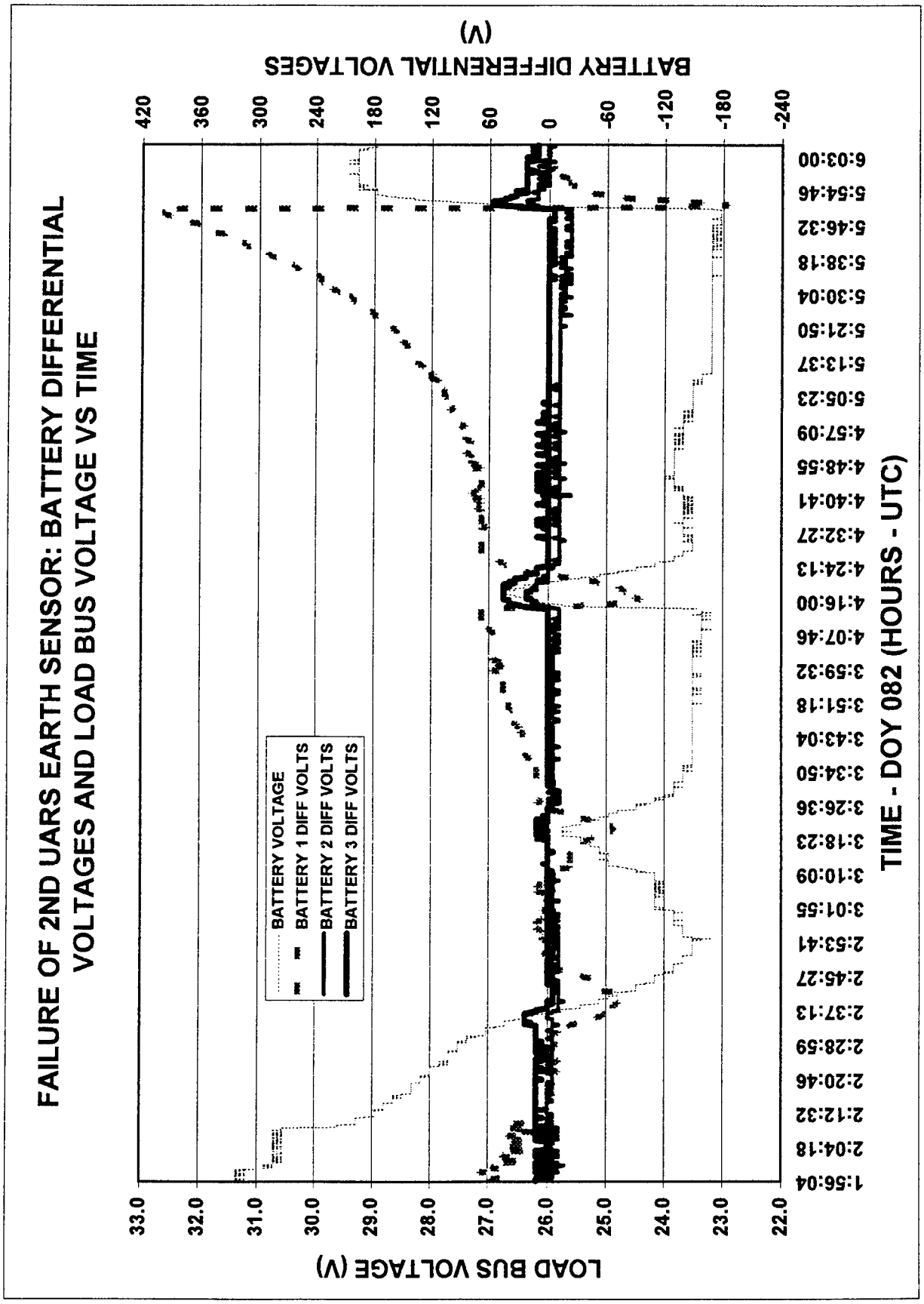
FAILURE OF 2ND UARS EARTH SENSOR: BATTERY DIFFERENTIAL VOLTAGES AND LOAD BUS VOLTAGE VS TIME
LOAD BUS VOLTAGE (V)
BATTERY DIFFERENTIAL VOLTAGES (V)
TIME - DOY 082 (HOURS - UTC)
BATTERY VOLTAGE
BATTERY 1 DIFF VOLTS
BATTERY 2 DIFF VOLTS
BATTERY 3 DIFF VOLTS
33.0
32.0
31.0
30.0
29.0
28.0
27.0
26.0
25.0
24.0
23.0
22.0
420
360
300
240
180
120
60
0
-60
-120
-180
-240
1:56:04
2:04:18
2:12:32
2:20:46
2:28:59
2:37:13
2:45:27
2:53:41
3:01:55
3:10:09
3:18:23
3:26:36
3:34:50
3:43:04
3:51:18
3:59:32
4:07:46
4:16:00
4:24:13
4:32:27
4:40:41
4:48:55
4:57:09
5:05:23
5:13:37
5:21:50
5:30:04
5:38:18
5:46:32
5:54:46
6:03:00

RECOVERY AND SUBSEQUENT PERFORMANCE

- Future operation of Attitude Control System thrusters now constrained to specific configurations
- S/A indefinitely "parked", near the S/C "noon" position
  - S/C orbital power profile constrained to a Cosine Power curve
  - Exploiting maximum S/A output power to maximize data collection by the remaining scientific instruments now requires careful monitoring and management
- Batteries dramatically converged in temperature delta, load-sharing and C/D ratio after the deep discharge event
  - Battery 1 half-battery differential voltage exceeded +728 mV on numerous occasions in the 7 days following the deep discharge event, then resumed a benign signature

SUMMARY

- UARS on-board batteries have experienced degraded performance since the first full-sun period
- UARS on-board batteries successfully endured a 60% DOD event arising from the failure of other S/C components
- UARS on-board batteries exhibited a relatively constant discharge voltage plateau at 23.04 volts (1.045 volts/cell) between 47% and 59% depth-of-discharge

Soft-Short Management and Remediation in 10-Year-Old NiCds in Geo Orbit

Nicanor A. Flordeliza, GE American Communications Satellites, Inc.
4 Research Way, Princeton , NJ 08540
Ronald W. Bounds, Aerospace Consulting Group Inc.
423 Terhune Road, Princeton NJ 08540

Abstract

After 10 years in Geo orbit, during the Spring 1993 eclipse season, soft shorts occurred in cells of two of the three batteries on the F2R spacecraft. On battery #1, the cell soft short turned suddenly into a hard short; the resulting sudden 1.2V fall in battery voltage and rise in temperature was observed via telemetry. On battery #3, the deleterious impact of its soft short increased day by day, manifesting itself as a drop in battery voltage part-way through each eclipse, causing high loading on the remaining good battery. This paper reports how by planned charge management, including applying (against-the-book) overcharge ratios (C/D) exceeding 1.75, the battery #3 cell soft short was "built down" until the cell voltage fade ceased. The problem with the battery #3 soft-shorted cell was fought with partial success throughout the latter half of the Fall 93 season, and the lessons learned were applied to alleviate the problem during the Spring 94 and Fall 94 eclipse seasons. The life of the spacecraft was successfully prolonged until it was retired in March 1995.

The F2R Battery System

The GE American Communications (Americom) F2R spacecraft was built by RCA Astro Space for a ten-year design life and was launched into Geosynchronous orbit on 9/8/83. The spacecraft carries 24 C-Band transponder channels for communications services over the continental USA. The power system is of the direct-energy-transfer type and uses partial array shunting to regulate the bus voltage to 35.3 volts in sunlight. During eclipse, the batteries discharge directly into the bus and the bus voltage is determined by the battery discharge voltages.

The F2R battery system is composed of three 22-cell Nickel-Cadmium batteries. The salient characteristics of the system are listed in Table 1. Figure 1 shows the two 11-cell packs of one battery, each pack composed of eleven rectangular prismatic, Nickel-Cadmium cells with 24 ampere-hour nominal capacity. The cells have Pellon 2505-ML non-woven nylon separators. The batteries are intended for operation at a Depth-of-Discharge (DOD) not to exceed 50%.

A functional block diagram of the F2R power system is shown in Figure 2. The batteries discharge into the bus via redundant individual parallel sets of Schottky diodes, which provide a low voltage drop -- typically 1.2 volts at 20 amps -- between each battery and the bus. Each battery may be independently charged at any one of 4 commandable charge rates (see Table 2) via dedicated redundant linear dissipative regulators operating from bus voltage. Battery temperatures are maintained between 0 and 15 degrees C by means of a passive battery thermal radiator design with the support of thermistor-controlled heaters to prevent going colder than 0 deg. C.

Table 1.

SATCOM F2R NI-CD BATTERY SYSTEM	
o	3 Batteries, 22 Cells Each
o	2 Packs / Battery, 11 Cells / Pack
o	Cell: Nickel Cadmium, prismatic, Capacity: 24 AH Nameplate
o	Separator: Non-Woven Nylon (Pellon 2505-ML)
o	Parallel Discharge via Redundant Diode circuits to Bus.
o	Bus voltage = 35.3 Volt, sunlight, regulated; 24-33 V in eclipse.
o	S/C load average = 820 watts
o	Battery max. design DOD = 50%
o	Eclipses: 88/year: 2 Seasons/year; 44 days per Season
o	Eclipse discharge duration: 5 to 72 minutes
o	Battery reconditioning via individual cell letdown resistors, 1.5 ohms/cell.
o	Launched 9/8/83 -- Retired 3/2/95
o	Spacecraft design life -- 10 years

Normal Operation and Battery Management

Figure 3 shows the battery discharge currents and sharing for the longest eclipse day (1992 day 266) of the Fall 1992 season. The 3 batteries began life well matched, with discharge currents balanced to within +/- 5% of the average current by means of matched sets of diodes and wiring. By 1991 and 1992, the performance of battery #1, seen here for day 92/266, had begun to diverge. Battery 1 began exhibiting a slower rise of current during the initial 5-10 minutes of discharge, as illustrated in Figure 3, but later on leveled out to provide a larger current and the greater ampere hour share of the 3 batteries. The battery voltages on 92/266 shown in Figure 4 were typical, with battery #3 exhibiting a voltage about 60 mV lower than #1 or #2. The ampere-hour outputs were in the ratio 34.29%, 33.88% and 31.83% for batteries 1, 2, and 3, respectively.

Typical battery management for this period (see Table 3) was to recharge after eclipse at the C/20 1.2 ampere rate to rollover for a C/D ratio of about 1.15, a period of about 10.5 hrs on the longest eclipse day, then switch to trickle charge for the remainder of the 23 hour sunlit period till the next eclipse. Figure 5 shows the battery temperatures and charge currents on the day 92/266. The battery temperatures were maintained between 0 and 15 degrees C, with an average temperature of 5 to 10 degrees.

Table 2.

BATTERY CHARGE RATES		
Rate	Designation	Current
C/10	HIGH	2.4 A.
C/20	NORMAL	1.2 A.
C/30	LOW	0.8 A.
C/60	TRICKLE	0.4 A.

Battery #1 and Battery #3 Problems Appear

At the start of the 1993 Autumnal Equinox (AE, Fall) eclipse season, the system performed normally with the batteries ampere-hour-sharing to within +/- 2% of the desired nominal 33% per battery. On day 93/248, the fifth day of the AE season, the first sign of trouble in Battery #1 appeared. On days 248 through 251, the discharge current of battery #1 fell to half its initial value after 40 minutes or so of discharge, and its ampere hour share decreased from 31% to below 27%. Figure 6 shows the battery currents on day 93/251, and the fade of battery #1. The battery discharge voltages are shown in Figure 7. Analysis showed that the battery #1 voltage was dropping in mid-discharge by an amount equivalent to one cell. Thus the energy of that one cell was being exhausted, and the cell was being driven daily into reversal.

A similar problem had been observed on Battery #3 during the Spring 93 season. During the middle days 93/076 to 93/079 of the VE93 season, battery #3 saw one cell fade out some 50-55 minutes into eclipse, with a halving of its current from 10 to 5 amps, thus causing the currents of the other two batteries to rise proportionately to support the load. The problem was at that time attributed to accidental under-charging. After 93/079, additional charging was applied to battery #3, which performed normally on 93/080 and subsequent days. thus apparently curing the voltage fade.

The Battery #1 Cell Hard-Short Failure

As a result of the battery #3 experiences in the VE 93 season, the first reaction as regards the battery #1 problem arising in the Fall 93 season was to provide additional charging. Figure 8 shows how battery #1 was charged at the 1.2 A C/20 rate to a safe 30-45 minutes past rollover after the 93/251 eclipse, then commanded to trickle charge.

Then, at 13:20 on day 251 during the trickle-charging period (see Figure 9) the voltage of battery #1 was observed to abruptly fall 1.2 volts, from 30.2 to 29 volts. Figure 8 shows that the decrease in voltage was accompanied by a sudden, transient, 3.5 deg. C temperature rise in battery #1 Pack B temperature, which had been below 12 deg.C up to the time of failure. It appeared that one cell in pack B had developed a hard short. Two hours later the spacecraft controllers briefly tried 40 minutes of 0.8 A charge to try to get the battery voltage to recover, but without success.

On the next day, 93/252, as Figure 10 shows, a dramatic reduction in performance was observed, and the change in the battery discharge current profiles indicated that something serious had indeed occurred in battery #1. The discharge current of battery #1 stayed around 6.6 amps, while the battery #2 and #3 currents were 13.4 and 12.7 amps respectively at end of discharge. On day 252, after the failure, battery #1 was now discharging only 5.5 ampere-hours and carrying but 19.2 % of the load, while batteries #2 and #3 were carrying 42% and 38.8% of the load, and

producing 12.05 and 11.13 ampere hours, respectively. The conclusion was inescapable: one cell of battery #1 had abruptly shorted out and discharged itself, during trickle charge on day 251, and we had observed it happen. Battery #1 now performed as a 21-cell battery. This performance of day 252 became the new typical baseline.

But then, on days 254 through 258, battery #1, though behaving as a 21-cell battery, exhibited an additional voltage fade and consequent further decrease in current share. We considered this to be due to a soft short, and battery #1 charging was gradually increased to try to overcome the effects of the short. and replace the charging current which was being drained away. On day 258, an unexpected sudden fade in battery #3 voltage combined with the voltage fade on battery #1 to result in an additional 0.8 v drop in bus voltage by the end of eclipse. Under these conditions, the potential threat of transponder uncommanded shutoffs caused by the low bus voltage made it necessary to examine the battery performance and micro-manage the recharging on a day to day basis.

The Battery #3 Situation Worsens

From day 271 and the days following, the situation on F2R rapidly became more serious as battery #3 now began incurring a voltage and current fade daily during each eclipse, like the fade seen on battery #1 on day 251. The battery #1 cell fade was corrected by performing more charging. The day 258 problem on battery #3 had been temporarily corrected by additional charging, but it came back on day 271 and stayed. A little more charging was tried on battery #3, but without clear effect. The onset of voltage fade occurred earlier each day, although the eclipses were becoming shorter in this second half of the eclipse season, and additional charging no longer seemed to benefit the situation. It appeared that the soft short was day by day becoming less soft and draining more energy. Battery consultants were called in. More and more credence was given to the theory that there was a soft short in Battery #3, but opinion was divided as to what might be done. Figure 11 shows the discharge current profiles on days 280, 281 and 282, and illustrates how, despite a cautious amount of increased charging , battery #3 was fading earlier and earlier each day.

Capacity Analyses Show A 1-Cell Voltage Fade

Analyses performed on TLM data for day 93/279 yielded the ampere-hour capacity curves shown in Figure 12. From these curves it is clear that battery #1 is one cell voltage below batteries #2 and #3 throughout the discharge. The voltage of battery #3 fades by one cell (1.15V) after about 7 ampere hours out. The decrease in battery #2 and #1 voltages after the fade of battery #3 is due to the increased load on those other batteries.

The problem persisted through to the end of the AE 93 season, when finally the discharge duration became so short as to not exhaust the available energy in the weak cell of Battery #3. The status and prognosis for the F2R batteries at the close of the AE93 season was not promising. The C/D ratio for battery #3 had been increased from 1.3 to 1.62 to little avail. The battery voltage fading problem had not been solved, but had resulted in the decision to intentionally reduce the bus load, and prevent undesirable and unintentional transponder shutoffs.

AE 93 End-Season Assessment

At the end of the AE93 season the following conclusions were drawn:

- Battery #1 has one cell failed shorted plus one weak cell which sometimes fades early.
- Battery #2 is performing normally, but its load is too high.
- Battery #3 has one cell which is weak and fading during each eclipse.
- The Battery #3 cell fade is progressive; starting earlier each day even if the C/D charge return at C/20 and C/30 rates is increased to 1.6.
- The fade is probably due to a "soft short" which bypasses/discharges an estimated 2 to 2.5 amp-hours of battery #3 capacity per day.

Effects of Cell Reversal on Cadmium Migration

A major concern was that driving the weak cell of battery #3 daily into reversal might potentially lead to cell shorting, as it had on Battery #1. J.Mrha et al (Ref. 6) indicate that overdischarge of a nickel-cadmium cell and prolonged operation in reversal can cause forming of cadmium "bridges" (dendrites) across the separator and may result in eventual shorting of the cell. Of direct import is the indication that if the cell reversal on overdischarge is observed to be small, i.e. less than 300 mV negative, it is a direct sign that there

is cadmium in the separator and that cadmium bridges may form on overdischarge. If the cadmium dendrites grow large enough, the short may develop to become permanent.

A New Spring, Old Problem

The beginning of the Spring (VE) 1994 season showed that the problem had not gone away. During the intervening winter season battery #3 had been reconditioned to 10 volts (instead of 2 v), as a precautionary measure. During days 1 (94/059) through 6 (94/065) of the season, battery #3 was fading earlier each day and its load share was diminishing.

The Americom Spacecraft Engineering Group and the Operations Group now began seriously experimenting with significantly greater amounts of overcharge than had previously been tried. This was done over the objections of some battery experts who emphasized the dangers of excessive overcharge. However, it seemed that the F2R batteries could indeed tolerate large amounts of overcharge, if the temperatures were monitored and the battery charge terminated if they got too hot. There appeared to be adequate overcharge protection left in the batteries, despite their age, and they were not negative-limited; thus the voltages on charge remained benign and did not approach the potentials for hydrogen evolution.

The Curve Turns

After considerable experimentation and raising the charge return C/D ratio bit by bit, signs of improvement were finally seen in the situation. Figure 13 shows the battery discharge currents for days 94/081 through 94/087, and shows how the battery #3 fading trend was reversed and pushed back. The battery discharge voltages for the day 94/084 are shown in Figure 14 for comparison. After day 94/080, charge returns of greater than 1.77, exclusive of trickle charge, were being applied to battery #3, as the table accompanying Figure 13 shows. This was being accomplished by a main charge at C10 or C/20 to rollover plus a boost charge at C/30, immediately prior to the next eclipse. On day 94/092, some 12 days after the middle of the VE 94 season, after maintaining the high C/D of > 1.8, battery #3 did not fade, because the time of fade was finally pushed to beyond the duration of discharge. This is shown by the discharge currents of Figure 15. The high daily charge return was continued to the end of the season, and battery #3 did not fade again. Aggressive charge management, together with some special analytical techniques (Ref. 2) which provided insight into the severity of the battery voltage fade, gave guidance to the amount of recharge desired.

Fall 1994 Eclipse Season Performance

For the Fall 94 season, additional battery recharge was not delayed until after the batteries exhibited a problem. Additional charge return was pumped into battery #3 right from the beginning of the season, as well as some additional charging into battery #1 (see Figure 19 C/D ratios). Figure 16 shows that the battery #3 performance on day 266, the day of longest discharge, was fully recovered. Battery #1 per-formance was however gradually degrading further as its current share shows. Figure 17 summarizes the Fall 1994 (Final) Eclipse season bus voltage performance, and includes the VE 94 season for comparison. The minimum load bus voltage was kept above the minimums recorded in VE 94.

Figure 18 presents the relative ampere hour performance of the three batteries for the AE and VE 94 seasons and shows how the ampere-hour output of battery 3 was kept high as a result of the aggressive C/D charge management applied. Figure 19 summarizes the C/D ratios applied in the Spring and Fall of '94 for recharging the batteries.

The battery system, as a result of this charge management effort, survived 1994. The effects of the soft short in battery #3 were alleviated and, we believe, the soft short itself was ameliorated. The charge management during the eclipse season as well as during the storage and reconditioning in the Winter and Summar seasons was conceived to try to minimize any growth in the suspected soft-shorting dendrites. The success of the charging policy and the improved performance of battery #3 bear out the validity of the plan.

RECOMMENDATIONS

Maintain fullest state-of-charge condition feasible. Avoid open-circuit stand -- store on trickle charge. Trickle Charge storage works to minimize dendrite or soft short formation. Avoid high temperatures and keep NiCds cool: Goal is 0 to +15 deg. C.

Consider changing the Reconditioning regime to 10 V instead of 2 V to minimize dendrite

formation. Dendrite formation appears to be related to slow discharge rates. See Eliason, Ref 4. Large amounts of overcharge should only be attempted with caution. Make sure NiCd's have adequate electrochemical overcharge protection (i.e. not negative limited). Do not exceed the hydrogen evolution potential.

CONCLUSIONS

The battery management goal had been to overcome the short term effects of the soft short in battery #3, as well as hopefully find a way to retard and if possible, reverse the trend of the growth of the soft short. The authors feel that the charge management philosophy used succeeded in diminishing and "building down" the shorting dendrites.

The performance of battery #3 was restored after the middle of the VE 94 season, and remained good for the Fall 94 season. The large amounts of overcharge applied, together with judicious trickle charge combined with absolutely minimizing any necessary periods of open-circuit stand, seem to have prevented the soft short from growing.

Acknowledgments:
The authors would like to acknowledge the assistance, contributions and discussions provided by Nick Chilelli, Steve Gaston, and Steve Schiffer of Lockheed-Martin Astro Space, Mark Halverson of GE-Americom and Guy Rampel, Consultant, as well as Jack Schmidt and the Spacecraft Analysts and Controllers at GE Americom Vernon Valley TT&C.

References:

1. Newell et al, *"Satellite Battery Reconditioning System and Method"*, US Patent #3,997,830, Dec 14, 1976.
2. R.Bounds, M.Halverson, *"A Method for Determination of In-Orbit Battery Internal Impedance"*, Proc. 28th IECEC, August 1993.
3. S.Gross, *"Unsolved Problems of Nickel-Cadmium Batteries"*, Proceedings of the 16th IECEC, Atlanta, 1981, Vol. 1, 177-181.
4. R.R. Eliason, *"Analysis of Aerospace Ni-Cd Battery Cells"*, 1977 GSFC Battery Workshop, NASA Conference Publ. 2041, 377-388.
5. Dr. P.P. McDermott, *"Cadmium Migration in Aerospace Nickel-Cadmium Cells"*, GSFC, March 1976, Report CR-144753, 24-26.
6. J.Mrha, M.Musilova and J.Jindra, (Heyrovsky Institute of the Czechoslovakia Academy of Sciences), *"On the Anomalous Behaviour of Deeply Discharged, Sealed Ni-Cd Cells"*, Journal of Power Sources, 8 (1982) 403-408.
7. W.R.Scott & D.W.Rusta, *"Sealed-Cell Nickel-Cadmium Battery Applications Manual"*, NASA Reference Publication RP-1052, December 1979, (NTIS N80-16095), 364-368.
8. F.Ford, G. Rao, and T.Yi, *"Handbook for Handling and Storage of Nickel-Cadmium Batteries"*, NASA Reference Publ.1326.

Table 3. Nominal Battery Management Plan

BATTERY MANAGEMENT PLAN	
Charge	Recharge at C/20 after Eclipse to C/D= 1.15 or rollover. Switch to Trickle charge for remainder of day. Charge batteries in parallel.
Discharge	Automatic on load demand exceeding array output. Batteries discharge in parallel, load sharing through design of discharge diode circuits.
Reconditioning	Recondition prior to each eclipse season. Discharge Battery to 2 V. via individual 1.5 ohms/cell Letdown Resistors.
Storage	Trickle Charge (C/60) at all times, non-eclipse operation. Open-Circuit if above 30 °C, 4 hrs max.
Thermal Control	Passive radiative, maintained above 2 °C by thermistor controlled pack heaters.

SATCOM 24 AH NICD FLIGHT BATTERY BY BUILT BY RCA ASTRO

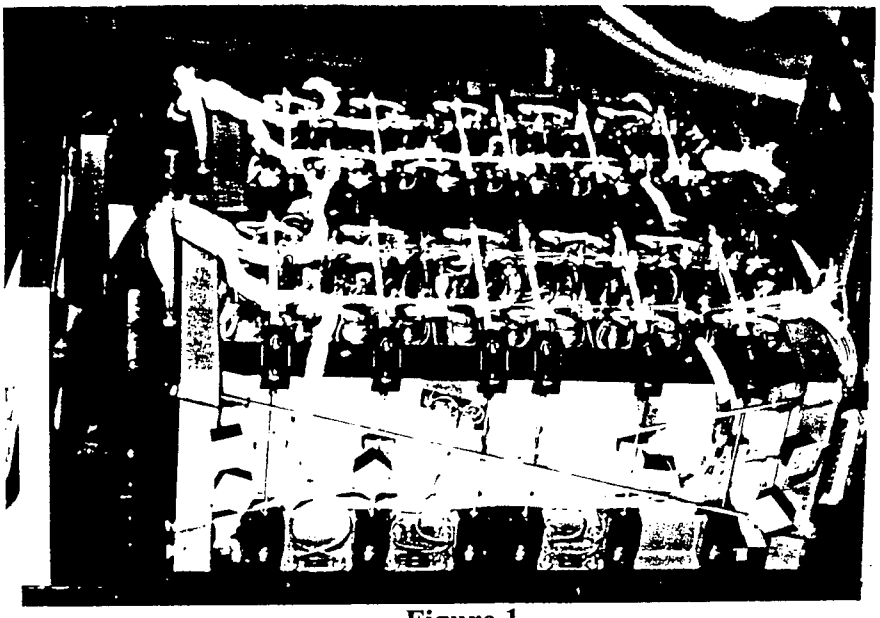

Figure 1

EPS FUNCTIONAL BLOCK DIAGRAM

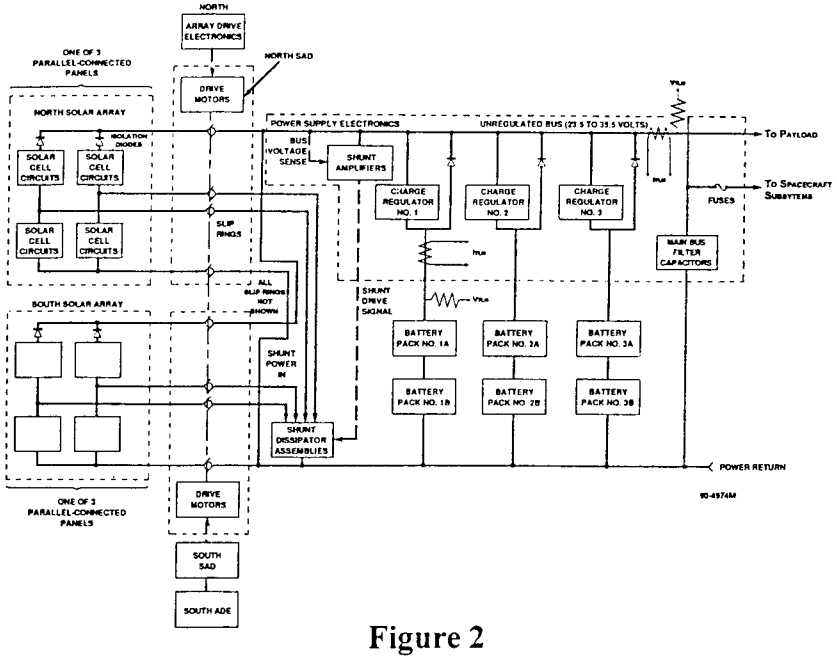

Figure 2

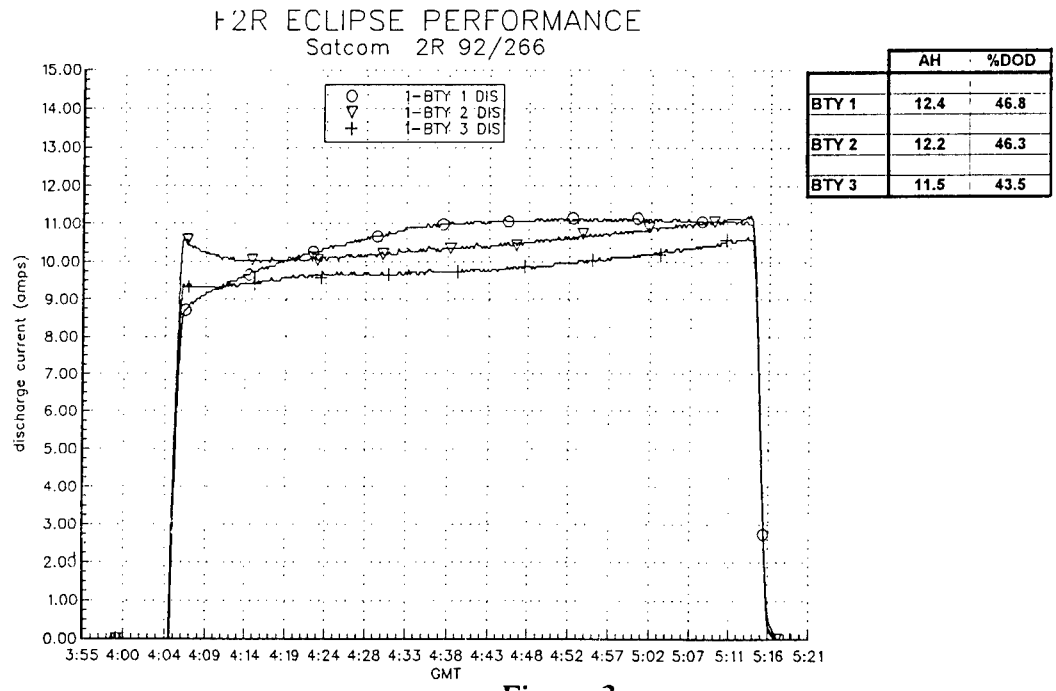

	AH	%DOD
BTY 1	12.4	46.8
BTY 2	12.2	46.3
BTY 3	11.5	43.5

Figure 3

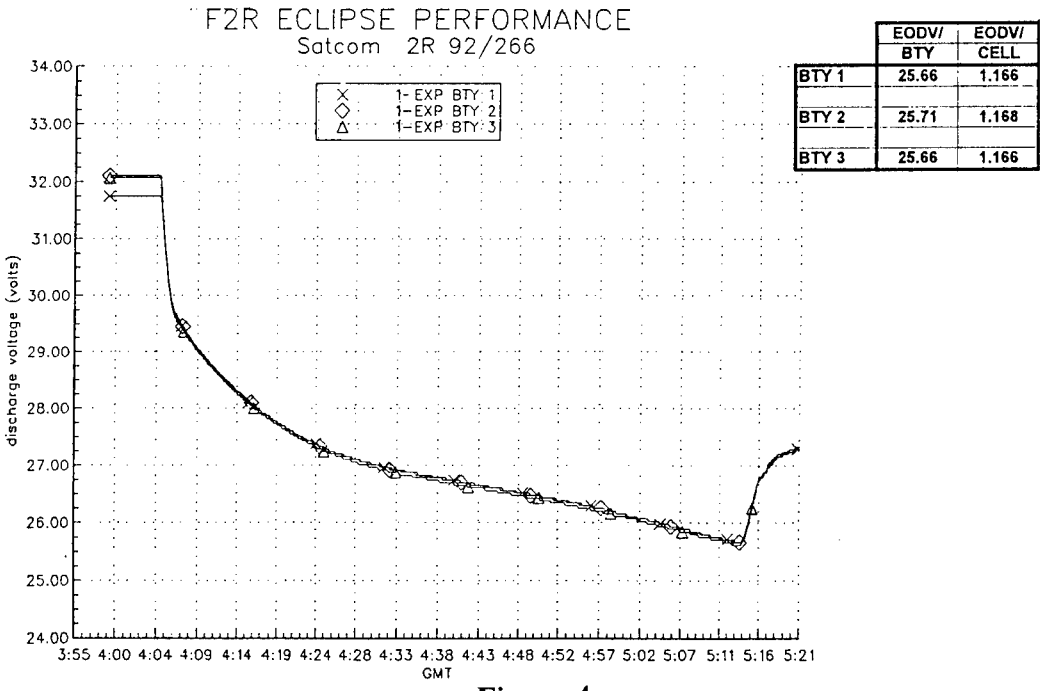

	EODV/ BTY	EODV/ CELL
BTY 1	25.66	1.166
BTY 2	25.71	1.168
BTY 3	25.66	1.166

Figure 4

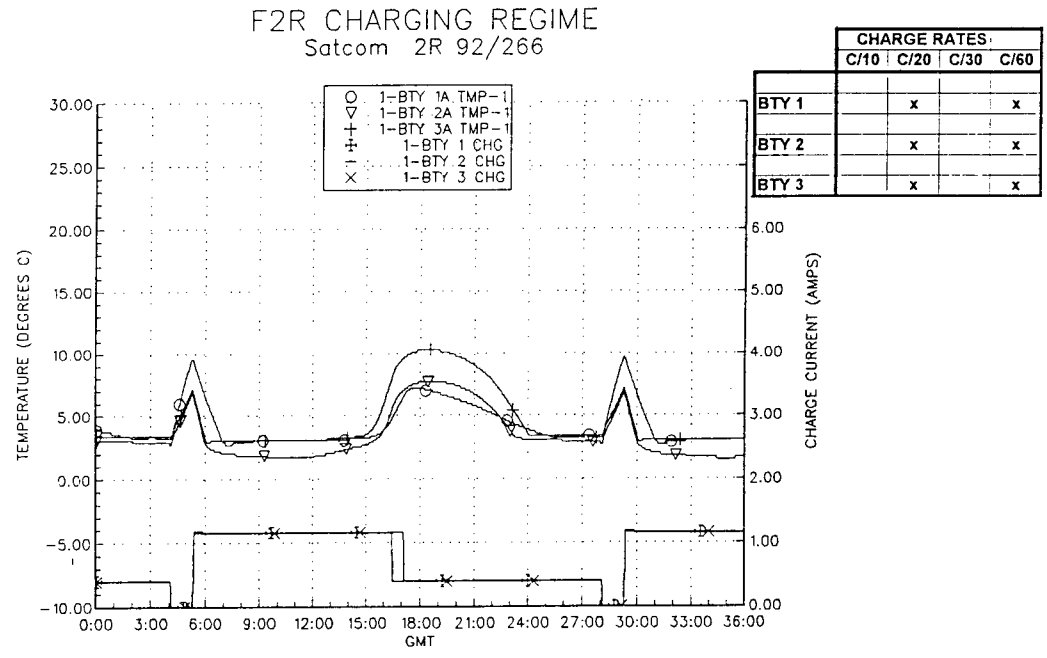

Figure 5

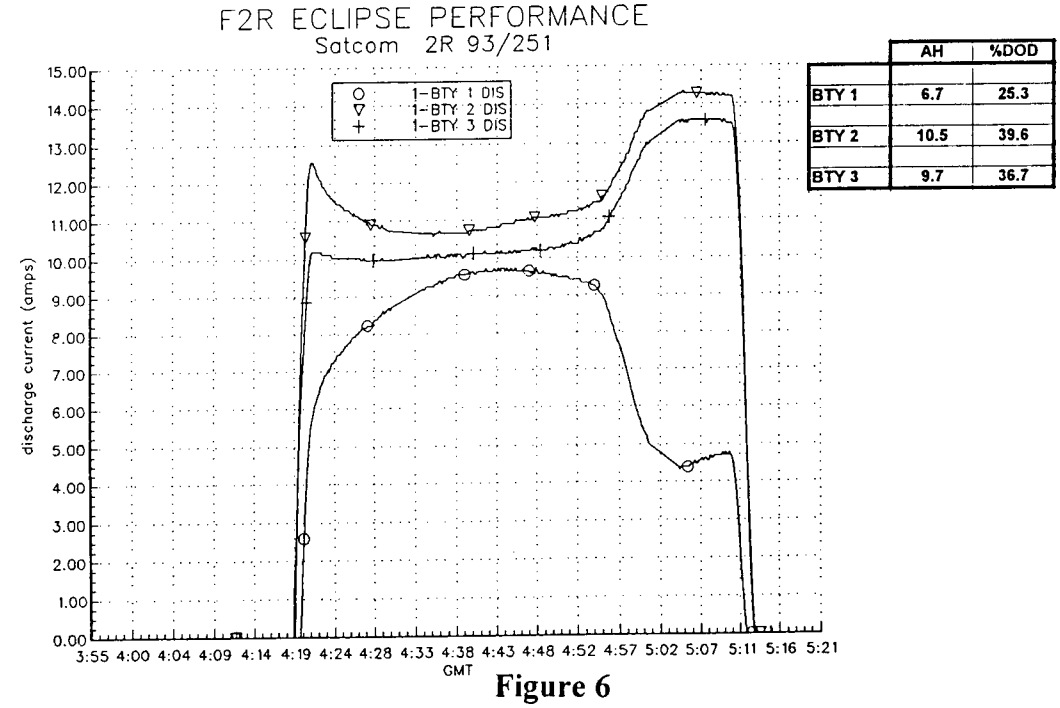

Figure 6

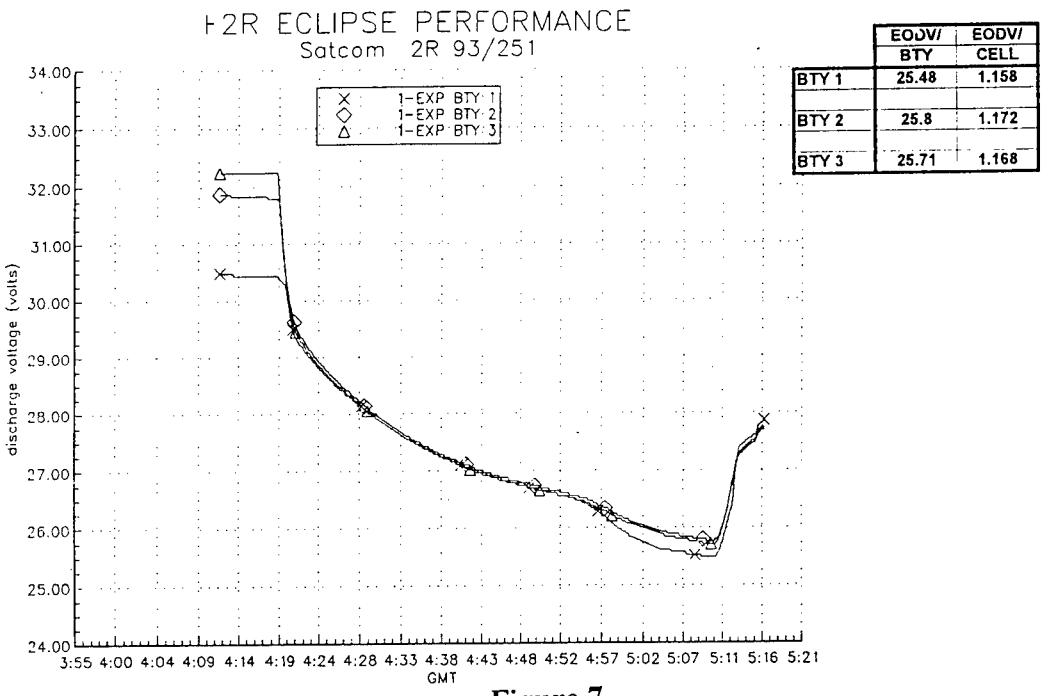

	EODV/ BTY	EODV/ CELL
BTY 1	25.48	1.158
BTY 2	25.8	1.172
BTY 3	25.71	1.168

Figure 7

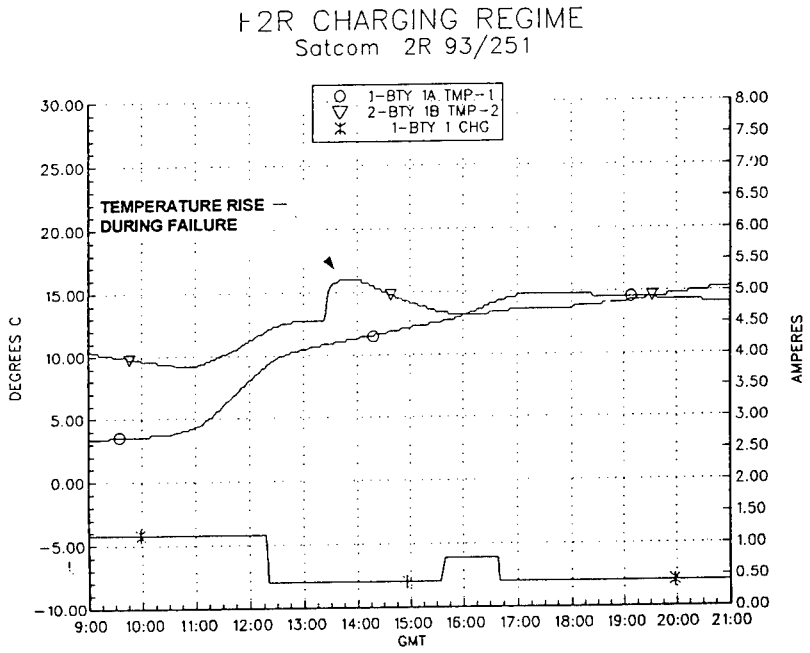

Figure 8

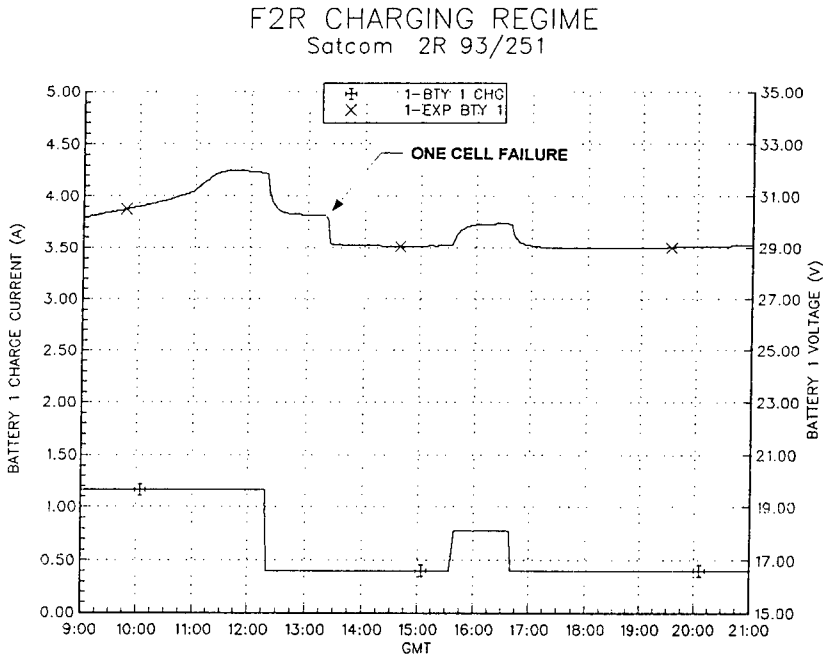

Figure 9

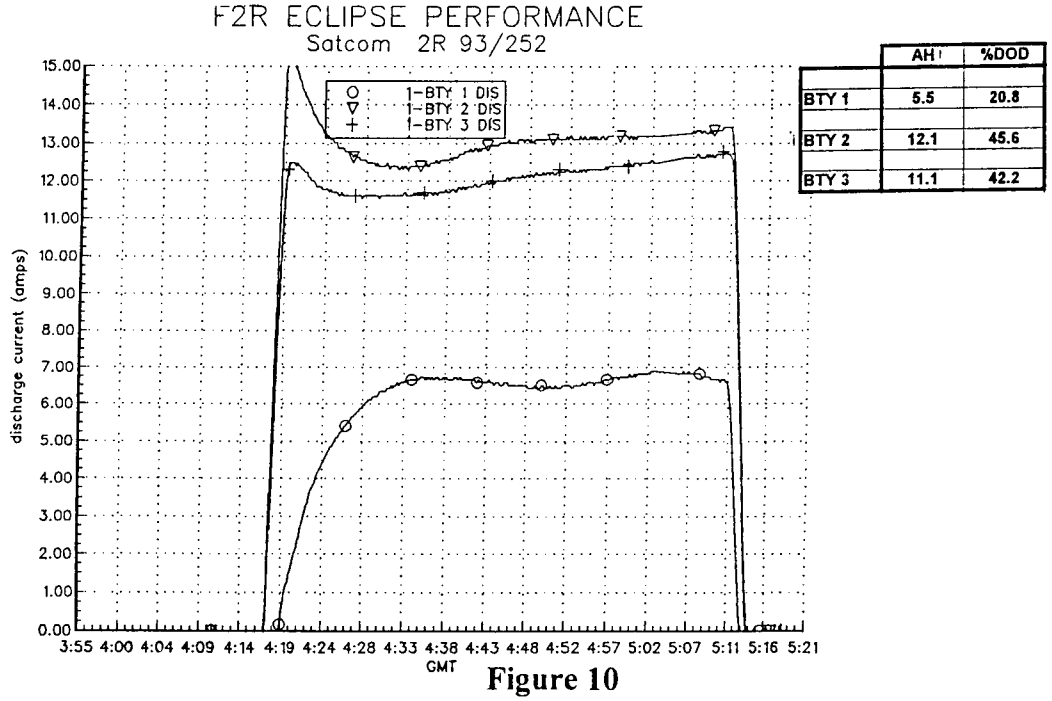

	AH	%DOD
BTY 1	5.5	20.8
BTY 2	12.1	45.6
BTY 3	11.1	42.2

Figure 10

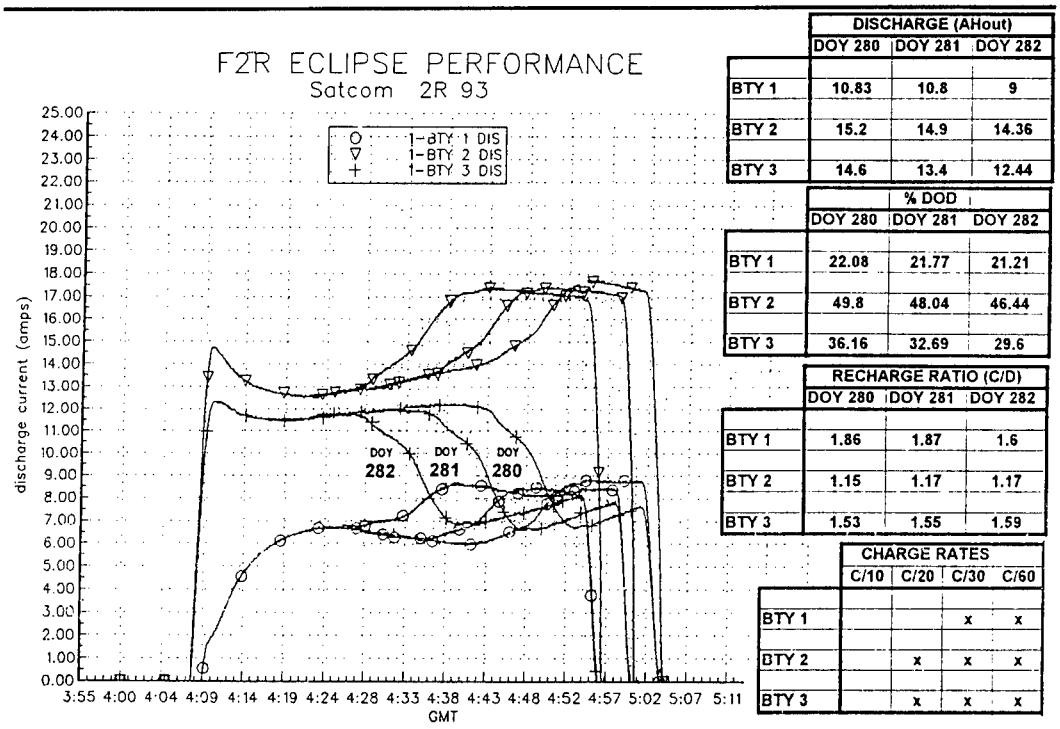

	DISCHARGE (AHout)		
	DOY 280	DOY 281	DOY 282
BTY 1	10.83	10.8	9
BTY 2	15.2	14.9	14.36
BTY 3	14.6	13.4	12.44

	% DOD		
	DOY 280	DOY 281	DOY 282
BTY 1	22.08	21.77	21.21
BTY 2	49.8	48.04	46.44
BTY 3	36.16	32.69	29.6

	RECHARGE RATIO (C/D)		
	DOY 280	DOY 281	DOY 282
BTY 1	1.86	1.87	1.6
BTY 2	1.15	1.17	1.17
BTY 3	1.53	1.55	1.59

	CHARGE RATES			
	C/10	C/20	C/30	C/60
BTY 1			x	x
BTY 2		x	x	x
BTY 3		x	x	x

Figure 11

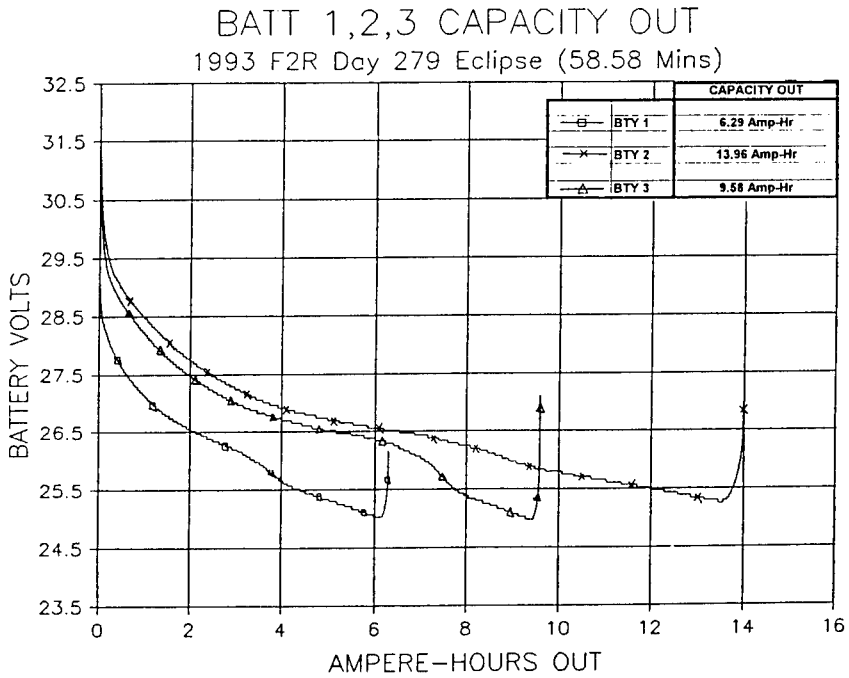

Figure 12

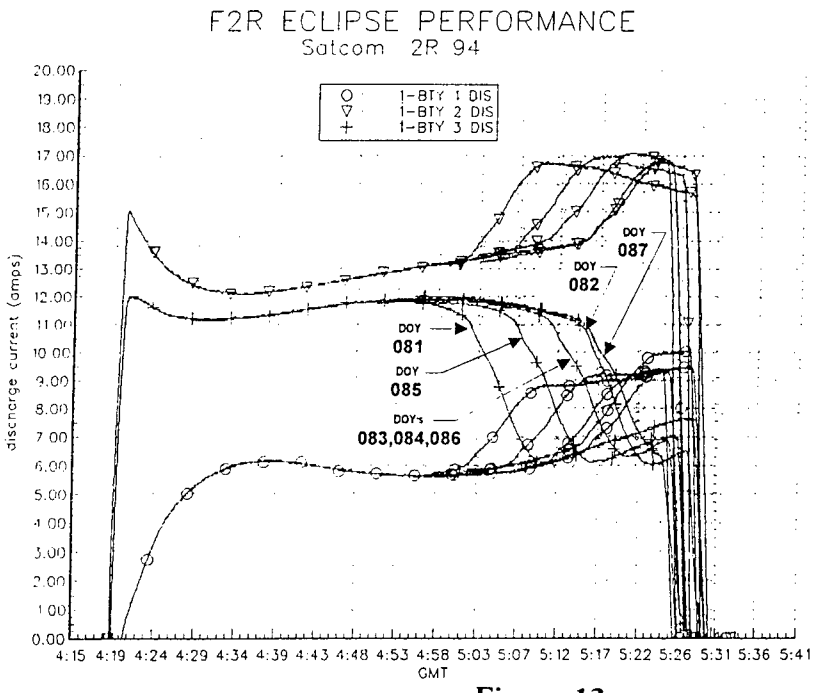

BATTERY 3	
DOY	C/D
80	1.77
81	1.71
82	1.88
83	1.79
84	1.8
85	1.78
86	1.83
87	1.85
88	1.83
89	1.81

BATT# 1 AVE. C/D @ 1.6
BATT# 2 AVE. C/D @ 1.15

Figure 13

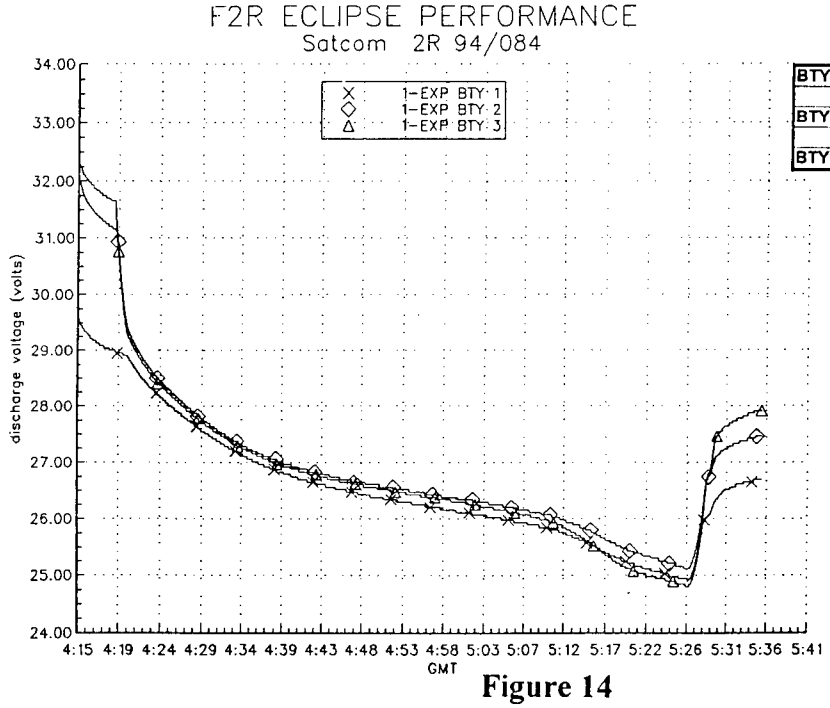

	EODV/ BTY	EODV/ CELL
BTY 1	24.94	1.129
BTY 2	25.16	1.143
BTY 3	24.85	1.129

Figure 14

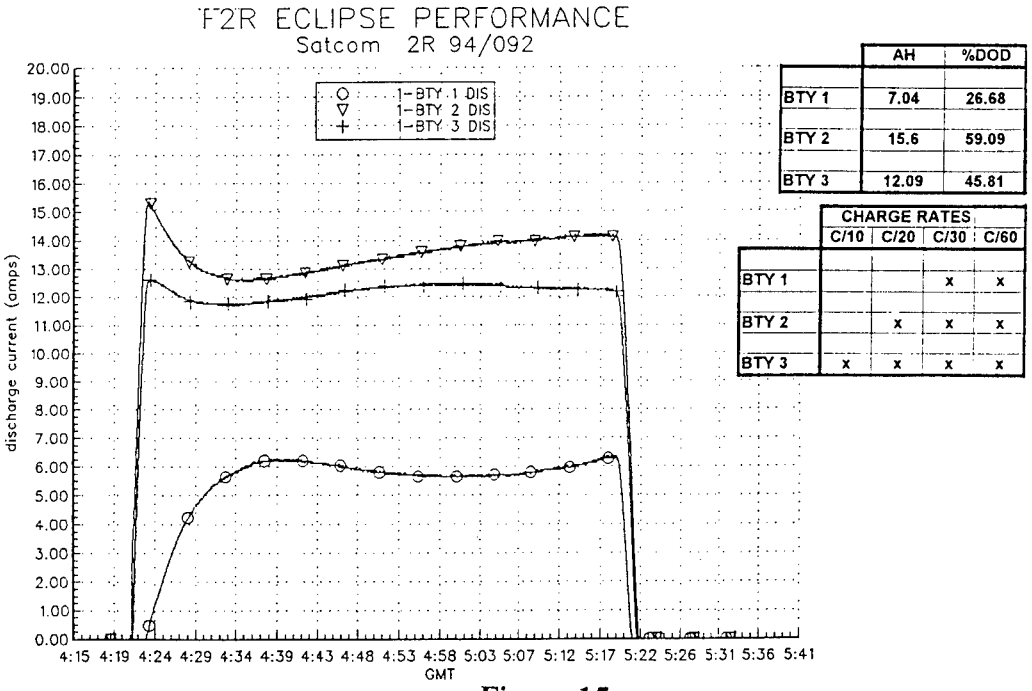

	AH	%DOD
BTY 1	7.04	26.68
BTY 2	15.6	59.09
BTY 3	12.09	45.81

	CHARGE RATES			
	C/10	C/20	C/30	C/60
BTY 1			x	x
BTY 2		x	x	x
BTY 3	x	x	x	x

Figure 15

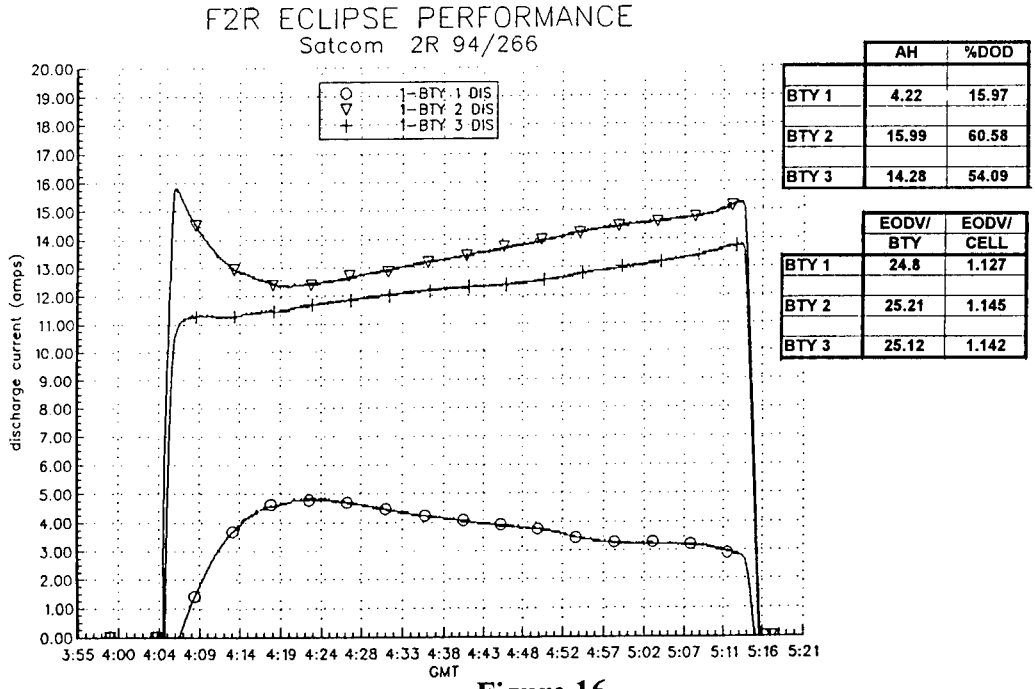

	AH	%DOD
BTY 1	4.22	15.97
BTY 2	15.99	60.58
BTY 3	14.28	54.09

	EODV/ BTY	EODV/ CELL
BTY 1	24.8	1.127
BTY 2	25.21	1.145
BTY 3	25.12	1.142

Figure 16

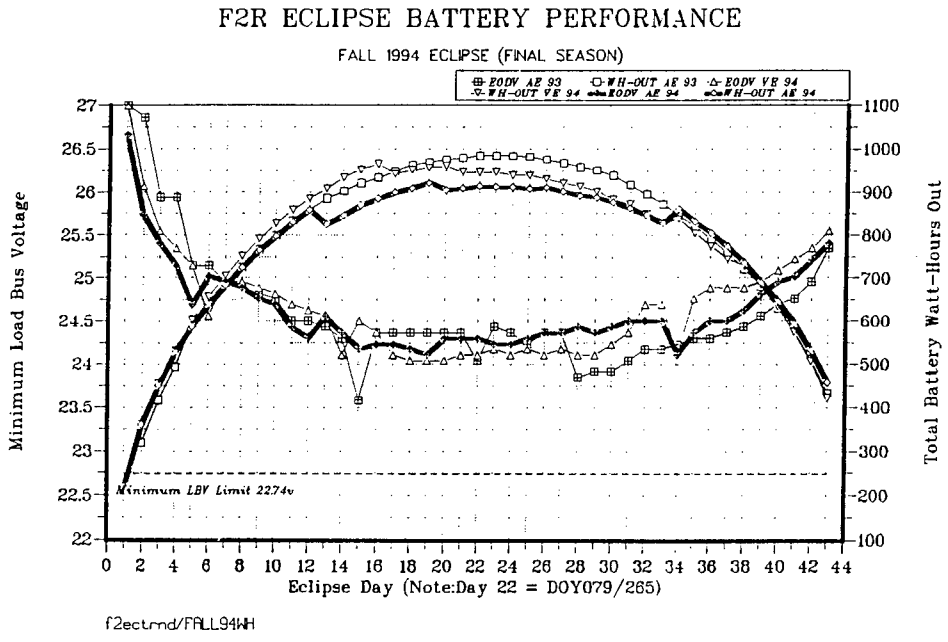

Figure 17

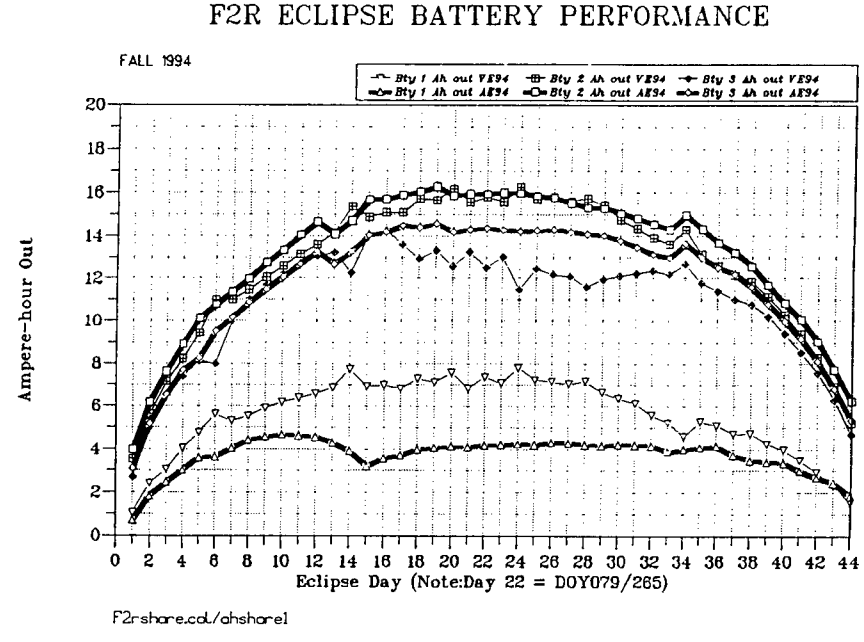

Figure 18

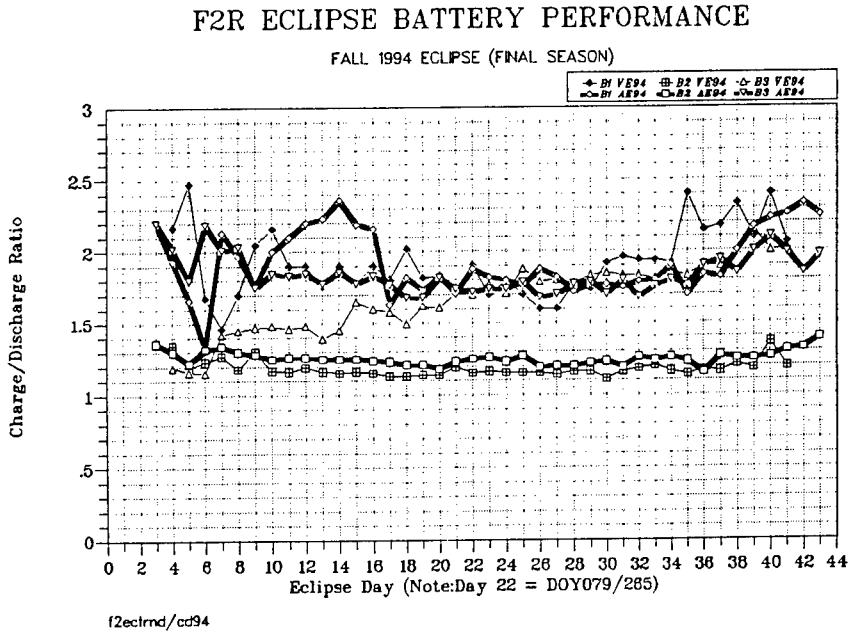
F2R ECLIPSE BATTERY PERFORMANCE
FALL 1994 ECLIPSE (FINAL SEASON)
B1 VE94
B2 VE94
B3 VE94
B1 AE94
B2 AE94
B3 AE94
Charge/Discharge Ratio
3
2.5
2
1.5
1
.5
0
0 2 4 6 8 10 12 14 16 18 20 22 24 26 28 30 32 34 36 38 40 42 44
Eclipse Day (Note:Day 22 = DOY079/285)
f2ectrnd/cd94

Figure 19

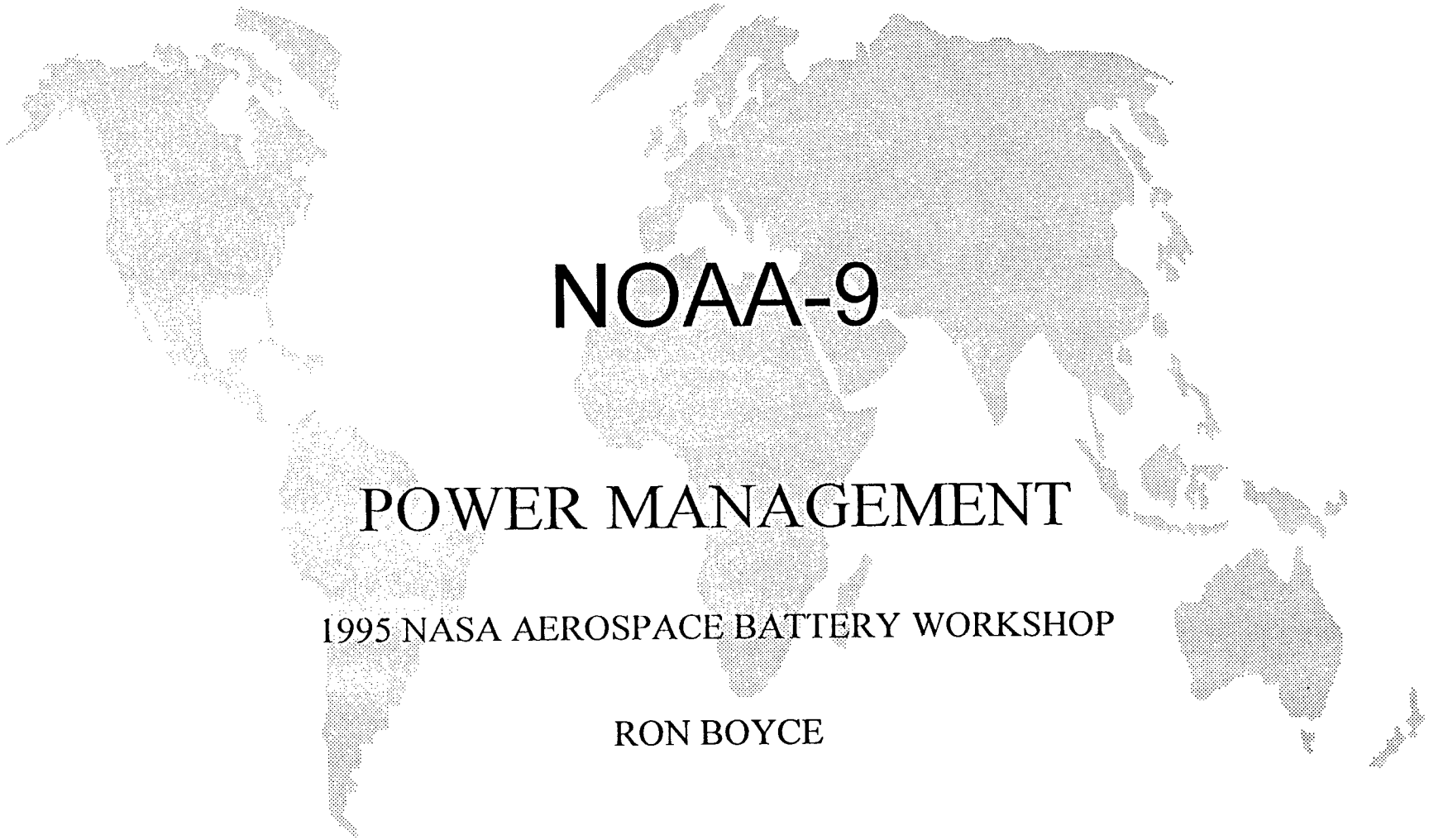

NOAA-9

POWER MANAGEMENT

1995 NASA AEROSPACE BATTERY WORKSHOP

RON BOYCE

NOAA - LOCKHEED MARTIN Eng. Support

NOAA-9 FACTS

- LAUNCHED 12 DEC.1984
- 3 - 26.5 AMP-HOUR BATTERIES IN 8 AND 9 CELL PACKS
- TYPICAL 12 TO 18 PERCENT D.O.D.
- PRESENT ECLIPSE PERIOD 32 MINUTES
- PACK TEMPERATURE CONTROL <5 DEG. >10 DEG. C
- BATT.#1 PRIME CHARGE REG. FAILED AFTER 1 YEAR
- BATT#2 PRIME CHARGE REG. FAILED AFTER 1.5 YEARS
- BATT#1 BACKUP CHARGE REGULATOR FAILED 2 AUG. 1995 (D.O.Y.214). PROBABLY CAUSED BY LOSS OF BUSS VOLTAGE REGULATION.

NOAA - LOCKHEED MARTIN Eng. Support

TOOLS USED

- CHARGE REGULATOR - VT CONTROL
- STORED COMMAND TABLE
  LIMIT BATTERY OVERCHARGE
- ARRAY OFFSET - LAG 55 TO 105 DEG.
  MAXIMUM OFFSET THAT ALLOWS FULL RECHARGE
- SADBIAS SOFTWARE
  MAINTAIN BUS REGULATION AS CHARGE I DECREASES
- POWER MONITOR SOFTWARE
  CHARGE STATE MONITOR & ANOMALY DETECTION

NOAA - LOCKHEED MARTIN Eng. Support

NOAA-09

- NOAA-9 POWER PLOT #1

ARRAY SHORT CIRCUIT PATCH I
ARRAY SHUNT DRIVE(BUS REG.)
ARRAY OFFSET CHANGE BY SADBIAS SOFTWARE

- N0AA-9 POWER PLOT #2

ARRAY TEMPERATURES
TELEMETRY ERROR DUE TO LOSS OF BUS REGULATION
PAYLOAD BUS I
PAYLOAD BUS V
BUS OVERVOLTAGE CAUSED BY BATTERY #2 COMMAND
TO TRICKLE CHARGE

NOAA - LOCKHEED MARTIN Eng. Support

PLOT NAME: NRT_OPS$HISPLOT_PLOT:N9PPLT1
TITLE: N9PLR1
DESCRIPTION: NOAA-9 POWER PLOT #1
SETUP FILENAME: NRT_OPS$HISPLOT_SETUP:N9PLR1
START/STOP TIME: 95/318/06:25:00.0 - 95/318/08:25:00.0

SCID: 09
PLOT CREATION DATE: 318/13:54:02
PLOT PRINT DATE: 318/14:54:23
SAMPLING PERIOD: 000/00:00:08.00

Y-DATA	CHAN	UNITS	TYPE	VS	X_DATA	CHAN	UNITS	TYPE	SYM	GPH
NSADARRI	FA256	AMP	EU		TIME		HRS			1
NSADSCI	FA268	MA	EU		TIME		HRS			1
NPSESHNV	FA260	VOL	EU		TIME		HRS			1
CSHUNT1	FSAT0	VOL	EU		TIME		HRS			1

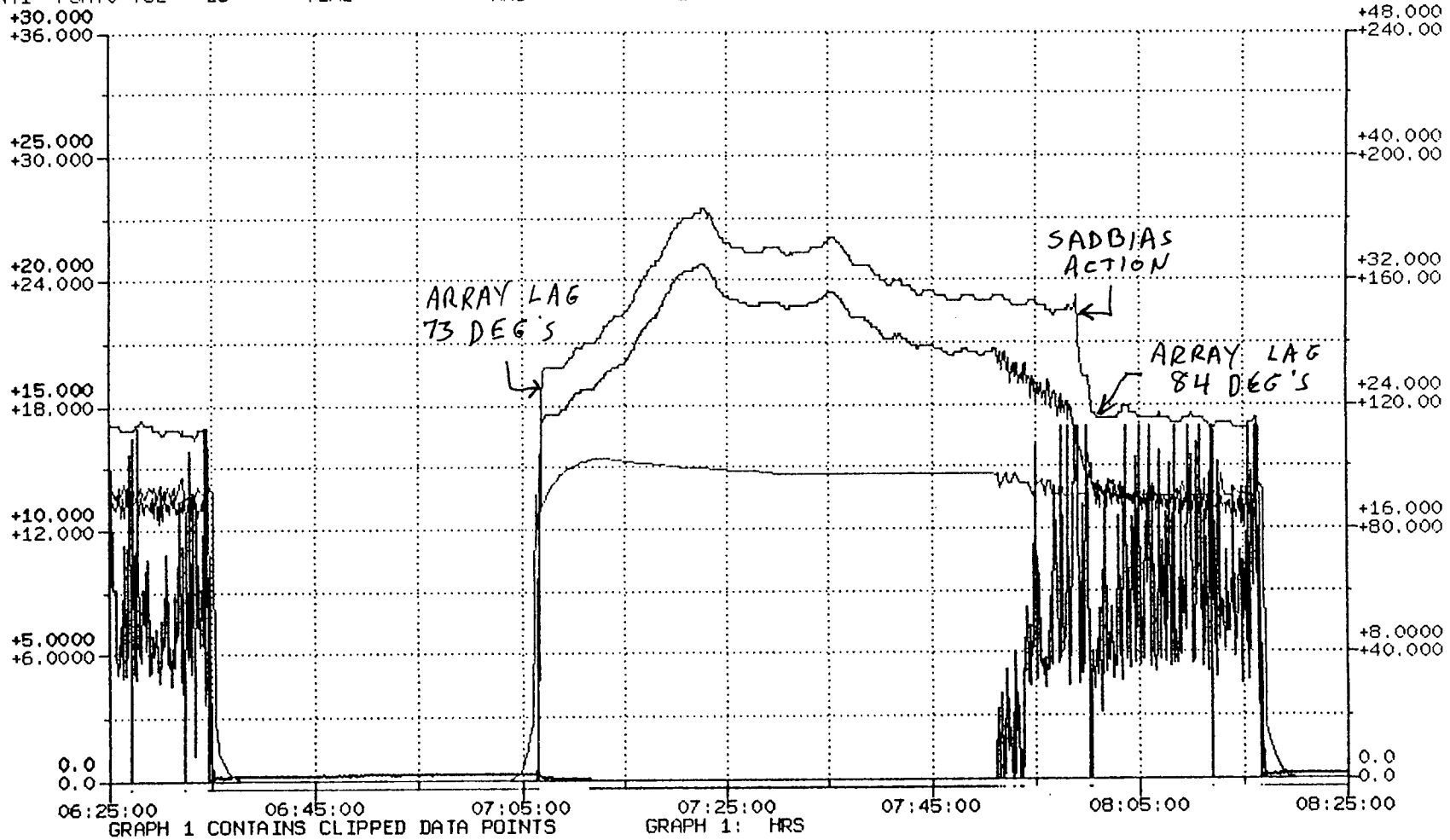

PLOT NAME: NRT_OPS$HISPLOT_PLOT:N9PPLT2
TITLE: N9PLR2
DESCRIPTION: NOAA-9 POWER PLOT #2
SETUP FILENAME: NRT_OPS$HISPLOT_SETUP:N9PLR2
START/STOP TIME: 95/318/06:25:00.0 - 95/318/08:25:00.0

SCID: 09
PLOT CREATION DATE: 318/13:56:04
PLOT PRINT DATE: 319/20:19:07
SAMPLING PERIOD: 000/00:00:08.00

Y-DATA	CHAN	UNITS	TYPE	VS	X_DATA	CHAN	UNITS	TYPE	SYM	GPH
CSALOWT	FSATO	DEG	EU		TIME		HRS		—	1
CSAHIT	FSATO	DEG	EU		TIME		HRS		—	1
NPSEBUSI	**FA296**	**AMP**	**EU**		**TIME**		**HRS**		**—**	**2**
NPSEBUSV	FA153	VOL	EU		TIME		HRS		—	2

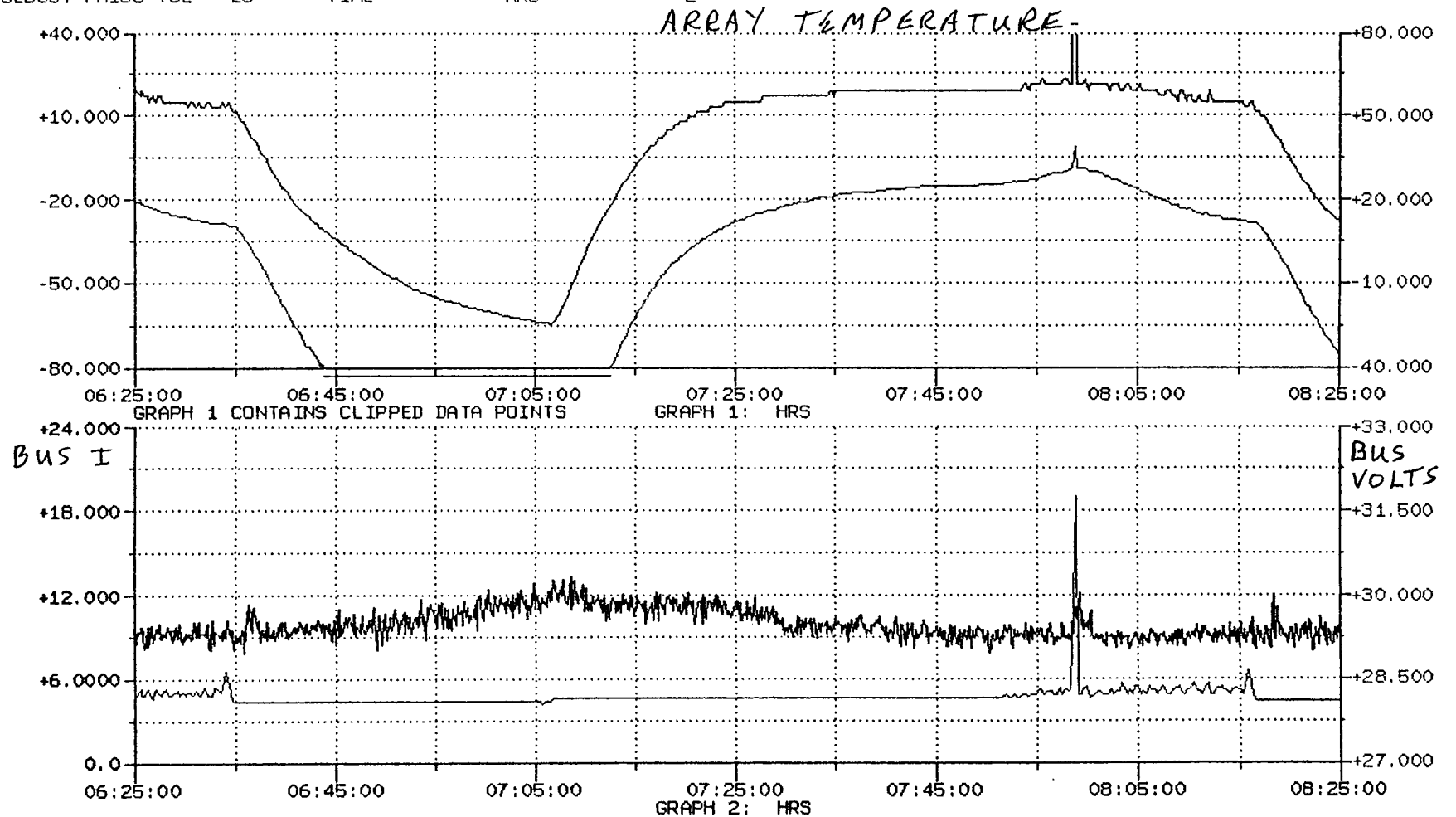

NOAA-9

- N0AA-9 POWER PLOT #3
- BATTERY #1 ORBIT SIGNATURE
  - VOLTS
  - DISCHARGE I
  - RECHARGE I
- NOT POSSIBLE TO RECHARGE DUE TO FAILED CHARGE REGULATORS- PRIME AND BACKUP

NOAA - LOCKHEED MARTIN Eng. Support

PLOT NAME: NRT_OPS$HISPLOT_PLOT:N9PPLT3
TITLE: N9PLR3
DESCRIPTION: NOAA-9 POWER PLOT #3
SETUP FILENAME: NRT_OPS$HISPLOT_SETUP:N9PLR3
SCID: 09
PLOT CREATION DATE: 318/13:58:20
PLOT PRINT DATE: 318/14:55:36
SAMPLING PERIOD: 000/00:00:08.00
SIARI/STOP TIME: 95/318/06:25:00.0 - 95/318/08:25:00.0

Y-DATA	CHAN	UNITS	TYPE	VS	X_DATA	CHAN	UNITS	TYPE	SYM	GPH
NBAT1V	FA480	VOL	EU		TIME		HRS		—	1
NBAT1DCH	FA332	AMP	EU		TIME		HRS		—	1
NBAT1CHI	FA300	AMP	EU		TIME		HRS		—	1

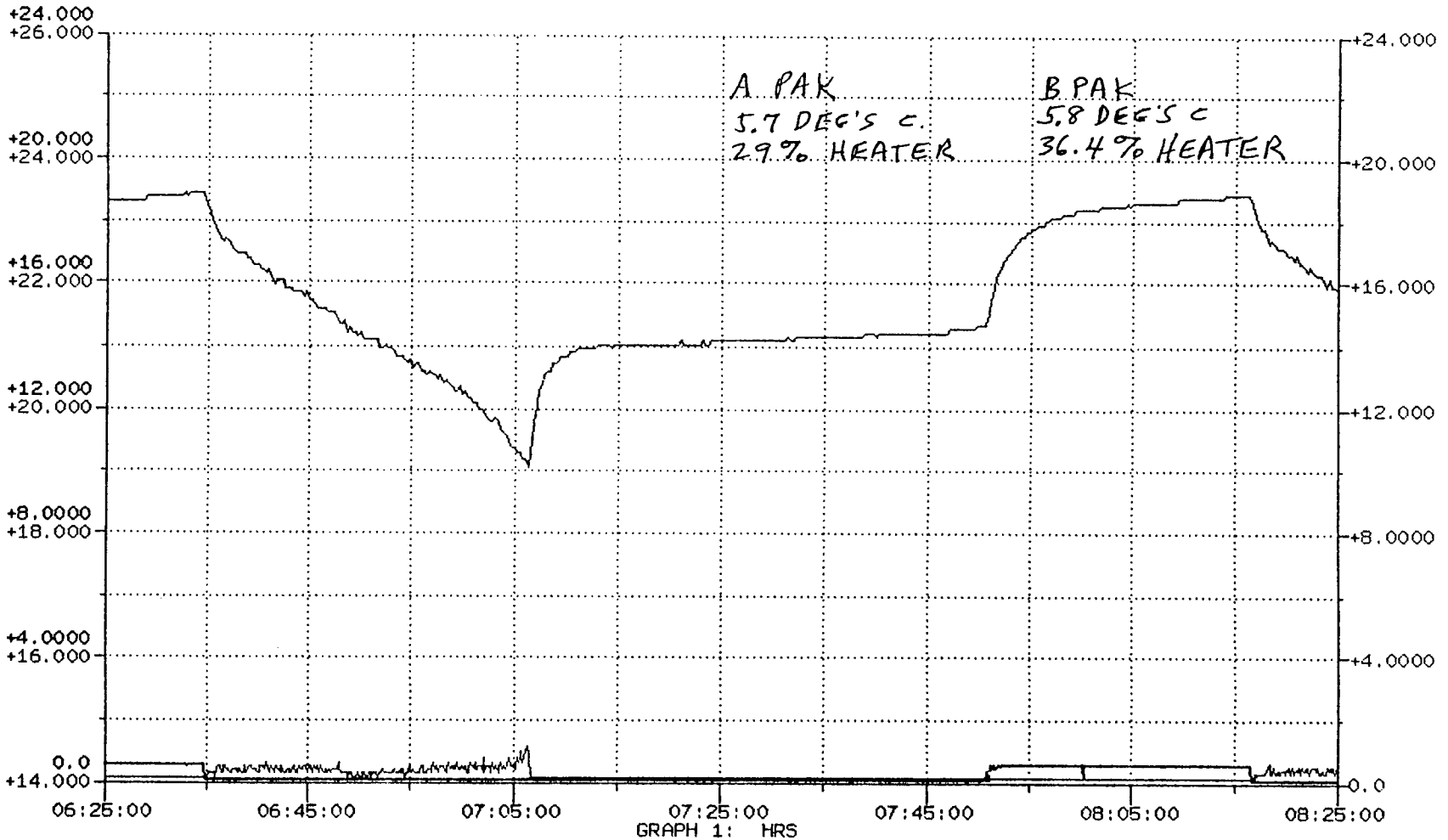

NOAA-9

- N0AA-9 POWER PLOT #4
  BATTERY #2 ORBIT SIGNATURE
- POOR DISCHARGE CHARACTER
- ABNORMAL RECHARGE SIGNATURE
  RECHARGE (AGAIN) LIMITED BY Stored Command Table
- HIGH C/D (~1.3 TO 1)

NOAA - LOCKHEED MARTIN Eng. Support

PLOT NAME: NRT_OPS$HISPLOT_PLOT:N9PPLT4
TITLE: N9PLR4
DESCRIPTION: NOAA-9 POWER PLOT 4
SETUP FILENAME: NRT_OPS$HISPLOT_SETUP:N9PLR4
SIARI/SIOP TIME: 95/318/06:25:00.0 - 95/318/08:25:00.0

SCID: 09
PLOT CREATION DATE: 318/14:00:05
PLOT PRINT DATE: 318/14:56:13
SAMPLING PERIOD: 000/00:00:08.00

Y-DATA	CHAN	UNITS	TYPE	VS	X_DATA	CHAN	UNITS	TYPE	SYM	GPH
NBAT2V	FA488	VOL	EU		TIME		HRS		—	1
NBAT2DCH	FA348	AMP	EU		TIME		HRS		—	1
NBAT2CHI	FA316	AMP	EU		TIME		HRS		—	1

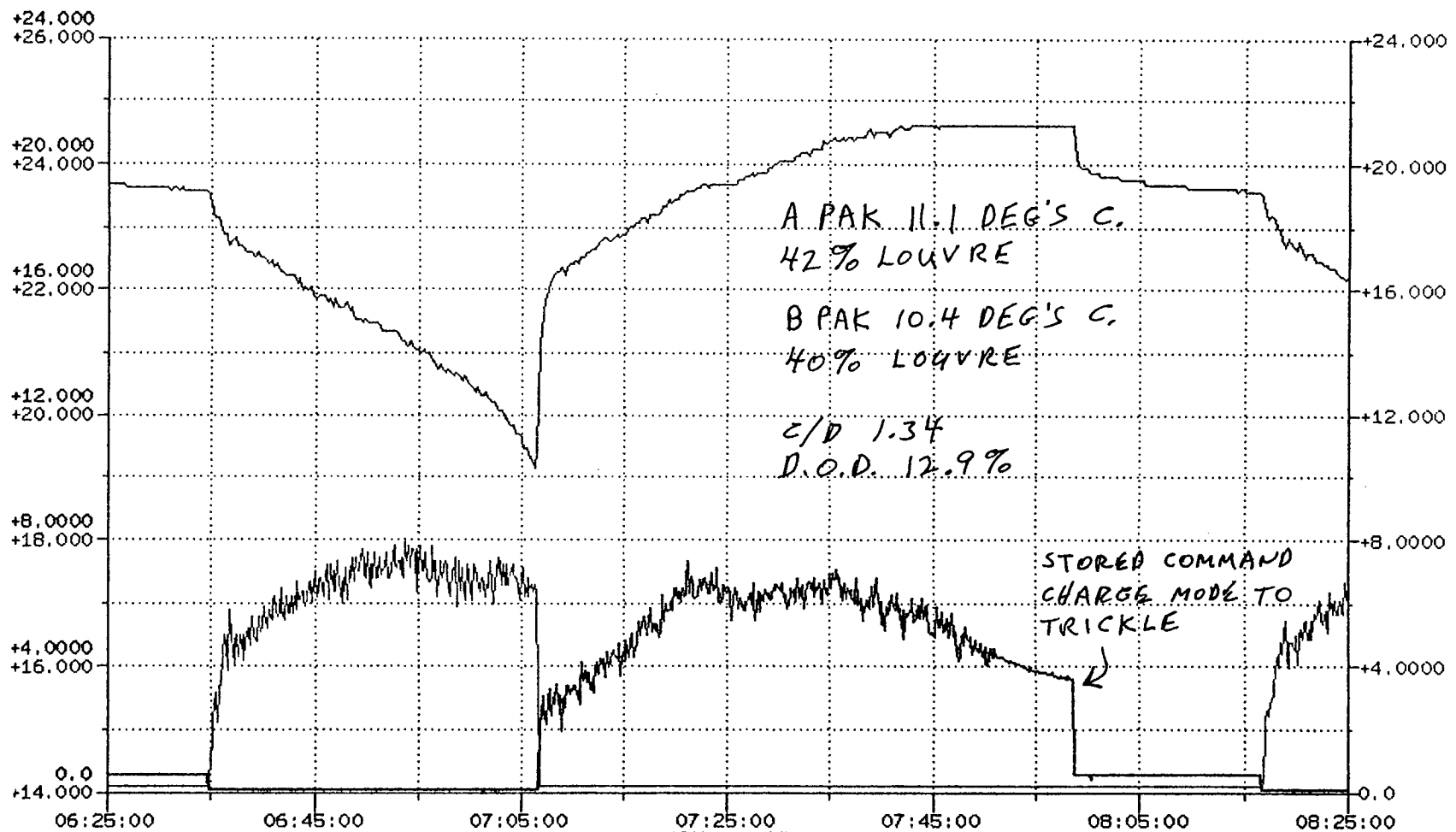

NOAA-9

- N0AA-9 POWER PLOT #5
- BATTERY #3 ORBIT SIGNATURE
- MAKES UP FOR POOR SIGNATURES OF BATTERY #2
- MAXIMUM ARRAY OFFSET (BY SADBIAS SOFTWARE)MUST BE LIMITED TO MAINTAIN CHARGE STATE OF THIS BATTERY.

- This battery has never exibited the overcharge characteristics that plague batteries 1 & 2. This battery was assembled from "lot 11" cells.

  One battery on NOAA-11 and three batteries on NOAA-10 were assembled from this lot and exhibit similar characteristsics.

NOAA - LOCKHEED MARTIN Eng. Support

PLOT NAME: NRT_OPS$HISPLOT_PLOT:N9PPLT5
TITLE: N9PLR5
DESCRIPTION: NOAA-9 POWER PLOT 5
SETUP FILENAME: NRT_OPS$HISPLOT_SETUP:N9PLR5
START/STOP TIME: 95/318/06:25:00.0 - 95/318/08:25:00.0

SCID: 09
PLOT CREATION DATE: 318/14:01:52
PLOT PRINT DATE: 318/14:56:46
SAMPLING PERIOD: 000/00:00:08.00

Y-DATA	CHAN	UNITS	TYPE	VS	X_DATA	CHAN	UNITS	TYPE	SYM	GPH
NBAT3V	FA472	VOL	EU		TIME		HRS			1
NBAT3DCH	FA284	AMP	EU		TIME		HRS			1
NBAT3CHI	FA276	AMP	EU		TIME		HRS			1

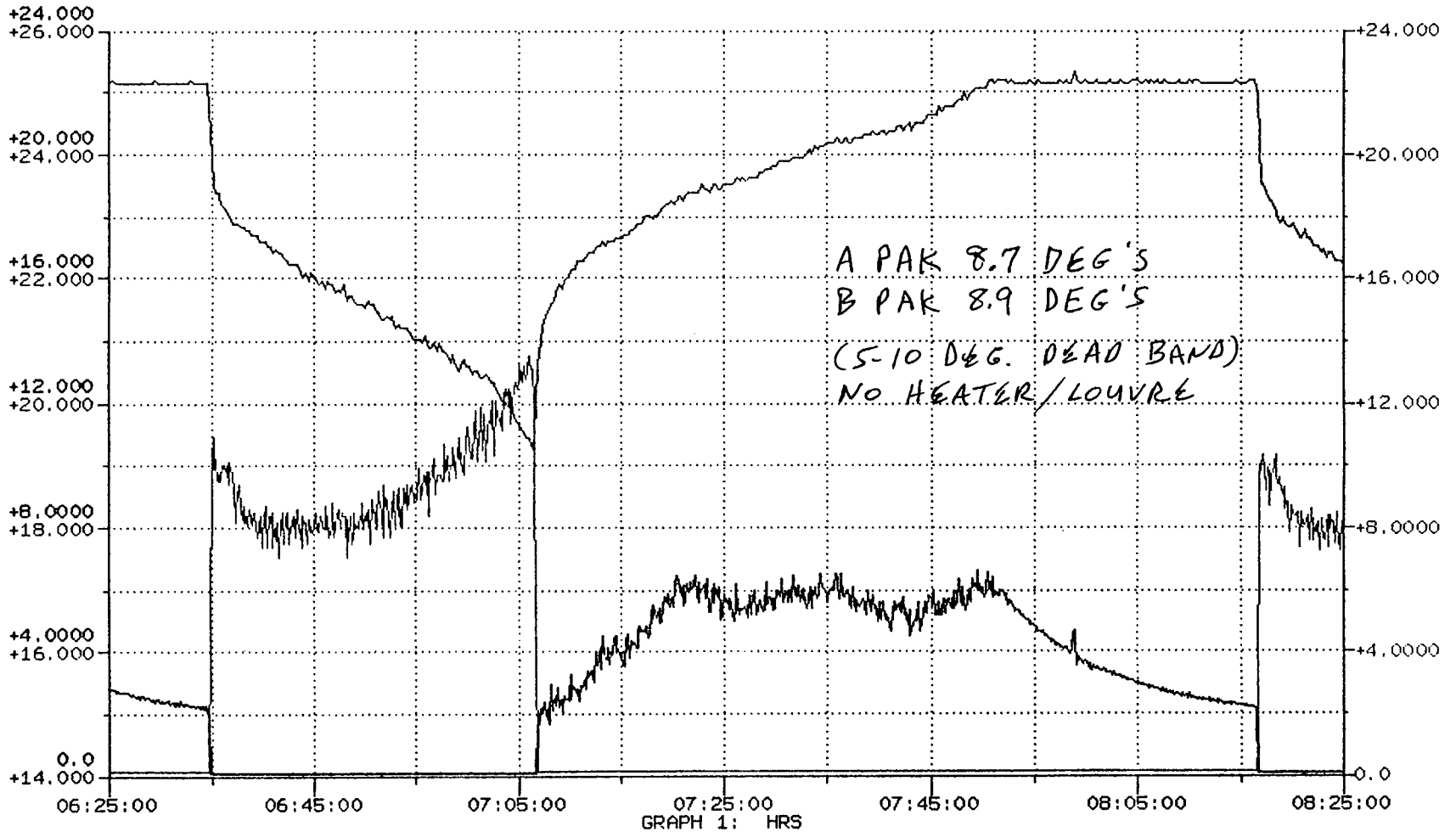

NOAA-9

- 12 HOUR PLOT OF BATTERY VOLTAGES
  INDICATES MINIMUM END OF NIGHT VOLTAGE
- MAXIMUM ARRAY CURRENT SIGNATURE
- MINIMUM END OF NIGHT VOLTS EVERY FOURTH REV.
  CAUSED BY TRANSMITTER AND RECORDER LOADS
  DURING DATA PLAYBACK

NOAA - LOCKHEED MARTIN Eng. Support

PLOT NAME: NRT_OPS$HISPLOT_PLOT:N9BATTV
TITLE: BATTERY VOLTS
DESCRIPTION: 12 HOUR PLOT
SETUP FILENAME: NRT_OPS$HISPLOT_SETUP:BATTERY
SCID: 09
PLOT CREATION DATE: 319/20:22:09
PLOT PRINT DATE: 319/20:32:09
SAMPLING PERIOD: 000/00:00:32.00
SIARI/SIOP TIME: 95/318/00:00:00.0 - 95/318/12:00:00.0

Y-DATA	CHAN	UNITS	TYPE	VS	X_DATA	CHAN	UNITS	TYPE	SYM	GPH	Y-DATA	CHAN	UNITS	TYPE	VS	X_DATA	CHAN	UNITS	TYPE	SYM	GPH
NBAT1V	FA480	VOL	EU		TIME		HRS			1											
NBAT2V	FA488	VOL	EU		TIME		HRS			1											
NBAT3V	FA472	VOL	EU		TIME		HRS			1											
NSADARRI	FA256	AMP	EU		TIME		HRS			1											

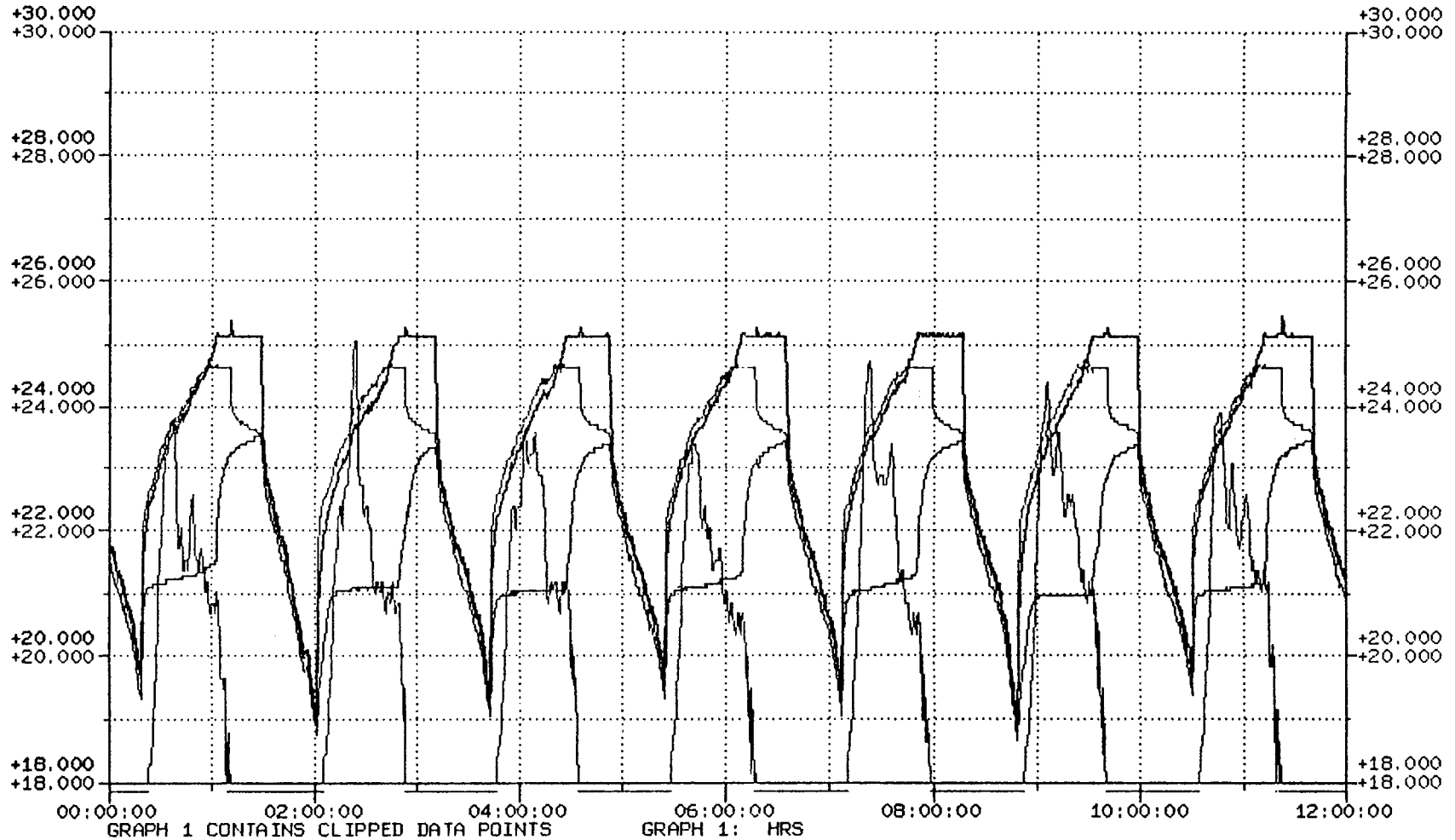

NOAA-9

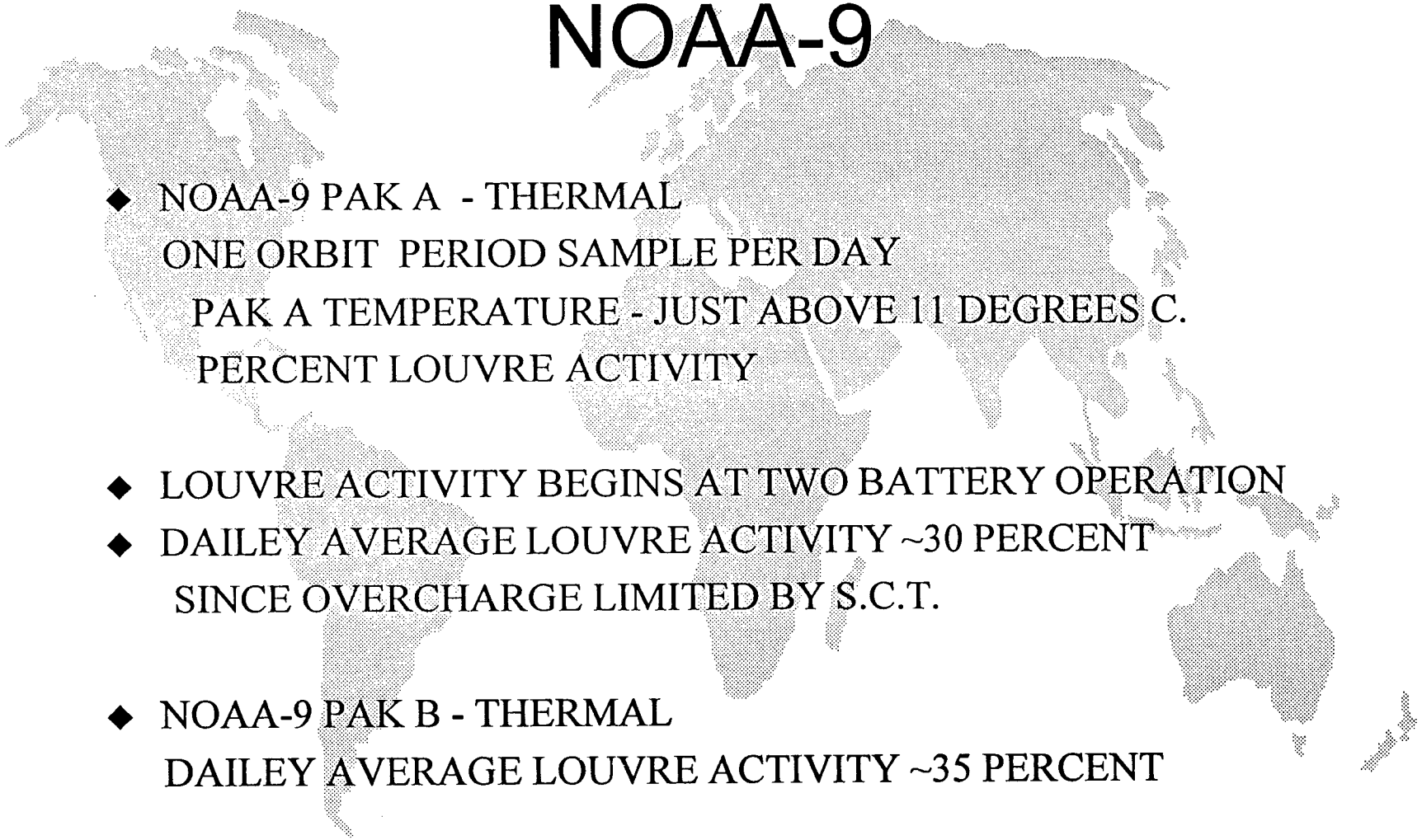

- NOAA-9 PAK A - THERMAL
  ONE ORBIT PERIOD SAMPLE PER DAY
  PAK A TEMPERATURE - JUST ABOVE 11 DEGREES C.
  PERCENT LOUVRE ACTIVITY

- LOUVRE ACTIVITY BEGINS AT TWO BATTERY OPERATION
- DAILEY AVERAGE LOUVRE ACTIVITY ~30 PERCENT
  SINCE OVERCHARGE LIMITED BY S.C.T.

- NOAA-9 PAK B - THERMAL
  DAILEY AVERAGE LOUVRE ACTIVITY ~35 PERCENT

NOAA - LOCKHEED MARTIN Eng. Support

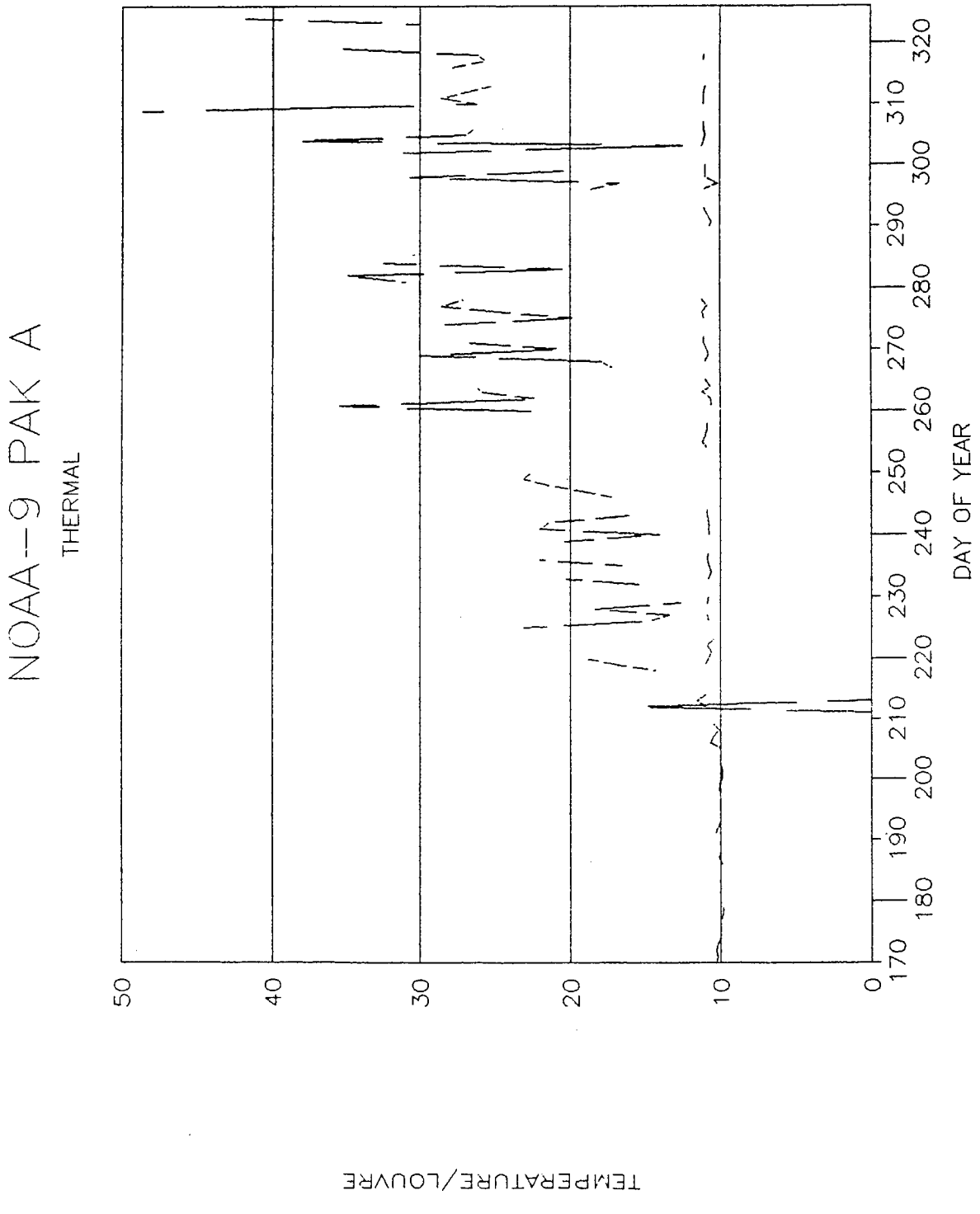
NOAA-9 PAK A
THERMAL
TEMPERATURE/LOUVRE
DAY OF YEAR
50
40
30
20
10
0
170
180
190
200
210
220
230
240
250
260
270
280
290
300
310
320

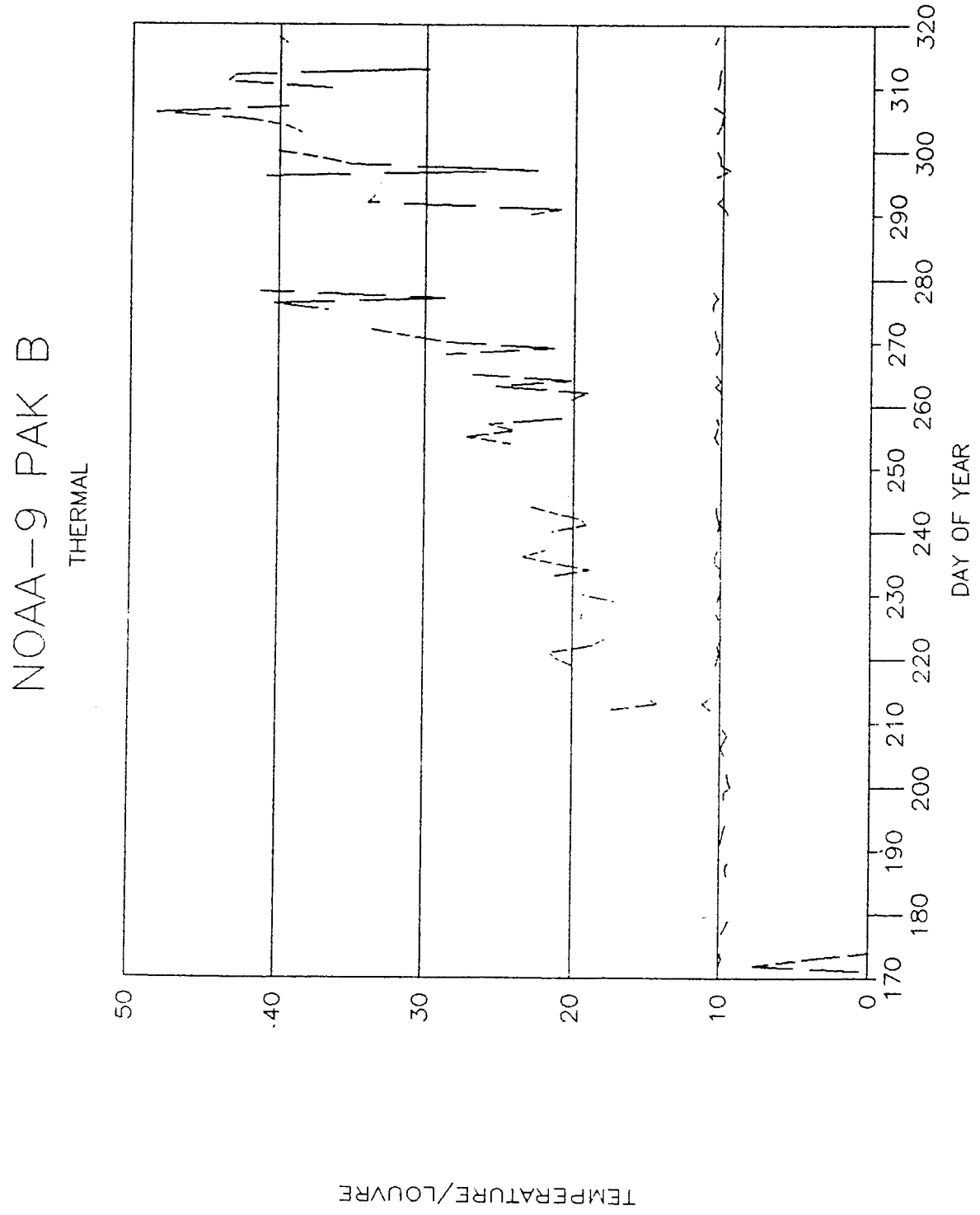
NOAA-9 PAK B
THERMAL
TEMPERATURE/LOUVRE
DAY OF YEAR
50
40
30
20
10
0
170
180
190
200
210
220
230
240
250
260
270
280
290
300
310
320

NOAA-9

- NOAA-9 BATT.#2 - C/D RATIO
  LARGE VARIATIONS CAUSED BY SINGLE ORBIT DATA
  AVERAGE C/D ~1.3

- DECREASE IN D.O.D. (BUS LOAD) CAUSE HARDWARE FAILURES OF 2 OCT. 1995 - BETWEEN D.O.Y 200 & 210

- NOAA-9 BATT.#2 AND #3 - DEPTH OF DISCHARGE
  INCREASE IN D.O.D. DUE TO TWO BATTERY OPERATION
  DECREASE OF BATTERY TWO DISCHARGE

NOAA - LOCKHEED MARTIN Eng. Support

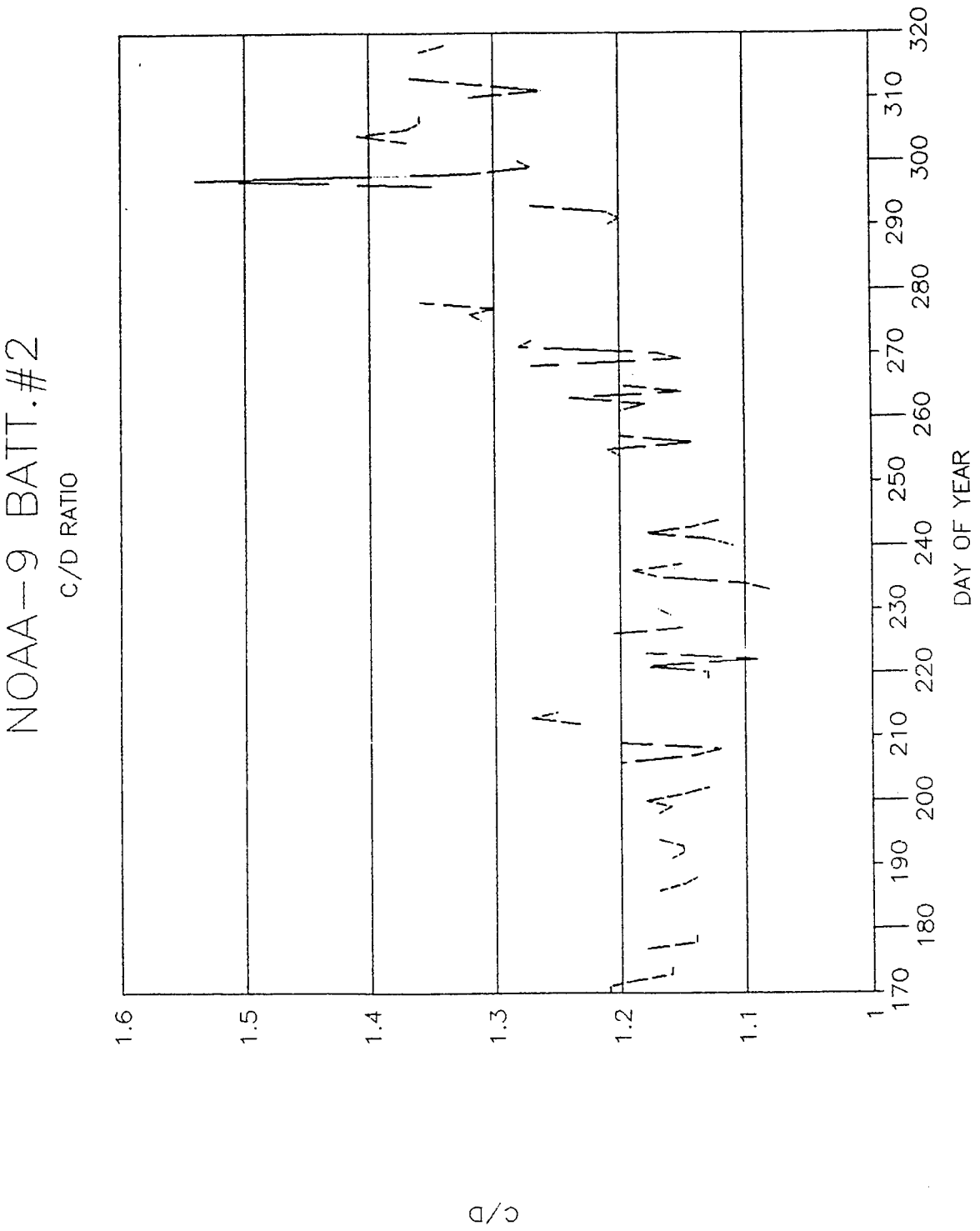
NOAA-9 BATT.#2
C/D RATIO
1.6
1.5
1.4
1.3
1.2
1.1
1
170
180
190
200
210
220
230
240
250
260
270
280
290
300
310
320
DAY OF YEAR
C/D

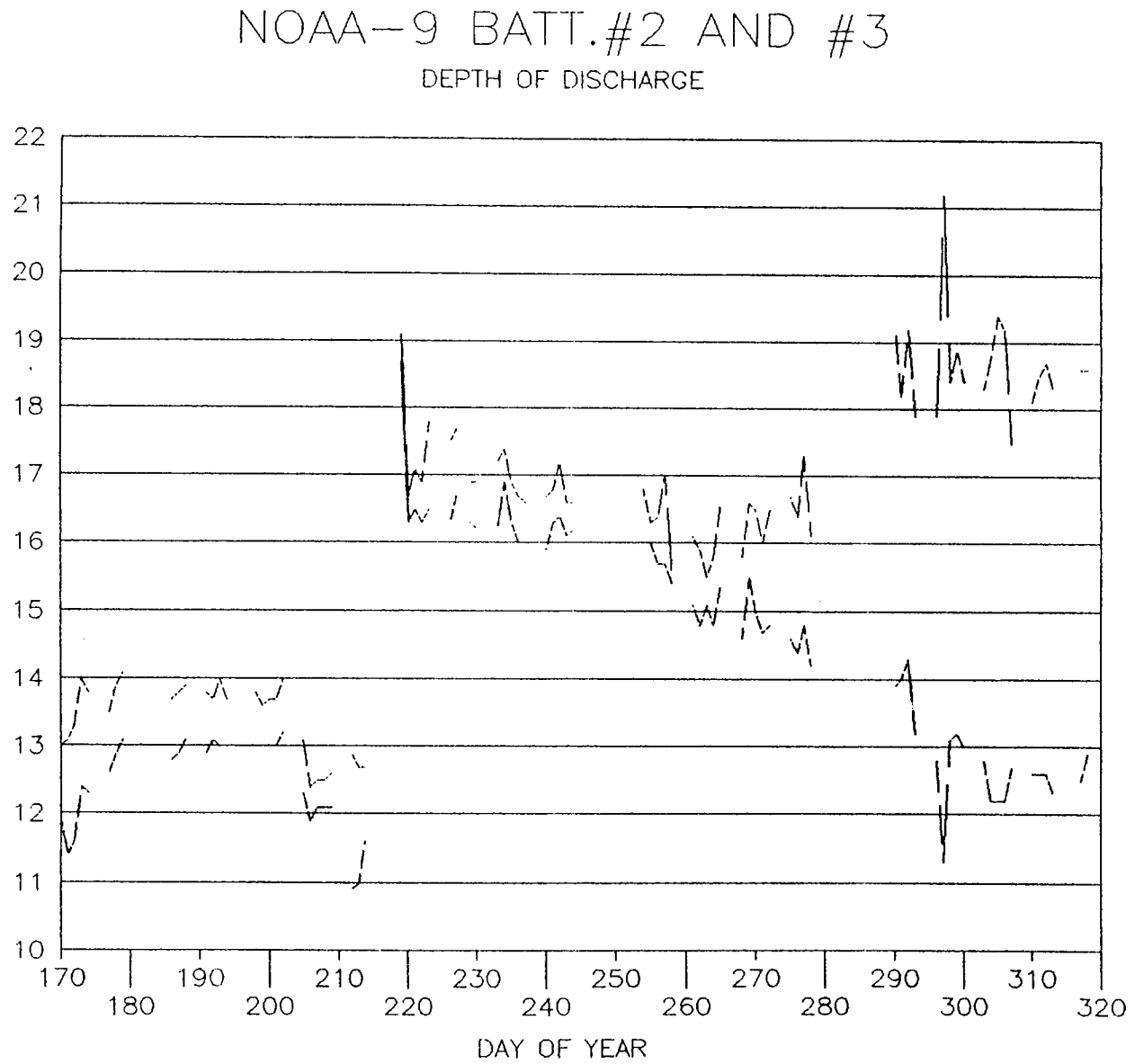
NOAA-9 BATT.#2 AND #3
DEPTH OF DISCHARGE
D.O.D. PERCENT OF 26.5
22
21
20
19
18
17
16
15
14
13
12
11
10
170
180
190
200
210
220
230
240
250
260
270
280
290
300
310
320
DAY OF YEAR

Nickel-Hydrogen Session

High Energy Density Micro-Fiber Based Nickel Electrode For Aerospace Batteries

Jennifer Franciso, Dennis Chiappetti and Dwaine Coates
Eagle-Picher Industries, Inc.
Joplin, Missouri

Abstract

The nickel electrode is the specific energy limiting component in battery systems such as nickel-hydrogen, nickel-metal hydride and nickel-zinc. Lightweight, high energy density nickel electrodes have been developed which deliver in excess of 180 mAh/g at the one-hour discharge rate. These electrodes are based on a highly porous, nickel micro-fiber (< 10 micron diameter) substrate, electrochemically impregnated with nickel-hydroxide active material. Electrodes are being tested both as a flooded half-cell and in full nickel-hydrogen and nickel-metal hydride cells. The electrode technology developed is applicable to commercial nickel-based batteries for applications such as electric vehicles, cellular telephones and laptop computers and for low-cost, high energy density military and aerospace applications.

Introduction

The nickel electrode is currently the specific energy limiting component in nickel-based battery systems. The focus of the present work is to develop an aerospace flight qualified nickel electrode. Rapid growth in earth-orbital satellite applications, including small satellites, and increasing spacecraft power system performance requirements have created a need for improved flight-qualified nickel-hydrogen (NiH_2) battery technology. However, these performance improvements must not compromise the inherent safety or reliability of the NiH_2 battery. A concerted effort is currently underway to improve NiH_2 performance while decreasing system cost. This effort involves work at the component, cell and full battery level. Component level development work includes performance enhancement and cost reduction at the basic electrode level, including the nickel/nickel-hydroxide electrode. Increased performance, with electrode specific energy (mAh/g) as the primary figure of merit, is the major goal of this effort. However, cost reduction is also an important part of the overall program.

Nickel/Nickel-Hydroxide Electrodes

There is considerable literature available on the nickel electrode in general. Several papers have been published on fiber-type nickel electrodes specifically *(1-4)*. Eagle-Picher has done considerable work in the past on fiber nickel electrodes *(5, 6)* and in conjunction with specific battery R&D programs *(7)*. To date, the active material loading obtained typically with fiber-based substrates has been relatively low. An additional problem is that the active material utilization has also typically been low. This results in an electrode with a relatively low specific energy (in terms of milliampere-hours per gram), even though the fiber substrate is lighter in weight than sintered nickel powder. The low loading and low utilization problems associated with previous fiber-based electrode substrate technology have been solved through a unique approach.

Nickel Electrode Substrate Material

Traditional aerospace qualified nickel electrodes use a sintered carbonyl nickel powder as the electrode substrate. This material forms a rigid, highly porous matrix into which the nickel-hydroxide active material can be introduced. Sintered nickel powder is very strong and dimensionally stable, but it contributes adversely to the overall electrode weight. This type of substrate may account for more than 50% of the total weight in a typical aerospace nickel electrode. A light weight substrate would greatly improve the electrode specific energy. The approach used in this development effort has been to utilize fiber-based nickel electrode substrates, prepared using proprietary micro-diameter metal fiber technology. This material is superior to prior fiber substrates based on the smaller fiber diameter, smaller equivalent pore size and dimensional stability. Two vendors which produce such substrates are Memtec America Corp. and Ribbon Technology Corp.

Electrode Active Material Impregnation

In order to form a working nickel electrode, nickel-hydroxide active material must be inserted into the porous substrate material. Aerospace applications, particularly space NiH_2 batteries, are the primary application for which this work is being performed. Therefore, the nickel-hydroxide active material insertion method primarily being investigated is a close

JF110895.PM5

variation of the aerospace electrochemical impregnation method. It is somewhat based on the nitrate reduction process, which has been previously described in the literature, with some important modifications. In general, the porous electrode substrate is cathodically polarized in a bath of aqueous nickel-nitrate. Process parameters such as temperature, flow, current density, solution concentrations, pH, additive concentrations and other parameters are precisely controlled with specified limits.

Electrochemical Impregnation Results

A wide variety of substrate samples have been impregnated under a variety of conditions, yielding equally diverse results. Typical electrode specific energy values obtained range from less than 100 milliampere-hours per gram (mAh/g) to more than 180 mAh/g. Other performance factors, such as dimensional stability, also vary over a wide range, depending on specific substrate and impregnation parameters. Initial microfiber substrate parameters are indicated for several different samples in Tables 1 and 3. The column labeled "Standard" is similar data for a standard aerospace grade nickel electrode. The sample physical size was four square inches (two inches by two inches). The initial substrate thickness was measured in five places using a dial micrometer. The average initial substrate thickness is indicated along with the standard deviation, which is a measure of substrate thickness uniformity. The substrate volume is simply based on the area multiplied by the thickness. The sample bulk porosity is calculated from this value, the substrate weight and the density of nickel (8.9 g/cc). The substrate porosity is defined as the ratio of void volume to electrode volume, expressed as a percentage.

Tables 2 and 5 indicate a similar set of electrode parameters after the electrochemical impregnation. The sample area is constant since there is no measurable change in the XY plane of the substrate. The thickness, however, does increase during the impregnation process. This is the result of filling the substrate voids with nickel-hydroxide active material. The substrate is dimensionally stable in the XY plane because of the way that the fibers are randomly oriented in this plane during the layering process. They are essentially interwoven in interlocking layers. The substrate is much less stable in the Z direction perpendicular to the electrode plane. Even though the substrate is sintered to provide additional strength in this direction, the forces involved in the active material changes that occur cannot be completely overcome. One of the major factors affecting ultimate electrode performance is this propensity towards thickness growth. Minimizing this effect is essential, particularly for a long life aerospace application, and is one of the major goals of the current study.

As shown in Tables 2 and 5, the impregnated electrode thickness increases from 9.6% for Sample G up to 61% for Sample A. This is considerably more than the corresponding increase observed in aerospace sintered powder electrodes. When the green electrodes are formed, additional thickness growth occurs as the result of active material expansion during the charge/discharge process. This ranges from less than 1.0% for Sample F up to 23% for Sample G (based on the percentage increase as compared to the impregnated thickness). This data shows that most of the thickness increase observed during electrode manufacturing occurs during the actual impregnation process step rather than during the electrical cycling formation step. For example, 94% of the total thickness increase in Sample F was due to the impregnation step (percentage of total thickness increase). This ranges down to only 27% for Sample G. The total increase in thickness for each finished electrode sample (due to both impregnation and formation) is also indicated and ranges from 9.6% for Sample J up to 82% for Sample A (based on the percentage compared to the initial unimpregnated thickness). In general, higher thickness growth is experienced with fiber electrodes than with sintered aerospace nickel electrodes. Considerable progress has been made in optimizing fiber substrate parameters to minimize this growth. Early electrode designs grew in thickness as much as 90% while more recent design iterations have been reduced to below 10%. While excessive thickness increase is not desirable, it is not necessarily prohibitive in an electrolyte starved compressed cell stack design, such as the NiH_2 cell. Some electrode thickness increase can be accommodated in the cell design.

Tables 3 and 6 show weight pick-up and active material loading data. Some active material weight is typically lost during the formation process due to simple extrusion and expulsion through vigorous gas evolution reactions that occur during the electrical cycling. Also, any surface loading is easily lost during this step. In some respect the measure of weight loss during formation is indicative of the efficacy of the impregnation step. A lower weight loss in formation indicates that the active material is more tightly held in the substrate pores and is not as easily lost during electrical cycling in KOH. The active material weight loss during formation (expressed as a percentage of the green impregnated pick-up) varies from 1.65% for Sample C up to 66% for Sample G. The final active material loading (grams of active material per cubic centimeter of electrode void volume) is calculated from the difference in the substrate weight and the final weight after formation. The actual grams of active material loaded into the substrate can be very accurately determined on an analytical balance. Finished loading ranged from 0.52 for Sample G up to 1.71 for Sample C.

The electrode flooded capacity is determined by cycling in KOH. The electrode is charged at a constant C/2 rate until 150% overcharge is reached. The electrode is then discharged at constant current at the C/2 rate and the time measured rela-

JF110895.PM5

tive to an end voltage (typically -1.2 VDC versus the nickel counter-electrode). The electrical capacity is then expressed in milliampere-hours. The electrode theoretical capacity is calculated from the finished active material weight in grams multiplied by 0.289 Ah/g, which is the theoretical energy density of the nickel-hydroxide electrochemical reaction, based on a one electron reaction (Ni^{++}/Ni^{+++}). The utilization is calculated based on the ratio of the actual capacity to the theoretical capacity, expressed as a percentage. State-of-the-art aerospace electrodes manufactured by Eagle-Picher typically yield about 120% of theoretical under these test conditions. This attests to the efficiency of the electrochemical impregnation process. Low utilization has typically been one of the major disadvantages of fiber substrates in the past (along with excessive active material bleeding and thickness growth). The utilization problem has been essentially solved during the development phase of this program. Fiber electrodes currently being developed are routinely yielding over 100% utilization.

The single biggest disadvantage of the nickel electrode in general can be conveniently expressed in terms of the ratio of active material in the electrode to inactive material in the electrode. In a state-of-the-art sintered nickel powder aerospace electrode, about 63% of the total weight of the nickel electrode is electrochemically inactive. This weight is comprised of the sintered nickel powder substrate and the nickel wire mesh current collector. These components provide no energy storage capacity in the electrode. Correspondingly only 37% of the electrode weight is electrochemically active material. This is the reason that although the active material has a theoretical energy density of 289 mAh/g, the nickel electrode is much lower, e.g. 120 mAh/g, which is about 42% of theoretical. By comparison, fiber nickel electrodes are up to 60% active mass. This corresponds to an electrode specific energy of 180 mAh/g, or about 62% of the theoretical specific energy of pure nickel active material. An increase in specific energy from 120 to 180 mAh/g, 42% to 62% of theoretical, makes a very significant increase in overall specific energy at the full cell and battery level. The fiber-based electrode therefore has the potential of significantly increasing the specific energy of the nickel-hydrogen cell.

Nickel-Hydrogen Cell Performance

Sample fiber-based nickel electrodes were built into sealed NiH_2 cells for performance analysis and testing. Standard flight quality NiH_2 cell components were used to insure that the nickel electrode was the only component variable. The cells were assembled in boilerplate pressure containment vessels which closely simulate the actual flight NiH_2 cell configuration. The cells were activated with 31% aqueous KOH. The cells were designed to be nickel electrode limited by supplying a hydrogen overcharge to the cell. The quantity of excess hydrogen active material, i.e. the hydrogen pressure precharge, was varied from 20 psi to 150 psi in order to investigate the effect of cell operating pressure on nickel electrode performance. A variety of electrical testing was performed, including charging and discharging at a wide variety of rates. Standard low-earth-orbit (LEO) cycling was also performed in order to characterize cell performance under a standard test regime.

Figure 1 shows a set of charge curves at constant current rates varying from 0.094C to 1.0 C. Full cell voltage (the nickel electrode versus the hydrogen electrode) is plotted as a function of state-of-charge (SOC), expressed as a percentage of full charge. The cell was charged on each test to about 150% to 160% SOC, corresponding to 50 to 60% overcharge. The charges were done at the indicated hydrogen precharge, either 20 psi or 50 psi. The test was done at ambient room temperature with no means of active cooling. There may be some thermal effects at the higher rates, however these effects are minimized by the large thermal mass of the boilerplate pressure vessel. This set of data characterizes the charge impedance and oxygen evolution characteristics of the nickel electrode. In general, the cell charges at a much lower full cell voltage than a standard nickel-hydrogen cell. This is, in part, because the cell is being operated at relatively low hydrogen pressure compared to a standard spaceflight cell. The cell voltage is a function of hydrogen pressure (per the Nernst Equation). The fiber nickel electrode shows very good charge efficiency over a wide range of charge rates, up to the one hour rate. Higher charge rates are yet to be investigated.

Figure 2 shows comparable discharge data. Full cell voltage is plotted as a function of the nickel electrode specific energy. Each test was performed at a constant 50 psi hydrogen to remove pressure as a variable and to insure that the cell remained nickel electrode limited. All testing was done at room temperature with no active cooling to the cell. Each discharge was performed at the indicated rate at constant current. Each discharge was preceded by a 0.1 C charge to 150% overcharge to eliminate any effects of charging on the subsequent discharge. The cell was discharged at rates ranging from 0.25 C (4 hour rate) up to 1.25 C, which is less than a one hour discharge. There is considerable variation in cell capacity at the different rates, which is normal for any type of battery. The nickel electrode delivers 160 mAh/g at the lowest rate and 100 mAh/g at the highest rate. At the standard 0.5 C discharge rate the electrode delivers about 150 mAh/g which is considerably better than a standard aerospace sintered electrode.

Figure 3 shows four discharge curves, plotting cell voltage versus discharge capacity (mAh/g). Each discharge was done at the 0.5 C constant current discharge rate and at a constant cell overpressure of 50 psi of hydrogen. Again, all testing was done at room ambient temperature. The charge current, prior to each discharge, was varied from 0.1 C to 1.0 C

JF110895.PM5

in order to investigate the effect of charge current on discharge performance. Each charge was performed at the indicated constant current rate to 150% overcharge, based on the cell discharge capacity. The data indicates that charge current has very little effect on the fiber nickel electrode charge efficiency. A cell charged in 1.5 hours at a high rate delivers nearly the same discharge capacity as the same cell charged at a low rate overnight for 15 hours. This shows excellent charge efficiency for the fiber nickel electrode (the limiting cell component in this case). The cell discharge plateau voltage remains unaffected by the charge rate.

Conclusion

Most of the specific work done was primarily directed towards aerospace nickel-hydrogen batteries. However, the nickel electrode technology developed is usable in a wide variety of nickel battery types for a wide range of applications. The traditional problems associated with fiber electrode substrates, such as low active material loading and low active material utilization, have been overcome. Optimized electrode substrate microstructure, micro-fiber diameters, small equivalent pore size and mat layering techniques have greatly improved the fiber electrode substrate. The electrochemical impregnation process allows more efficient active material loading into the substrate and yields higher active material utilization. Electrodes yielding up to 180 milliampere-hours per gram, with utilizations of more than 100% have been prepared on a laboratory scale. Scale-up to full flight-weight nickel-hydrogen cells is underway.

References

1. *Metal-Carbon Composite Electrodes From Fiber Precursors*, Kohler, D. A., et.al., 24th IECEC, 1989, p.1441.

2. *Characterization and Cycle Tests of Lightweight Nickel Electrodes*, D.L. Britton, ECS Proceedings Volume 90-4, 1990.

3. *Development of Lightweight Nickel Electrodes for Zinc/Nickel Oxide Batteries*, W. Taucher, et.al., 186th ECS Meeting, 1994.

4. *Connection of the Charge Efficiency and Self-Discharge of the Fibrous Nickel Electrode With the Structure of the Support*, R. Rouget, et.al., ECS Proceedings Volume 90-4, 1990.

5. *Development of Fiber-Based Nickel Hydroxide Electrodes for Nickel-Iron Batteries,* M.J. Vanderpool, et.al., ECS Proceedings Volume 90-4, 1990.

6. *Advances in Lightweight Nickel Electrode Technology*, D.K. Coates, et.al., Space Electrochemical Research and Technology, NASA Lewis, 1988.

7. *Advanced Dependent Pressure Vessel (DPV) Nickel-Hydrogen Spacecraft Battery Design*, D. Coates, et.al., 19th International Power Sources Symposium, 1995.

Figure 1. Fiber nickel electrode NiH_2 cell voltage as a function of charge current.

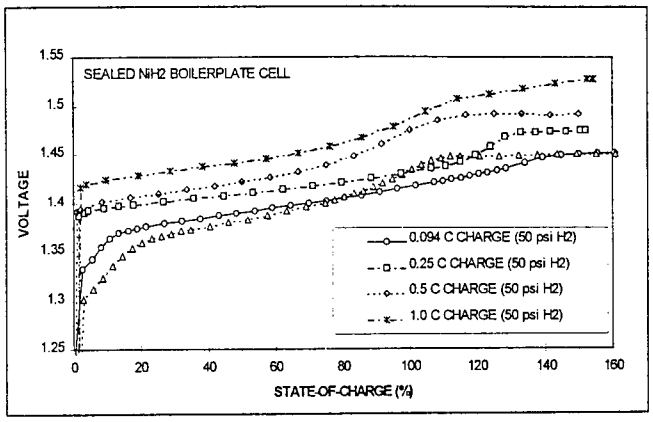

Figure 2. Fiber electrode specific energy as a function of discharge rate in a sealed NiH_2 cell.

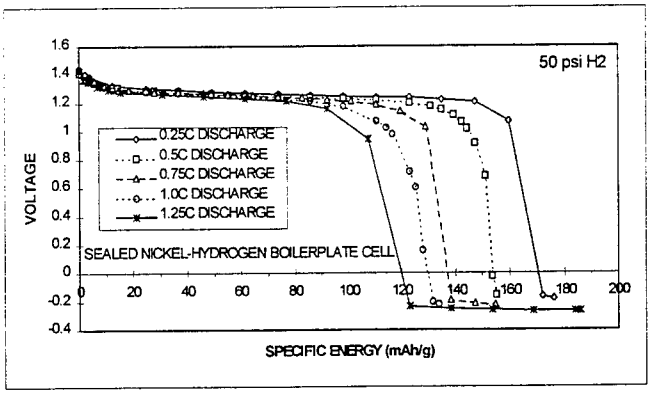

Figure 3. The effect of charging current on cell discharge voltage and capacity.

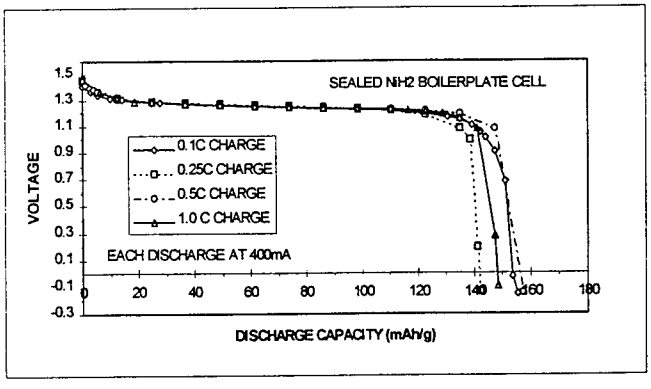

JF110895.PM5

Table 1 Initial Microfiber Substrate Parameters

	Standard	Sample A	Sample B	Sample C	Sample D
Approx. Size (in^2)	7.9	4	4	4	4
Initial Volume (cc)	3.88	1.45	1.152	1.483	1.396
Initial Porosity (%)	80.0	83.77	76.1	83.1	82.4
Initial Void Volume (ccvv)	2.94	1.21	0.877	1.22	1.15
Avg. Initial Thk. (in)	0.030	0.0221	0.0176	0.0226	0.0213
Std. Dev. (X1000)	na	0.33	0.44	1.04	1.86

Table 2 Microfiber Substrate Parameters After Electrochemical Impregnation and Formation Process

	Standard	Sample A	Sample B	Sample C	Sample D
Avg. Impreg. Thk. (in)	na	0.0356	0.0267	0.0289	0.0247
Std. Dev. (X1000)	na	3.75	2.24	2.46	2.58
Thk. Growth Imp. (in)	na	0.0135	0.0092	0.0063	0.0034
Thk. Growth Imp. (%)	na	61.09	52.1	27.9	16
Avg. Thk. Finished (in)	0.031	0.0402	0.0284	0.0308	0.0266
Std. Dev. (X1000)	na	4.57	3.35	2.68	3.17
Final Void Volume (cc)	3.05	2.40	1.59	1.77	1.34
Final Porosity (%)	80.0	91.08	85.22	87.6	84.5
Thk. Growth Formation (in)	na	0.0046	0.0017	0.0019	0.0019
Thk. Growth Formation (%)	na	12.92	6.4	6.5	8.9
Thk. Inc. Due to Imp (%)	na	74.59	84.3	77	64.2
Total Thk. Increase (in)	0.001	0.0181	0.0108	0.0082	0.0053
Total Thk. Inc. Finished (%)	5.88	81.90	61.6	36.2	24.9

Table 3 Active Material Weight Pick-up/Loading and Electrochemical Capacity/Utilization Data

	Standard	Sample A	Sample B	Sample C	Sample D
Init. Substrate Wt. (g)	8.61	2.0928	2.4488	2.2328	2.191
Impregnated (Green) Wt. (g)	na	na	5.2507	5.3091	4.4721
Impregnated Pick-up (g)	na	na	2.8019	3.0763	2.5511
Finished (Formed) Wt. (g)	13.64	5.7732	4.8889	5.2584	3.9215
Finished Pick-up (g)	5.03	3.6804	2.4401	3.0256	1.7305
Formation Wt. Loss (%)	na	na	12.9	1.65	12.3
Loading (g/ccvv)	1.65	1.53	1.53	1.71	1.29
Flooded Capacity (Ah)	1.74	1.04	0.75	0.74	0.5
Theoretical Capacity (Ah)	1.45	1.06	0.71	0.87	0.5
Utilization (%)	120	97.78	106	85.1	100
Active Mass (%)	36.87	63.75	49.9	57.5	44.1
Inactive Mass (%)	63.13	36.25	50.1	42.5	55.9
Specific Energy (mAh/g)	127.85	180.14	153.4	140.7	127.5
Energy Density (mAh/cc)	434.33	394.61	403	366	287

**na=not applicable*

JF110895.PM5

Table 4 Initial Microfiber Substrate Parameters

	Sample E	Sample F	Sample G	Sample H	Sample I	Sample J
Approx. Size (in^2)	4	4	4	4	4	4
Initial Volume (cc)	1.99	1.93	1.77	1.86	1.82	2.38
Initial Porosity (%)	83.06	83.23	84.41	84.08	88.51	85.04
Initial Void Volume (ccvv)	1.65	1.61	1.49	1.56	1.61	2.02
Avg. Initial Thk. (in)	0.0303	0.0295	0.027	0.0283	0.0278	0.0363
Std. Dev. (X1000)	0.33	2.36	1.56	na	na	na

Table 5 Microfiber Substrate Parameters After Electrochemical Impregnation and Formation Process

	Sample E	Sample F	Sample G	Sample H	Sample I	Sample J
Avg. Impreg. Thk. (in)	0.0354	0.0328	0.0296	na	na	na
Std. Dev. (X1000)	2.36	1.94	1.61	na	na	na
Thk. Growth Imp. (in)	0.0051	0.0033	0.0026	na	na	na
Thk. Growth Imp. (%)	16.83	11.19	9.63	na	na	na
Avg. Thk. Finished (in)	0.0396	0.033	0.0365	0.0376	0.0391	0.0398
Std. Dev. (X1000)	1.59	0.93	2.39	na	na	na
Final Void Volume (cc)	2.26	1.84	2.12	2.17	2.35	2.25
Final Porosity (%)	87.03	85.00	88.47	88.01	91.83	86.36
Thk. Growth Formation (in)	0.0042	0.0002	0.0069	na	na	na
Thk. Growth Formation (%)	11.86	0.61	23.31	na	na	na
Thk. Inc. Due to Imp (%)	54.84	94.29	27.37	na	na	na
Total Thk. Increase (in)	0.0093	0.0035	0.0095	0.0093	0.0113	0.0035
Total Thk. Inc. Finished (%)	30.69	11.86	35.19	32.86	40.65	9.64

Table 6 Active Material Weight Pick-up/Loading and Electrochemical Capacity/Utilization Data

	Sample E	Sample F	Sample G	Sample H	Sample I	Sample J
Init. Substrate Wt. (g)	2.9958	2.8873	2.4562	2.6294	1.8631	3.1681
Impregnated (Green) Wt. (g)	na	6.9453	5.6849	na	na	na
Impregnated Pick-up (g)	na	4.058	3.2287	na	na	na
Finished (Formed) Wt. (g)	6.6584	5.0933	3.5555	5.9915	4.925	6.1871
Finished Pick-up (g)	3.6626	2.206	1.0993	3.3621	3.0619	3.019
Formation Wt. Loss (%)	na	45.64	65.95	na	na	na
Loading (g/ccvv)	1.62	1.20	0.52	1.55	1.30	1.34
Flooded Capacity (Ah)	0.87	0.87	0.56	1.02	0.93	0.96
Theoretical Capacity (Ah)	1.06	0.64	0.32	0.97	0.88	0.87
Utilization (%)	82.19	136.46	176.27	104.98	105.10	110.03
Active Mass (%)	55.01	43.31	30.92	56.11	62.17	48.80
Inactive Mass (%)	44.99	56.69	69.08	43.89	37.83	51.20
Specific Energy (mAh/g)	130.66	170.81	157.50	170.24	188.83	155.16
Energy Density (mAh/cc)	335.11	402.13	234.02	413.78	362.80	367.92

**na=not applicable*

JF110895.PM5

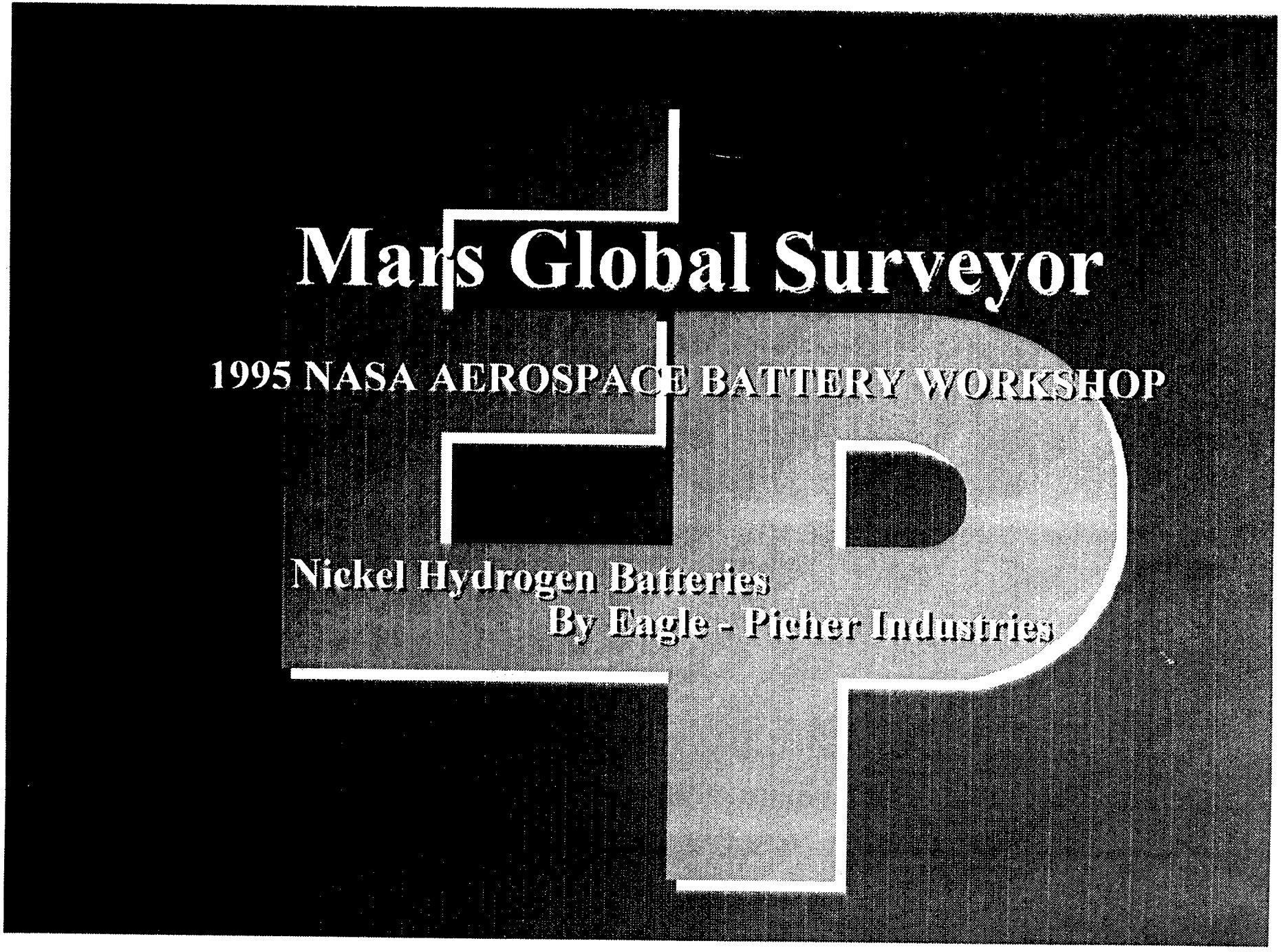
Mars Global Surveyor
1995 NASA AEROSPACE BATTERY WORKSHOP
Nickel Hydrogen Batteries
By Eagle - Picher Industries

EAGLE PICHER
NASA Battery Conference

Mars Global Surveyor

Presentation

- MARS GLOBAL SURVEYOR
- TWO CELL CPV DESIGN SUMMARY
- CPV PERFORMANCE SUMMARY
- BATTERY DESIGN SUMMARY
- ELECTRONICS SUMMARY
- BATTERY PERFORMANCE SUMMARY
- QUESTIONS AND ANSWERS

D. GINDER ; EAGLE PICHER INDUSTRIES; NOVEMBER 1995

EAGLE PICHER
NASA Battery Conference

Mars Global Surveyor

MGS Satellite Objectives

COURTESY OF LOCKHEED MARTIN & JET PROPULSION LABORATORIES

- NASA's NEXT INTERPLANETARY MISSION
- COMPLETE AS MUCH OF THE MARS OBSERVER MISSION AS POSSIBLE
  - » SURFACE CHARACTERIZATION
  - » SURFACE COMPOSITION AND THERMOPHYSICAL PROPERTIES
  - » DETERMINE TOPOGRAPHY, GEODETIC FIGURE, & GRAVITATIONAL FIELDS
  - » ESTABLISH NATURE OF MAGNETIC FIELDS, AND MAP CRUSTAL REMNANT FIELDS
  - » MONITOR GLOBAL WEATHER AND THERMAL STRUCTURE OF THE ATMOSPHERE
  - » STUDY SURFACE-ATMOSPHERIC INTERACTIONS
- USE AS MUCH EXISTING H/W FROM MO. AS FEASIBLE
- PROVIDE MULTIPLE YEARS OF ON-ORBIT RELAY COMMUNICATIONS CAPABILITY FOR MARS LANDERS AND ATMOSPHERIC VEHICLES
- SUPPORT PLANNING FOR FUTURE MARS MISSIONS THROUGH DATA ACQUISITION

EAGLE PICHER
NASA Battery Conference

Mars Global Surveyor

Eagle Picher Program Philosophy

- TEAM APPROACH
  - » PRODUCTION, ENGINEERING, QUALITY INVOLVEMENT AS A PRODUCT TEAM
  - » LOCKHEED MARTIN AND JPL INVOLVED AS TEAM MEMBERS
  - » SELECTION OF MOTIVATED TEAM ORIENTED INDIVIDUALS
- BETTER (HIGHER QUALITY); FASTER (REDUCED SCHEDULE), CHEAPER (LOWER COST DUE TO TEAMWORK APPROACH
- REDUCED PAPERWORK BY IMPLEMENTING "WHAT MAKES SENSE ATTITUDE", THE WAY WE HAVE ALWAYS DONE IT DOESN'T NECESSARILY MAKE IT THE BEST WAY
- DOCUMENT RED LINE CAPABILITY THROUGH QUAL. BUILD
- CONSTANT COMMUNICATION AMONG TEAM

EAGLE PICHER
NASA Battery Conference

Mars Global Surveyor

Battery Program Requirements

- DESIGN A NICKEL HYDROGEN SYSTEM COMPATIBLE WITH EXISTING NICAD MARS OBSERVER BASED SPACECRAFT COMPONENTS
- PHYSICAL CHARACTERISTICS MUST FIT WITHIN THE ENVELOPE ALLOTTED FOR THE NICAD SYSTEM
- 20 VOLT BATTERY
- 5 + YEAR MISSION
- HIGH RELIABILITY
- QUALIFICATION BATTERY DELIVERY IN 11 MONTHS TO SUPPORT S/C TESTING
- E/P TO PERFORM ALL DESIGN, ANALYSIS, AND QUALIFICATION OF BATTERY

EAGLE PICHER
NASA Battery Conference

Mars Global Surveyor

CPV Design Summary

- EPI MANTECH
- 23 mil PRESSURE VESSELS
- COMMON PRESSURE VESSEL
- RABBIT EAR TERMINALS (60° INCLUDED ANGLE)
- 30 mil SLURRY POSITIVES
- 32 ELECTRODE COUPLES (16 PER STACK)
- DOUBLE LAYER ZIRCAR
- ZIRCONIUM WALL WICK
- 31% KOH
- NICKEL PRE-CHARGED
- 800 PSI MAXIMUM DESIGN PRESSURE
- MASS: 1291g MAX / CPV

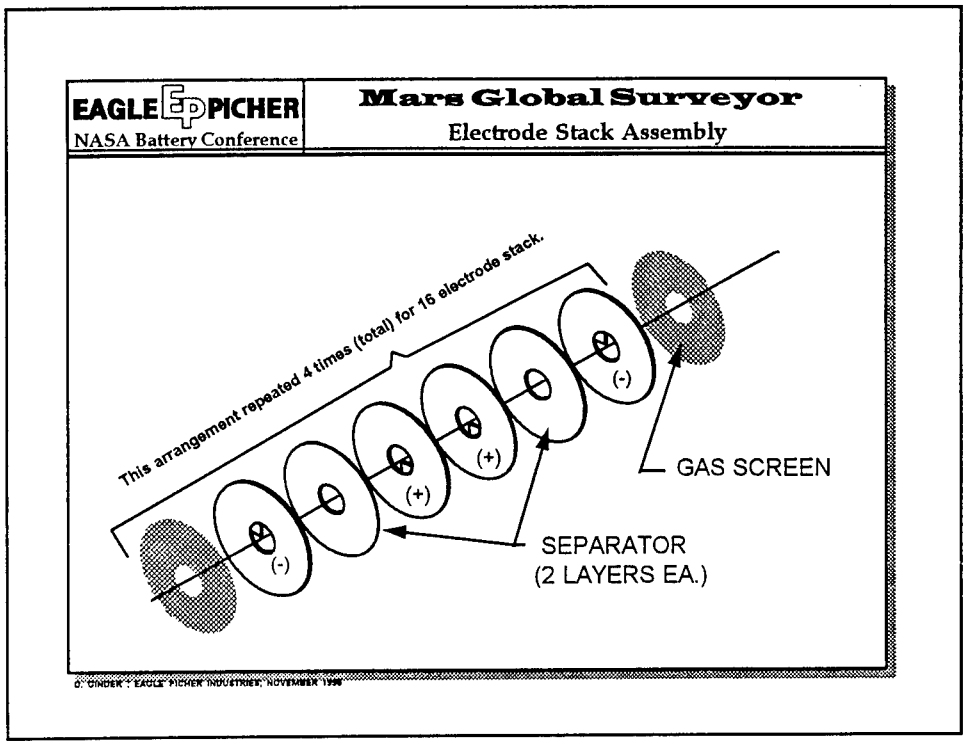

This slide shows a typical single electrode stack sequence used on nickel hydrogen cells. The MGS cell incorporates a double layer zircar separator for increased cycle life. This arraignment is repeated four times to complete a 16 electrode stack.

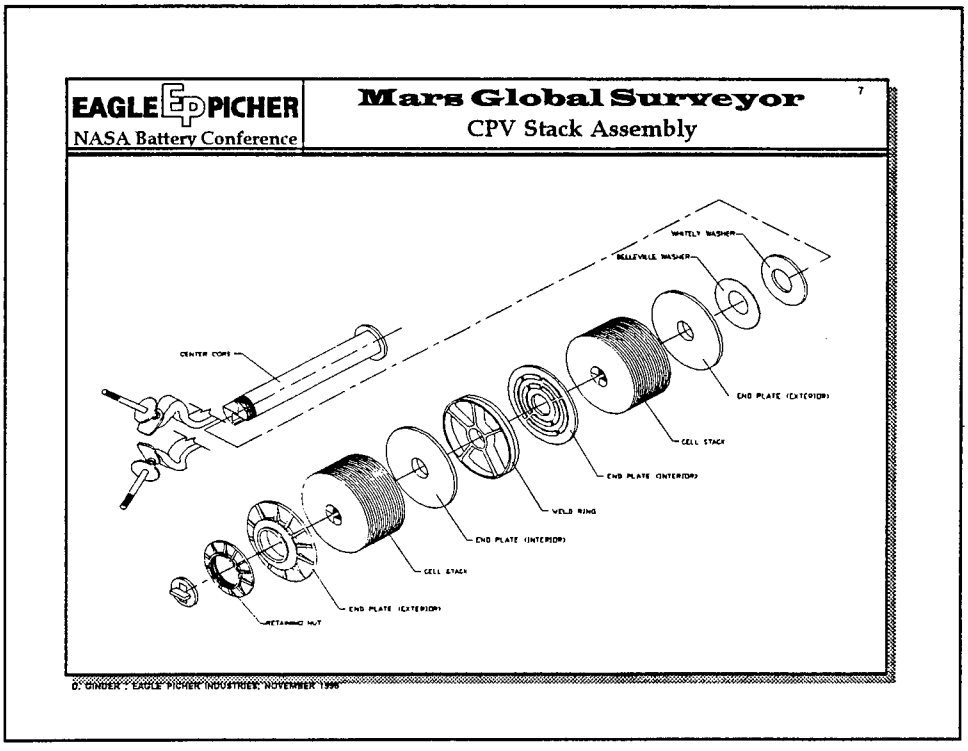

The MGS cell is termed a double stack Common Pressure Vessel or CPV. The CPV accommodates a double stack of 16 electrodes on a cell core which is separated by a weld ring. The two stacks are wired in series which doubles the voltage at the terminals when compared to an IPV or Independent Pressure Vessel. The CPV is then encapsulated with the a dome and cylinder and girth welded to the weld ring. This weld ring is the structural load carrying member of the stacks to the CPV "can".

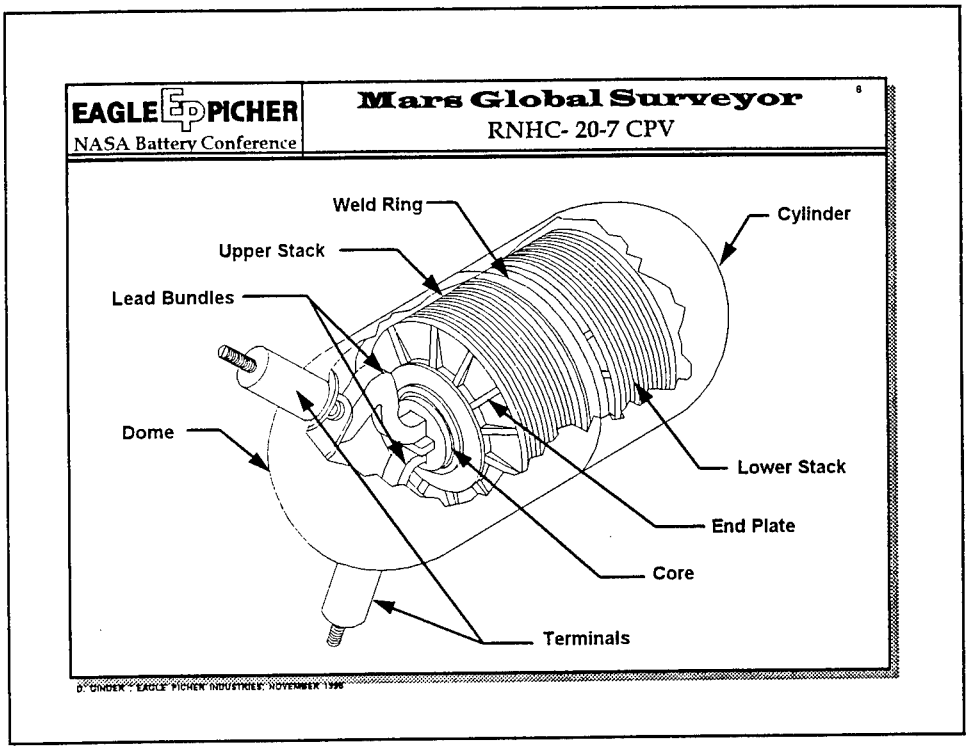

Shown is a cut-away view of the completed CPV showing the two lead bundles protruding through the core and welded to the CPV terminals

EAGLE PICHER

NASA Battery Conference

Mars Global Surveyor

RNHC 20-7 CPV Outline

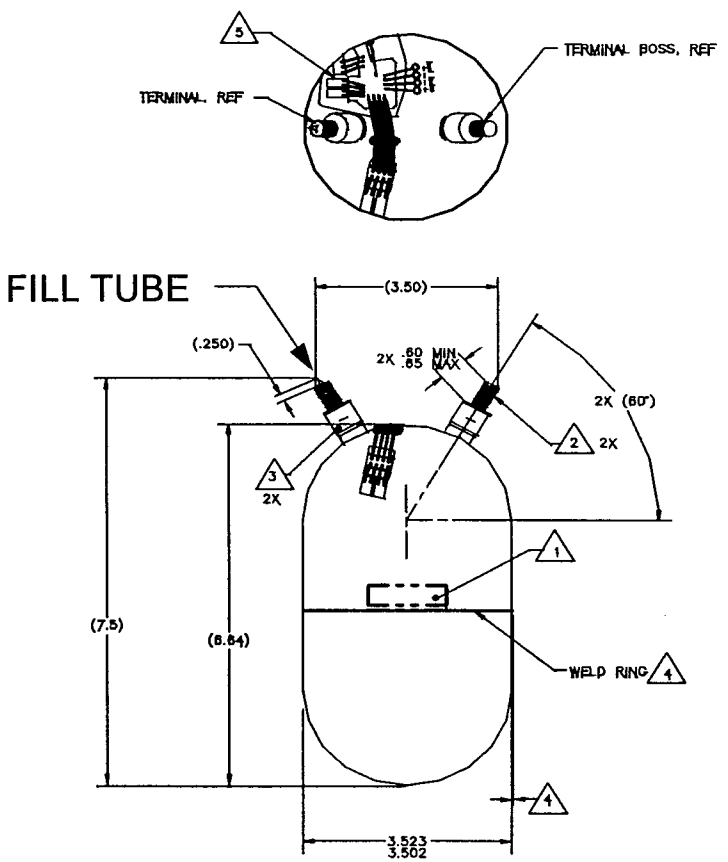

Design Features

- Compact Design- 20 A-HR / 2 Cell CPV
- Strain Gage Conf.
- Boss Fill Tube
- 60° Angle Terminals
- Design Wt. 1253g Max. Wt. 1290g

EAGLE EPICHER
NASA Battery Conference

Mars Global Surveyor

RNHC-20-7 CPV Performance Summary

- ALL TEST RESULTS AVERAGED FROM 20 CPV'S DURING ATP
- ALL CAPACITIES TO 2.0 VOLTS (1.0 VOLT PER CELL STACK)
- CAPACITY @ 25° = 19.66 A-HR
- CAPACITY @ 10°C = 22.05 A-HR
- CAPACITY @ -5° = 24.24 A-HR
- CHARGE RETENTION CAPACITY = 19.40 A-HR (88%)
- OVERCHARGE = 3.07 VOLTS (AFTER 24 HOURS @ 2 AMPERE RATE @ 10°C)
- PRESSURE VESSEL CYCLES 92,000
- BURST 3800 PSI (4.75X); CYCLE/BURST 3700 PSI (4.63X)
- ENERGY DENSITY PER CPV = 44.0 W-H/KG

D. GINDER ; EAGLE PICHER INDUSTRIES; NOVEMBER 1995

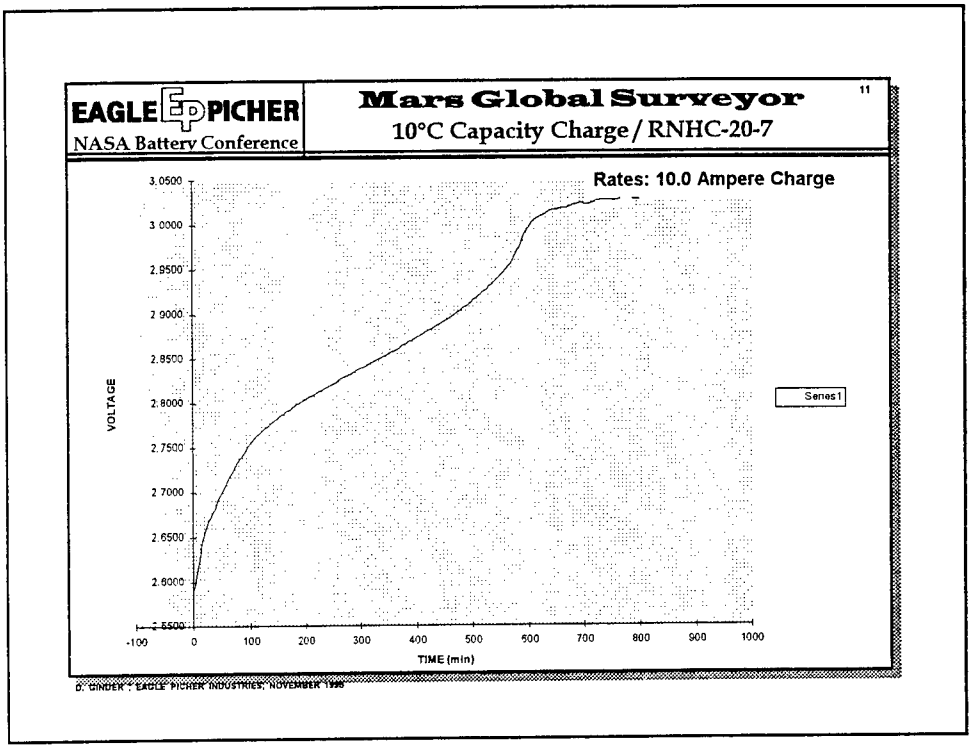

Charge voltage curve with respect to time for one of the MGS CPV's. Data was taken during cell acceptance testing. The test values used were from the 10°C capacity test cycle number 5.

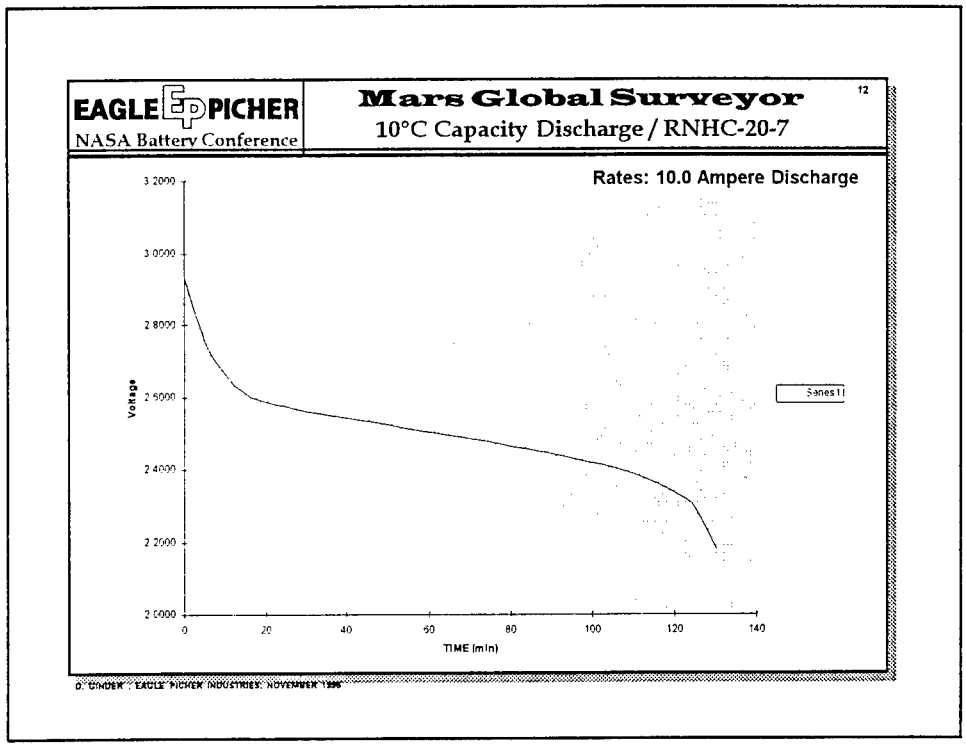

Discharge voltage curve with respect to time for one of the MGS CPV's. Data was taken during cell acceptance testing. The test values used were from the 10° C capacity test cycle number 5.

EAGLE PICHER
NASA Battery Conference

Mars Global Surveyor

Battery Design Objectives

- MEET OR EXCEED ALL PD REQUIREMENTS
- USE EXISTING TECHNOLOGIES
- MODULAR BATTERY DESIGN
- HIGH RELIABILITY HARDWARE
- PARALLEL FABRICATION OF COMPONENTS
- LOW SCHEDULE RISK CONFIGURATIONS
- TEAM EFFORT WITH CUSTOMER (DESIGN OPTIMIZATION)
- DESIGN FOR MANUFACTURABILITY
- REDUCED PART COUNT

EAGLE PICHER
NASA Battery Conference

Mars Global Surveyor

Battery Design Features

- MODULAR ASSEMBLY
- DUAL STRAIN GAUGE ELECTRONICS
- S.G. POWER MODULATOR (High reliability S-Class H/W)
- RADIATIVE AND CONDUCTIVE HEAT TRANSFER SYSTEM
  - » THERMAL SLEEVES FOR CONDUCTION
  - » HIGH EMISSIVITY (CPV'S AND BASE PLATE)
  - » LOW EMISSIVITY COATINGS ON DOMES
- 8 HORIZONTALLY MOUNTED CPV's PER BATTERY
- HEATERS AND HEATER CONTROL MODULES (HCM)
- THERMISTORS
- RESISTOR MODULE
- WEIGHT-OPTIMIZED STRUCTURE (CPV MOUNTING AND BASE PLATE)
- POWER AND TELEMETRY CONNECTORS (PIGTAIL CONFIGURATION)
- PRECISION MACHINED ALUMINUM BASE PLATE (6061-T6 Al)

D. GINDER ; EAGLE PICHER INDUSTRIES; NOVEMBER 1995

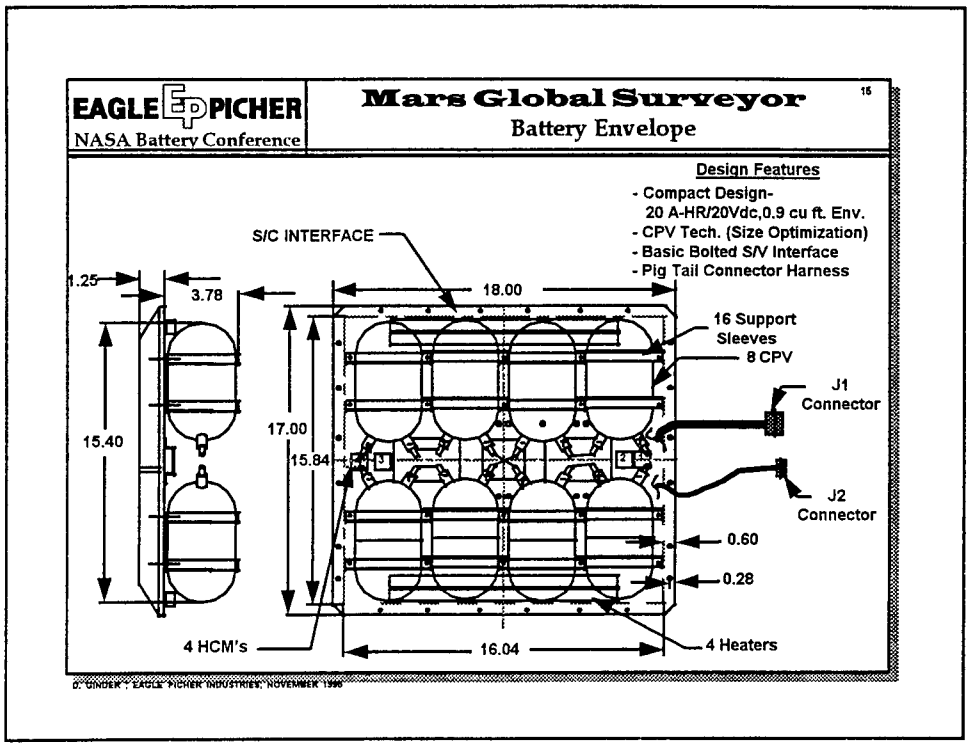

Total battery envelope is 5"x17"x18" with 0.75 inches constituting the base plate. The top of the structural supports for the 3.5" CPV's are a mere 3.78 inches above the surface of the base plate. One of the biggest challenges was packaging of the battery components in the allocated space.

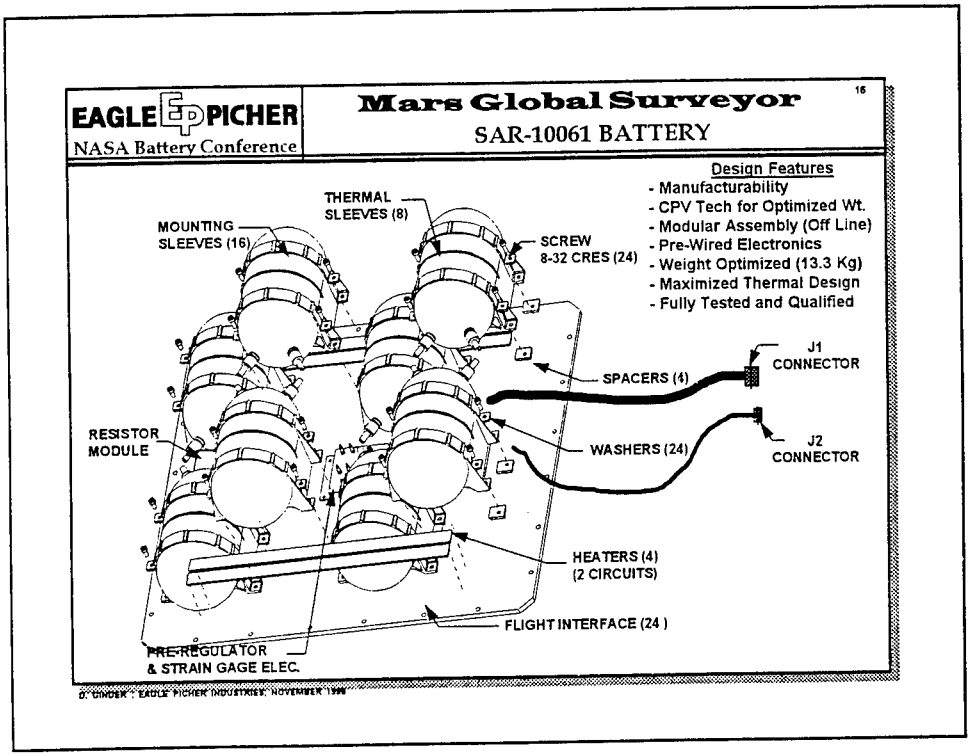

The MGS battery is a complete power storage system ready for installation onto the spacecraft. Telemetry is provided to the spacecraft computer for battery voltage, battery half pack voltage, temperature for charge control, temperature for thermal control, cell pressure on a 0 to 5 volt range. Other features include 4 Kapton heaters (2) in the primary circuit and (2) in the secondary. Four heater control modules controlling the 4 heater strings. Strain gage per-regulator and dual strain gage amplifiers. Cells are cross wired between the two center cells to create 2 opposing magnetic field loops in order to cancel/reduce the electromagnetic fields generated by the cell interconnects. The telemetry and power are interfaced to the spacecraft via two light weight (outer shell composite - EMI) breech-Lok connectors.

EAGLE PICHER
NASA Battery Conference

Mars Global Surveyor

ELECTRONICS SUMMARY

- DUAL STRAIN GAGE AMPLIFIERS
- SINGLE STRAIN GAGE POWER PRE-REGULATOR
- RESISTOR MODULE
  - » V/T CURVE RESISTORS
  - » SIGNAL PROTECTION
  - » GROUND SUPPORT EQUIPMENT POWER INTERRUPT
- TRICKLE CHARGE RESISTOR
- HEATER CONTROL MODULES (CUSTOMER SUPPLIED)
- KAPTON HEATERS (44 WATTS TOTAL POWER)

EAGLE PICHER

NASA Battery Conference

Mars Global Surveyor

Strain Gage Amplifier

Input power:	14 - 16 VDC	
Strain gage excitation:	approximately 10.0 VDC	
Internal circuit power:	approximately 10.0 VDC	
* Amplified output:	discharged cell; approximately 0.2 VDC charged cell; approximately 5.0 VDC	
Current draw: (approximately)	strain gage assembly;	0.028 A
	strain gage electronic assembly;	0.004 A
	Total:	0.032 A
Size:	2.25 x 2.25 x .5	
Weight:	19 g	
Voltage regulator:	per MIL-M-38510/117	
Operational amplifier:	per MIL-M-38510/110	
Resistor:	per MIL-R-55182/1 and MIL-R-39008/4	
Diode:	per MIL-S-19500/116	
Capacitor:	per MIL-C-39014/01 and MIL-C-39014/02	
Printed circuit board:	per MIL-P-55110	

Design Features

- Printed Circuit Board
- Compact Design
- Flight Heritage (No-Fail.)
- Light Weight = 19grams
- Robust Design
- MIL Standard Parts

EAGLE PICHER
NASA Battery Conference

Mars Global Surveyor

Strain Gage Pre-Regulator

19

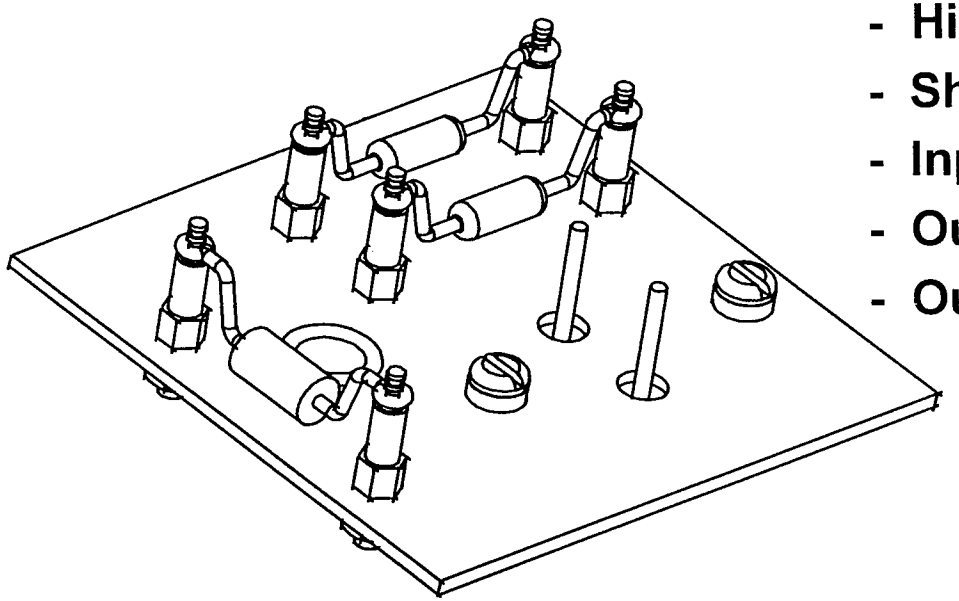

Design Features

- Compact Design
- Simplified Design
- High Reliability Comp.
- Short Fabrication
- Inputs: 16-36 Volts
- Output: 15 Volts ± 5%
- Output Tolerance ± .25%

EAGLE PICHER
NASA Battery Conference

Mars Global Surveyor
Battery Performance Summary

- ALL TEST RESULTS PERFORMED ON QUAL. BATTERIES
- ALL CAPACITIES CALCULATED @ FIRST CPV TO 2.0 VOLTS
- CAPACITY @ 20°C = 20.87 A-HR
- CAPACITY @ 10°C = 23.56 A-HR
- CHARGE RETENTION @ 10°C = 21.98 A-HR (93.3%)
- CAPACITY @ -5°C = 25.37 A-HR
- RANDOM VIB. SUCCESSFULLY COMPLETED TO 13.5 g's RMS
- PYRO SHOCK SUCCESSFULLY COMPLETED TO 1100 g's
- BATTERY MASS @ 13.25 KG (29.15 lbs)
- ENERGY DENSITY PER BATTERY = 35.56 WH/KG
- PACKING FACTOR = (13.3/8(1253))=1.33

D. GINDER ; EAGLE PICHER INDUSTRIES; NOVEMBER 1995

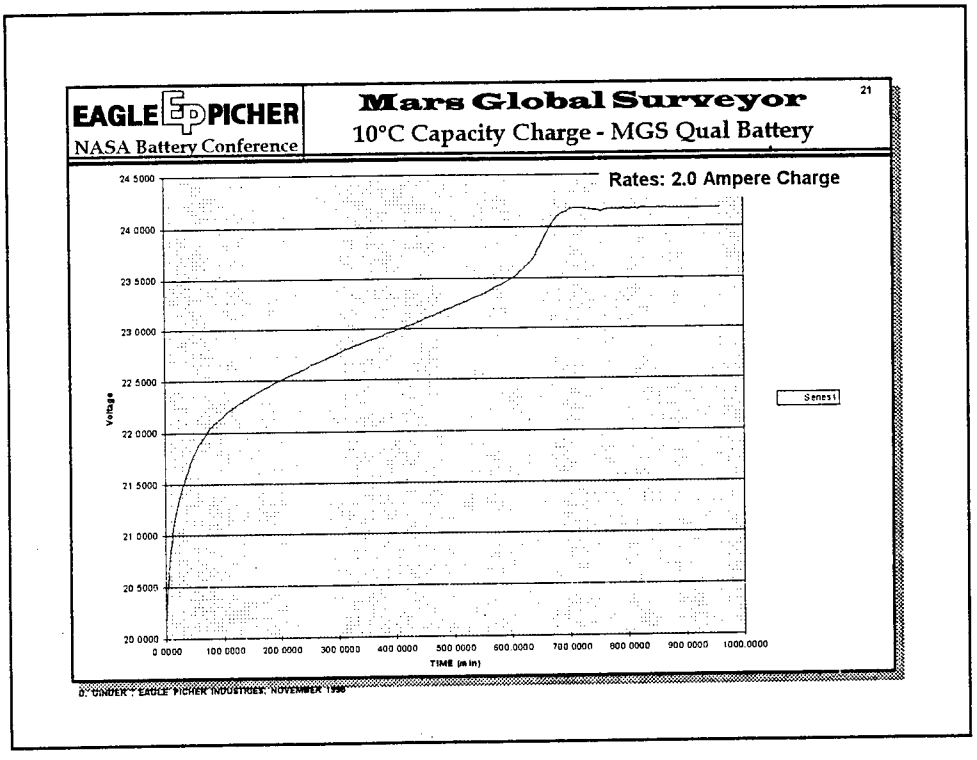

Charge voltage curve with respect to time for the MGS battery. Data was taken during the battery acceptance testing. The test values used were from the 10° C capacity test prior to charge retention.

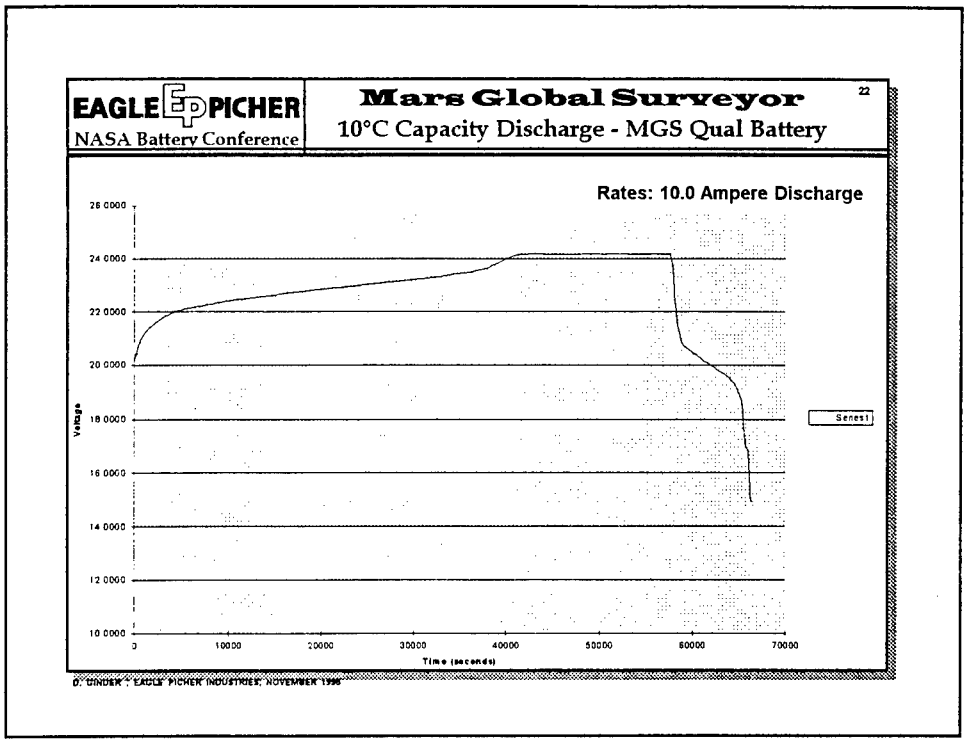

Discharge voltage curve with respect to time for the MGS battery. Data was taken during the battery acceptance testing. The test values used were from the 10° C capacity test prior to charge retention.

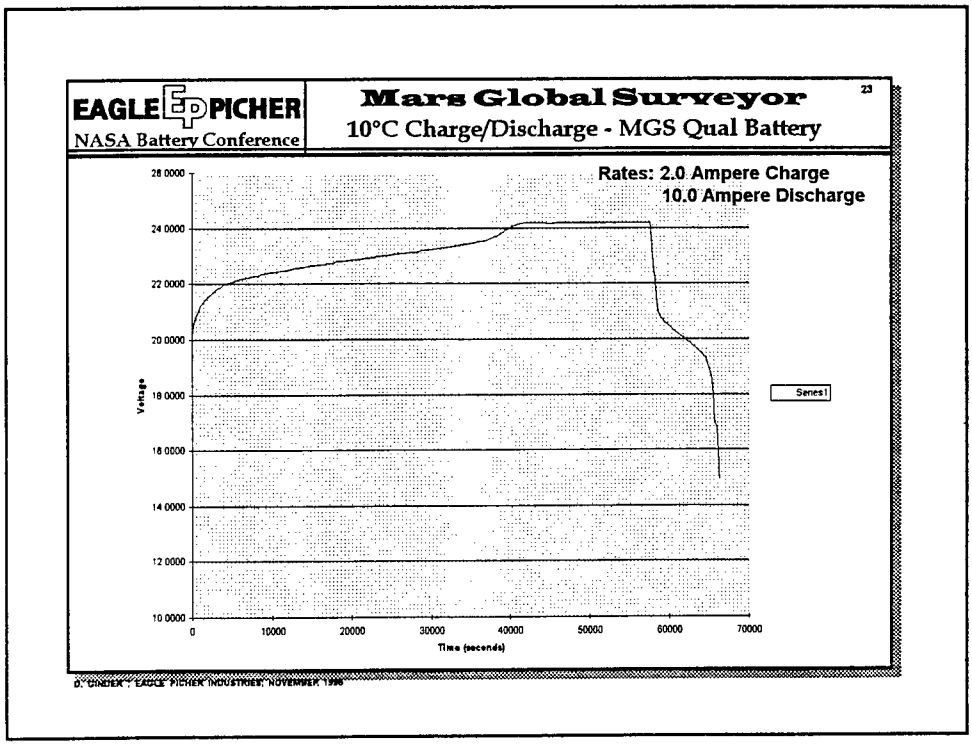

This chart combines the charge / discharge curve of the preceding charts to give an overall view of the 10°C test cycle. Upon completion of each electrical cycle the CPV's are independently resistor drained to 0.2 volts with a 0.4 ohm resistor.

EAGLE PICHER
NASA Battery Conference

Mars Global Surveyor

QUESTIONS AND ANSWERS

AIR FORCE NiH2 IPV STORAGE TESTING

1995 NASA BATTERY WORKSHOP

CAPT SHAWN SMELLIE
CAROLE A. HILL

This paper was prepared by Capt Shawn Smellie (Phillips Lab) and Carole Hill (Aerospace Corporation). This paper discusses the USAF Phillips Laboratory Nickel Hydrogen IPV storage test. This test is being performed at the Naval Surface Warfare Center (NSWC) at Crane Indiana. The authors would like to acknowledge the support of NSWC Crane in conducting this test and in the preparation of this presentation.

AIR FORCE NiH2 IPV STORAGE TESTING

- INTRODUCTION
- OBJECTIVES
- CONDITIONS
- STATUS/DATA
- RESULTS
- OBSERVATIONS & CONCLUSION

In overview, this paper will cover the objectives and conditions of the storage test. The status of the stored and cycling cells will be discussed. The results of the post storage acceptance tests will be presented. Voltage, current, and temperature data will be presented for the storage period. The last part of the paper will be a conclusion and observations from our initial evaluation.

AIR FORCE NiH2 IPV STORAGE TESTING

INTRODUCTION

AIR FORCE NiH2 IPV TEST PROGRAM
- STORAGE TEST IS ONE PORTION OF THE TEST PROGRAM

TWO CELL PACKS STORED FOR 5 YEARS
- COMPLETED APR 95

TWO CELL PACKS CYCLING AT 25% DOD
- FIVE YEARS OF CYCLE DATA

The storage test is just one component of the USAF Phillips Laboratory Nickel Hydrogen IPV Test Program. The plan was to store cells for a defined period and cycle matching cells to determine the effect on cycle life. The storage period was complete in Apr 95 and the cycling cells have achieved five years of real time LEO cycling.

AIR FORCE NiH2 IPV STORAGE TESTING

OBJECTIVES

- INVESTIGATE CELL STORAGE METHODS
  - 2 MANUFACTURERS
  - 2 CONDITIONS

- LOOK AT EFFECTS STORAGE MODE HAS ON BATTERY AND CELL CYCLE LIFE
  - COMPARE TO CYCLE LIFE DATA
  - COMPARE TO CYCLE PROFILE DATA

There are two main objectives of the storage test. The first is to investigate various storage methods on NiH2 cells. This was accomplished using two different manufacturers and two different storage methods or conditions. The second objective was to determine the effect of storage method on cycle performance and cycle life. This will be accomplished using matching cells cycling at 25% depth of discharge. Individual cycle performance as well as cycle life comparisons will be made.

AIR FORCE NiH2 IPV STORAGE TESTING

CONDITIONS

- TWO SETS OF TEN CELLS (EPI-CS & GATES)
  - 150 AH, 4.5 INCH
  - FIVE CELLS FROM EACH MANUFACTURER
  - DESIGNED POSITIVE PRE-CHARGE BASED ON SPECIFICATION
- THREE STORED DISCHARGED AT OPEN CIRCUIT
  - DISCHARGED AT C/50 TO 0.1 VOLTS
  - DISCHARGED AT C/100 TO 0.1 VOLTS
  - 1 OHM RESISTOR FOR 16 HOURS
- TWO STORED AT CONSTANT POTENTIAL
  - DISCHARGED AT C/50 TO 0.1 VOLTS
  - DISCHARGED AT C/100 TO 0.1 VOLTS
  - 1 OHM RESISTOR TO 0.5 VOLTS
  - 0.7 VOLTS APPLIED POTENTIAL

The cells used for this test were manufactured by EPI-CS and Gates. The cells are 150 Ahr capacity and 4.5 inch in diameter. The open circuit test condition was selected because of its simplicity in implementing and actual use. The constant potential test condition was selected based on electrochemical reactivity of the NiH2 cell.

AIR FORCE NiH2 IPV STORAGE TESTING

CONDITIONS CONT.

- TWO FIVE CELL PACKS CYCLING AT 25% DOD
- ROOM TEMPERATURE
  - NO ACTIVE CONTROL
- DURATION OF TEST: FIVE YEARS
  - VOLT & TEMP RECORDED WEEKLY
  - CURRENT RECORDED ON CELLS AT CONSTANT POTENTIAL

The cells were not designed for LEO testing and that is why they are being cycled at 25% depth of discharge. The matching cells being cycled were treated the same prior to the storage period. The test is being conducted at room temperature and is not actively controlled. The storage duration was set at five years and data is recorded weekly.

AIR FORCE NiH2 IPV STORAGE TESTING

CONDITIONS CONT. - CELL SERIAL NUMBERS

	OPEN CIRCUIT	CONSTANT POTENTIAL
EPI-CS	1,4,12	6,11
GATES	2,4,10	5,8

CYCLING CELLS: EPI (3,5,9,10,14), GATES (1,3,6,7,9)

This chart shows the cell serial numbers and where the cells were placed in the test matrix. These serial numbers match up with the data presented later in the paper.

AIR FORCE NiH2 IPV STORAGE TESTING

STATUS/DATA

- STORAGE PERIOD COMPLETED
- ACCEPTANCE TESTS REPEATED
- BEGIN LIFE CYCLE EVALUATION
- DATA
  - PL TEST MATRIX TABLE
  - CRANE TREND PLOTS
  - CONSTANT POTENTIAL
  - CELL CURRENT FOR CONSTANT POTENTIAL
  - OPEN CIRCUIT VOLTAGE
  - TEMPERATURE

The five year storage period was complete in Apr 95. The cells remained under storage conditions until Jun 95. At that point the acceptance test was repeated for the stored cells. The cells were placed on LEO life cycle evaluation at 25% depth of discharge in Sep 95. Data recorded during the storage period will be presented as follows: constant potential, cell current, open circuit voltage, and temperature. This data is in the form of trend plots. Also included in the data is the Phillips Lab test matrix table and Crane trend plots for the cycling cells and the stored cells.

Air Force NiH_2 LEO Life Test
Phillips Laboratory

Manufacturer	Pack #	Rated Capacity	Design	Temp Deg C	DOD†	Ave EODV	# Cycles Completed	# Cells
Gates	5000G	50 Ah	Alt/31%	-5	53%	>0.8	39175	10/4
Gates	5002G	50 Ah	Alt/31%	10	54%	>0.7	39882	10/10
Hughes	5000H	50 Ah	BtB/31%	-5	50%	>1.2	41211	10/10
Hughes	5002H	50 Ah	BtB/31%	10	49%	>1.0	41738	10/9
Yardney	5000Y	50 Ah	Alt/31%	-5	41%	>1.0	46468	10/9
Yardney	5003Y	50 Ah	Alt/31%	10	25%	>1.1	34959	5/5
Eagle-Picher (CS)	5402E	90 Ah	Alt/31%	10	40%	>1.2	39751	8/8
Hughes	5402H	90 Ah	Alt/31%	10	40%	>1.1	39504	5/5
Gates	5402G	90 Ah	Alt/31%	10	40%	>1.2	39715	8/8
Yardney	5402Y	110 Ah	Alt/31%	10	40%	>1.1	21106	9/4
Gates	5000A	150 Ah	BtB/31%	10	25%	>1.1	31749	5/5
Eagle-Picher (CS)	5000C	150 Ah	BtB/31%	10	25%	>1.1	31873	5/5
Eagle-Picher (J)	3214E	50 Ah	BtB/26%	10	40%	>1.1	12928	10/10
Eagle-Picher (J)	3314E	50 Ah	Alt/31%	10	40%	>1.1	13464	10/10
Eagle-Picher (J)	3316E	50 Ah	BtB/31%	10	60%	>1.1	13402	10/10
Eagle-Picher (J)	3254E	50 Ah	BtB/26%	-5	40%	>1.2	13296	10/10
Yardney	3214Y	50 Ah	Alt/26%	10	40%	>1.2	12601	10/10
Yardney	3254Y	50 Ah	Alt/26%	-5	40%	>1.1	12518	10/10
Gates	5001A	150 Ah	BtB/31%	10	25%°	>1.2	1198	5/5
Eagle-Picher (CS)	5001C	150 Ah	BtB/31%	10	25%°	>1.2	891	5/5
Eagle-Picher (J)	BL25	50 Ah	BtB/31%	10	40%‡	>1.2	26652	10/9
Eagle-Picher (J)	5002E	50 Ah	BtB/31%	10	40%	>1.2	28086	7/7
Eagle-Picher (J)	P321E	50 Ah	BtB/26%	10	40%‡	>1.2	11399	10/10
Eagle-Picher (J)	3001C	50 Ah	BtB/26% Alt/31%	10	40%*	>1.0	7627	4/4

† Depth of discharge based on nameplate **Current: 20 Nov 95**

‡ Pulse Test Cells ° Storage Test Cells

* State of Charge Cells

NSWC Crane Pack ID 5000C 5 cells

Voltage/Pressure/Recharge EOC/EOD Trend Plot 08/28/91 - 10/23/95

EPI-C 150 AmpHr 4.5" 25% DOD 10 Deg C Moved from PACK 5000A (Cells 6-10)

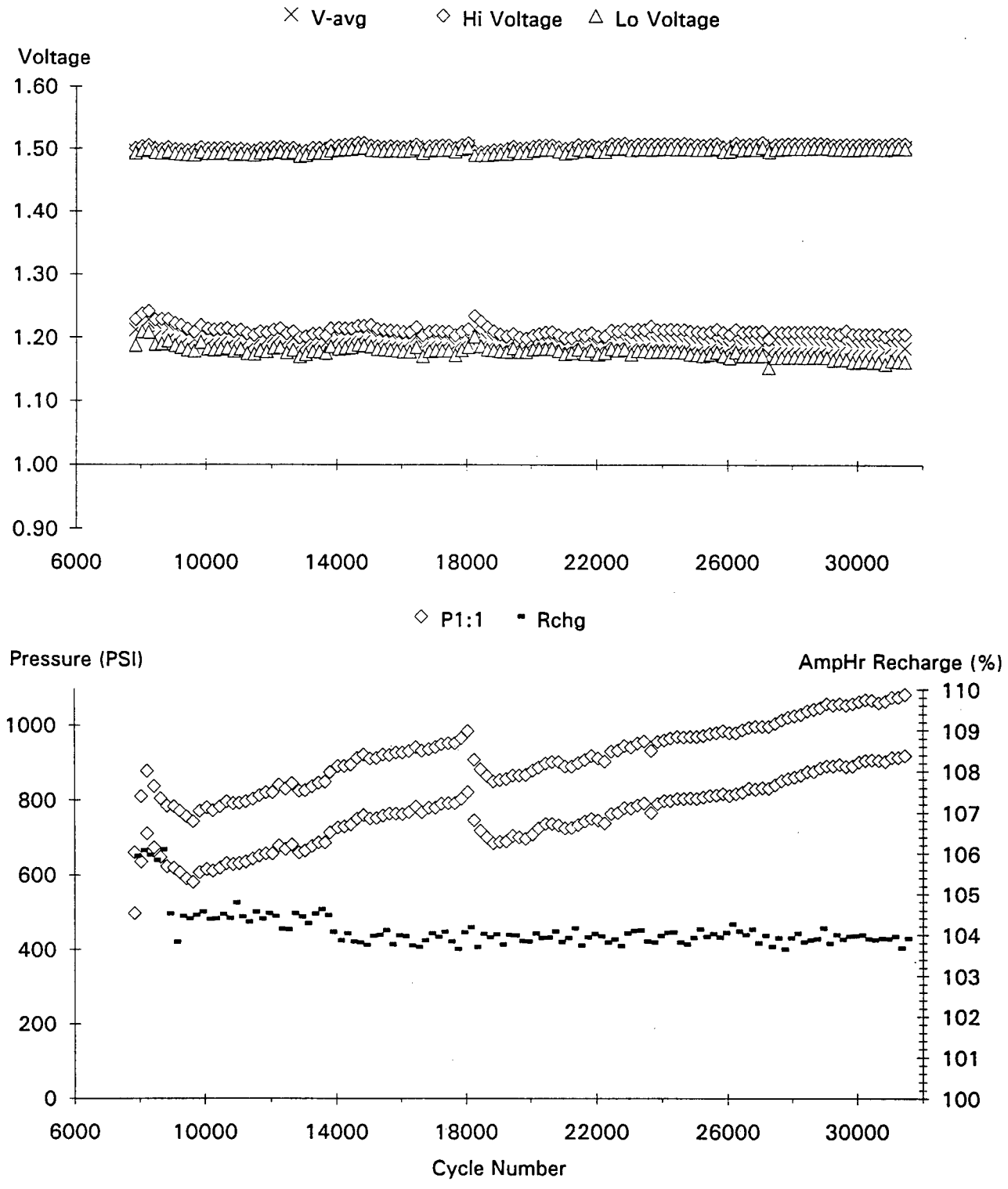

NSWC Crane **Pack ID 5001C** **5 cells**

Voltage/Pressure/Recharge EOC/EOD Trend Plot 09/26/95 - 10/29/95

EPI-C 150 AmpHr 4.5" 25% DOD 10 Deg C Moved from PACK 5000A (Cells 6-10)

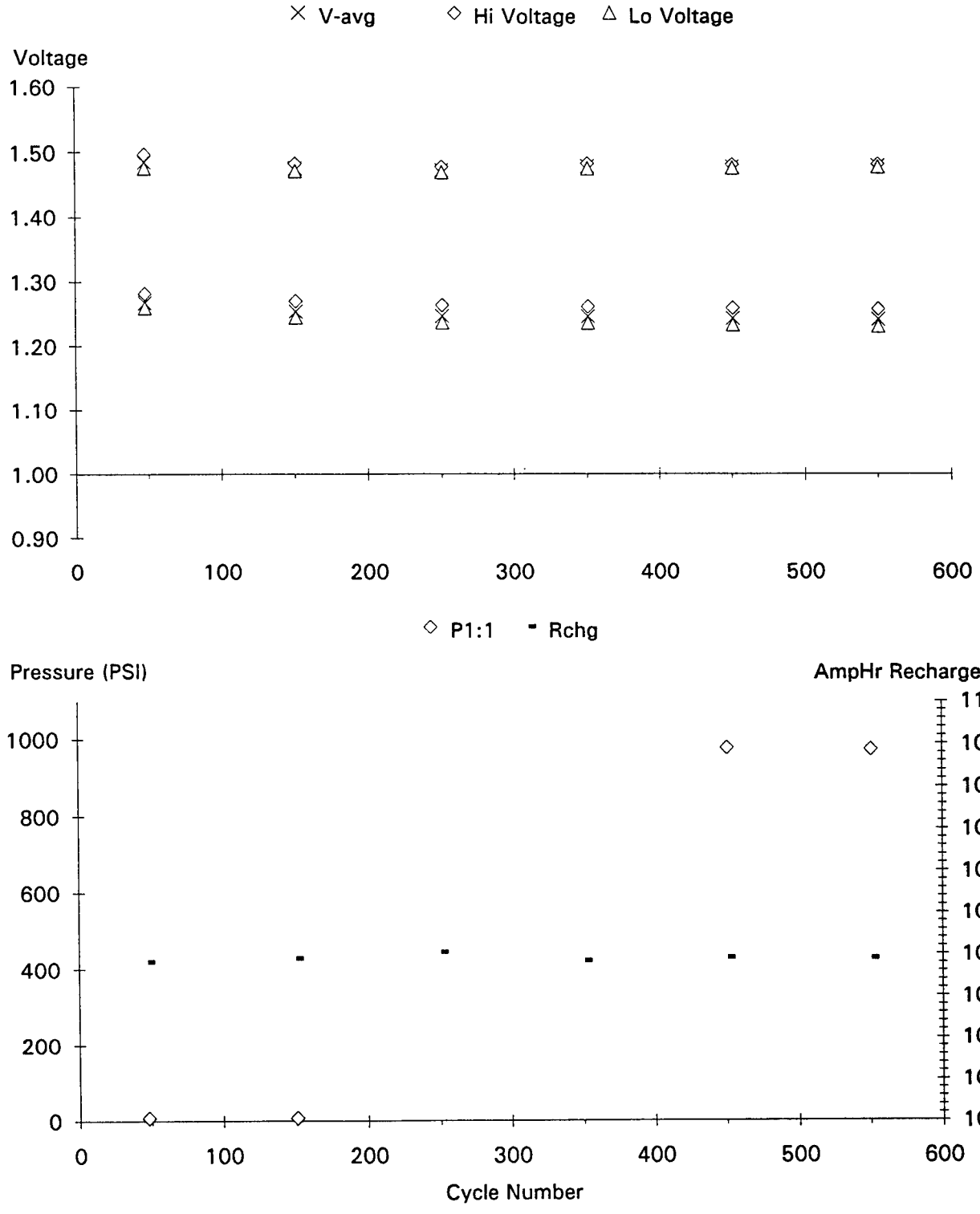

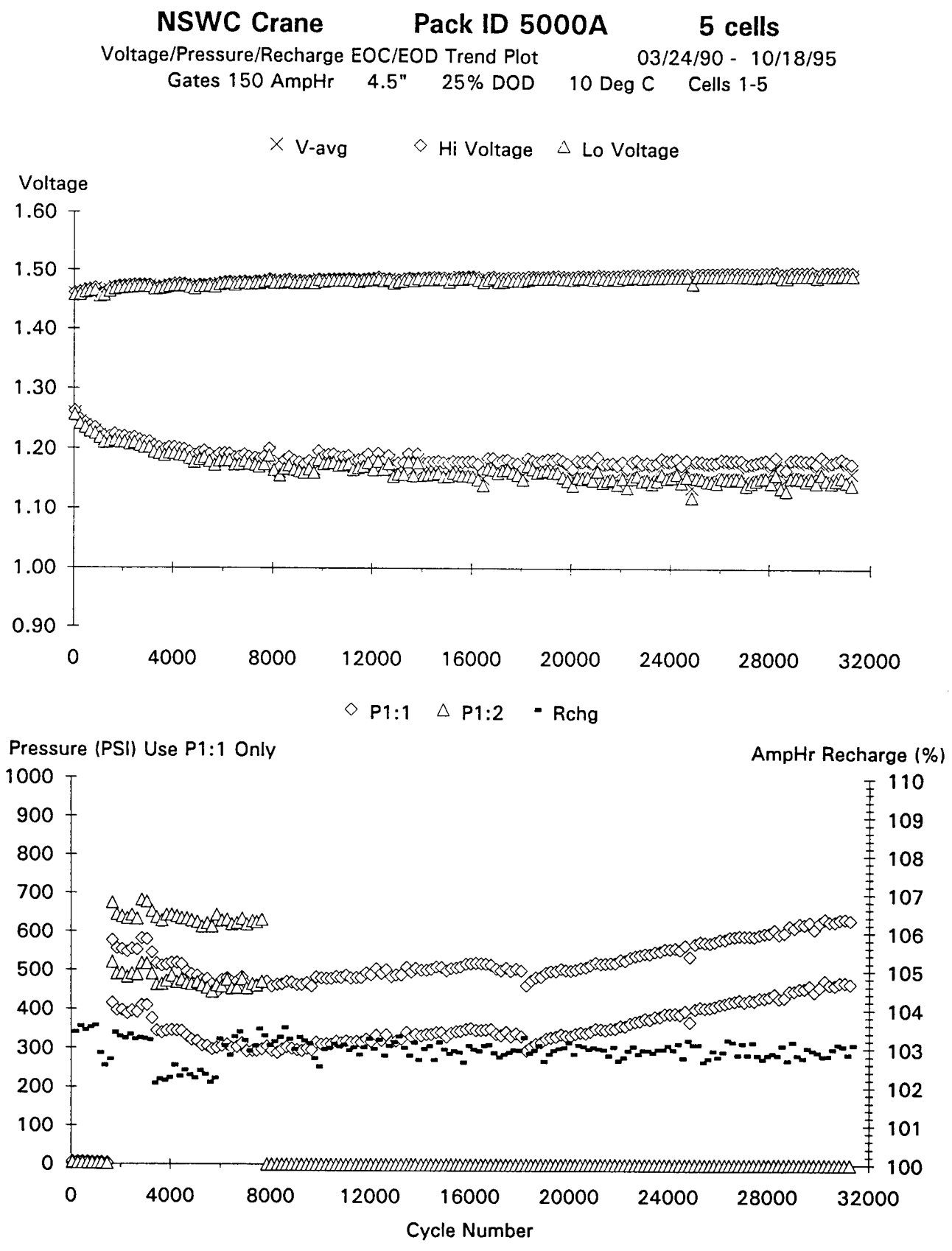
NSWC Crane
Pack ID 5000A
5 cells
Voltage/Pressure/Recharge EOC/EOD Trend Plot
03/24/90 - 10/18/95
Gates 150 AmpHr 4.5" 25% DOD 10 Deg C Cells 1-5
V-avg
Hi Voltage
Lo Voltage
Voltage
1.60
1.50
1.40
1.30
1.20
1.10
1.00
0.90
0
4000
8000
12000
16000
20000
24000
28000
32000
P1:1
P1:2
Rchg
Pressure (PSI) Use P1:1 Only
AmpHr Recharge (%)
1000
900
800
700
600
500
400
300
200
100
0
110
109
108
107
106
105
104
103
102
101
100
Cycle Number

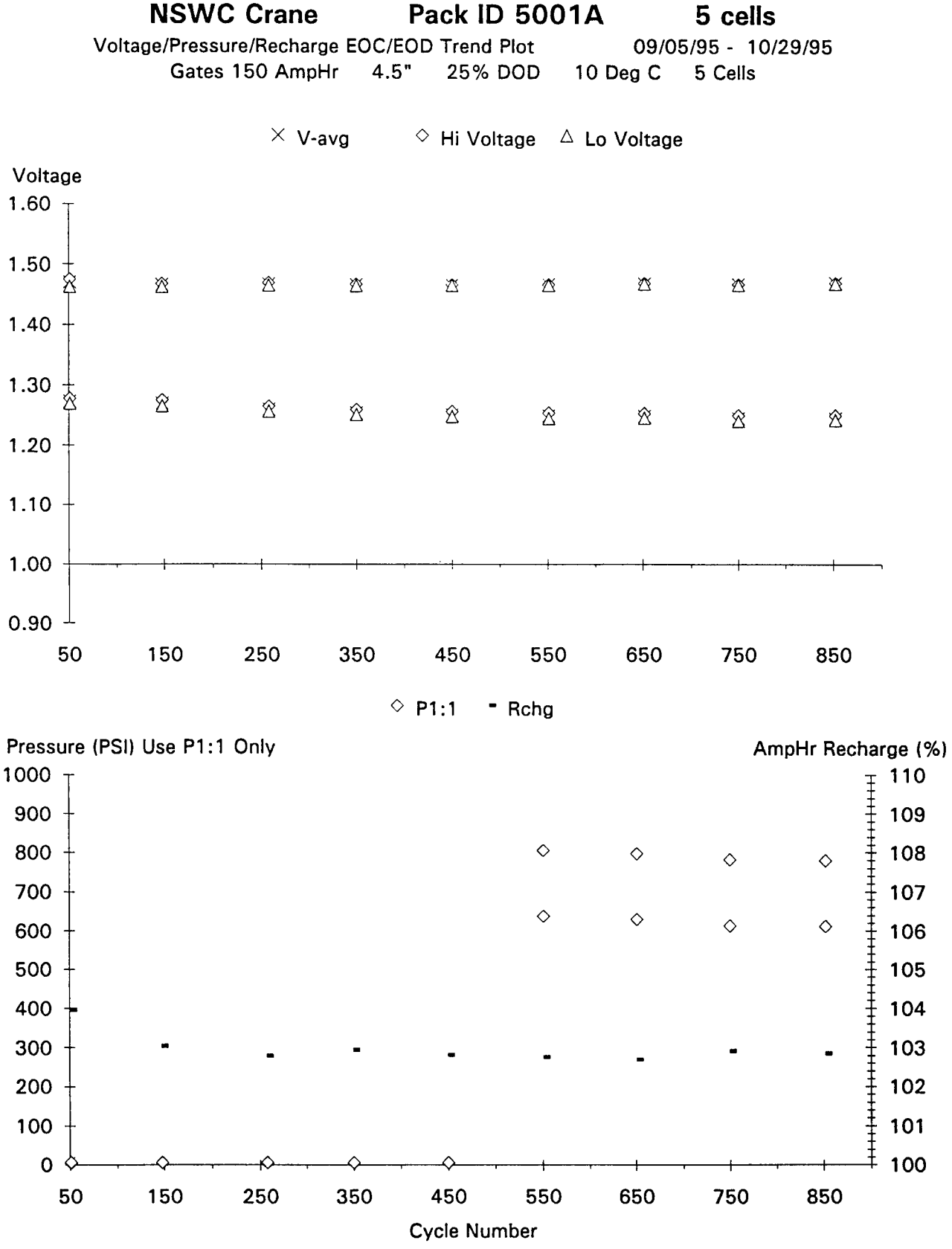
NSWC Crane Pack ID 5001A 5 cells
Voltage/Pressure/Recharge EOC/EOD Trend Plot 09/05/95 - 10/29/95
Gates 150 AmpHr 4.5" 25% DOD 10 Deg C 5 Cells
× V-avg ◇ Hi Voltage △ Lo Voltage
Voltage
1.60
1.50
1.40
1.30
1.20
1.10
1.00
0.90
50 150 250 350 450 550 650 750 850
◇ P1:1 - Rchg
Pressure (PSI) Use P1:1 Only
AmpHr Recharge (%)
1000
900
800
700
600
500
400
300
200
100
0
110
109
108
107
106
105
104
103
102
101
100
50 150 250 350 450 550 650 750 850
Cycle Number

AIR FORCE NiH2 IPV STORAGE TESTING

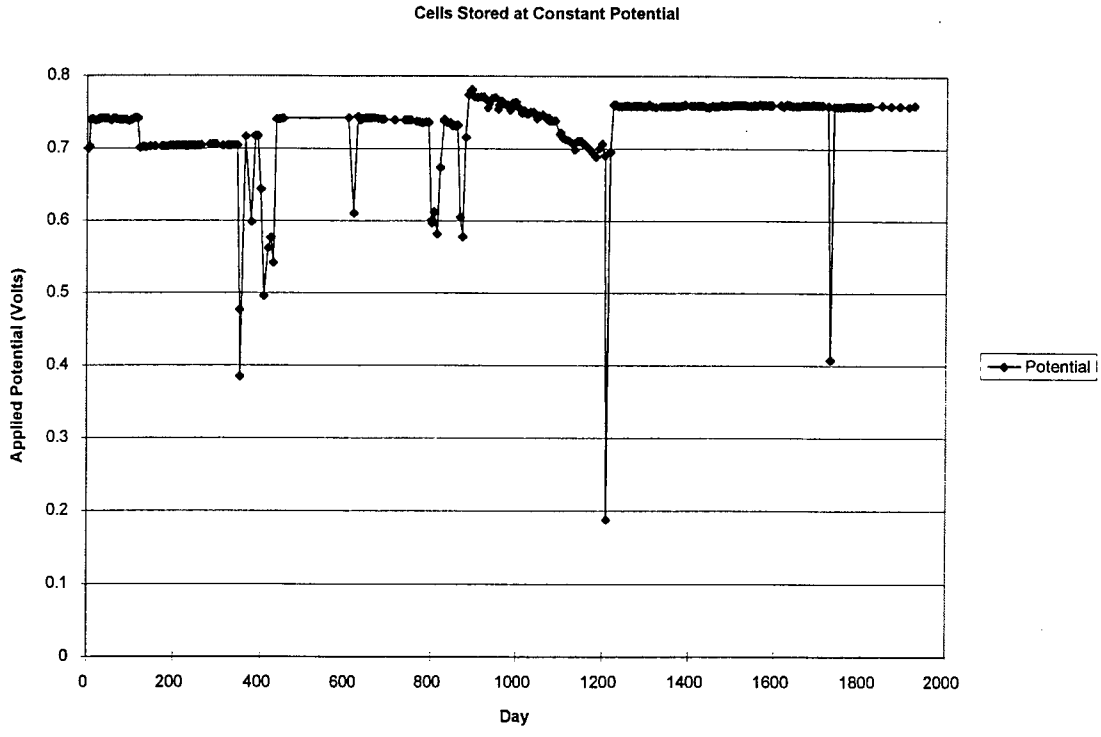

This chart shows the data for the applied potential for the duration of the storage period. The target potential was 0.7 volts. The major deviations can be attributed to test equipment problems.

AIR FORCE NiH2 IPV STORAGE TESTING

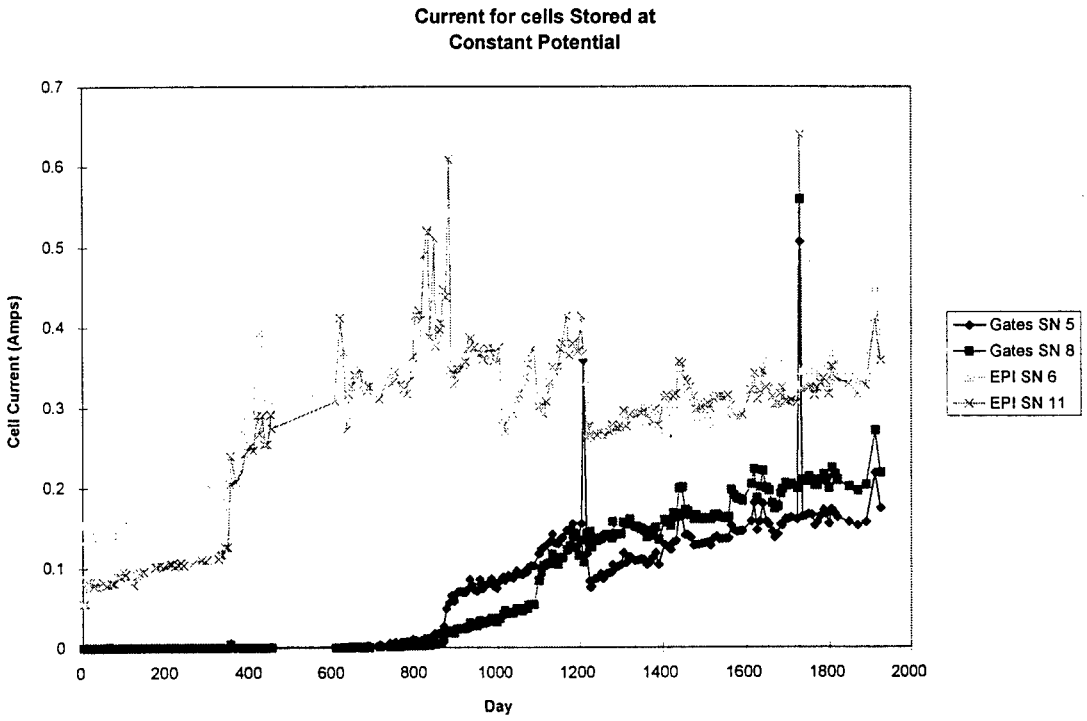

This chart is a plot of cell current for the cells stored at constant potential. The Gates cells show positive precharge until about 800 days. It appears the EPI cells were not positive precharge at the start.

AIR FORCE NiH2 IPV STORAGE TESTING

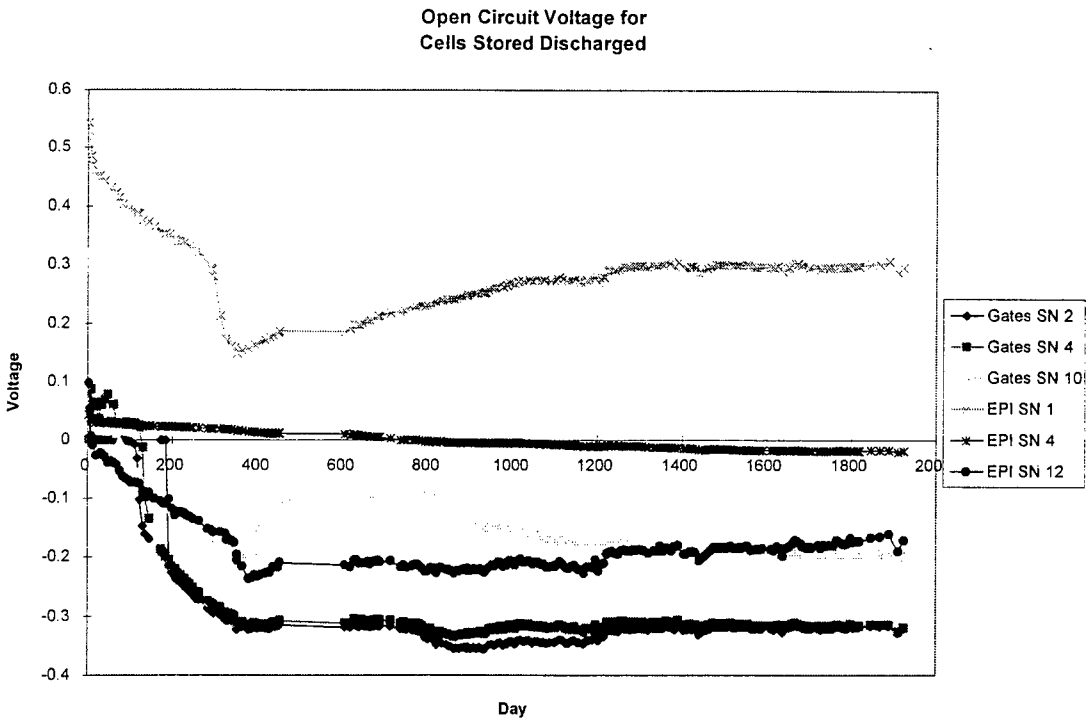

This chart shows the measured open circuit voltage for the cells stored discharged. This data will require further analysis to determine its significance.

AIR FORCE NiH2 IPV STORAGE TESTING

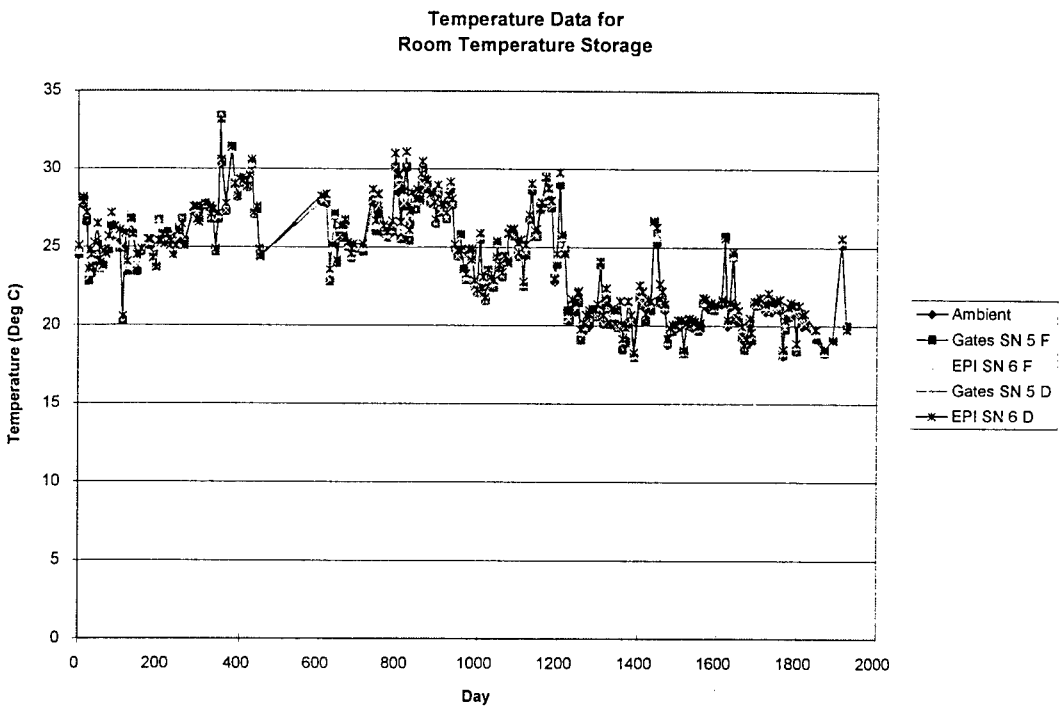

This chart is temperature data for two of the cells being stored at room temperature. Measurements are being made on the dome and flange. The data indicates the cell temperatures do not deviate from the ambient room temperature.

AIR FORCE NiH2 IPV STORAGE TESTING

RESULTS

- CAPACITY TO 1.0V COMPARISONS, 10 DEG C
  - PRE AND POST STORAGE
- 72 HOUR OPEN CIRCUIT STAND
- EPI AND GATES CYCLE 500 COMPARISON
  - STORED CELLS AND CYCLING CELLS
- CAPACITY CHECK VOLTAGE PROFILE, 10 DEG C
  - EPI - OPEN CIRCUIT STORAGE
  - GATES - CONSTANT POTENTIAL

The results that will be presented in this paper are listed above. There is a bar graph showing pre and post storage capacity to 1.0V for all ten cells that were stored. Data is also presented for the 72 hr open circuit stand test. Plots were generated comparing initial cycle profiles for cells stored and the cycling cells. This comparison is at cycle 500 due to the limited cycle data for the stored cells. The final graphs presented are capacity check voltage profiles for the two cell manufactures and the two test conditions. These plots are for the 10 deg C capacity check.

AIR FORCE NiH2 IPV STORAGE TESTING

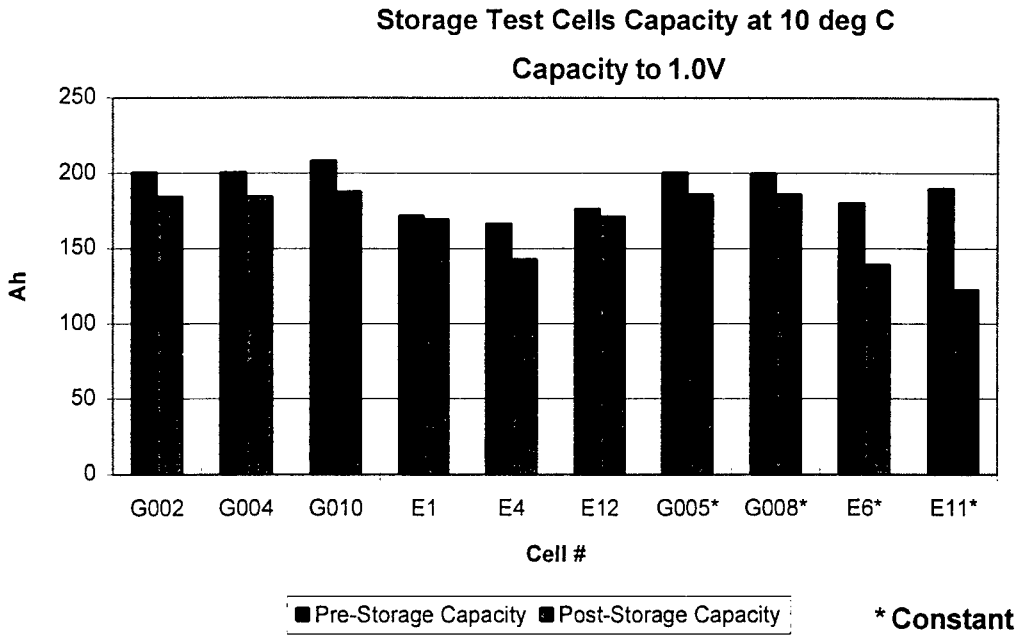

* Constant Potential

This chart is a plot of capacity data to 1.0V before and after storage. This 10 deg C check is representative of the data for other temperatures. The results for all temperatures and both manufacturers show less capacity after storage. The more significant loss for the EPI cells stored at constant potential needs to be investigated. The * indicates the cells stored at the constant potential test condition. This data does show the more significant extra capacity designed into the Gates cells.

AIR FORCE NiH2 IPV STORAGE TESTING

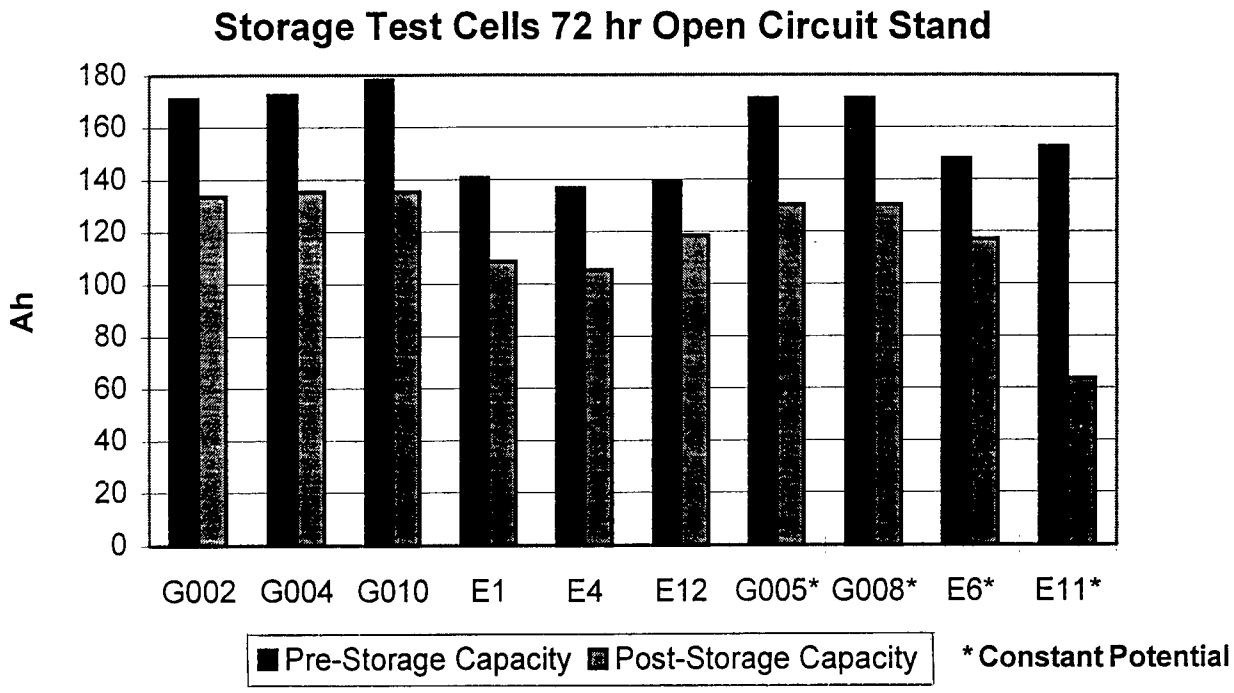

The 72 hour open circuit stand test was repeated after storage. This data shows even more clearly the capacity over design of the Gates cells. This data requires further analysis to determine its significance.

AIR FORCE NiH2 IPV STORAGE TESTING

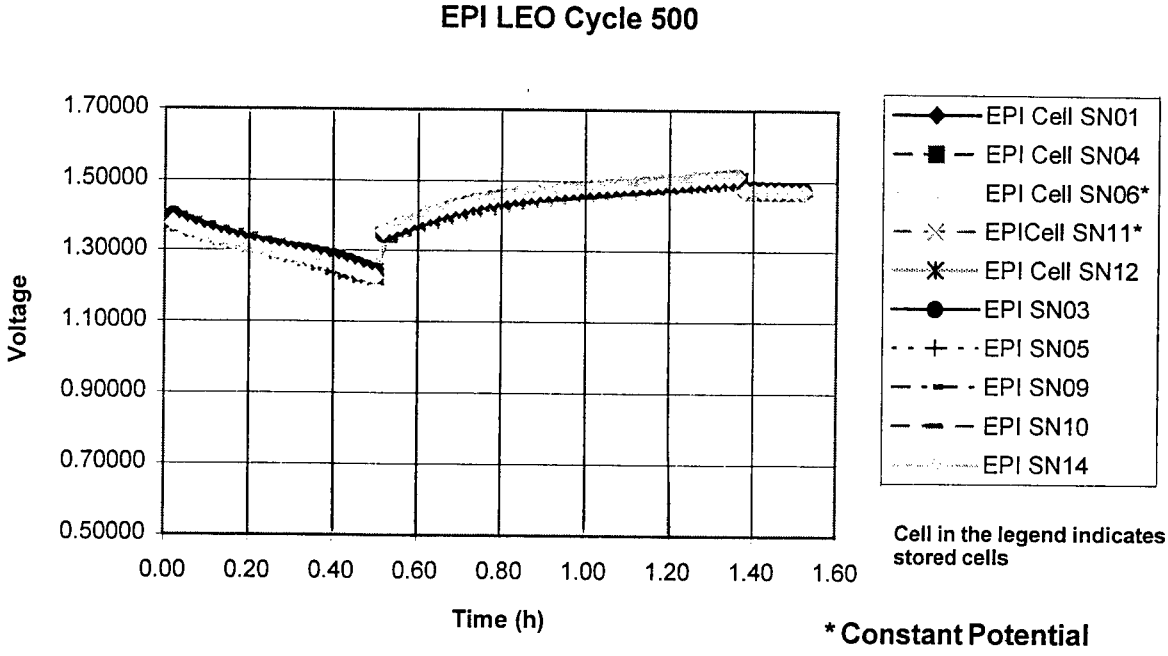

A LEO cycle comparison was made between cycling cells and cells stored for five years. The comparison was made at cycle 500. This graph shows data for EPI cells. At this early point the data looks very good.

AIR FORCE NiH2 IPV STORAGE TESTING

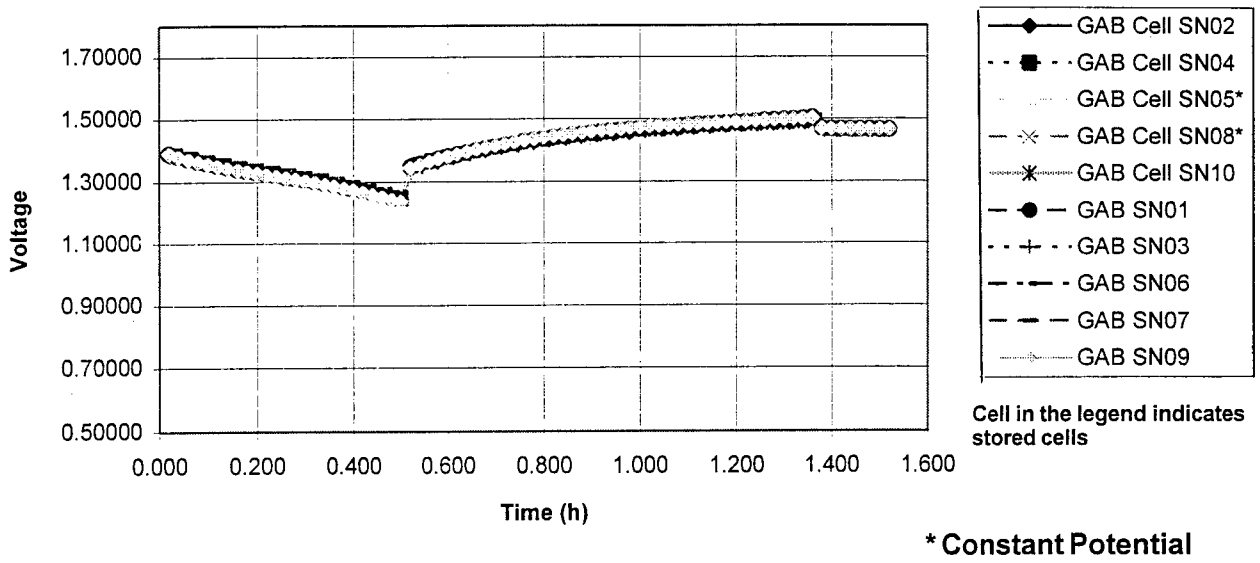

A LEO cycle comparison was made between cycling cells and cells stored for five years. The comparison was made at cycle 500. This graph shows data for Gates cells. At this early point the data looks very good.

AIR FORCE NiH2 IPV STORAGE TESTING

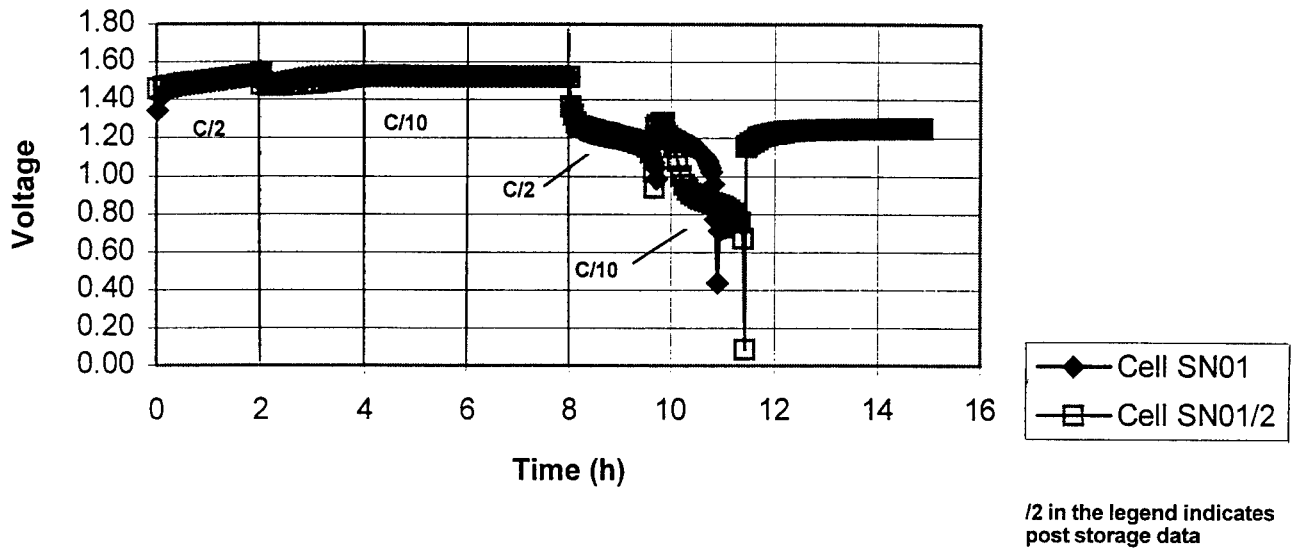

/2 in the legend indicates post storage data

This chart is a plot of a voltage profile for a 10 deg C capacity check. The data is for EPI cells stored under the open circuit test condition. The different rates are shown on the graph. This data is representative of the other temperatures and storage conditions. The data indicates an increase in capacity at the low rate discharge.

AIR FORCE NiH2 IPV STORAGE TESTING

GATES

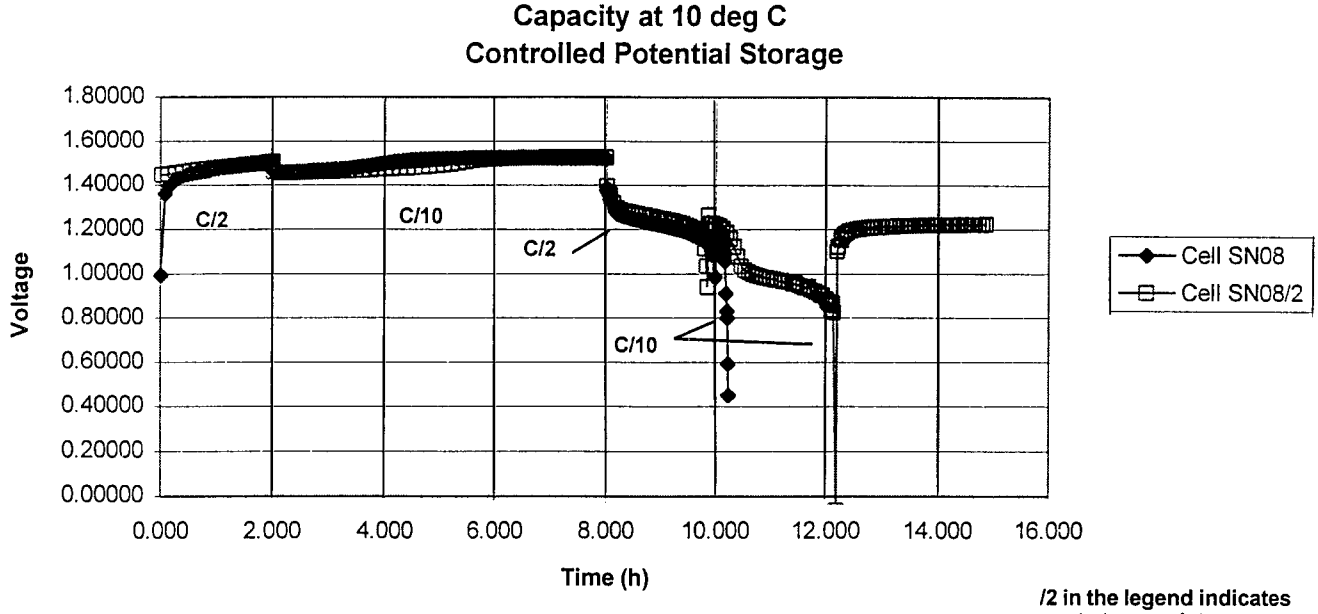

/2 in the legend indicates post storage data

This chart is a plot of a voltage profile for a 10 deg C capacity check. The data is for Gates cells stored under the constant potential test condition. The different rates are shown on the graph. This data is representative of the other temperatures and storage conditions. The data indicates an increase in capacity at the low rate discharge.

AIR FORCE NiH2 IPV STORAGE TESTING

OBSERVATIONS & CONCLUSION

- EVIDENCE THAT EPI CELLS WERE NOT POSITIVE PRE-CHARGE
- GATES CELLS CHANGE OR LOSE POSITIVE PRECHARGE AFTER 800 DAYS
- AT CYCLE 500 THE VOLTAGE PROFILES LOOK GOOD BETWEEN STORED AND NON-STORED CELLS
- DECREASE IN CAPACITY TO 1.0V FOR ALL CELLS AND ALL TEMP
- CAPACITY CHECK VOLTAGE PROFILE INDICATES INCREASE IN CAPACITY AT LOW RATE (C/10)

- BASED ON PRELIMINARY ANALYSIS
- MORE ANALYSIS WILL BE PERFORMED IN FUTURE
- THE STORAGE TEST PROGRAM IS ZERO FUNDED AFTER FY95 FUNDS EXPENDED (Jan 96)

This chart lists some of our observations from our initial evaluation of the data. More analysis will be necessary to confirm these observations. The observation of the precharge status is based on the cell current data. The decrease in capacity to 1.0V was evident in all the cells at all temperatures and is shown with the 10 deg C data. The capacity check voltage profiles show the increase in capacity at low rates for the stored cells.
The funding information is presented to keep the space power and battery community informed regarding this test.

HUBBLE SPACE TELESCOPE ONBOARD BATTERY PERFORMANCE

Presented to
1995 NASA AEROSPACE BATTERY WORKSHOP

Presented By
Gopalakrishna M. Rao
Harry Wajsgras
Space Power Applications Branch
NASA/Goddard Space Flight Center
Greenbelt, Maryland, USA 20771
and
Hari Vaidyanathan
COMSAT Laboratories
Clarksburg, Maryland 20871
and
Jon D. Armontrout
Lockheed-Martin
Electrical Power Products
Sunnyvale, California 94089

November 29, 1995

HST

- Six 88 Ah Ni-H2 batteries in two three-battery modules (Flight Spare Module(FSM) and Flight Module 2(FM2))
- Common bus for all batteries to operate at a common voltage
- 22 series cells per battery
- Positive plate fabrication
  - FSM in 2 - 6/88
  - FM2 in 6 - 11/88
- Cell activation
  - FSM in 1/89
  - FM2 in 3/89
- Launched on 4/24/90

CELL DESIGN SUMMARY

AF "Pineapple Slice" Cell Design with the Following Components:

- 48 Dry Sintered Nickel Positive Electrodes (0.035 in. thick)
- 48 Platinum Negative Electrodes (0.006 in. thick)
- Zirconium Oxide Cloth Separators and Gas Screens
- Polysulfone End Plates, Core and Retaining Nut
- Belleville and Whiteley Washers
- Inconel 718 Pressure Vessel (0.040 in. thick)
- Zirconium Oxide Pressure Vessel Wall Wick
- Inconel 718 Terminal Bosses and Weld Ring
- Injection Molded Nylon Terminal Seals

CELL DIAGRAM

BATTERY SPECIFICATION

SIX BATTERY SYSTEM	MAXIMUM DOD 14%	WITH ONE BATTERY FAILED
BATTERY CAPACITY AT 0°C	88 AMP-HR	AT 15 AMP (C/6) DISCHARGE RATE
MAX. DISCHARGE CURRENT	20 AMPERES	TO 26.5 VOLTS DC AT BATTERY
PEAK DISCHARGE CURRENT	30 AMPERES	FOR 10 SECONDS MAXIMUM
CHARGING RANGES	5.0 TO 18.0 AMPERES	DURING ORBITAL OPERATIONS
ORBITAL LIFE	FIVE YEARS	

BATTERY DIAGRAM

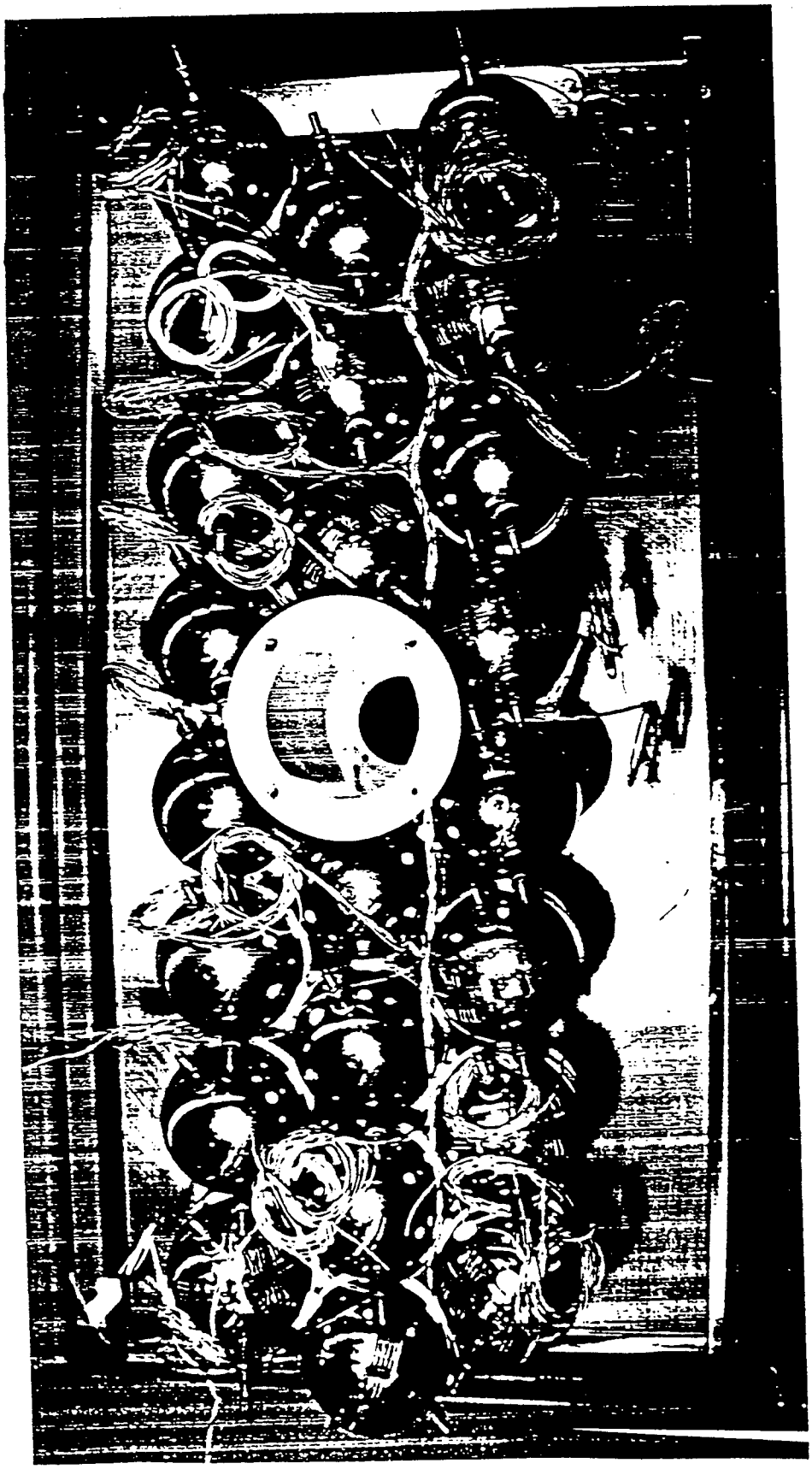

BATTERY MODULE

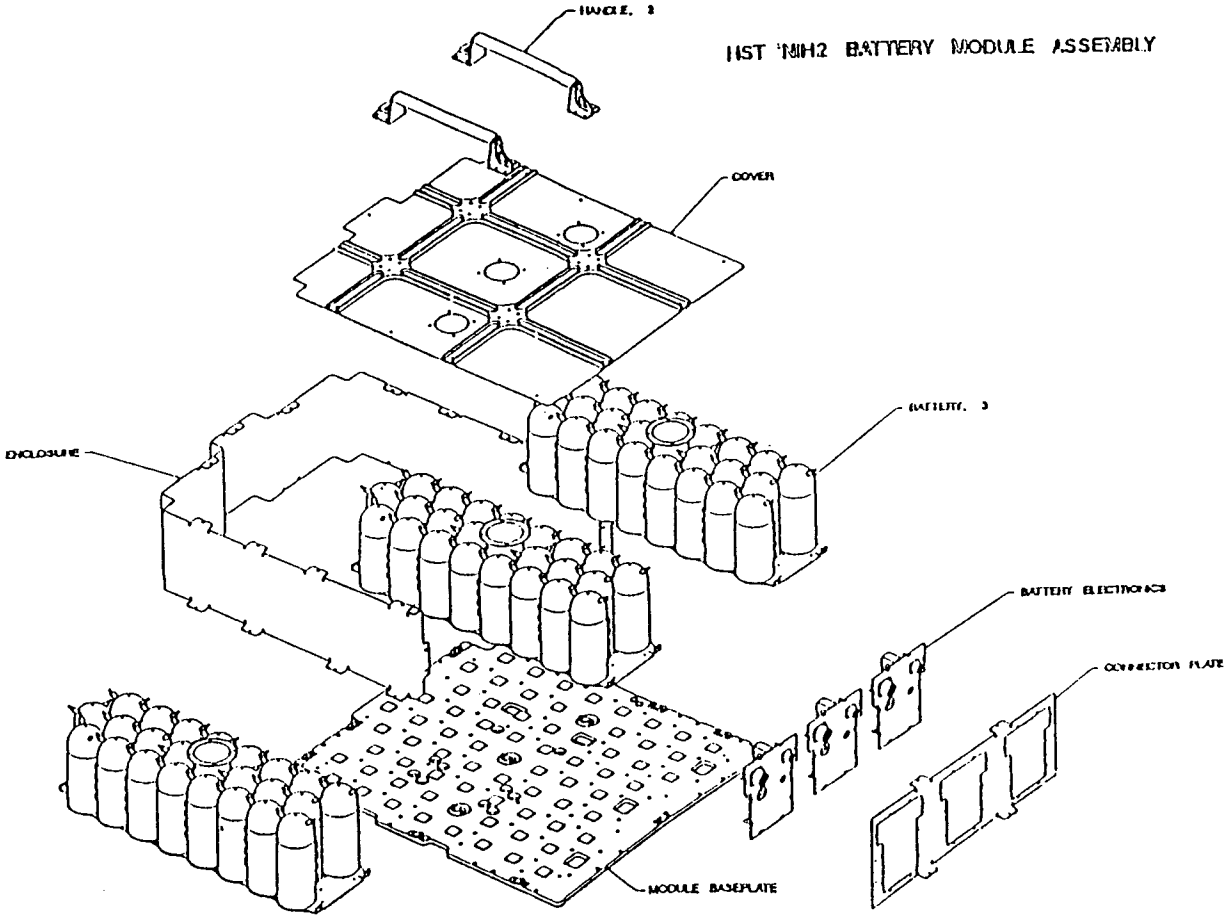

SIMPLIFIED BLOCK DIAGRAM

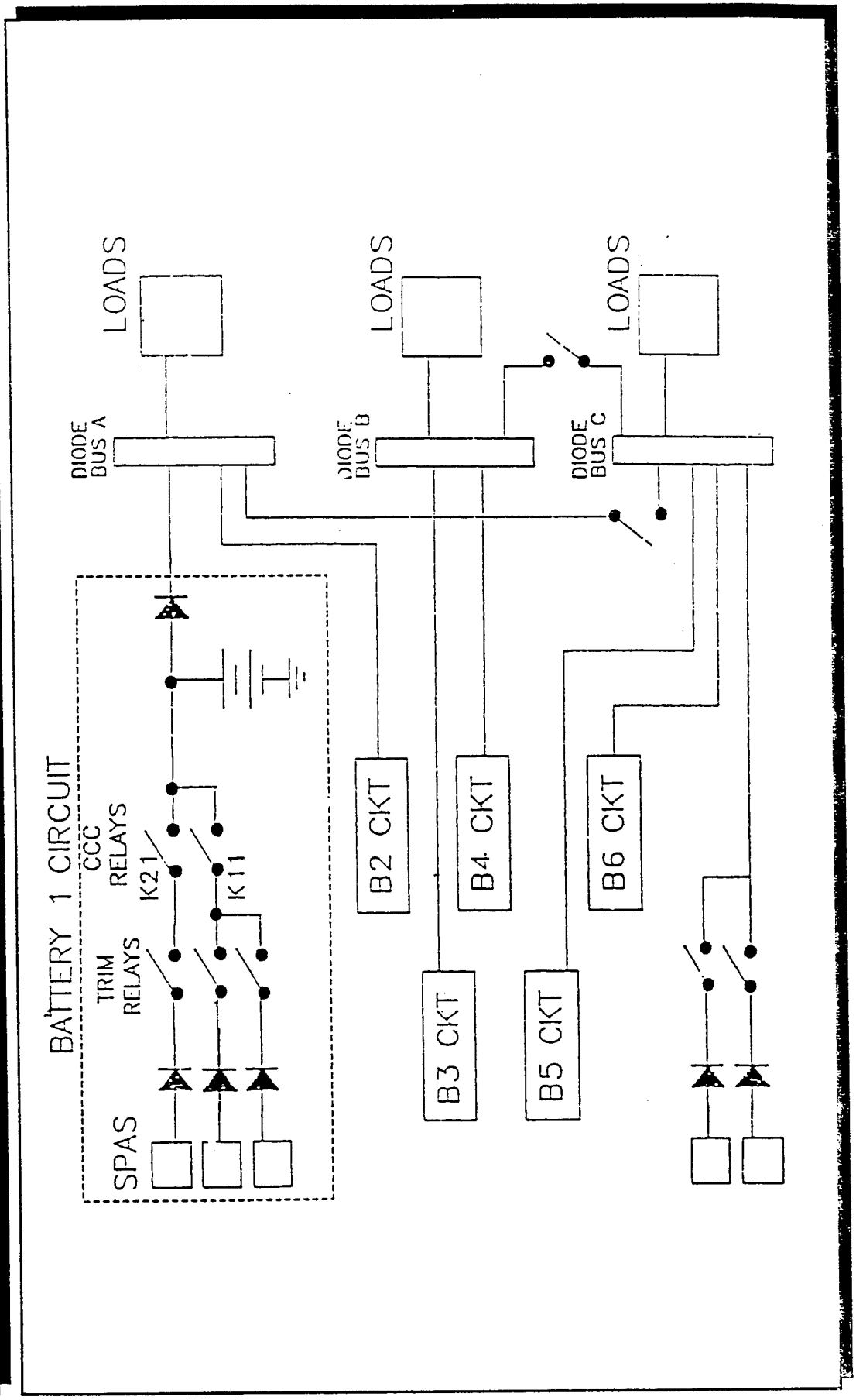

CCC K1 AND K2 LEVEL VT CURVES

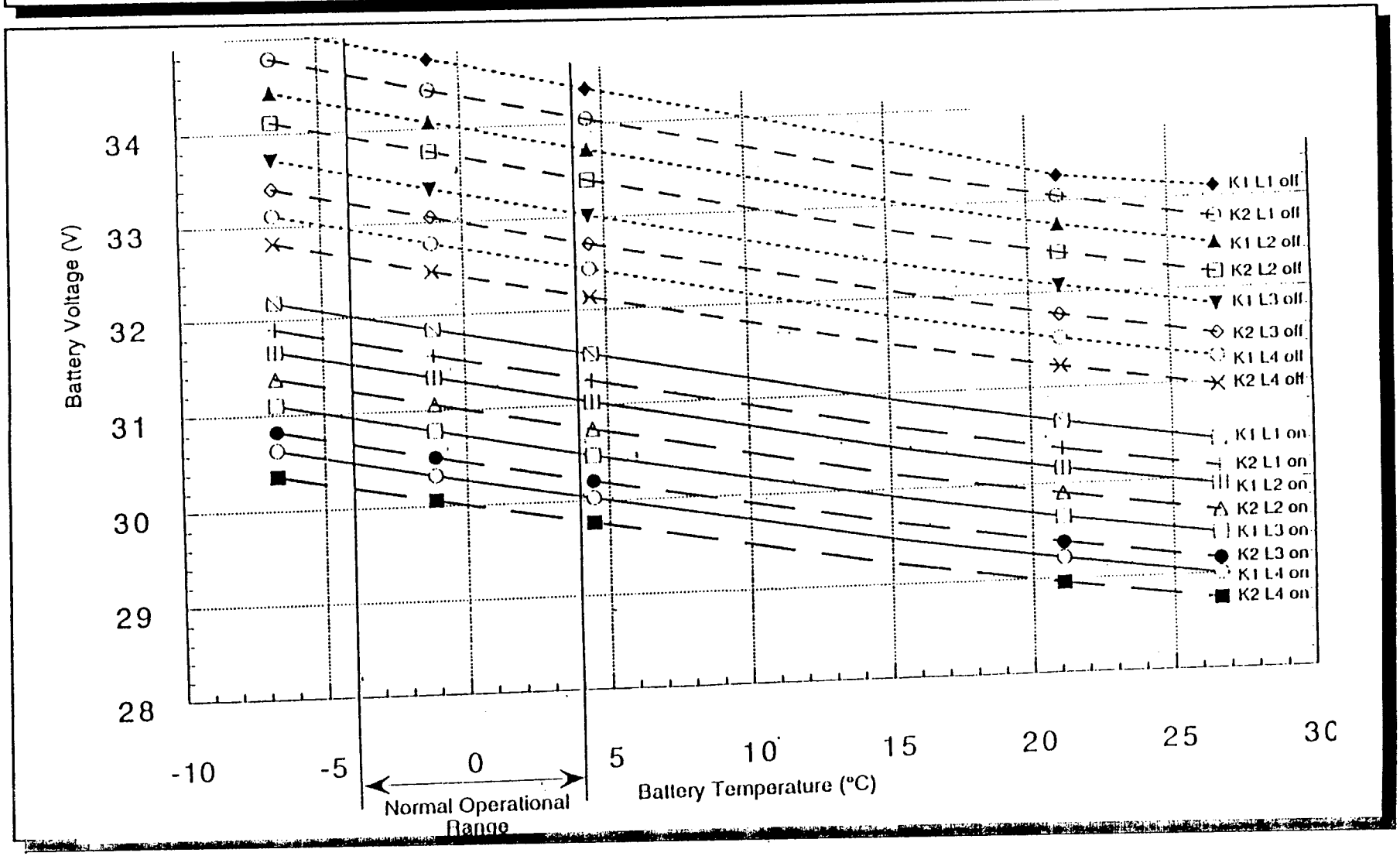

SYSTEM CONSTRAINTS

THERMAL: DISSIPATION OF HEAT GENERATED IN BATTERY CONDUCTED THROUGH TWO INCH HONEYCOMB PANEL PRIOR TO RADIATING TO SPACE

LOUVERS AND MLI ON BAY DOOR INSTALLED ON EXTERIOR BAY DOOR SURFACE TO REDUCE BATTERY HEATER DUTY CYCLES

BATTERIES IN INTIMATE PROXIMITY AND THERMALLY COUPLED

TEMPERATURE OPERATING RANGE: -5°C TO 20°C

ELECTRICAL: MAXIMUM CHARGE VOLTAGE 34.3 VOLTS DC (SYSTEM CONSTRAINT)
THIS TRANSLATES TO 1.56 VOLTS DC PER CELL
(THERMAL LIMITATION IS 1.53 VOLTS PER CELL)
MINIMUM DISCHARGE VOLTAGE 26.5 VOLTS DC (SYSTEM CONSTRAINT)
THIS TRANSLATES TO 1.20 VOLTS DC PER CELL AND WAS
SECONDARY REASON FOR ADJUSTING ELECTROLYTE CONC.

OPERATING PARAMETERS

Parameter	Value
Temperature	0° ± 3°C
Charge Rate (max)	18A
Charge Control	V/T level K1L4
Total Load	1625 to 2,400 W
Reconditioning Load	5.1 Ω/22-cell battery
Discharge Mode	All batteries in parallel

ONBOARD BATTERY MANAGEMENT

- 15 Charge and Discharge Cycles per Day
- The Constant Current Charge to Preselected VT Level With a Recharge Ratio of 1.05
- Battery Cycles Between 70- and 88-Percent State-of-Charge
- Periodic Reconditioning of the Batteries

CURRENT STATUS

- Five Years of Nominal Performance
- Hardware Mode Operation at VT Level K1L4
- Complete 29874 Eclipse Orbits
- Depth of Discharge ranged between 5 to 8.5%
- System Capacity = 450Ah
- Operating Temperature = 0 ± 3 degrees
- Average Recharge Ratio about 1.05
- Last Reconditioning - November 16-17, 95 on Battery #2, Coulombic Capacity to 26.4V about 72.4Ah

VARIATION OF EOD VOLTAGE WITH CYCLING

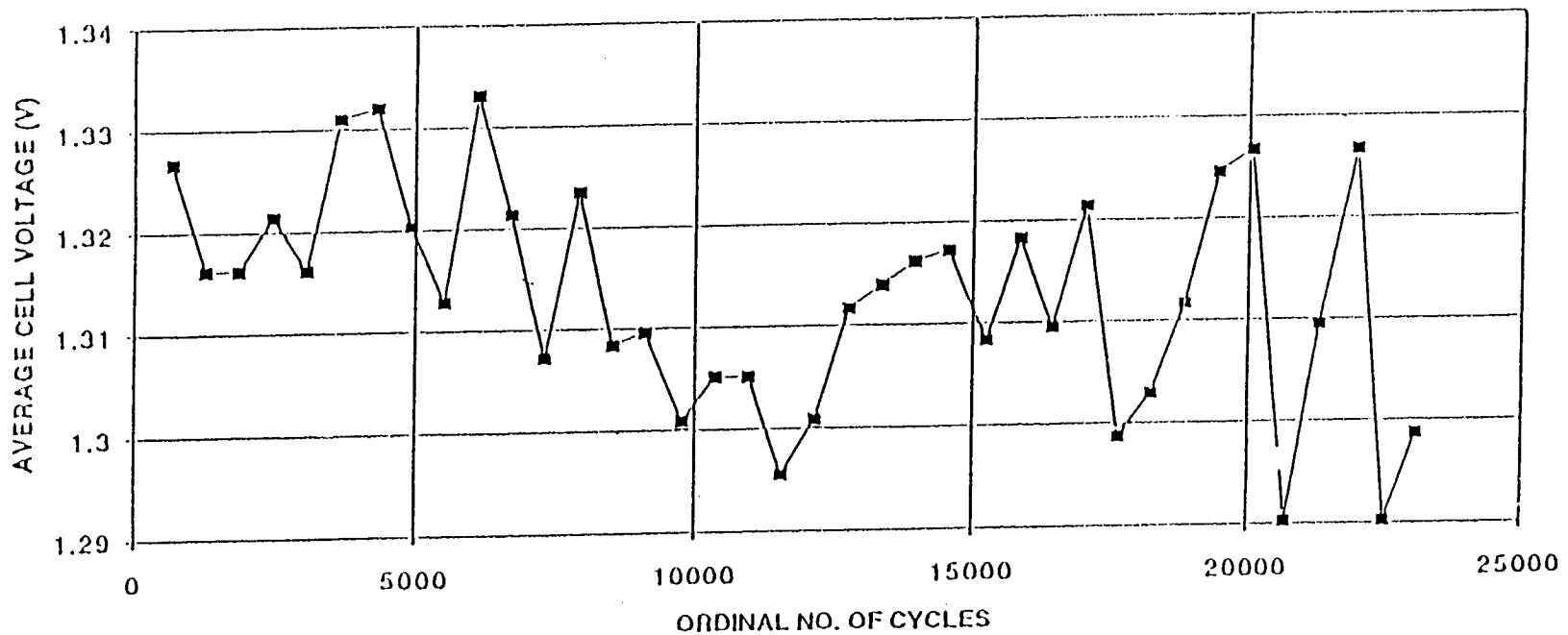

DEVIATION IN EOD VOLTAGE WITH CYCLING

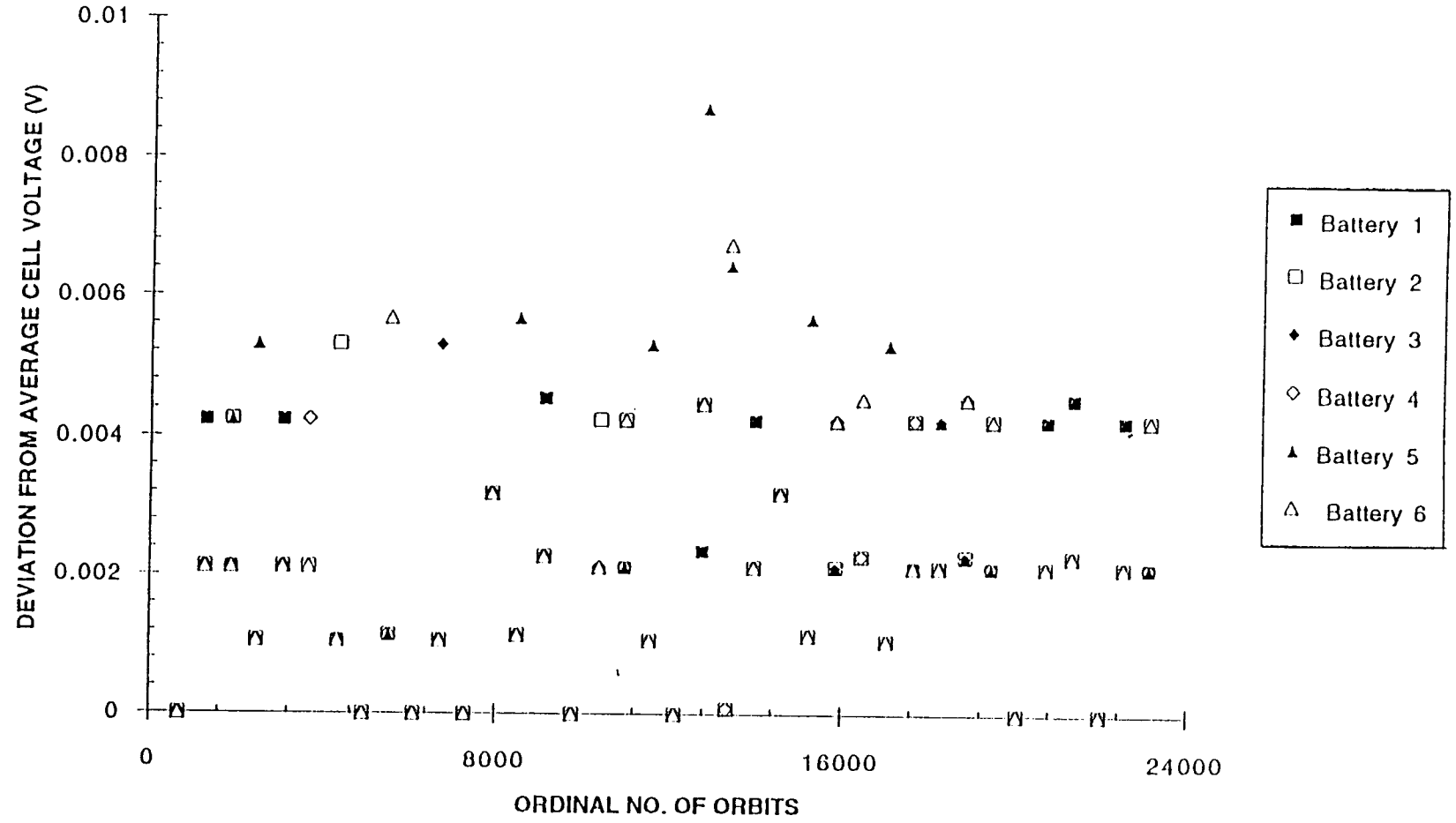

VARIATION OF TEMPERATURE WITH CYCLING

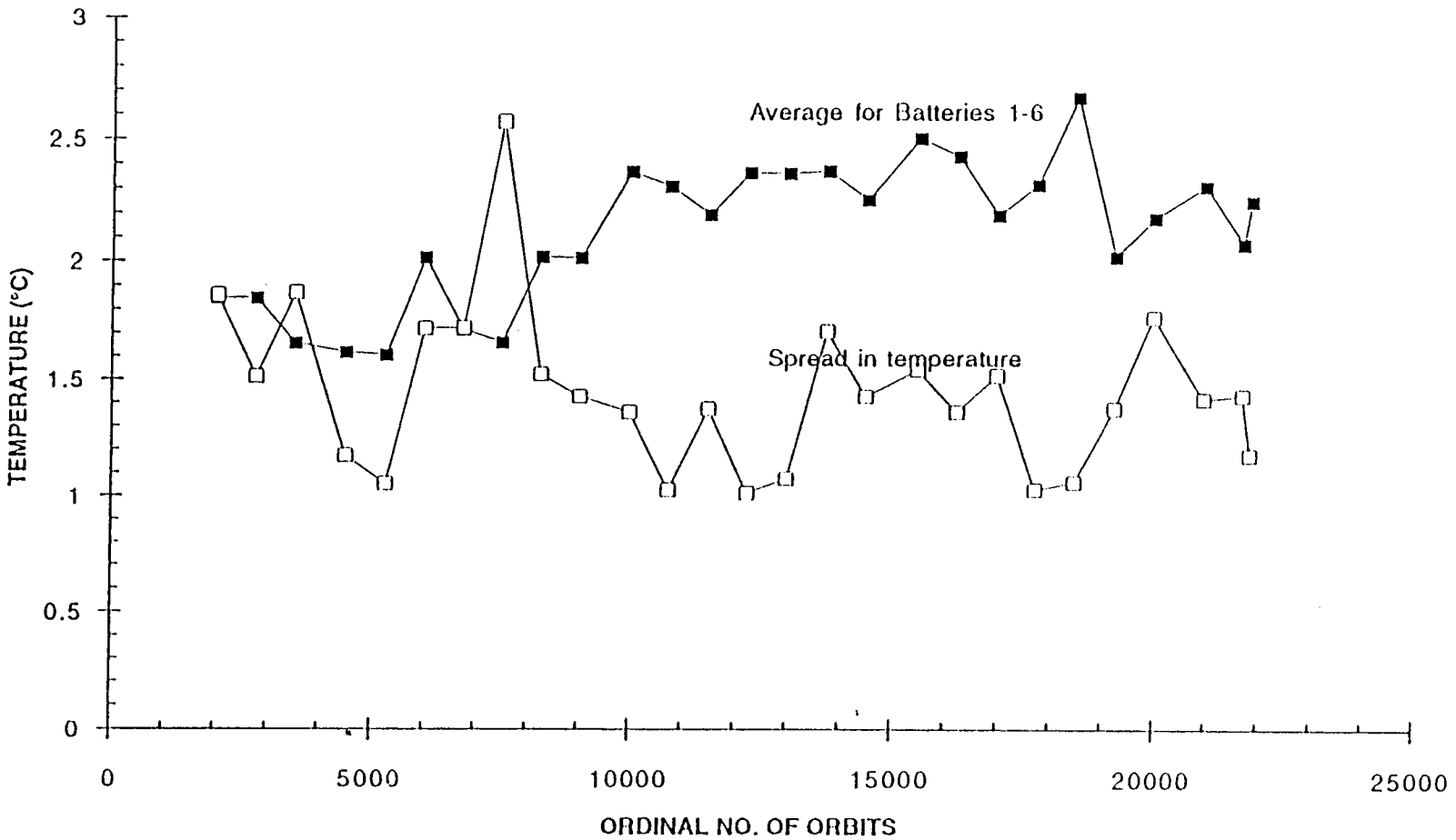

VARIATION OF DEPTH OF DISCHARGE WITH CYCLING

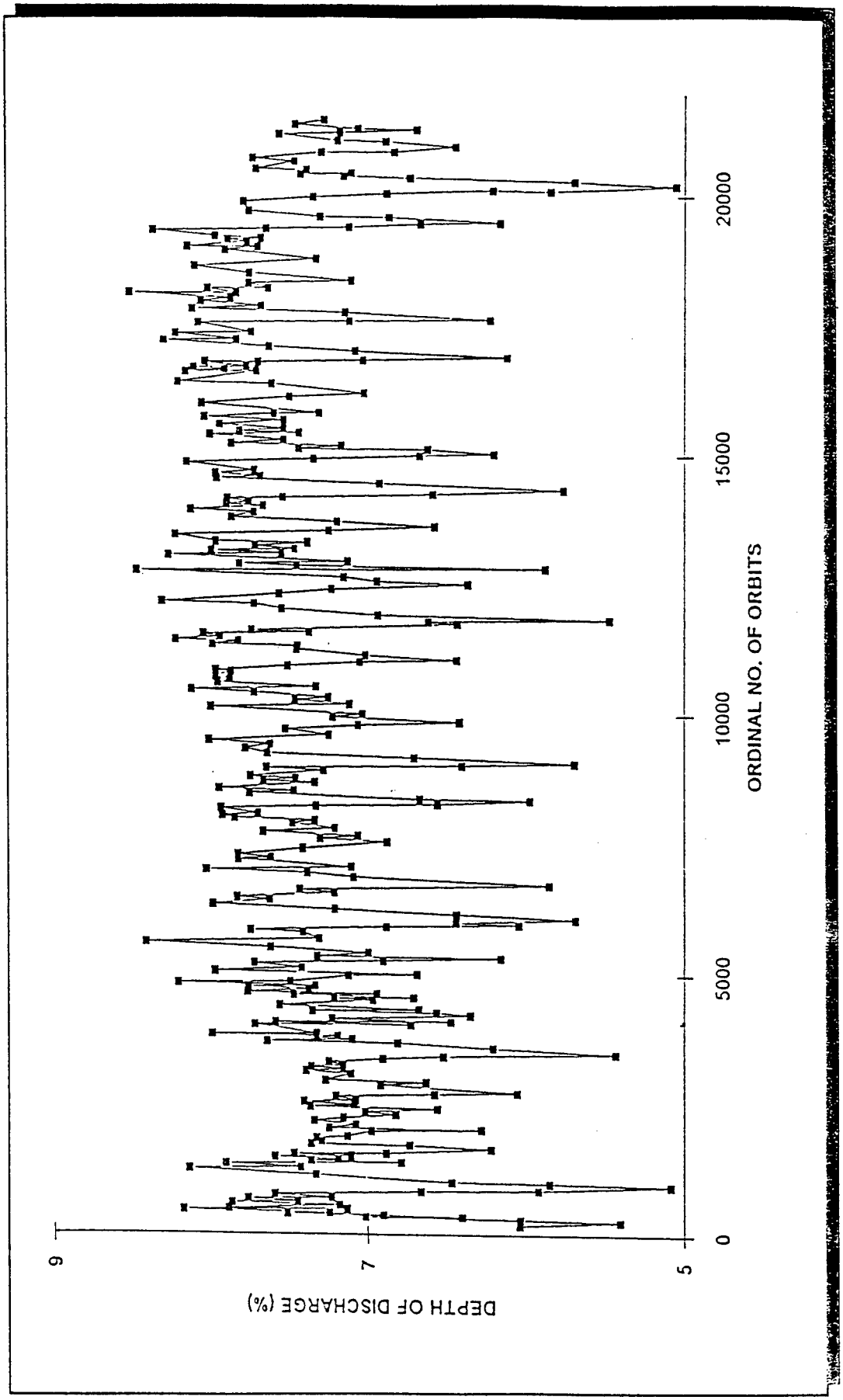

VARIATION OF RECHARGE RATIO WITH CYCLING FOR BATTERY 1

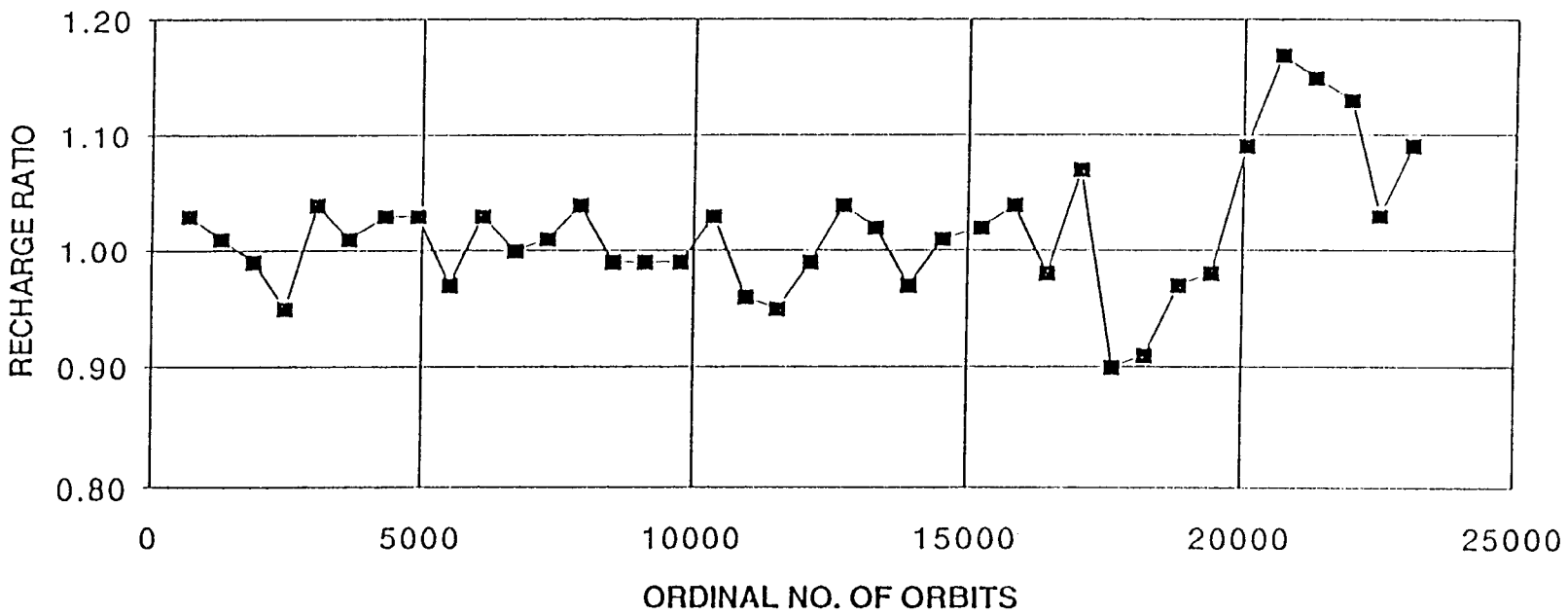

VARIATION OF PRESSURE WITH CYCLING FOR BATTERY 3

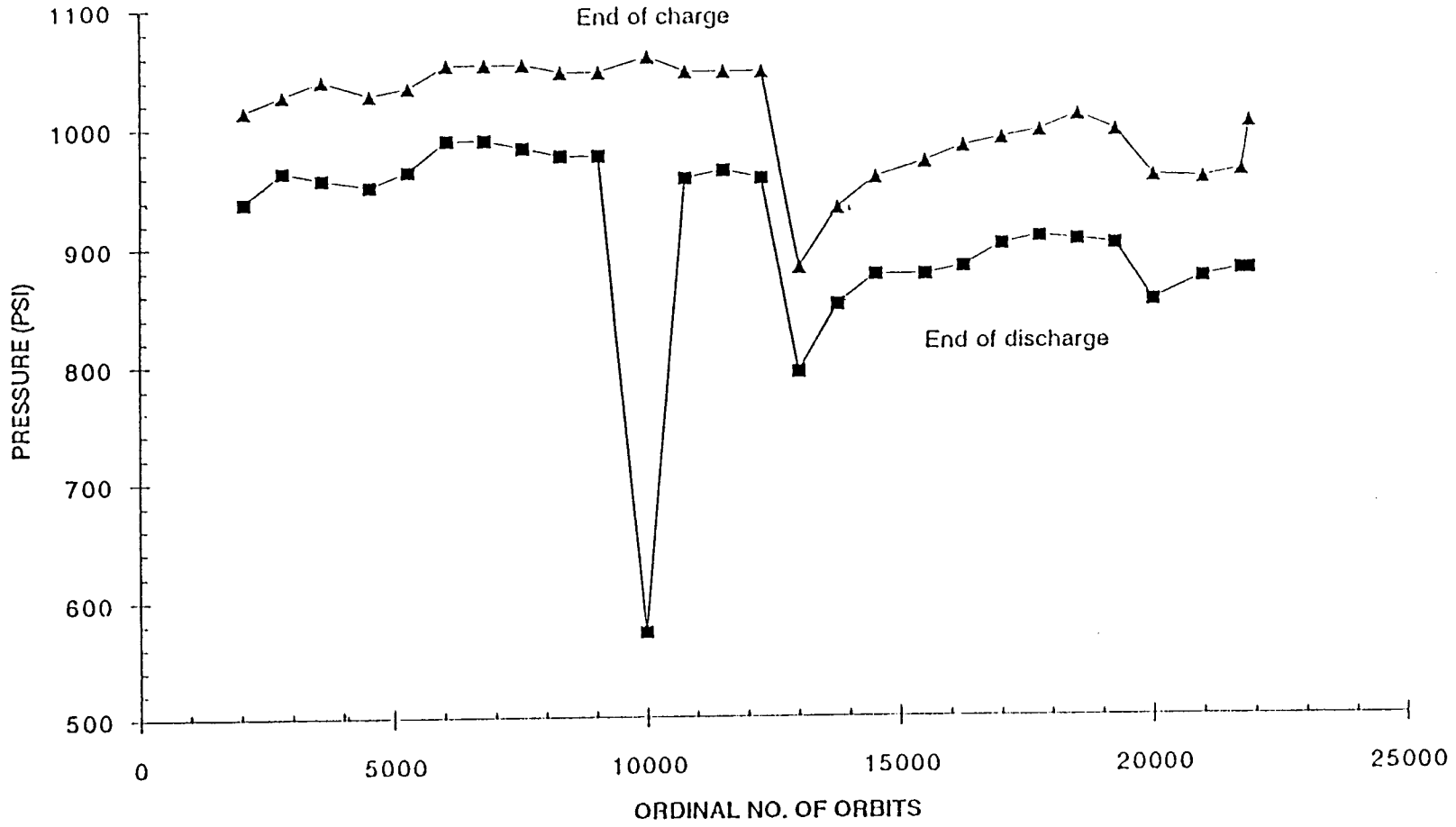

BATTERY LOAD SHARING (PERCENT)

Battery No.	Orbit 100	Orbit 21,050
1	16.5	16.9
2	17.2	17.5
3	16.8	17.0
4	16.7	16.6
5	16.2	16.0
6	16.2	16.0

PERFORMANCE SUMMARY

- The Cell Voltage Is Declining at the Rate of 6.99×10^{-4} mV/cycle
- The Temperature Gradient is Negligible.
- The Load Sharing is in the Expected Range.
- The Preselected Voltage for Charge Termination Is Appropriate for the Time Being
- The End of Charge Pressure has Increases of 9.5 - 29.5 psi for Batteries 1, 4, 5 and 6 and Decreased by 13 - 38 psi for Batteries 2 and 3.
- The Average Capacity of the Batteries to 26.4 V has Decreased by 19%

RECONDITIONING PARAMETERS

BATTERY NO.	RECONDITIONING DATE	CYCLES	VOLTAGE LIMIT V/T LEVEL	SUNLIGHT TIME (min)	CAPACITY CALCULATED FROM CURRENT TO 26.4 V (Ah)	CAPACITY CALCULATED FROM PRESSURE TO 26.4 V (Ah)	END OF RECONDITIONING VOLTAGE (V)
1	12/90	3,383	1.504	69.0	94.2	93.0	19
	8/94	21,900	1.488	62.0	80.4	94.4	15
	7/95	28,410	1.488	63.8	74.5	81.5	15
2	8/92	12,940	1.504	61.3	88.5	94.0	13
	12/94	23,700	1.488	69.8	79.3	82.2	15
	11/95	30,330	1.488	68.3	72.4	76.4	15
3	8/92	12,940	1.504	61.3	85.6	92.3	13
	4/95	25,500	1.488	61.4	73.5	82.2	15
4	12/90	3,383	1.504	69.0	88.0	93.4	19
5	8/92	12,940	1.504	61.6	94.0	102.6	13
	2/95	24,600	1.488	61.2	78.3	94.8	15
6	8/92	12,940	1.504	61.2	88.3	93.9	13
	10/94	22,890	1.488	65.5	74.6	86.5	15
	9/95	29,270	1.488	64.1	70.5	74.2	15

RECONDITIONING: Battery 2 Current Profile

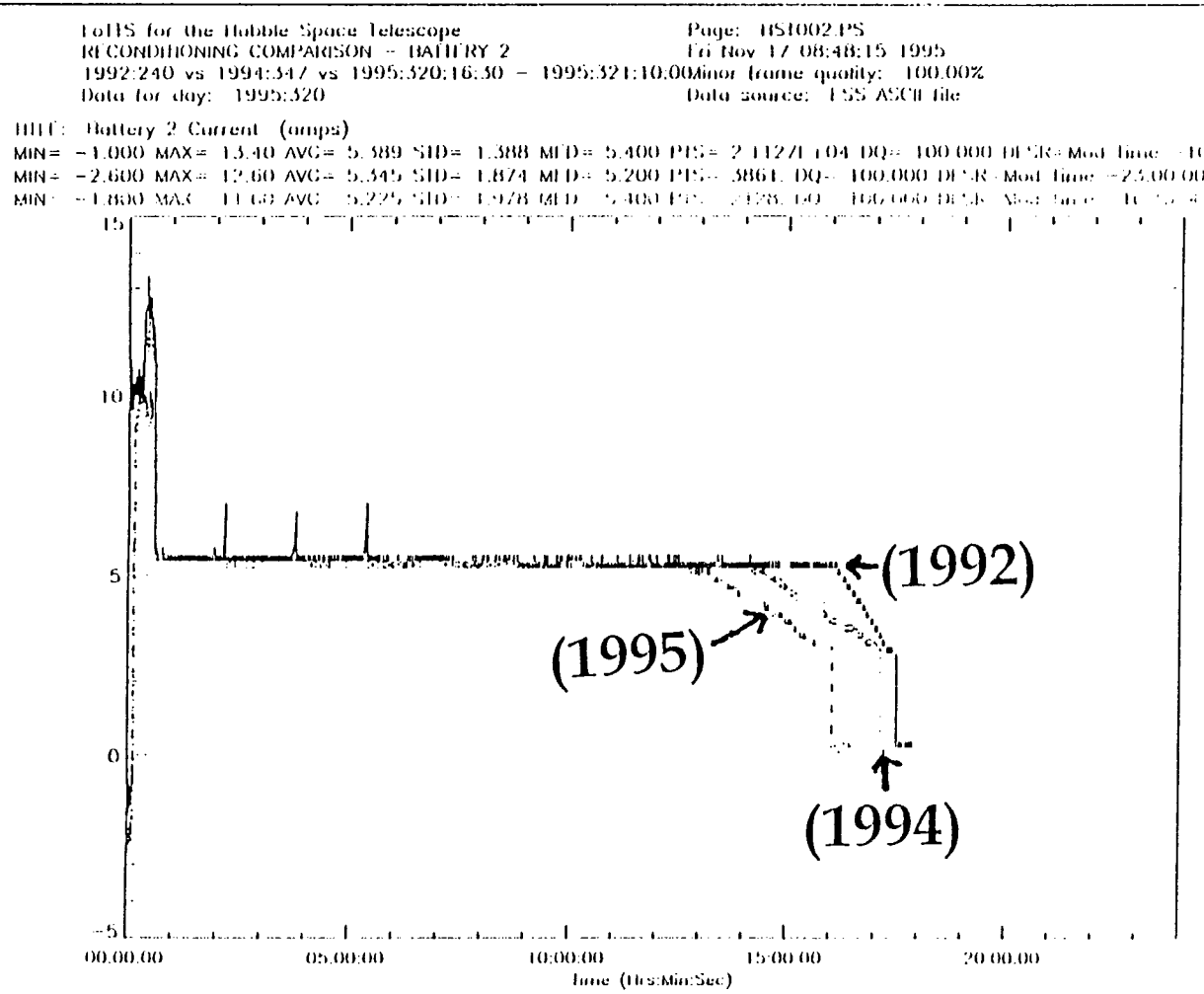

RECONDITIONING: Battery 2 Pressure Profile

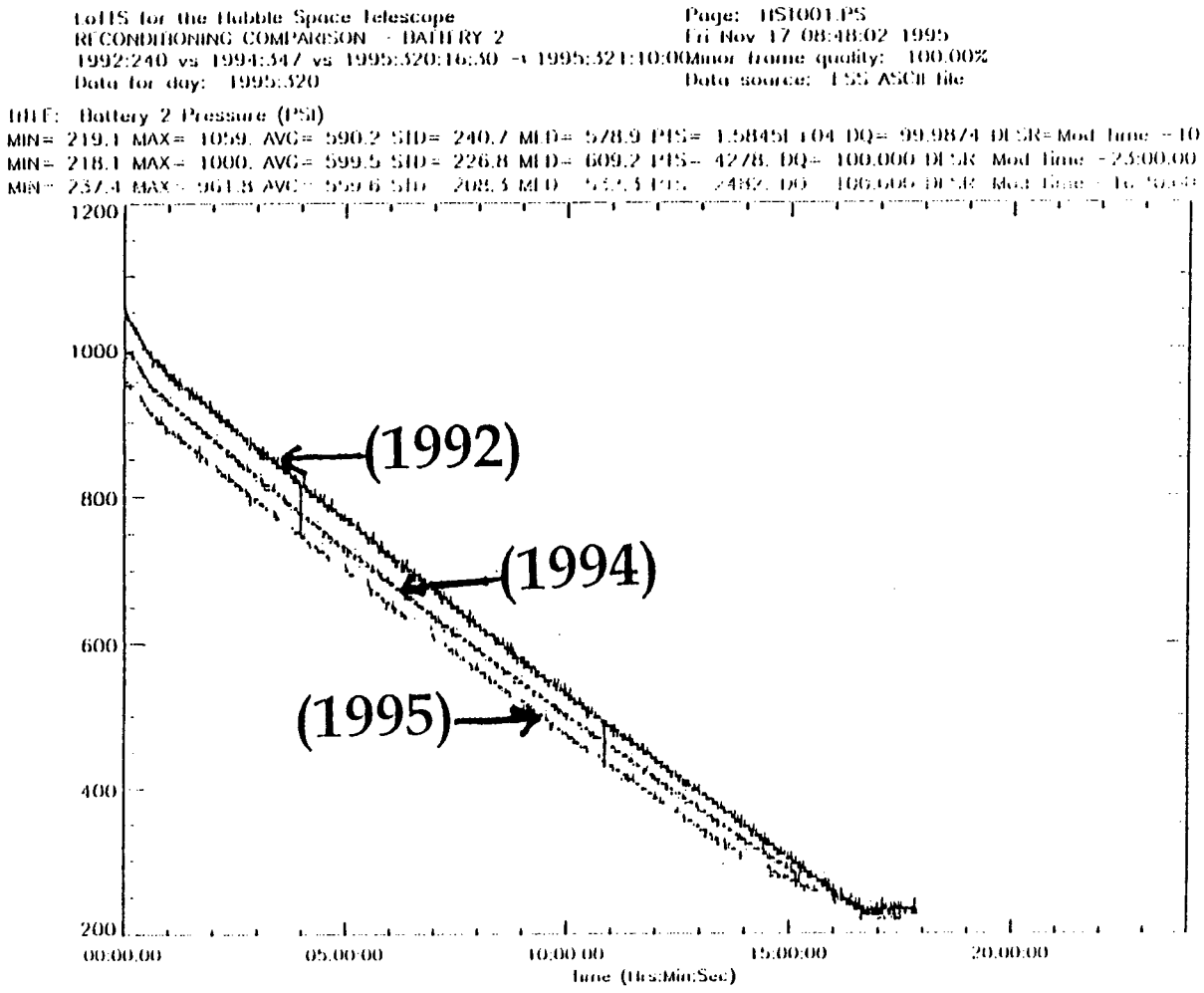

RECONDITIONING: Battery 2 Voltage Profile

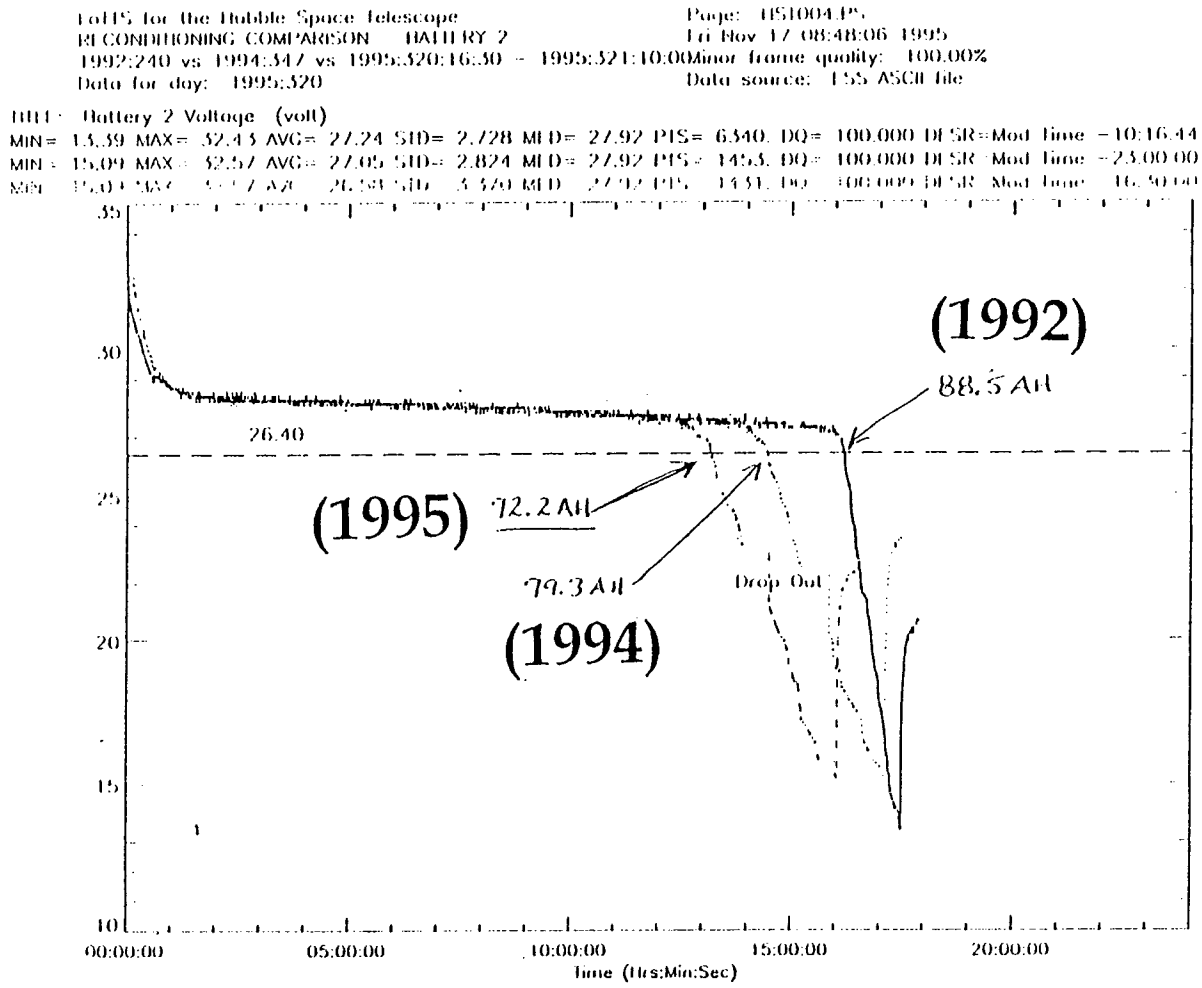

RECONDITIONING CAPACITY DATA

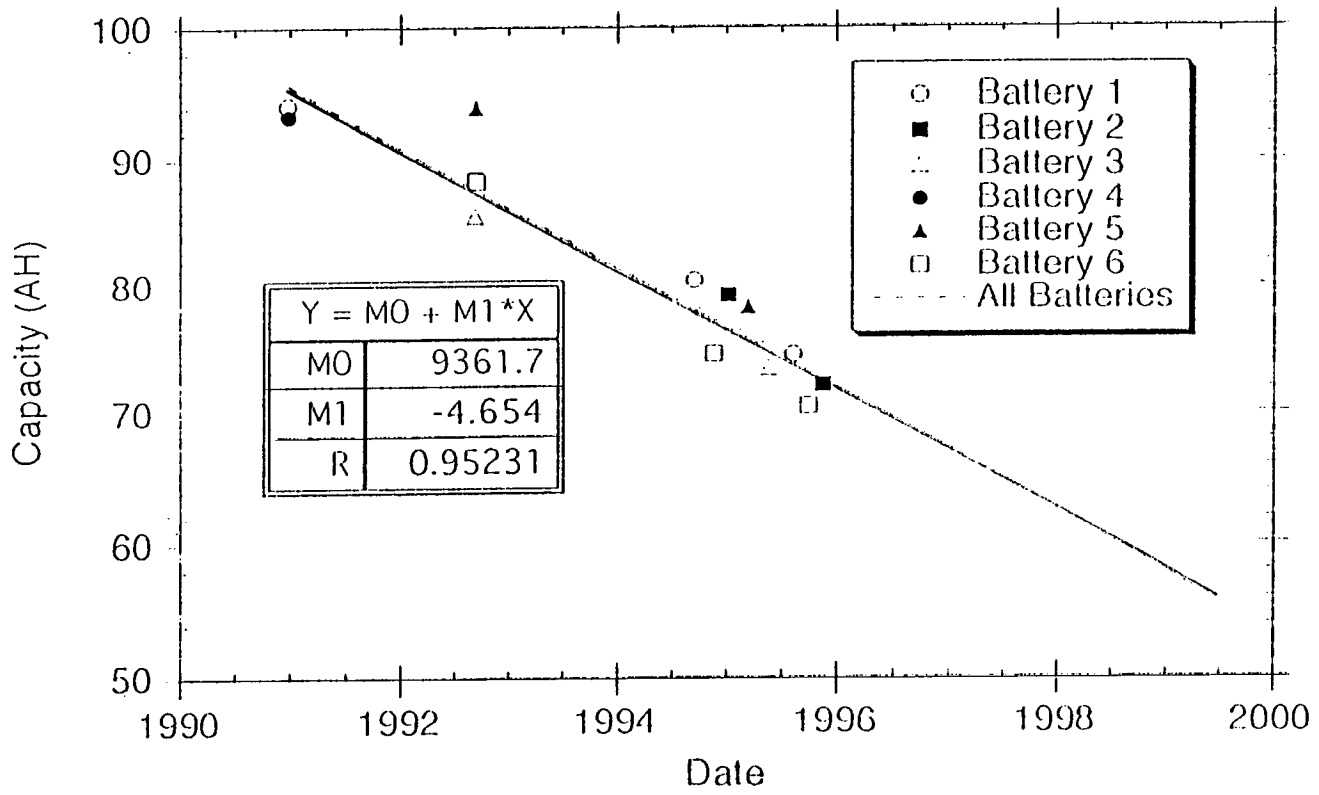

CONCLUSIONS

- The Batteries exhibit a High Level of Performance in Voltage, Capacity, and Pressure with Stable Recharge Ratio, Temperature and Load Sharing.
- In Orbit Performance does not raise Concern on Life Expectancy up to Nine Years. Additional Data would be required to further Quantify the Capacity Degradation.
- The Capacity Loss in the Batteries may be due to Premature Battery Charge Termination at Lower VT Level (K1L4); Operating Batteries on Secondary Heaters and/or at higher VT Levels are under Consideration . The Capacity Loss due to Corrosion of Nickel Sinter may not be precluded.

SINGLE BATTERY POWER SUBSYSTEMS: ON–LINE RECONDITIONING

R.F. TOBIAS
TRW SPACE AND ELECTRONICS GROUP
REDONDO BEACH, CALIFORNIA

THE 1995 NASA AEROSPACE BATTERY WORKSHOP
THE HUNTSVILLE HILTON
HUNTSVILLE, ALABAMA
NOVEMBER 28 - 30 , 1995

BACKGROUND

- DETAILED TRADE STUDIES CONDUCTED AT TRW SHOW THAT THE ELECTRICAL POWER SUBSYSTEM (EPS) ARCHITECTURE THAT OFFERS THE HIGHEST RELIABILITY, LOWEST WEIGHT AND LOWEST COST IS A SINGLE NICKEL-HYDROGEN BATTERY, SINGLE BUS APPROACH

- FOR A SINGLE NICKEL-HYDROGEN BATTERY SYSTEM CELL REDUNDANCY IS REQUIRED

  - EXTRA CELLS ARE ADDED TO THE SERIES CONNECTED CELLS IN ORDER TO ALLOW FOR CELL FAILURES

  - CELL BYPASS CIRCUITRY IS INCLUDED FOR EACH CELL IN ORDER TO ALLOW A CELL TO FAIL "OPEN"

BACKGROUND (CON'T)

- TRADITIONAL DEEP DISCHARGE RECONDITIONING (BATTERY RECONDITIONED OFF-LINE TO A VOLTAGE OF LESS THAN 1.0 VOLT/CELL) CAN NOT BE PERFORMED BECAUSE THE BATTERY IS DIRECTLY CONNECTED TO THE BUS

- TODAY'S PRESENTATION ADDRESSES AN ON-LINE APPROACH TO RECONDITIONING (" SHALLOW" RECONDITIONING)
  -- LIMITED DATA WILL BE PRESENTED DEMONSTRATING BATTERY PERFORMANCE ENHANCEMENT

SINGLE BUS, SINGLE BATTERY

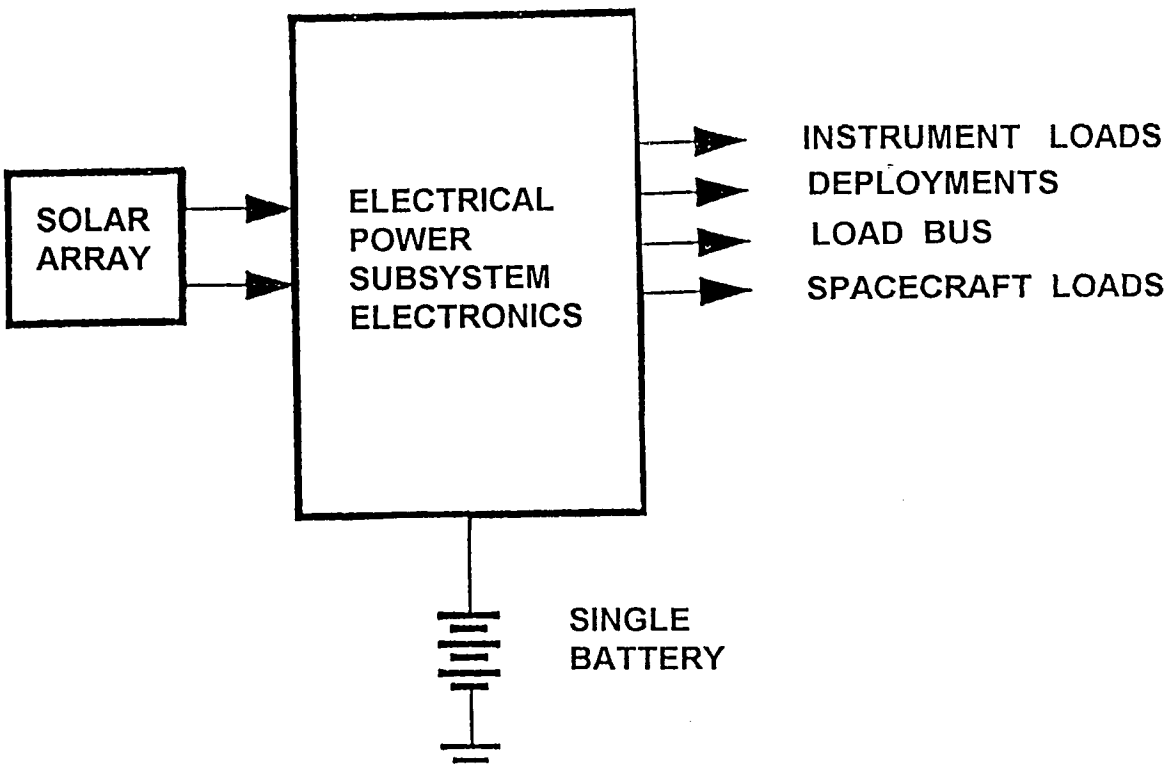

SPACECRAFT BATTERY RECONDITIONING

- RECONDITIONING REFERS TO A DEEP DISCHARGE
  - LOW RATE DISCHARGE (≈ C/100) TO A CUTOFF VOLTAGE SIGNIFICANTLY LESS 1.0 VOLT/CELL FOLLOWED BY CHARGING AT AN APPROPRIATE RATE WITH ADEQUATE OVERCHARGE

- NICKEL-CADMIUM RECONDITIONING
  - RECONDITIONING IN GEO
    - -- HAS BECOME STANDARD PRACTICE
    - -- MAINTAINS CAPACITY AND VOLTAGE PERFORMANCE
  - RECONDITIONING IN LEO
    - -- USUALLY DIFFICULT AND EXPENSIVE
    - -- LIMITED BENEFITS

- NICKEL-HYDROGEN RECONDITIONING

  - RECONDITIONING IN GEO IS CONTROVERSIAL

    -- INTELSAT USES RECONDITIONING (COMSAT CELL DESIGN)

    -- HUGHES DOES NOT UTILIZE RECONDITIONING ON THEIR STANDARD PRODUCT

    -- RCA (LOCKHEED-MARTIN) INCLUDES RECONDITIONING CAPABILITY IN THEIR POWER SUBSYSTEM BUT DOES NOT RECONDITION IN NORMAL OPERATION

    -- TRW'S POSITION IS THAT RECONDITIONING IS NOT REQUIRED

  - RECONDITIONING IN LEO

    -- PRESENTLY IMPLEMENTED ON THE ONLY NiH2 BATTERY EQUIPPED SPACECRAFT IN OPERATION : HST (USED AS CHECK ON THE STATE-OF-HEALTH)

NICKEL-HYDROGEN LIFE TESTING

- GEO LIFE TESTING SHOWS VERY LITTLE DIFFERENCE IN EODV WITH OR WITHOUT RECONDITIONING (HUGHES - INTELSAT VI DATA)

- EXTENSIVE CYCLE LIFE TESTING OF NiH2 UNDER LEO CYCLING REGIMES HAS BEEN CONDUCTED

  -- EAGLE-PICHER
  -- HUGHES
  -- CRANE

- MANY OF THESE TESTS ARE ONGOING
- NORMAL LEO TESTING DOES NOT INCLUDE RECONDITIONING
- LIFE CYCLING DATA IS SHOWN ON THE FOLLOWING FIGURE

Nickel Hydrogen Battery Reconditioning

HUGHES INTELSAT VI DATA

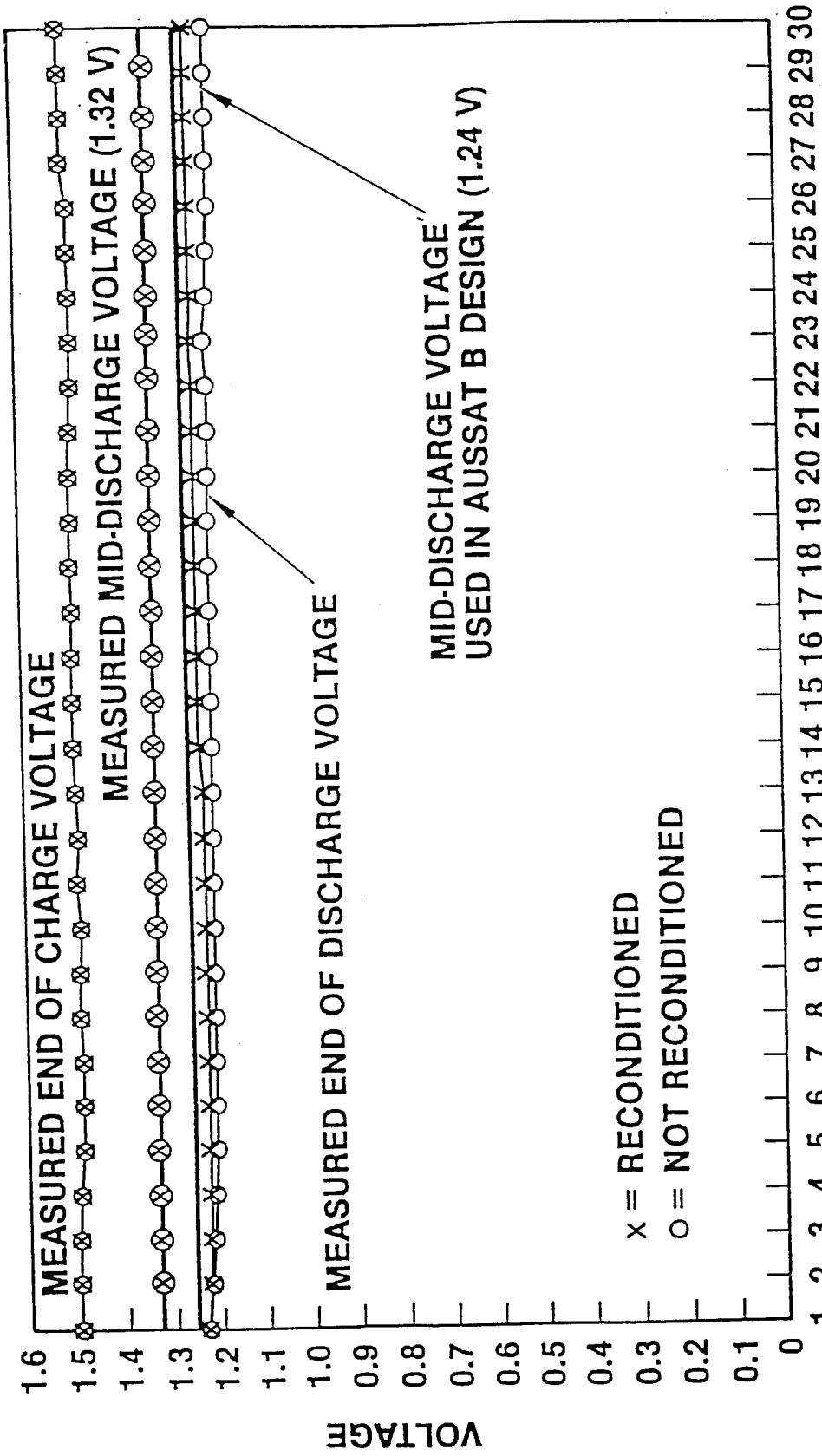

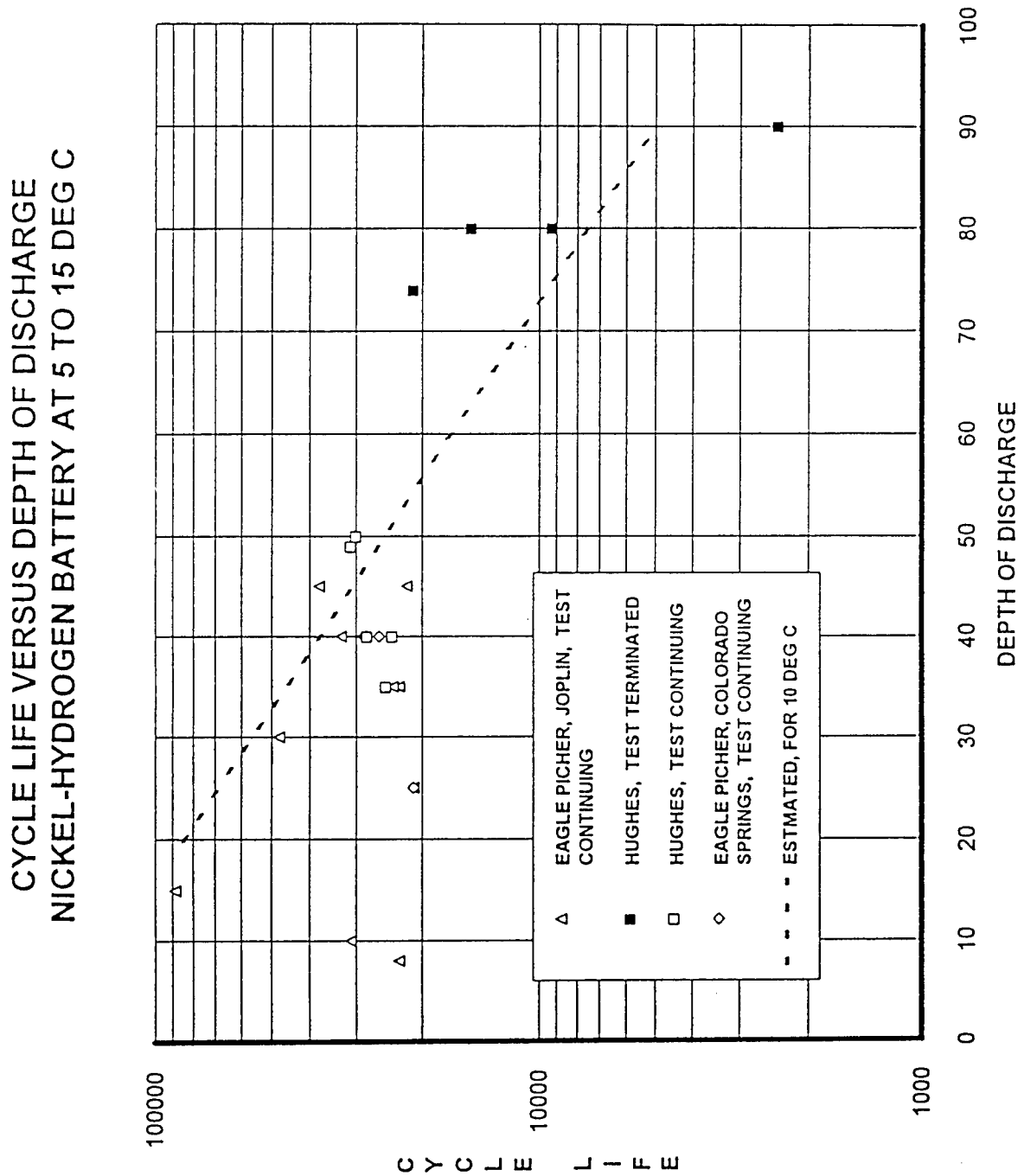
CYCLE LIFE VERSUS DEPTH OF DISCHARGE
NICKEL-HYDROGEN BATTERY AT 5 TO 15 DEG C
CYCLE LIFE
100000
10000
1000
0
10
20
30
40
50
60
70
80
90
100
DEPTH OF DISCHARGE
EAGLE PICHER, JOPLIN, TEST CONTINUING
HUGHES, TEST TERMINATED
HUGHES, TEST CONTINUING
EAGLE PICHER, COLORADO SPRINGS, TEST CONTINUING
ESTMATED, FOR 10 DEG C

NICKEL-HYDROGEN LEO CYCLING TEST DATA

(4.5 INCH DIAMETER CELLS)

CELL CAPACITY	DOD %	CYCLES NO.	EODV VOLTS
90	40	> 36,000	> 1.1
150	25	> 29,000	> 1.1
100	40	> 33,000	> 1.2
150	25	> 29,000	> 1.1

NICKEL-HYDROGEN LIFE TESTING (CON'T)

- THIS FIGURE INDICATES THAT NiH2 TECHNOLOGY HAS LONG LIFE AND STABLE VOLTAGE WITHOUT RECONDITIONING

- LIFE PREDICTIONS ARE SENSIVE TO NUMBER OF CYCLES AS SHOWN. LIFE IS ALSO SENSITIVE TO TEMPERATURE, TYPE OF CHARGE CONTROL AND CALENDAR LIFE SINCE ACTIVATION

- CURVE FOR CYCLE LIFE vs DOD PREDICTS APPROXIMATELY A SIX YEAR LIFE AT 40% DOD

LEO ON-LINE RECONDITIONING DATA

- **TEST CONDITIONS**
  - -- 90 MINUTE CYCLE (30 Minute Discharge + 60 Minute Charge)
  - -- 10° C
  - -- 40% DOD
- **ON-LINE RECONDITIONING RESULTED FROM TEST EQUIPMENT FAILURES**
  - -- CHARGE CYCLE LASTED ONLY 30 MINUTES
  - -- DOD INCREASED TO 55% FOR THE FOLLOWING CYCLE
- **RESULTS**
  - -- END OF DISCHARGE VOLTAGE INCREASED (Approximately 15 Cycles to Reach Maximum EODV)
  - -- INCREASED EODV LASTED FOR APPROXIMATELY 300 CYCLES

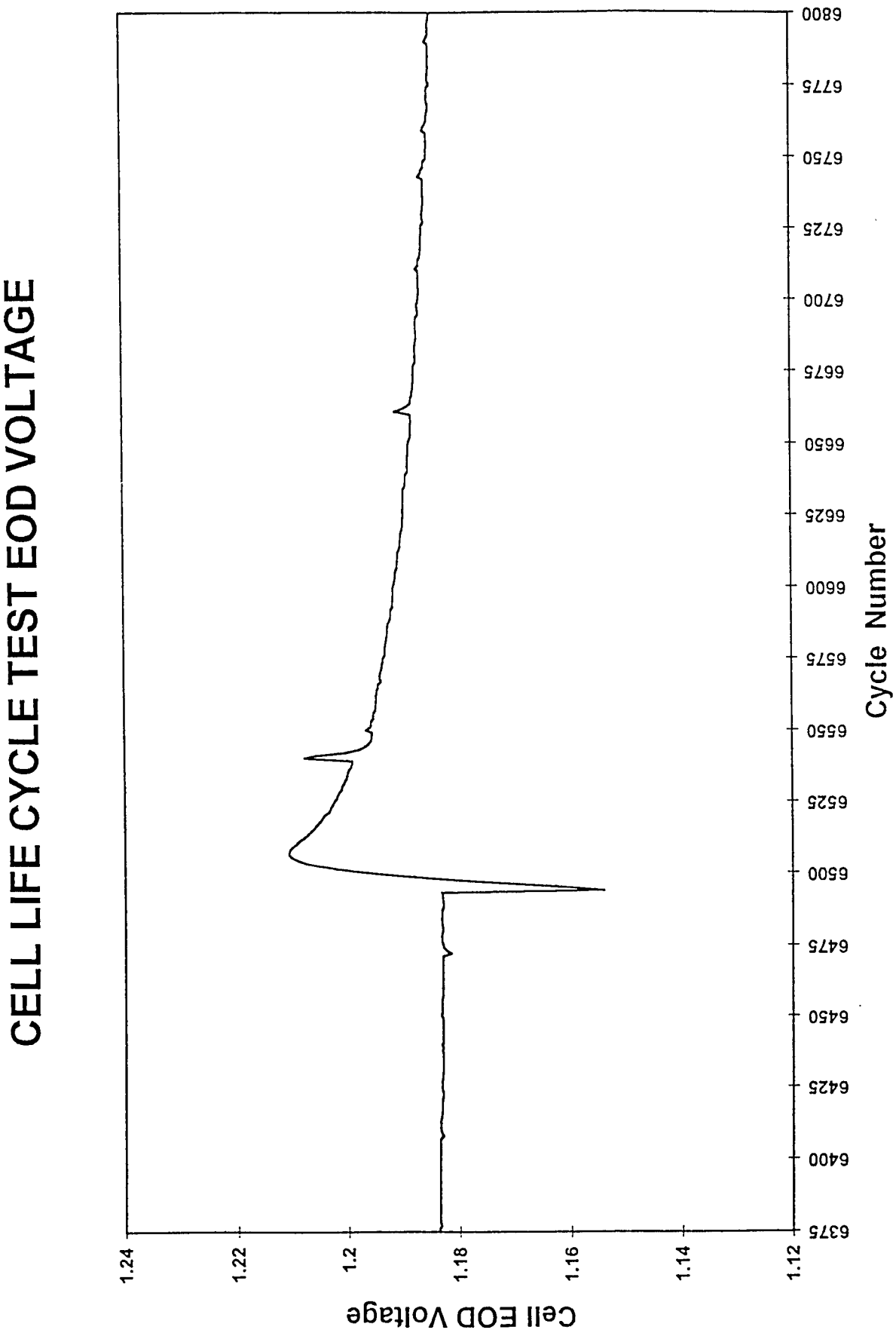
CELL LIFE CYCLE TEST EOD VOLTAGE
Cell EOD Voltage
1.24
1.22
1.2
1.18
1.16
1.14
1.12
Cycle Number
6375
6400
6425
6450
6475
6500
6525
6550
6575
6600
6625
6650
6675
6700
6725
6750
6775
6800

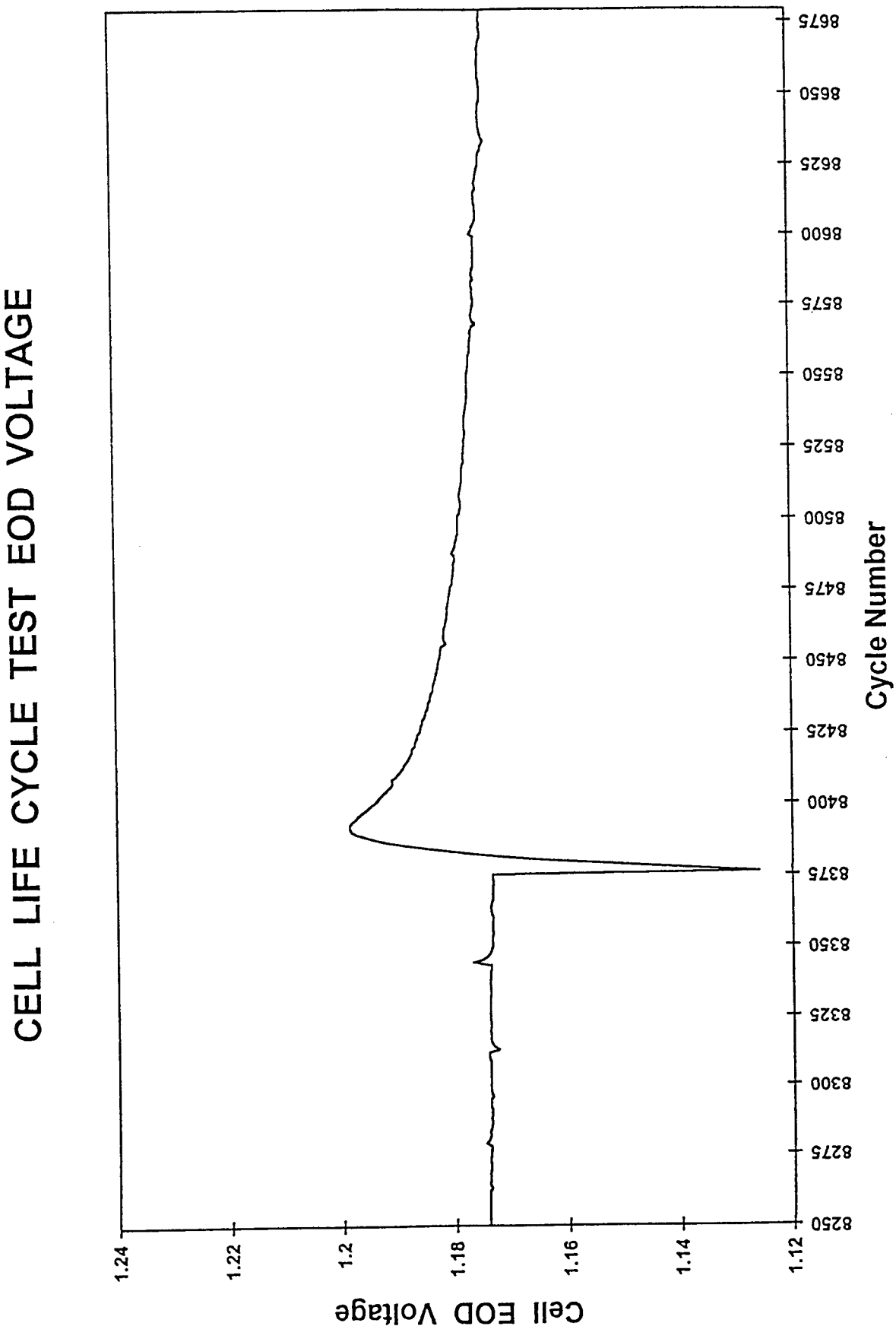
CELL LIFE CYCLE TEST EOD VOLTAGE
Cell EOD Voltage
1.24
1.22
1.2
1.18
1.16
1.14
1.12
Cycle Number
8250
8275
8300
8325
8350
8375
8400
8425
8450
8475
8500
8525
8550
8575
8600
8625
8650
8675

GEO ON–LINE RECONDITIONING DATA

- TEST CONDITIONS
  - GROUND TEST SIMULATION WHICH INCLUDED A 20% DOD SUNLIGHT DISCHARGES IN ADDITION TO THE USUAL ECLIPSE DISCHARGES
- ON-LINE RECONDITIONING RESULTED FROM THE REGULAR ECLIPSES
- RESULTS
  - DAILY DISCHARGE EODV DECREASES SLIGHTLY DURING THE FIRST SIX DAYS AND INCREASES SIGNIFICANTLY AFTER THE SEVENTH DAY
    - EODV DECREASES DURING THE FIRST SIX DAYS IS DUE TO NORMAL PERFORMANCE
    - SUBSEQUENT EODV INCREASE OCCURS BECAUSE BATTERY IS BEING RECONDITIONED PRIOR TO EACH DAILY DISCHARGE BY THE ECLIPSES WHICH ARE INCREASING DEEPER THAN THE DAILY DISCHARGES

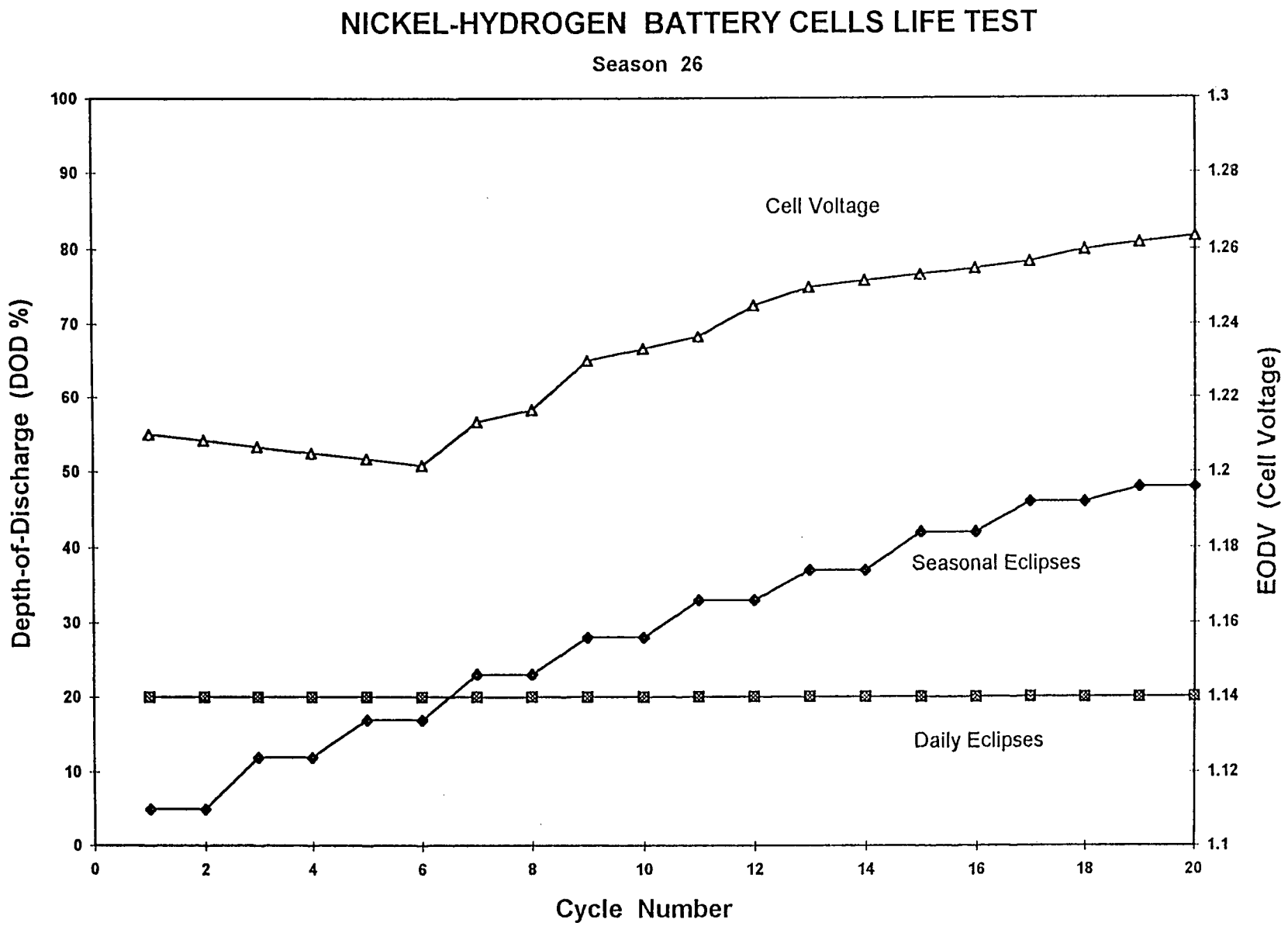
NICKEL-HYDROGEN BATTERY CELLS LIFE TEST
Season 26
Depth-of-Discharge (DOD %)
EODV (Cell Voltage)
Cycle Number
Cell Voltage
Seasonal Eclipses
Daily Eclipses
0
10
20
30
40
50
60
70
80
90
100
1.1
1.12
1.14
1.16
1.18
1.2
1.22
1.24
1.26
1.28
1.3
0
2
4
6
8
10
12
14
16
18
20

RECONDITIONING -- SINGLE BATTERY ARCHITECTURE

- CONCLUSION FROM AVAILABLE DATA IS THAT LONG LIFE AND STABLE VOLTAGE IS REALIZABLE WITH THE BASELINE ARCHITECTURE (SINGLE BATTERY, SINGLE BUS) WITHOUT THE NEED FOR RECONDITIONING
  - CONSERVATIVE BATTERY DESIGN IS ASSUMED RELATIVE TO THE DEPTH-OF-DISCHARGE VS LIFE CYCLE REQUIREMENT, AS WELL AS ORBITAL OPERATING TEMPERATURES
- EPS ARCHITECTURE INCLUDES THE CAPABILITY FOR ON-LINE RECONDITIONING IN THE UNLIKELY EVENT THAT ANOMALOUS BATTERY VOLTAGE DEGRADATION OCCURS

ON–LINE RECONDITIONING

- APPROACH CONSISTS OF INCREASING THE BATTERY DOD BEYOND THE NOMINAL ECLIPSE DISCHARGE DOD WHILE MAINTAINING THE BATTERY ON-LINE

- TO RECONDITION THE BATTERY
  - GROUND CONTROLLER SWITCHES THE EPS TO MANUAL MODE AND LIMITS THE CHARGE CURRENT PROFILE TO A LOW VALUE UNTIL THE BATTERY DOD INCREASES TO THE DESIRED LEVEL
  - BATTERY CHARGE CONTROL CAN THEN BE REINITIALIZED AND NORMAL OPERATION RESUMED

ON–LINE RECONDITIONING (CON'T)

- **PROTECTION AGAINST INADVERTENT PROBLEMS (UNEXPECTED LOADS) DURING ON-LINE RECONDITIONING**

  – FAULT MANAGEMENT PROVISIONS IN THE FLIGHT SOFTWARE (FSW) PROVIDE CONTINUOUS PROTECTION (SAME AS DURING NORMAL OPERATION)

    THE FSW MONITORS THE STATE-OF-CHARGE AND TRIGGERS AN EMERGENCY RESPONSE IF CHARGE BECOMES TOO LOW. WHEN TRIGGERED, THE FSW PUTS THE SPACECRAFT INTO SAFE MODE (SHEDS DISCRETE LOADS) AND RETURNS SYSTEM TO FULL BATTERY CHARGE

  – GROUND MONITORS THE TELEMETRY AND CONFIRMS THAT THE RATE OF DISCHARGE OVER SEVERAL ORBITS IS AS EXPECTED
  - GROUND CAN TERMINATE THE DISCHARGE CYCLES EARLY AND RETURN TO NORMAL CHARGING

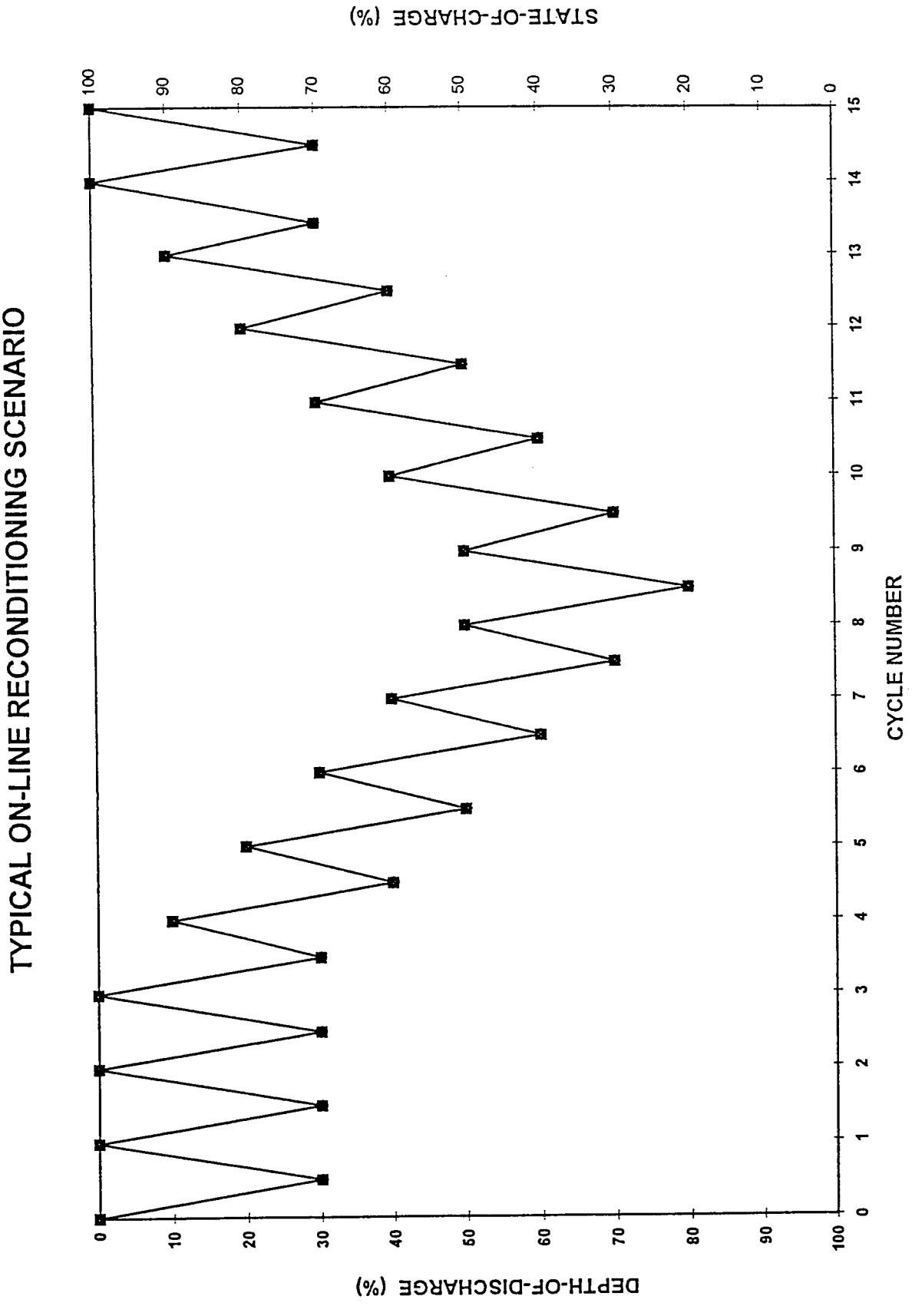
TYPICAL ON-LINE RECONDITIONING SCENARIO
DEPTH-OF-DISCHARGE (%)
STATE-OF-CHARGE (%)
CYCLE NUMBER
0
10
20
30
40
50
60
70
80
90
100
0
1
2
3
4
5
6
7
8
9
10
11
12
13
14
15

SUMMARY

- TEST DATA SHOWS THAT VOLTAGE PERFORMANCE IMPROVEMENT CAN BE ACHIEVED WITH ON-LINE RECONDITIONING OF NICKEL-HYDROGEN BATTERIES IN LEO ORBIT
  - DATA INDICATES THAT VOLTAGE IMPROVEMENT MAY LAST ONLY A FEW HUNDRED CYCLES
- ADDITIONAL TESTING IS REQUIRED TO DETERMINE IF AN OPTIMUM RECONDITIONING PROCESS CAN BE DEVELOPED TO ENHANCE THE DISHARGE VOLTAGE OVER A GREATER NUMBER OF CYCLES

FUTURE ACTIVITIES

- AS PART OF THE EOS COMMON PROGRAM TRW WILL BUILD AN ENGINEERING MODEL (EM) BATTERY MODULE ASSEMBLE (BMA)
  - THE BMA WILL BE A COMPLETE 1/2 BATTERY INCLUDING NiH2 BATTERY CELLS, CELL BYPASS SWITCHES, AND THERMAL CONTROL SYSTEM
  - THE 12 160 Ah NiH2 CELLS WILL BE PROCURED TO THE SAME SPECIFIATIONS AND STANDARDS THAT ARE PLANNED FOR FLIGHT UNITS

- THIS EM BMA WILL UNDERGO QUALIFICATION LEVEL ENVIRONMENTAL TESTING- (VIBRATION, THERMAL VACUUM, ETC.)

- SUBSEQUENT TO THE QUALIFICATION LEVEL TESTING THE BMA WILL BE PUT INTO A SIMULATED LEO LIFE TEST (30% DOD, 65/35 MIN CHARGE/DISCHARGE CYCLES, 10° C)
  - THE BMA WILL BE ELECTRICALLY DIVIDED INTO 3 GROUPS OF 4 CELLS EACH
  - ONE GROUP WOULD BE CYCLED WITHOUT RECONDITIONING
  - ONE GROUP WOULD BY CYCLED WITH PERIODIC ($\approx$ EVERY 1000 CYCLES) DEEP DISCHARGE RECONDITIONING ($<$ 1.0 VOLT/CELL)
  - ONE GROUP WOULD BE CYCLED WITH PERIODIC SHALLOW DISCHARGE RECONDITIONING ($\approx$ 8 0 % DOD)

FUTURE ACTIVITIES (CON'T)

- IT IS OUR BELIEF THAT THESE TESTS WILL SHOW THE FOLLOWING
  - NiH2 BATTERY CELLS WHEN PROPERLY PROCURED AND MANAGED ON ORBIT DO NOT REQUIRE RECONDITIONING FOR LEO APPLICATONS
  - RECONDITIONING OF NiH2 CELLS IN LEO RESULTS IN ONLY TEMPORARY ENHANCEMENT IN EODV (A FEW HUNDRED CYCLES)
  - IN LEO SHALLOW DISCHARGE RECONDITIONING IS JUST AS EFFECTIVE AS DEEP DISCHARGE RECONDITIONING

NICKEL-HYDROGEN BATTERY STATE OF CHARGE DURING LOW RATE TRICKLE CHARGING

C. LURIE and S. FOROOZAN
TRW SPACE AND ELECTRONICS GROUP
REDONDO BEACH, CALIFORNIA

J. BREWER and L. JACKSON
NASA GEORGE C. MARSHALL SPACE FLIGHT CENTER
MARSHALL SPACE FLIGHT CENTER, ALABAMA

THE 1995 NASA AEROSPACE BATTERY WORKSHOP
THE HUNTSVILLE HILTON
HUNTSVILLE, ALABAMA
NOVEMBER 28 - 30, 1995

BACKGROUND

- THE AXAF-I PROGRAM HAS BEEN INVESTIGATING TECHNIQUES FOR MANAGING NICKEL-HYDROGEN BATTERY STATE OF CHARGE, DURING PRELAUNCH AND LAUNCH OPERATIONS, IN THE ABSENCE OF ACTIVE COOLING

- THE OVERALL CONCLUSION OF THESE INVESTIGATIONS IS THAT HIGH STATE OF CHARGE CAN BE ACHIEVED AND MAINTAINED, IN THE ABSENCE OF ACTIVE COOLING, UTILIZING

  - ADIABATIC CHARGING, AND

  - LOW RATE TRICKLE CHARGING

- THE ADIABATIC CHARGING TECHNIQUE WAS PRESENTED AT THE 1994 NASA BATTERY WORKSHOP AND LOW RATE TRICKLE CHARGING WAS DISCUSSED AT THE 1995 IECEC

- TODAY'S PRESENTATION ADDRESSES STEADY STATE BATTERY CAPACITY AND TEMPERATURE, DURING LOW RATE TRICKLE CHARGING, IN A SIMULATED PRELAUNCH AMBIENT ENVIRONMENT

CONT'D

The NASA AXAF-I program requires high battery state of charge at launch. Traditional approaches to providing high state of charge, during prelaunch operations, require significant battery cooling. The use of active cooling, in the AXAF-I prelaunch environment, was considered and proved to be difficult to implement and very expensive. Accordingly alternate approaches were considered. An approach utilizing adiabatic charging and low rate trickle charge, was investigated and proved successful.

References:

Lurie, C., Foroozan, S., Brewer, J., and Jackson, L., 1994, "Adiabatic Charging of Nickel-Hydrogen Batteries," Proceedings, 27th NASA Aerospace Battery Workshop, Marshall Space Flight Center, Huntsville, AL, pp. 581-598

Lurie, C., Foroozan, S., Brewer, J., and Jackson, L., 1995, "Nickel-Hydrogen Battery State of Charge Management in the Absence of Active Cooling," Proceedings, 30th Intersociety Energy Conversion Engineering Conference, American Society of Mechanical Engineers, Orlando, FL, pp. 143-148.

BACKGROUND CONT'D

- THE ABILITY TO PREDICT BATTERY TEMPERATURE IS IMPORTANT BECAUSE STATE OF CHARGE IS A STRONG FUNCTION OF TEMPERATURE.
- PREDICTION OF BATTERY TEMPERATURE REQUIRES KNOWLEDGE OF THE BATTERY HEAT CAPACITY, DISSIPATION, AND COOLING.
- THE AXAF-I BATTERY MOUNTING CONFIGURATION PROVIDES EFFECTIVE THERMAL ISOLATION IN TERMS OF CONDUCTIVE AND RADIATIVE HEAT TRANSFER. BATTERY COOLING, IN THE PRELAUNCH ENVIRONMENT, IS LIMITED TO HEAT TRANSFERRED TO THE AIR IN CONTACT WITH THE BATTERY.
- HEAT TRANSFER FROM THE BATTERY, AS INTEGRATED INTO THE SPACECRAFT, TO THE AMBIENT AIR IS DIFFICULT TO MODEL.
- ACCORDINGLY A SIX-CELL MODULE, SIMULATING BATTERY THERMAL CHARACTERISTICS, WAS DESIGNED AND FABRICATED. THIS MODULE WAS MOUNTED IN A STRUCTURE SIMULATING THE THERMAL ENVIRONMENT THE BATTERY WOULD EXPERIENCE, IN THE SPACECRAFT, DURING PRELAUNCH OPERATIONS.

During extended periods of low rate trickle charge, steady state battery capacity is a function of trickle charge rate and temperature. The trickle charge rate is known; therefore, if the steady state temperature can be predicted, the steady state capacity can be predicted. Steady state battery temperature can be predicted if the battery heat capacity, dissipation, and cooling are known. Battery heat capacity and dissipation are easily determined. However, cooling is difficult to model in the prelaunch environment, because, as integrated into the spacecraft, battery cooling is limited to heat transferred from the battery to the ambient air in contact with the battery. Therefore battery cooling data were determined experimentally.

The approach included designing and building a battery module and structure simulating the thermal environment the battery would experience, in the spacecraft, during the prelaunch operations, and trickle charging the battery module at trickle charge rates in the range C/250 to C/1000.

TEST ARTICLES

- TESTING WAS PERFORMED ON A SIX-CELL MODULE DESIGNED TO SIMULATE FLIGHT BATTERY STEADY STATE THERMAL CHARACTERISTICS

- TEST CELL DEFINITION

CELL PART NUMBER	RNH 30-9
RATED CAPACITY (Ah)	30
STACK CONFIGURATION	BACK-TO-BACK
POSITIVE ELECTRODE	0.030", SLURRY
SEPARATOR	ZIRCAR, 2 LAYERS
ELECTROLYTE (%, FINAL)	31
OPERATING PRESSURE (psi)	475
STRAIN GAUGE	YES
TERMINAL CONFIGURATION	AXIAL
WEIGHT (gms)	1010
PRECHARGE	POSITIVE

The battery module consists of six flight-design cells mounted in aluminum thermal sleeves with mechanical and thermal properties similar to flight hardware. The thermal sleeves are mounted on an aluminum plate closely simulating the flight battery baseplate.

The cells are Eagle Picher RNH 30-9 nickel-hydrogen cells with components and design characteristics common to many Eagle Picher cells presently in operation.

SIX-CELL MODULE
TRICKLE CHARGE TEST SET UP

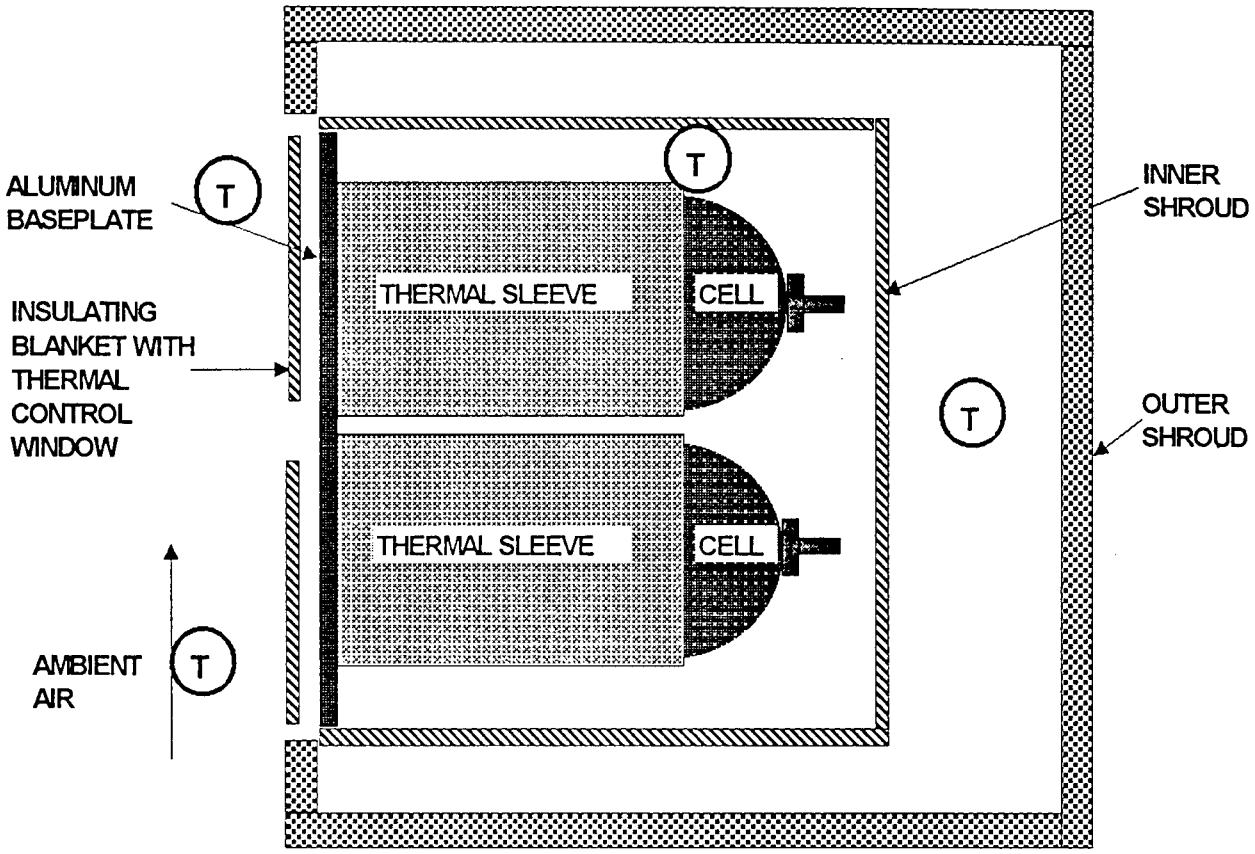

The six-cell module was mounted in a structure designed to simulate the portions of the spacecraft and shuttle bay that will influence battery temperature during prelaunch operations. The six-cell module was mounted with its baseplate 90° to the floor. The baseplate was covered with a flight type MLI insulating blanket in which a thermal control window, scaled for the six-cell module, was cut. The module was enclosed in an inner shroud simulating the MLI battery doghouse used on the spacecraft. The total assembly was then enclosed in an outer shroud simulating the spacecraft structure and the shuttle bay. Multiple thermocouples measured temperatures of the ambient air, module baseplate, individual cells, and air inside the shrouds.

C/500 RATE TRICKLE CHARGE
TEMPERATURE DATA

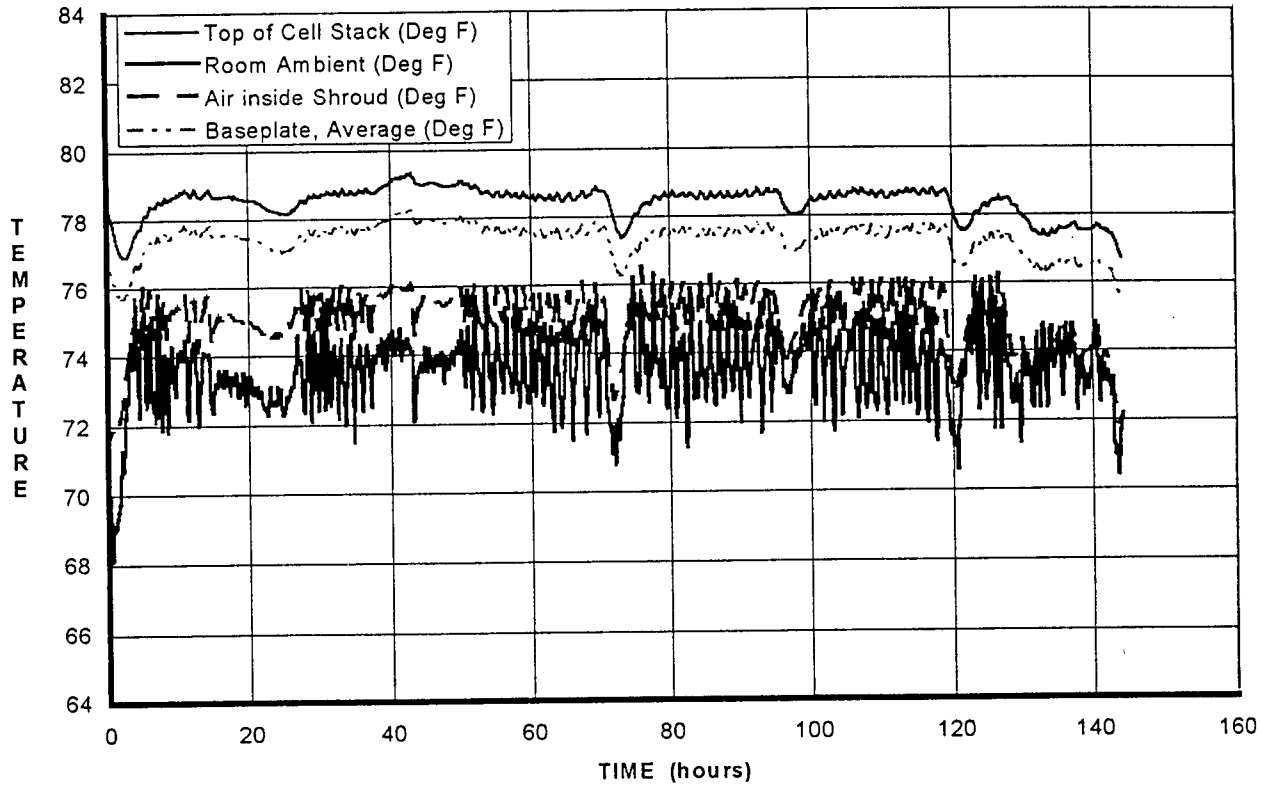

Typical temperature data is shown for the C/500 rate trickle charge case. In this case the average top-of-the-cell-stack temperature was 78.5°F and the average room ambient air temperature was 73.5°F. The air inside the shroud remained approximately 2°F above the room ambient air temperature. The module baseplate was approximately 1°F cooler than the top-of-the-cell-stack temperature, which is consistent with the battery thermal model.

All measured temperatures track the excursions in the room ambient air temperature. These excursions are caused by cycling of the test facility heating and ventilating system. Consideration was given to running the test in a thermally controlled, e.g., constant temperature, environment. This was not done because much of the prelaunch period will be in facilities with similar temperature variability.

C/500 RATE TRICKLE CHARGE
TEMPERATURE INCREASE

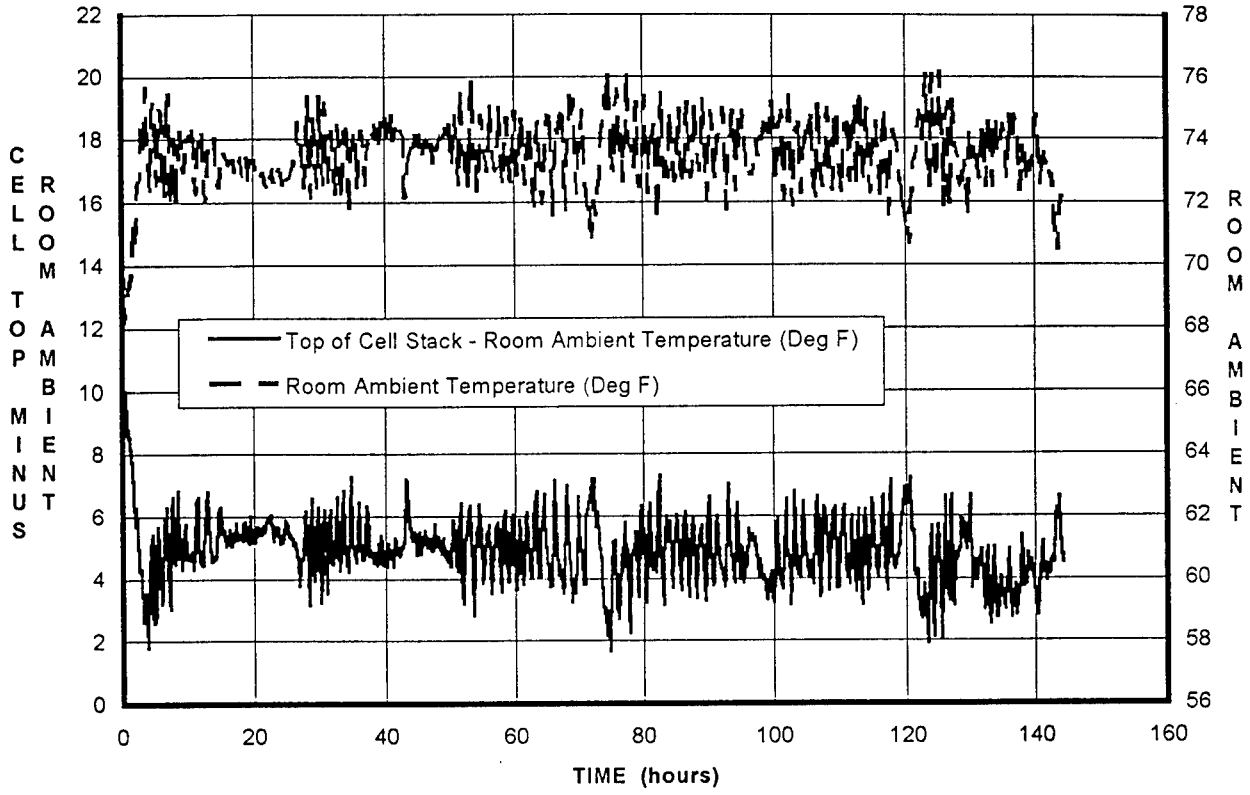

Analysis of the temperature data shown on the previous chart yields the difference between the top-of-the-cell-stack temperature and the room ambient air temperature. This difference is the temperature increase of the battery above its ambient and is shown in the chart above. At the C/500 trickle charge rate, the battery temperature is shown to be approximately 5.5°F above the ambient room air temperature.

The average temperature increases, observed at the various trickle charge rates run, are stable and reproducible.

C/500 RATE TRICKLE CHARGE
STEADY STATE CAPACITY

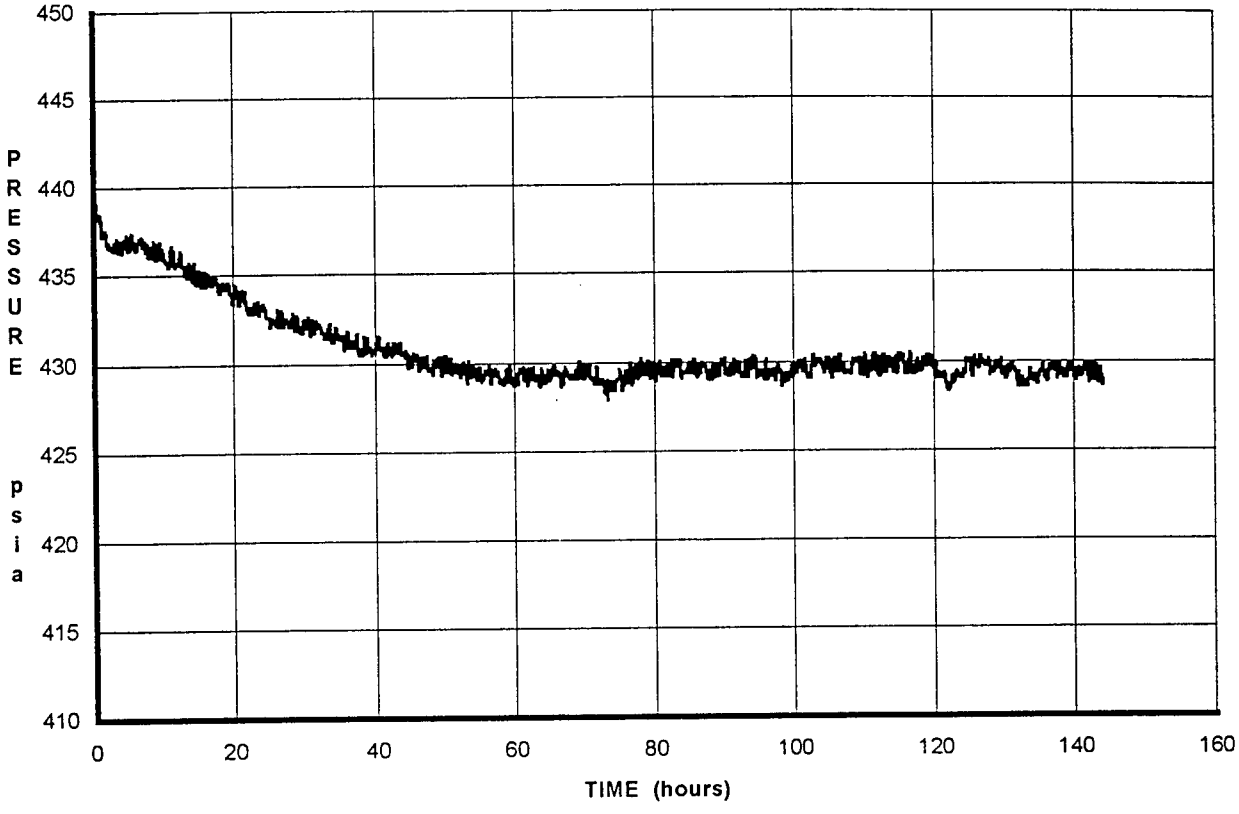

Capacity stability was tracked using cell internal pressure data. The correlation between steady state cell internal pressure and capacity is excellent. The chart above shows the six-cell module capacity stabilizing after approximately 50 hours of trickle charge at the C/500 rate.

The higher initial pressure is the result of an extended period of trickle charge, at the C/300 rate, which preceded the C/500 rate trickle charge shown.

C/250 RATE TRICKLE CHARGE
STEADY STATE CAPACITY

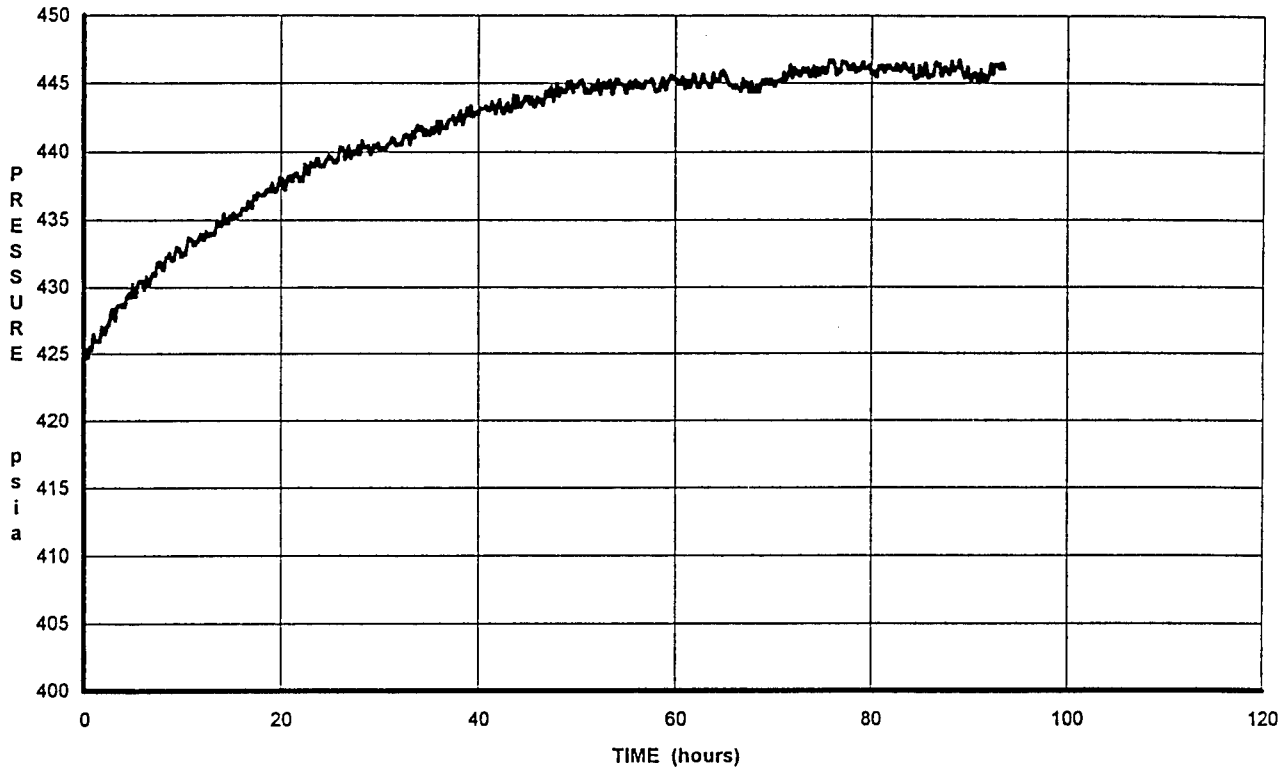

The previous chart showed the battery module capacity decreasing from a higher state of charge and stabilizing at a state of charge consistent with the C/500 rate trickle charge at the ambient room air temperature. The curve shown above demonstrates that the battery can accept charge at low trickle charge rates. At the C/250 trickle charge rate the six-cell module capacity increased slowly and stabilized after approximately 70 hours.

Steady state capacity, during low rate trickle charge, is a function of trickle charge rate and temperature, and will be achieved starting from either a higher or lower state of charge.

OPEN CIRCUIT STAND
SELF DISCHARGE

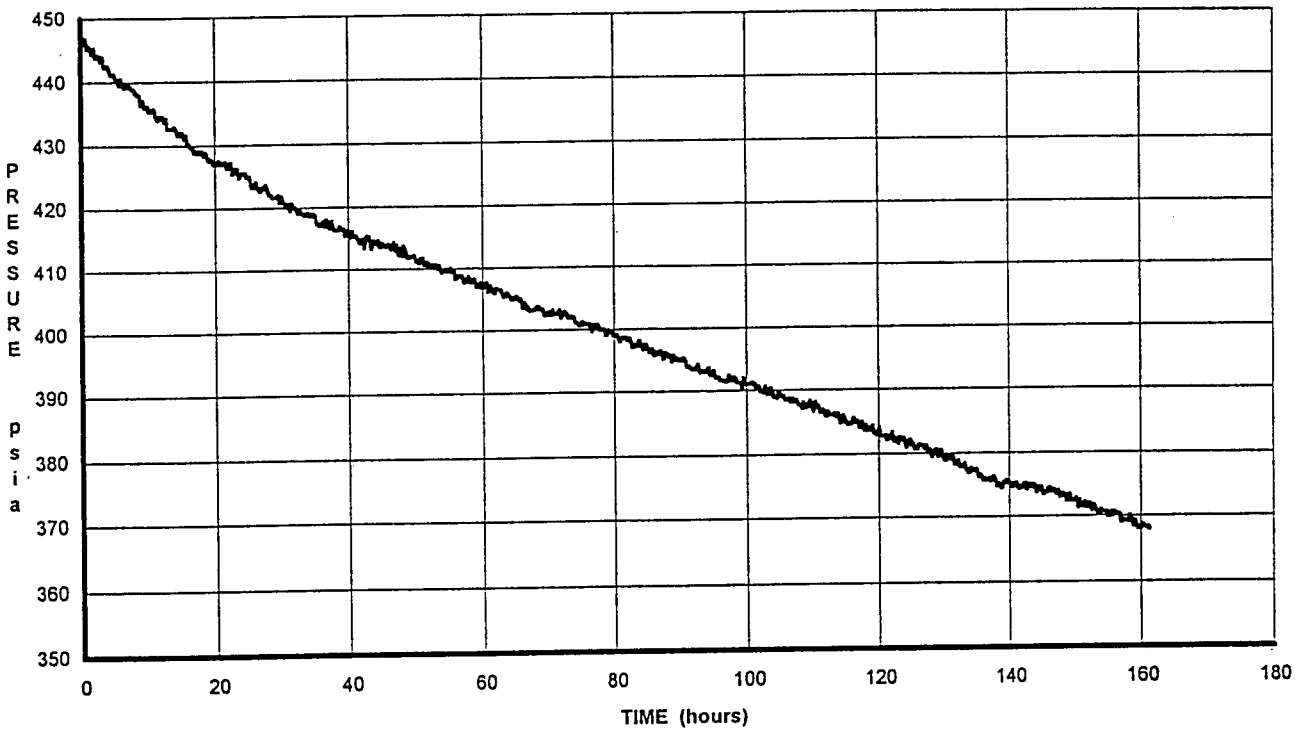

The open circuit stand case is shown to demonstrate that, in the absence of trickle charge current, the capacity decreases at an approximately constant rate after the first day.

STEADY STATE CAPACITY

FUNCTION OF TRICKLE CHARGE RATE AND TEMPERATURE

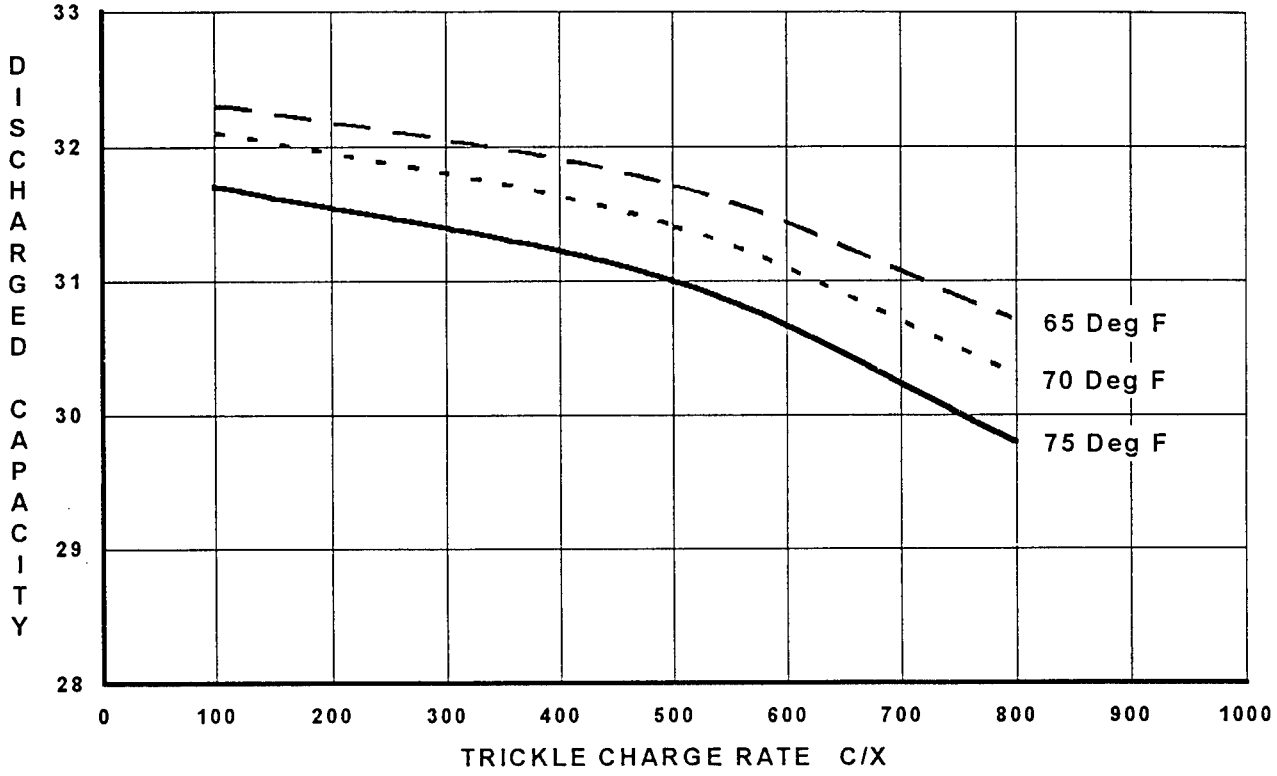

This chart summarizes the low rate trickle charge data obtained at temperatures of 65°F, 70°F, and 75°F over a range of trickle charge rates from C/100 to C/800. The curves are not continued beyond C/800 because the self discharge rate becomes larger than the trickle charge rate in that region. Cell capacities were approximately 32 Ah at 68°F. Accordingly the data indicates that a trickle charge rate of C/100 maintains nominal capacity at room temperature. It is interesting to note that the steady state capacity, at a trickle charge rate of C/500 is only 3% lower than the steady state capacity at the C/100 rate, for the configuration tested. This can be highly significant for applications in which the ability to cool is limited.

C/1000 RATE TRICKLE CHARGE
TEMPERATURE DATA

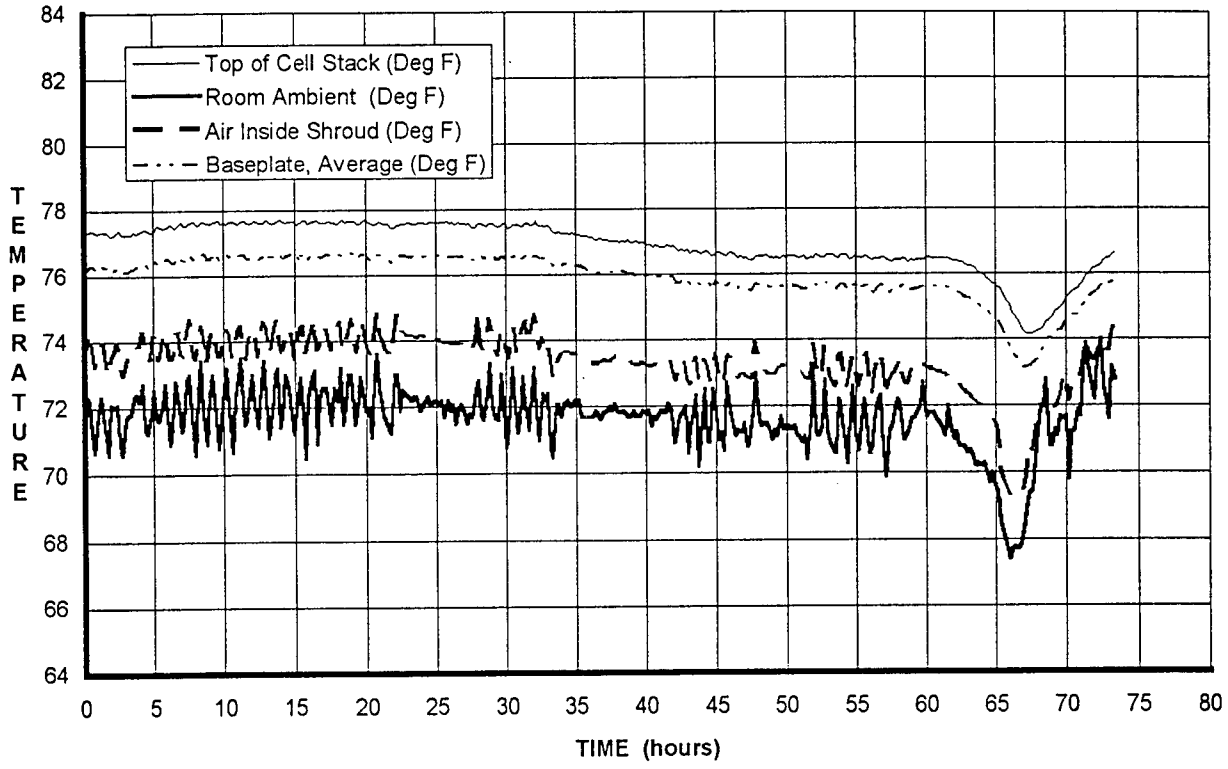

The C/1000 rate trickle charge data shown above is similar to the C/500 rate trickle charge data shown previously, except that the temperature increase is lower, at approximately 4.5°F. The significant difference between cell temperature and room ambient air temperature, at this very low rate trickle charge, is a result of the limited cooling in the simulated prelaunch environment.

OPEN CIRCUIT STAND
TEMPERATURE DATA

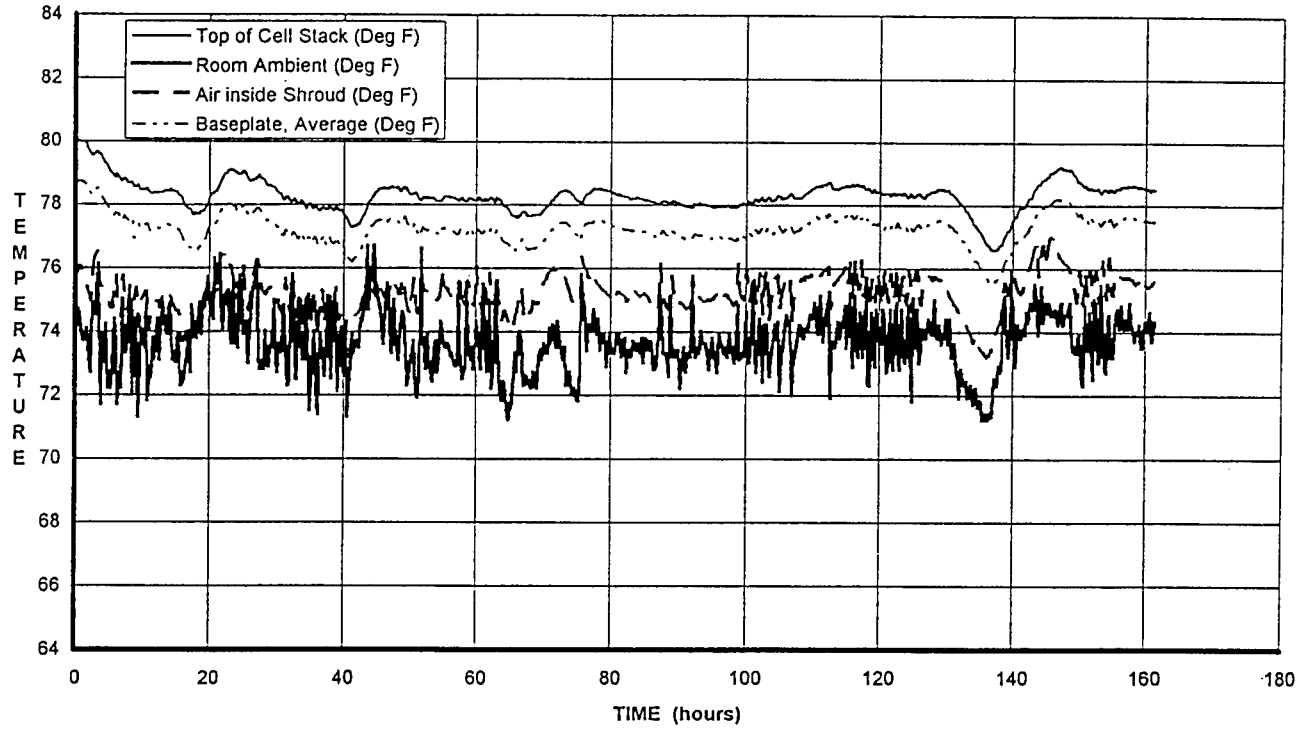

The open circuit stand temperature data shown above demonstrates that significant dissipation occurs as a result of self discharge processes. It is interesting to note that the temperature increase observed during open circuit stand, 4.3°F, and the temperature increase observed during the C/1000 rate trickle charge (shown on the previous chart), 4.5°F, are very close. In fact, all temperature increases observed at trickle charge rates in the C/800 to C/1200 range are within a few tenths of a degree Fahrenheit. It appears that heating, due to trickle charge processes, becomes constant when the trickle charge rate drops below the self discharge rate.

SELF DISCHARGE RATE
AS A FUNCTION OF TEMPERATURE

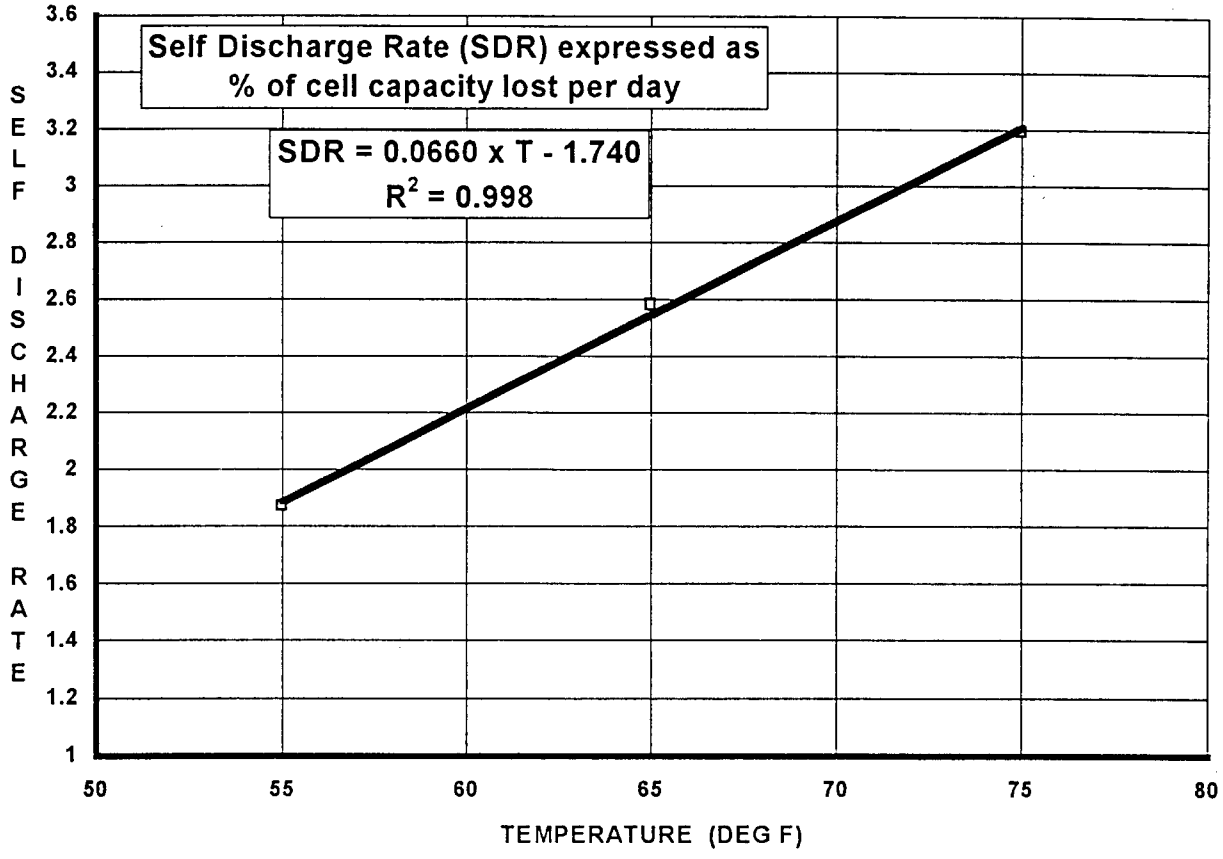

The self discharge rate for these cells has been determined and is shown above. The self discharge rate is expressed as the average per cent of cell capacity lost per day and includes the more rapid initial loss occurring during the first several hours of open circuit stand.

At an average room ambient air temperature of 72°F the average self discharge rate is C/750.

TEMPERATURE INCREASE
AS A FUNCTION OF TRICKLE CHARGE RATE

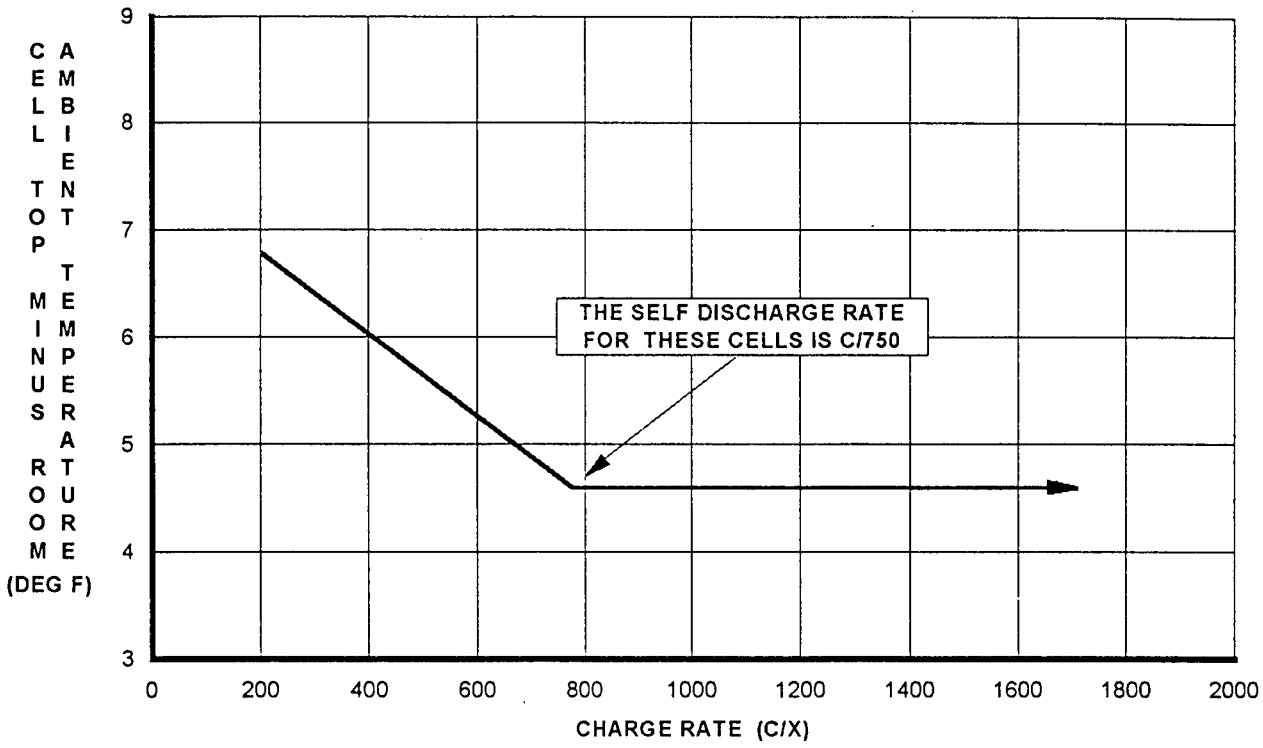

This chart summarizes the temperature increase data obtained at the various trickle charge rates run. The curve shows two linear segments intersecting at a trickle charge rate very close to the previously determined C/750 self discharge rate.

SUMMARY

- BATTERY TEMPERATURE INCREASE, DUE TO LOW RATE TRICKLE CHARGING, HAS BEEN DETERMINED EXPERIMENTALLY, USING A SIX-CELL BATTERY MODULE IN A TEST SETUP SIMULATING THE ANTICIPATED AXAF-I PRELAUNCH ENVIRONMENT.

- TEST RESULTS INDICATE

  - TRICKLE CHARGE RATES LESS THAN OR EQUAL TO THE SELF DISCHARGE RATE DO NOT INCREASE DISSIPATION BEYOND THAT DUE TO THE SELF DISCHARGE.

  - SIGNIFICANT TRICKLE CHARGE RATES (~C/500) RESULT IN BATTERY TEMPERATURES ONLY A FEW DEGREES (F) HIGHER THAN OBSERVED DURING PERIODS OF OPEN CIRCUIT STAND.

PERFORMANCE FEATURES OF 22-CELL, 19Ah SINGLE PRESSURE VESSEL NICKEL HYDROGEN BATTERY

Presented to
1995 NASA AEROSPACE BATTERY WORKSHOP

Presented By
Gopalakrishna M. Rao
Space Power Applications Branch
NASA/Goddard Space Flight Center
Greenbelt, Maryland, USA 20771
and
Hari Vaidyanathan
COMSAT Laboratories
Clarksburg, Maryland 20871

November 29, 1995

SPV NICKEL-HYDROGEN BATTERY

TECHNOLOGY DESCRIPTION

- Serially Connected Individual Ni-H2 Cells
- A Single Pressure Vessel
- A common Hydrogen Atmosphere
- Maintains Commonalty with Electrical Power Subsystem Interface Topology with Individual Pressure Vessel (IPV) Ni-H2 Battery and NiCd Battery
  - INTELSAT V IPV (1983)
  - Hubble Space Telescope IPV (1989)

SPV NICKEL-HYDROGEN BATTERY

ADVANTAGES

- About 50% Increase in Specific Energy Density
- About 50% Increase in Life
- About 10% Increase in Depth of Discharge (DoD)
- Comparable Cost
- Higher Reliability

SPV NICKEL-HYDROGEN BATTERY

ELECTRICAL INTERFACE

- Similar In-orbit Management Procedures for SPV Ni-H2 Battery and NiCd Battery
- Similar Charge Rates and Recharge Ratios for SPV Ni-H2 Battery and NiCd Battery
- Charge Control Methods such as V/T limit, ampere-hour integration, etc Applicable for SPV Ni-H2 Battery
- Pressure as a state-of-charge Indicator for SPV Ni-H2 Battery Available

SPV NICKEL-HYDROGEN BATTERY

MECHANICAL INTERFACE

- **Footprint**
  - 19 Ah SPV NI-H2 Battery about 42.75 cm x 31.1 cm x 31.1 cm
  - 19 Ah Super NiCd battery about 38.4 cm x 33 cm x 12.7 cm
- **Weight**
  - 19 Ah SPV NI-H2 Battery about 16 kg
  - 19 Ah Super NiCd battery about 21.4 kg
- **Size Baseplate to Accommodate the Larger Footprint of SPV NI-H2 Battery**

SPV NICKEL-HYDROGEN BATTERY

Development Strategy

- 22 Cylindrical Individual Ni-H2 Cells
- 28 ± 6 Volts
- 19 Ah Capacity
- 12.62 kg in Weight
- 10 in diameter and 16.825 in length
- 300 psi Operating Pressure

SPV NICKEL-HYDROGEN BATTERY

DESIGN FEATURES

VENDOR	SPECIFIC ENERGY WH/Kg	ENERGY DENSITY WH/L	NUMBER OF CELLS	CELL CONTAINER	GAS DIFFUSION MECHANISM
EPI/Butler	40.66	36.89	22	Heat Sealed Dual Plastic Bag	Gore-Tex Membranes
EPI/Joplin	35.64	29.97	22	Rigid Cell Case Made of Lustran	Porous Teflon Plugs on the Cell Cover

COMMON FEATURES:

- Inconel Battery Case
- Ziegler Seals
- Zircar Separator
- 31% KOH
- Polypropylene Absorber
- Slurry Sintered Aqueous E. I. Positives

EPI/BUTLER ATP DATA

ACCEPTANCE PLAN	CAPACITY TO 22V	EOC PRESSURE	NOTES
Functional 10° C Capacity	21.5 Ah	243.7 PSIA	
Room Temp (20° C) Capacity	19.3 Ah	232.7 PSIA	
Charge Retention	18.5 Ah	239.7 PSIA	End of Rest Pressure 217.7 PSIA
10° Capacity	20.5 Ah	238.7 PSIA	
Charge Retention	19.6 Ah	238.7 PSIA	91.1% Retained
10° Capacity			Test Aborted - Equipment Problem
Peak Load 10° C			9.5A = 27.65V 38A = 24.07V 9.5A = 25.38V

EPI/BUTLER ATP DATA - CONTD.

ACCEPTANCE PLAN	CAPACITY TO 22V	EOC PRESSURE	NOTES
10° Capacity	20.3 Ah	238.7 PSIA	
Room Temp (20° C) Capacity	18.6 Ah	232.7 PSIA	
Charge Retention	17.9 Ah	237.7 PSIA	End of Rest Pressure = 213.7 PSIA
10° Capacity	19.8 Ah	235.7 PSIA	
30° Capacity	15.1 Ah	216.7 PSIA	
20° Capacity	17.3 Ah	233.7 PSIA	
10° Capacity	19.7 Ah	242.7 PSIA	
0° Capacity	20.19 Ah	239.7 PSIA	
Room Temp (20° C) Capacity	17.8 Ah		

EPI/JOPLIN ATP DATA

	DATE	VOLTAGE	TO 22V
FUNCTIONAL 10° C 16 HR. CHARGE AT 2.5 AMPS 12.5 AMP DISCHARGE TO 19V /SHORT DOWN TO 2.2 V	10/11/94	33.4	31.3
ROOM TEMP. CAP. 25° C 16 HR. CHARGE AT 2.5 AMPS 12.5 AMP DISCHARGE TO 19V /SHORT DOWN TO 2.2 V	10/11/94	32.1	26.0
CHARGE RETENTION 10° C 16 HR. CHARGE AT 2.5 AMPS 72 HR. OPEN CIRCUIT STAND 12.5 AMP DISCHARGE TO 19V /SHORT DOWN TO 2.2 V	10/16/94	33.4	27.5
PEAK LOAD 10° C 16 HR. CHARGE AT 2.5 AMPS 50 AMP PULSE FOR 1 MIN. 1 HR INTO DISCHARGE 12.5 AMP DISCHARGE TO 19V /SHORT DOWN TO 2.2 V	10/17/94	33.2	30.5
PEAK LOAD 10° C 16 HR. CHARGE AT 2.5 AMPS 50 AMP PULSE FOR 1 MIN. 1 HR INTO DISCHARGE 12.5 AMP DISCHARGE TO 19V /SHORT DOWN TO 2.2 V	10/18/94	33.3	30.3
FUNCTIONAL 10° C 16 HR. CHARGE AT 2.5 AMPS 12.5 AMP DISCHARGE TO 19V /SHORT DOWN TO 2.2 V	10/19/94	33.3	30.2
ROOM TEMP. CAPACITY 25° C 16 HR. CHARGE AT 2.5 AMPS 12.5 AMP DISCHARGE TO 19V /SHORT DOWN TO 2.2 V	10/20/94	32.2	26.7
CHARGE RETENTION 10° C 16 HR. CHARGE AT 2.5 AMPS 72 HR. OPEN CIRCUIT STAND 12.5 AMP DISCHARGE TO 19V /SHORT DOWN TO 2.2 V	10/24/94	33.3	27.7
30° C CAPACITY CYCLE 16 HR. CHARGE AT 2.5 AMPS 12.5 AMP DISCHARGE TO 19V /SHORT DOWN TO 2.2 V	10/26/94	31.7	21.4

EPI/JOPLIN ATP DATA - CONTD.

		DATE	VOLTAGE	TO 22V
20°C CAPACITY CYCLE 16 HR. CHARGE AT 2.5 AMPS 12.5 AMP DISCHARGE TO 19V /SHORT DOWN TO 2.2 V		10/27/94	32.8	29.0
10°C CAPACITY CYCLE 16 HR. CHARGE AT 2.5 AMPS 12.5 AMP DISCHARGE TO 19V /SHORT DOWN TO 2.2 V		10/28/94	33.5	30.1
0°C CAPACITY CYCLE 16 HR. CHARGE AT 2.5 AMPS 12.5 AMP DISCHARGE TO 19V /SHORT DOWN TO 2.2 V		10/29/94	34.3	30.3
OVERCHARGE -5°C 48 HR CHARGE AT 1.25 A 12.5 AMP DISCHARGE TO 19V /SHORT DOWN TO 2.2 V		10/30/94	34.1	37.3
20C CAPACITY CYCLE 16 HR. CHARGE AT 2.5 AMPS 12.5 AMP DISCHARGE TO 19V /SHORT DOWN TO 2.2 V		11/1/94	32.3	28.1
CHARGE RETENTION 10° C 16 HR. CHARGE AT 2.5 AMPS 72 HR. OPEN CIRCUIT STAND 12.5 AMP DISCHARGE TO 19V /SHORT DOWN TO 2.2 V		11/6/94	33.3	26.8
FUNCTIONAL 10° C 16 HR. CHARGE AT 2.5 AMPS 12.5 AMP DISCHARGE TO 19V /SHORT DOWN TO 2.2 V		11/6/94	33.3	30.8
THERMAL VAC (CYCLE AND SOAK)				
3 CYCLES AT EACH TEMPERATURE 55 MIN. CHARGE AT 8.6 AMPS 35 MIN. DISCHARGE AT 12.9 AMPS	30C	11/12/94	32.2	N/A
	10C	11/13/94	33.4	N/A
	-10C	11/13/94	35.3	N/A
12.5 AMP DISCHARGE TO 19V /SHORT DOWN TO 2.2 V				

COMSAT QTP DATA

VENDOR	CAPACITY, AH	PERCENT CAPACITY RETAINED AFTER 3 DAYS OF SELF DISCHARGE AT 10°C	AVERAGE DISCHARGE VOLTAGE AT C/2 RATE	INTERNAL RESISTANCE Milliohms
EPI/Joplin	24.5	90.2	27.513V	80
EPI/Butler	20.2	92.6	27.782V	55

COMSAT QTP DATA - CONTD.

ITEM	EPI(JOPLIN) SPV	EPI(BUTLER) SPV
ELECTROLYTE LEAK	NO LEAK	NO LEAK
CAPACITY AT 10°C, AH	24.5	20.2
CAPACITY AT 25°C,AH	22.3	16
CAPACITY AT 10°C,AH	24.5	20.2
CAPACITY AFTER 72 HR,AH	22.1	18.7
PEAK LOAD(38A) TEST,V	23.95	24.11
FINAL FUNCTIONAL		
CAPACITY AT 10°C, AH	24.7	20.5
CAPACITY AT 20°C, AH	23.9	17
CAPACITY AFETR 72 HR,AH	22.2	18.4
CAPACITY AT -10°C, AH	24.9	21.9
CAPACITY AT 30°C,AH	19	16.8
CAPACITY AT 20°C,AH	23.9	18.5
CAPACITY AT 10°C,AH	24.3	21.4
CAPACITY AT 0°C,AH	24.5	23.1

COMSAT QTP DATA - CONTD.

BUTLER 10 C CAPACITY - INITIAL FUNCTIONAL

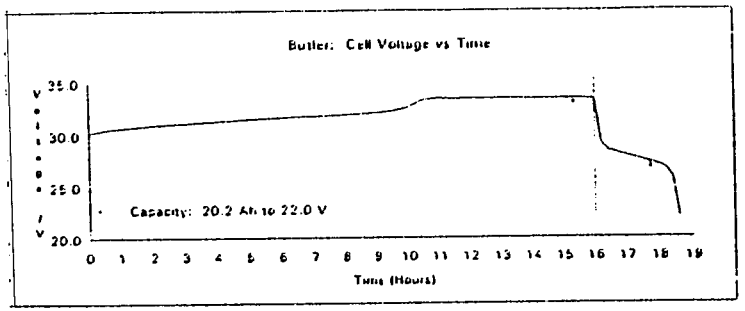

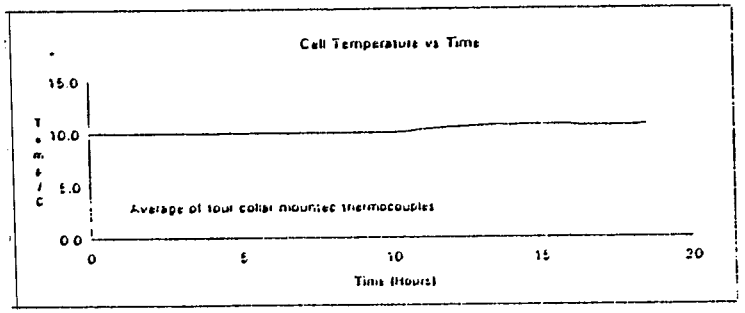

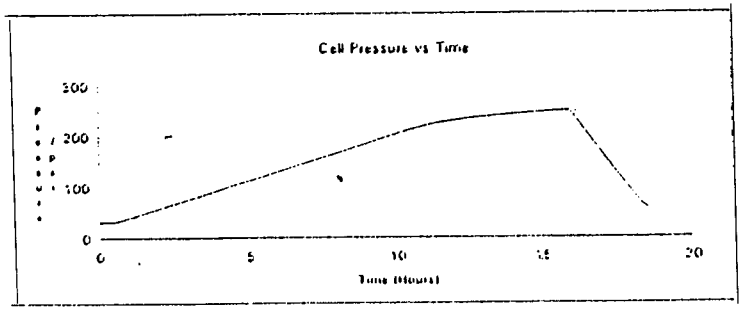

EPI 10 C CAPACITY - INITIAL FUNCTIONAL

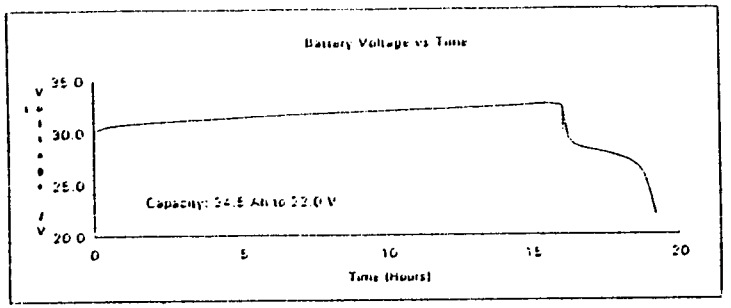

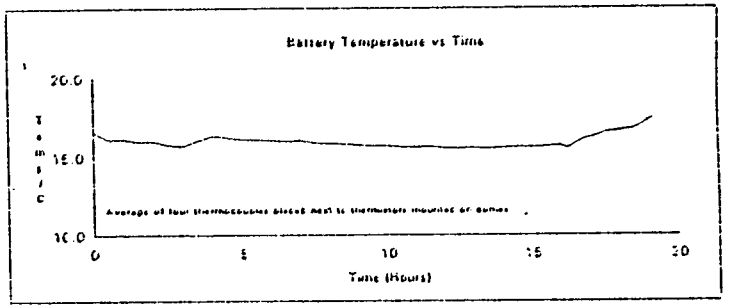

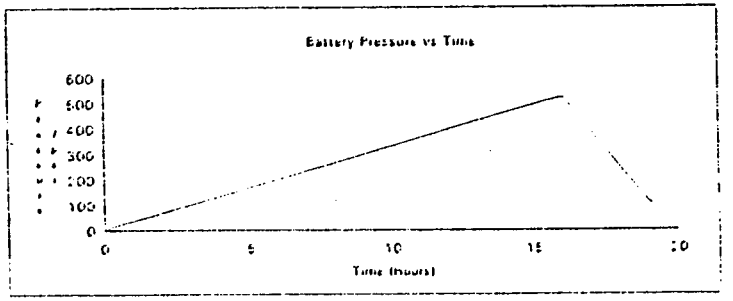

COMSAT QTP/ENVIRONMENTAL TEST SUMMARY

- THERMAL SOAK TESTS YIELDED STABLE EOC VOLTAGE
- THE EOD VOLTAGE WAS REPRODUCABLE AT 30°C, 10°C, AND -10°C WITH VALUES OF 27.66, 28.22, AND 27.1 VOLTS, RESPECTIVELY.
- THE BATTERIES MET THE SPECIFIED REQUIREMENTS WHEN SUBJECTED TO RANDOM VIBRATION, LOW LEVEL SINE AND SINE SWEEP VIBRATION.

COMSAT QTP DATA - CONTD.

BUTLER 10 C CAPACITY - FINAL FUNCTIONAL

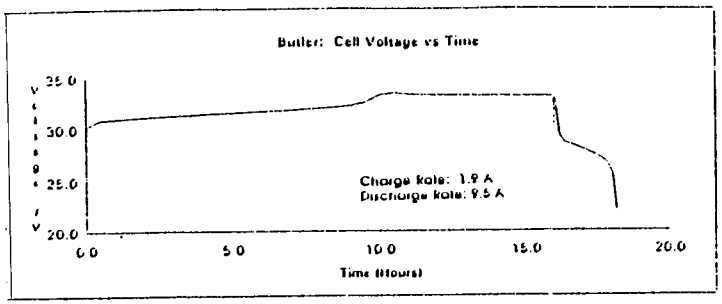

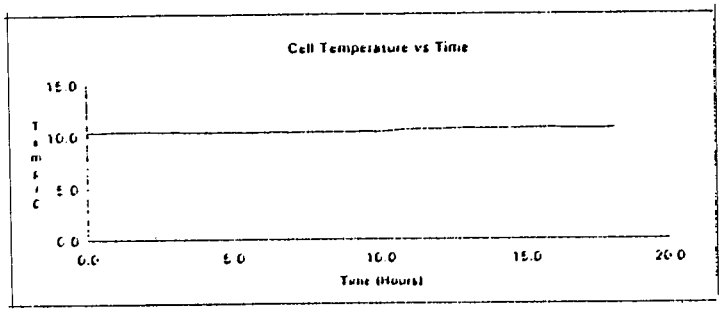

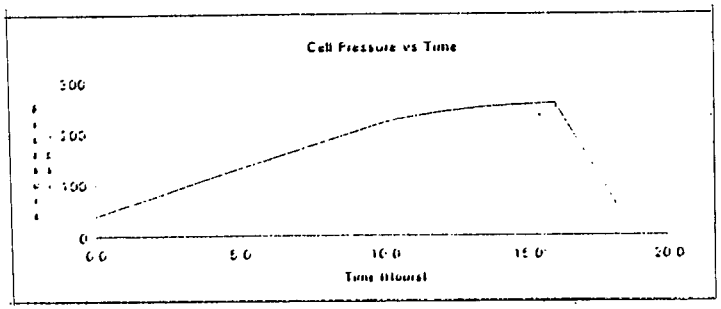

EPI 10°C CAPACITY - FINAL FUNCTIONAL

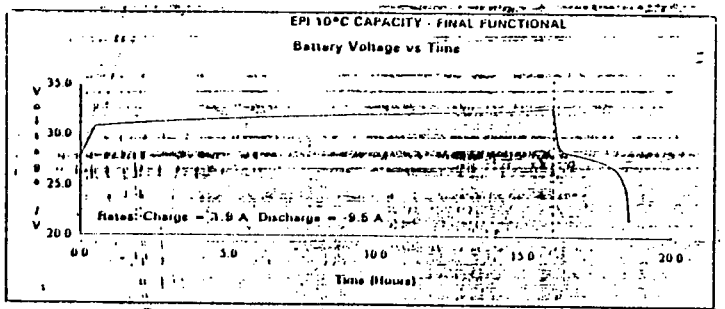

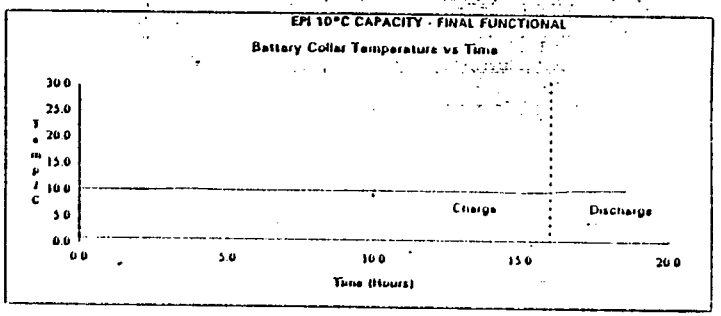

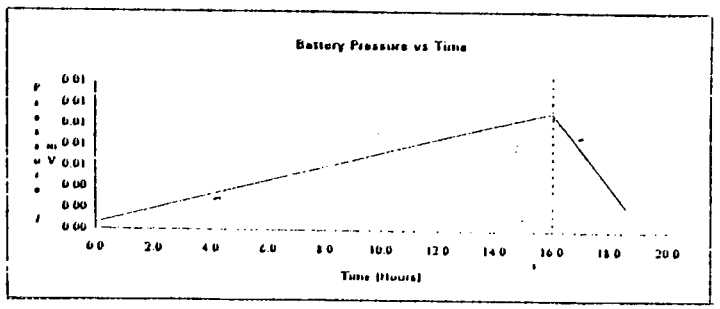

LEO TEST CONDITIONS

- 30 MINUTES DISCHARGE AND 60 MINUTES CHARGE REGIMES
- 0.6C CHARGE RATE WITH TAPER AT 1.473 V/CELL (VT CONTROL) TO A RECHARGE RATIO OF 1.05 (AHI C/D CONTROL). THEN STEP TO TRICKLE AT C/100 FOR THE REMAINDER OF 60 MINUTES
- 0.8C DISCHARGE RATE
- FORTY PERCENT DEPTH OF DISCHARGE
- BATTERY TEMPERATURE CONTROLLER AT 20°C USING COOLANT JACKET
- 16 CYCLES PER DAY

BUTLER LEO CYCLE PROFILES

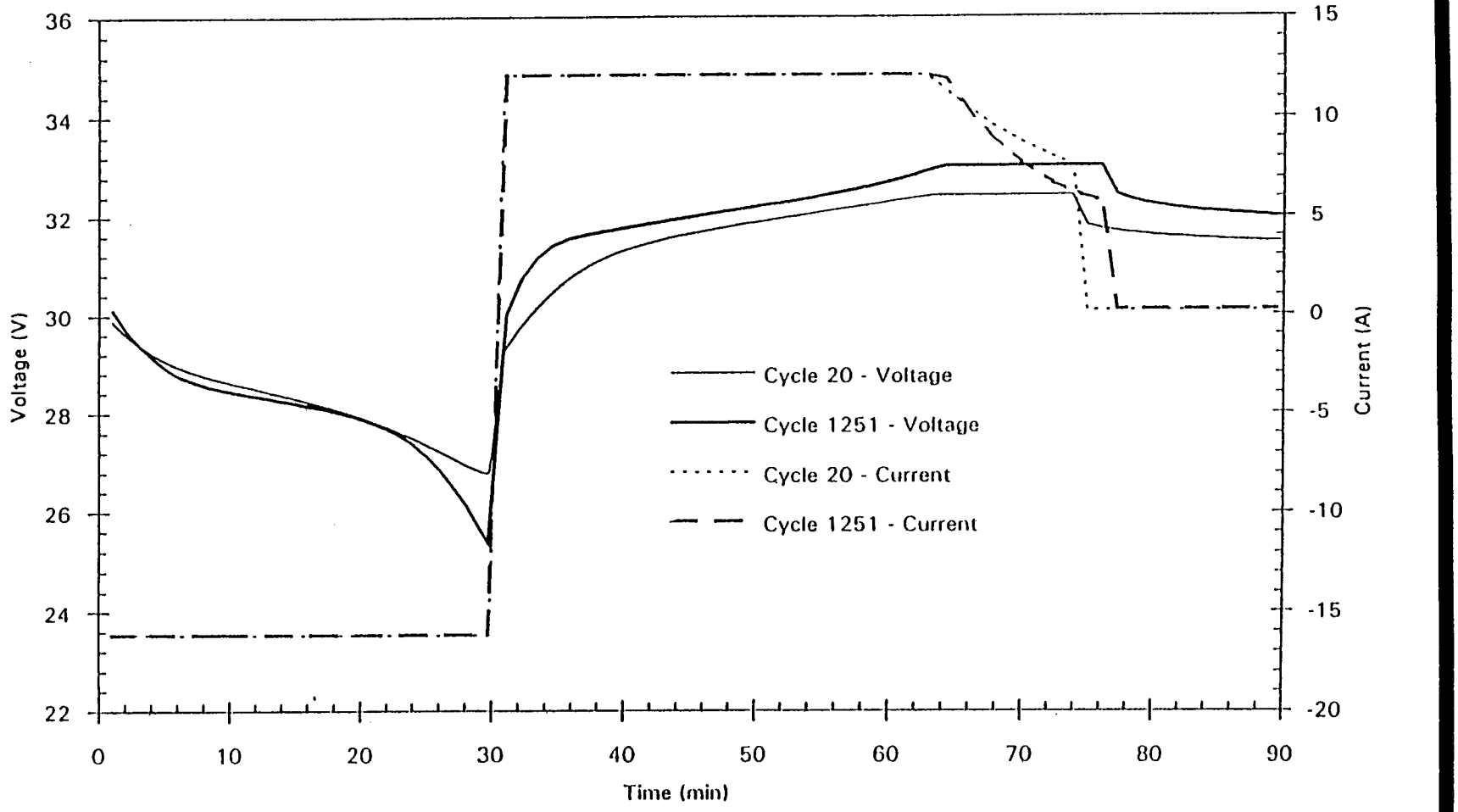

JOPLIN LEO CYCLE PROFILES

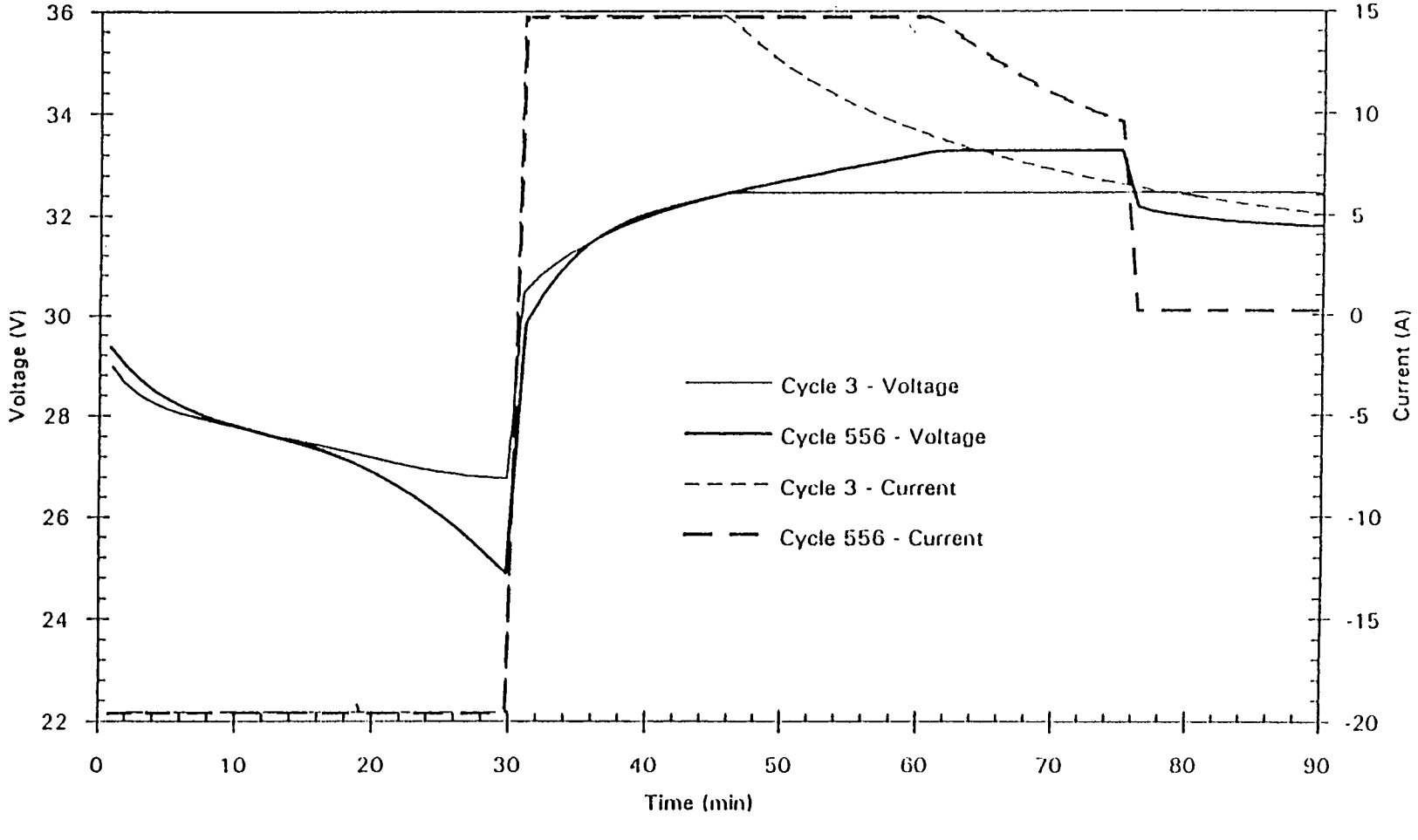

CONCLUSIONS

- TWO 22-CELL 19Ah NiH2 SPV QUAL BATTERIES, ONE EACH FROM EPI/JOPLIN AND EPI/BUTLER, WERE DESIGNED AND PROCURED.
- THE TWO BATTERIES DIFFER IN THE CELL ENCAPSULATION TECHNOLOGY, STACK PRELOAD AND ACTIVATION PROCEDURE.
- BOTH THE BATTERIES MET THE SPECIFIED REQUIREMENTS WHEN SUBJECTED TO QUALIFICATION TESTING.
- TO DATE BUTLER AND JOPLIN BATTERIES COMPLETED 2100 AND 1300 LEO CYCLES, RESPECTIVELY, WITH NOMINAL PERFORMANCE .

Battery and Nickel Electrode Modeling Focused Session

JPL

FIRST PRINCIPLES NICKEL-CADMIUM AND NICKEL HYDROGEN SPACECRAFT BATTERY MODELS

P. TIMMERMAN, B.V. RATNAKUMAR, S. DISTEFANO

JET PROPULSION LABORATORY
CALIFORNIA INSTITUTE OF TECHNOLOGY
PASADENA, CALIFORNIA

PRESENTED TO 1995 NASA BATTERY WORKSHOP
HUNTSVILLE, ALABAMA
NOVEMBER 28-30, 1995

STATUS

NICKEL-CADMIUM MODEL OPERATIONAL

INCLUDES TWO PHASE POSITIVE ELECTRODE
PREDICTIONS ARE VERY CLOSE TO ACTUAL DATA

NICKEL-HYDROGEN MODEL IS OPERATION, BUT NEEDS ADDITIONAL WORK

TWO PHASE POSITIVE ELECTRODE NOT YET INCLUDED
PREDICTIONS ARE UNACCEPTABLE

BOTH MODES RUN ON UNIX AND MACINTOSH COMPUTERS

NICKEL-CADMIUM MODEL IS AVAILABLE TO NASA USERS

TWO PHASE NICKEL HYDROGEN MODEL IS EXPECTED SHORTLY

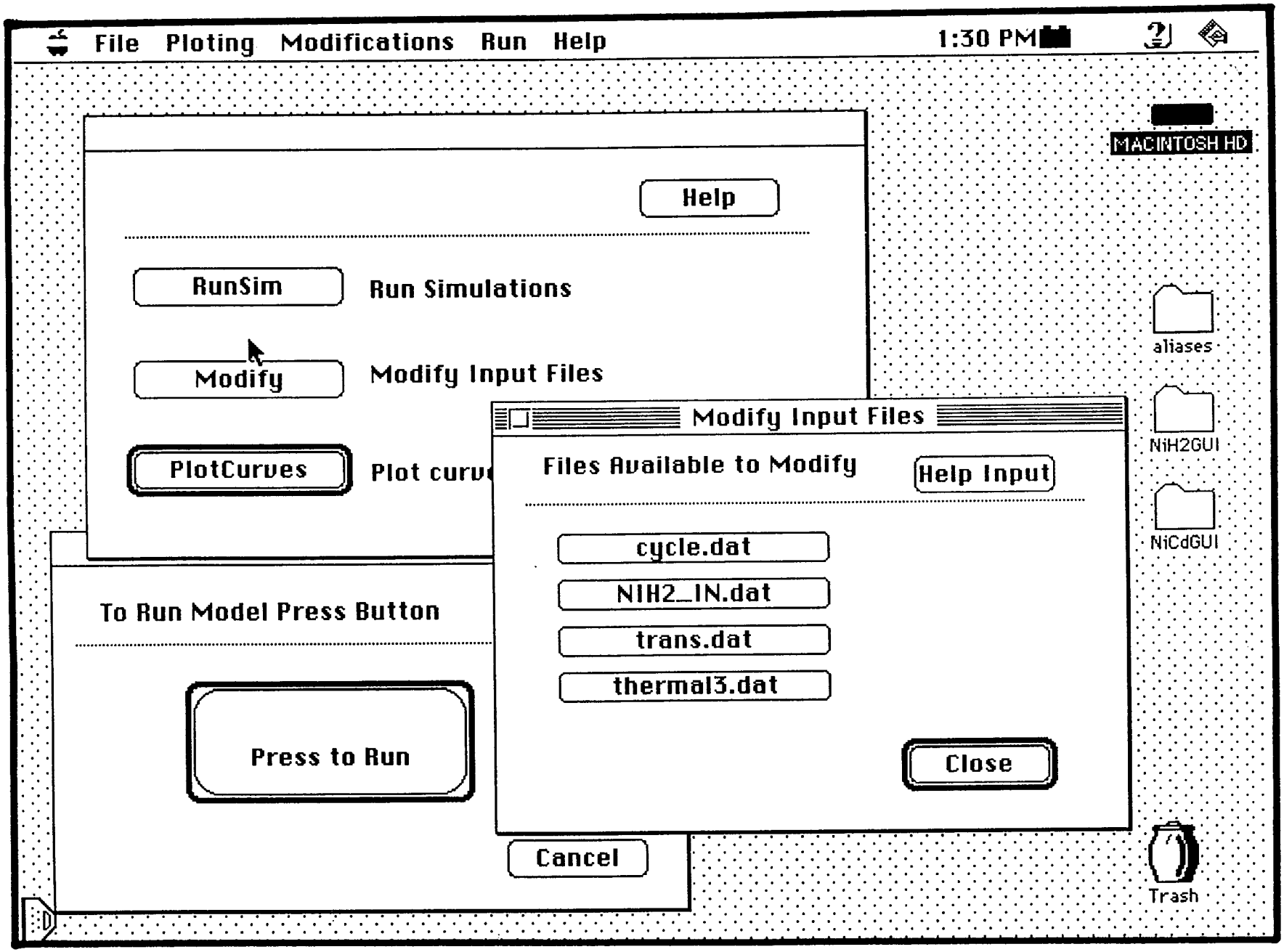
File Ploting Modifications Run Help
1:30 PM
MACINTOSH HD
Help
RunSim
Run Simulations
Modify
Modify Input Files
PlotCurves
Plot curv
aliases
NiH2GUI
NiCdGUI
Modify Input Files
Files Available to Modify
Help Input
cycle.dat
NIH2_IN.dat
trans.dat
thermal3.dat
Close
To Run Model Press Button
Press to Run
Cancel
Trash

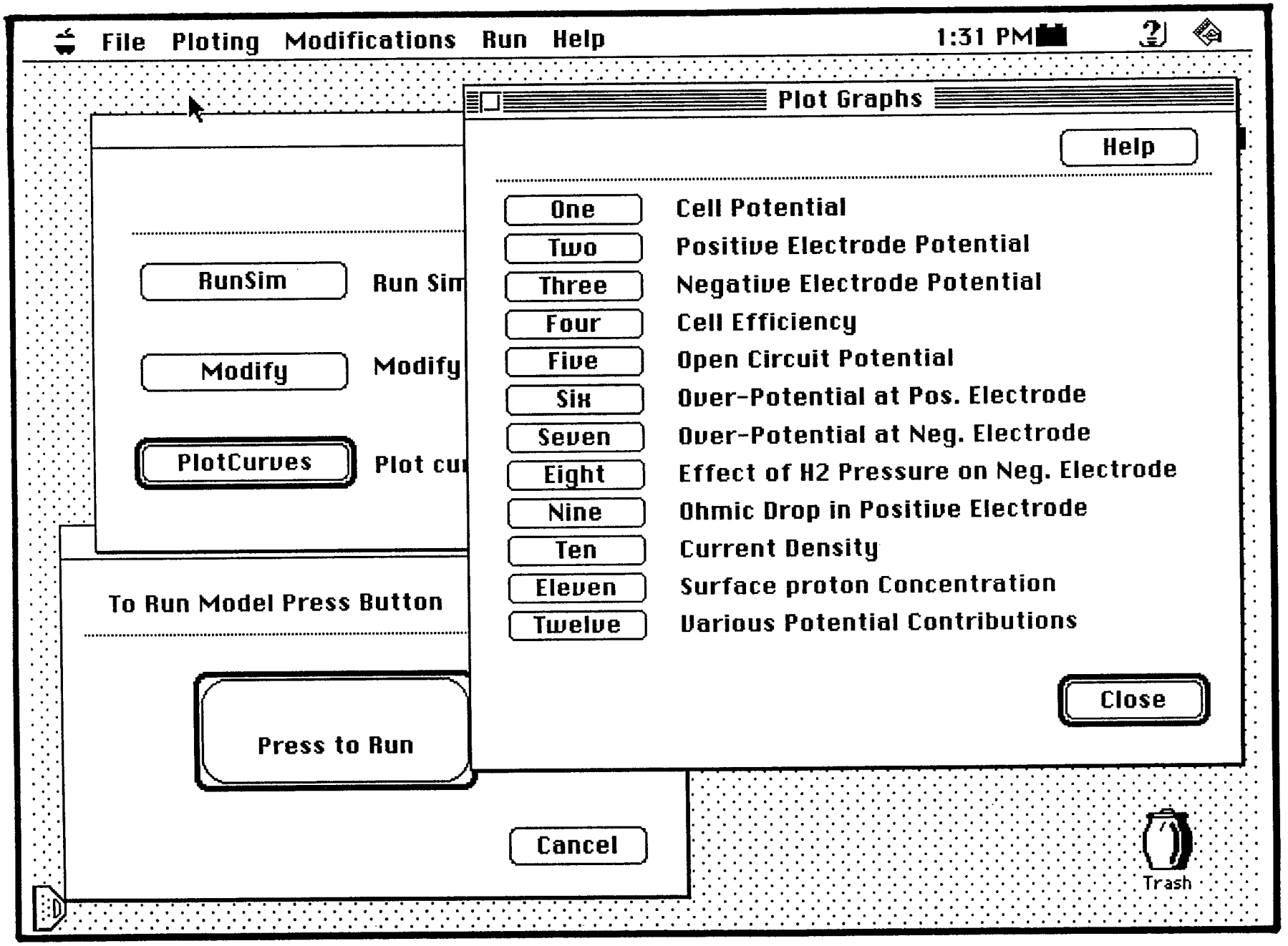
File Ploting Modifications Run Help
1:31 PM
Plot Graphs
Help
RunSim
Run Sim
Modify
Modify
PlotCurves
Plot cu
To Run Model Press Button
Press to Run
Cancel
One
Cell Potential
Two
Positive Electrode Potential
Three
Negative Electrode Potential
Four
Cell Efficiency
Five
Open Circuit Potential
Six
Over-Potential at Pos. Electrode
Seven
Over-Potential at Neg. Electrode
Eight
Effect of H2 Pressure on Neg. Electrode
Nine
Ohmic Drop in Positive Electrode
Ten
Current Density
Eleven
Surface proton Concentration
Twelve
Various Potential Contributions
Close
Trash

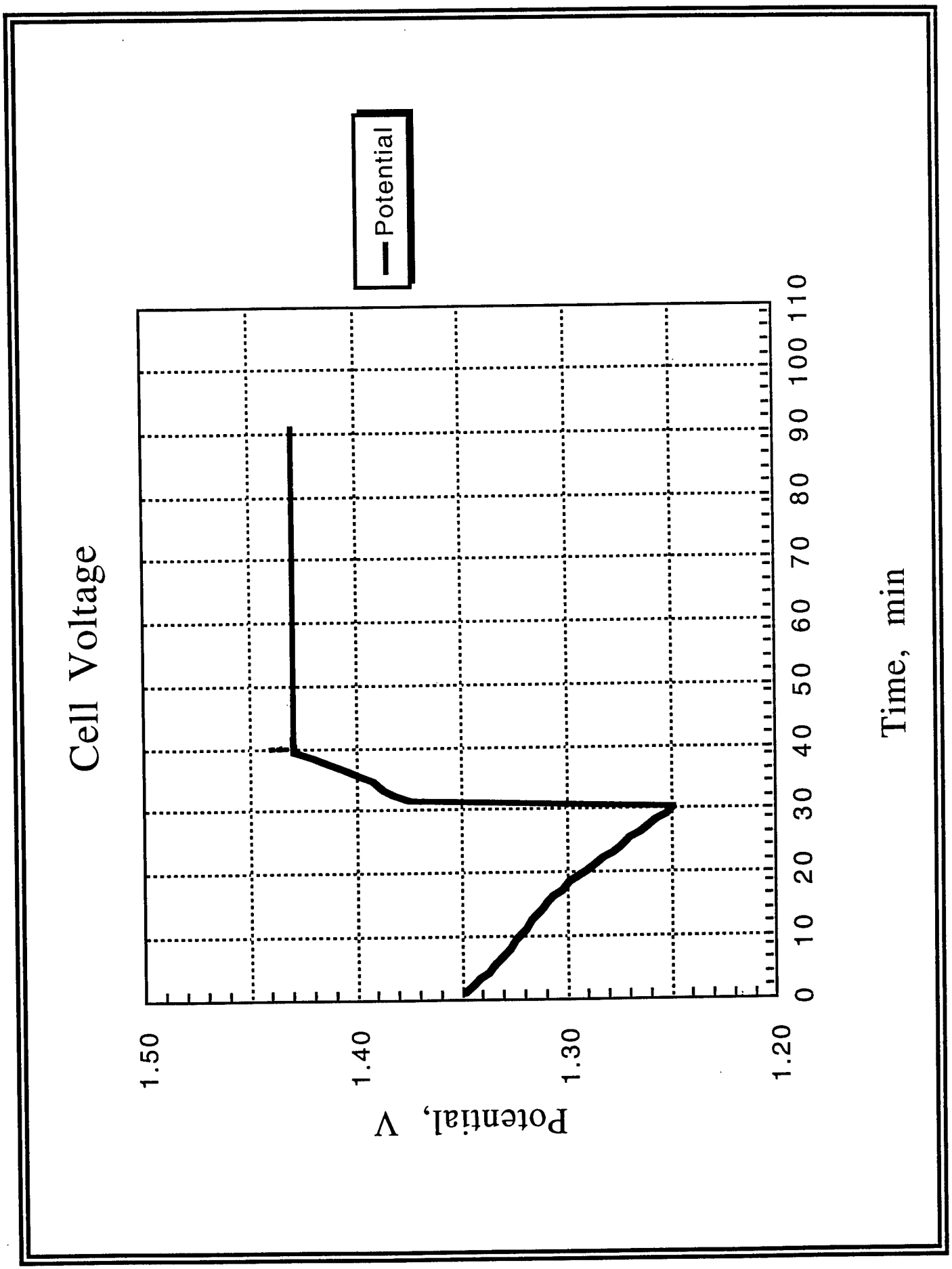
Cell Voltage
Potential
Potential, V
1.50
1.40
1.30
1.20
0 10 20 30 40 50 60 70 80 90 100 110
Time, min

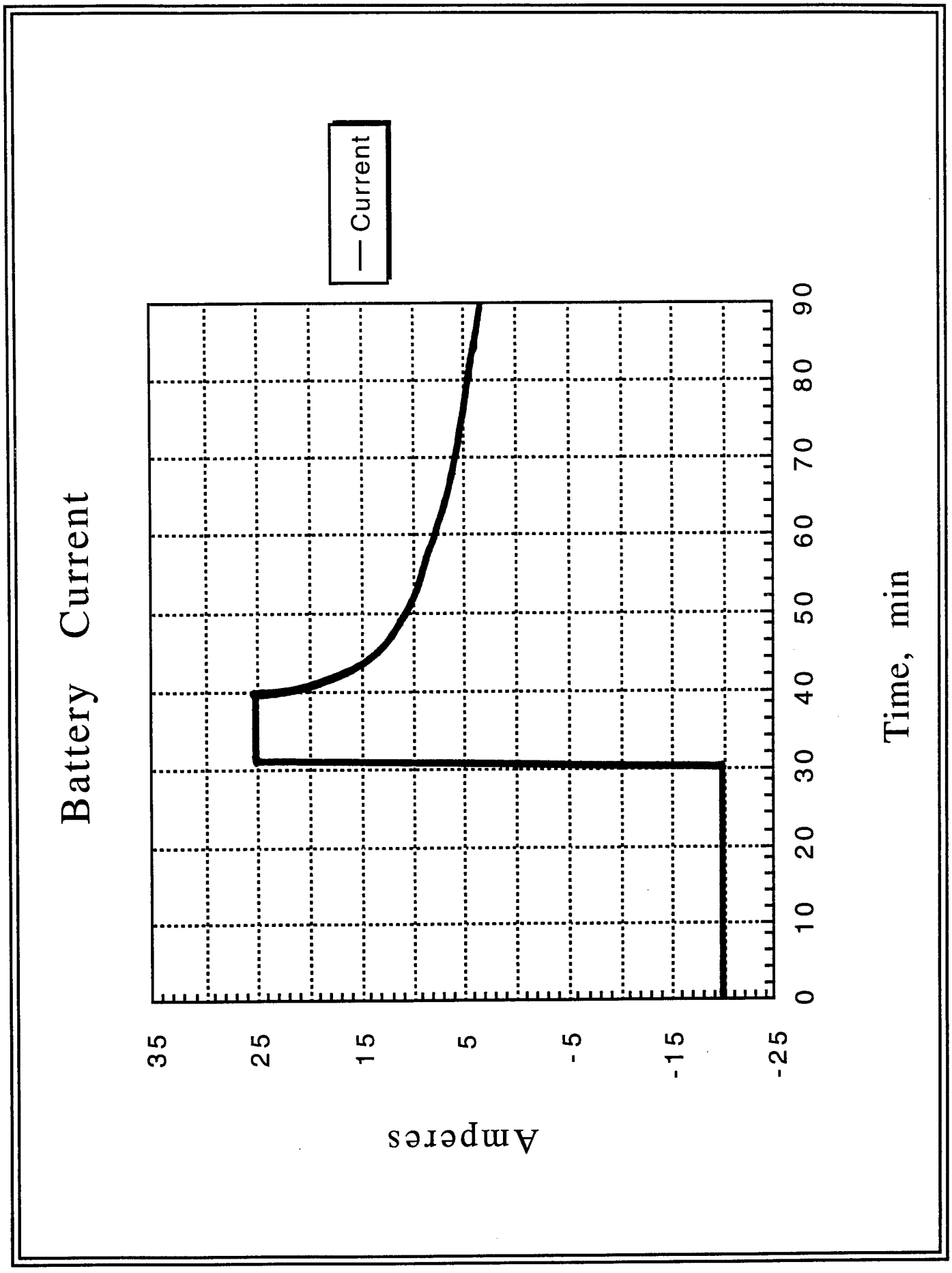
Battery Current
— Current
Amperes
35
25
15
5
-5
-15
-25
0
10
20
30
40
50
60
70
80
90
Time, min

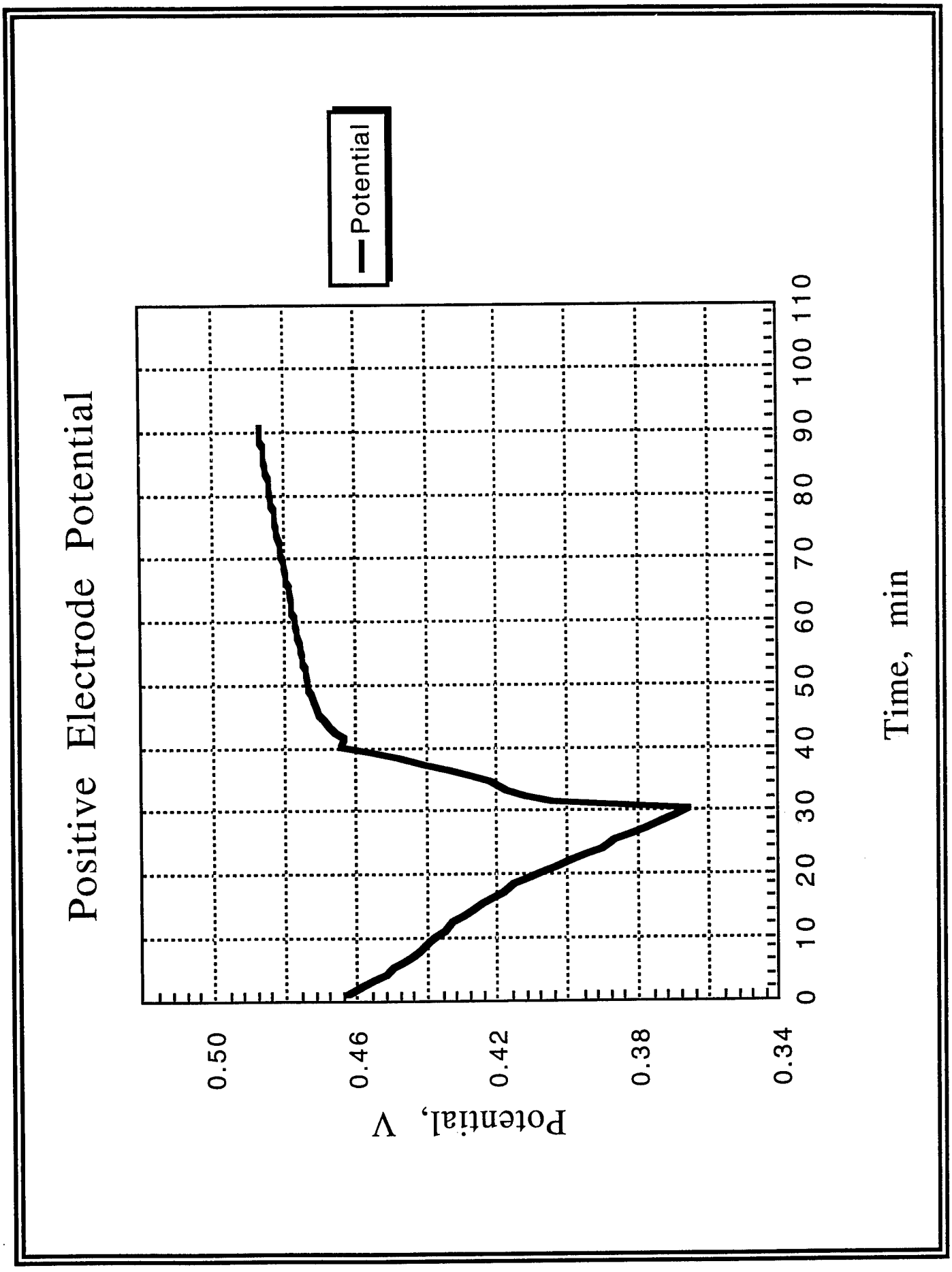
Positive Electrode Potential
Potential
Potential, V
0.50
0.46
0.42
0.38
0.34
0 10 20 30 40 50 60 70 80 90 100 110
Time, min

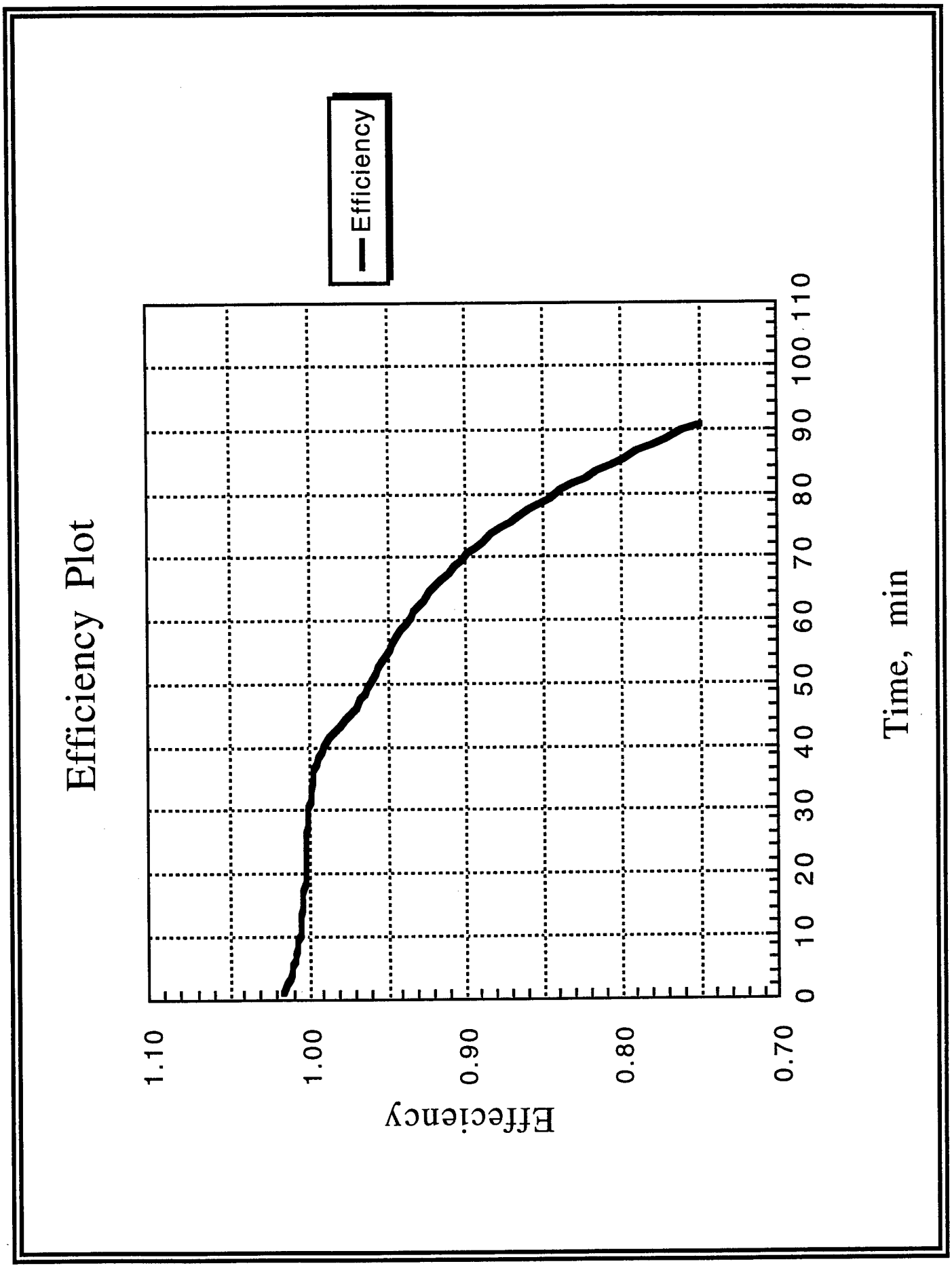
Efficiency Plot
Efficiency
1.10
1.00
0.90
0.80
0.70
Effeciency
0
10
20
30
40
50
60
70
80
90
100
110
Time, min

Predicted Versus Actual Discharge Voltages: Topex 50AH, C/2 Rate

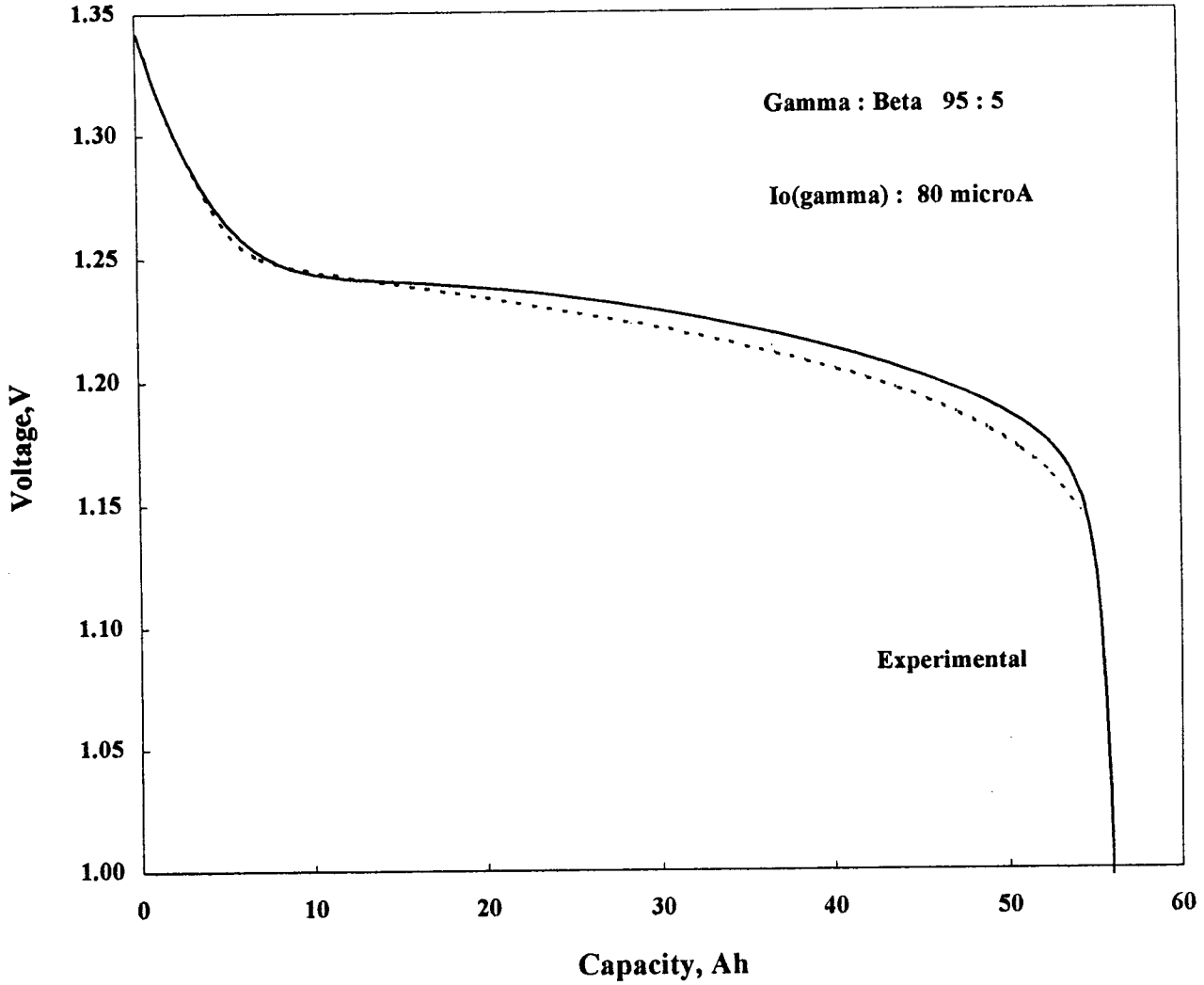

ACKNOWLEDGMENT

The work described here was carried out at the Jet Propulsion Laboratory, California Institute of Technology, under contract with the National Aeronautics and Space Administration.

This work is also part of the NASA Battery Program sponsored by the Office of the NASA Chief Engineer.

Mathematical Models for Electrochemical Impregnation of Nickel Electrodes

Chien-Hsien Ho, Gowri S. Nagarajan,
Mahesh Murthy and J.W. Van Zee

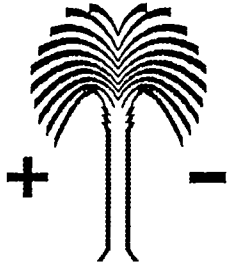

Center for Electrochemical Engineering
Department of Chemical Engineering
University of South Carolina

J.W. Van Zee, University of South Carolina
Presented at the NASA Battery Workshop

Nov. 29, 1995

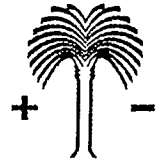

Outline

- Motivation
- **Impregnation Models for Porous Plaques**
  - Single Step Precipitation Model
  - Two-Step Tetramer Precipitation Model
- **Film Growth Model for Planar Experiments** - Not Presented
- **Vapor-Liquid Equilibrium of Impregnation Baths** - Not Presented

Objectives for Impregnation Model

- Predict the impregnation conditions for uniform loading
  - Study process as a function of
  - current, thickness, concentration & temperature
- Develop quality control tools for electrode manufactures
  - reproducibility, predictability & variability
  - based on first principles
  - characterization methologies:
    - » *in-situ* & nondestructive
- Basis for predicting performance of batteries with
  - non-uniform loadings

J.W. Van Zee, University of South Carolina
Presented at the NASA Battery Workshop

Nov. 29, 1995

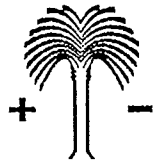

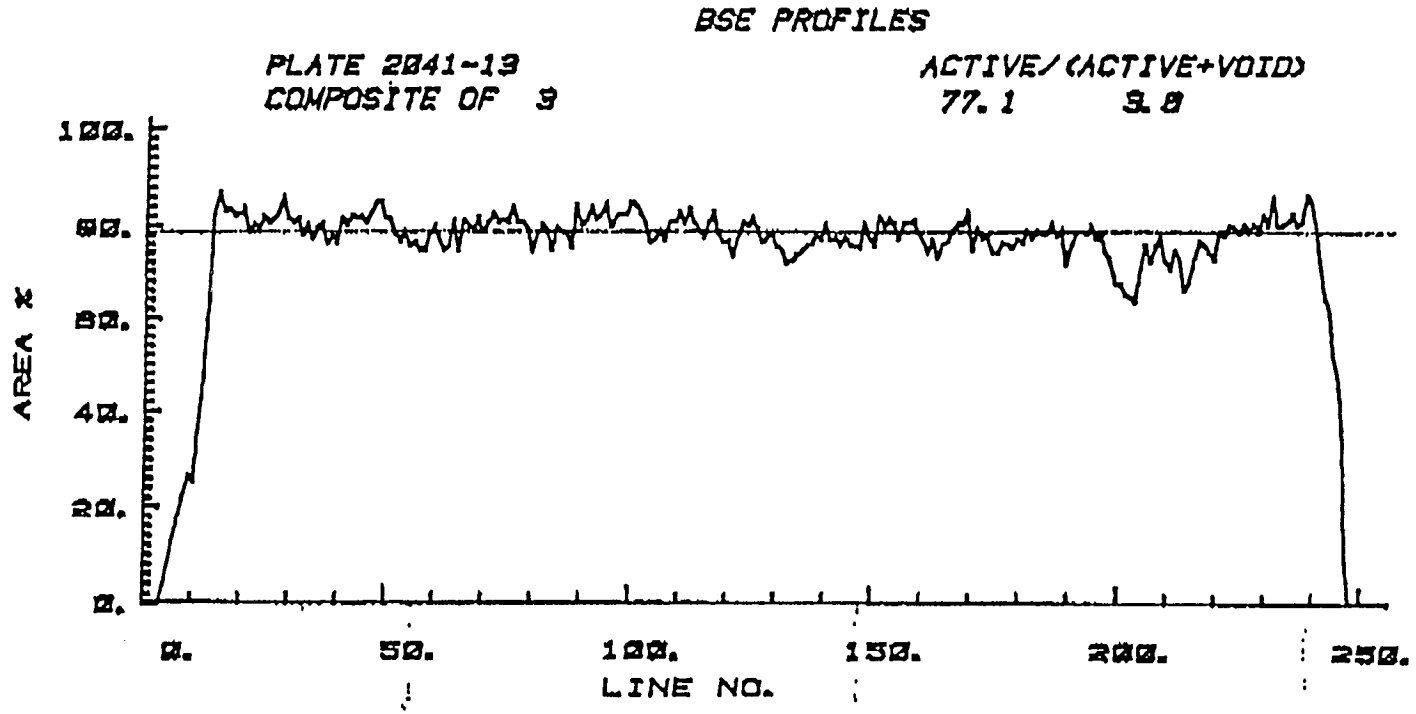

Plate impregnated in a fresh bath exhibiting more uniform loading

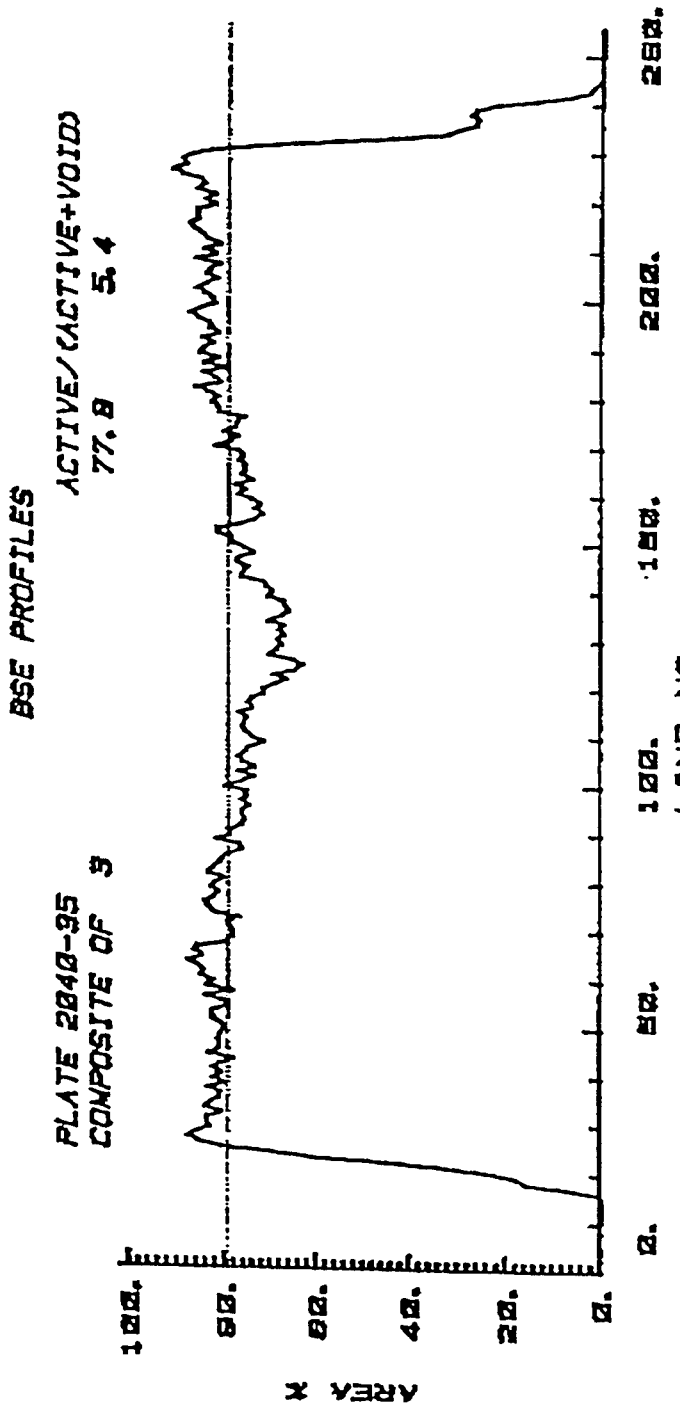

Plate impregnated in an aged bath exhibiting enhanced loading near the outer surfaces and depleted loading near the center.

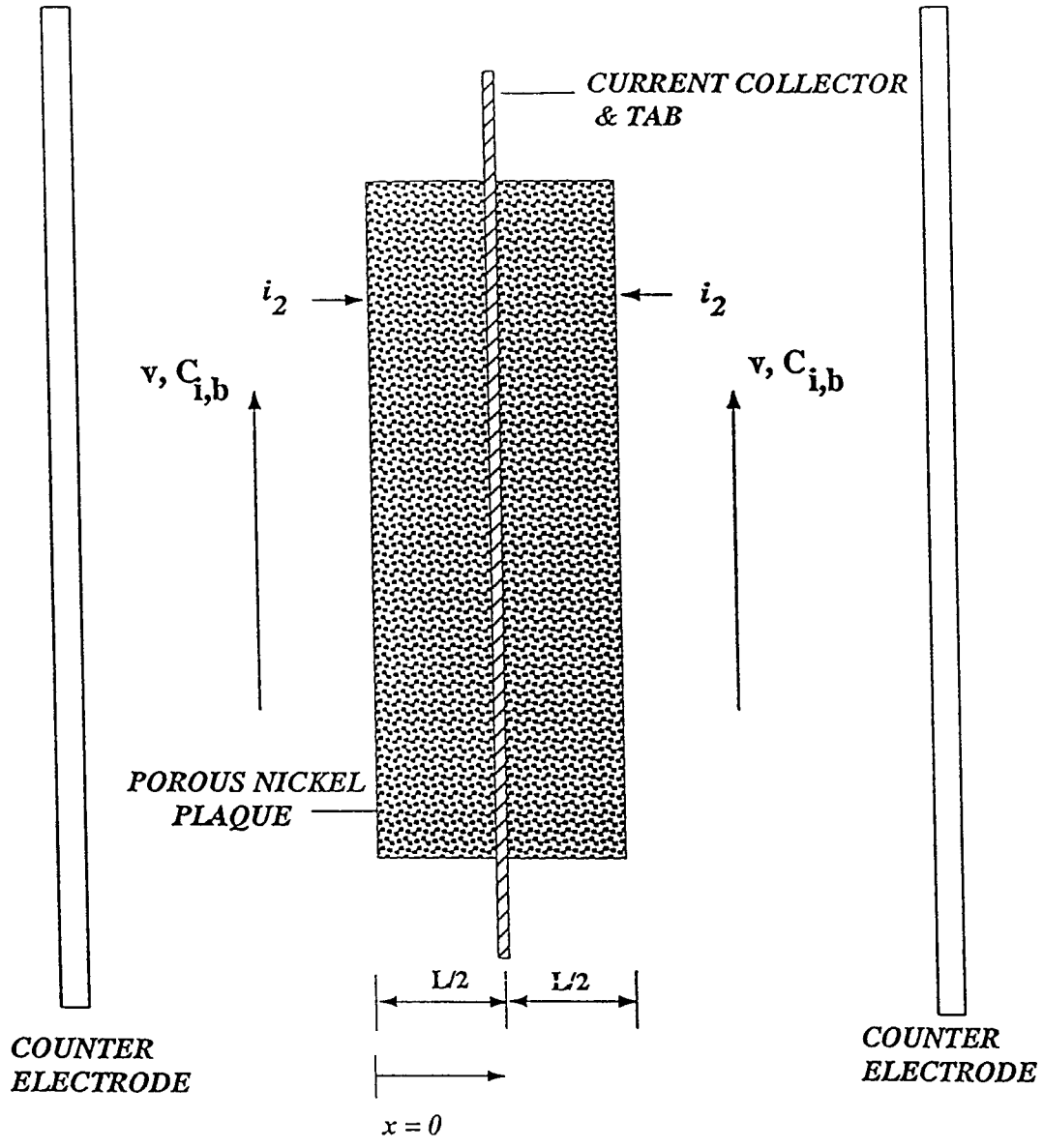

Figure 1. SCHEMATIC OF POROUS NICKEL PLAQUE

Butler-Volmer Kinetic Expression

$$\nabla \cdot i_2 = \frac{\partial i_2}{\partial x} = a i_o \left[\theta_{OH^-}^{9/8} \exp\left(\frac{\alpha_a F}{RT}\eta\right) - \theta_{NO_3^-}^{1/8} \exp\left(-\frac{\alpha_c F}{RT}\eta\right)\right]$$

$$\theta_{OH^-} = \frac{C_{OH^-}}{C_{ref}} \quad : \quad \theta_{NO_3^-} = \frac{C_{NO_3^-}}{C_{ref}} \quad : \quad \eta = \phi_1 - \phi_2 - U_{ref}$$

Mass Balance Expression

$$\frac{\partial \epsilon C_i}{\partial t} = -\frac{s_i}{nF}\frac{\partial i_2}{\partial x} + \frac{D_i}{\tau}\frac{\partial}{\partial x}\left(\epsilon \frac{\partial C_i}{\partial x}\right) + \frac{z_i D_i F}{\tau RT}\left(\frac{\partial}{\partial x}\left(\epsilon C_i \frac{\partial \phi_2}{\partial x}\right)\right) + R_i$$

Equilibrium and Precipitation Reactions

$Ni^{2+} + 2OH^- = Ni(OH)_2 \downarrow$ $\quad K_{sp} = 1.6 \times 10^{-23}\ (mol/cc)^3$

$Ni^{2+} + OH^- = 1/4Ni_4(OH)_4^{4+}$ $\quad K = 2.10 \times 10^{12}\ (mol/cc)^{-7/4}$

$OH^- + 1/4Ni_4(OH)_4^{4+} = Ni(OH)_2$ $\quad K = 3.38 \times 10^{-11}\ (mol/cc)^{-5/4}$

Nickel and Ammonia Equilibrium

$NH_3 + H_2O = OH^- + NH_4^+$ $\quad K = 1.76 \times 10^{-8}\ (mol/cc)$

$Ni^{2+} + 6NH_3 = Ni(NH_3)_6^{2+}$ $\quad K = 10^{8.74}\ M$

$Ni^{2+} + NH_3 = Ni(NH_3)^{2+}$ $\quad K = 10^{2.8}\ (mol/cc)^{-7/4}$

Cobalt and Ammonia Equilibrium

$Co^{2+} + 6NH_3 = Co(NH_3)_6^{2+}$ $\quad K = 10^{5.11}\ M$

$Co^{2+} + NH_3 = Co(NH_3)^{2+}$ $\quad K = 10^{2.11}\ M$

$Co^{2+} + OH^- = Co(OH)^+$ $\quad K = 2.24 \times 10^7\ (mol/cc)^{-1}$

$Co^{2+} + 2OH^- = Co(OH)_2 \downarrow$ $\quad K_{sp} = 1.3 \times 10^{-24} (mol/cc)^3$

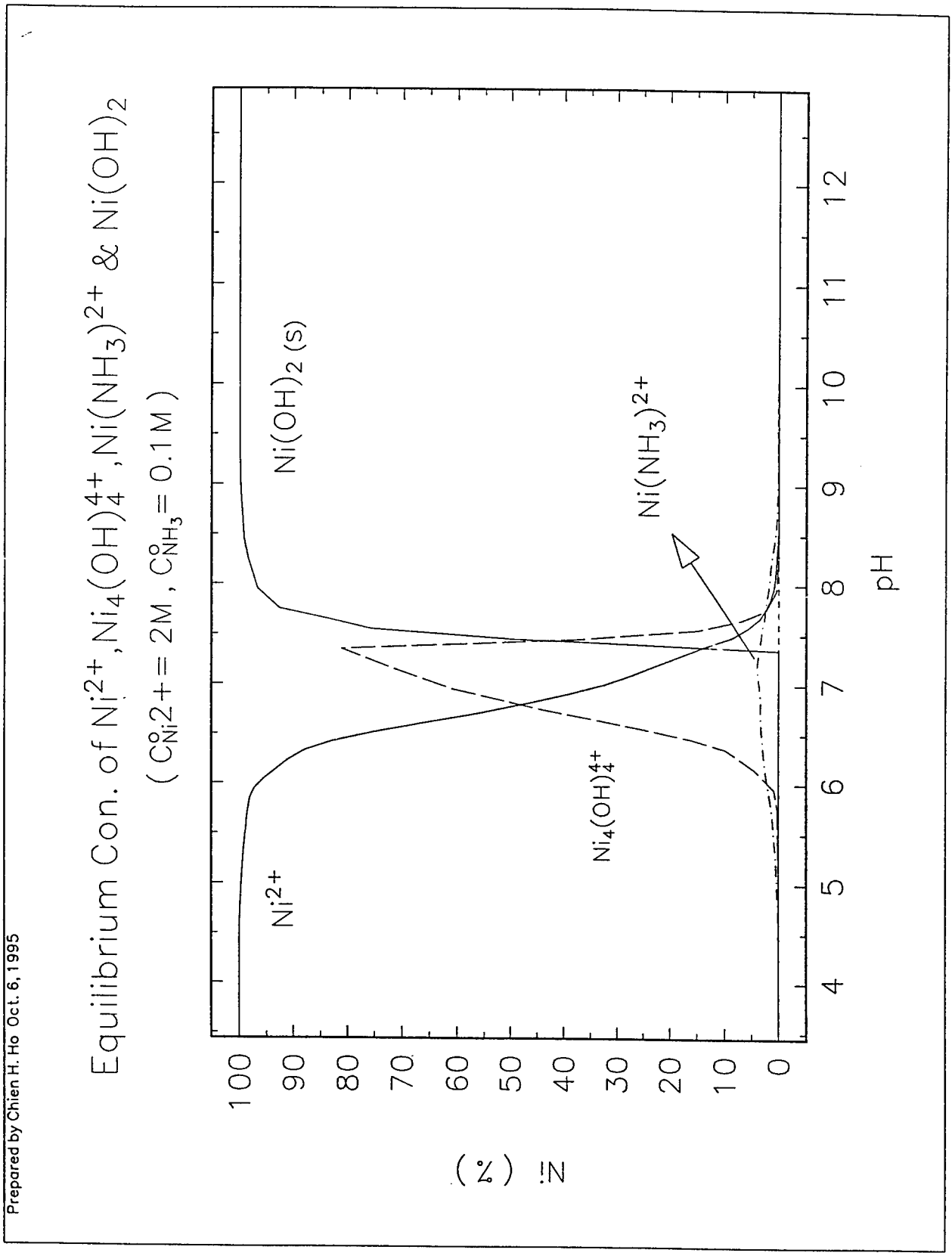
Equilibrium Con. of Ni^{2+}, $Ni_4(OH)_4^{4+}$, $Ni(NH_3)^{2+}$ & $Ni(OH)_2$
($C^o_{Ni}2+ = 2M$, $C^o_{NH_3} = 0.1\,M$)
Prepared by Chien H. Ho Oct. 6, 1995
Ni^{2+}
$Ni_4(OH)_4^{4+}$
$Ni(NH_3)^{2+}$
$Ni(OH)_2$ (s)
Ni (%)
pH
100
90
80
70
60
50
40
30
20
10
0
4
5
6
7
8
9
10
11
12

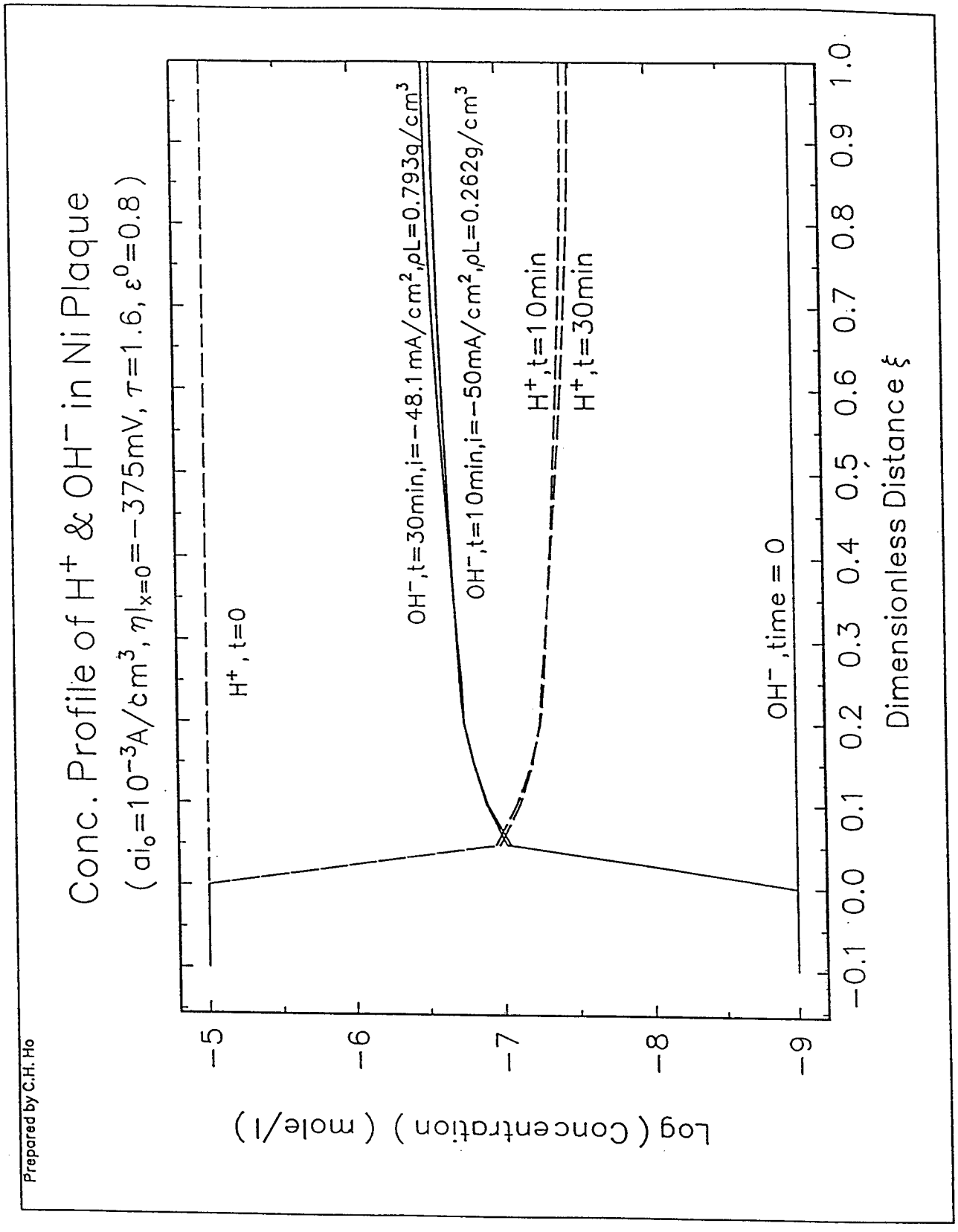
Conc. Profile of H+ & OH- in Ni Plaque
(ai0=10-3A/cm3, η|x=0=-375mV, τ=1.6, ε0=0.8)
H+, t=0
OH-,t=30min,i=-48.1mA/cm2,ρL=0.793g/cm3
OH-,t=10min,i=-50mA/cm2,ρL=0.262g/cm3
H+,t=10min
H+,t=30min
OH-,time = 0
Log (Concentration) (mole/l)
-5
-6
-7
-8
-9
-0.1 0.0 0.1 0.2 0.3 0.4 0.5 0.6 0.7 0.8 0.9 1.0
Dimensionless Distance ξ
Prepared by C.H. Ho

Flux Expression

- Inside Porous Region

$$\frac{N_i}{\varepsilon} = -\frac{D_i}{\tau}\frac{\partial c_i}{\partial x} - \frac{z_i D_i F c_i}{\tau RT}\frac{\partial \phi_2}{\partial x}$$

- Outside Porous Region

$$\frac{\partial c_i}{\partial x} = \frac{N_M k_i}{D_i}\left(c_{i,x=0} - c_{i,b}\right)$$

where $$k_i = \frac{N_{Nu} D_i}{2S}$$

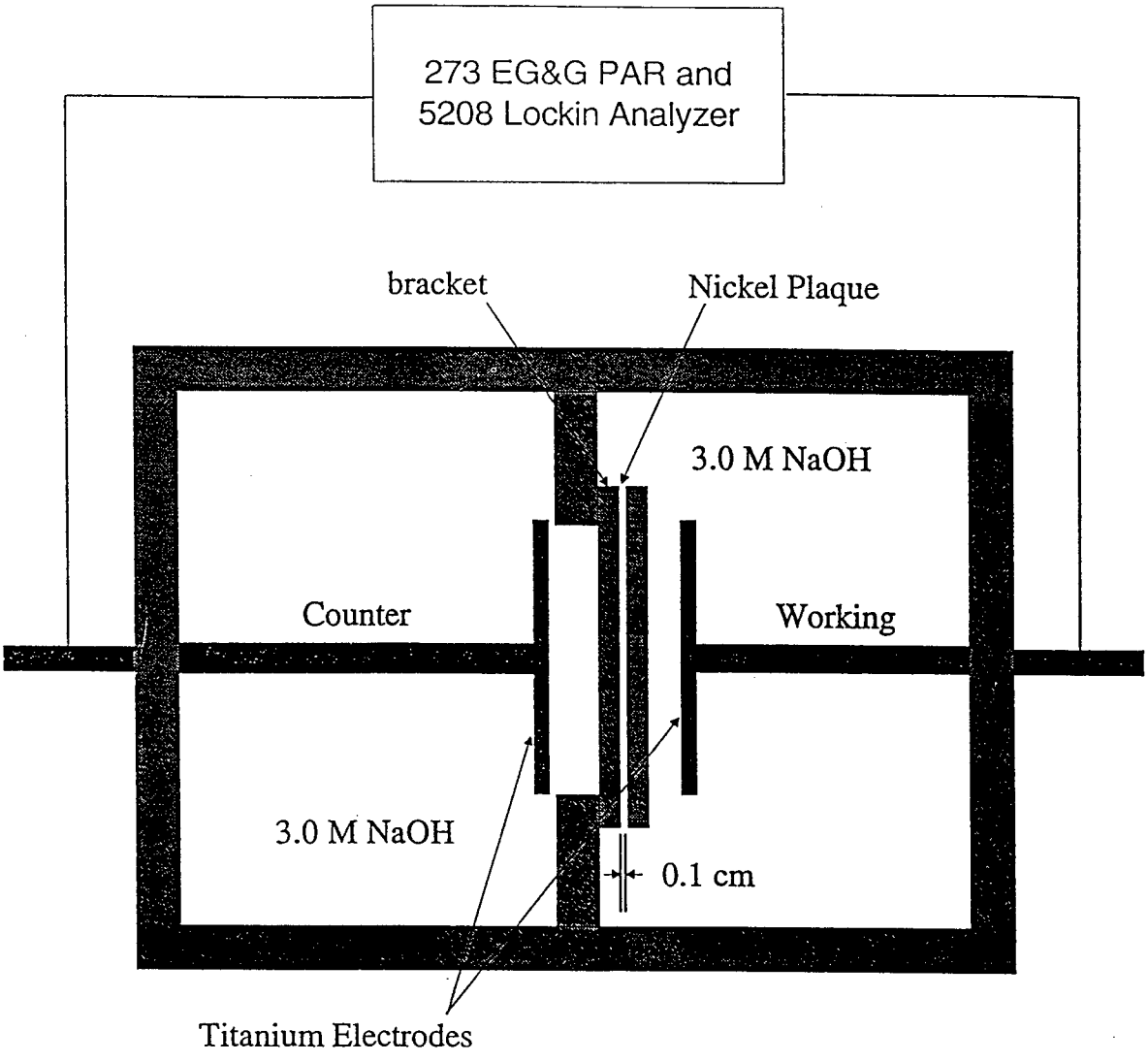

$$N_M = \frac{\tau}{\varepsilon} = \frac{r}{r_o}$$

Experimental Set-Up for the determination of the MacMullin Number for the Nickel Plaques.

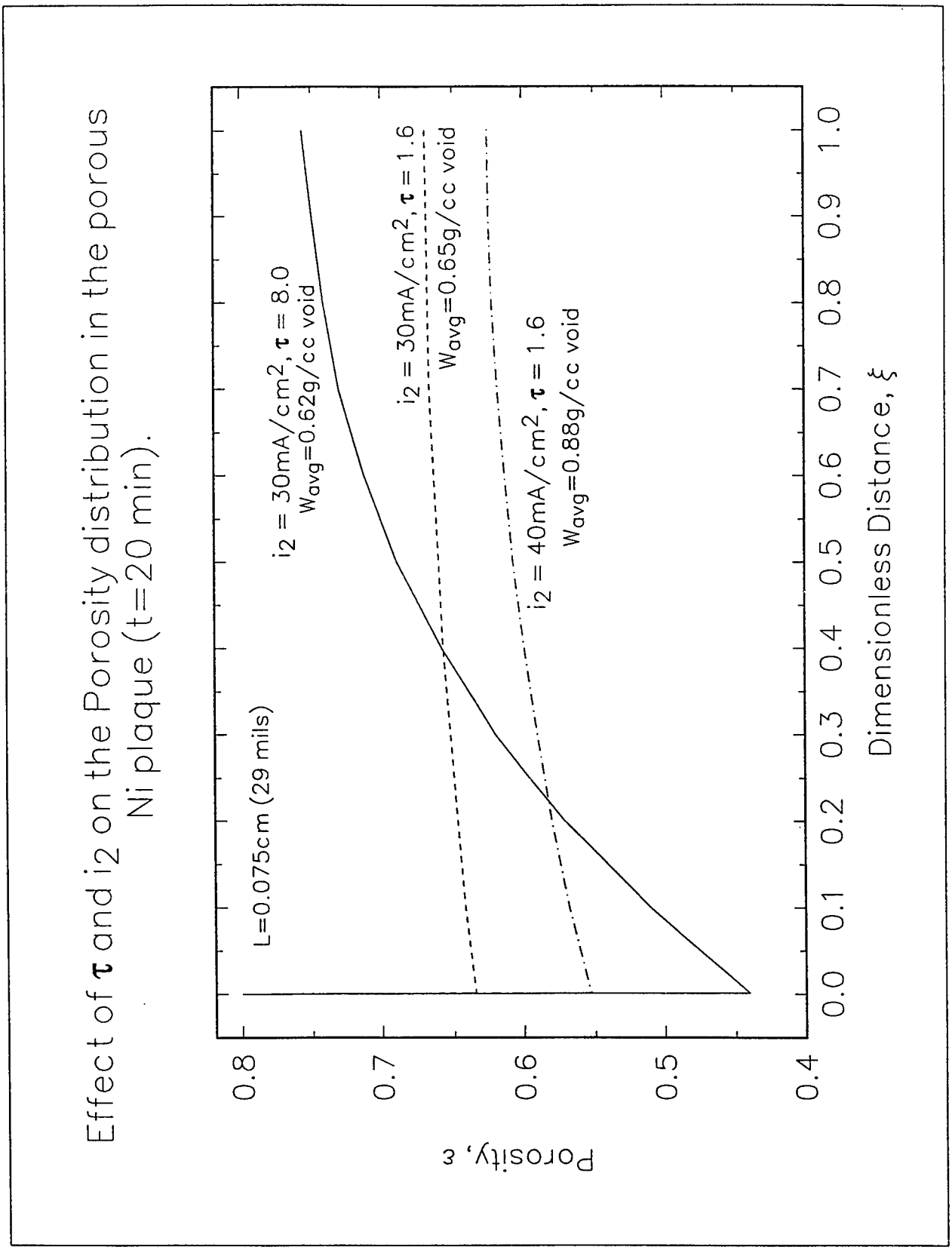
Effect of τ and i2 on the Porosity distribution in the porous Ni plaque (t=20 min).
L=0.075cm (29 mils)
i2 = 30mA/cm2, τ = 8.0
Wavg=0.62g/cc void
i2 = 30mA/cm2, τ = 1.6
Wavg=0.65g/cc void
i2 = 40mA/cm2, τ = 1.6
Wavg=0.88g/cc void
Porosity, ε
Dimensionless Distance, ξ
0.8
0.7
0.6
0.5
0.4
0.0
0.1
0.2
0.3
0.4
0.5
0.6
0.7
0.8
0.9
1.0

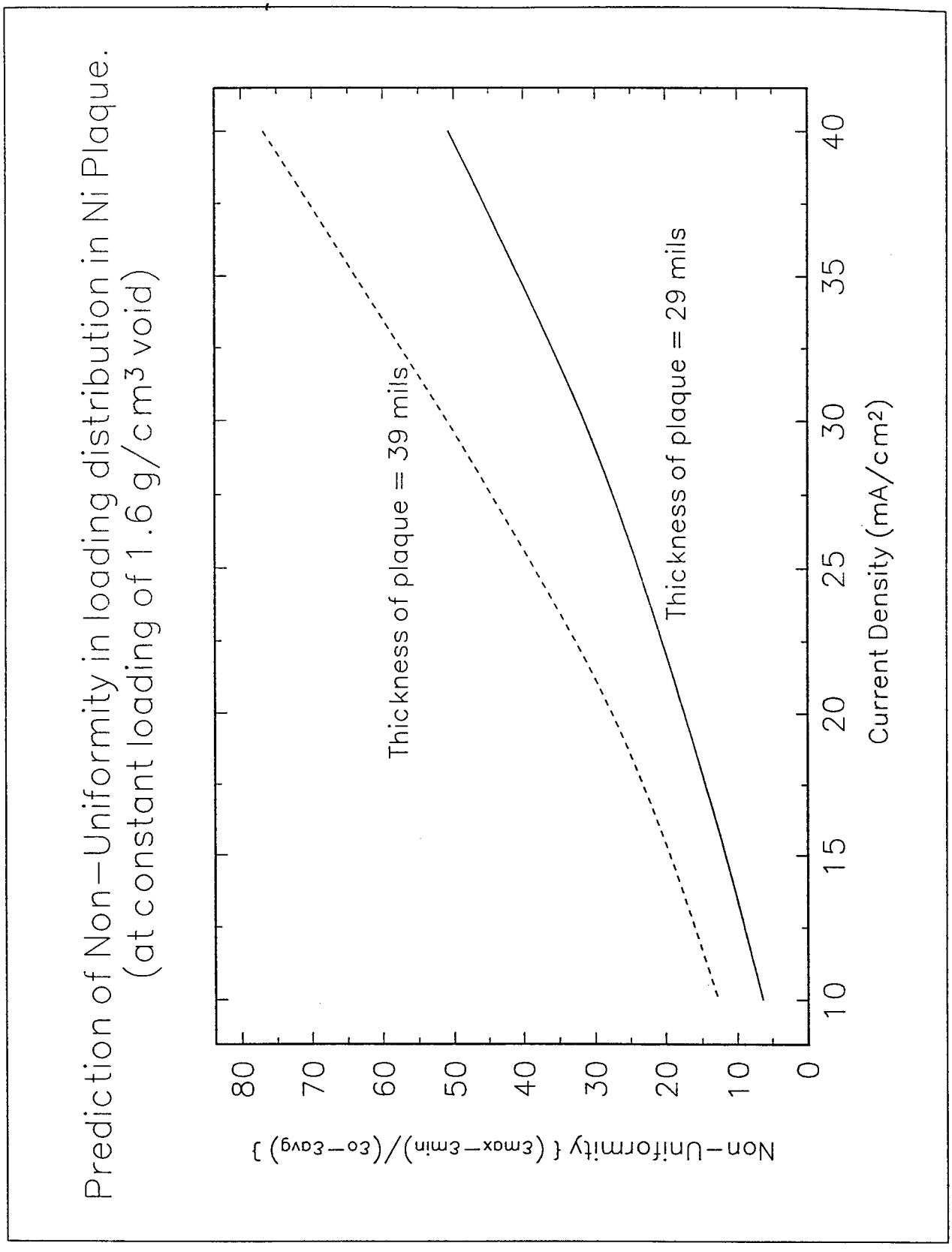
Prediction of Non–Uniformity in loading distribution in Ni Plaque.
(at constant loading of 1.6 g/cm³ void)
Non–Uniformity { (εmax–εmin)/(εo–εavg) }
Current Density (mA/cm²)
Thickness of plaque = 39 mils
Thickness of plaque = 29 mils
0
10
20
30
40
50
60
70
80
10
15
20
25
30
35
40

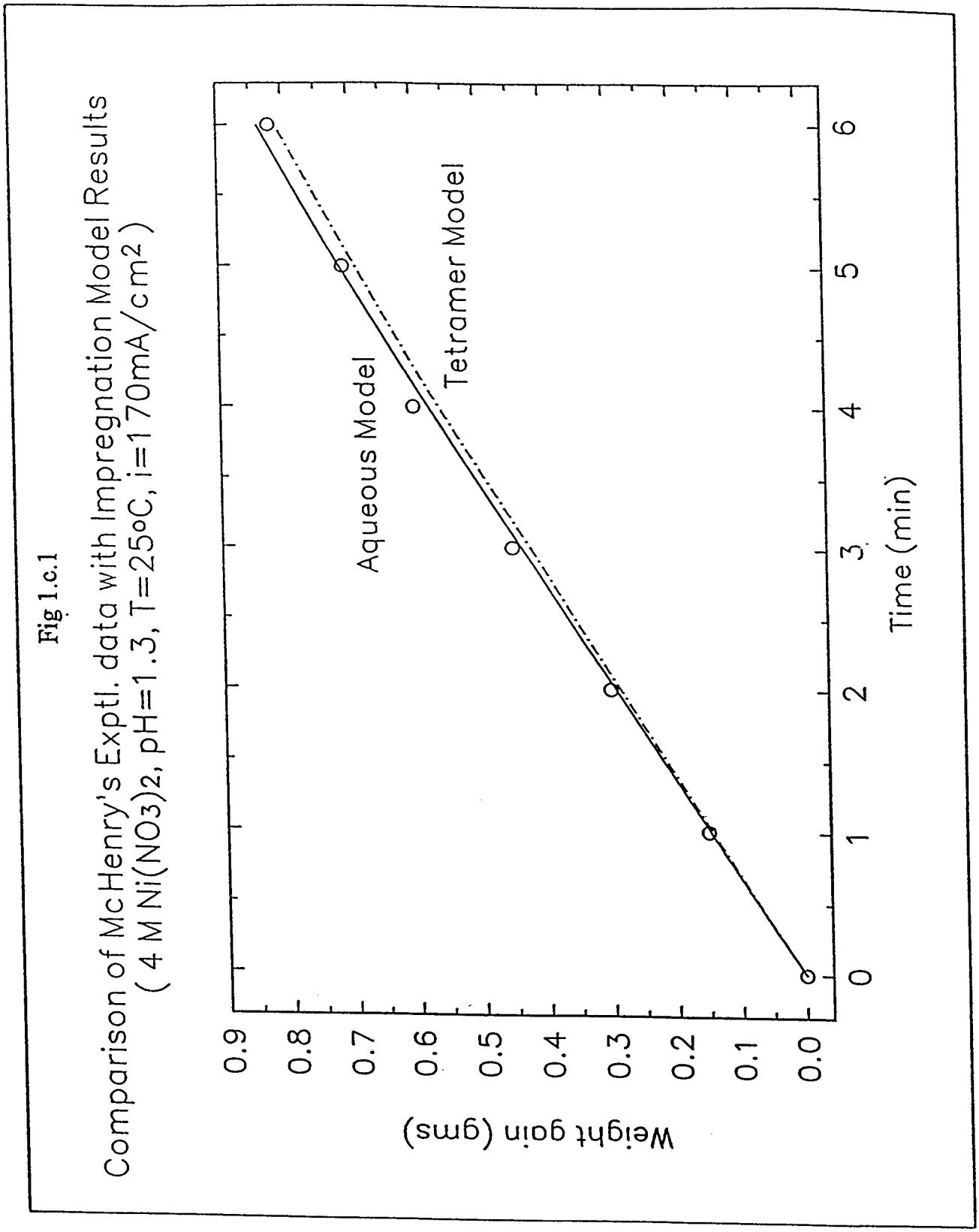
Comparison of McHenry's Exptl. data with Impregnation Model Results
(4 M Ni(NO3)2, pH=1.3, T=25°C, i=170mA/cm2)
Aqueous Model
Tetramer Model
Weight gain (gms)
Time (min)
0.0
0.1
0.2
0.3
0.4
0.5
0.6
0.7
0.8
0.9
0
1
2
3
4
5
6

Fig 1.c.1

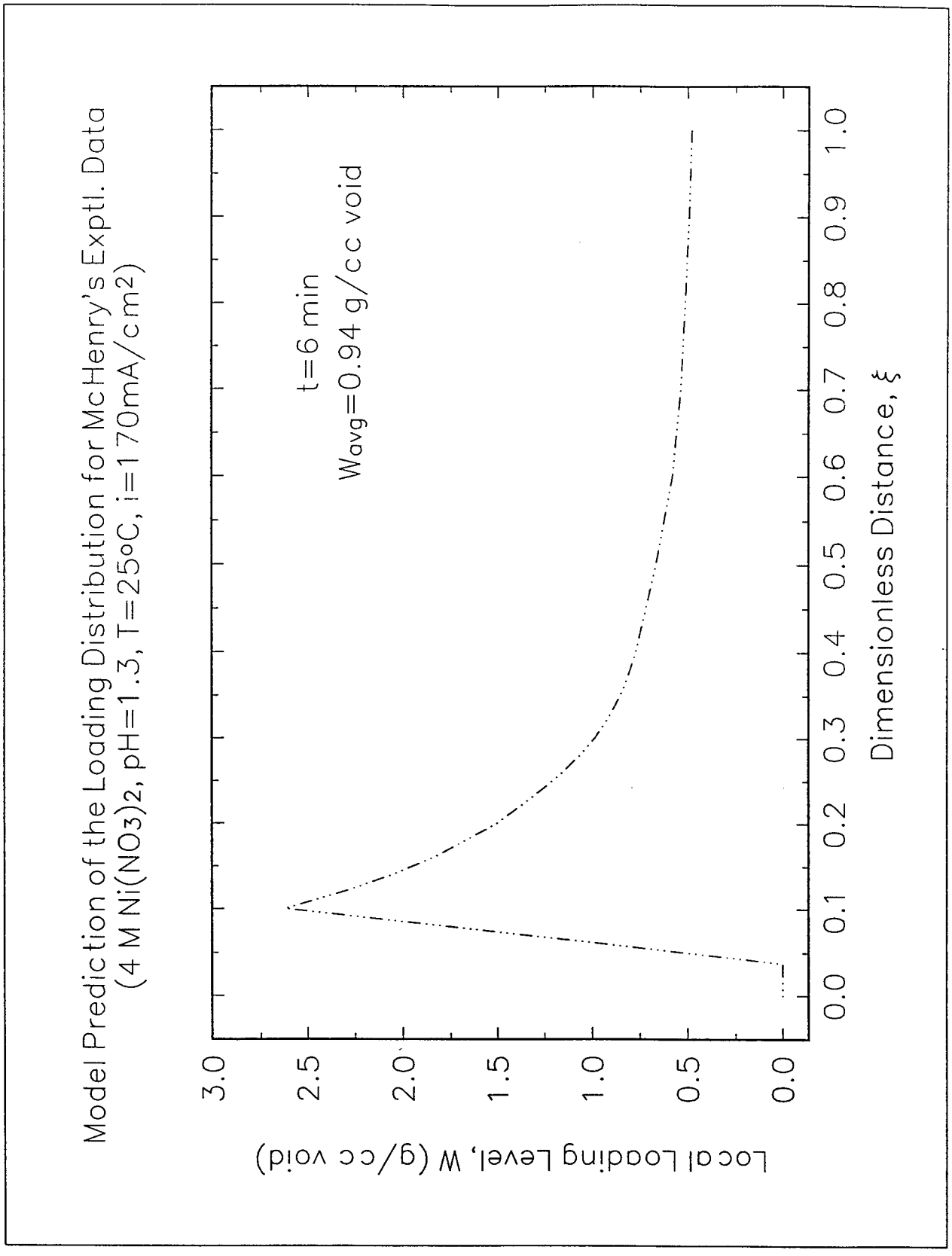
Model Prediction of the Loading Distribution for McHenry's Exptl. Data
(4 M Ni(NO3)2, pH=1.3, T=25°C, i=170mA/cm2)
t=6 min
Wavg=0.94 g/cc void
Local Loading Level, W (g/cc void)
Dimensionless Distance, ξ
0.0
0.5
1.0
1.5
2.0
2.5
3.0
0.0
0.1
0.2
0.3
0.4
0.5
0.6
0.7
0.8
0.9
1.0

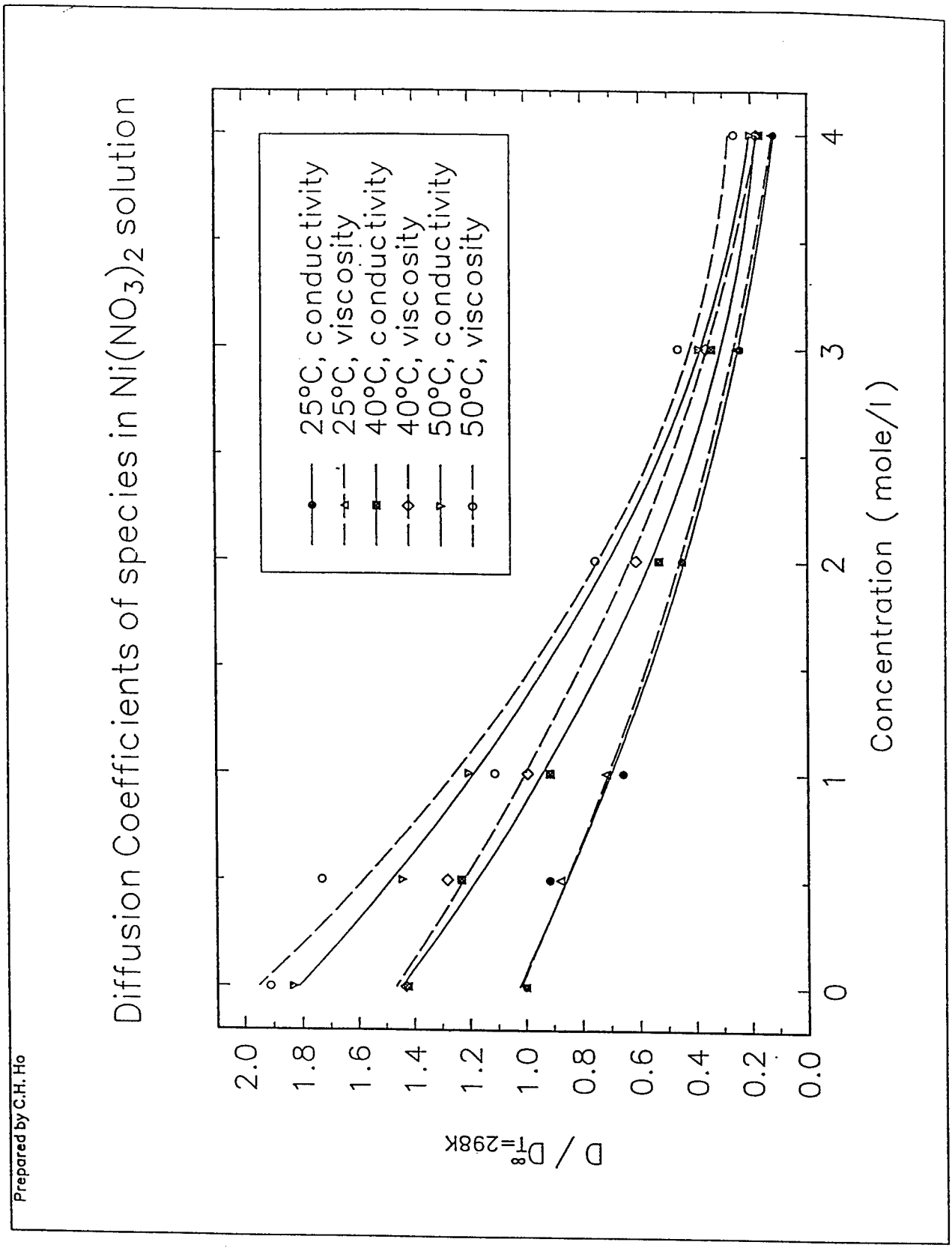
Diffusion Coefficients of species in $Ni(NO_3)_2$ solution
Prepared by C.H. Ho
25°C, conductivity
25°C, viscosity
40°C, conductivity
40°C, viscosity
50°C, conductivity
50°C, viscosity
$D / D^{\circ}_{T=298K}$
Concentration (mole/l)
0.0
0.2
0.4
0.6
0.8
1.0
1.2
1.4
1.6
1.8
2.0
0
1
2
3
4

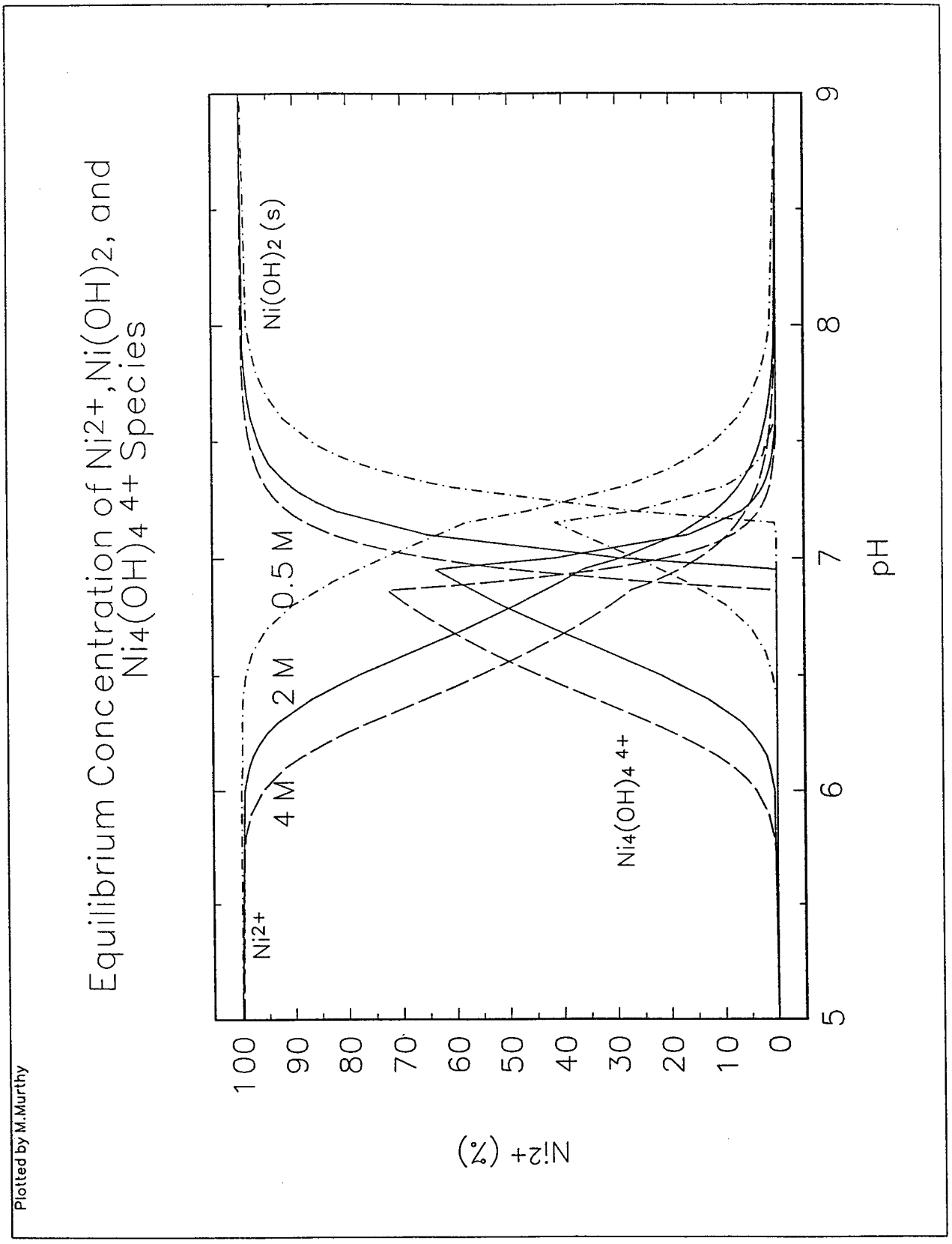
Equilibrium Concentration of Ni2+, Ni(OH)2, and Ni4(OH)4 4+ Species
Plotted by M.Murthy
Ni2+ (%)
pH
Ni2+
4 M
2 M
0.5 M
Ni(OH)2 (s)
Ni4(OH)4 4+
100
90
80
70
60
50
40
30
20
10
0
5
6
7
8
9

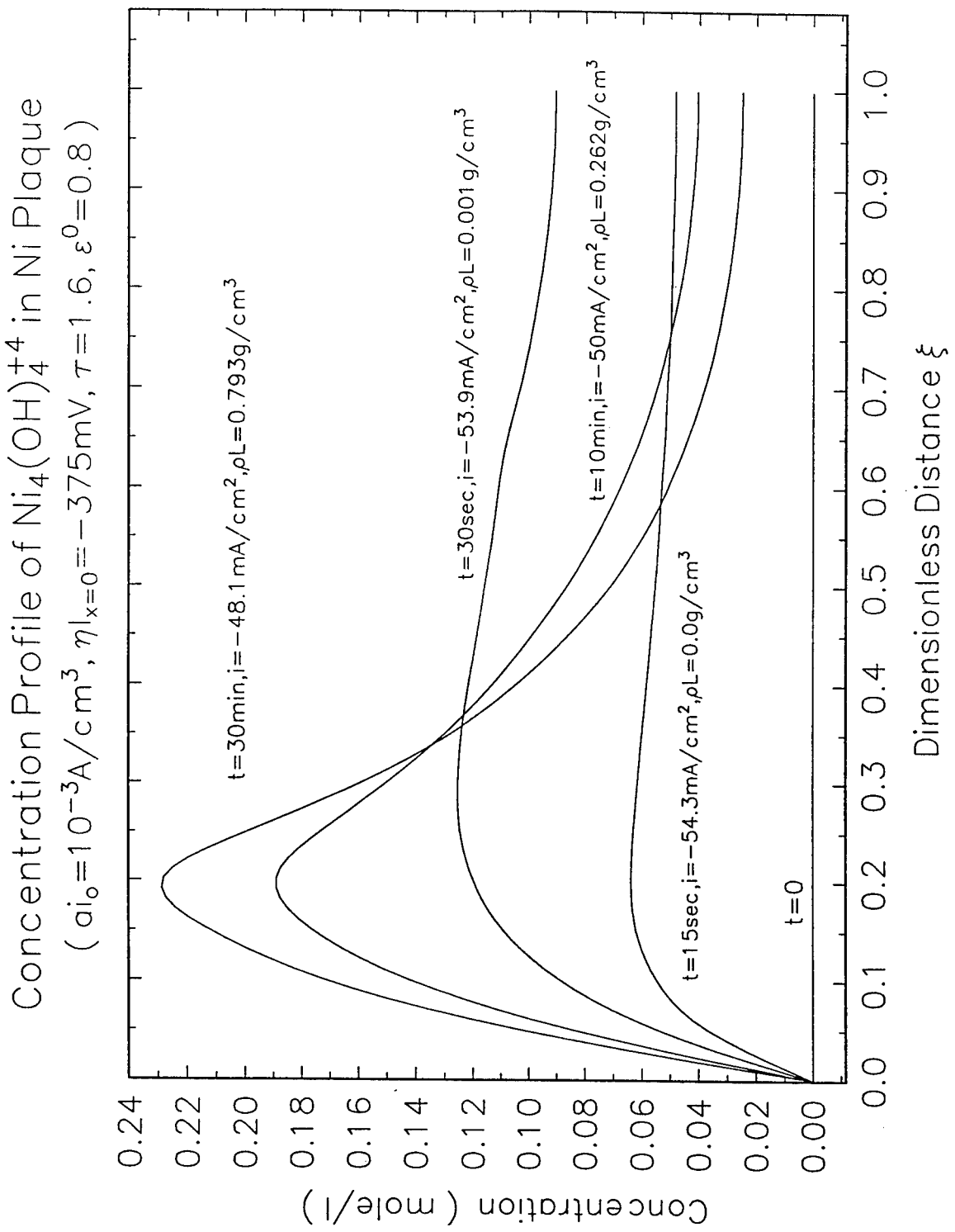
Concentration Profile of $Ni_4(OH)_4^{+4}$ in Ni Plaque
($ai_o=10^{-3}A/cm^3$, $\eta|_{x=0}=-375mV$, $\tau=1.6$, $\varepsilon^0=0.8$)
t=30min,i=−48.1mA/cm²,ρL=0.793g/cm³
t=30sec,i=−53.9mA/cm²,ρL=0.001g/cm³
t=10min,i=−50mA/cm²,ρL=0.262g/cm³
t=15sec,i=−54.3mA/cm²,ρL=0.0g/cm³
t=0
Concentration (mole/l)
0.00
0.02
0.04
0.06
0.08
0.10
0.12
0.14
0.16
0.18
0.20
0.22
0.24
Dimensionless Distance ξ
0.0
0.1
0.2
0.3
0.4
0.5
0.6
0.7
0.8
0.9
1.0

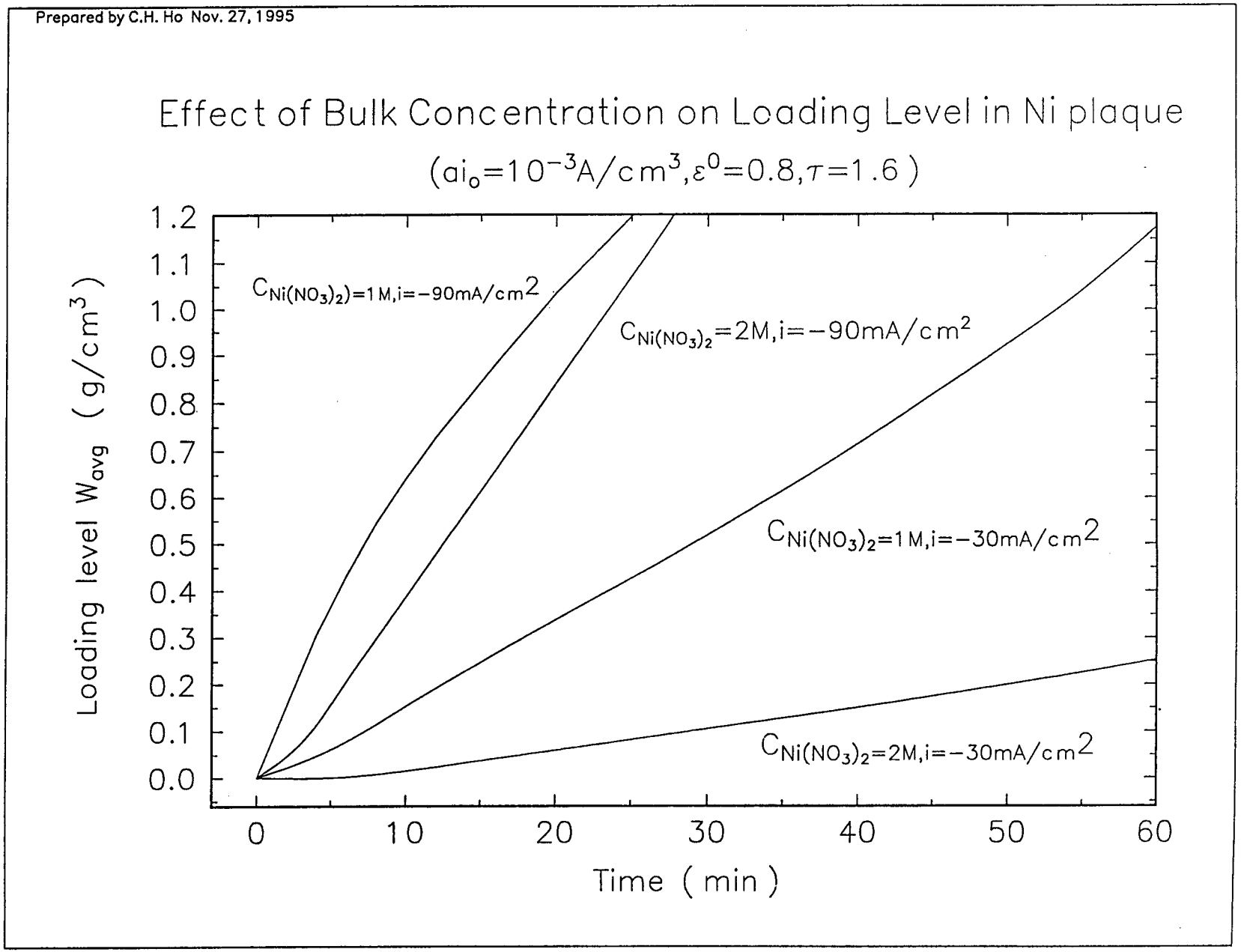
Prepared by C.H. Ho Nov. 27, 1995
Effect of Bulk Concentration on Loading Level in Ni plaque
($ai_o=10^{-3}A/cm^3, \varepsilon^0=0.8, \tau=1.6$)
Loading level W_{avg} (g/cm^3)
Time (min)
$C_{Ni(NO_3)_2}$=1 M, i=−90mA/cm^2
$C_{Ni(NO_3)_2}$=2M, i=−90mA/cm^2
$C_{Ni(NO_3)_2}$=1 M, i=−30mA/cm^2
$C_{Ni(NO_3)_2}$=2M, i=−30mA/cm^2
0.0
0.1
0.2
0.3
0.4
0.5
0.6
0.7
0.8
0.9
1.0
1.1
1.2
0
10
20
30
40
50
60

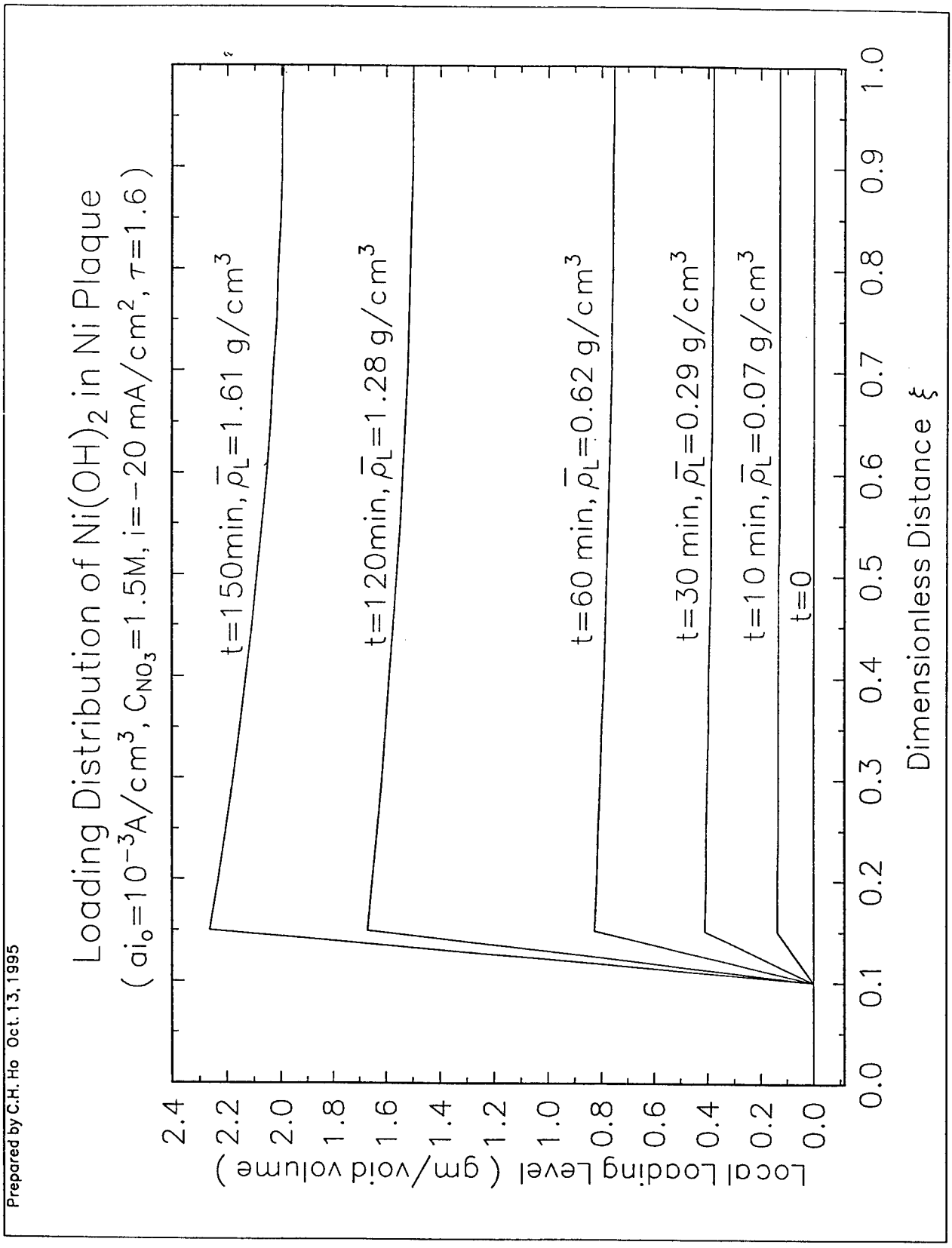
Loading Distribution of $Ni(OH)_2$ in Ni Plaque
($ai_o=10^{-3}A/cm^3$, $C_{NO_3}=1.5M$, $i=-20\ mA/cm^2$, $\tau=1.6$)
Prepared by C.H. Ho Oct. 13, 1995
t=150min, $\bar{\rho}_L=1.61\ g/cm^3$
t=120min, $\bar{\rho}_L=1.28\ g/cm^3$
t=60 min, $\bar{\rho}_L=0.62\ g/cm^3$
t=30 min, $\bar{\rho}_L=0.29\ g/cm^3$
t=10 min, $\bar{\rho}_L=0.07\ g/cm^3$
t=0
Local Loading Level (gm/void volume)
Dimensionless Distance ξ
0.0
0.2
0.4
0.6
0.8
1.0
1.2
1.4
1.6
1.8
2.0
2.2
2.4
0.1
0.3
0.5
0.7
0.9

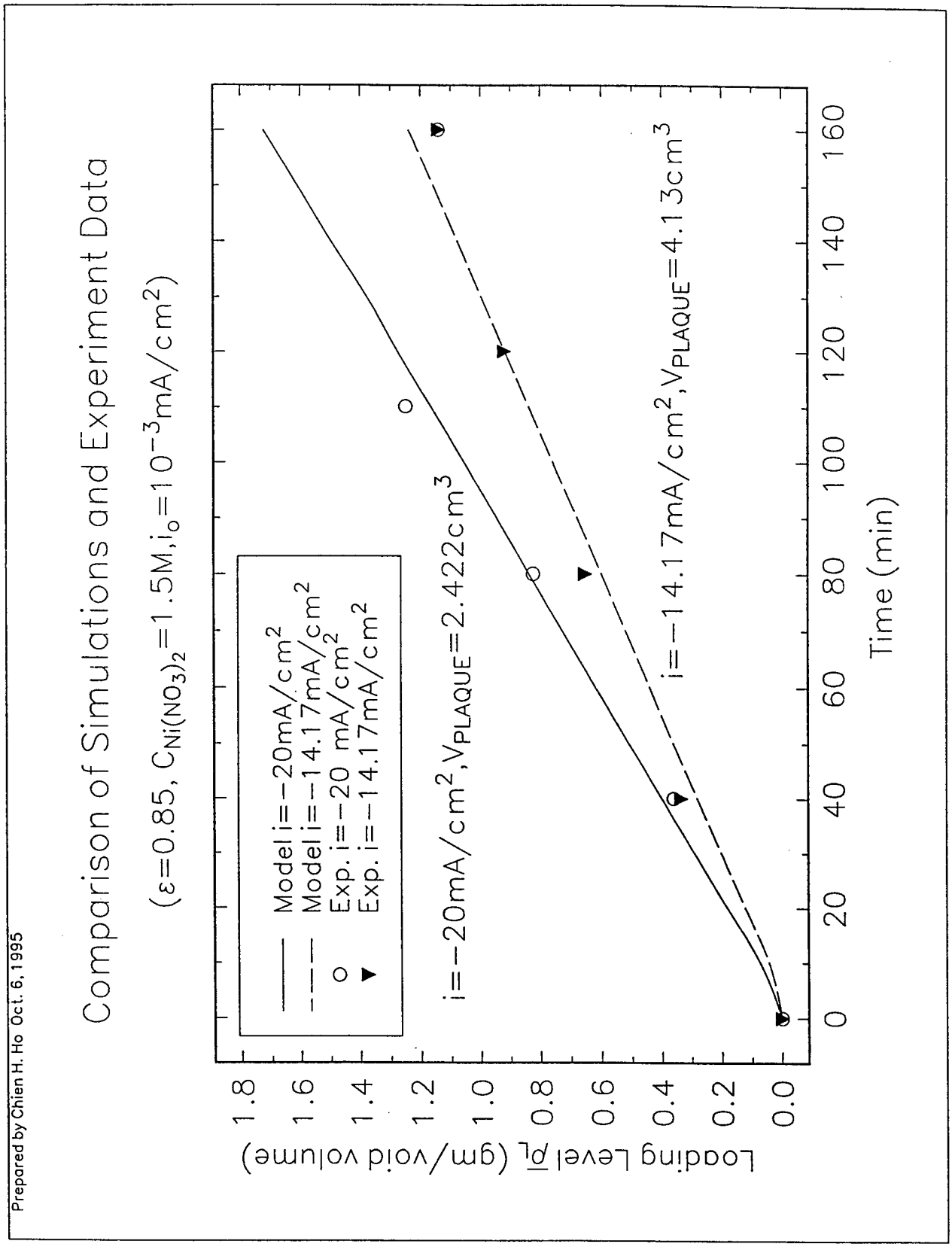
Comparison of Simulations and Experiment Data
(ε=0.85, $C_{Ni(NO_3)_2}$=1.5M, $i_o=10^{-3}$mA/cm^2)
Model i=−20mA/cm^2
Model i=−14.17mA/cm^2
Exp. i=−20 mA/cm^2
Exp. i=−14.17mA/cm^2
i=−20mA/cm^2, V_{PLAQUE}=2.422cm^3
i=−14.17mA/cm^2, V_{PLAQUE}=4.13cm^3
Loading Level $\bar{\rho}_L$ (gm/void volume)
Time (min)
0.0
0.2
0.4
0.6
0.8
1.0
1.2
1.4
1.6
1.8
0
20
40
60
80
100
120
140
160
Prepared by Chien H. Ho Oct. 6, 1995

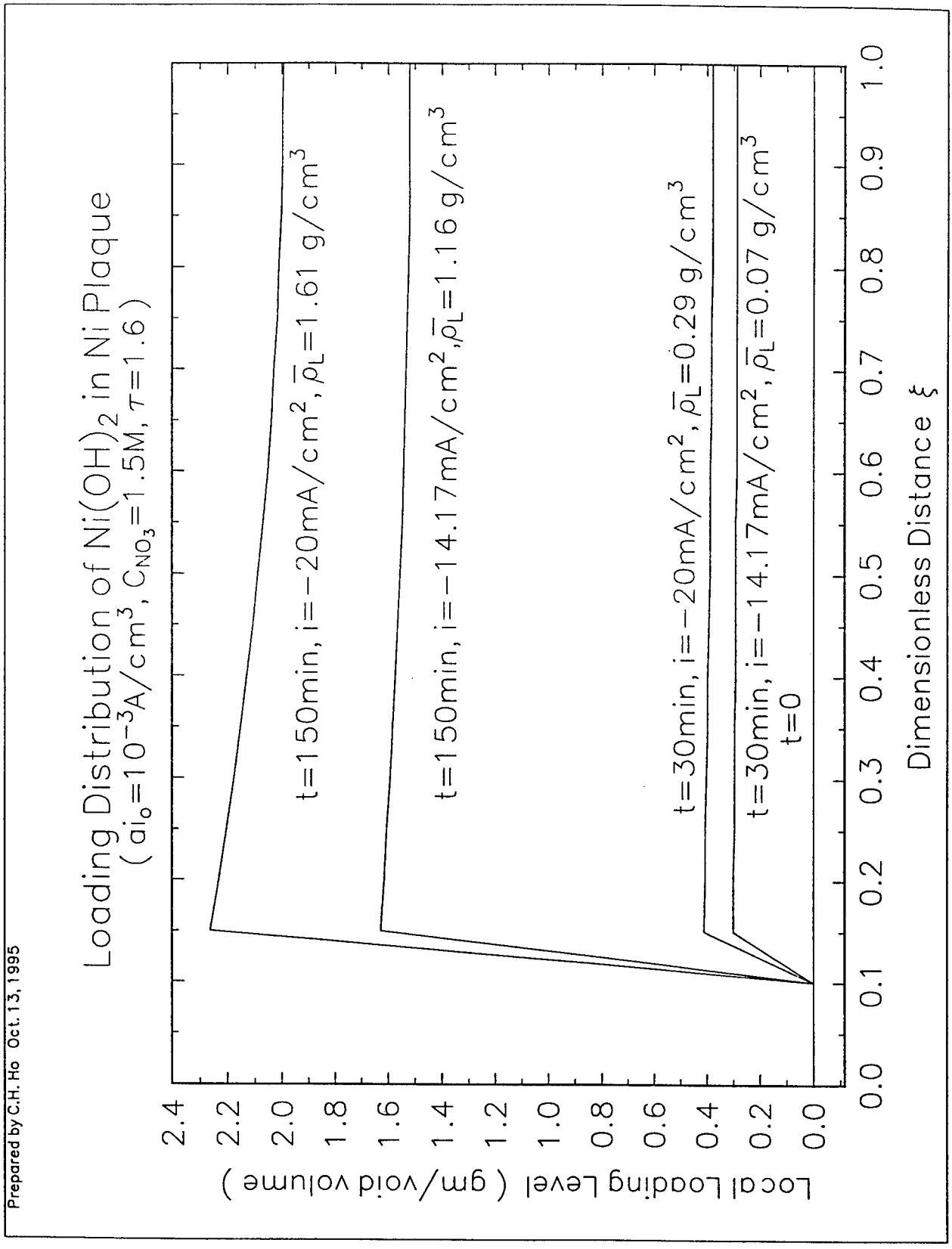
Loading Distribution of $Ni(OH)_2$ in Ni Plaque
($ai_o=10^{-3}A/cm^3$, $C_{NO_3}=1.5M$, $\tau=1.6$)
Prepared by C.H. Ho Oct. 13, 1995
t=150min, i=−20mA/cm², $\bar{\rho}_L$=1.61 g/cm³
t=150min, i=−14.17mA/cm², $\bar{\rho}_L$=1.16 g/cm³
t=30min, i=−20mA/cm², $\bar{\rho}_L$=0.29 g/cm³
t=30min, i=−14.17mA/cm², $\bar{\rho}_L$=0.07 g/cm³
t=0
Local Loading Level (gm/void volume)
Dimensionless Distance ξ
0.0
0.2
0.4
0.6
0.8
1.0
1.2
1.4
1.6
1.8
2.0
2.2
2.4
0.1
0.3
0.5
0.7
0.9

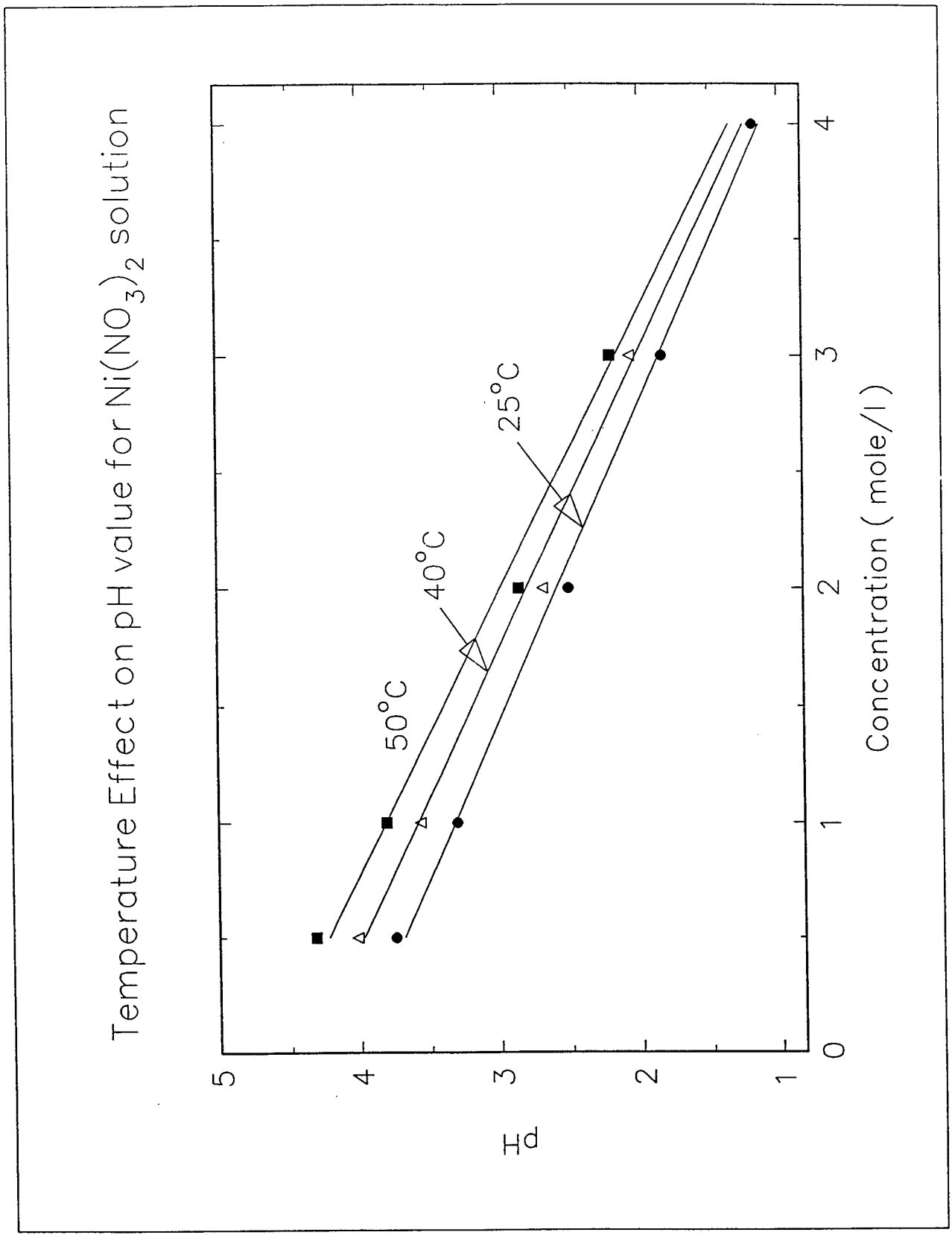
Temperature Effect on pH value for $Ni(NO_3)_2$ solution
pH
Concentration (mole/l)
50°C
40°C
25°C
5
4
3
2
1
0
1
2
3
4

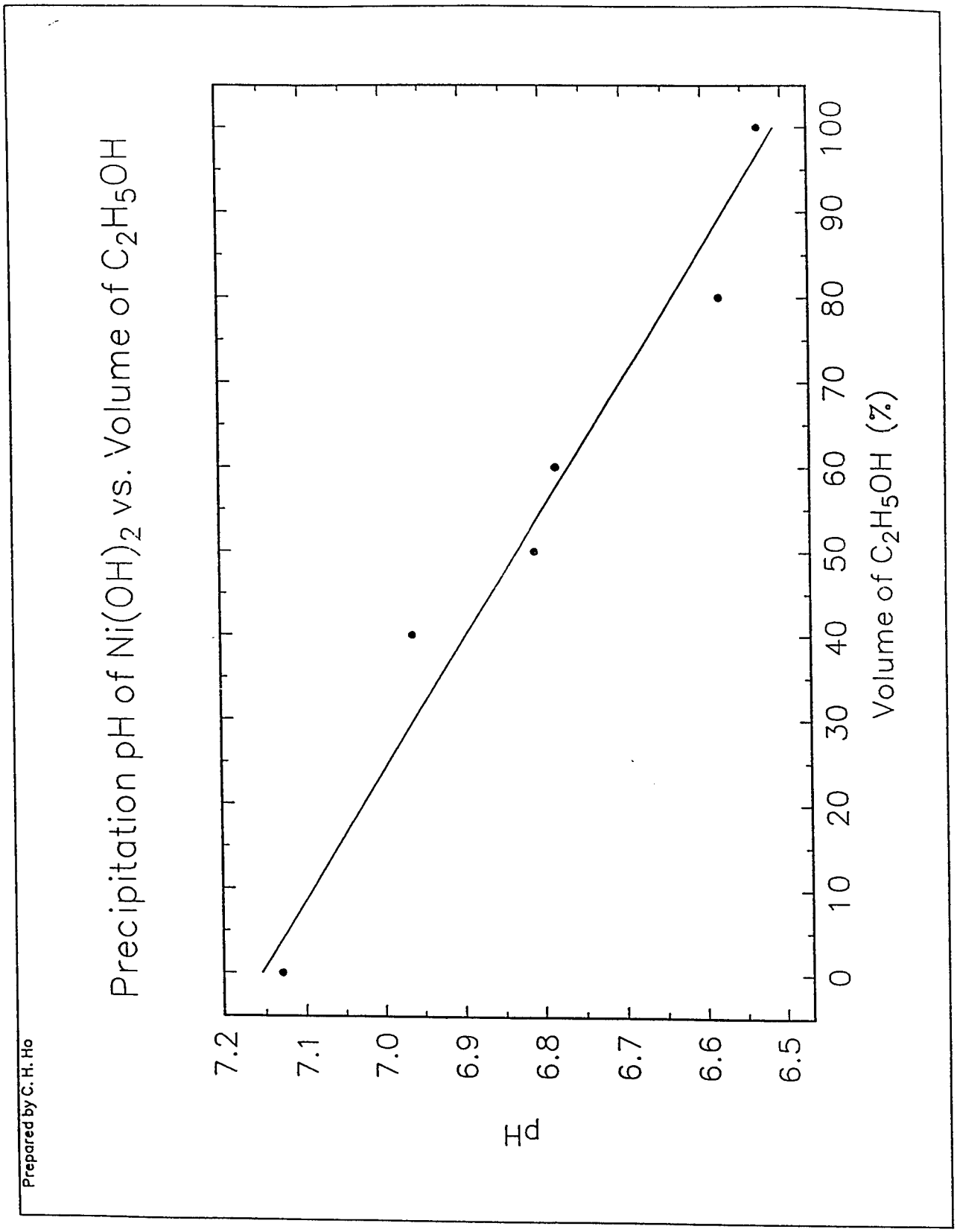
Precipitation pH of $Ni(OH)_2$ vs. Volume of C_2H_5OH
Prepared by C. H. Ho
pH
7.2
7.1
7.0
6.9
6.8
6.7
6.6
6.5
0
10
20
30
40
50
60
70
80
90
100
Volume of C_2H_5OH (%)

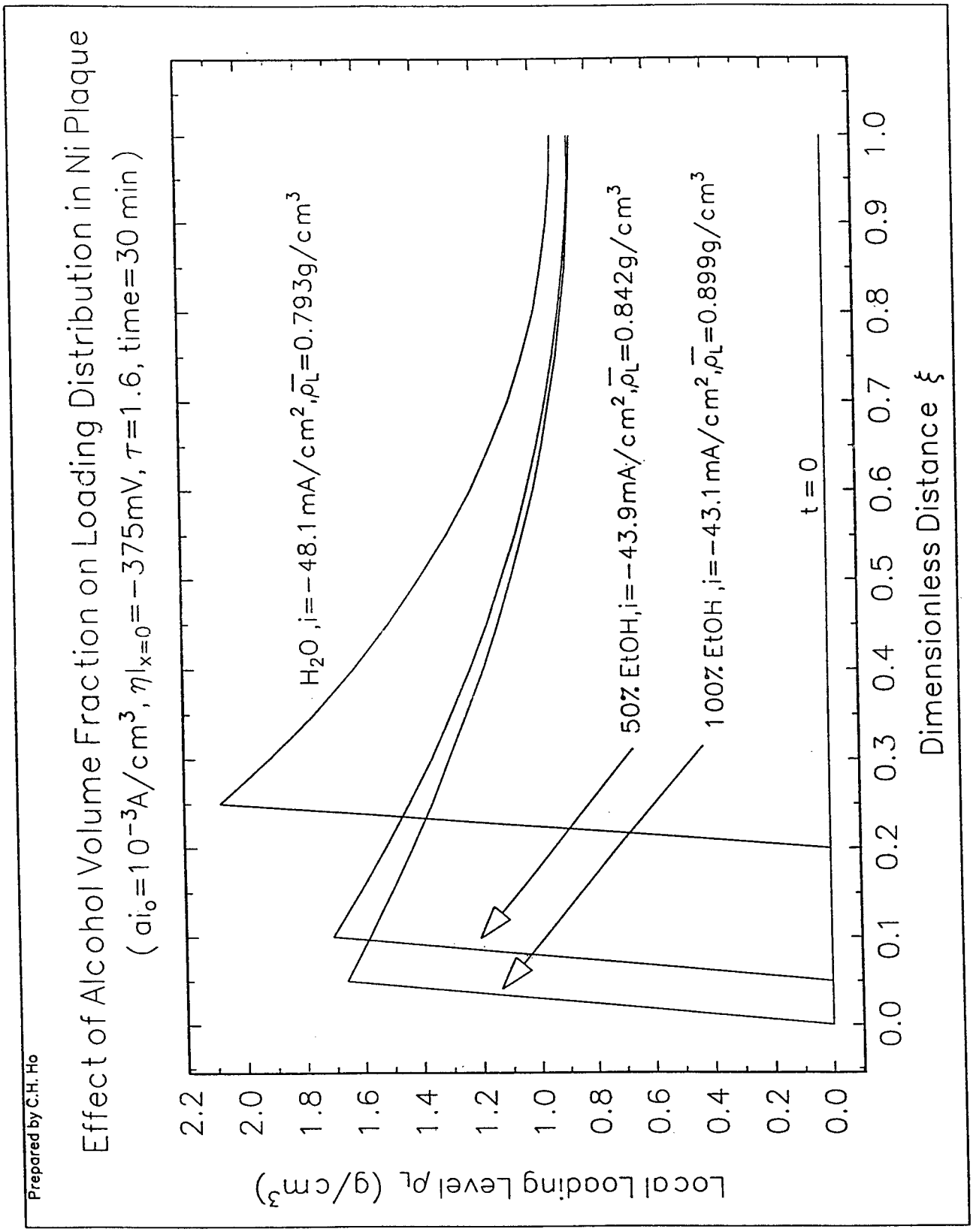
Effect of Alcohol Volume Fraction on Loading Distribution in Ni Plaque
($ai_o=10^{-3}A/cm^3$, $\eta|_{x=0}=-375mV$, $\tau=1.6$, time=30 min)
Prepared by C.H. Ho
H_2O ,i=−48.1 mA/cm², $\bar{\rho_L}$=0.793g/cm³
50% EtOH,i=−43.9mA/cm², $\bar{\rho_L}$=0.842g/cm³
100% EtOH ,i=−43.1 mA/cm², $\bar{\rho_L}$=0.899g/cm³
t = 0
Local Loading Level ρ_L (g/cm³)
Dimensionless Distance ξ
0.0
0.2
0.4
0.6
0.8
1.0
1.2
1.4
1.6
1.8
2.0
2.2
0.1
0.3
0.5
0.7
0.9

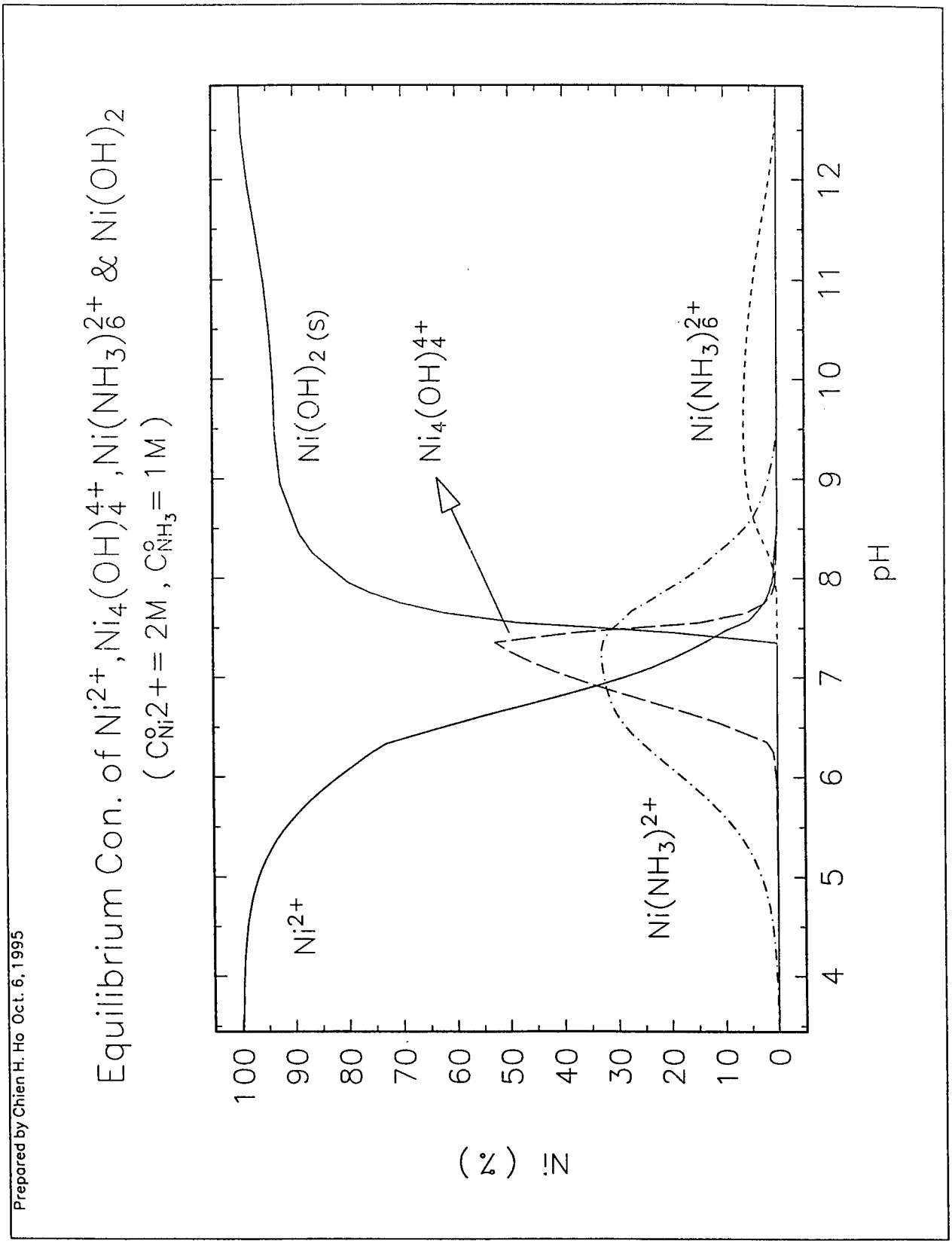
Equilibrium Con. of Ni^{2+}, $Ni_4(OH)_4^{4+}$, $Ni(NH_3)_6^{2+}$ & $Ni(OH)_2$
($C^o_{Ni}2+ = 2M$, $C^o_{NH_3} = 1M$)
Prepared by Chien H. Ho Oct. 6, 1995
Ni^{2+}
$Ni(OH)_2$ (s)
$Ni_4(OH)_4^{4+}$
$Ni(NH_3)^{2+}$
$Ni(NH_3)_6^{2+}$
Ni (%)
pH
100
90
80
70
60
50
40
30
20
10
0
4
5
6
7
8
9
10
11
12

Effect of Ammonia on Nickel Hydroxide Film Deposition

1 M $Ni(NO_3)_2$ Solutions

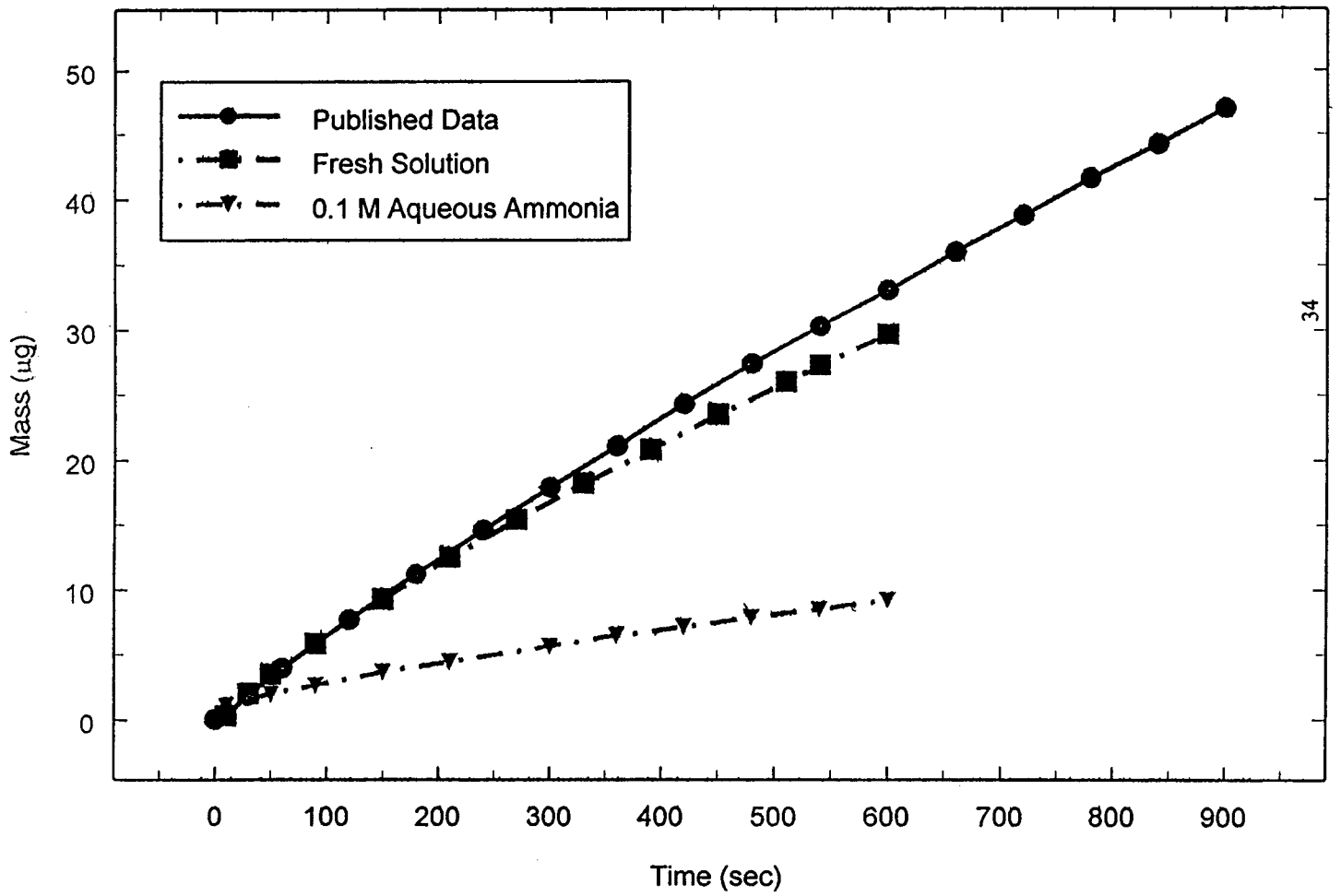

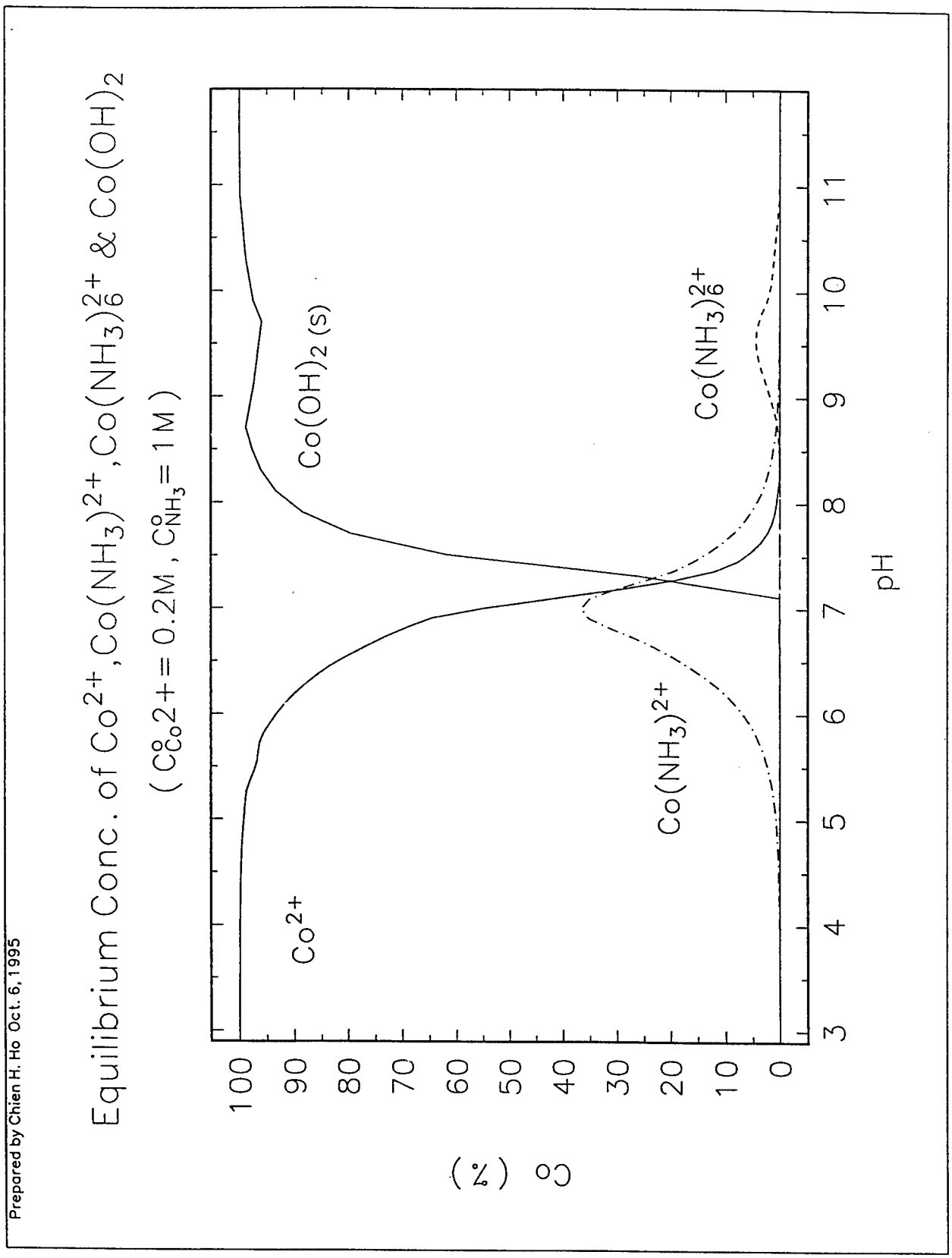
Equilibrium Conc. of Co^{2+}, $Co(NH_3)^{2+}$, $Co(NH_3)_6^{2+}$ & $Co(OH)_2$
($C^o_{Co}2+ = 0.2M$, $C^o_{NH_3} = 1M$)
Prepared by Chien H. Ho Oct. 6, 1995
Co^{2+}
$Co(NH_3)^{2+}$
$Co(OH)_2$ (s)
$Co(NH_3)_6^{2+}$
Co (%)
pH
100
90
80
70
60
50
40
30
20
10
0
3
4
5
6
7
8
9
10
11

Short Term Goals (6 months)

- Include Ammonia-Nickel Complexes and Decomposition Kinetics
- Simulate Chemical Changes to Bath for Multiple Impregnations
- Predict Distribution of Codeposition Hydroxide Products
- Predict Distribution of Codeposited Anions

J.W. Van Zee, University of South Carolina
Presented at the NASA Battery Workshop

Nov. 29, 1995

Near Term Goals (1 year)

- Verify Model with Production Data
  - Requires USC-Industry Interaction
- Develop User Friendly Interface
- Improve Assumptions Not Accepted by Industrial Community
- Export Beta-Version of Model to Industrial Sites
  - USC Personnel Train Production Engineers
- Identify Next Generation of Production Anomalies to be Included

J.W. Van Zee, University of South Carolina
Presented at the NASA Battery Workshop

Nov. 29, 1995

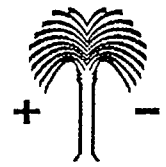

USC's Vision for Paradigm Shift

- Develop a Process for Model Development Consisting of
  - Feedback from Industry
  - Experimental Designs
  - Model Refinement
- Develop *a-priori* Predictive Capabilities
- Develop Mechanistic Understanding

J.W. Van Zee, University of South Carolina
Presented at the NASA Battery Workshop

Nov. 29, 1995

Nickel Hydrogen and Silver Zinc Battery Cell Modeling at The Aerospace Corporation

Albert H. Zimmerman
Electronics Technology Center
The Aerospace Corporation
El Segundo, California 90245

Abstract

A nickel hydrogen battery cell model has been fully developed and implemented at The Aerospace Corporation. Applications of this model to industry needs for the design of better cells, power system design and charge control, thermal management, and long-term performance trends will be described. Present efforts will be described that are introducing the silver and zinc electrode reactions into this model architecture, so that the model will be able to predict performance for not only silver zinc cells, but also nickel zinc, silver hydrogen, and silver cadmium cells. The silver zinc cell modeling effort is specifically designed to address the concerns that arise most often in launch vehicle applications: transient response, power-on voltage regulation, hot or cold operation, electrolyte spewing, gas venting, self-discharge, separator oxidation, and oxalate crystal growth. The specific model features that are being employed to address these issues will be described.

Nickel Hydrogen Cell Model

The most widely used rechargeable battery cell in modern spacecraft power systems is the nickel hydrogen battery cell. In spite of its excellent cycle life capability, nickel hydrogen battery cell designs are continually being changed to meet specific needs of programs. For example, small changes in cell capacity needs are accommodated by stacking more plates, higher current needs by reducing cell resistance, longer cycle life needs by lowering electrolyte concentration, improved thermal management needs by using recombination wall wicks, etc. To evaluate the effects of these seemingly small changes on cell performance, both short-term and long-term, good battery cell performance models are required. During the past three years, at The Aerospace Corporation we have developed a general modeling architecture that is suitable for modeling all chemical and physical processes in a battery cell, utilizing the actual three-dimensional porous or solid structures of the real cell components. We have programmed into this simulation architecture, all the processes that are known to influence the behavior of the nickel hydrogen battery cell. This detailed model for the nickel hydrogen battery cell has been described previously in detail,[1-3] and therefore will not be re-iterated here. The conclusion from this effort has been that, as the processes and component structures included in the model converged an accurate description of the nickel hydrogen cell, the cell performance predicted by the model also converged to that of the real nickel hydrogen cell. For

example, Fig. 1 shows I/V curves predicted by the model in comparison to repeated measurements for 50Ah battery cells at 10 deg C. The results in Fig. 1 show first that it is quite difficult to distinguish model predictions from real data for this model, and second that the variability in repeated performance measurements is greater than the deviation from the model predictions. This comparison provides only one of the many levels of validation that have been applied to this model.

A second type of model validation that has been applied to our nickel hydrogen model, tests its ability to predict long term performance capability. The long term performance of nickel hydrogen cells is often limited by the swelling of the nickel electrode and the changes in structure or electrolyte distribution that accompany the swelling. This can be easily modeled simply by evaluating the effect of different structural changes on cell performance. For example, Fig. 2 indicates the usable power available from a standard MANTECH design nickel hydrogen cell as a function of the amount of the free volume filled with electrolyte. Clearly this design is quite robust, with nearly a 40% increase in stack volume due to swelling being tolerated before usable power drops precipitously. This is consistent with life test data for this design, which typically show core breakage or short circuit failure modes before that due to electrolyte redistribution. However, with other cell designs, margins for electrolyte re-distribution can be much less. Fig. 3 indicates electrolyte margins for three common generic cell designs, as predicted by out cell model. The margins in Fig. 3 agree with the general trends seen in life test data, for which standard asbestos separator cells cannot tolerate much positive swelling (i.e. high DOD cycling) without developing a high resistance. With a single layer of zircar separator, while margins are increased, electrolyte re-distribution is still a potential failure mode that is not expected in cells with two layers of zircar separator.

This nickel hydrogen cell model has, for the past year, been applied to all the major issues that our customers and their suppliers have been concerned about. For nickel hydrogen batteries the most common concerns have been related to understanding the temperature profiles and state of charge of charged batteries that are awaiting launch, or during spacecraft integration and test. Figure 4 indicates a typical prediction of battery temperature following termination of trickle charge, then termination of cooling 2 hr later. The temperature climbs as self-discharge occurs, until active system cooling is activated at about 90 deg F. Where comparisons with test data are available, the model predictions of battery state of charge are within about 1% of that indicated by either pressure or subsequent discharge.

Another common use of our nickel hydrogen cell model is the generation of performance data for a specific cell design before that cell is produced and available for a complete characterization test, which incidentally requires 4-5 months of testing if all goes well. The I/V curves in Fig.1 provide a glimpse into the type of data that is readily obtained. The performance data generated in 1-2 weeks of model simulations can be used to accurately choose charge control parameters, thermal control design, and other aspects of power system design, as well as for planning mission operations. The cost and schedule benefits associated with not having to envelope all conditions that the batteries may see with test data, particularly early in the development process, can be enormous. Our nickel hydrogen battery model has been used to explore component and cell technology improvements. For example, the overall effects of different lightweight nickel electrode designs on cell performance have been evaluated before any cells with these advanced components were built. In other cases new cell designs were modeled before any cells were built, in several cases discovering cell design issues that are very likely to have contributed to early failure if the cells had been built and tested as originally planned.

Finally, our nickel hydrogen cell model has been applied to generating a fully computer

designed nickel hydrogen cell. The goal in this optimization process was to stay within the range of components typically used in existing nickel hydrogen cells, but to allow the computer model to arrange them in the best possible way. The design that emerged is a cell with about 65 Ah of predicted capacity, but with the same usable energy above 1.2 volts (C/2 discharge rate) as a 100 Ah cell. The cell is predicted to have 40% lower internal impedance that a typical MANTECH nickel hydrogen cell, and should exhibit approximately 50% of the degradation rate during cycling at a common depth-of-discharge. A number of the design changes in this new cell had not been previously considered, and were found by the computer to be desirable due to interactions between changes in other components configurations. Test cells are now being assembled by a prominent cell manufacturer, so that the performance features expected of this design can be evaluated by test. It is clear even now, in this situation, that a good modeling capability has shortened the development process by at least one iteration of design and test.

The battery simulation software that contains the latest version of this nickel hydrogen battery model is called Battery Cell Model (BCM) 2.11a. While not now available for general release, a 2-disk demonstration version of the software is available, and shows the capabilities of the simulation software, as well as providing detailed documentation of how the cell is modeled. The software can be installed to run on any 486 or 586 based PC, although it runs much more efficiently on a 100MHz or better 586. Any specific nickel hydrogen battery or cell simulations can presently be done at Aerospace to support our customers.

Silver Zinc Cell Model

In today's spacecraft power systems, the batteries that generate the most performance and reliability issues, after nickel hydrogen, are the silver zinc batteries commonly used in launch vehicles and in many other support applications. The typical issues related to silver zinc batteries have to do with transient response, power-on voltage regulation, hot or cold operation, electrolyte spewing, gas venting, self-discharge, separator oxidation, and shorting from oxalate crystal growth. Evaluation of the kinds of processes included in our nickel hydrogen cell model, suggested that the same modeling approach could accurately address many of these critical issues for silver zinc battery cells. Our approach is to use the same generic model architecture, which is a finite element, finite difference approximation technique. We will preserve the capability to model the actual three-dimensional structures of both the silver and zinc electrodes, since these structures have been found to be essential for accurately modeling the high current behavior, transient response, and voltage regulation characteristics of the cell.

This model is now being developed as an extension of the earlier nickel hydrogen based software (initially being referred to as BCM 3.00), with the addition of appropriate chemical and electrochemical processes for the silver and zinc electrodes. This will allow these electrodes to be combined with the existing nickel, hydrogen, or cadmium electrode models to model nickel zinc, silver cadmium, or silver hydrogen cells. This upgrade will require a new approach to modeling porous electrodes. In both the silver and zinc electrodes, the porous structure of the electrode is actually formed by the active material on a wire grid structure. Thus, these electrodes must be modeled to allow the porous structure to be electrochemically converted during charge and discharge. This situation is clearly different from the nickel and cadmium electrodes, where to first order, the sinter provides a fixed substrate that does not rapidly change during charge/discharge operation.

Fortunately, the generic modeling architecture places no constraints on how the current or chemicals are distributed either within individual finite elements, or across collections of them. Thus the appropriate silver and zinc electrode modules may be readily inserted into the existing software structure.

Additional changes must be made in the mass transport modules. Convective mass transport will look much like that in a nickel hydrogen cell (pressures are lower), except that the operation of a vent valve will be included through the use of a vent valve element. This element will use a module that mimics the behavior of a cell vent valve. Clearly, this operation, when dynamically combined with the convective transfer during cell venting, can simulate electrolyte spewing from the cell vent. Diffusive mass transport must include the movement of argentate, zincate, and oxalate species, as well as the highly concentrated hydroxide ions which dominate diffusive transport. The transport of ions through a semi-permeable separator membrane will also be included through the use of an appropriate separator element. All processes must include appropriate temperature coefficients to allow operation up to temperatures of 250 deg F, an end of discharge temperature that can easily be reached in a large high-rate silver zinc cell.

The development process for this silver zinc cell model is expected to be 1-2 years. This development procedure is being used to some extent as a benchmark to evaluate how the general battery modeling capabilities can be best expanded to include other types of batteries. Systems of particular interest for such extensions are not only the advanced lithium primary and secondary battery types, but also commercially important batteries such as lead-acid and alkaline manganese oxide-zinc cells. Clearly this approach to modeling battery cells can be extended to these other systems if sufficient need for accurate battery cell modeling can be identified.

References

1. A. Zimmerman, *Proc. of the 29th IECEC*, American Inst. of Aeronautics and Astronautics, ISBN 1-56347-091-9, Vol. 4, 1994, p. 63.
2. A. Zimmerman and M. Quinzio, *Proc. of the 1994 NASA Aerospace Battery Workshop*, NASA Conf. Pub. 3292, 1994, p. 177.
3. A. Zimmerman and M. Quinzio, *Proc. of the Fourth European Space Power Conf.*, ESA SP-369, Vol. 2, 1995, p. 443.

Acknowledgement

The Aerospace Corporation supported this work under the Aerospace Supported Research (ASR) Program. This support is gratefully acknowledged.

FIGURE 1. I/V Curves at 10°C for Model NiH_2 Cell

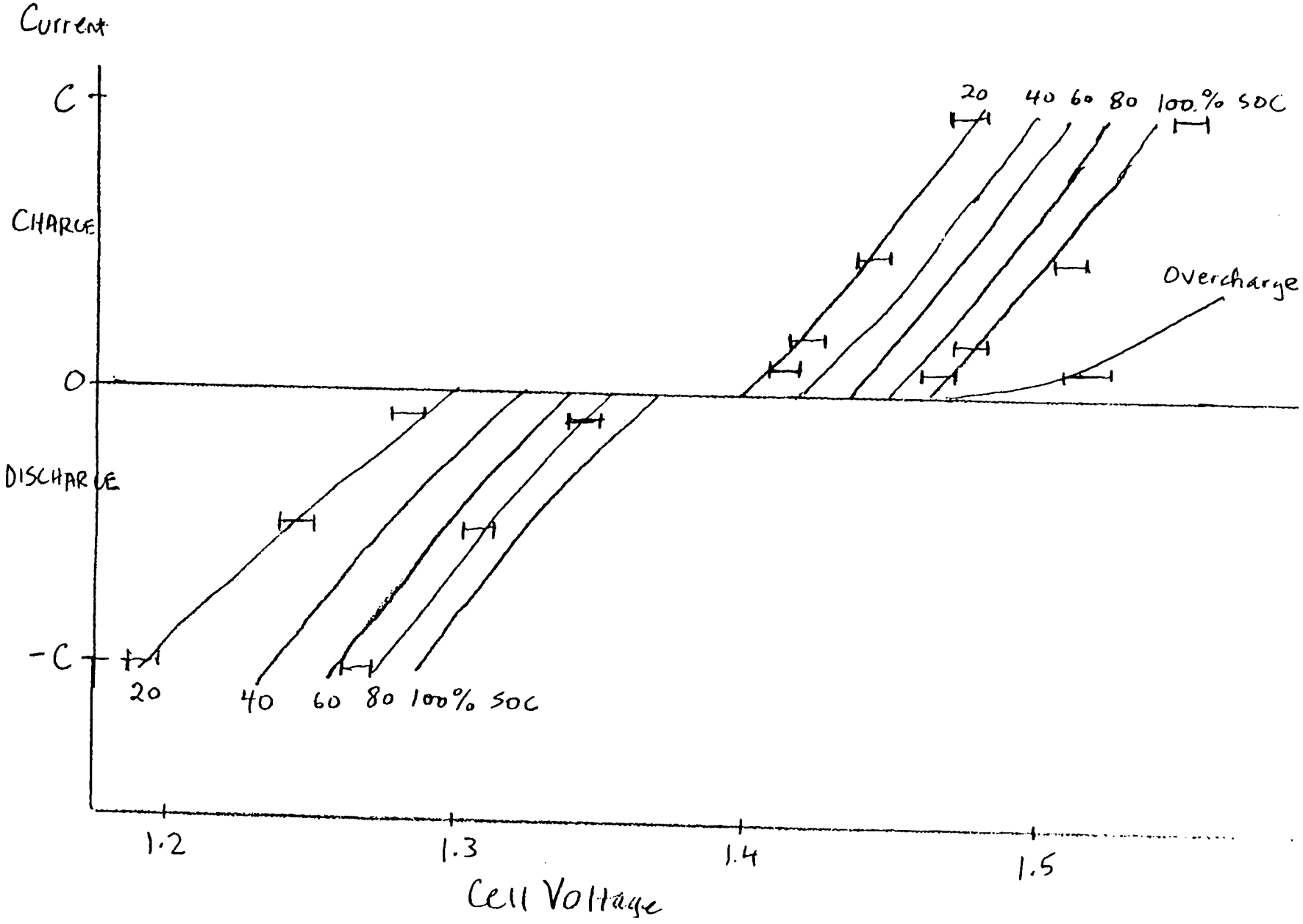

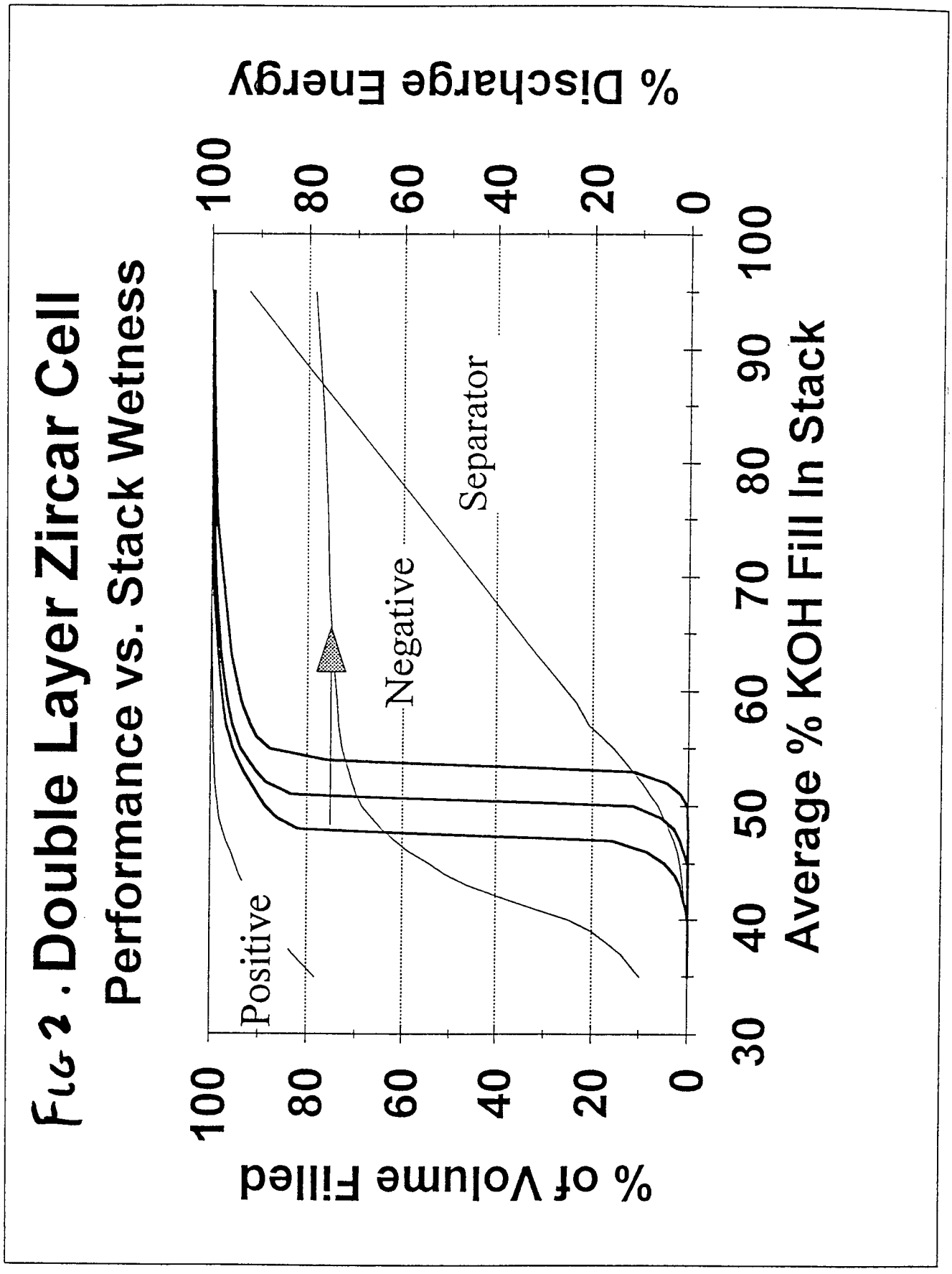
Fig 2. Double Layer Zircar Cell
Performance vs. Stack Wetness
% Discharge Energy
100
80
60
40
20
0
% of Volume Filled
100
80
60
40
20
0
Positive
Negative
Separator
30
40
50
60
70
80
90
100
Average % KOH Fill In Stack

FIG. 3

NiH_2 Cell Model Can Predict Operational Margins for Different Cell Designs

- Model indicates large differences in electrolyte margin for different cell designs

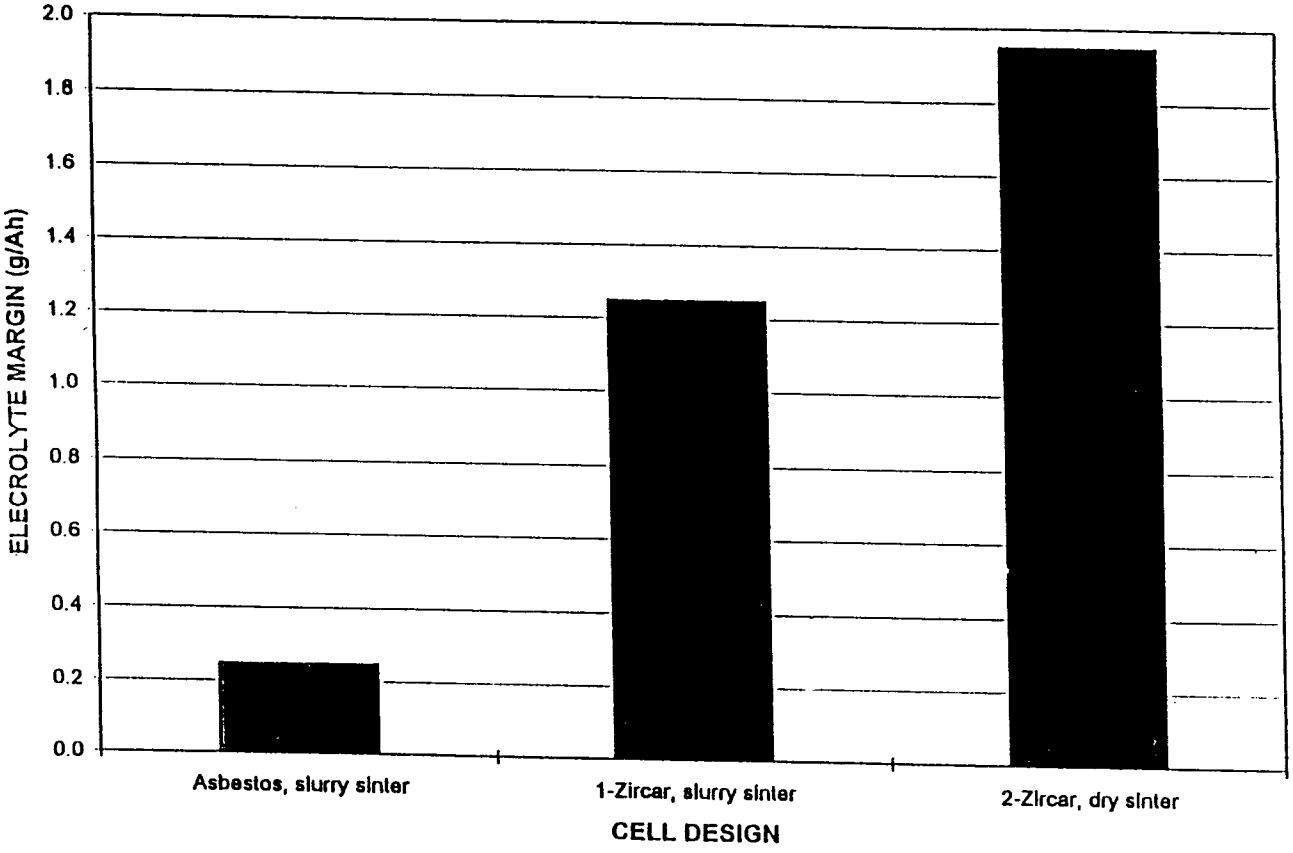

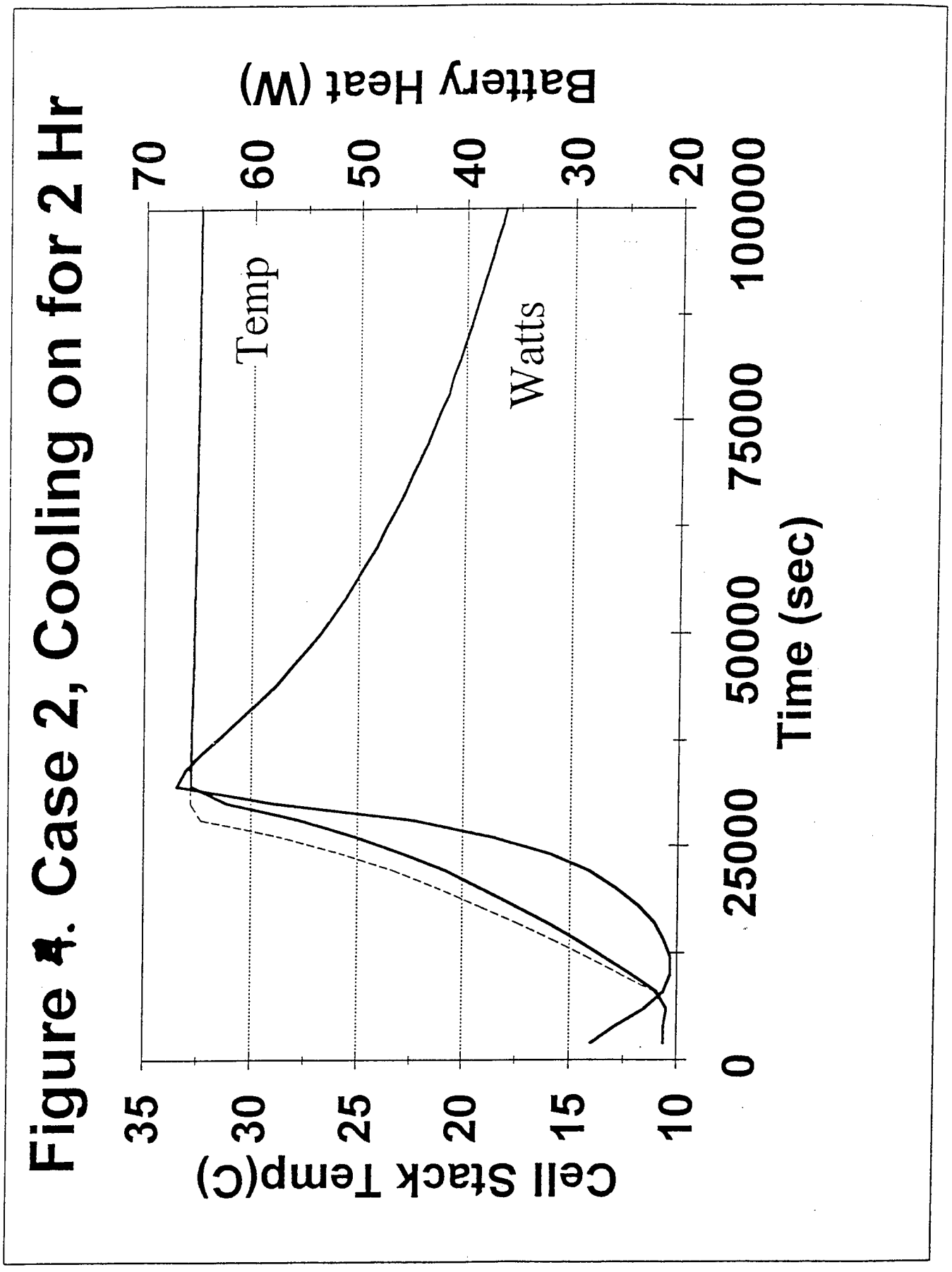
Figure 4. Case 2, Cooling on for 2 Hr
Cell Stack Temp(C)
35
30
25
20
15
10
Battery Heat (W)
70
60
50
40
30
20
Temp
Watts
0
25000
50000
75000
100000
Time (sec)

Mathematical Modeling of a Nickel/Hydrogen Cell

Pauline De Vidts, Javier Delgado

&

Ralph E. White

Center for Electrochemical Engineering

Department of Chemical Engineering

University of South Carolina

November 1995

Objective

Develop a mathematical model based on fundamental principles to simulate the dynamic behavior of a nickel/hydrogen cell.

Outline

- Description of the model
- Solution of the model and description of the software
- Simulations and case studies
- Summary
- Current and future work

A Nickel/Hydrogen Battery

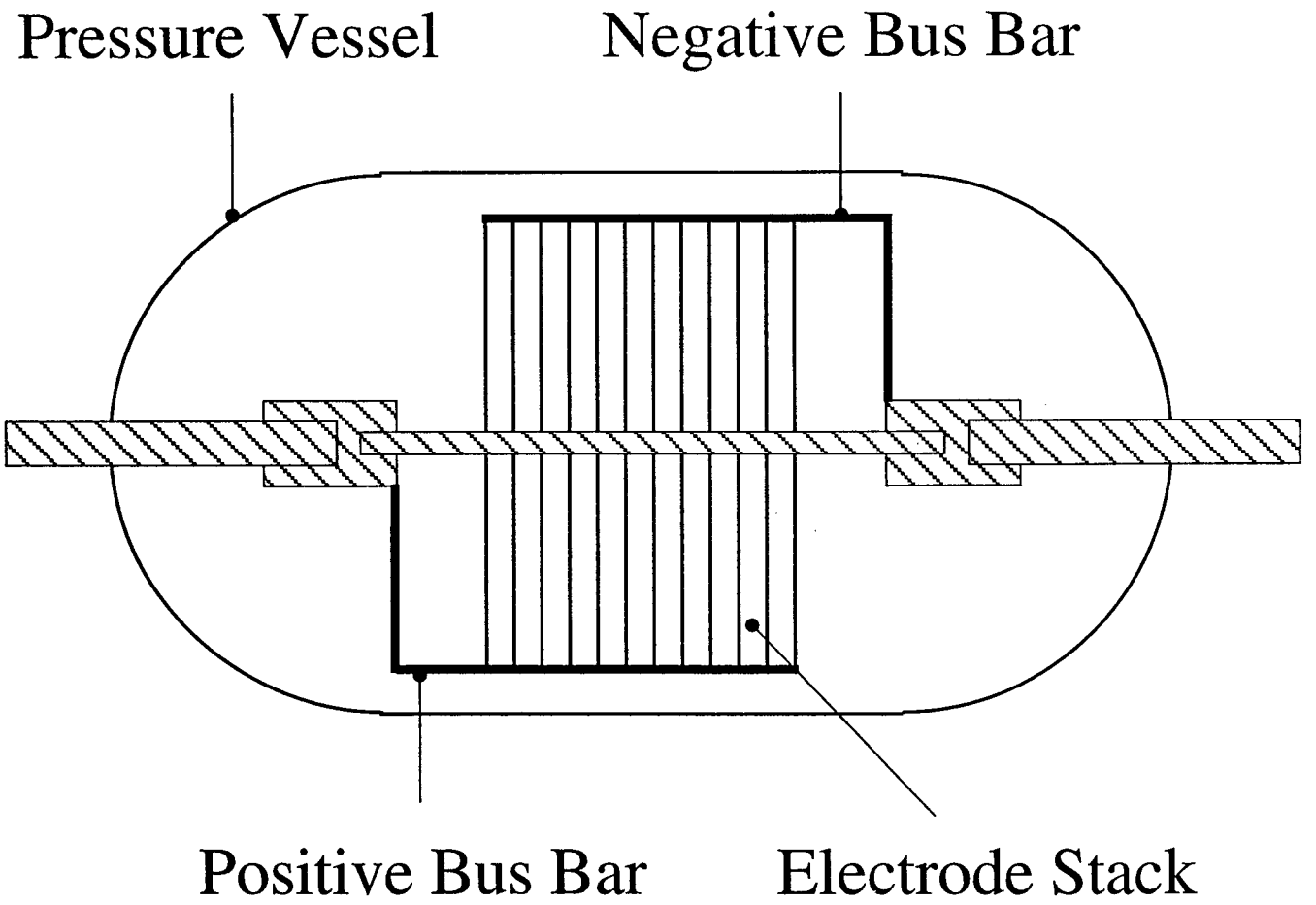

A Nickel/Hydrogen Unit Cell

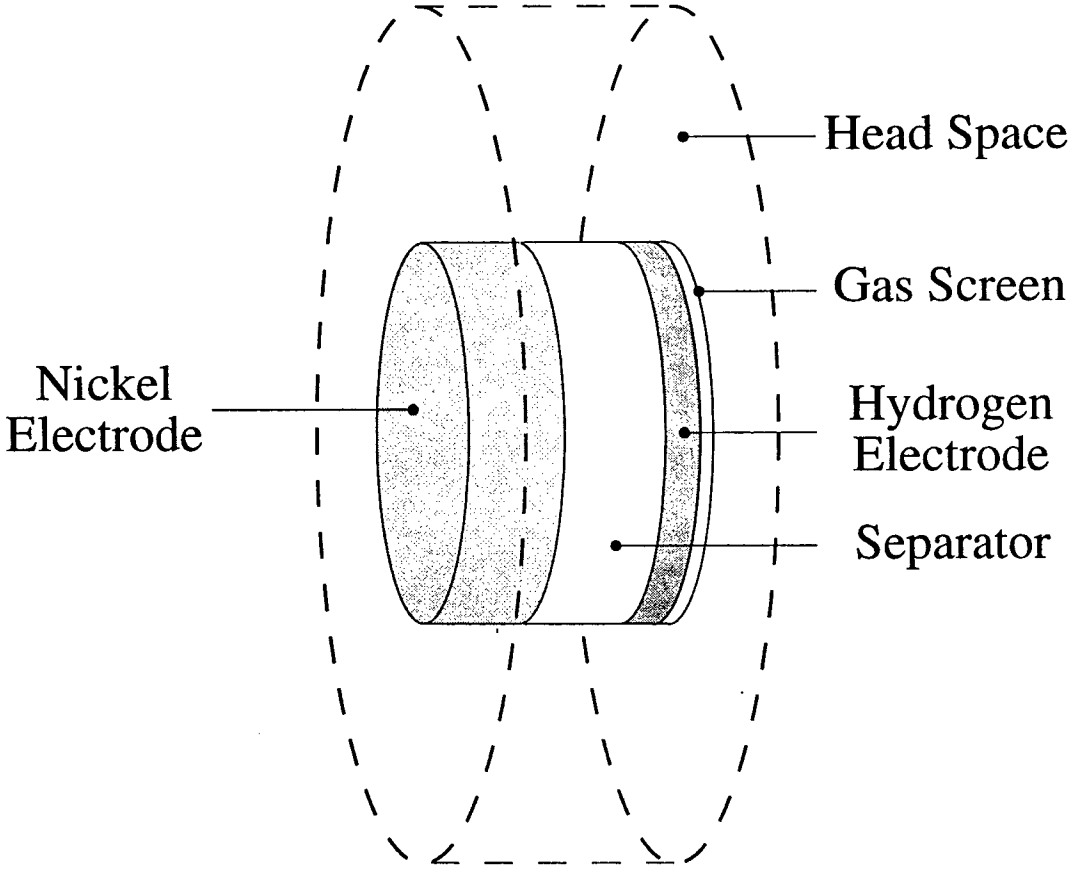

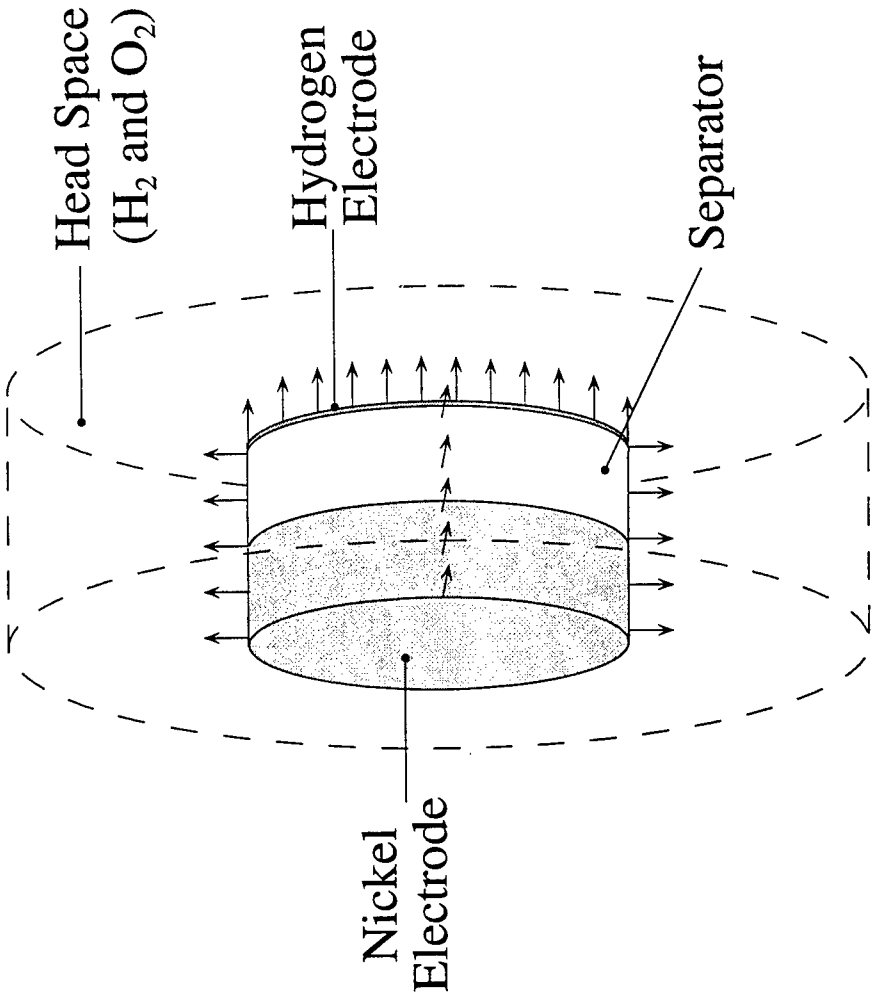
Head Space
(H_2 and O_2)
Hydrogen
Electrode
Separator
Nickel
Electrode

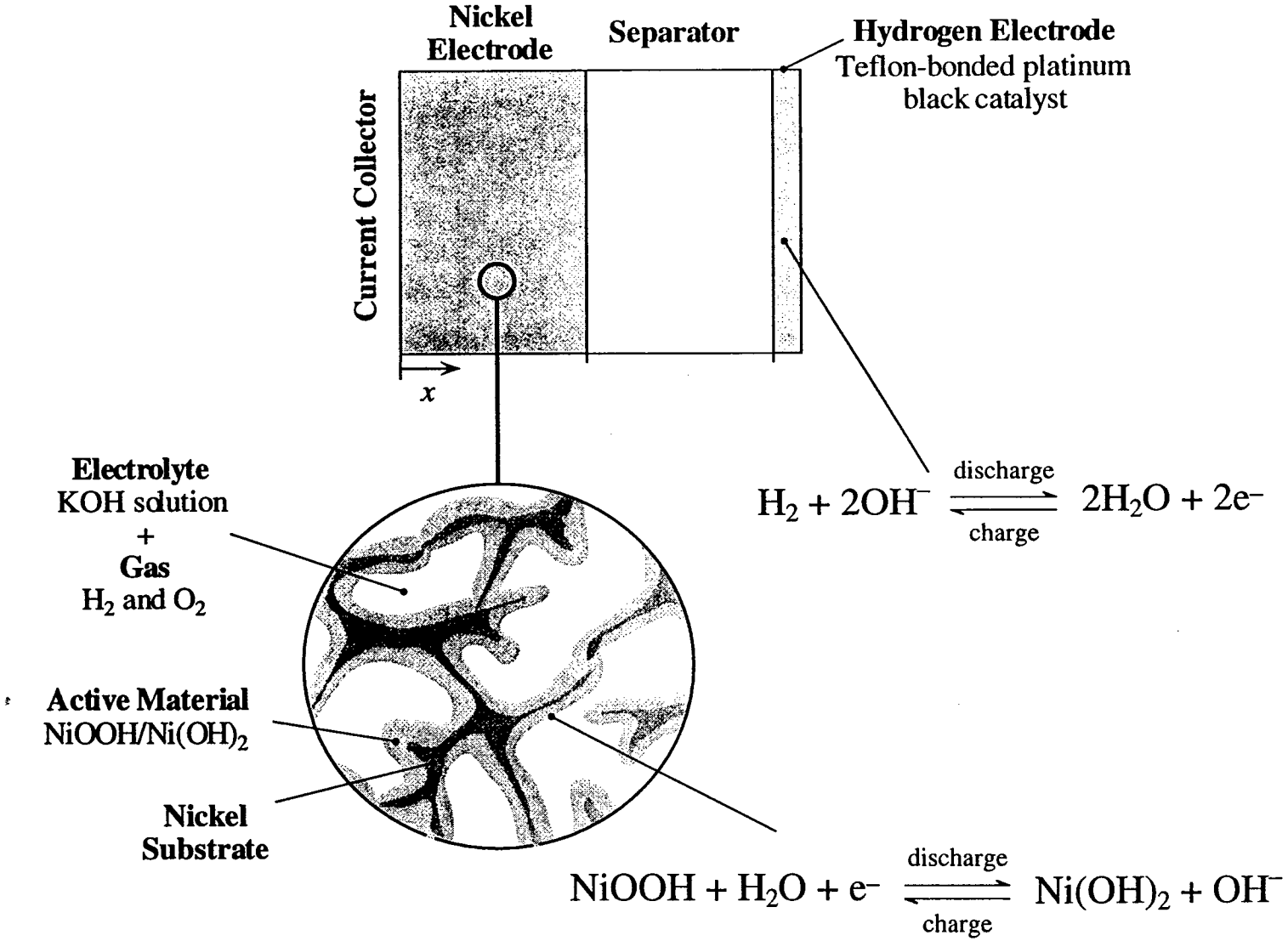
Nickel Electrode
Separator
Hydrogen Electrode
Teflon-bonded platinum black catalyst
Current Collector
x
Electrolyte
KOH solution
+
Gas
H_2 and O_2
Active Material
$NiOOH/Ni(OH)_2$
Nickel Substrate
$H_2 + 2OH^- \rightleftharpoons 2H_2O + 2e^-$
discharge
charge
$NiOOH + H_2O + e^- \rightleftharpoons Ni(OH)_2 + OH^-$
discharge
charge

Representation of the Nickel/Hydrogen Cell

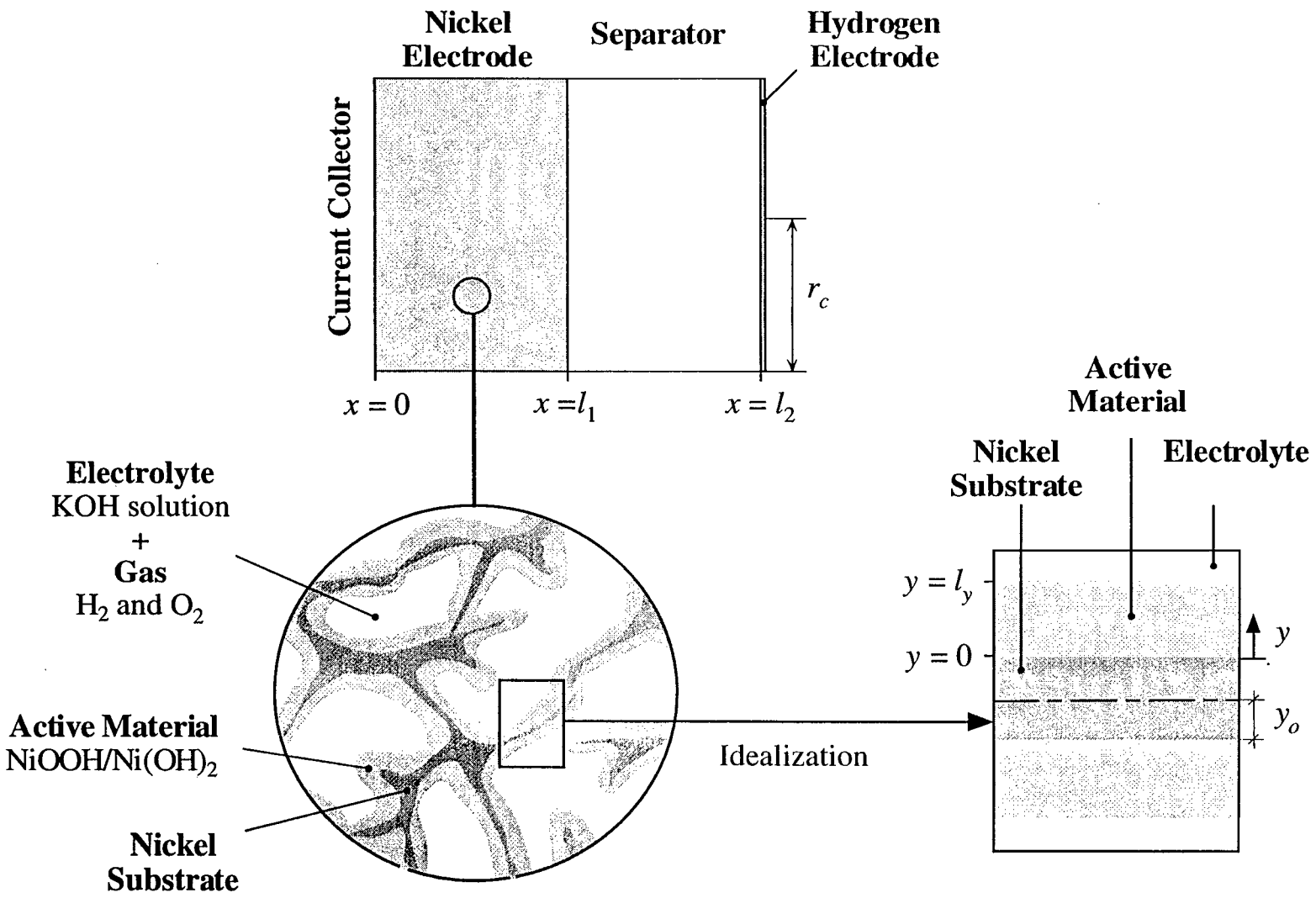

The Nickel Reaction

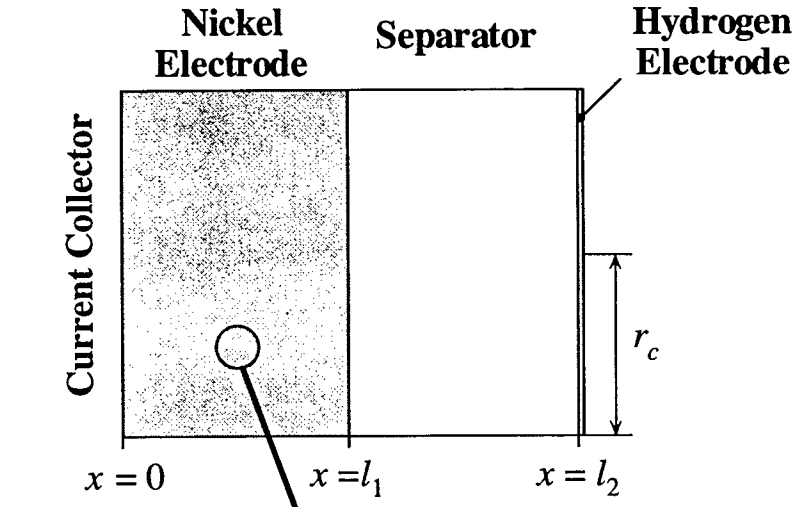

$$H_2O \rightleftharpoons H^+ + OH^-$$

$$NiOOH + H^+ + e^- \underset{\text{charge}}{\overset{\text{discharge}}{\rightleftharpoons}} Ni(OH)_2$$

$$NiOOH + H_2O + e^- \underset{\text{charge}}{\overset{\text{discharge}}{\rightleftharpoons}} Ni(OH)_2 + OH^-$$

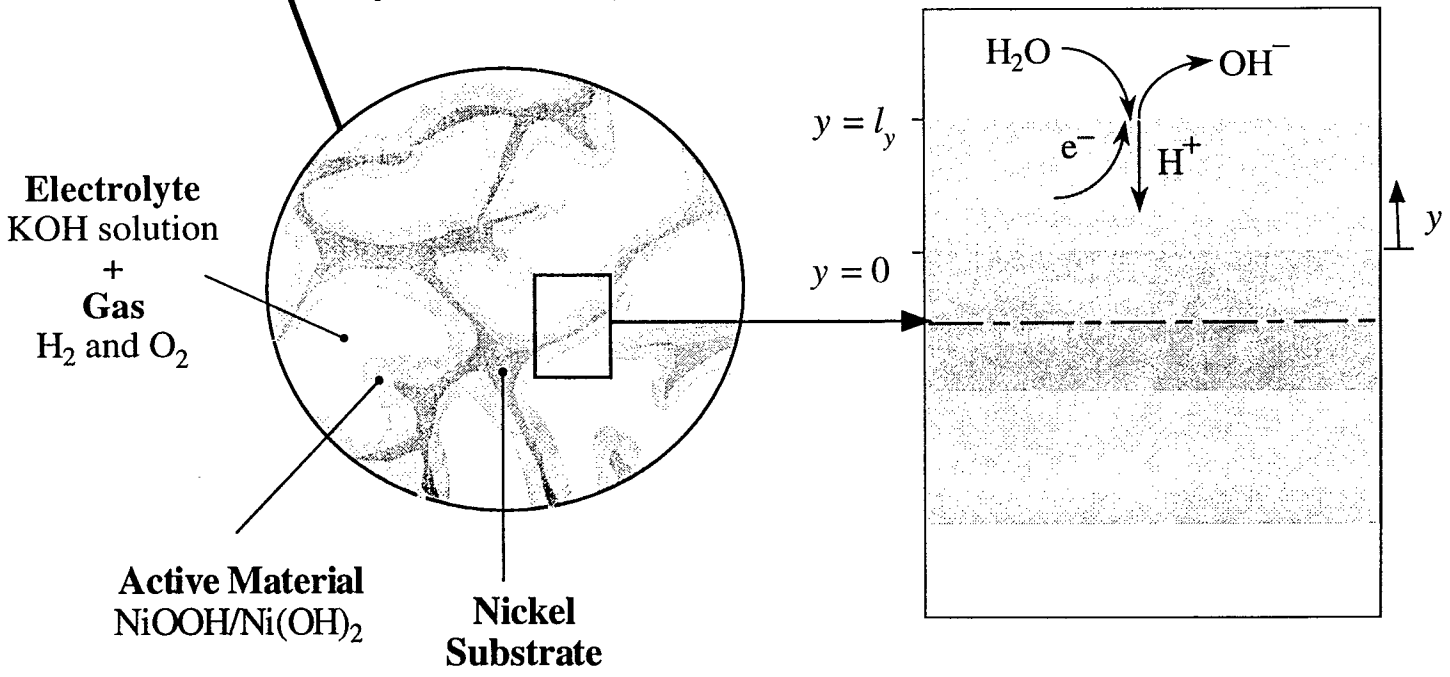

Main Features of the Model

- Consider three phases for the relevant species.
- Use of local volume averaging technique for porous media applied to porous electrodes.
- Addition of energy balance to allow the consideration of thermal effects.
- New numerical method to improve solution accuracy and execution speed.
- Improved software implementation to allow easy interaction with systems models.

Model Assumptions

- Porous media is represented as continua – volume averaging
- Non-porous active material
- Solid matrix of nickel electrode is represented as collection of cylinders
- Pseudo-two dimensional representation of the nickel electrode
- Pores of nickel electrode and separator are filled with liquid and gas
- Gas phase consists of hydrogen and oxygen
- Hydrogen electrode is treated as a flat plate electrode
- Uniform temperature inside the cell

Electrode Reactions

Reactions at the Nickel Electrode

Main reaction: $$NiOOH + H_2O + e^- \underset{\text{charge}}{\overset{\text{discharge}}{\rightleftarrows}} Ni(OH)_2 + OH^-$$

Side reactions: $$\frac{1}{2}O_2 + H_2O + 2e^- \rightleftarrows 2OH^-$$

$$2H_2O + 2e^- \rightleftarrows H_2 + 2OH^-$$

Reactions at the Hydrogen Electrode

Main reaction: $$H_2 + 2OH^- \underset{\text{charge}}{\overset{\text{discharge}}{\rightleftarrows}} 2H_2O + 2e^-$$

Side reaction: $$2OH^- \rightleftarrows \frac{1}{2}O_2 + H_2O + 2e^-$$

Model Equations

- Material Balance $\frac{\partial \varepsilon c_i}{\partial t} = -\nabla \cdot \mathbf{N}_i + R_i \quad i = OH^-, H_2, O_2$
- Electroneutrality $\sum_i z_i c_i = 0$
- Ohm's Law $\mathbf{i} = -\kappa \nabla \phi$
- Modified Ohm's Law $\mathbf{i} = -\kappa \nabla \phi - \kappa f(c_{OH^-}) \nabla \ln c_{OH^-}$
- Conservation of Charge $\frac{\partial q}{\partial t} = -\nabla \cdot \mathbf{i}$
- Energy Balance

$$m_{cell} c_{p,cell} \frac{dT}{dt} = -\left\{\begin{array}{c}\text{heat transfered}\\ \text{to the surroundings}\end{array}\right\} + \left\{\begin{array}{c}\text{heat produced by}\\ \text{the reactions}\end{array}\right\} + \left\{\begin{array}{c}\text{electrical}\\ \text{work}\end{array}\right\} + \left\{\begin{array}{c}\text{work caused by}\\ \text{changes in pressure}\end{array}\right\}$$

- The rates of reaction are written as Butler-Volmer expressions

Solution of the Model and Description of the Software

- The model consists of a system of partial differential equations with multiple spatial regions.
- Use the numerical method of lines (MOL) to solve de model, which transforms the system of partial differential equations into a system of mixed differential/algebraic equations (DAEs).
- Use DASSL, which is an specialized code designed to solve the DAEs
- The solution obtained with DASSL is:

  more accurate
  faster
  more robust

  than traditional methods (e.g., finite differences, Crank-Nicolson)
- Software needs moderate computational requirements (high-end PC, such as Power Macintosh)

Other models solved using a similar methodology include

- Isothermal Nickel/Hydrogen cell
  De Vidts, 1995; De Vidts, Delgado, and White, submitted to the *Journal of the Electrochemical Society*

- Nickel/Metal-hydride electrode under discharge
  De Vidts and White, *Conference on NASA Centers for Commercial Development of Space*, 1995

- Nickel/Metal-hydride cell under discharge
  De Vidts, Delgado, and White, to appear in the *Journal of the Electrochemical Society.*

- Nickel/Metal-hydride cell performance
  De Vidts, Delgado, and White, in preparation

- Nickel/Cadmium cell performance
  De Vidts and White, *Journal of the Electrochemical Society. 142*, 1509–1519, **1995.**

- Film nickel electrode model
  Streinz, Motupally, Delgado, and Weidner, in preparation

Model Capabilities

The model can be used to simulate:

- cell voltage
- cell pressure (hydrogen and oxygen)
- temperature
- heat generation
- partial current densities
- electrolyte concentration, potential, and current profiles

The user can manipulate operating conditions, such as,

- rates of charge and discharge
- periods of stand-by
- external temperature
- cycling

Design parameters can be modified; for example,

- Initial conditions
  - state of charge
  - pressure
  - temperature
  - loading
- Cell dimensions
- Electrolyte concentration
- Electrode and Separator properties
  - porosity
  - active area
- Mass transfer
- Heat transfer
- Other properties can also be modified upon request; for example, physical and chemical properties of separator and electrolyte

Simulations and Case Studies

Isothermal

- Comparison with experimental data
- Prediction of second discharge plateau
- Effect of initial pressure
- Prediction of optimal charging rate

Simulations and Case Studies (cont.)

Non-Isothermal

- Effect of thermal effects on cell behavior during a charge/discharge cycle
- Potential
- Pressure
- Temperature
- Heat generation

Parameter Values

Electrolyte concentration	26% wt
Initial hydrogen pressure	52 atm
Initial oxygen pressure	trace (charge) 0.05 atm (discharge)
Temperature	25°C
Theoretical capacity of the nickel electrode	32.5×10^{-3} Ah/cm^2
Nickel electrode thickness	0.072 cm
Separator thickness	0.04 cm
Cell radius	2.5 cm
Head space volume	87.7 cm^3
Heat transfer coefficient	3×10^{-3} W/cm^2 K
Specific surface area of the substrate in the nickel electrode	2×10^3 cm^2/cm^3
Porosity of the nickel electrode	0.5
Porosity of the nickel substrate phase in the separator	0.86
Porosity of the liquid phase in the separator	0.65
Porosity of the gas phase in the separator	0.2

Cell Voltage during Discharge
Comparison with Experimental Data

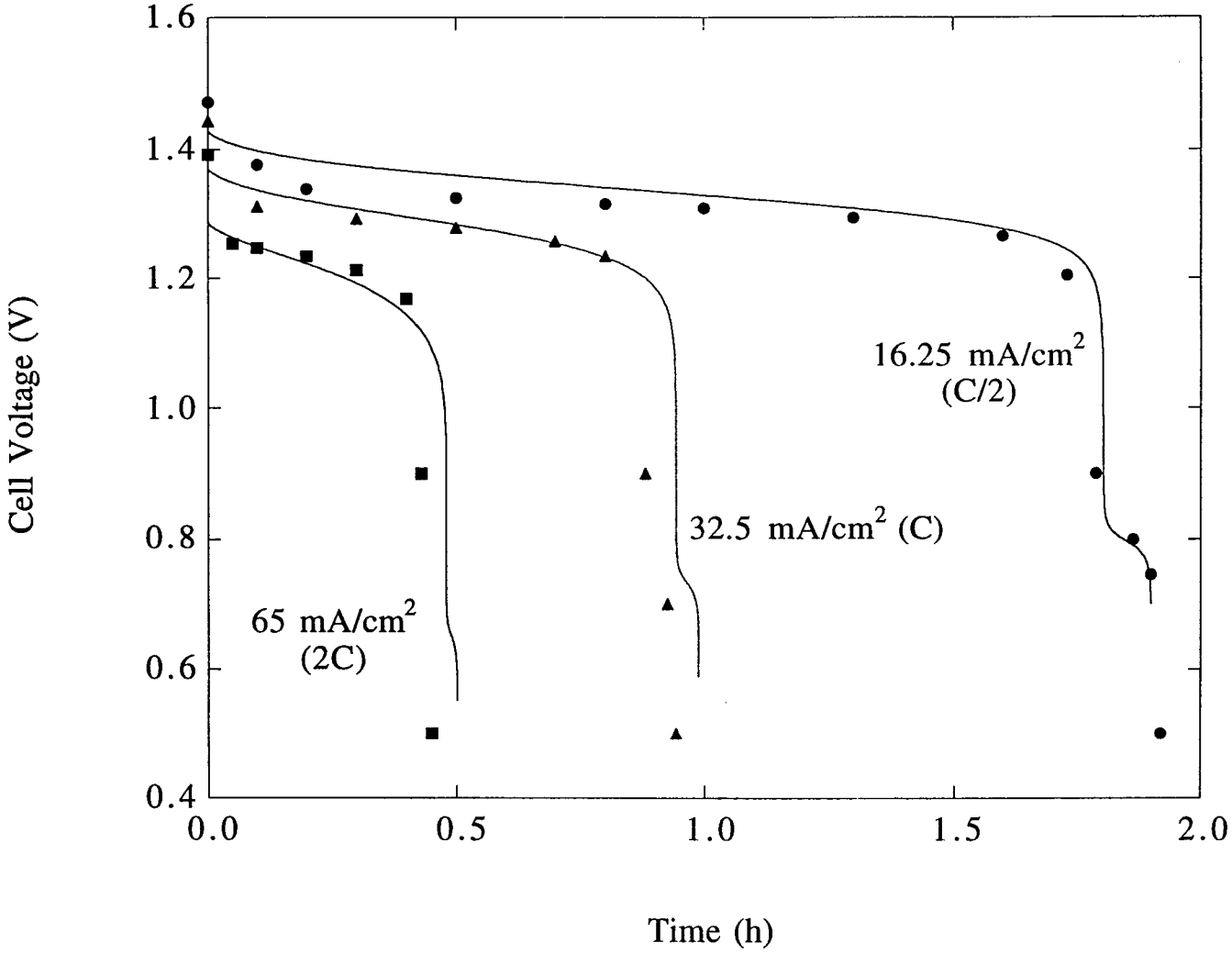

Cell Pressure during Discharge
Comparison with Experimental Data

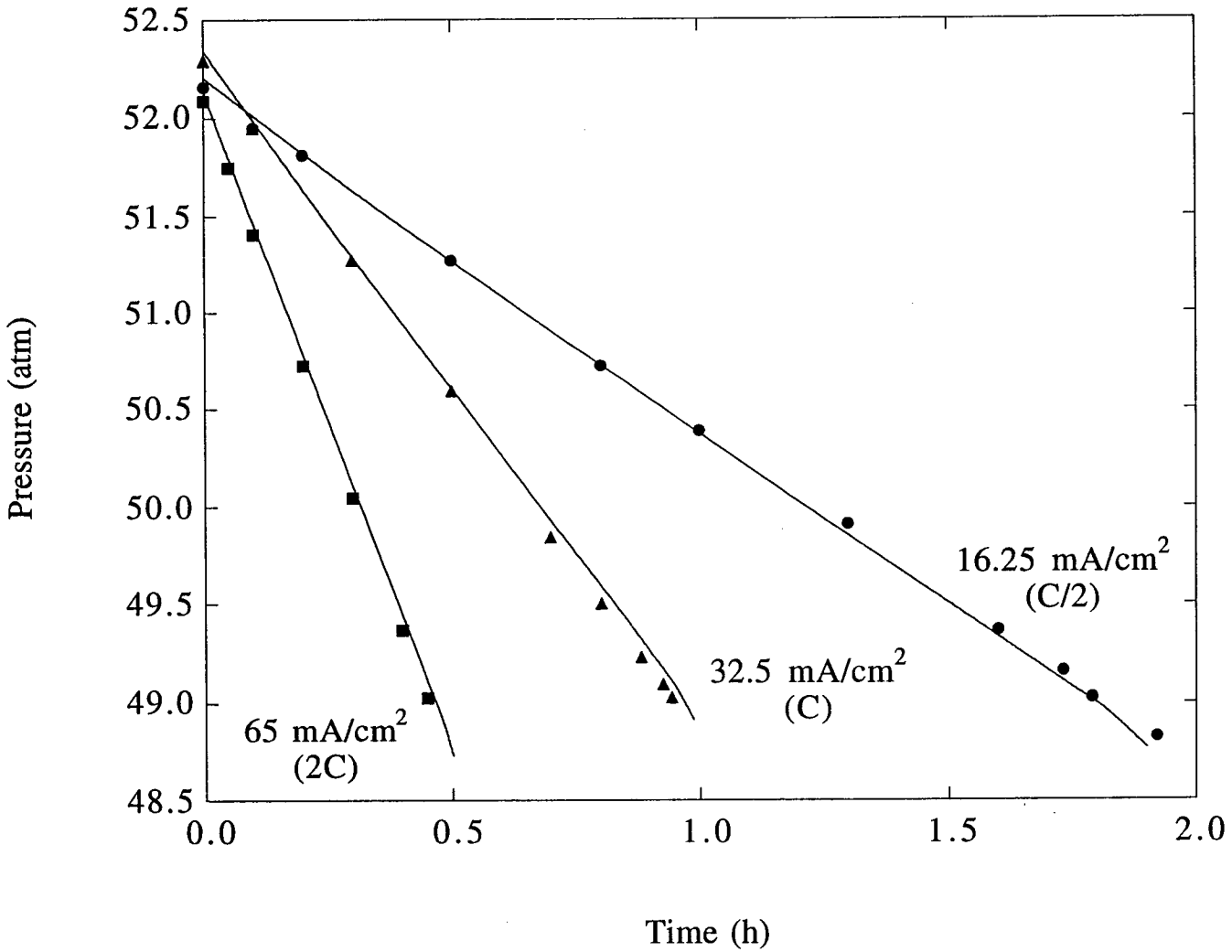

Cell Voltage during Charge
Comparison with Experimental Data

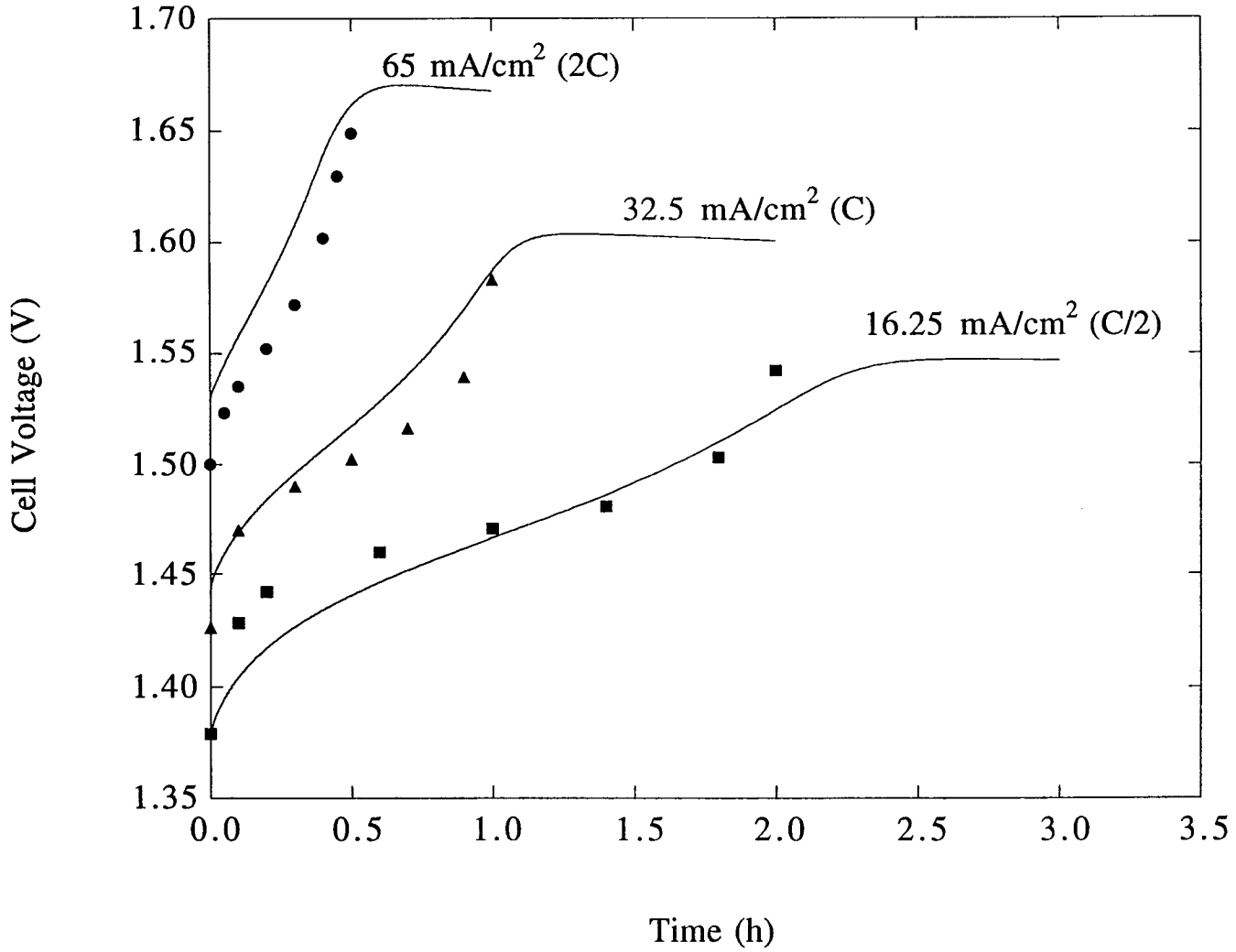

Cell Pressure during Charge
Comparison with Experimental Data

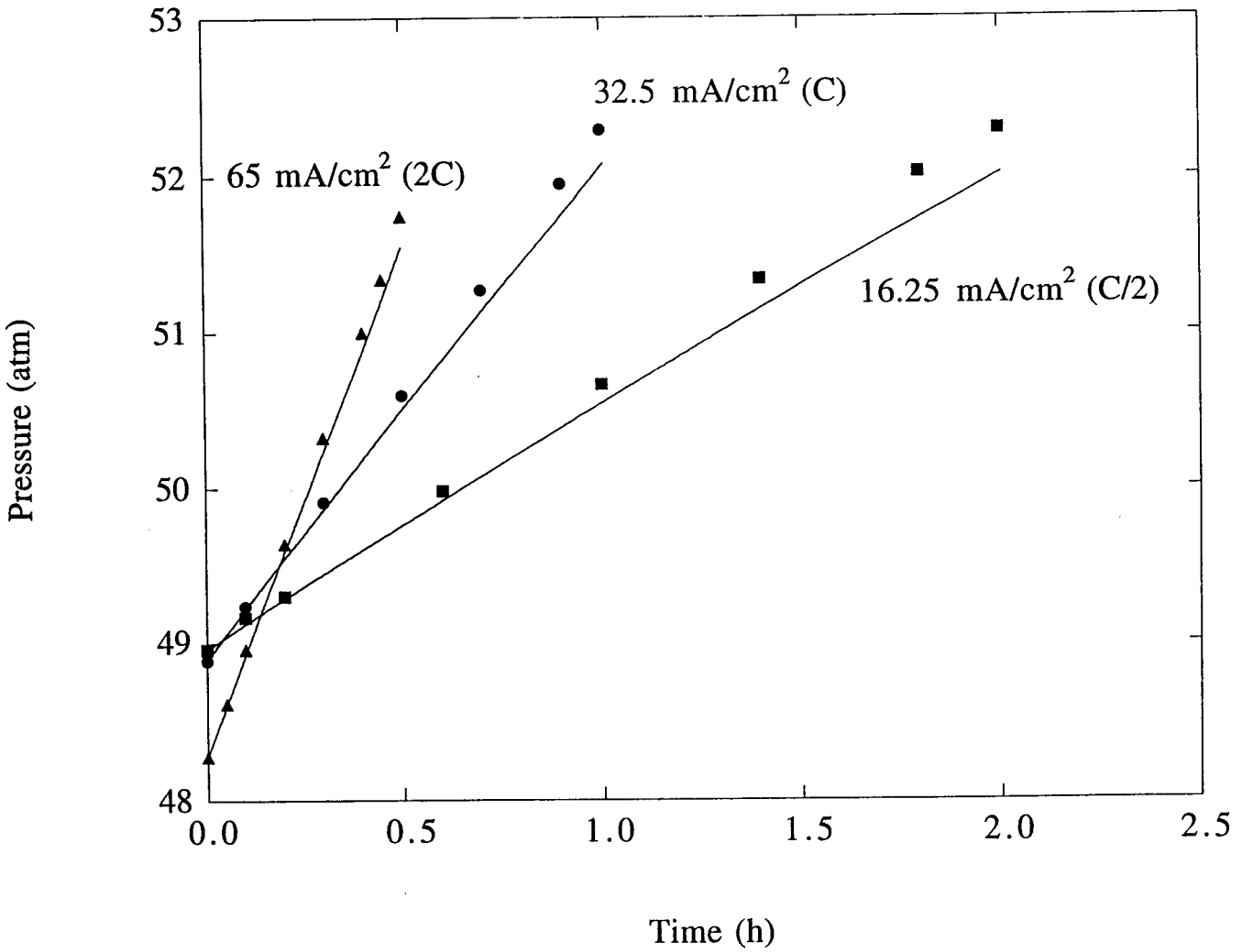

Second Discharge Plateau

- A second discharge plateau is predicted if there is oxygen accumulation.

- Role of oxygen on appearance of the plateau has been verified experimentally on a film electrode (J. Weidner and co-workers).

Cell Voltage during Discharge

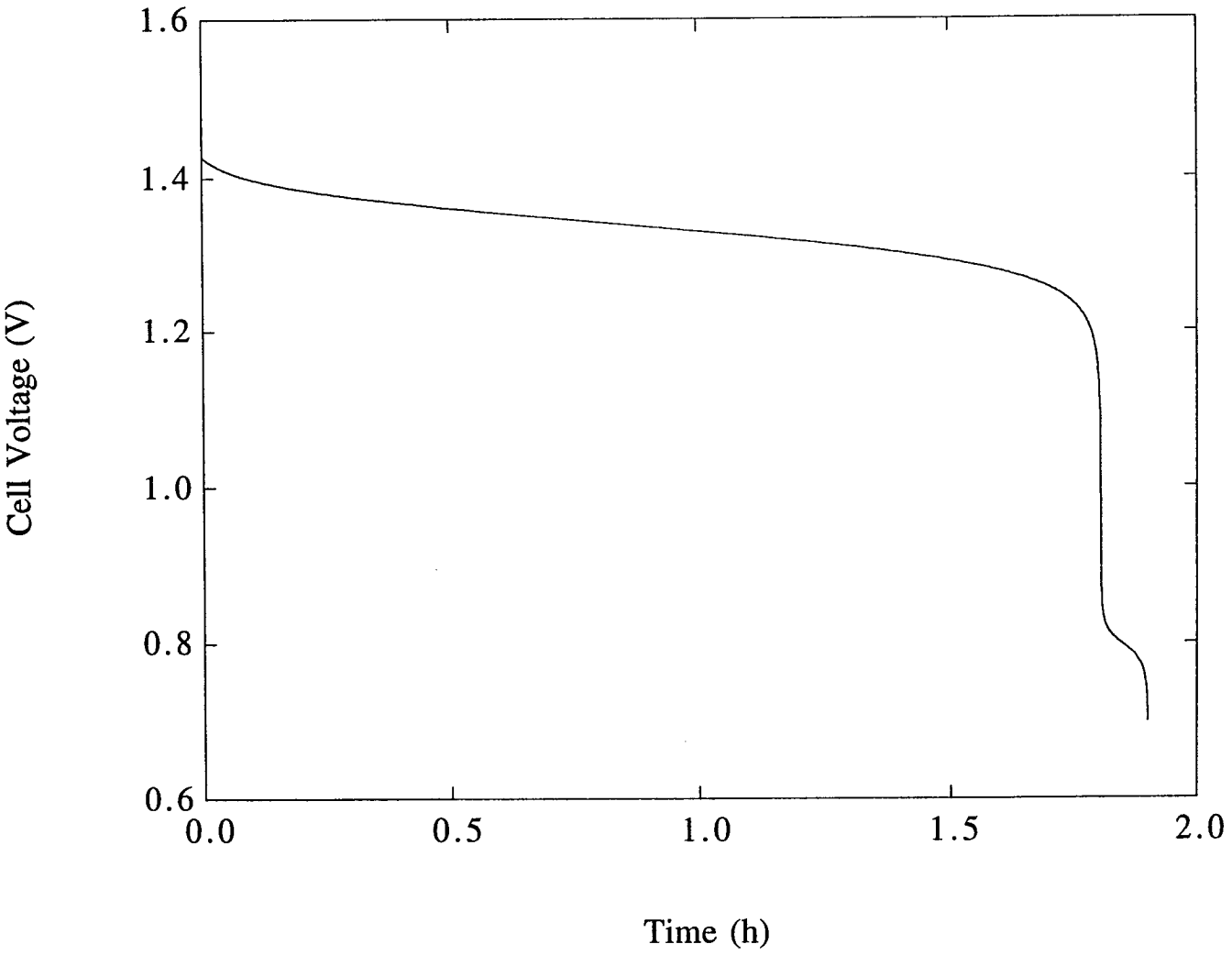

Reaction Current Densities during Discharge

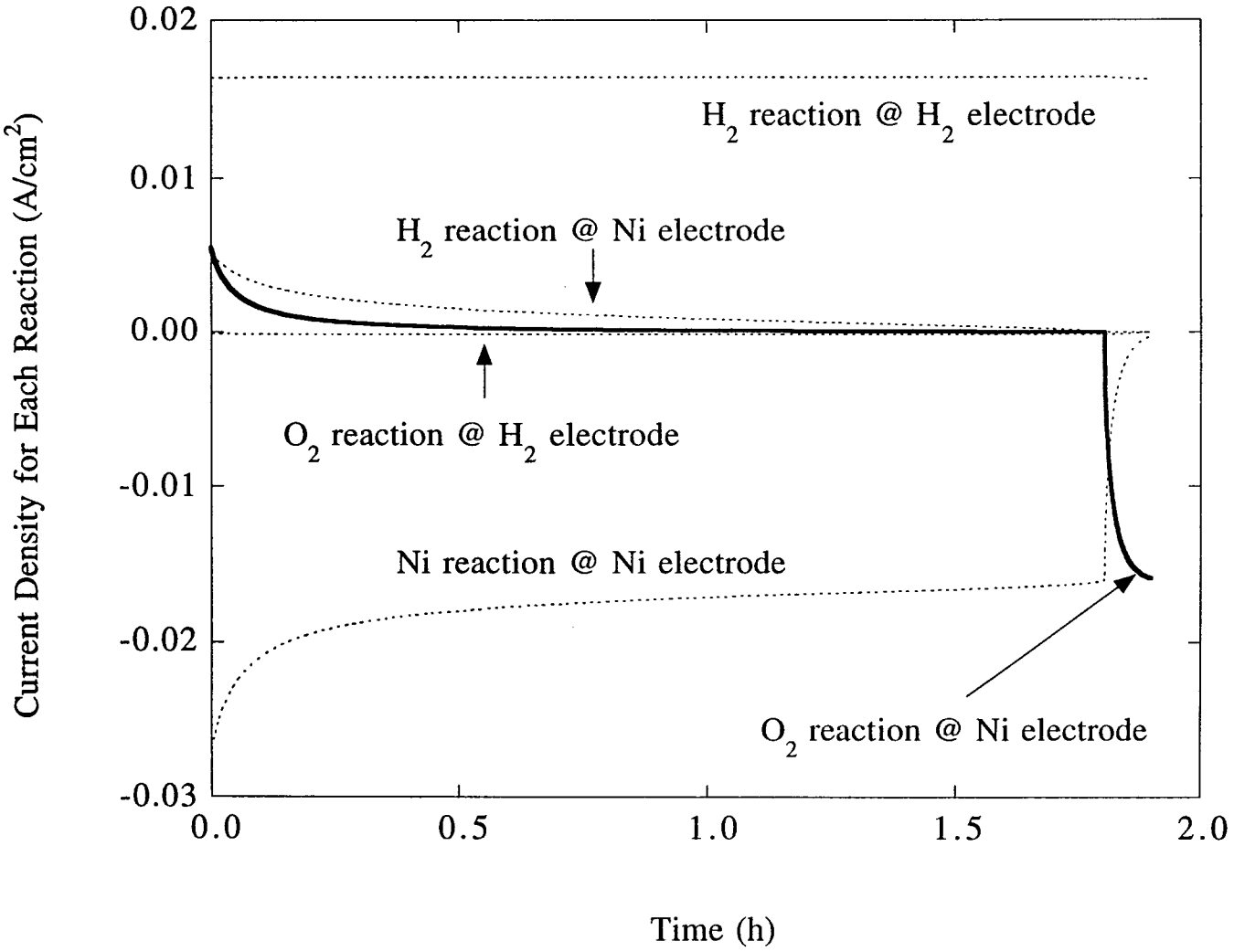

Oxygen Partial Pressure during Discharge

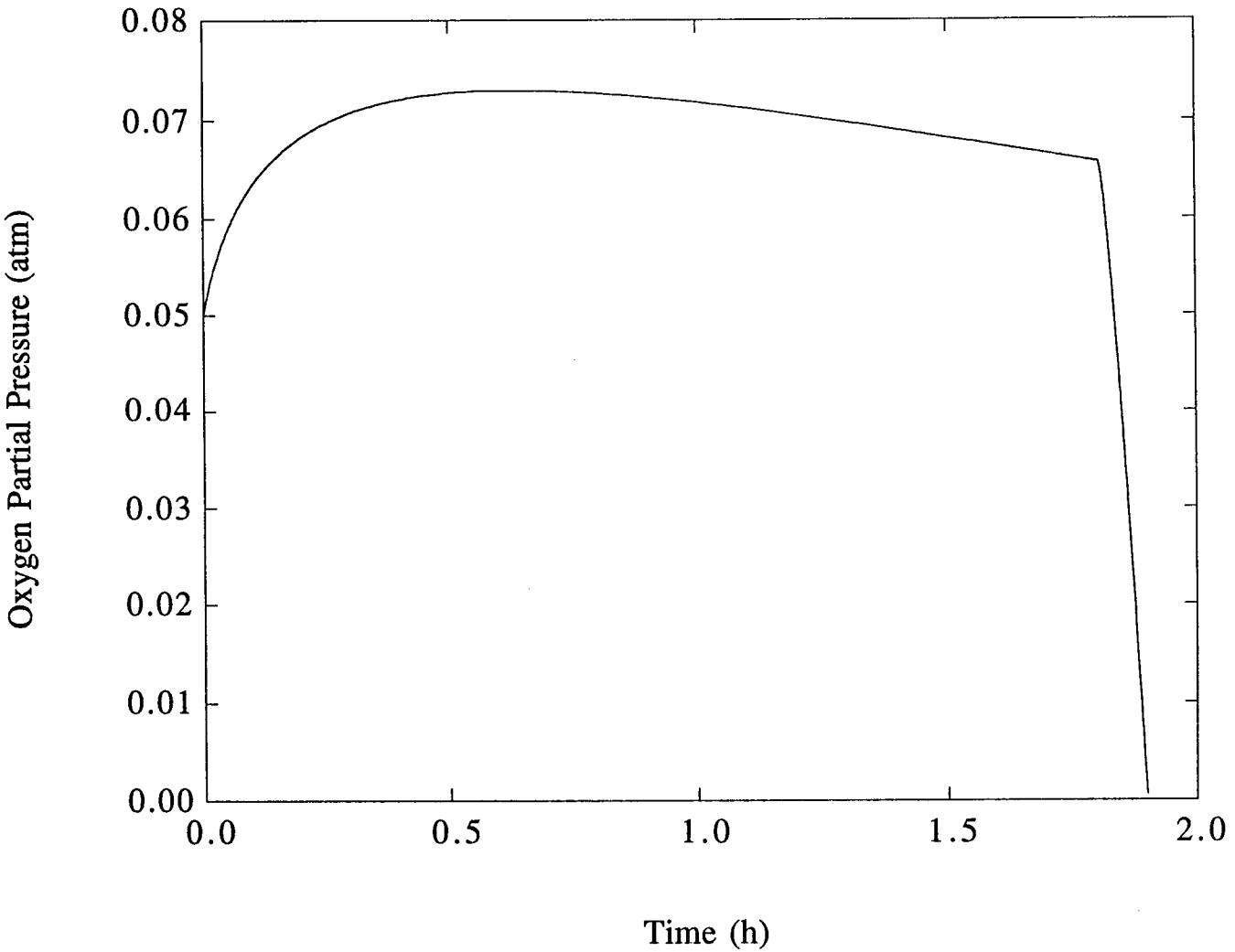

Second Discharge Plateau

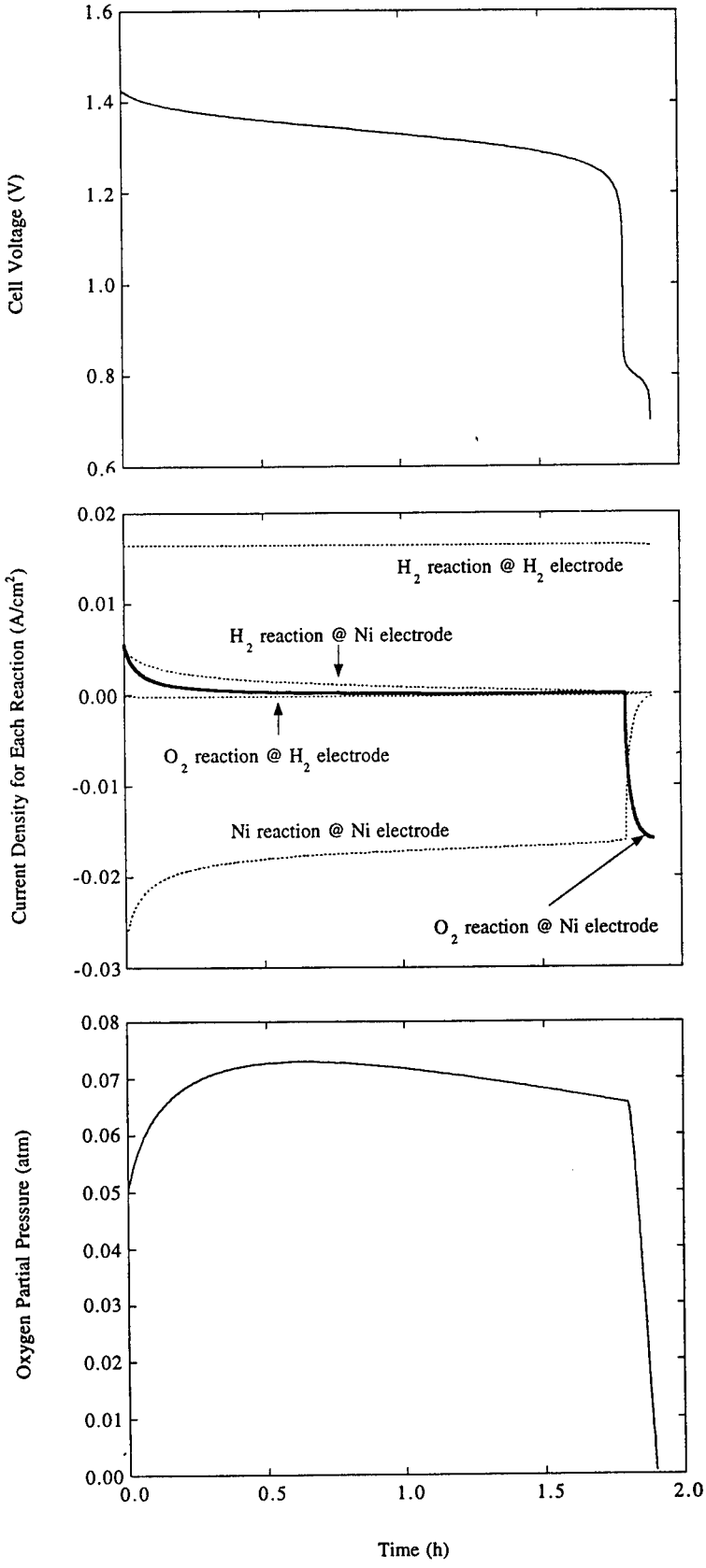

Effect of Initial Oxygen Pressure

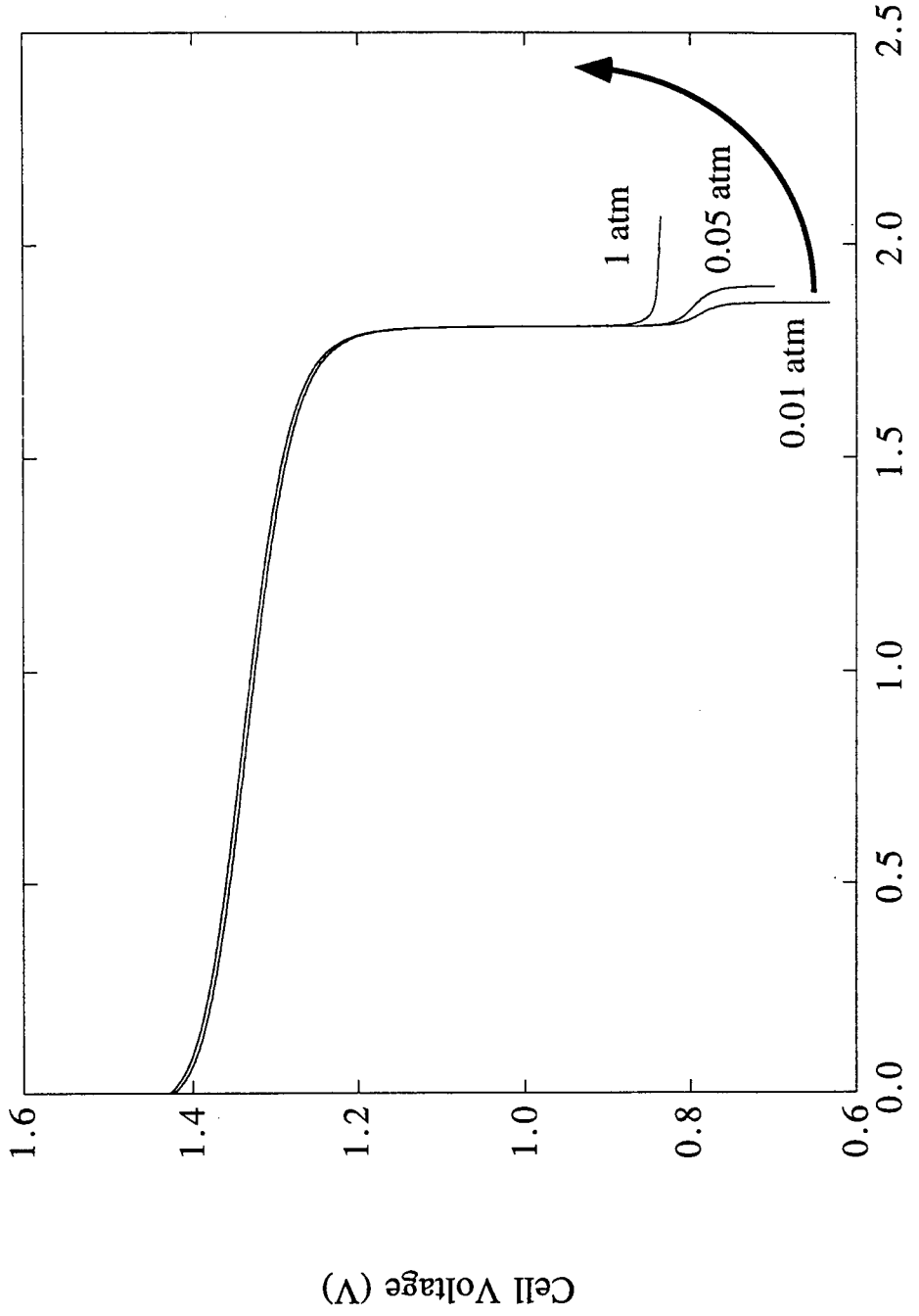

Effect of Initial Hydrogen Pressure

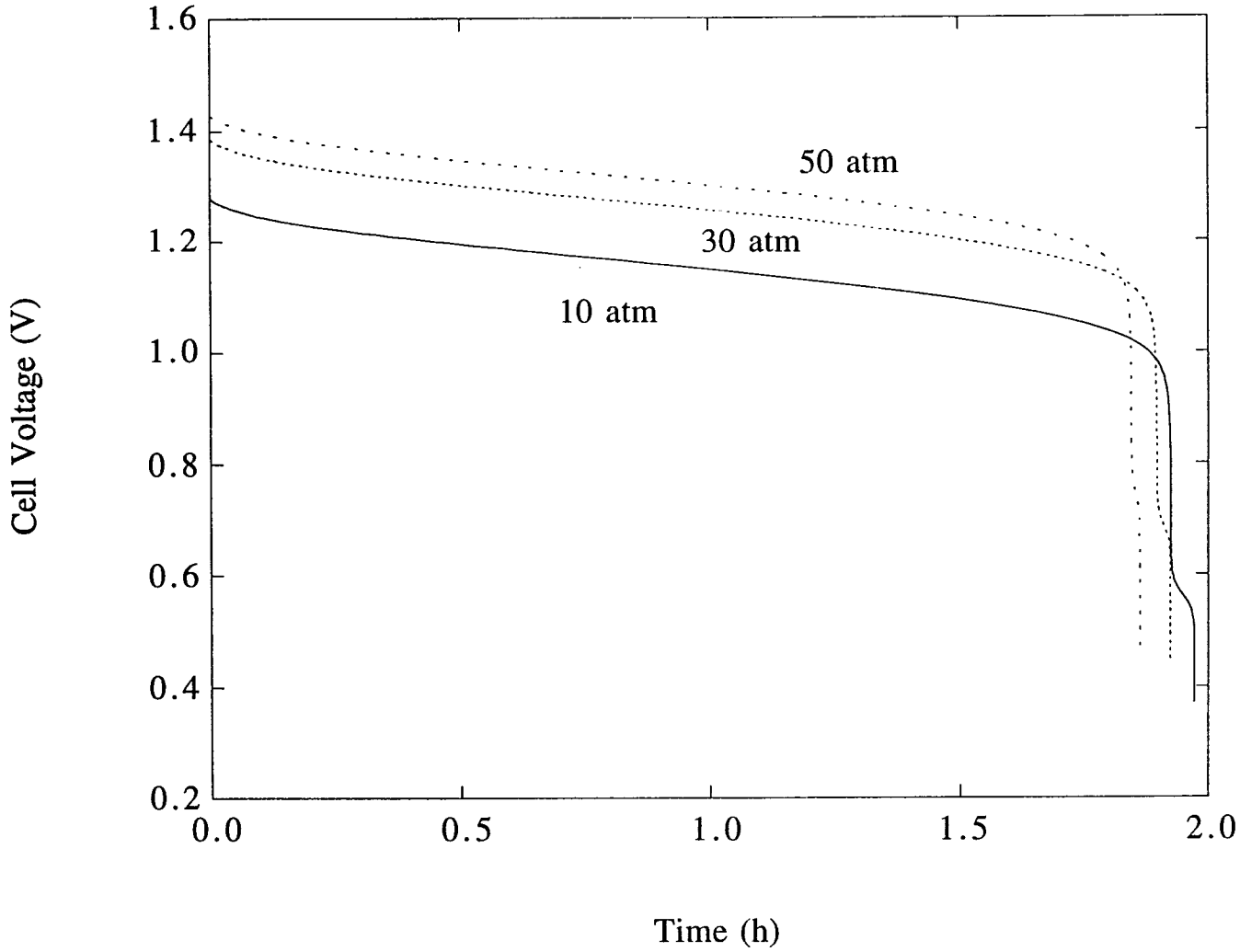

Effect of Applied Current on Final State of Charge

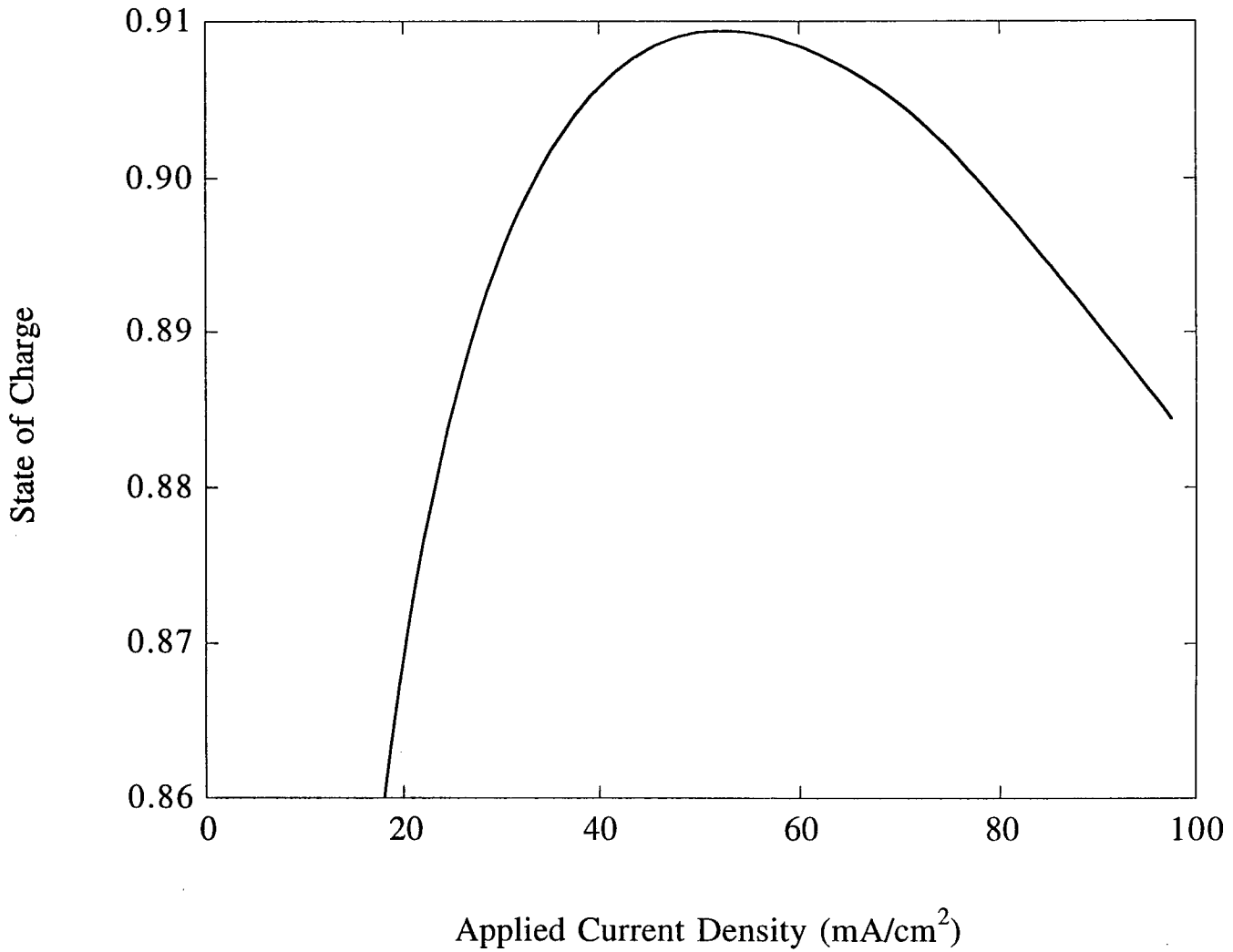

Charge/Discharge Voltage Profiles under Non-Isothermal Conditions

C/10 charge for 16 h followed by a C/2 discharge

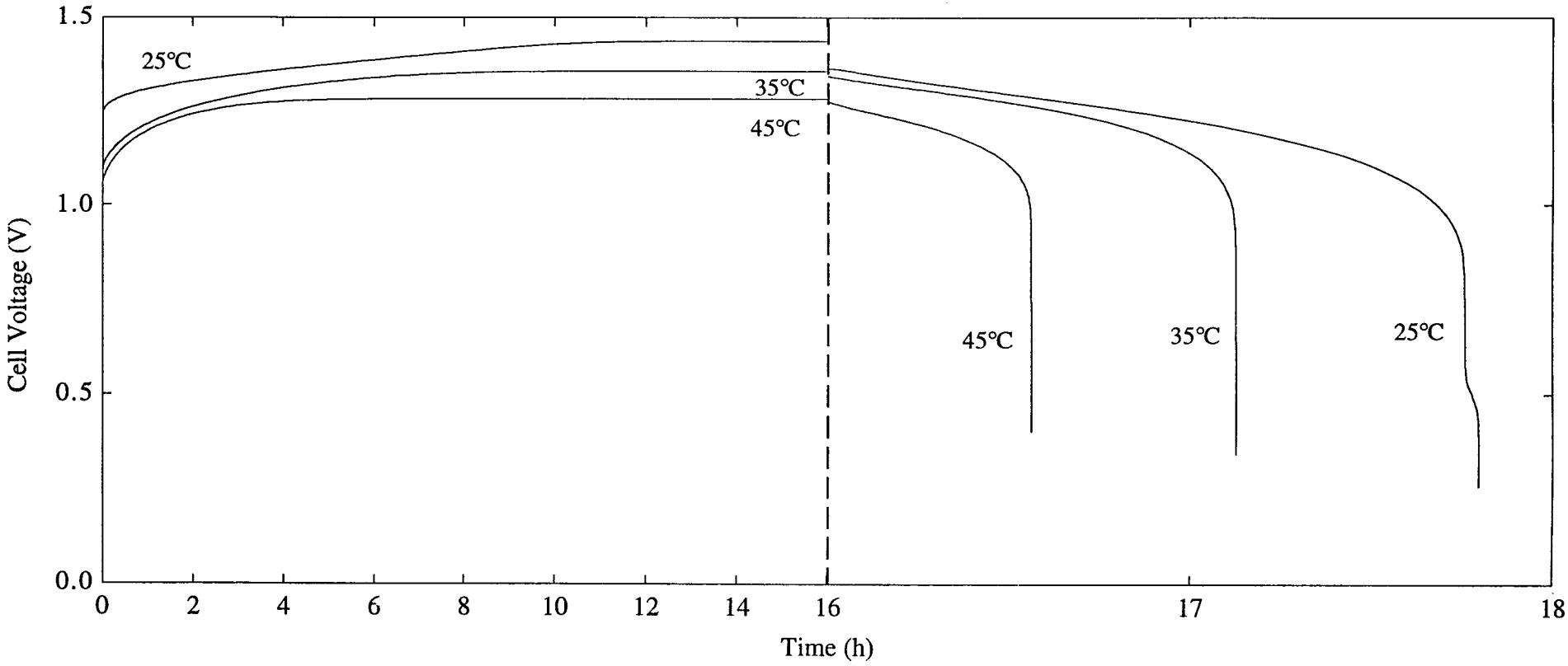

Charge/Discharge Pressure Profiles under Non-Isothermal Conditions

C/10 charge for 16 h followed by a C/2 discharge

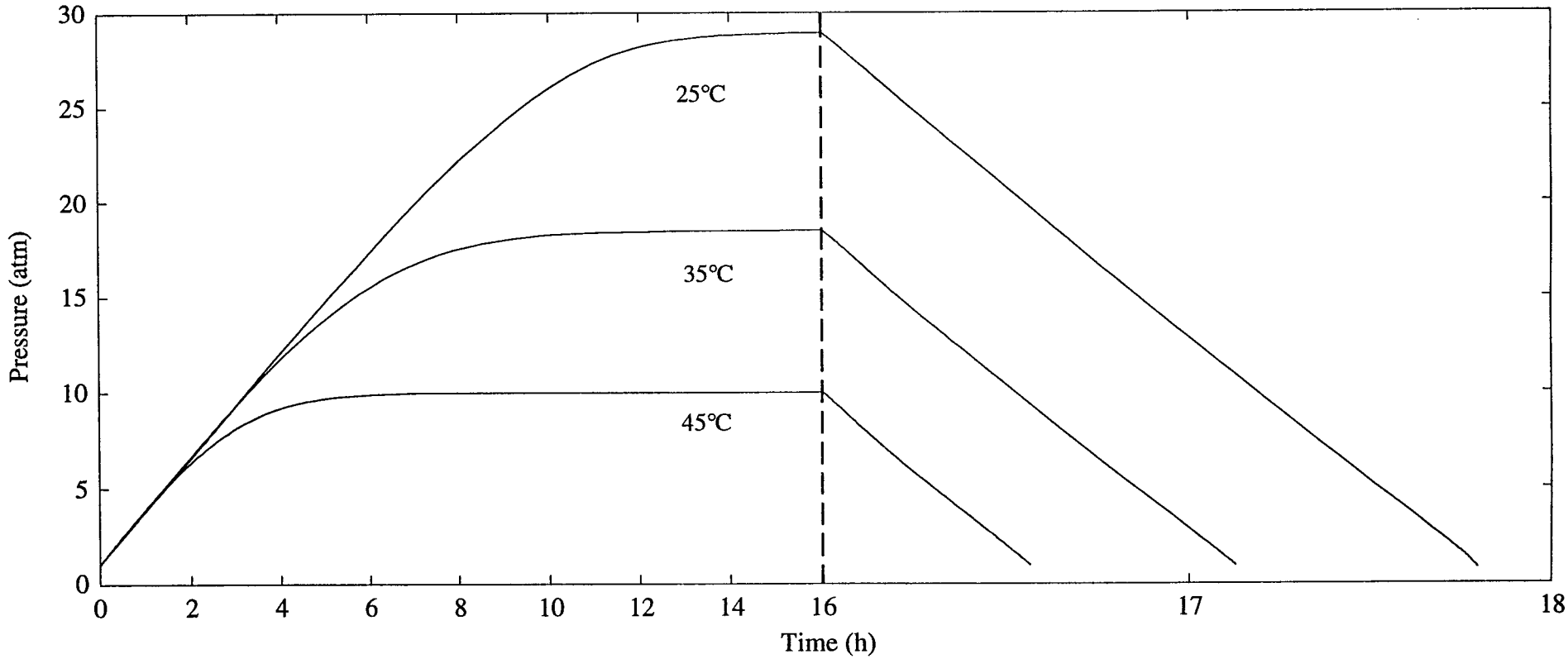

Charge/Discharge Temperature Profiles under Non-Isothermal Conditions

C/10 charge for 16 h followed by a C/2 discharge

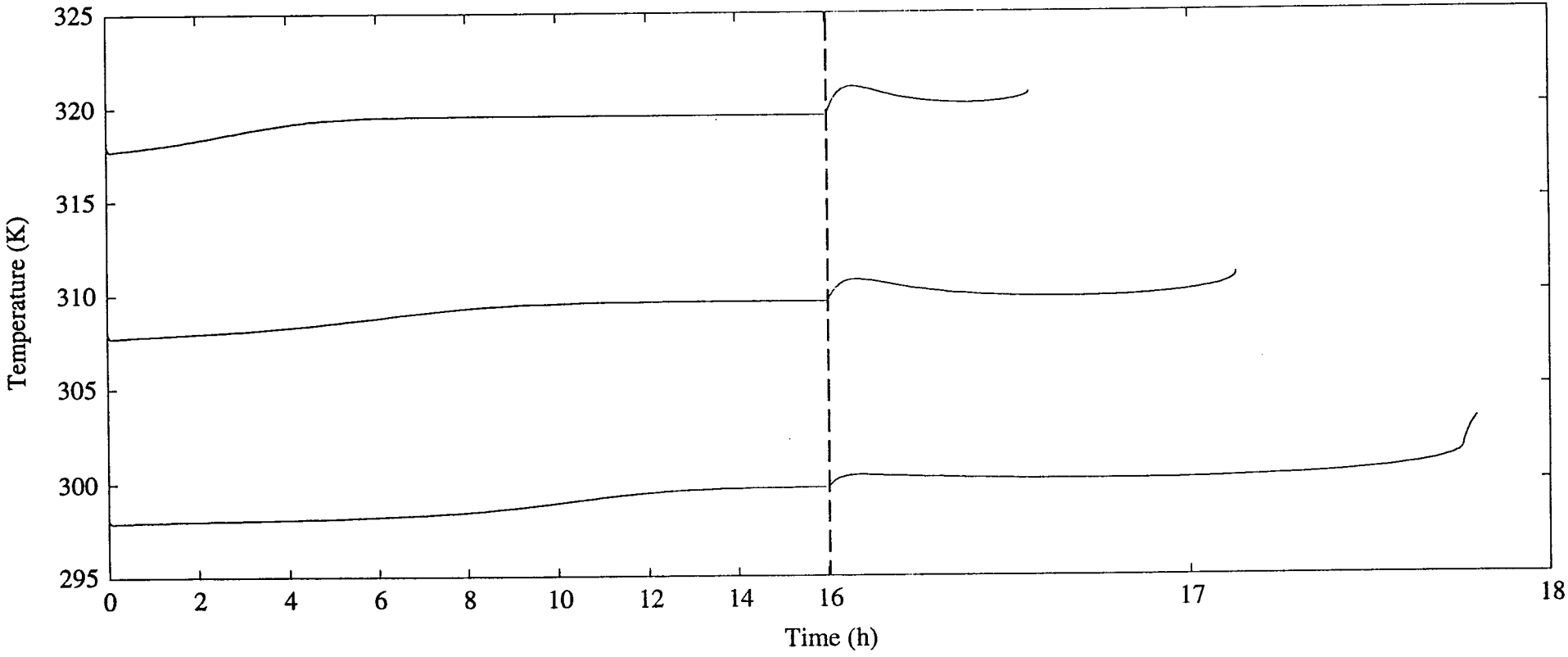

Charge/Discharge Heat Generation Profiles under Non-Isothermal Conditions

C/10 charge for 16 h followed by a C/2 discharge

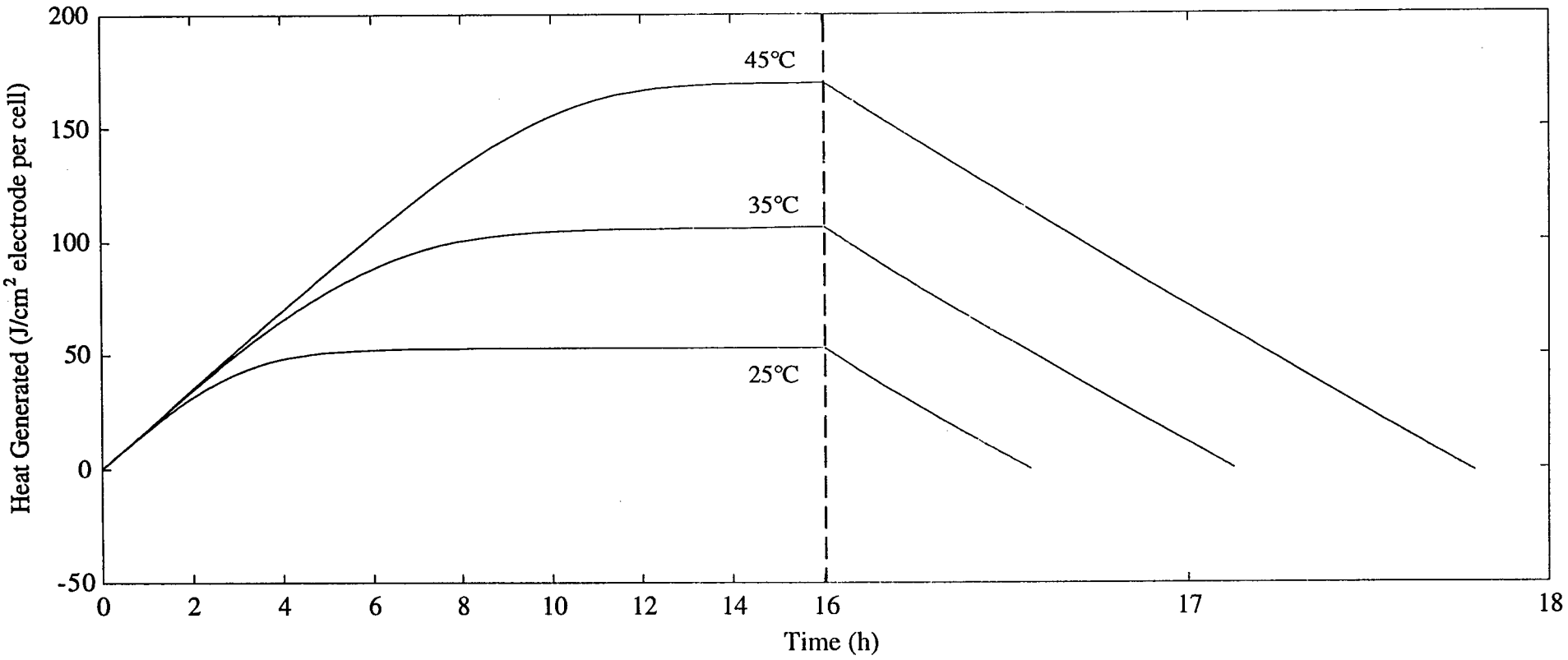

Summary

- Developed a first-principles model for the nickel-hydrogen cell with thermal effects.
- Simulations obtained using the model are in agreement with experimental data.
- The model helped unveil a possible explanation for the second discharge plateau: oxygen accumulation in the cell.
- The model predicts an optimum rate of charge that maximizes the charging efficiency of the cell.
- The non-isothermal predictions agree qualitatively with experimental evidence.

Current Work

- User's Manual for the software
- Refinement of kinetic parameters and expressions

  open circuit/self-discharge
  over-charge
  heats of reaction and temperature dependence

- Measurement of oxygen and hydrogen in the head space
- Improvement of the software to optimize execution speed and memory requirements.

Recommendations for Future Work

Modeling

- Refine kinetic expressions for the electrode reactions for discharge and charge.
- Include the effect of water vapor in the gas phase.
- Include the effect of wall wicks inside the cell.
- Test a model of the nickel electrode based on a two phase approach (Huggins, *Solid States Ionics*, 1994).
- Recirculating cell design.

Recommendations for Future Work (cont.)

Modeling (cycling and storage)

- Select the degradation mechanisms that need to be included; for example:

  cobalt depletion of the nickel electrode
  oxidation of the platinum electrode
  corrosion of nickel substrate
  changes in active surface area
  cracking of the solid materials

- Determine the effect of temperature on the degradation mechanisms.

- Include degradation mechanisms into the model.

Recommendations for Future Work (cont.)

Experimental

- Measure relevant cell species inside a single cell during operation.
- Place wall wicks inside the single cell to test their effect and compare to the model predictions.
- Run cycling experiments with single cells and batteries.
- Post-mortem analysis of the cycled cells.
- Develop quantitative relationships to account for degradation mechanisms.

NiH_2 Battery Model Requirements

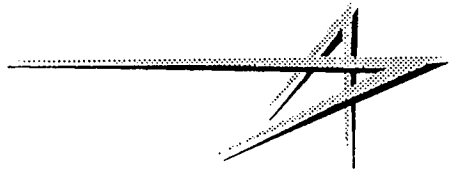

D.P. Hafen and J.D. Armantrout
Lockheed Martin Missiles and Space

Presented at NASA Marshall Battery Workshop
Huntsville, Alabama
Nov. 28-30, 1995

DATE: 11/8/95
ORIGINATOR: D. HAFEN

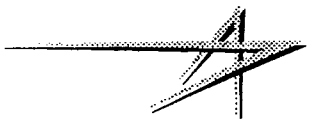

NiH_2 BATTERY MODEL REQUIREMENTS

INTRODUCTION

- Voltage Prediction model needed for various purposes
  - System sizing
  - Assessment of system performance
  - Battery selection
  - Assignment of batteries to physical location
  - Operations
- Overview of requirements
  - What we want model to do
  - How it can be used

DATE: 11/8/95
ORIGINATOR: D. HAFEN

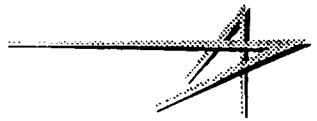

NiH_2 BATTERY MODEL REQUIREMENTS

WHAT WE WANT MODEL TO DO

- Provide battery performance measures
  - Voltage
  - Efficiency
  - Heat Generation
  - Self Discharge
- Inputs which will change for each call to routine
  - Current
  - State-of-Charge
  - Temperature
- Inputs which will be constant for a given computer run
  - Battery Age
  - State of deconditioning
  - Design (sinter type, porosity, loadings, electrolyte etc.)
- Model need to correlate with test performance
  - Voltage vs. time
  - Capacity
  - Impedance
  - Charge Retention

DATE: 11/8/95
ORIGINATOR: D. HAFEN

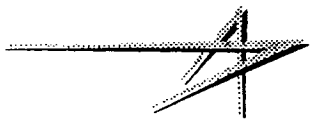

NiH_2 BATTERY MODEL REQUIREMENTS

How the model can be used

- Needs to interface with multi-battery system simulation which contains models for other components (solar array, diodes, wiring, loads, charge controller)
- Energy balance
- Thermal management
- Interaction of parallel batteries which load share
  - Different temperatures
  - Different capacities
  - Different impedances

EAGLE-PICHER POWER SYSTEMS DEPARTMENT

REQUIREMENTS FOR A NICKEL ELECTRODE IMPREGNATION MODEL

ROLAN C. FARMER, DARREN SCOLES AND DAVID F. PICKETT

GENERAL REQUIREMENTS

- MUST SIMULATE PRODUCTION PROCESS
- CAPABLE OF USE BY PRODUCTION PERSONNEL
- CAN AID IN SOLUTION OF PRODUCTION ANOMALIES
- MUST YIELD CREDIBLE RESULTS EASILY VERIFIED BY EXPERIMENT
- ASSUMPTIONS IN MODEL ACCEPTED BY INDUSTRIAL COMMUNITY

MUST SIMULATE PRODUCTION PROCESS

- MUST SIMULATE DEPOSITION INTO PRODUCTION TYPE NICKEL SUBSTRATE WITH APPROXIMATE DIMENSIONS:
  - INITIAL SURFACE AREA OF SUBSTRATE ~0.1 SQ. METERS PER GRAM
  - OVERALL POROSITY OF ~80%
  - PORE DIAMETER 8 TO 20 MICROMETERS
  - PORE LENGTH 0.2 TO 1.0 MILLIMETERS
- CHEMICAL DEFINITION OF DEPOSIT MUST BE MADE
  - NOT ALL DEPOSIT IS ALWAYS $Ni(OH)_2$
  - RATIO OF ACTIVE MATERIAL AND RESIDUAL DEPOSITS SUCH AS NITRATE WOULD BE HELPFUL
- CHEMICAL DEFINITION OF DEPOSITION BATH AFTER X IMPREGNATIONS SHOULD BE MADE

CAPABLE OF USE BY PRODUCTION PERSONNEL

- FINAL FORM OF MODEL SHOULD BE CAPABLE OF BEING USED BY PRODUCTION FOREMAN OR PRODUCTION ENGINEER
- IN CASE OF DIFFICULTIES "HOT LINE" FOR ASSISTANCE SHOULD BE AVAILABLE
  - PLANT ENGINEERING PERSONNEL COULD ASSIST WITH PROPER ORIENTATION
- PRODUCTION PERSONNEL HAVE TO BE COMFORTABLE USING MODEL
  - CREDIBLE RESULTS SHOULD COME OUT OF MODEL

CAN AID IN RESOLUTION OF PRODUCTION ANOMALIES

- CAN PREDICT OUTCOME OF ERRONEOUS CURRENT/VOLTAGE SETTINGS
- CAN PREDICT OUTCOME OF USING OUT OF SPECIFICATION CONCENTRATIONS AND pH VALUES
- CAN PREDICT LIMITED EFFECT OF IMPURITIES
- ANY MAJOR DEVIATION IN PROVEN PROCESS WILL REQUIRE QUALIFICATION

MUST YIELD CREDIBLE RESULTS EASILY VERIFIED BY EXPERIMENT

- MODEL RESULTS, IF DIFFERENT THAN PRODUCTIONS, SHOULD BE EASILY RATIONALIZED
- VERIFICATION WITH SIMPLE EXPERIMENT IS ALWAYS HELPFUL

ASSUMPTIONS IN MODEL MUST BE ACCEPTED BY INDUSTRIAL COMMUNITY

- IN GENERAL INDUSTRY SKEPTICAL OF MATHEMATICAL MODELS' ACCURACY IN PREDICTION OF PHYSICAL WORLD
- SKEPTICISM WILL ONLY BE OVERCOME BY SUCCESS OF MODEL IN MAKING VIABLE SIMULATIONS
- ONCE ACCEPTED NO OTHER ALTERNATIVE (SUCH AS "HAND WAVING") WILL BE ACCEPTED

CONCLUSIONS & FINAL COMMENTS

- IN GENERAL, AEROSPACE COMMUNITY IS SKEPTICAL OF BATTERY MODELS
  - TEND TO RELY ON HARD EXPERIMENTAL DATA
  - MODELS TEND TO BE "AFTER THE FACT" AND ONLY TRACK EXPERIMENTAL RESULTS
- MODELS ARE USEFUL IN ORGANIZING ENGINEERING AND SCIENTIFIC DATA IN A LOGICAL SEQUENCE, BUT
  - BATTERY ENGINEERS LACK MATHEMATICAL BACKGROUND TO FOLLOW MECHANISMS
  - PREDICTION SUCCESS NEEDS IMPROVEMENT
- ANY PREDICTION BY A MODEL MAY TAKE YEARS TO QUALIFY AND BE ACCEPTED

Nickel-Cadmium Session

GOOD AND BAD FEATURES OF Ni-Cd CELL DESIGNS

Sidney Gross

Northwest Engineering Consultants
7201 - 26 Ave. N. E.
Seattle, WA 98115
Tel. 206-522-2223

OUTLINE

CORROSION
ELECTROLYTE MANAGEMENT
OXYGEN REDUCTION
NITRATE ION
MATERIALS
PERFORMANCE

CREDITS

Baars
Baumgartner
Billerbeck
Casey
Fleischer
Jyas
Lim
Lunn
Maurer
McDermott
Ohta
Okada
Vaidyanathan
Verzwyvelt

THE GOOD AND THE BAD

In brief, bad designs and processes for spacecraft Ni-Cd cells are those have been used in the past, and good ones are those we should be using in the future. Bad designs and processes are those that are difficult to control closely or which associated with them employ processes that are injurious to long life. As will be shown in following charts, both chemical impregnation (CI) and electrochemical impregnation (EI) qualify as being "bad". Mechanical impregnation, which involves neither nitric acid nor nitrates is superior, and can be done in a variety of ways.

The substrates used are not in themselves harmful, but are considered to be "bad" if their pore structure is so small and of a type that it requires CI or EI. Metal coated plastic fibers, as in FNC, are "good", as well as some other fibers, felts, foams, and some newer structures.

THE GOOD AND THE BAD
(For Spacecraft)

"BAD" IMPREGNATION

- Chemical Impregnation (CI)
- Electrochemical Impregnation (EI)

GOOD IMPREGNATION

- Pasting
- Vibration dipping in slurry
- Plastic bonding (Cd only)

"BAD" SUBSTRATE

- Any very small pore nickel requiring CI or EI (sinter, super fiber, etc.)

GOOD SUBSTRATE

- FNC (fibrous nickel-cadmium)
- Some other fibers/felts
- Some foams

CORROSION

Corrosion of the nickel sinter or substrate can occur during chemical impregnation or during cycling. Theoretically, it can be prevented during electrochemical impregnation, but in practice some does occur there as well. Some of the problems that result are listed.

CORROSION:

a) FROM ACID DURING CHEMICAL IMPREGNATION

b) FROM DEPASSIVATION BY NO_3^-, Cl^-, & CO_3^{-2} DURING CYCLING

1. *VOLTAGE DEPRESSION'* - Helps form Ni_5Cd_{21}, creating voltage depression.
2. *Ni SWELLING & SEPARATOR DRYOUT'* - Extra capacity plus weakening helps enable thickening of the Ni electrode.
3. *OVERCHARGE PROTECTION'* - The source of oxygen is reduction of $Cd(OH)_2$ to Cd. Reduces overcharge protection, creates cell unbalance.
4. *WEAKENING'* - Electrode structure is weakened.
5. *RESISTANCE'* - Add electrical resistance, increases polarization, more heat generation.
6. *CELL MISMATCH'* - Cell mismatch results from unequal increase in positive capacity.
7. *NO COBALT'* - Ni active material produced contains no Cobalt.
8. *KOH CONCENTRATION'* - Some water is consumed, increases KOH concentration, can reduce life.

NICKEL CORROSION DURING CHEMICAL IMPREGNATION

Corrosion during CI is caused by attack of the nickel by the nitric acid present. The hydroxyl ions so produced are either neutralized by the nitric acid or react to directly form nickel hydroxide.

NICKEL CORROSION DURING CHEMICAL IMPREGNATION

$$4\,Ni + HNO_3 + 6\,H_2O \longrightarrow 4\,Ni^{+2} + NH_3^{+} + 9\,OH^{-}$$

$9OH^-$: Either neutralized by HNO_3

or

directly forms $Ni(OH)_2$

***Mechanical Impregnation*: No acid, no nitrate, no corrosion.**

CORROSION DURING CHEMICAL IMPREGNATION

Two especially serious results of corrosion during CI are accelerated thickening of the cadmium electrode, and creation of nickel ions which are the precursor to the formation of Ni_5Cd_{21}. This intermetallic material is the principal cause of voltage depression in the cadmium electrode toward the end of discharge.

For the nickel electrode, corrosion weakens the structure, and also adds more active material within each pore. Discharge results in a volume increase of the active material. The weakened structure is less able to tolerate this volume increased, especially since some of the pore volume is now occupied by newly created active material. These are important causes of thickening due to corrosion during CI.

To minimize corrosion during impregnation, plates sometimes are partially oxidized. A compromise must be struck between too much and too little. Though this is helpful, corrosion still occurs during CI.

CORROSION DURING CHEMICAL IMPREGNATION

Nickel Electrode - - **Helps enable electrode thickening**

Cadmium electrode - - **Helps form Ni_5Cd_{21}, creating voltage depression**

VOLTAGE DEPRESSION ARISING FROM CHEMICAL IMPREGNATION

Voltage depression during the latter part of discharge of Ni-Cd cells is sometimes referred to as a second plateau. When a reference electrode is used and voltages of both the nickel electrode and the cadmium electrode are obtained, it becomes clear that the cadmium electrode is the source of the voltage depression. This has been shown to be the result of the formation Ni_5Cd_{21} and is a result of the use of chemical impregnation.

VOLTAGE DEPRESSION ARISING FROM CHEMICAL IMPREGNATION

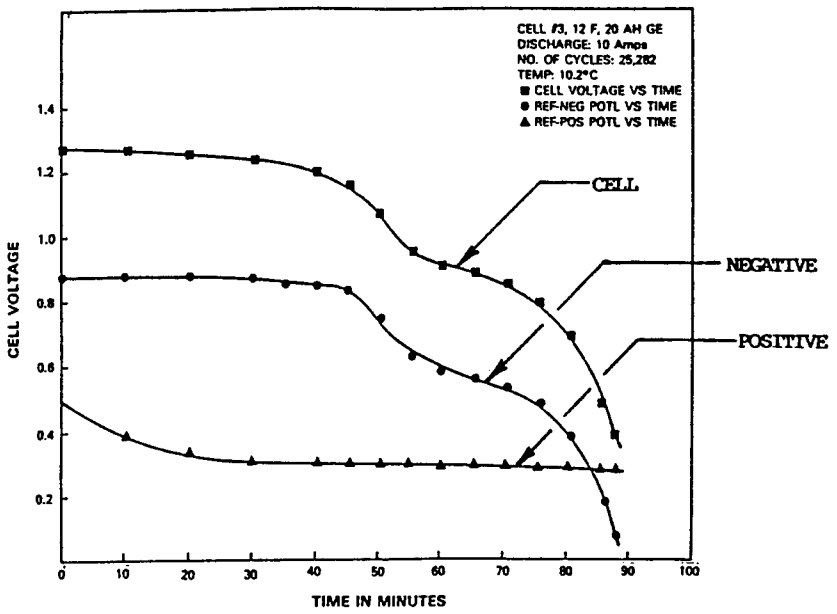

NICKEL CORROSION DURING CYCLING

Nickel does not corrode in KOH unless there are ionic impurities present. Key among these depassivating ions in Ni-Cd cells are nitrate, chloride, and carbonate ions. Nitrate ions cannot be completely washed out following chemical impregnation, and carbonate enters due to exposure of the plates wetted with KOH to the atmosphere. Some chloride ions can also find their way into the cells. It has also been found that once corrosion has occurred, further corrosion occurs much more readily.

By contrast, there usually is no corrosion of nickel during cycling when mechanical impregnation is employed. This is due to the fact that no depassivating ions need be used in the impregnation slurry or paste.

NICKEL CORROSION DURING CYCLING

$$Ni + 1/2\ O_2 + H_2O \text{ ----------> } Ni(OH)_2$$

***Chemical Impregnation*: Corrosion assisted by presence of NO_3^-, Cl^-, and CO_3^{-2}**

***Mechanical Impregnation*: Usually no corrosion. Depassivating ions not present in best designs.**

CORROSION WEAKENS NICKEL SUBSTRATE

As would be expected, the greater the amount of corrosion of the nickel substrate, the weaker the substrate becomes. However, strength is important in resisting forces which tend to thicken the electrode.

CORROSION WEAKENS NICKEL SUBSTRATE

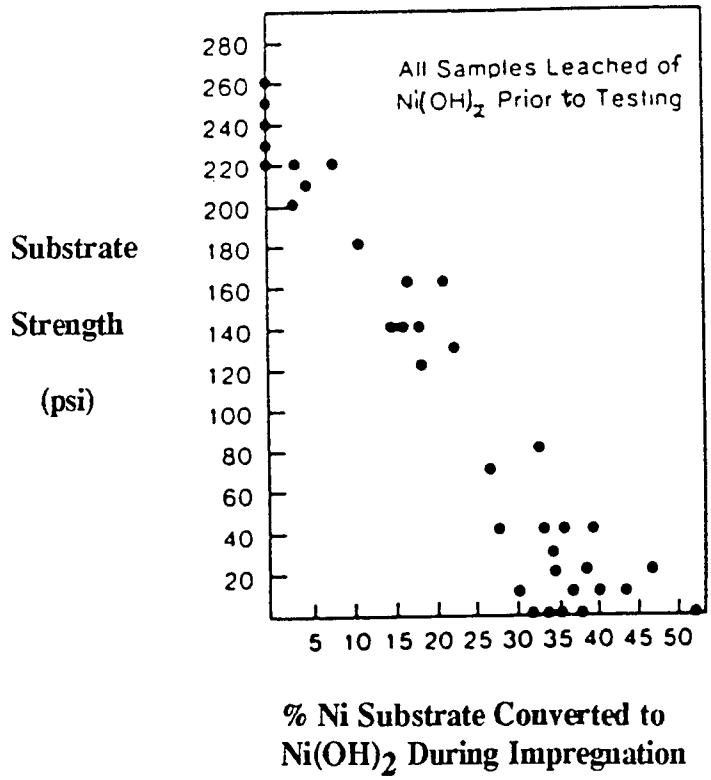

SWELLING OF CI NICKEL ELECTRODES

Swelling of sinter-based electrodes shown here, whether impregnated chemically or electrochemically, has long been a problem. Swelling is worse on heavily loaded plates, and on sinter plaques that have been weakened by corrosion from chemical impregnation.

Some mechanically impregnated electrodes will also swell. Of all the available technologies, FNC electrodes appear to have the least problems with swelling due to the combinations of the ability to load electrodes precisely, the lack of corrosion during impregnation, the high strength of the fiber structure, and the ability for elastic flexing as opposed to stretching or breaking.

SWELLING OF CHEMICALLY IMPREGNATED NICKEL ELECTRODES

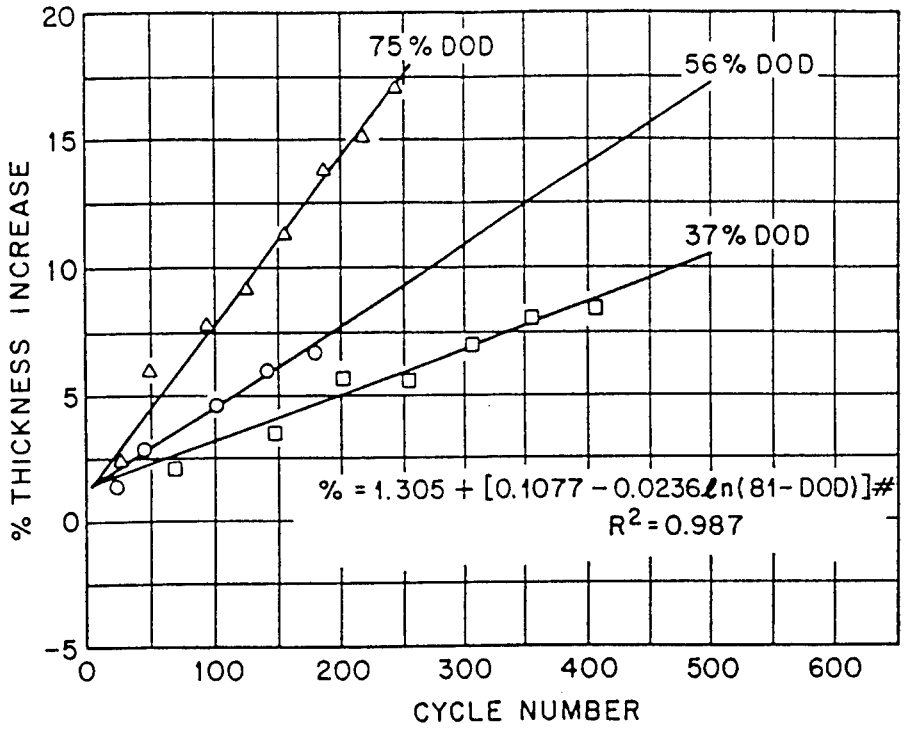

ELECTROLYTE GOING TO POSITIVE ELECTRODE DRYS OUT SEPARATOR

The amount of electrolyte in the separator diminishes with operating time of cells. This is a direct result of the expansion of the positive electrode. Having a finer pore size distribution than the separator, the swollen positive electrodes rob the separator of some of its electrolyte, even drying it out in worst cases.

ELECTROLYTE GOING TO POSITIVE ELECTRODE DRYS OUT SEPARATOR

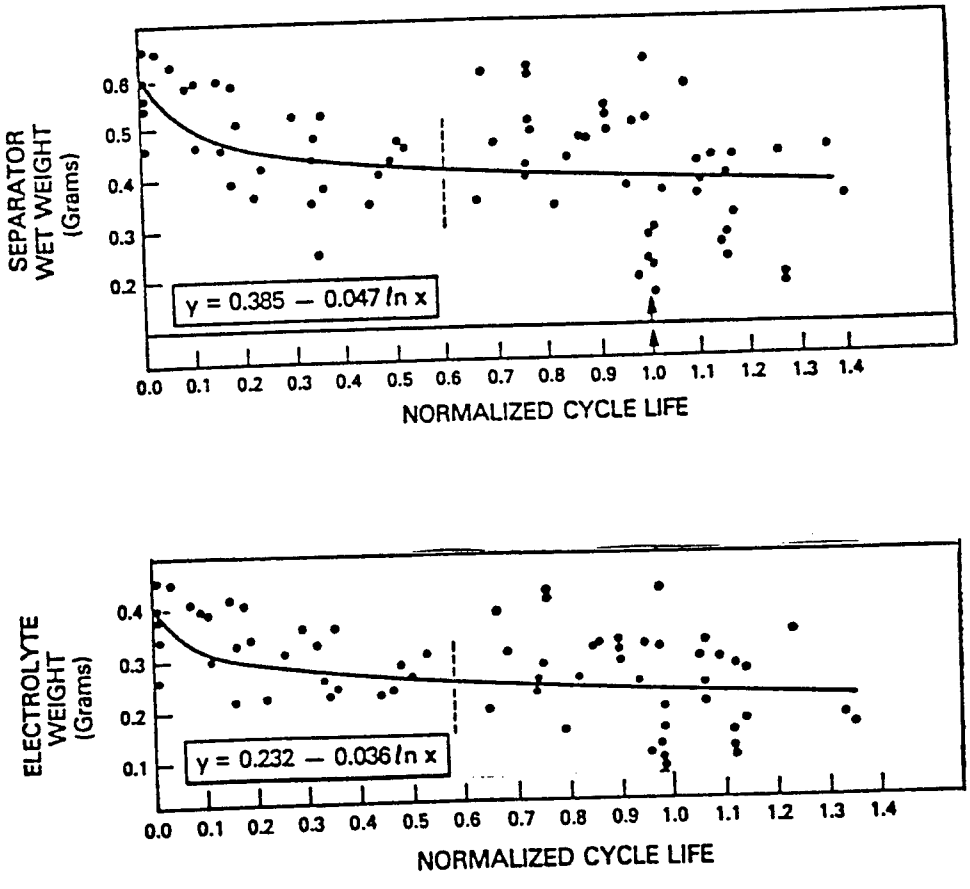

INHERENT BAD ELECTROLYTE MANAGEMENT OF PELLON SEPARATOR

As a consequence of the different capillarity of nickel electrodes versus pellon separator, the separator drys out much sooner than the positive electrode as the available electrolyte in the cell diminishes. This is the exact opposite of what is best. The ideal situation is for the separator to dry out last, for a cell cannot function with no electrolyte in the separator, but it can function when the electrolyte in the electrodes is reduced.

INHERENT BAD ELECTROLYTE MANAGEMENT OF PELLON SEPARATOR

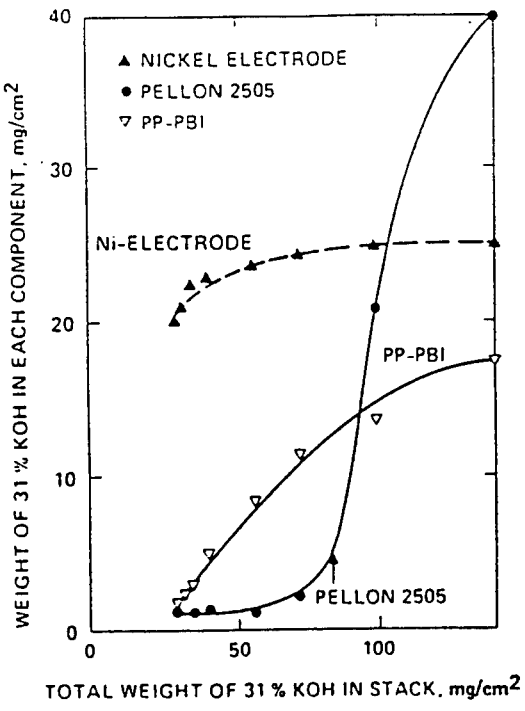

ELECTROLYTE MANAGEMENT CAN BE MARGINAL WITH SINTER CELLS

Data from this group of cells has produced a correlation between early failures and low amount of electrolyte in the cell. There is only a small difference in electrolyte quantity between success and failure. The cell manufacturer cannot correct the problem by adding more electrolyte, for the cells would exceed their high pressure limits if they would do so. With the allowable margin for error being very small and with a manufacturing process that is inherently difficult to precisely control, one can expect that problems like this might occur from time to time.

ELECTROLYTE MANAGEMENT CAN BE MARGINAL WITH SINTER CELLS

Data from Gates 50 AH Cell Separator Qual Tests show that early failures resulted from cells with electrolyte quantity on the low side.

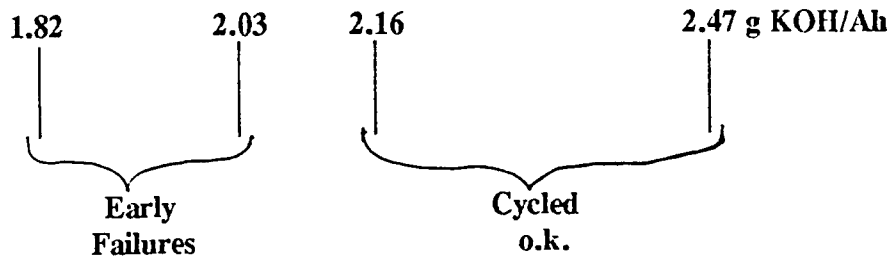

CONVENTIONAL: KOH AMOUNT IS RESTRICTED TO LIMIT PRESSURE

The cell test data shown here are not for aerospace cells, but they illustrate the principle. As electrolyte content in cells is increased, the cell pressure observed during overcharge increases. To avoid excessive operational pressure under worse case conditions, the amount of electrolyte must be limited. A typical limit is shown. For best electrical performance of the cell, however, it would be best if considerably more electrolyte could be added. That is not practical with the presently design sinter cells because of the limited rates of oxygen reduction. Thus, to achieve the goal of the use of a greater amount of electrolyte, a better means for oxygen reduction must be found. That requires turning one's back on the old technology, and the development of new technology.

CONVENTIONAL: KOH AMOUNT IS RESTRICTED TO LIMIT PRESSURE

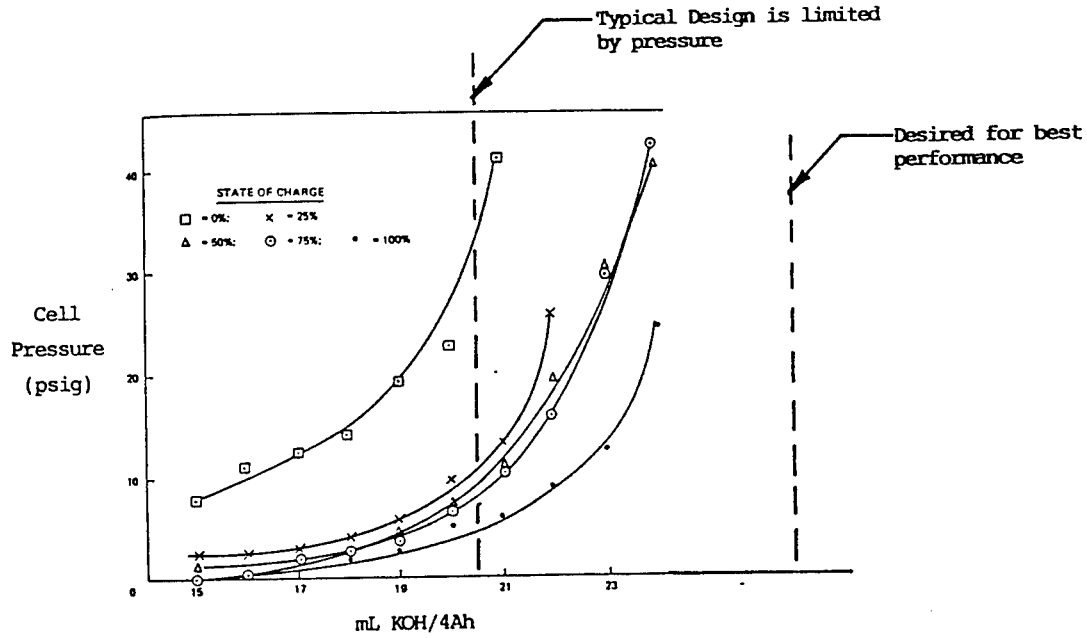

PHYSICAL SYSTEM REQUIRED FOR ELECTROCHEMICAL O_2 REDUCTION

The basic requirement for oxygen reduction is that oxygen come in contact with a metal that is wetted with KOH, and that the metal be connected electrically to the cadmium electrode. Thus, there are numerous methods available to implement these basic requirements.

PHYSICAL SYSTEM REQUIRED FOR ELECTROCHEMICAL O_2 REDUCTION

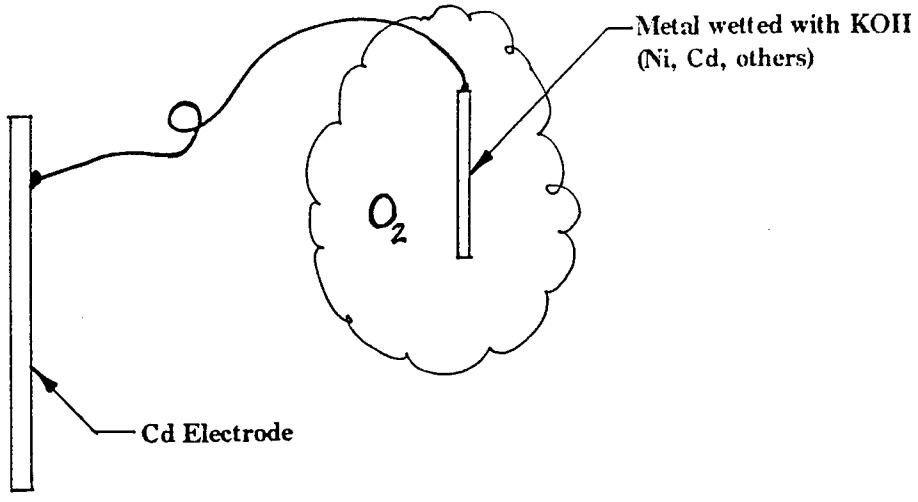

SINTERED Ni-Cd CELL IMPLEMENTATION OF O_2 REDUCTION

The method of implementation commonly used for oxygen reduction is shown below. Oxygen is transported from the nickel electrode to the cadmium electrode through a porous separator with an open, large pore size structure. Metal spots on the cadmium electrode are the sites for oxygen reduction. Only a small fraction of the total metal in the electrode participates in oxygen reduction.

SINTERED Ni-Cd CELL IMPLEMENTATION OF O_2 REDUCTION

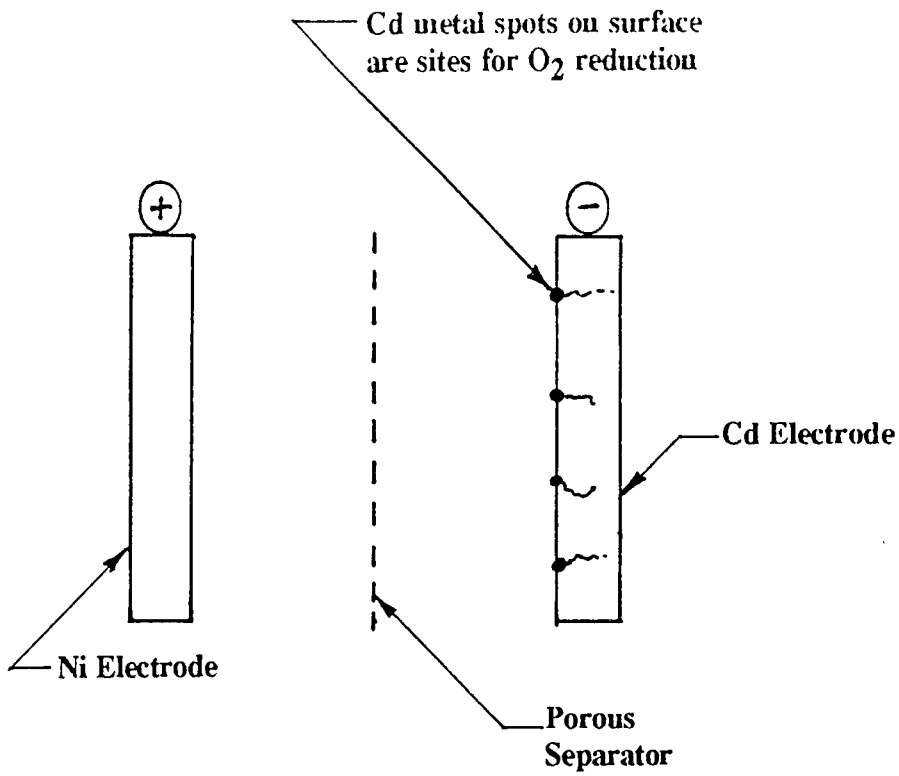

IMPLEMENTATION OF ADVANCED O_2 REDUCTION DESIGN (FNC)

Only one company offers spacecraft Ni-Cd cells with an advance design for oxygen reduction. That is ACME, which uses FNC technology, and at the same time employs mechanical impregnation, which we want. Based on an early suggestion by Baars, the Ni-plated plastic fibers used in the substrate are placed in the center of split negative electrodes. The pore size of the insert is large, so it does not easily flood, even though considerably more electrolyte is used than with conventional sinter cells. In spite of the large amount of electrolyte, this oxygen reduction system is so efficient that cells typically operate with negative pressure during overcharge.

IMPLEMENTATION OF ADVANCED O_2 REDUCTION DESIGN (FNC)

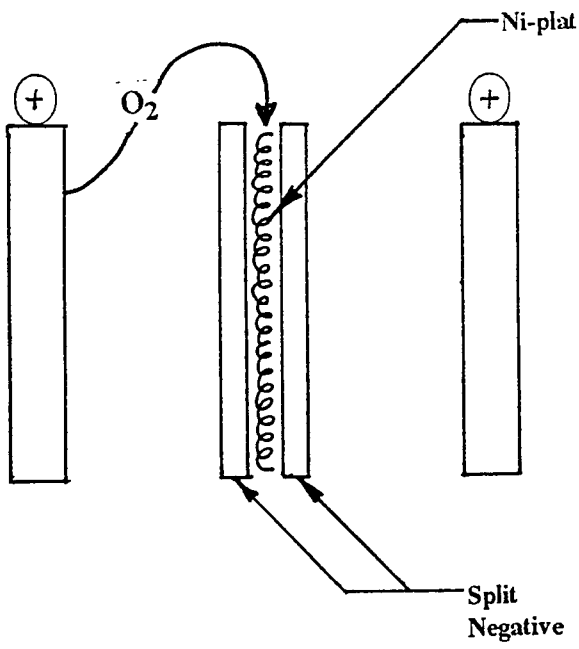

Design Allows:

- o Much greater amount of KOH
- o Very low pressure

*Baars (1958) proposed Ni gauze

COMPARISON OF O_2 REDUCTION – SINTER vs. FNC

Although typically the FNC design operates below one atmosphere, hence has negative pressure, a worse case design condition will have pressures close to one atmosphere. By contrast, sinter technology is usually not less then ten atmospheres for worst cases. When one considers conditions outside the normal specification that might arise during an anomaly, then the pressure for both designs would be increased, but might be catastrophic for the sinter design.

The advance design permits a lighter weight battery and much tolerance for extreme conditions. However, as useful as that may be, the key advantage it offers is that it enables the use of a large quantity of electrolyte.

COMPARISON OF O_2 REDUCTION – SINTER vs. FNC

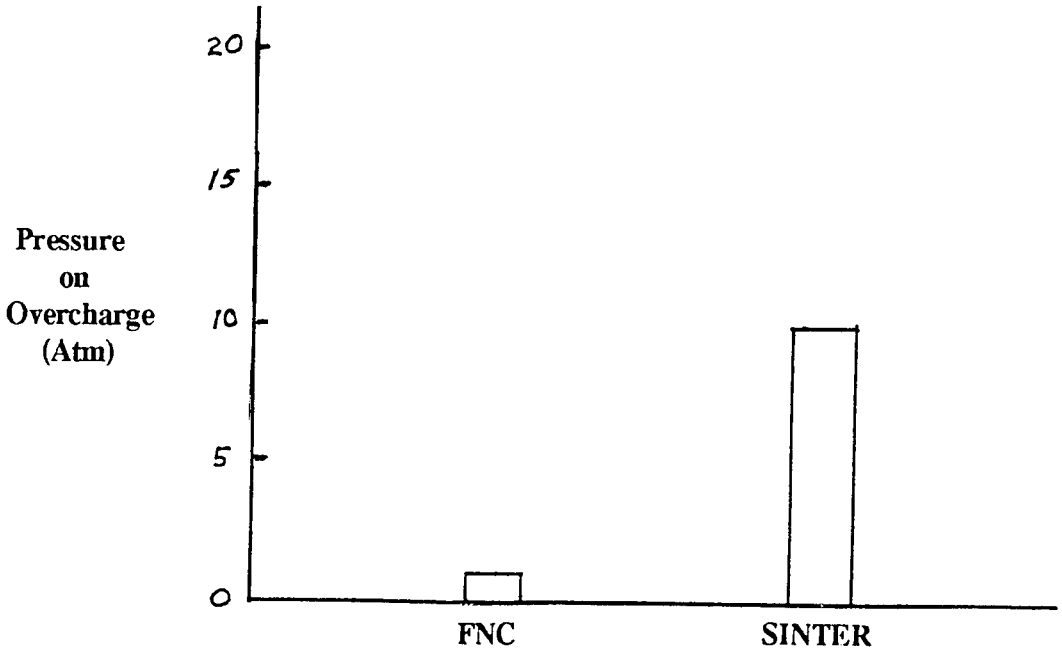

SUMMARY OF EFFECTS OF IMPROVED O_2 REDUCTION

Cell designs with advanced oxygen reduction have roughly nine important advantages over sinter technology. A key factor is that the advanced technology separates the functions of oxygen reduction and cell performance. Compromise is not needed between these two important requirements. An open-structure separator is not needed, which permits the use of a separator with tiny pores that will practically stop cadmium migration. Non-Nylon separator does not degrade and can be made in wettable versions. Since the cell performance is not very sensitive to the amount of electrolyte used, a much larger quantity can be used than in classical sinter cells. The problem of varying amount of electrolyte from cell to cell is eliminated. Separator dryout is also eliminated, and electrical performance and thermal performance are much improved.

SUMMARY OF EFFECTS OF IMPROVED O_2 REDUCTION

BASIC CONSIDERATIONS

1. Sinter cells require compromise between O_2 reduction and performance/life
2. Advanced technology separates these two functions. Compromise not needed.
3. Open-structure separator not needed.

PERFORMANCE

4. Non-Nylon separator doesn't degrade;with tiny pores, practically stops Cd migration.
5. Fast O_2 reduction, invariant with life. Pressure usually is negative.
6. Design not much sensitive to electrolyte amount. Large quantity can be used.
7. Variable amount of electrolyte cell-to-cell eliminated.
8. Separator dryout problem is avoided.
9. Electrical performance is improved.

NITRATE BATH CORRODES NICKEL

Though it is recognized that the nitric acid used in chemical impregnation is corrosive to nickel, it is not always recognized that nitrate compounds are also corrosive. This is an important principle, because whether the impregnation process is chemical or electrochemical, it is very difficult, perhaps impossible, to remove all the nitrate from the bath. Thus, corrosion can occur even after the impregnation has long been completed. In the example shown, the nickel hydroxide comes from two sources. One is from the conversion from nickel nitrate. The second is from corrosion of the nickel, which as shown here can be the greater of the two.

NITRATE BATH CORRODES NICKEL

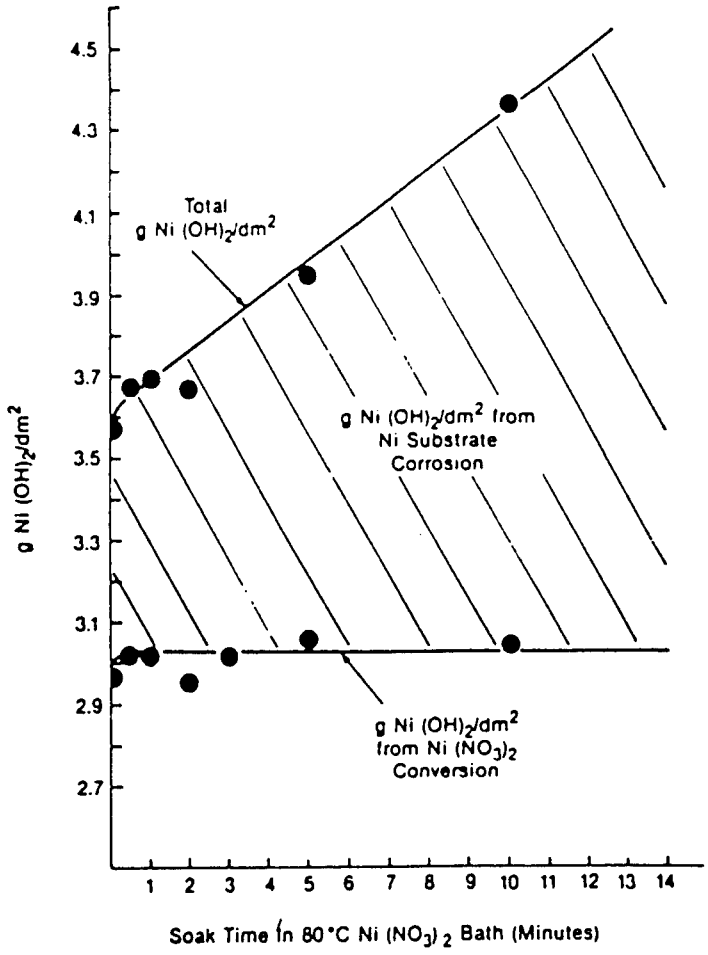

THE NITRATE SHUTTLE

In addition to the encouragement of corrosion, nitrate remaining within the cell is very detrimental to self discharge. That occurs through a mechanism known as the Nitrate Shuttle, discovered by Casey. The process starts at the cadmium electrode with nitrate ion discharging part of the electrode by reaction with metallic cadmium. The biproduct nitrite ion shuttles across to the nickel electrode where it reacts with the charged species to discharge it. This regenerates the nitrate ion, which then is free to continue the process. With a shuttle process, the nitrate ion is not consumed and continues unobstructed its nefarious work of slowly discharging the Ni-Cd cell.

THE NITRATE SHUTTLE

Nitrate discharges the cadmium electrode:

$$NO_3^- + Cd + H_20 \text{ ----------> } Cd(OH)_2 + NO_2^-$$

Nitrite discharges the nickel electrode:

$$NO_2^- + NiOOH + H_2O \text{ ----------> } Ni(OH)_2 + NO_3^-$$

NITRATE ION REDUCES CHARGE RETENTION IN Ni-Cd CELLS

This figure shows two examples of the nitrate shuttle obtained by addition of small amounts of nitrate ion in the cell. The reference line shows no nitrate addition. The two curves showing a loss of capacity with time are for the addition of silver nitrate and potassium nitrate, 0.005 and 0.007 M, respectively. It is clear that it is only a matter of time when the nitrate shuttle will completely discharge the cell. The message, of course, is that this problem can be avoided by using a mechanical impregnation process that does not use nitrates.

NITRATE ION REDUCES CHARGE RETENTION IN Ni-Cd CELLS

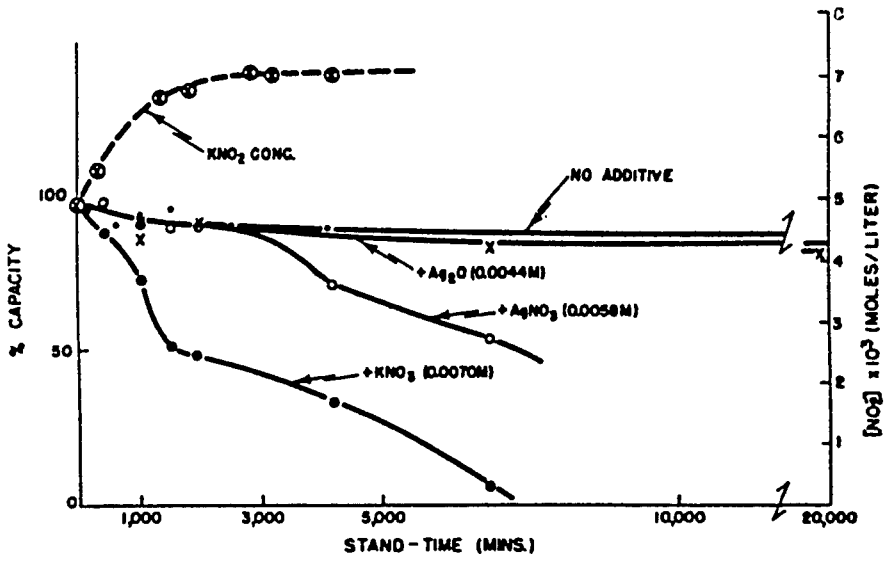

WEIGHT LOSS OF NYLON SEPARATOR IN 34% KOH

In the earliest days of the space program, a thorough study was made of candidate separators for sealed Ni-Cd cells by Gould. This study gave low marks to Nylon because of its poor stability. None the less, the study acknowledged that Nylon could be used, for most of the other candidates had their shortcomings, too. The industry therefore made a poor start with Nylon and never did much to improve the situation. Bell Laboratories also conducted early tests showing the limitations of Nylon. The data shown here by Lim shows Nylon instability at elevated temperature, and when these data are extrapolated to room temperature they show there are problems at that temperature, also.

WEIGHT LOSS OF NYLON SEPARATOR IN 34% KOH

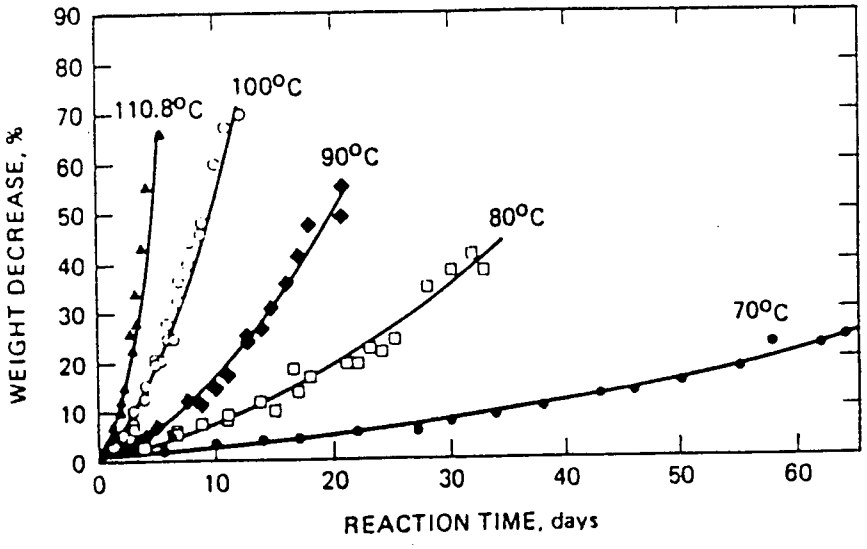

CARBONATE INCREASE WITH ECLIPSE SEASON

When Nylon degrades, one of the by-products is carbonate ion. People have long played games with carbonate contamination, and seem to have become used to it in cells. In the few occasions where nearly carbonate free cells were made and tested, however, the cells had very long lifetimes, though no doubt other factors contributed to that. The data here show that the carbonate buildup is hardly a trace impurity, and implies that there has been a significant degradation of the Nylon separator to produce this much carbonate.

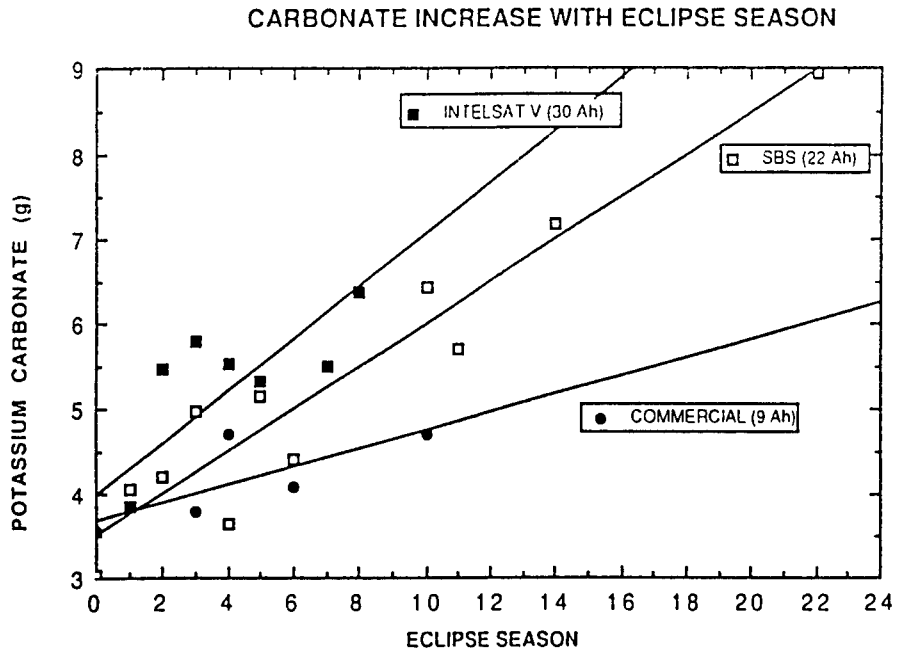

POROUS SEPARATORS ALLOW HYDRAULIC TRANSPORT OF Cd

Operation of the sealed Ni-Cd system results in a cyclic release and return of water to the nickel electrode. Nothing similar to that occurs at the cadmium electrode, except that during the time water is being generated, the cadmium electrode is becoming more porous and can absorb some of the excess electrolyte. The net effect is a back and forth sloshing of liquid between the two electrodes, passing each time through the open network separator. When this process is observed in time-lapse photography, as was done at WPAFB, it is reminiscent of the waves produced by a wave-making machine. Cadmium particles can clearly be seen quickly carried about by this hydraulic transport mechanism.

POROUS SEPARATORS ALLOW HYDRAULIC TRANSPORT OF Cd

Water Release and Return -- $Ni(OH)_2 + OH^- \underset{\text{Disch}}{\overset{\text{Chg}}{\rightleftharpoons}} NiOOH + H_2O + e^-$

Change in porosity of negative -- $Cd(OH)_2 + 2e^- \underset{\text{Disch}}{\overset{\text{Chg}}{\rightleftharpoons}} Cd + 2OH^-$

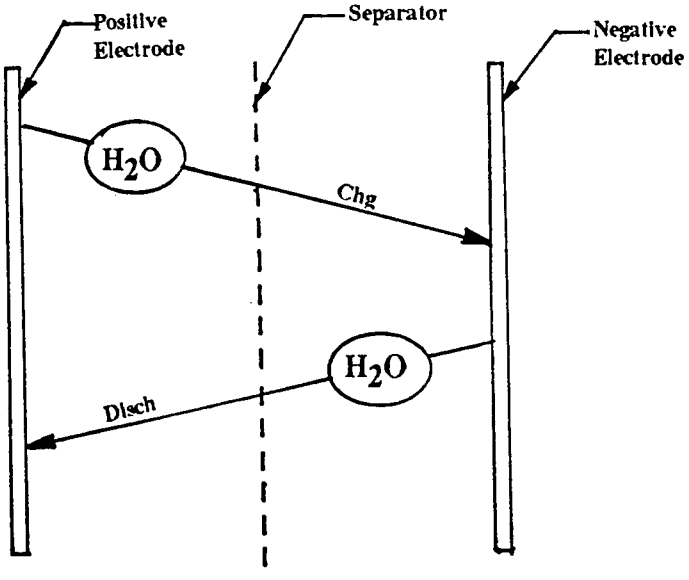

DENSITY OF NICKEL HYDROXIDE ACTIVE MATERIAL

As research continues to push the energy density of the Ni-Cd system closer to its limit, not in aerospace, but in other endeavors, many problems arise that must be overcome. One of the ways to overcome some of the problems is the use of suitable additives. In this figure, we see that the addition of Zn and Cd to nickel hydroxide is useful in helping to stabilize density of active material with cycling. This is only an example, however, to point out the use of additives in improving the technology.

When impregnation of active material is by either chemical or electrochemical impregnation, there is no way additives can be mixed uniformly with the nickel hydroxide or cadmium hydroxide that are produced. This can be a brick wall to progress. By contrast, mechanical impregnation is ideally suited to the incorporation of additives.

DENSITY OF NICKEL HYDROXIDE ACTIVE MATERIAL

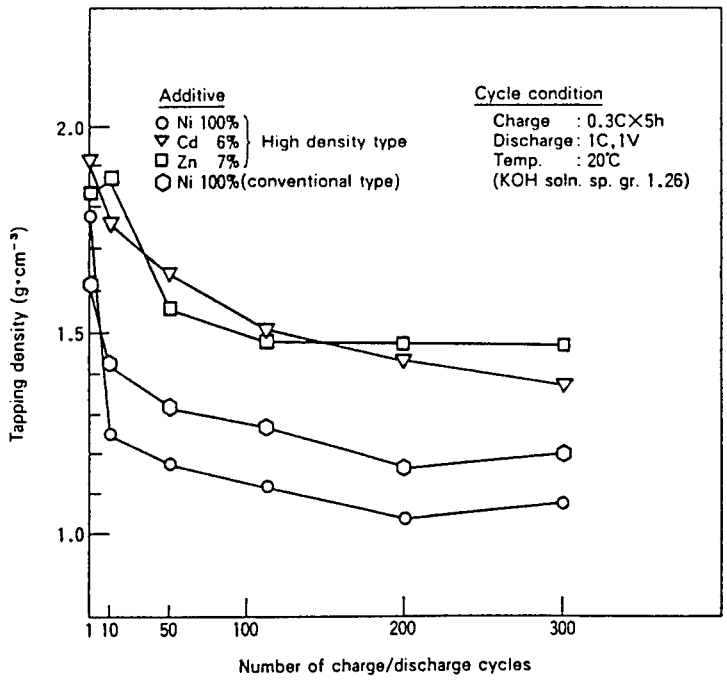

SUCCESSIVE CHEMICAL IMPREGNATION OF NICKEL ELECTRODES

Chemical impregnation is a step loading process in which the amount of loading is a function of the number of steps used. That means that it is difficult to precisely load to a predetermined amount. The problem becomes even more difficult when it is noted that the utilization efficiency with CI is also not highly predictable. Thus, you can get somewhere near the capacity you want with chemical impregnation, but don't have high standards.

SUCCESSIVE CHEMICAL IMPREGNATION OF NICKEL ELECTRODES

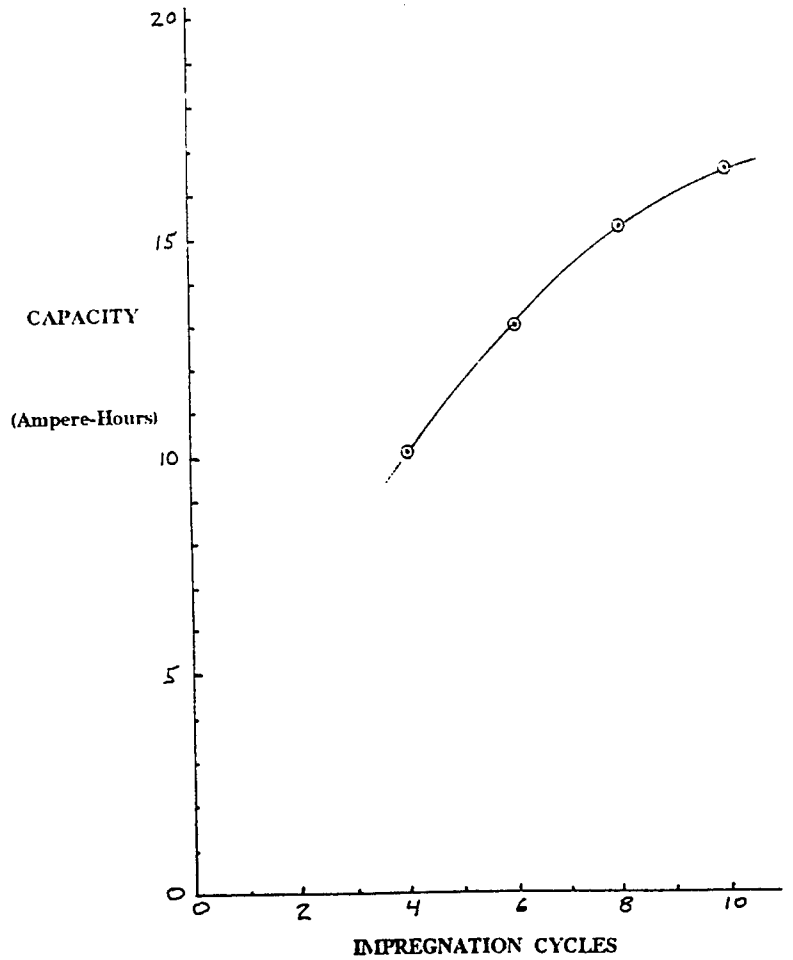

PRECISE LOADING WITH MECHANICAL IMPREGNATION

Mechanical impregnation is capable of loading fairly precisely. Since for some processes the utilization efficiency is close to 100%, it is possible to manufacture electrodes very close to the desired capacity.

An important factor is that the substrate used can have a known, well controlled porosity. This is impregnated with a liquid slurry or paste of known water/solids content. Loading of active material is therefore accurately known. When the water is removed by drying, the expected loading level is closely confirmed by weighing or chemical analysis.

PRECISE LOADING WITH MECHANICAL IMPREGNATION

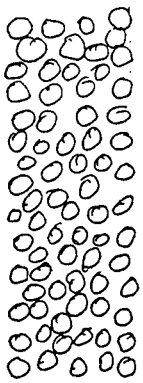

Substrate of known, well controlled porosity is used.

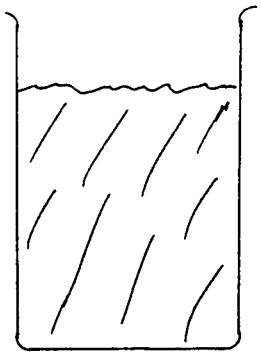

Liquid slurry or paste of known water/solids content is impregnated into substrate.

Water removed by drying. Loading is accurately known.

PRE-MANUFACTURED $Ni(OH)_2$ IS BEST

The technology associated with the nickel hydroxide used for mechanical impregnation is a whole science unto itself. Much progress have been made in this area. One of the advances is the development of processes to manufacture the powder with spherically shaped particles, this having been found to have superior properties for loading. Another advance has been the development of ways to incorporate cobalt compounds very evenly in each particle, which improves performance. In this regard, the technology has moved beyond the old fashioned cobalt hydroxide and uses mixtures of various cobalt oxides, hydroxides and metal. Similarly, zinc and cadmium metal additions can be useful, and can also be pre-incorporated, again being done very uniformly. Pre-incorporation not only assures a precise mixture of additives, but it eliminates some of the preparation steps at the battery plant, including the need for waste water and its treatment. Of course, all these advances are unavailable for chemical or electrochemical impregnation processes.

PRE-MANUFACTURED $Ni(OH)_2$ IS BEST

- Spherical geometry is superior
- Cobalt compounds pre-incorporated
- Zn and/or Cd pre-incorporated
- High capacity, >90% theoretical
- Waste water problems eliminated

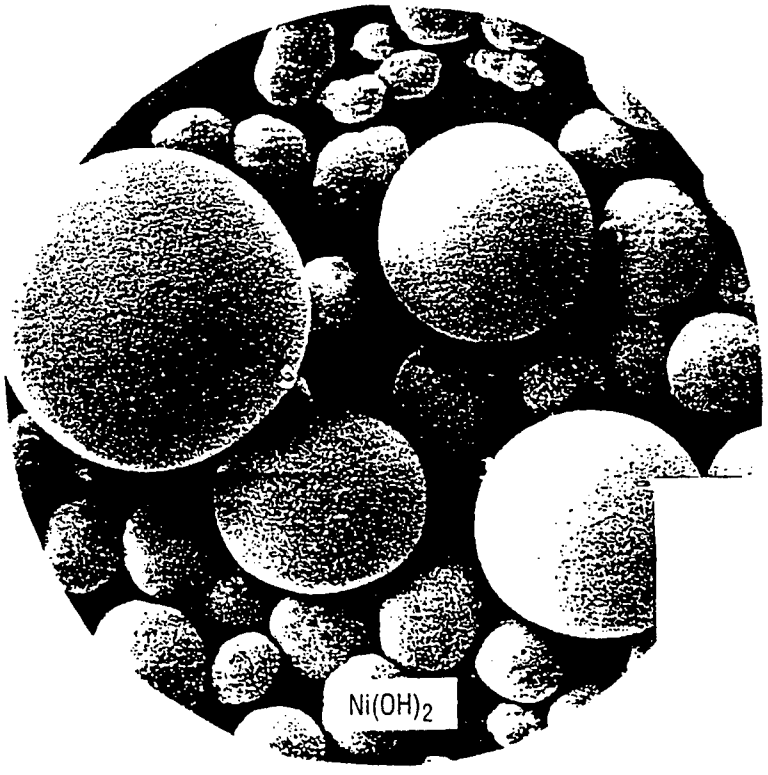

COBALT IS BEST ADDED BY COATING IT ON $Ni(OH)_2$ PARTICLES

Cobalt suboxide is a superior form of cobalt for addition to nickel hydroxide. A special process has been developed by one of the suppliers of nickel hydroxide that results in very high utilization of cobalt's benefits, using this superior form of cobalt. This involves first coating of sub-micron particles, followed by a formation charge, which incorporates the cobalt within the structure. Superior methods of cobalt addition such as this are available only to methods that use mechanical impregnation.

COBALT IS BEST ADDED BY COATING IT ON $Ni(OH)_2$ PARTICLES

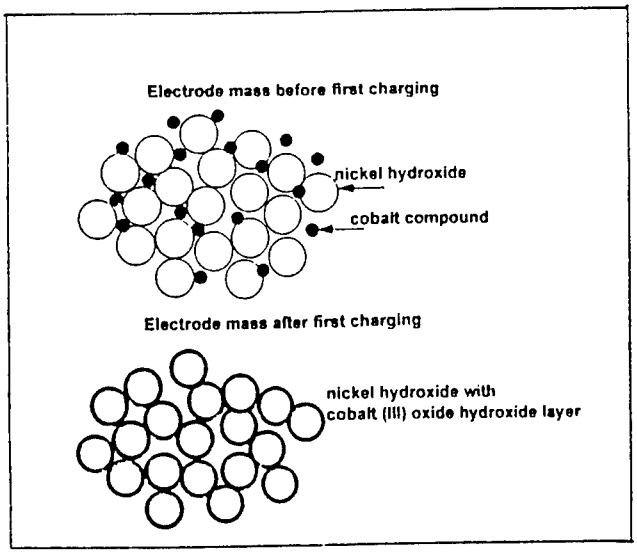

Cobalt compounds (suboxide) coat the $Ni(OH)_2$ particles during formation

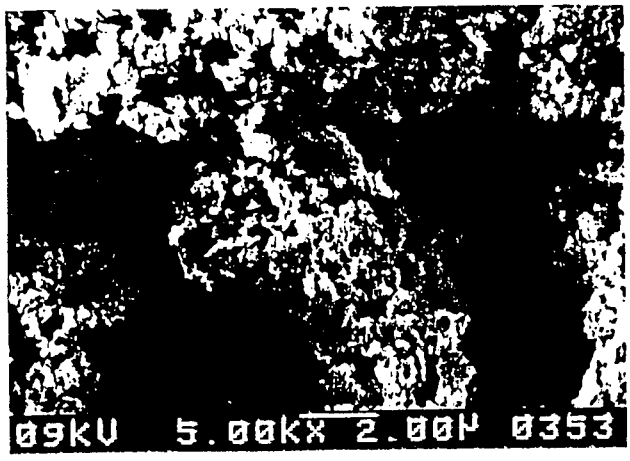

Electron micrograph of cobalt suboxide showing largely sub-micron particles

ADDITIVES TO IMPROVE UTILIZATION OF $Ni(OH)_2$ AT 45°C

High temperature operation of nickel cadmium cells can be significantly improved by the use of additives to the nickel hydroxide. This figure shows the effect of various additives at 45°C. To obtain the benefit of any additive, it must be mixed intimately with the nickel hydroxide prior to impregnation. That is readily accomplished with mechanical impregnation, but is not practical with chemical or electrochemical impregnation.

ADDITIVES TO IMPROVE UTILIZATION OF $Ni(OH)_2$ AT 45°C

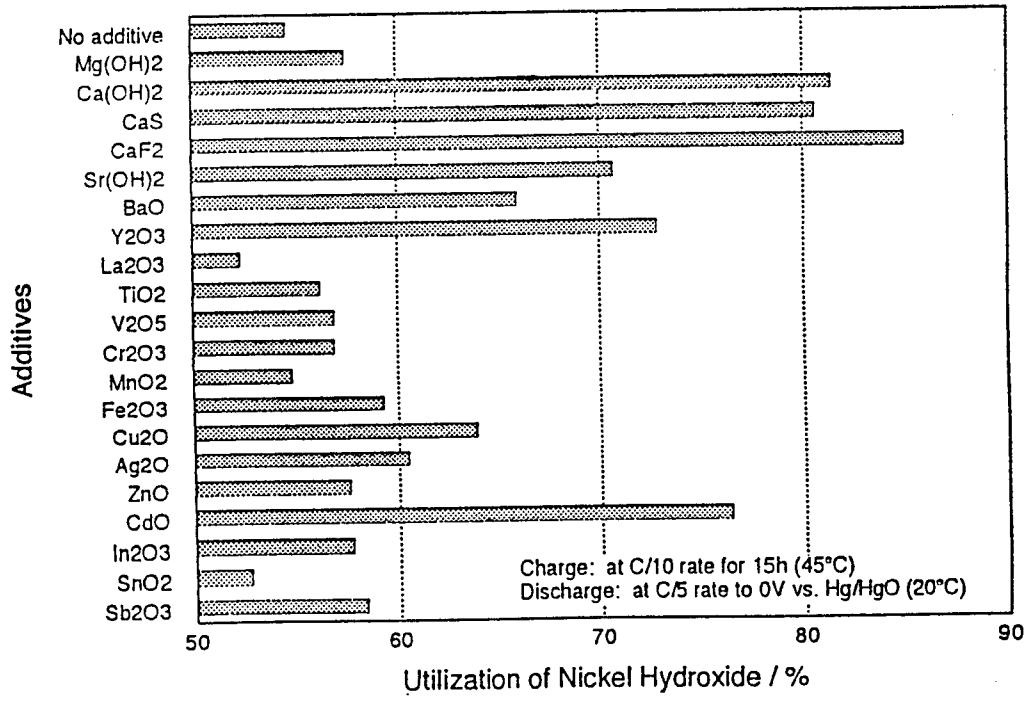

CAPACITY LOSS OF EI Ni ELECTRODES STORED DISCHARGED

Although electrochemical impregnation (EI) has some important advantages over chemical impregnation, one of its serious drawbacks is it's very poor storage performance in the discharged state. This has been a serious problem in nickel hydrogen technology, but is also a serious problem for nickel cadmium technology. There are ways around this deficiency, such as continuous trickle charged storage, but these have their disadvantages as well. The need for long storage is a basic requirement for spacecraft Ni-Cd cells, and cells made with electrochemical impregnation fall short of the mark in meeting this requirement.

CAPACITY LOSS OF EI Ni ELECTRODES STORED DISCHARGED

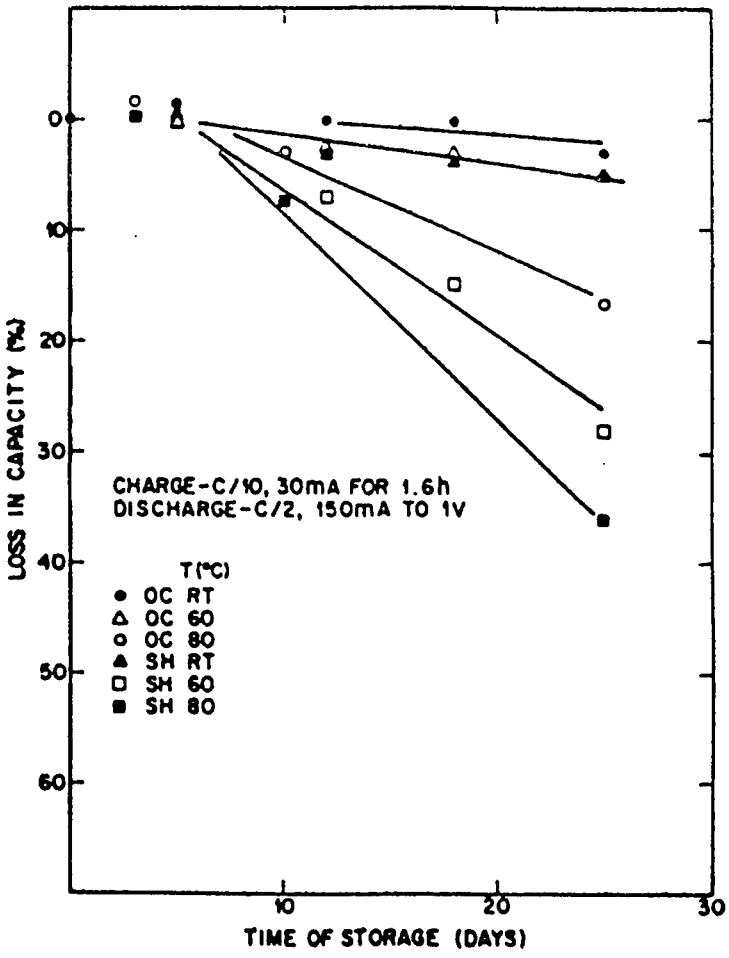

HIGH POWER PERFORMANCE OF 45 Ah Ni-Cd CELLS

High power capability is an important requirement of spacecraft Ni-Cd batteries. Unfortunately, this requirement is not always identified as such, because often it appears in association with some failure mode. During failures, it is often required that bus voltage not fall below some minimum, such as 22 volts or more at the battery when high current is drawn. This is about 1.1 volt per cell. With conventional Ni-Cd cells, this can limit the current draw to about 200 amperes. Sometimes this is insufficient. For such demands, the higher current capability of fiber nickel-cadmium technology is a distinct advantage.

HIGH POWER PERFORMANCE OF 45 Ah Ni-Cd CELLS

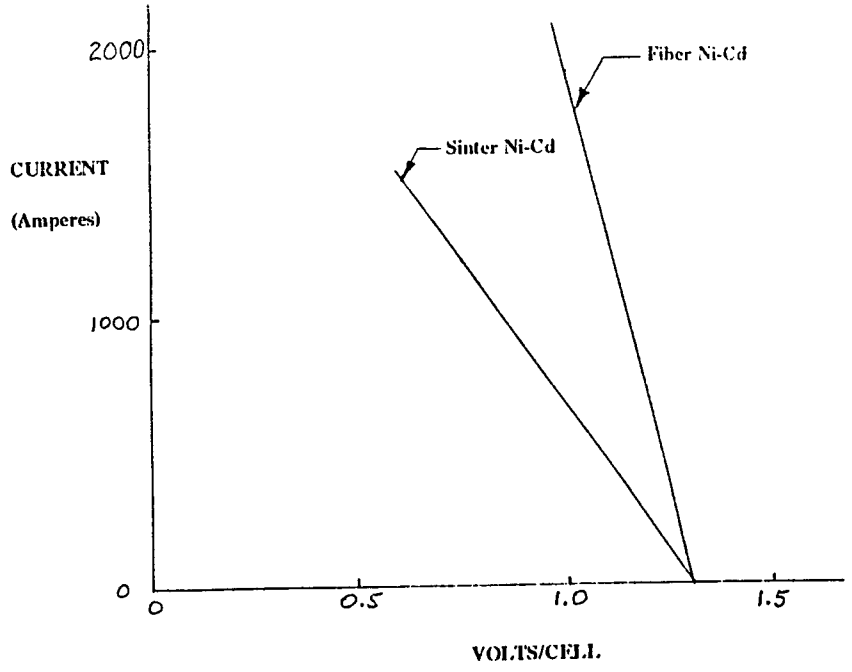

TOLERANCE TO HYDROGEN GASSING

Though it is not a common requirement for Ni-Cd cells to tolerate the generation of hydrogen gas, there are some occasions when such tolerance is important. Often this is for some failure mode or off-design condition. Design for this has not been an option in the past, because cells with this capability were not available. Today such cells are available (ACME FNC), so whether or not to use this feature is now a choice the user can make. The special electrode used is very small, so the penalty in using this is very slight.

TOLERANCE TO HYDROGEN GASSING

PROBLEM: Hydrogen can form in cells under special conditions, creating high pressure.

HYDROGEN GASSING CONDITIONS

- o Overcharge at high rate
- o Overcharge of degraded cells
- o Charge at low temp after high temp use
- o Charge at very low temp
- o Reversal of weak cell in battery

SOLUTION: For applications where this is a concern, add a special hydrogen recombination element.

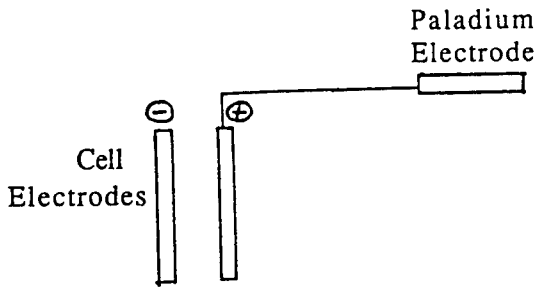

THE REACTION

$$1/2\ H_2 + OH^- \longrightarrow H_2O + e^-$$

CAPACITY INCREASE OF AA SIZE SEALED Ni-Cd CELLS

Whereas energy density of spacecraft Ni-Cd cells has remained nearly constant for the past 30 years, commercial Ni-Cd technology has made large strides in improving energy density, using mechanical impregnation. The data on this chart has not been updated, but the present capacity is about 1000 mAh. This is over a factor two improvement. Some of these gains could be applied to spacecraft cell technology, but likely only to those employing mechanical impregnation.

CAPACITY INCREASE OF AA SIZE SEALED Ni-Cd CELLS

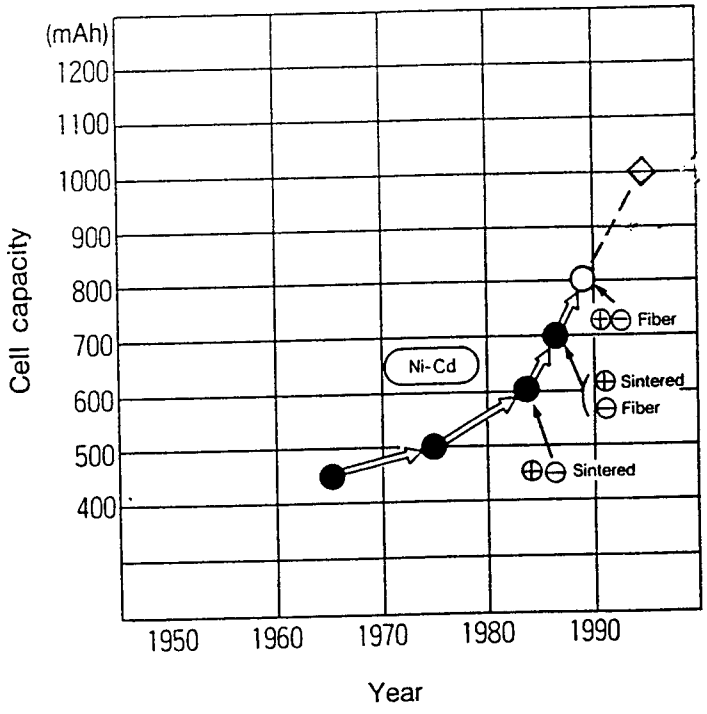

MAKING PROGRESS HAPPEN

It is clear that genuine progress in spacecraft Ni-Cd technology requires movement away from sinter technology and selecting to use mechanical impregnation technology. Reliance on the government to champion this progress almost surely will not work. The reason really is not because of small budgets, but because this is probably not the kind of thing they want to do. It doesn't sound flashy or exotic. In other words, the government most likely does not want to do this.

The answer then is that users of spacecraft batteries must control their own destiny, and do this themselves. Work with the suppliers that show good promise, and do your own testing. This need not be a costly endeavor, but nothing is free. If you have problems with setting up a program, try use of consultants.

Once you take the first step, the rest is easy.

MAKING PROGRESS HAPPEN

DON'T DEPENT ON TIIE GOVERNMENT

- o Their batting average is low
- o Ni-Cd is not exotic
- o They really don't want to seriously work Ni-Cd

DO IT YOURSELVES

- o Control your own destiny
- o Work with suppliers with advanced technology, quality people, and modern manufacturing.
- o Obtain and test their products
- o Try rigorous side by side tests
- o Look for degradation within cells as well as cyle life
- o Use good consultants

SELECTING NICD FLIGHT CELLS FOR THE NOAA/TIROS PROGRAM

USING VENDOR TEST DATA AND LIFE-CYCLE TEST DATA

Presented to
1995 NASA AEROSPACE BATTERY WORKSHOP

By
Mark R. Toft
Space Power Applications Branch
NASA Goddard Space Flight Center

November 28 - 30, 1995

INTRODUCTION

- Two 5-cell pre-acceptance test packs of Gates Aerospace Batteries (GAB) 47 AH NiCd cells (Pack 0347N from Lot 3 and Pack 0647N from Lot 6) began mission-profile life-cycle testing at the Naval Surface Warfare Center (NSWC) in Crane, IN during October 1993.
- The Lot 3 cell pack began to exhibit low charge voltage in one cell by cycle 2450 (~6 months after the beginning of cycling), following a period of reduced discharge
  - This first cell was removed from testing around cycle 2880
  - A second cell was removed for the same reason around cycle 3880 and testing was temporarily halted

INTRODUCTION - continued

- The Lot 6 cell pack began to exhibit low charge voltage in one cell by cycle 3020 (~7.5 months after the beginning of cycling), also following a period of reduced discharge
  - Subsequent and repeated divergences (despite reconditioning) made it necessary to remove three of the five cells from testing near cycle 4400.
  - The remaining two cells were combined into a single 5-cell pack with the three Lot 3 cells.
- Pack 0647N resumed mission-profile testing with a combination of Lot 3 and Lot 6 cells.
  - Two Lot 3 cells quickly diverged and pack testing was terminated after only 350 cycles.

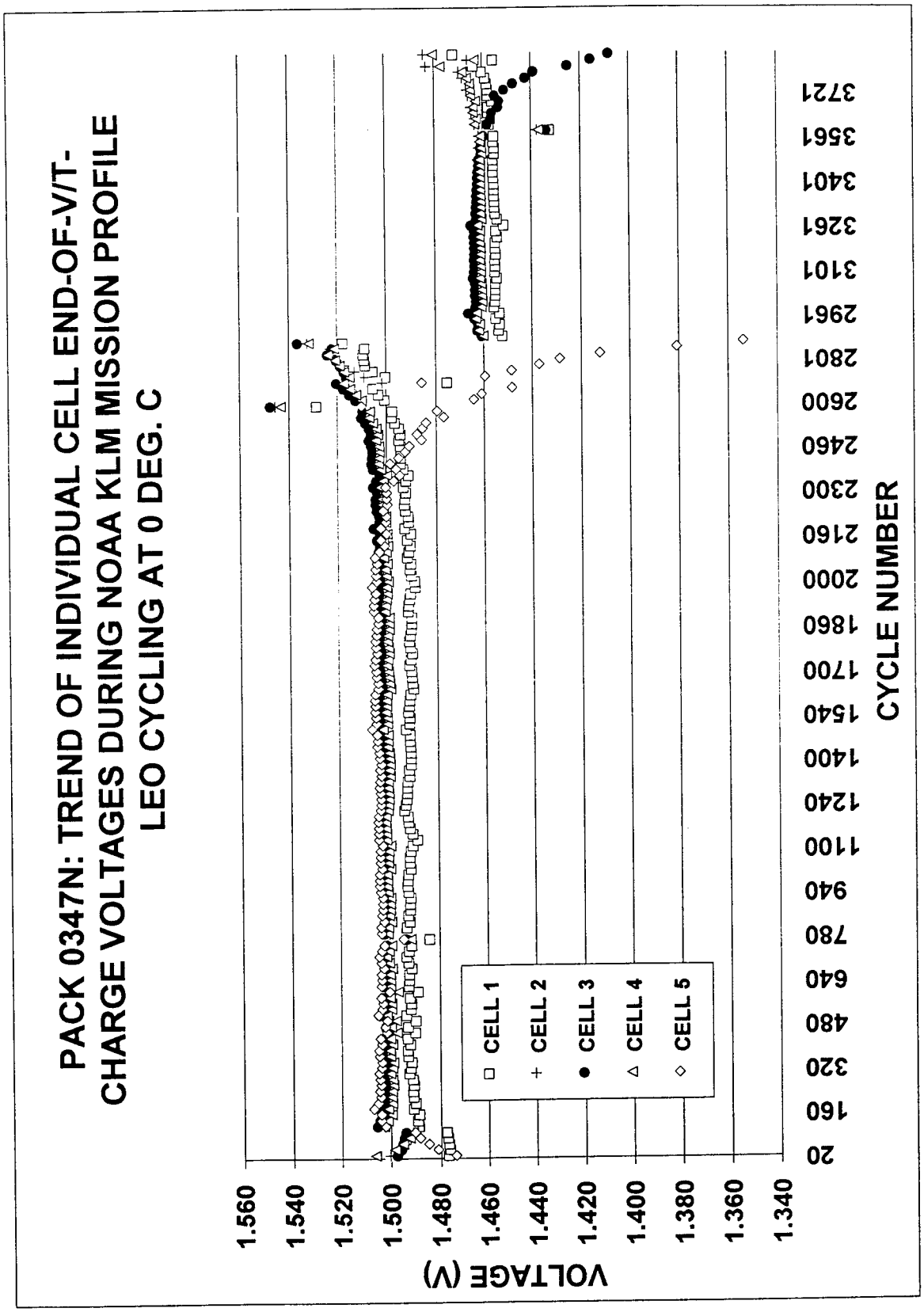
PACK 0347N: TREND OF INDIVIDUAL CELL END-OF-V/T-
CHARGE VOLTAGES DURING NOAA KLM MISSION PROFILE
LEO CYCLING AT 0 DEG. C
VOLTAGE (V)
1.560
1.540
1.520
1.500
1.480
1.460
1.440
1.420
1.400
1.380
1.360
1.340
CYCLE NUMBER
20
160
320
480
640
780
940
1100
1240
1400
1540
1700
1860
2000
2160
2300
2460
2600
2801
2961
3101
3261
3401
3561
3721
CELL 1
CELL 2
CELL 3
CELL 4
CELL 5

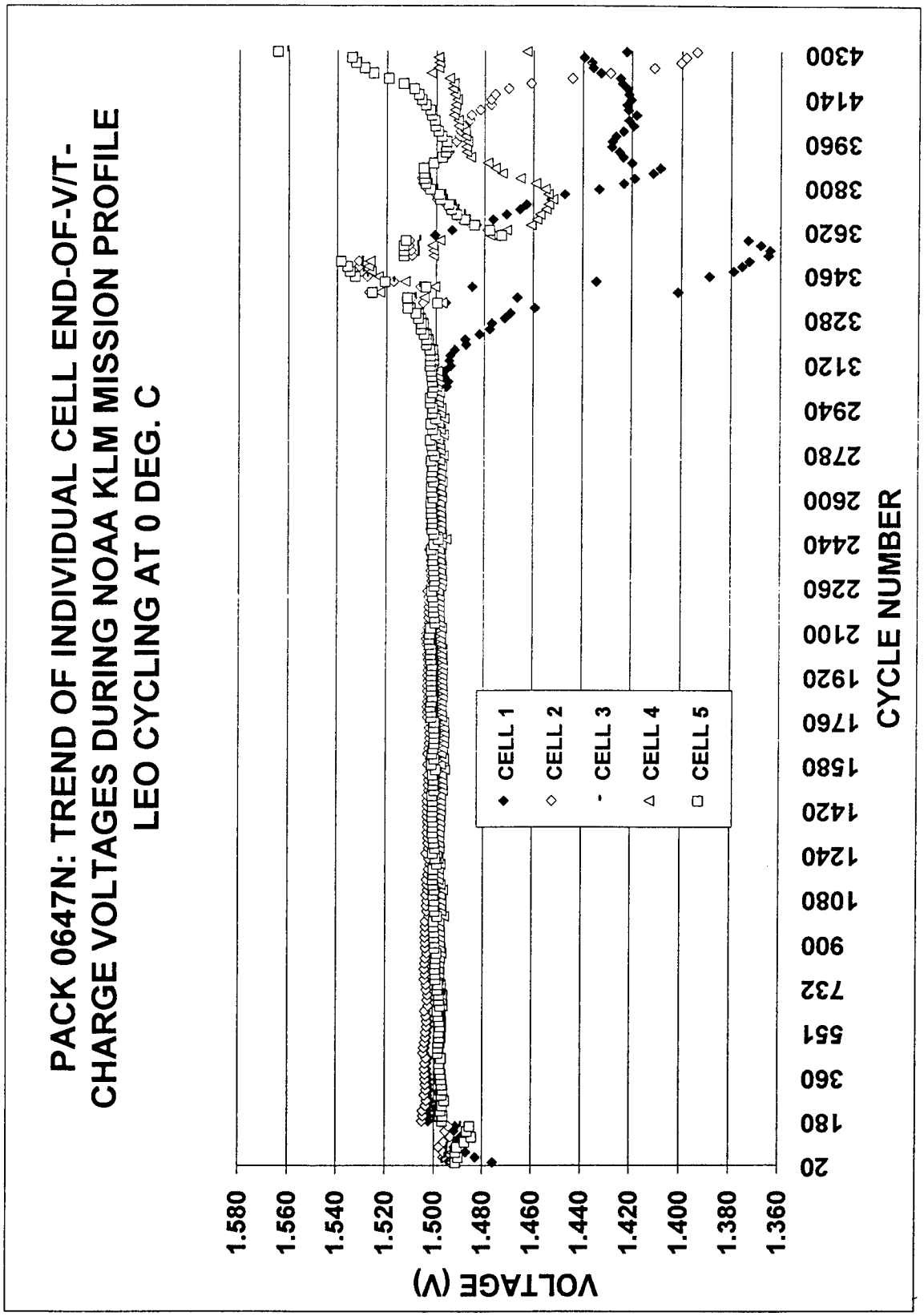
PACK 0647N: TREND OF INDIVIDUAL CELL END-OF-V/T-
CHARGE VOLTAGES DURING NOAA KLM MISSION PROFILE
LEO CYCLING AT 0 DEG. C
VOLTAGE (V)
1.580
1.560
1.540
1.520
1.500
1.480
1.460
1.440
1.420
1.400
1.380
1.360
CYCLE NUMBER
20
180
360
551
732
900
1080
1240
1420
1580
1760
1920
2100
2260
2440
2600
2780
2940
3120
3280
3460
3620
3800
3960
4140
4300
CELL 1
CELL 2
CELL 3
CELL 4
CELL 5

INTRODUCTION - continued

- Spacecraft battery manufacturer requested NASA/GSFC technical direction in September 1994 (after initial cell failures) to distinguish the bad cells from the flight cells.
  - Cells undergoing two electrolyte removals (versus one for most cells) were initially suspect as they were the first to exhibit voltage divergence.
    - A minimum of one electrolyte removal is required for cells of this design (Teflon-treated negative electrodes)
    - Cells with single electrolyte removal subsequently diverged.
  - The issue became: Was poor performance unique to the pre-accept cells or a lot-wide problem?

METHODOLOGY

- Review cell vendor test data from both lots and look for similarities among the divergent cells.
  - High voltages
  - High pressures
  - Low capacities
- Review life-cycle test data from NASA Standard 50 AH NiCd battery cells that exhibited voltage divergence:
  - Look for similarities in the pattern of voltage divergence:
    - Low charge voltage in life-cycle testing, followed by low discharge voltage.
    - Voltage divergence following period(s) of reduced discharge and/or increased overcharge.

METHODOLOGY - continued

- Review cell vendor test data from NASA Standard 50 AH NiCd battery cells that exhibited voltage divergence in life-cycle testing:
  - Employ lessons learned from previous investigations by emphasizing test data that may point up weaknesses in negative electrode performance.
  - Look for similarities among the divergent cells:
    - High voltages
    - High pressures
    - Low capacities
- Working from the combined database of the two designs, devise a method for effectively predicting long-term NiCd cell performance from cell vendor data.

METHODOLOGY - continued

- RESULTS: Specific points from the cell vendor's data, which are related to fundamentals of NiCd cell chemistry (primarily oxygen recombination) and electrical performance (voltage and capacity), when sampled at key points (in both Pre-ATP and ATP), CAN be related to long-term LEO life-cycle performance.
- The specific cell-vendor data points are:
  - a Formation cycle #1 - pressure at 0 hours, [Ideally between -25 inHg and -30 inHg]
  - b Formation cycle #4 - pressure at 0 hours, [Ideally between -25 inHg and -30 inHg]
  - c Formation cycle #4 - pressure at 4 hours, [Ideally between -25 inHg and -30 inHg]

METHODOLOGY - continued

- **Key cell-vendor data points (continued):**
  - d **Formation cycle #4 - End-of-charge pressure. [Ideally as low as possible]**
  - e **Formation cycle #4 - Capacity (C/2 discharge time, in minutes) to 1.0 volt. [Ideally, 120 minutes]**
  - f **Negative precharge - Total vent time. [Ideally, but within reason, as high as possible]**
  - g **0 °C Capacity Test - End-of-charge pressure. [Ideally, the lower the better]**
  - h **0 °C Capacity Test - Peak charge voltage. [Ideally, in the range of 1.500 V to 1.515 V]]**

METHODOLOGY - continued

- **Screening Factors:**
  1. "Pressure Growth Factor" (PGF) = "b-a"; should be a low number or may indicate build-up of oxygen.
  2. "Oxygen Recombination Factor" (ORF) = "c-b"; should be a low number or may indicate presence of oxygen.
  3. Formation cycle #4 - End-of-charge pressure; = "d", should be low, or may indicate inefficient oxygen recombination.
  4. Formation cycle #4 - Capacity (C/2 discharge time, in minutes) to 1.0 volt; = "e", should approach 120 minutes, or may indicate poor negative plate performance.
  5. Negative precharge - Total vent time; = "f", should be as high as possible, or may indicate inefficient oxygen recombination and poor negative plate performance.
  6. 0 °C Capacity Test - End-of-charge charge pressure; = "g", should be low, or may indicate inefficient oxygen recombination and poor negative plate performance.
  7. 0 °C Capacity Test - Peak charge voltage; = "h", should be low, or may indicate poor negative plate performance.

METHODOLOGY - continued

47AB01 Lot 6 Data

S/N	1. PGF (inHg)	2. ORF (inHg)	3. (PSIG)	4. (minutes)	5. (minutes)	6. (PSIG)	7. (VOLTS)
1	14	11	20	109	2160	40	1.535
6	6	6	7	110	2809	26	1.531
14	6	5	5	111	3528	25	1.532
19	11	9	21	110	1509	32	1.531
27	7	5	7	112	2652	35	1.531
33	6	4	2	111	4027	26	1.533

47AB01 Lot 3 Data

S/N	1. PGF (inHg)	2. ORF (inHg)	3. (PSIG)	4. (minutes)	5. (minutes)	6. (PSIG)	7. (VOLTS)
1	2	0	3	118	3795	20	1.520
9	4	1	7	117	6878	45	1.526
20	7	-1	20	112	2150	55	1.523
24	4	4	10	115	5285	22	1.521
33	3	1	8	120	3796	41	1.526
40	10	8	14	113	2300	50	1.526

METHODOLOGY - continued

- **Cell Rankings:** (6 is worst, 1 is best)

47AB01 Lot 6

S/N	Factor 1.	Factor 2.	Factor 3.	Factor 4.	Factor 5.	Factor 6.	Factor 7.	TOTAL SCORE
1	6	6	5	6	5	6	6	40
6	2	4	3.5	4.5	3	2	2	21
14	2	2.5	2	2.5	2	1	4	16
19	5	5	6	4.5	6	4	2	32.5
27	4	2.5	3.5	1	4	5	2	22
33	2	1	1	2.5	1	3	5	15.5

47AB01 Lot 3

S/N	Factor 1.	Factor 2.	Factor 3.	Factor 4.	Factor 5.	Factor 6.	Factor 7.	TOTAL SCORE
1	1	2	1	2	4	1	1	12
9	3.5	3.5	2	3	1	4	4	21
20	5	1	6	6	6	6	3	33
24	3.5	5	4	4	2	2	2	22.5
33	2	3.5	3	1	3	3	4	19.5
40	6	6	5	5	5	5	4	36

VERIFICATION

- NOAA/TIROS 47 AH Lot 6 and Lot 3 life-cycle test cells failed in the exact order predicted by the screening method rankings; even after the remaining "good" cells from the two original packs were combined into a single test pack.
- When applied to NASA Standard 50 AH cell lots that have already produced cells with similar voltage divergence early in life-cycle testing, the screening method confirmed that cells with high screening scores are the same cells that diverged early in life-cycle tests.

VERIFICATION - continued

Lot-S/N	TOTAL SCORE	RESULTS
6-1	40	**Failed 1st**
6-19	32.5	**Failed 2nd**
6-27	22	GAB DPA CELL
6-6	21	**Failed 3rd**
6-14	16	nominal
6-33	15.5	nominal
3-40	36	**Failed 1st**
3-20	33	**Failed 2nd**
3-24	22.5	**(Failed in combined pack)**
3-9	21	**(Failed in combined pack)**
3-33	19.5	GAB DPA CELL
3-1	12	nominal

VERIFICATION - continued

NSWC PACK #	LOT #	MISSION	TEST REGIME	CYCLE NUMBER OF SIGNIFICANT DIVERGENCE
6051A	LOT 16 (PRE-ACCEPT)	EUVE	CGRO MISSION	FIRST CELL 3989; SECOND CELL 10625
6051B	LOT 17 (PRE-ACCEPT)	CGRO MPS-2	CGRO MISSION	FIRST CELL (LOW EODV ONLY) 11825
6051H	LOT 1	CGRO MPS-1	STRESS	FIRST CELL ~6900
6052B	LOT 2	UARS	UARS MISSION	FIRST CELL ~4400

VERIFICATION - continued

PACK - S/N	TOTAL SCORE	RESULTS?
6051A - 79 (Lot 16)	33	**Failed 1st**
6051A - 34	31	nomimal
6051A - 3	26	**Failed 2nd**
6051A - 90	26	nomimal
6051A - 60	22	nomimal
6051B - 63 (Lot 17)	32.5	**First and only failure**
6051B - 90	30.5	nomimal
6051B - 35	27	nomimal
6051B - 50	24.5	nomimal
6051B - 89	17	nomimal
6051B - 20	15.5	nomimal

VERIFICATION - continued

- Life-test cells are indicated by black squares. The first cell to diverge was the second-highest-scoring cell of the five stress-test life-cycle test cells.

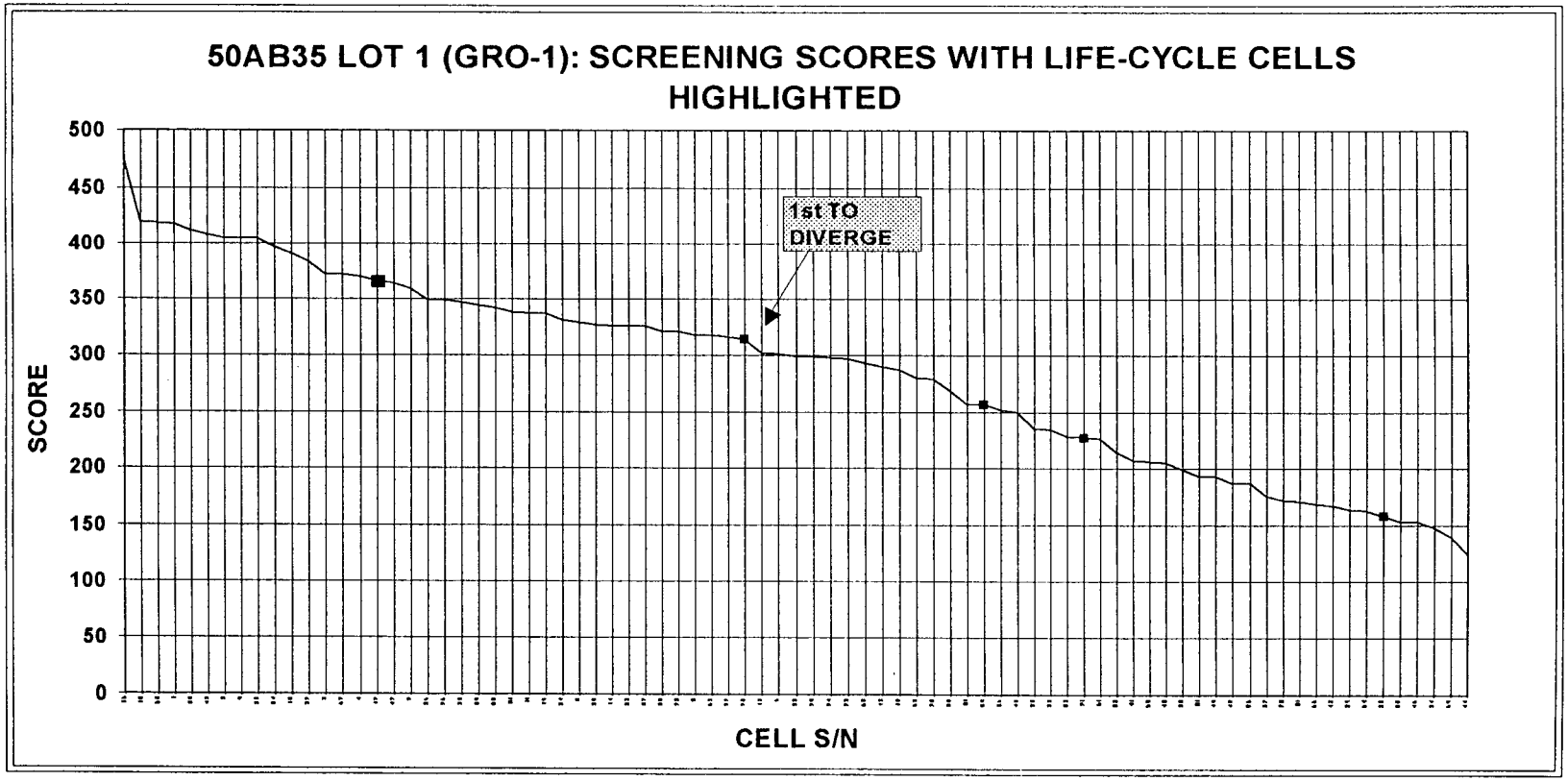

VERIFICATION - continued

- The first three cells to diverge were the three of the four highest-scoring cells of the five mission simulation life-cycle test cells.

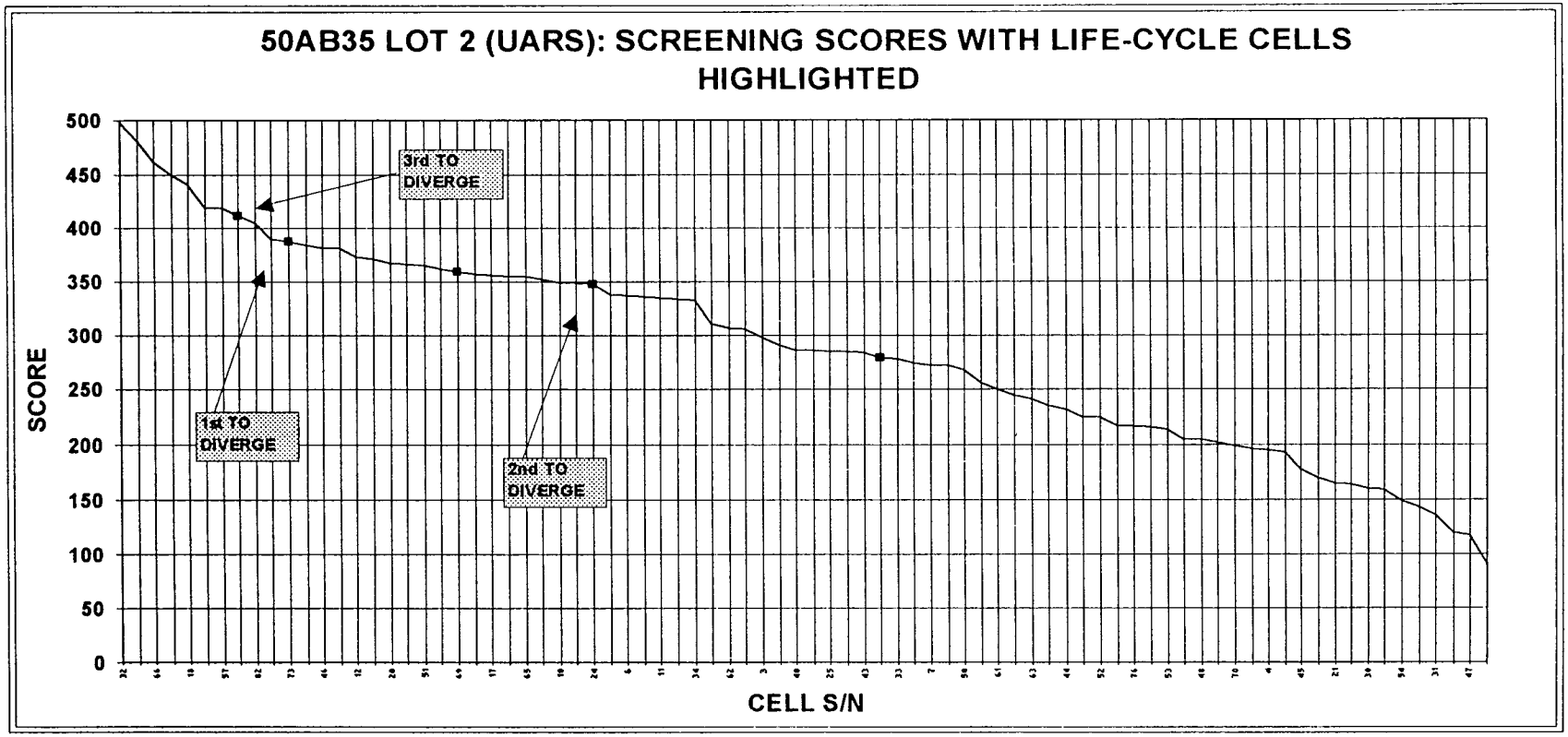

VERIFICATION - continued

- Frequency histogram of cell scores for a lot with known performance problems. Some of the cells scoring high are documented to have performed poorly in life-cycle testing; others are suspected of performing poorly in on-orbit batteries.

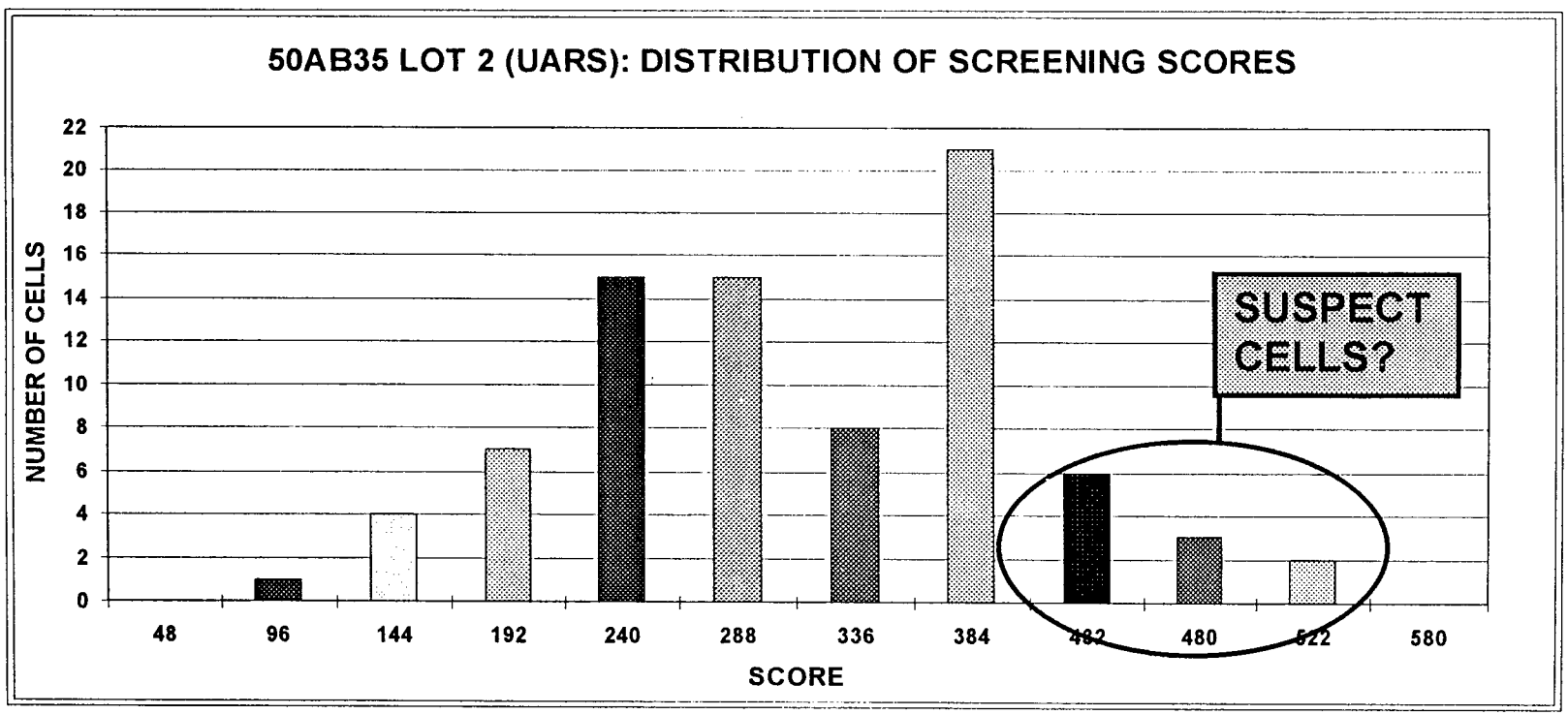

VERIFICATION - continued

- Frequency histogram of scores for a lot with NO known performance problems (except Pre-accept cells). It is documented that none of the cells scoring high have performed poorly in life-cycle testing; and on-orbit performance of batteries from this cell lot has been nominal.

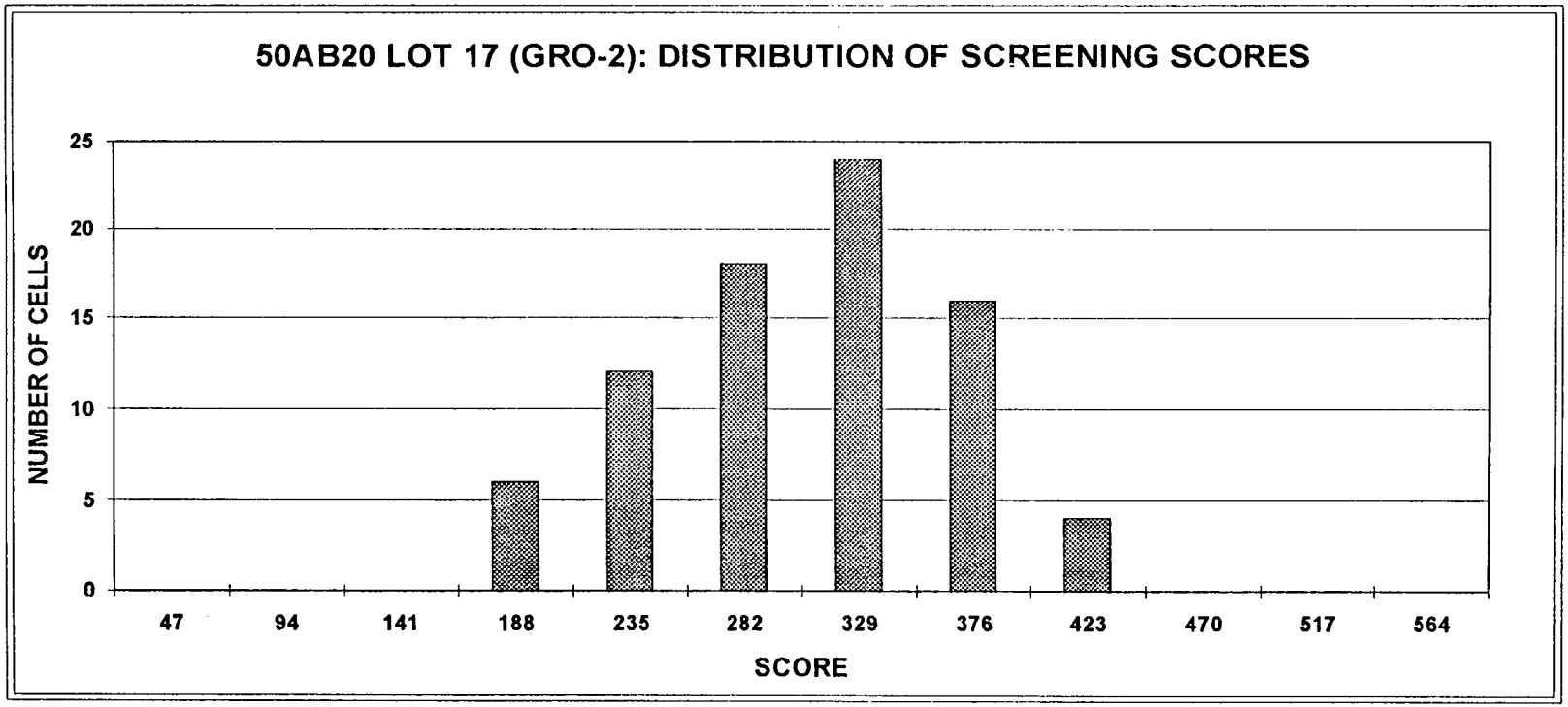

APPLICATION

- Tabulate the 7 data points for each of 60+ cells for NOAA/ TIROS KLM program (47AB01 Lot 6) and rank all cells from best to worst.
  - Worst cells (highest scoring) were excluded from flight battery cell selection; five of these cells were earmarked for a dedicated life-cycle test pack.
  - Acceptable cells (scoring medium to high) may be OK for flight cell usage; some of these cells were earmarked for a second life-cycle test pack.
  - Best cells (scoring low) were used for flight battery cell selection and flight spare cells; some were also earmarked for the second life-cycle test pack. The results from this second pack would be used to determine if the batteries manufactured from the screened flight cells were flightworthy.

APPLICATION - continued

- Cells with highest scores are non-flight and should be life-cycle tested.
- Use cells with medium to medium-high scores for flight and life-cycle test.
- Use cells with low to medium-high scores for flight use, flight spares and life-cycle test.

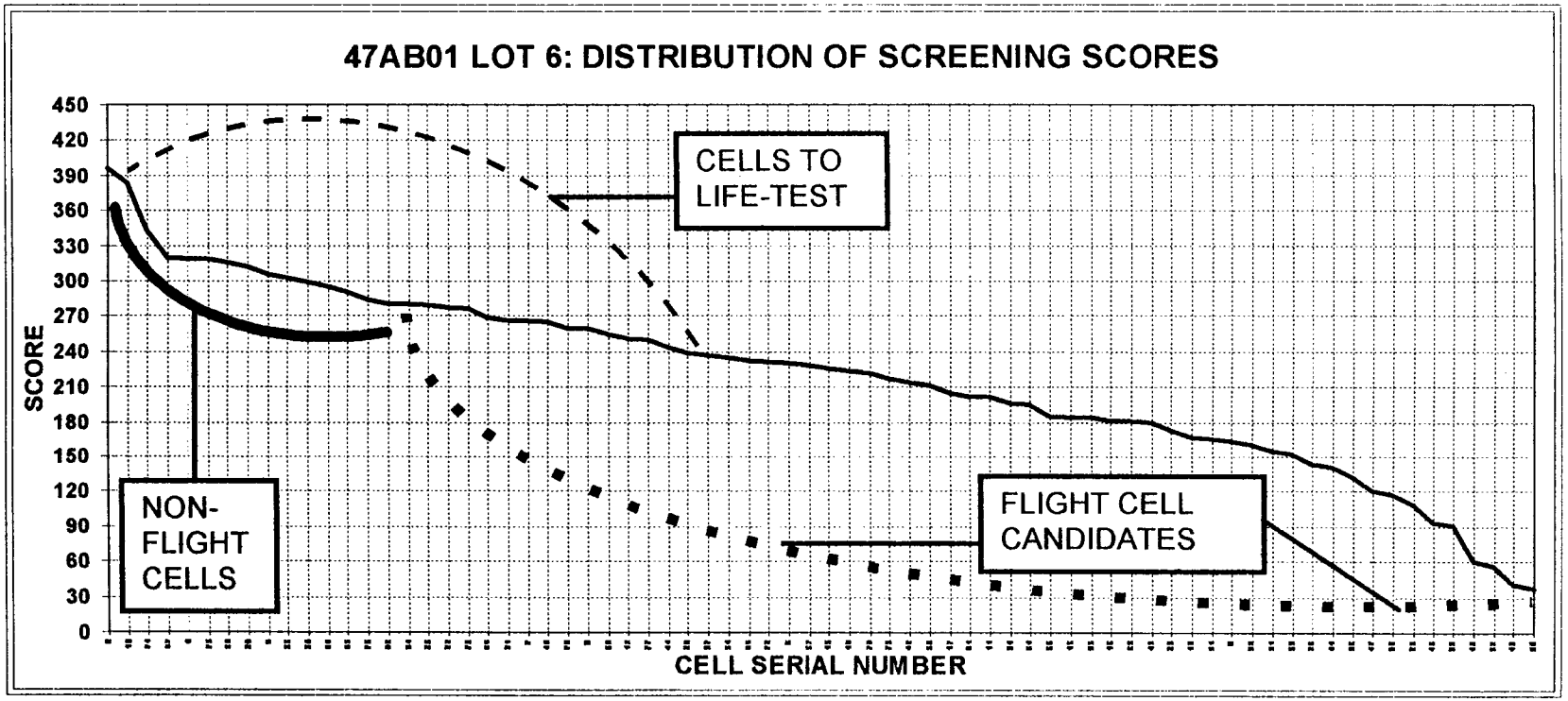

APPLICATION - continued

- 500+ cells of GAB/SAB "Florida manufacture" have been shipped to France for future activation and potential use in NASA and other U.S. Government programs.
  - Early activation of a few dry-stored cells (i.e. pre-acceptance) is recommended for all customers with Florida-fabricated NiCd cells stored in France.
  - Application of this screening method is recommended for all future activations of dry-stored cell lots:
    - Require SAFT-France to provide cell data previously provided by GE/GAB/SAB (both Pre-ATP and ATP).
    - Use required data to identify flight cell candidates and cell life-test candidates; further use data to identify and segregate cells exhibiting suspicious performance.

REPEATING LIFE-CYCLE TESTING ON NOAA/TIROS LOT 6 CELLS USING SCREENED CELLS

- Pack 0648N cells selected to produce early anomalous performance.
- Pack 0649N cells selected to produce long-term nominal performance.

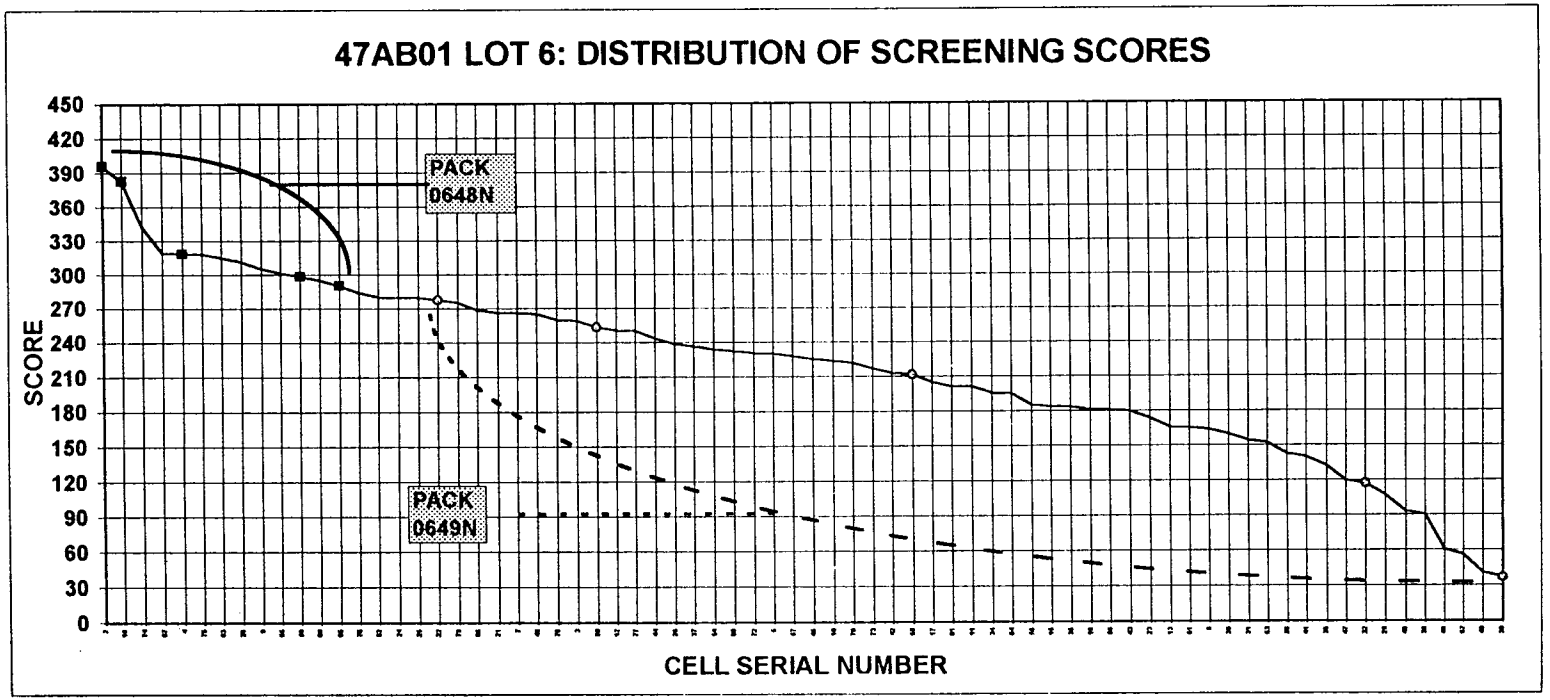

REPEATING LIFE-CYCLE TESTING ON NOAA/TIROS LOT 6 CELLS USING SCREENED CELLS (CONTINUED)

- Test conditions retained from original testing of Pre-accept packs 0347N and 0647N:
  - 0 °C
  - 9.84 Amp sunrise charge current (maintained to V/T limit)
  - Mission-profile depth-of-discharge varies from ~20% down to ~11% and back to ~20% in ~36 weeks
- Test conditions changed from original testing of Pre-accept packs 0347N and 0647N:
  - Transition from taper charge to trickle charge at 1.03 C/D ratio, instead of 1.05
  - Use a V/T limit of 1.47 V/cell for DOD's between 16% and 20% (instead of 1.50 V/cell at all DOD's) and 1.45 V/cell for DOD's below 16%

REPEATING LIFE-CYCLE TESTING ON NOAA/TIROS LOT 6 CELLS - PACK 0648N

- Pack 0648N began to exhibit anomalous voltages in all cells at cycle 1100. This voltage divergence grew and C/D ratios grew large enough to warrant reconditioning at cycle 2182
  - Cells resistively let-down to 0.060V/cell (average), then recharged (60 Ah returned) and put back in cycling (all per anticipated on-orbit procedures)
- Voltage divergence, accompanied again by ever-increasing end-of-charge currents and C/D ratios dictated a second reconditioning at cycle 2650.
  - Cells resistively let-down to 0.060V/cell (average), then recharged (55 Ah returned) and put back in cycling
- Cell #2 (S/N 4) was electrically removed from the pack at cycle 2707 due to renewed voltage divergence (cell #2 was the main reason for the prior two reconditionings); the other cells continued testing until a new divergence pattern developed, exceeding 100 mV. The pack was discontinued at cycle 2820.

REPEATING LIFE-CYCLE TESTING ON NOAA/TIROS LOT 6 CELLS - PACK 0649N

- Pack 0649N began exhibiting erratic charge voltage in cell #4 (S/N 58) at cycle 2100 following a test interruption.
  - Voltage divergence approached 55 mV at end-of-charge
  - C/D ratios did not increase (unlike pack 0648N)
  - End-of-charge currents did not increase (unlike pack 0648N)
  - The remaining four cells equally made up the voltage difference
- Pack 0649N cycling continued except that the V/T level was not raised from 1.45 V/cell to 1.47 V/cell when the DOD increased from ~15% to ~16% per the test plan.
- The V/T level was raised at cycle 2831, shortly after the DOD was increased from ~16% to ~17%, and cell #4 (S/N 58) reconverged with the cell voltages of the rest of the pack within 200 cycles. Cycling continues on otherwise unaffected.

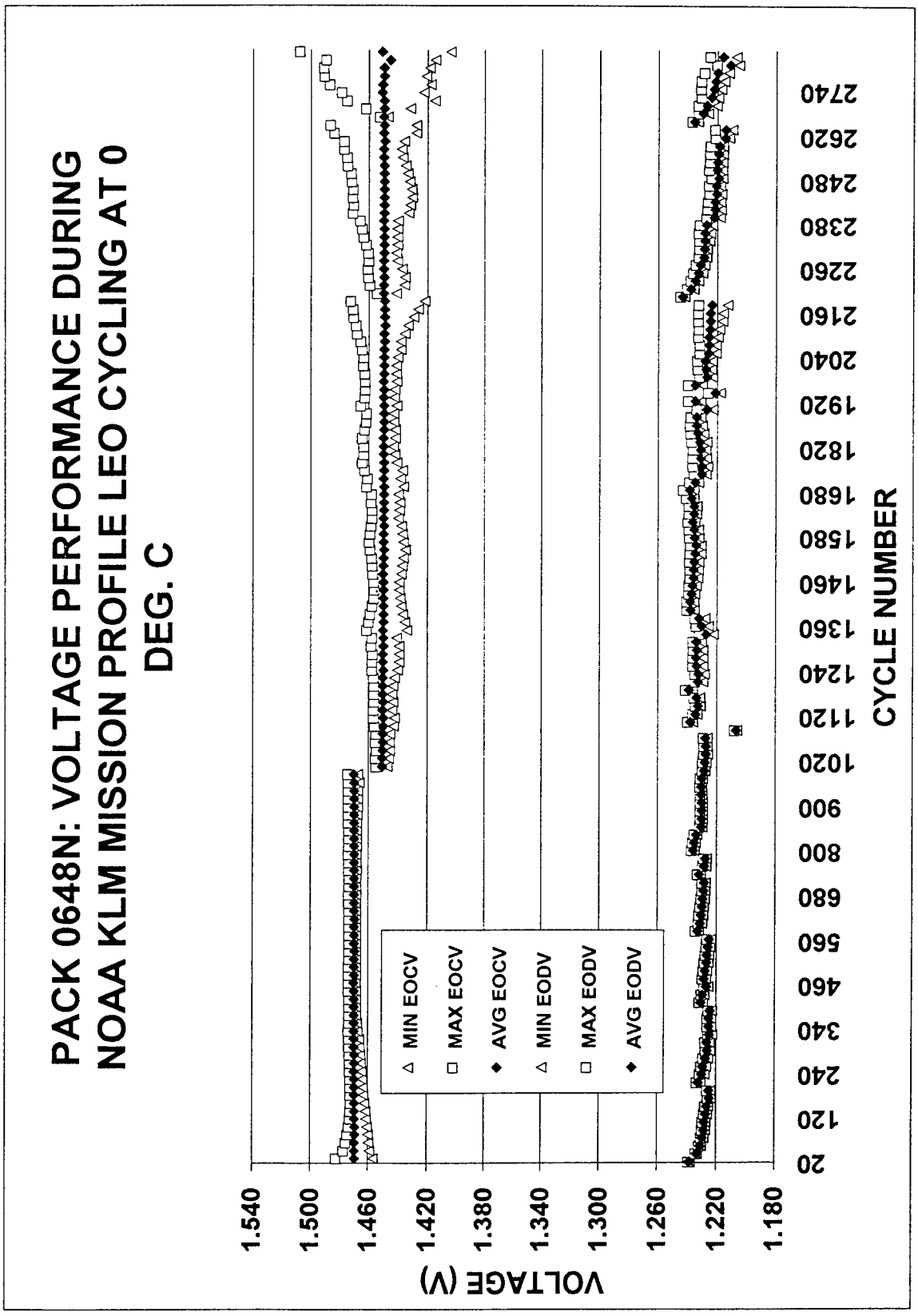
PACK 0648N: VOLTAGE PERFORMANCE DURING
NOAA KLM MISSION PROFILE LEO CYCLING AT 0
DEG. C
VOLTAGE (V)
1.540
1.500
1.460
1.420
1.380
1.340
1.300
1.260
1.220
1.180
CYCLE NUMBER
20
120
240
340
460
560
680
800
900
1020
1120
1240
1360
1460
1580
1680
1820
1920
2040
2160
2260
2380
2480
2620
2740
MIN EOCV
MAX EOCV
AVG EOCV
MIN EODV
MAX EODV
AVG EODV

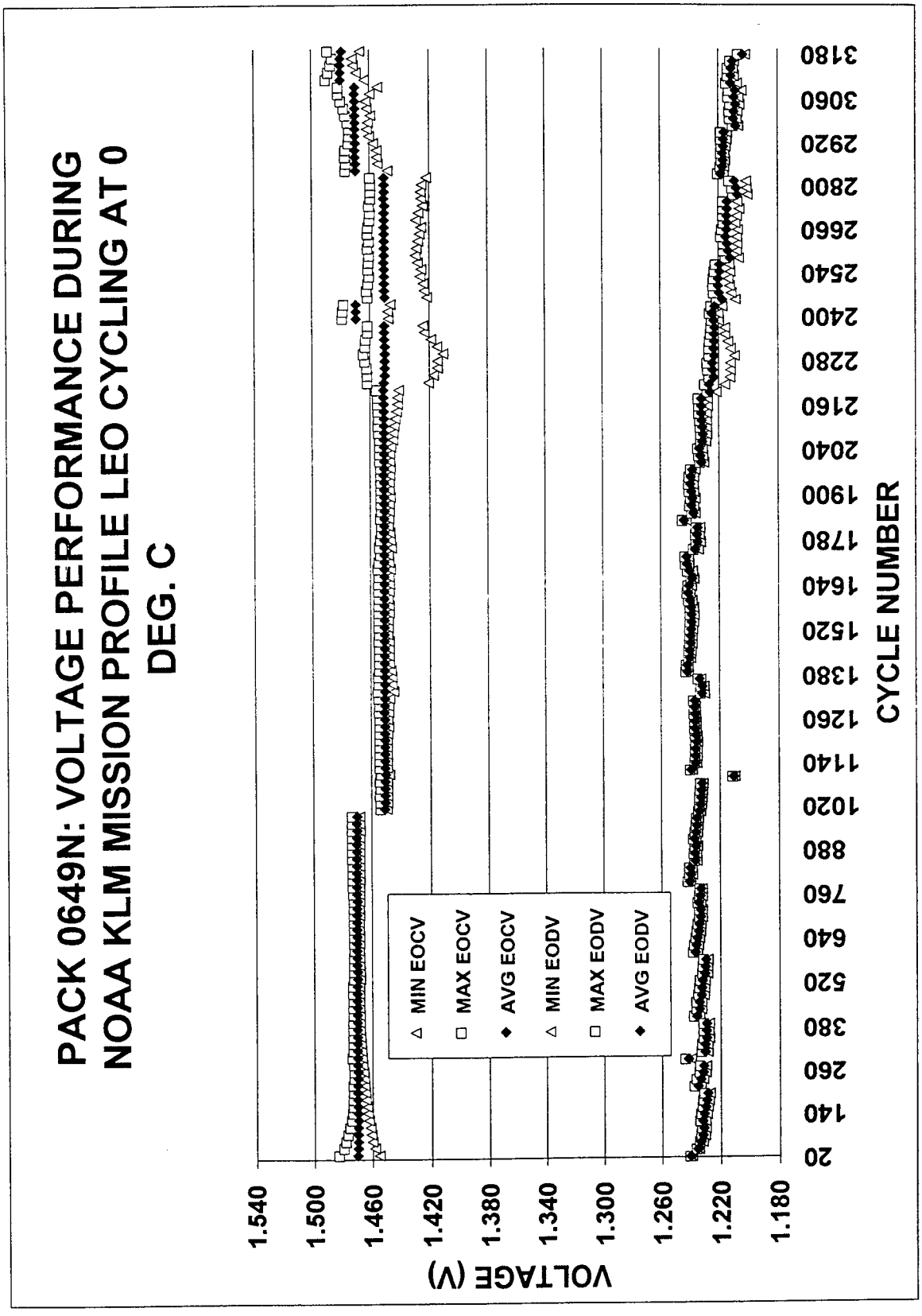
PACK 0649N: VOLTAGE PERFORMANCE DURING
NOAA KLM MISSION PROFILE LEO CYCLING AT 0
DEG. C
VOLTAGE (V)
1.540
1.500
1.460
1.420
1.380
1.340
1.300
1.260
1.220
1.180
CYCLE NUMBER
20
140
260
380
520
640
760
880
1020
1140
1260
1380
1520
1640
1780
1900
2040
2160
2280
2400
2540
2660
2800
2920
3060
3180
MIN EOCV
MAX EOCV
AVG EOCV
MIN EODV
MAX EODV
AVG EODV

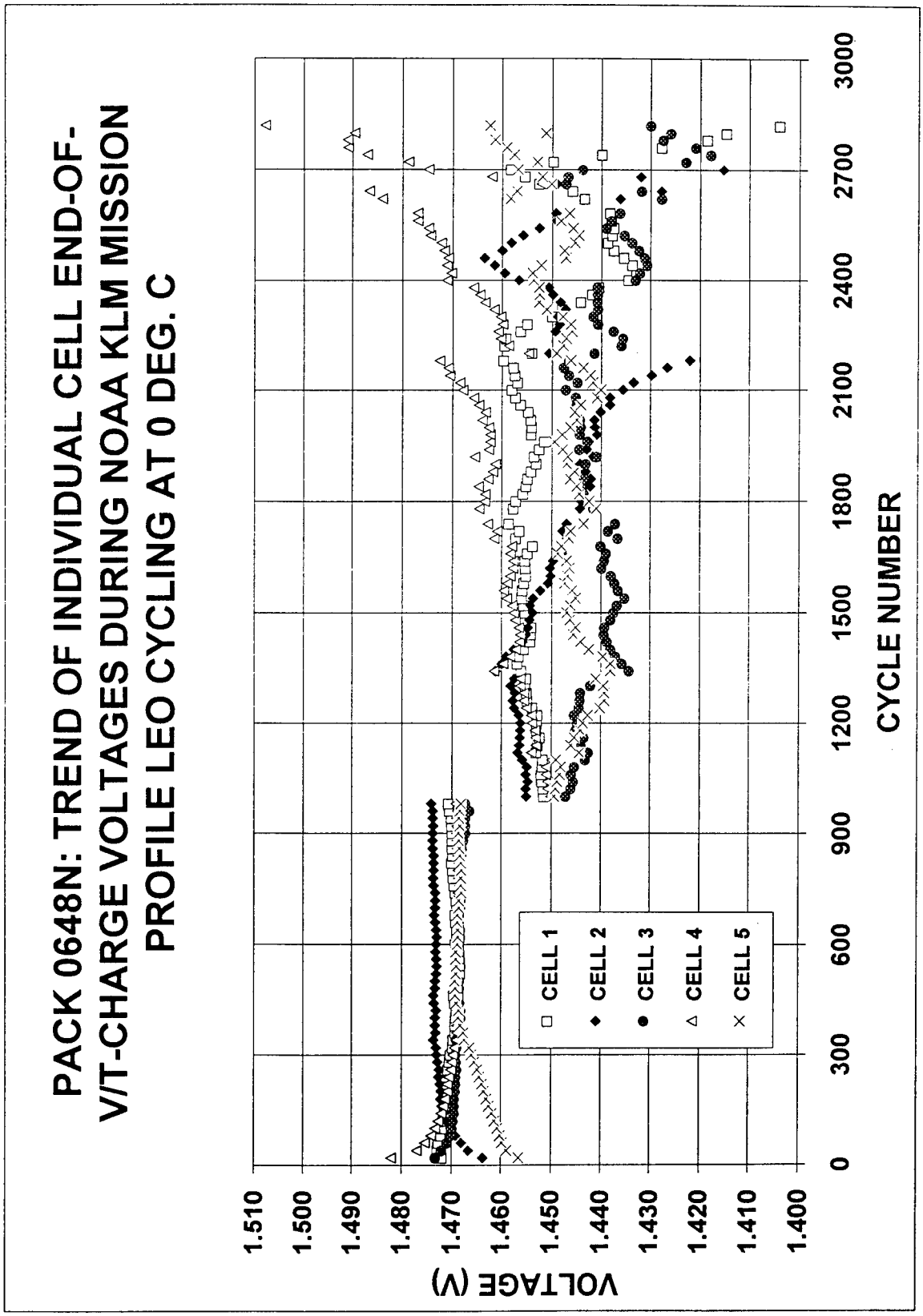
PACK 0648N: TREND OF INDIVIDUAL CELL END-OF-V/T-CHARGE VOLTAGES DURING NOAA KLM MISSION PROFILE LEO CYCLING AT 0 DEG. C
VOLTAGE (V)
1.510
1.500
1.490
1.480
1.470
1.460
1.450
1.440
1.430
1.420
1.410
1.400
0
300
600
900
1200
1500
1800
2100
2400
2700
3000
CYCLE NUMBER
CELL 1
CELL 2
CELL 3
CELL 4
CELL 5

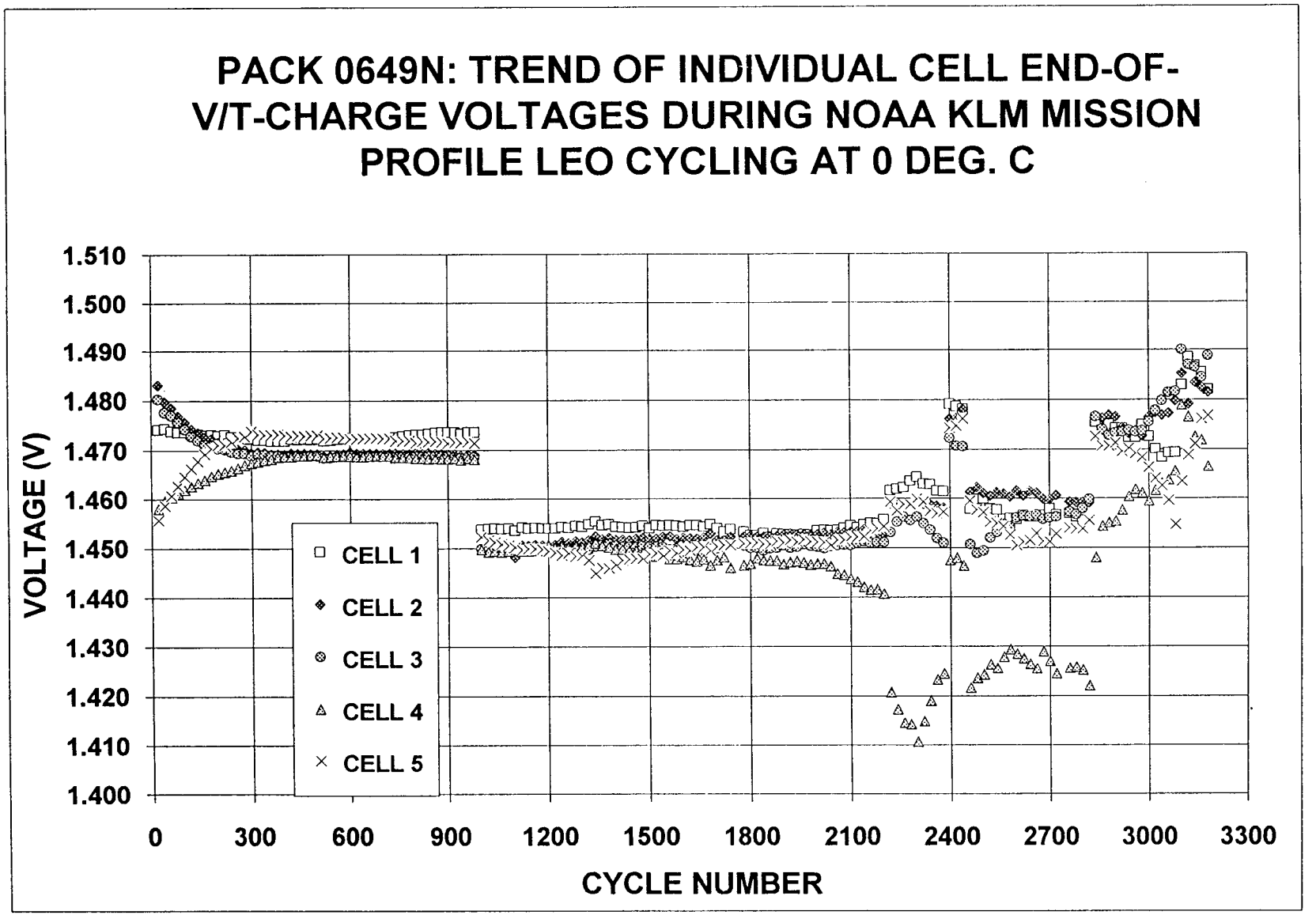
PACK 0649N: TREND OF INDIVIDUAL CELL END-OF-V/T-CHARGE VOLTAGES DURING NOAA KLM MISSION PROFILE LEO CYCLING AT 0 DEG. C
VOLTAGE (V)
1.510
1.500
1.490
1.480
1.470
1.460
1.450
1.440
1.430
1.420
1.410
1.400
CELL 1
CELL 2
CELL 3
CELL 4
CELL 5
0
300
600
900
1200
1500
1800
2100
2400
2700
3000
3300
CYCLE NUMBER

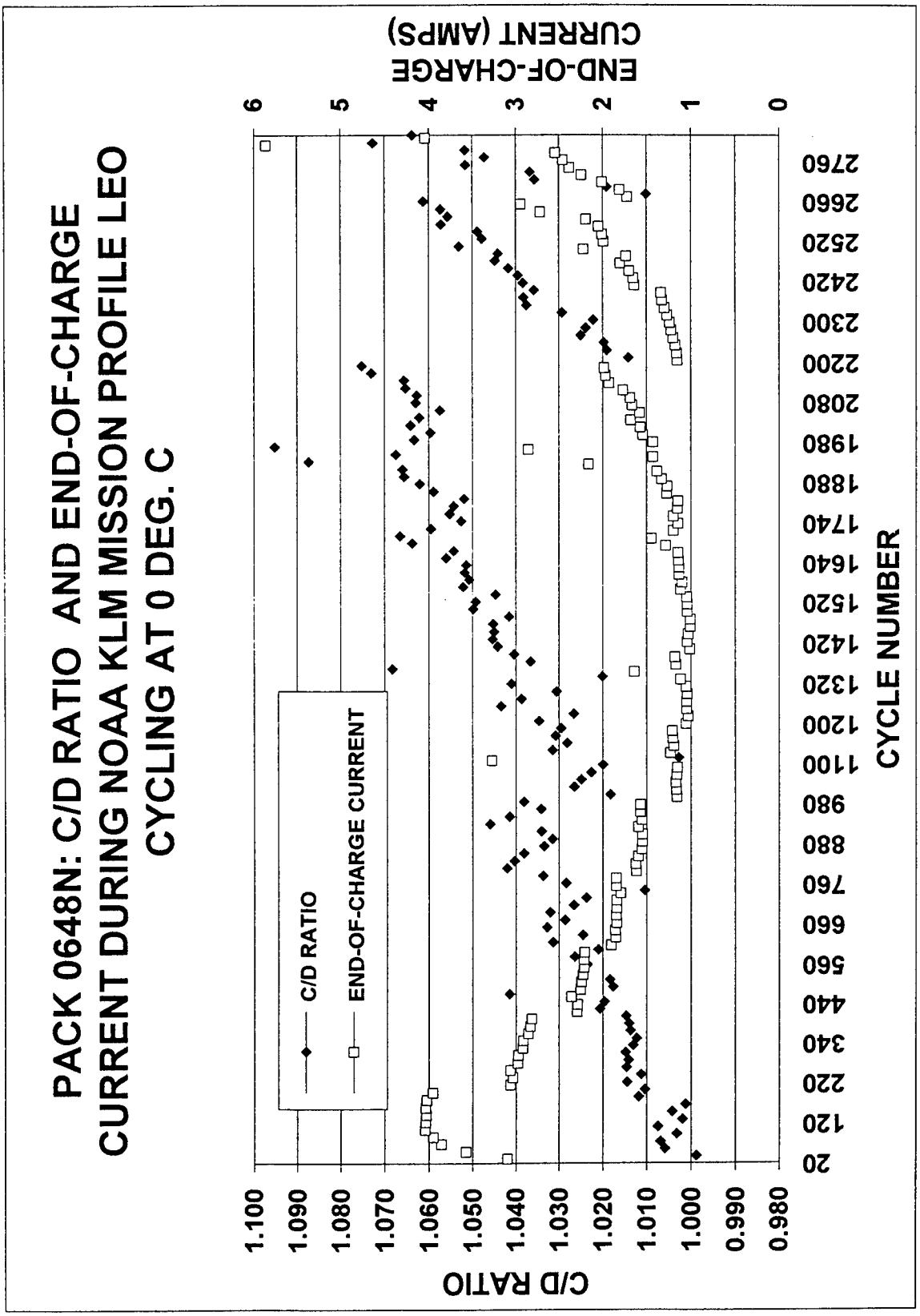
PACK 0648N: C/D RATIO AND END-OF-CHARGE CURRENT DURING NOAA KLM MISSION PROFILE LEO CYCLING AT 0 DEG. C
C/D RATIO
END-OF-CHARGE CURRENT (AMPS)
CYCLE NUMBER
C/D RATIO
END-OF-CHARGE CURRENT
1.100
1.090
1.080
1.070
1.060
1.050
1.040
1.030
1.020
1.010
1.000
0.990
0.980
6
5
4
3
2
1
0
20
120
220
340
440
560
660
760
880
980
1100
1200
1320
1420
1520
1640
1740
1880
1980
2080
2200
2300
2420
2520
2660
2760

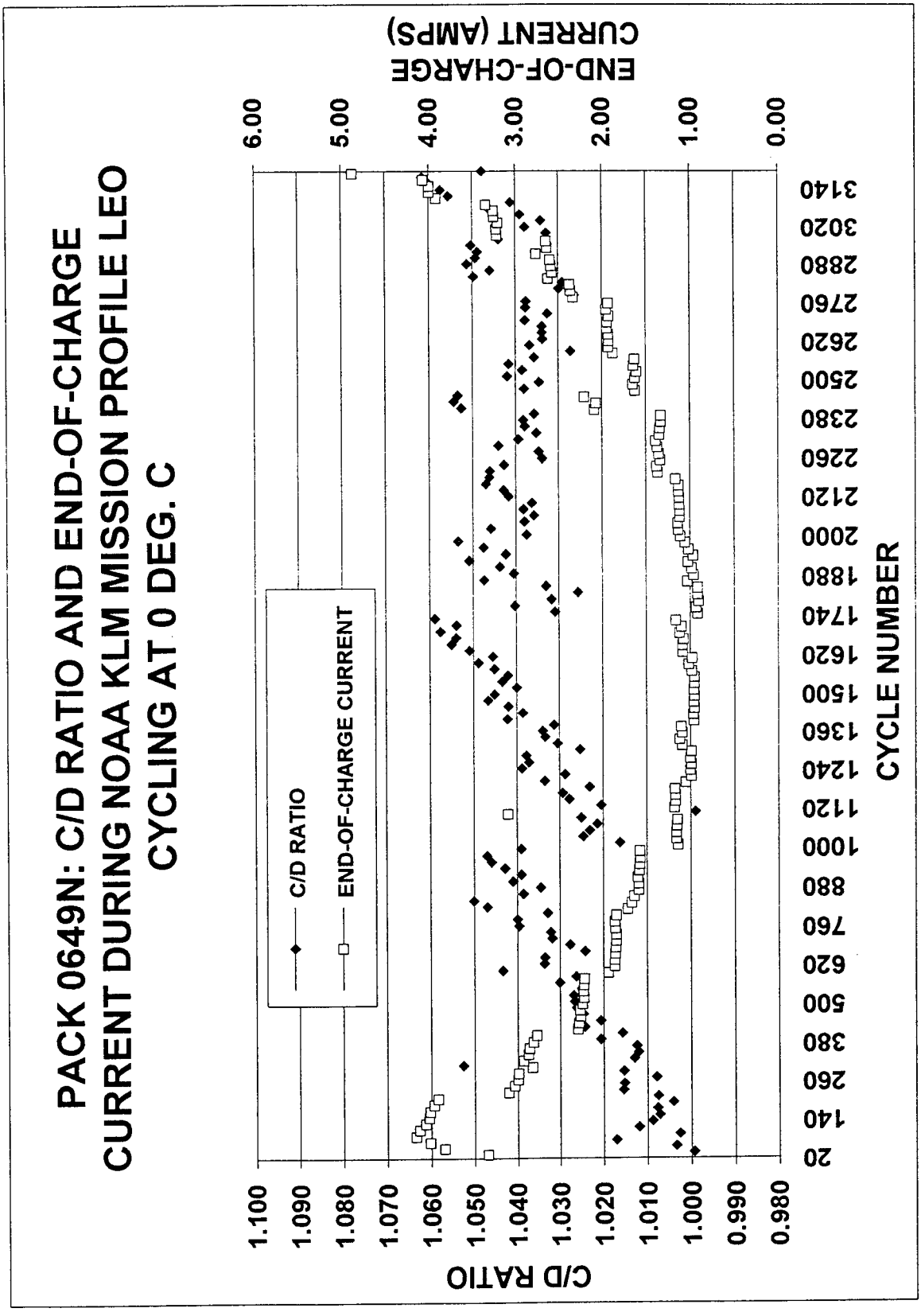
PACK 0649N: C/D RATIO AND END-OF-CHARGE CURRENT DURING NOAA KLM MISSION PROFILE LEO CYCLING AT 0 DEG. C
C/D RATIO
END-OF-CHARGE CURRENT (AMPS)
CYCLE NUMBER
C/D RATIO
END-OF-CHARGE CURRENT
1.100
1.090
1.080
1.070
1.060
1.050
1.040
1.030
1.020
1.010
1.000
0.990
0.980
6.00
5.00
4.00
3.00
2.00
1.00
0.00
20
140
260
380
500
620
760
880
1000
1120
1240
1360
1500
1620
1740
1880
2000
2120
2260
2380
2500
2620
2760
2880
3020
3140

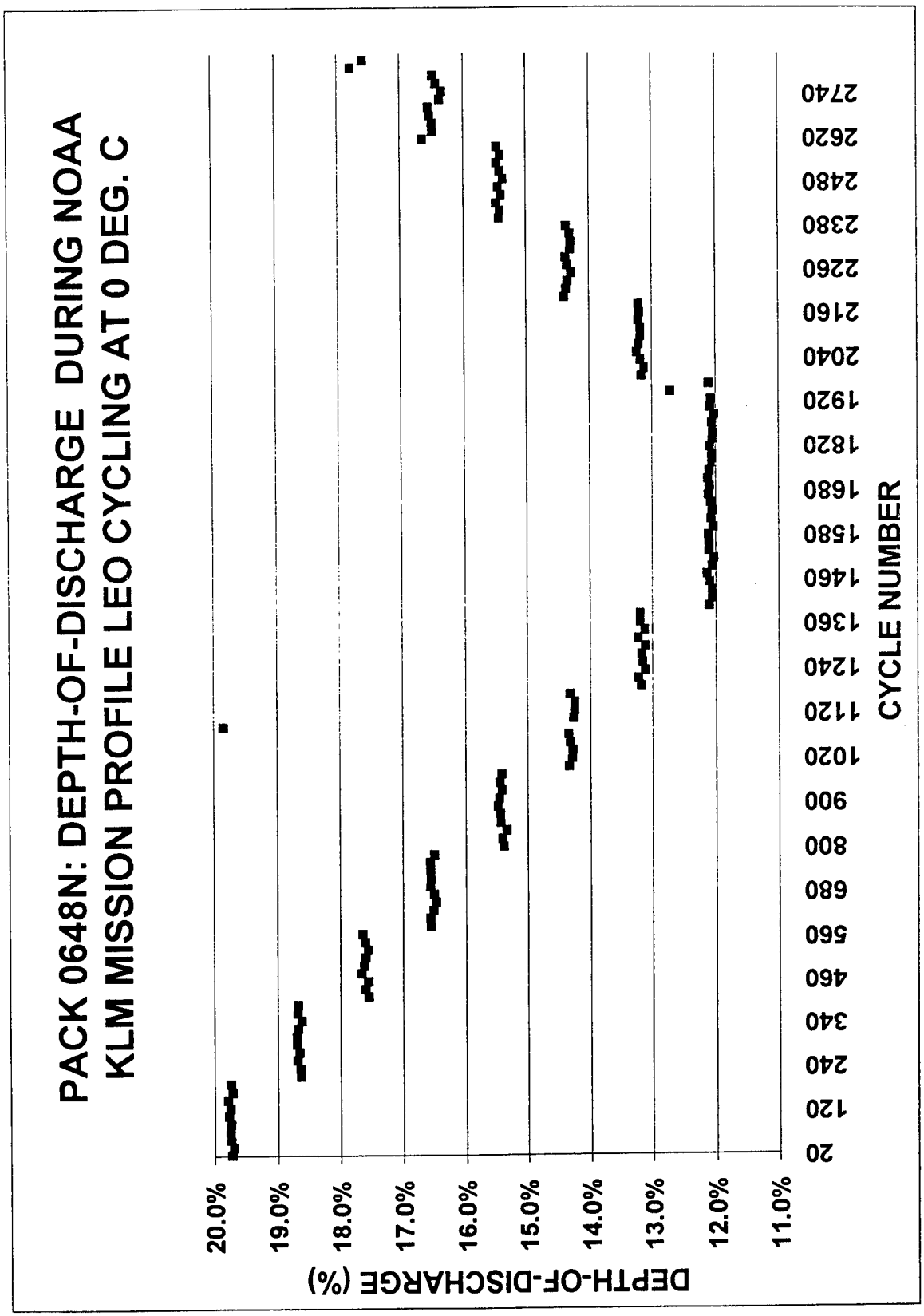
PACK 0648N: DEPTH-OF-DISCHARGE DURING NOAA
KLM MISSION PROFILE LEO CYCLING AT 0 DEG. C
DEPTH-OF-DISCHARGE (%)
20.0%
19.0%
18.0%
17.0%
16.0%
15.0%
14.0%
13.0%
12.0%
11.0%
CYCLE NUMBER
20
120
240
340
460
560
680
800
900
1020
1120
1240
1360
1460
1580
1680
1820
1920
2040
2160
2260
2380
2480
2620
2740

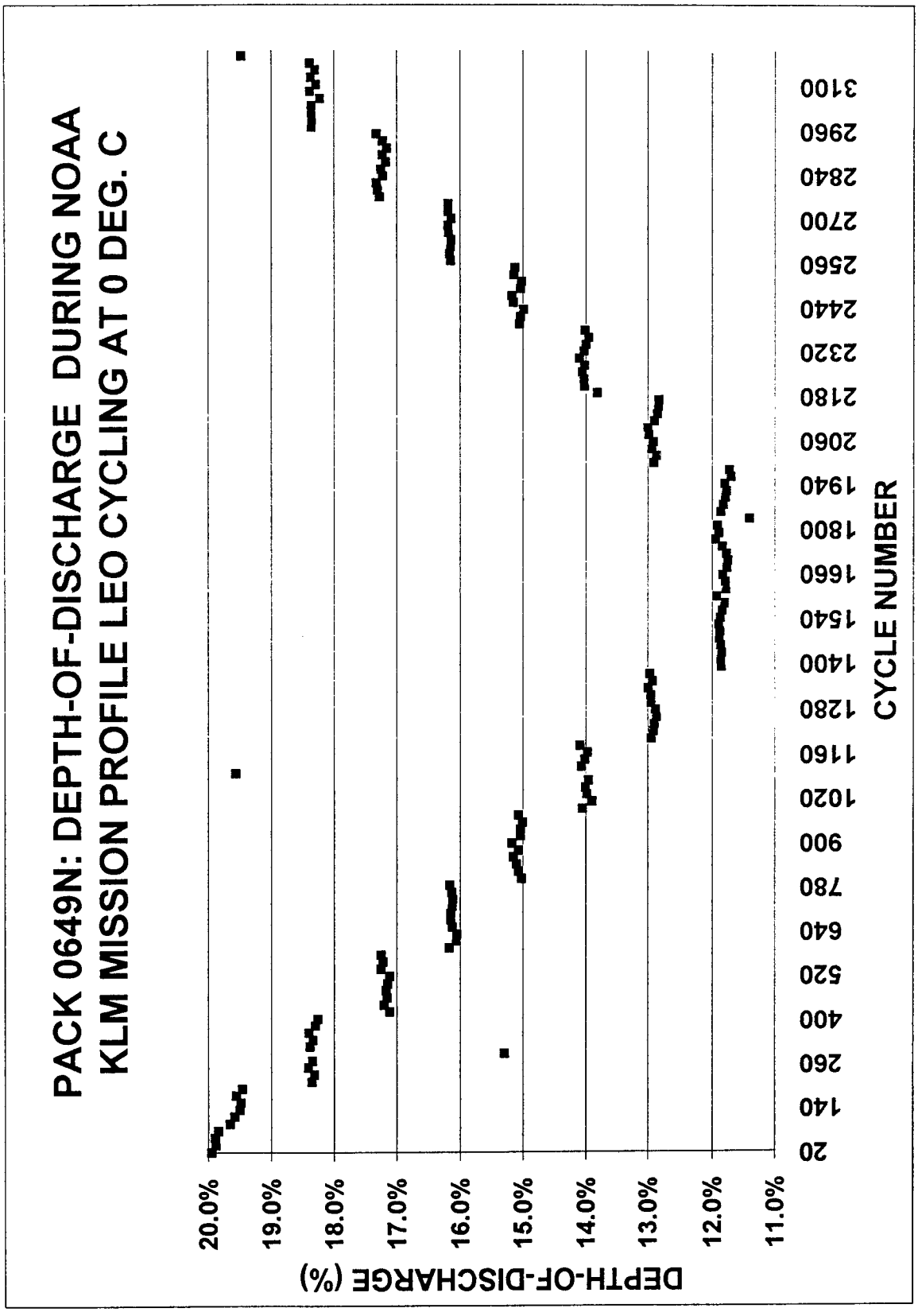
PACK 0649N: DEPTH-OF-DISCHARGE DURING NOAA
KLM MISSION PROFILE LEO CYCLING AT 0 DEG. C
DEPTH-OF-DISCHARGE (%)
20.0%
19.0%
18.0%
17.0%
16.0%
15.0%
14.0%
13.0%
12.0%
11.0%
CYCLE NUMBER
20
140
260
400
520
640
780
900
1020
1160
1280
1400
1540
1660
1800
1940
2060
2180
2320
2440
2560
2700
2840
2960
3100

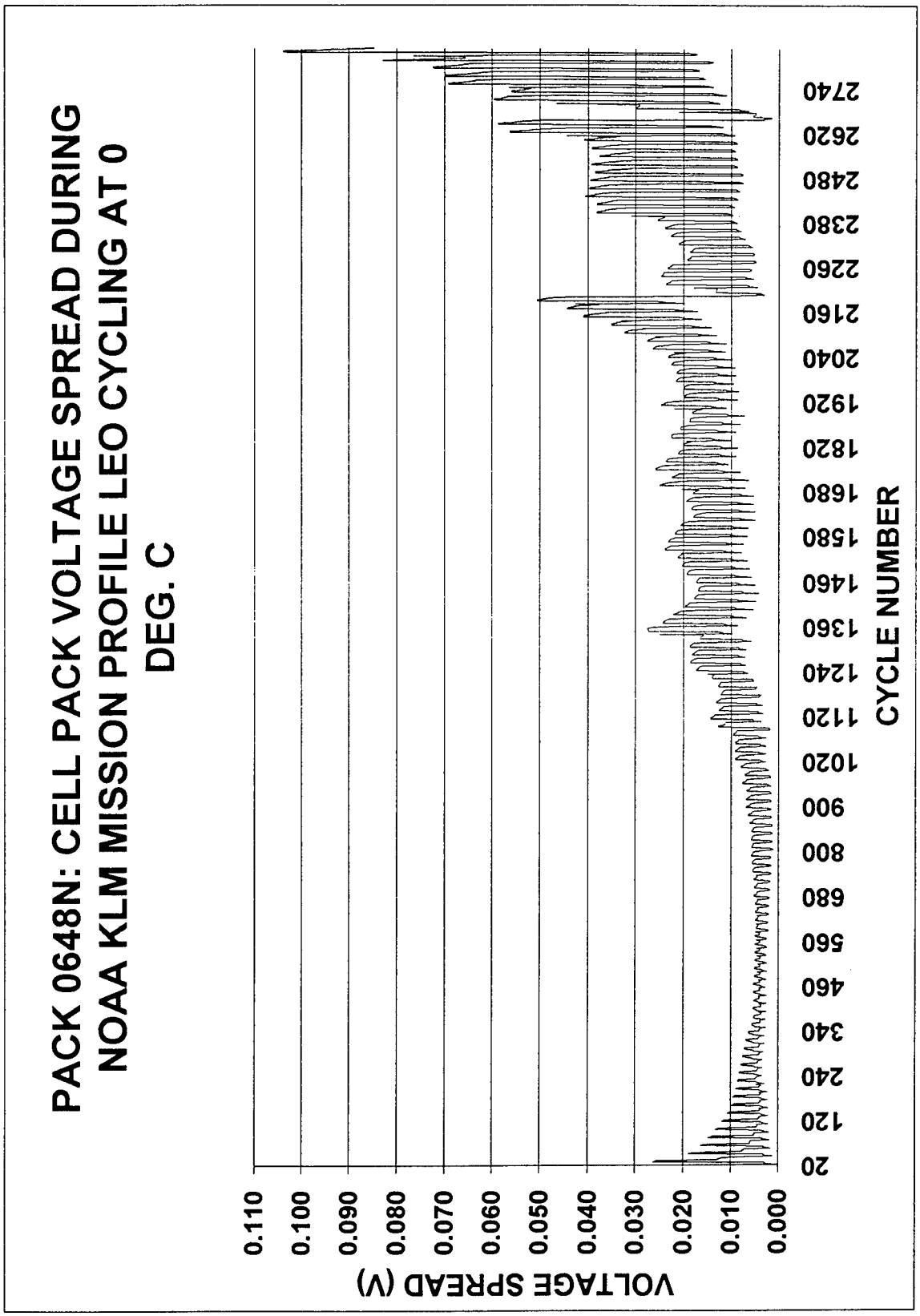
PACK 0648N: CELL PACK VOLTAGE SPREAD DURING
NOAA KLM MISSION PROFILE LEO CYCLING AT 0
DEG. C
VOLTAGE SPREAD (V)
0.110
0.100
0.090
0.080
0.070
0.060
0.050
0.040
0.030
0.020
0.010
0.000
CYCLE NUMBER
20
120
240
340
460
560
680
800
900
1020
1120
1240
1360
1460
1580
1680
1820
1920
2040
2160
2260
2380
2480
2620
2740

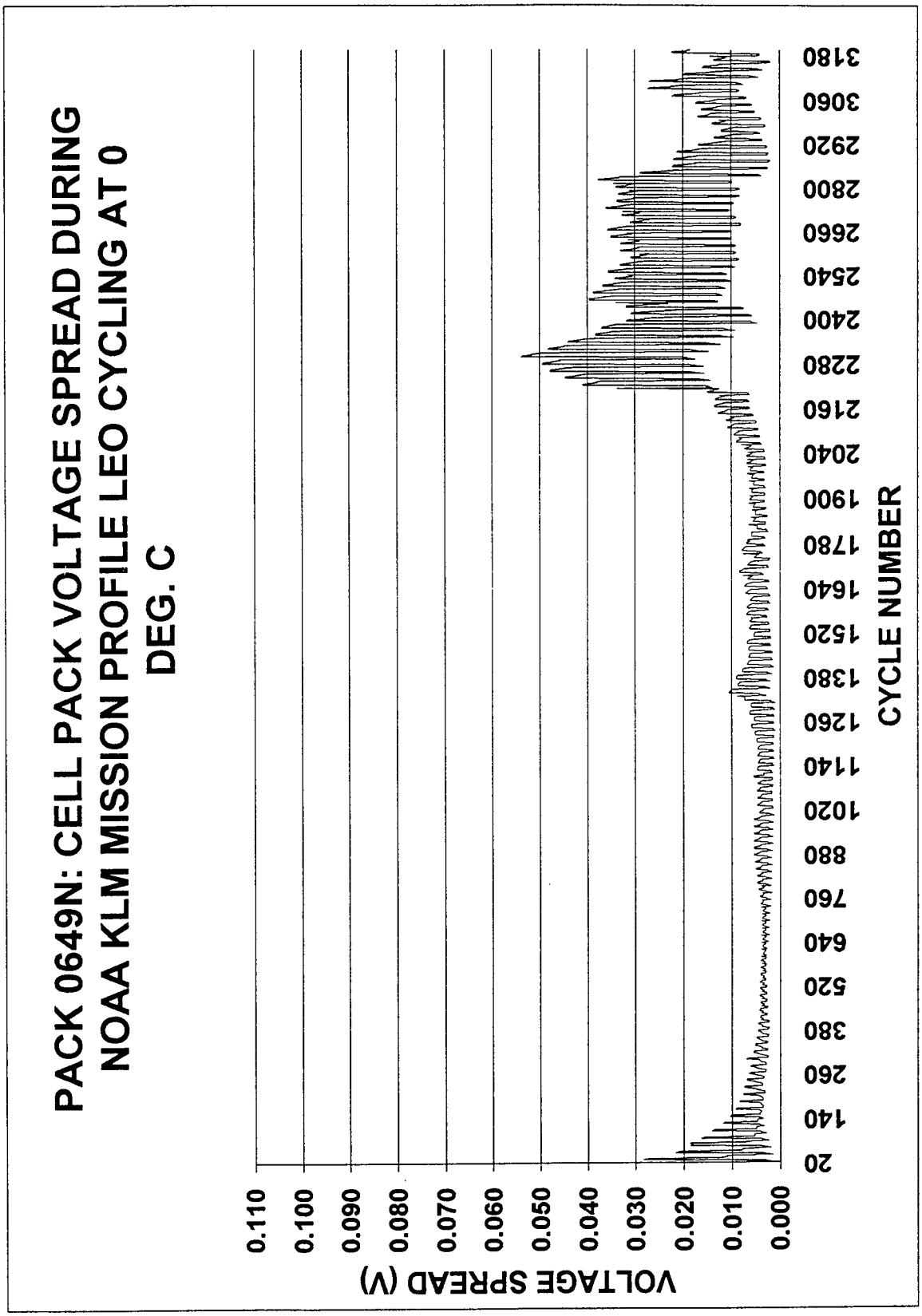
PACK 0649N: CELL PACK VOLTAGE SPREAD DURING
NOAA KLM MISSION PROFILE LEO CYCLING AT 0
DEG. C
VOLTAGE SPREAD (V)
0.110
0.100
0.090
0.080
0.070
0.060
0.050
0.040
0.030
0.020
0.010
0.000
CYCLE NUMBER
20
140
260
380
520
640
760
880
1020
1140
1260
1380
1520
1640
1780
1900
2040
2160
2280
2400
2540
2660
2800
2920
3060
3180

SUMMARY

- The simplest and most basic cell vendor data, whether it is from NiH_2, Lithium Ion, NiMH, Sodium Sulphur, or Advanced NiCd cell suppliers, may provide the best clues about a battery cell's future performance.
  - The fundamental electrochemical reactions of a particular battery cell technology provide key information for judging long-term performance potential.
  - Pressure, voltage and capacity measurements provide the fundamental measures for almost any energy storage technology.
- Cell vendor data may supply all that is needed to be known about a particular cell vendor's product (regardless of technology) and it's long-term performance capabilities.

CONCLUSIONS

- Data from Standard NiCd battery cell vendors appears to be useful for identifying defective cells.
- A potentially useful method has been developed to screen cells for flight battery use and identify prime candidate cells for life-cycle testing.
- Similar screening techniques may find application in the newer energy storage technologies.

NASA Battery Testbed: A Designed Experiment for the Optimization of LEO Battery Operational Parameters

F. Deligiannis
D. Perrone
S. Di Stefano

NASA Aerospace Battery Workshop
November 30, 1995

OUTLINE

- NASA BATTERY TESTBED BACKGROUND, CAPABILITIES AND RATIONALE
- DESIGNED EXPERIMENT TO OPTIMIZE LEO BATTERY MANAGEMENT
- IMPLEMENTATION / RESULTS
- SUMMARY

BACKGROUND

- NASA LOW-EARTH-ORBITING SATELLITES HAVE BEEN UTILIZING THE 50-Ah NASA STANDARD NICKEL CADMIUM BATTERY FOR THE LAST TWO DECADES
- DURING 1992 SEVERAL SATELLITES USING THE NASA STANDARD NiCd BATTERIES EXPERIENCED PERFORMANCE ANOMALIES DURING FLIGHT
- NOVEL BATTERY MANAGEMENT TECHNIQUES HAD TO BE IMPLEMENTED TO RECOVER BATTERY PERFORMANCE
- THE NASA BATTERY TESTBED WAS ESTABLISHED TO SYSTEMATICALLY EVALUATE VARIOUS BATTERY MANAGEMENT TECHNIQUES

TESTBED CAPABILITIES

- TESTBED CURRENTLY CONFIGURED TO HANDLE THREE 22-CELL 50 Ah NiCd BATTERIES IN PARALLEL
- ORBITAL PROFILES ARE SIMULATED AND IMPLEMENTED THROUGH COMPUTER HARDWARE/ SOFTWARE
- TYPICAL CHARGE/DISCHARGE MODES CAN BE IMPLEMENTED (CONSTANT CURRENT, CONSTANT POWER, CONSTANT VOLTAGE, ETC.)
- POWER AND ORBIT PROFILES ARE EASILY VARIED
- MONITORING AND DATA COLLECTION OF INDIVIDUAL CELL VOLTAGES, BATTERY CURRENTS, TEMPERATURES, & VOLTAGES

TYPICAL TESTBED OPERATION

(5% DOD, 20 AMP PEAK, 5°C, V/T 5, 110 MIN. ORBIT)

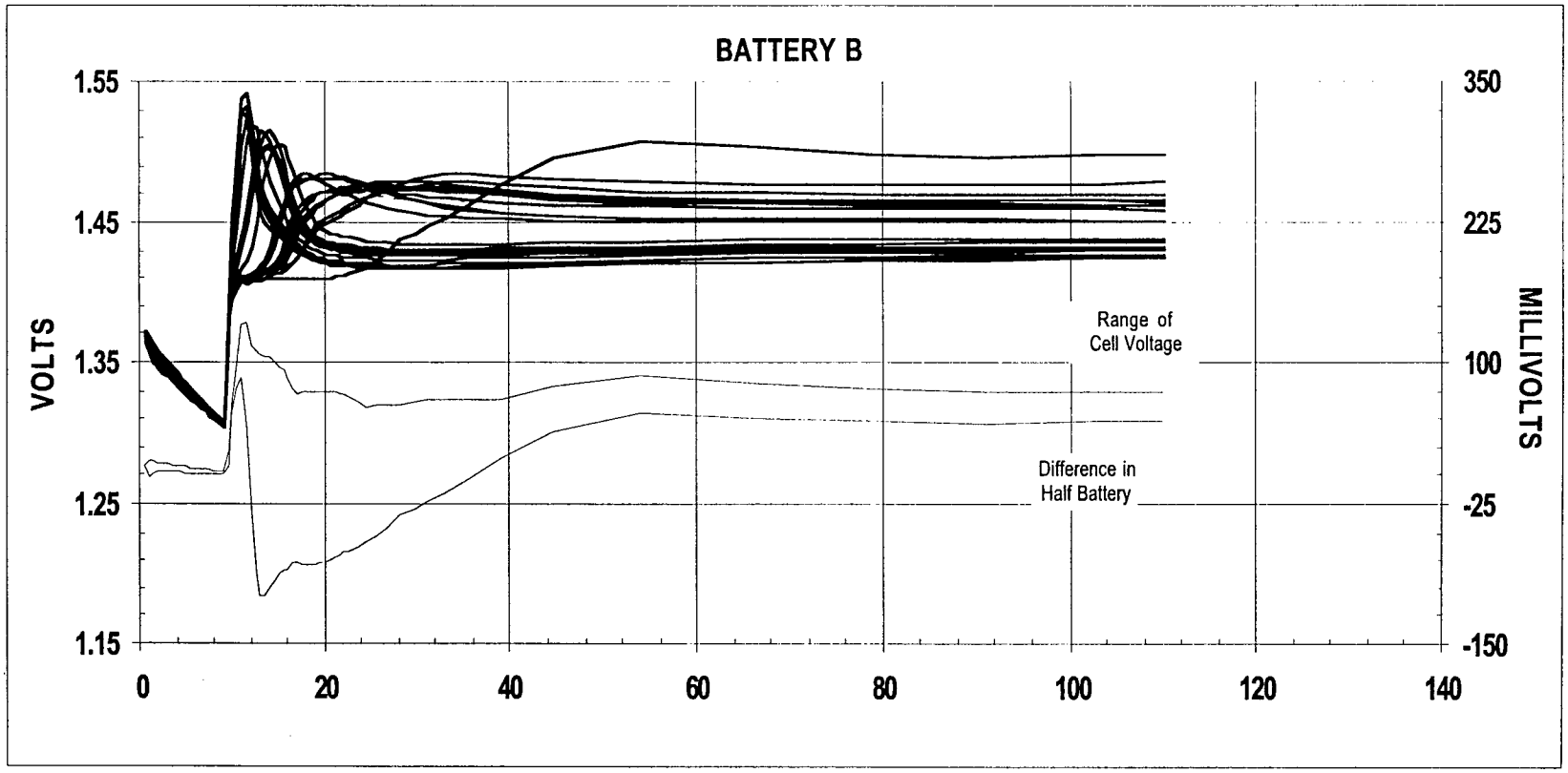

TYPICAL TESTBED OPERATION

(25%DOD, 20 AMP PEAK, 10°C. V/T 2, 100 MIN. ORBIT)

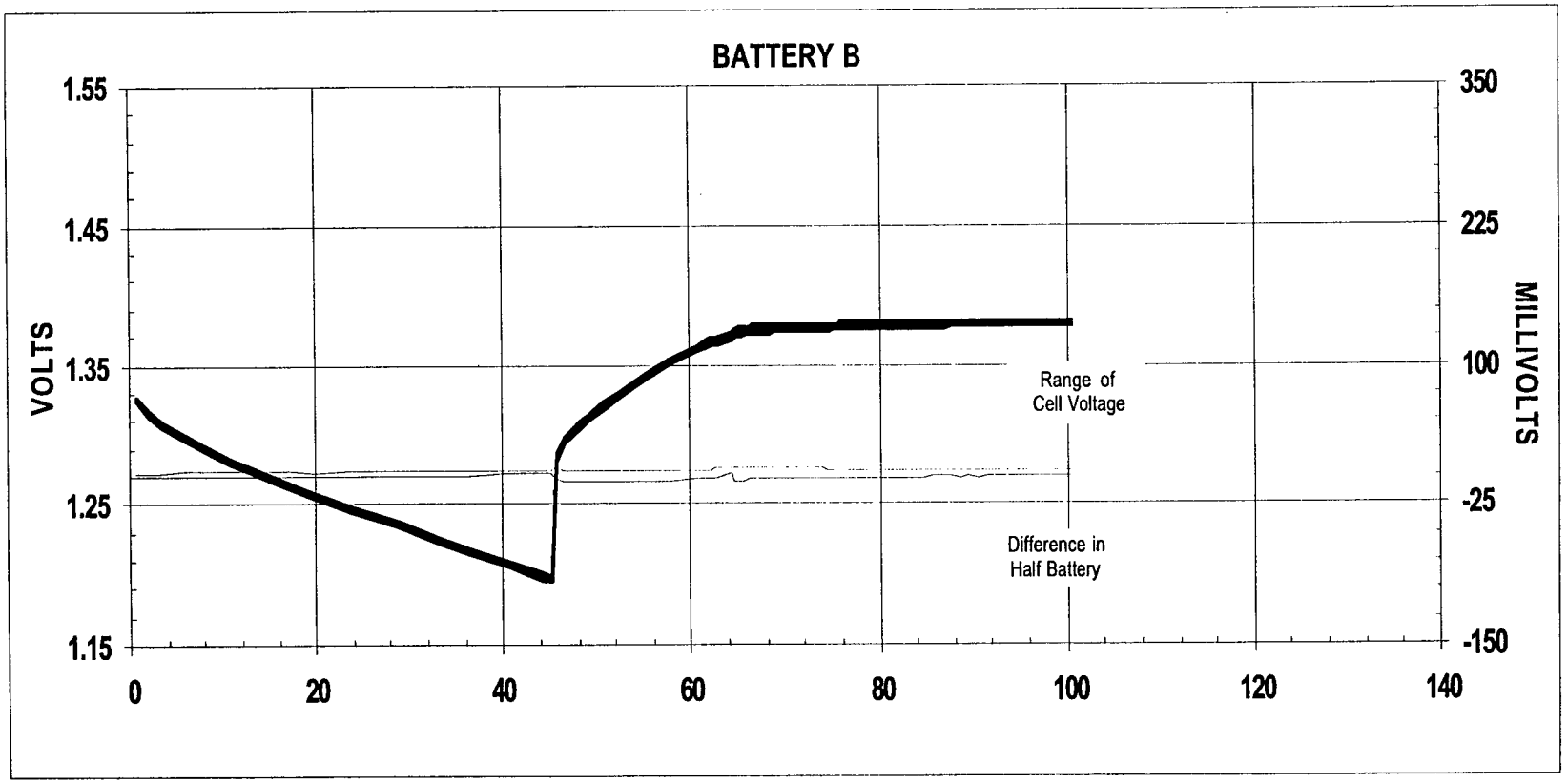

Robust Design - Macro Modeling Approach

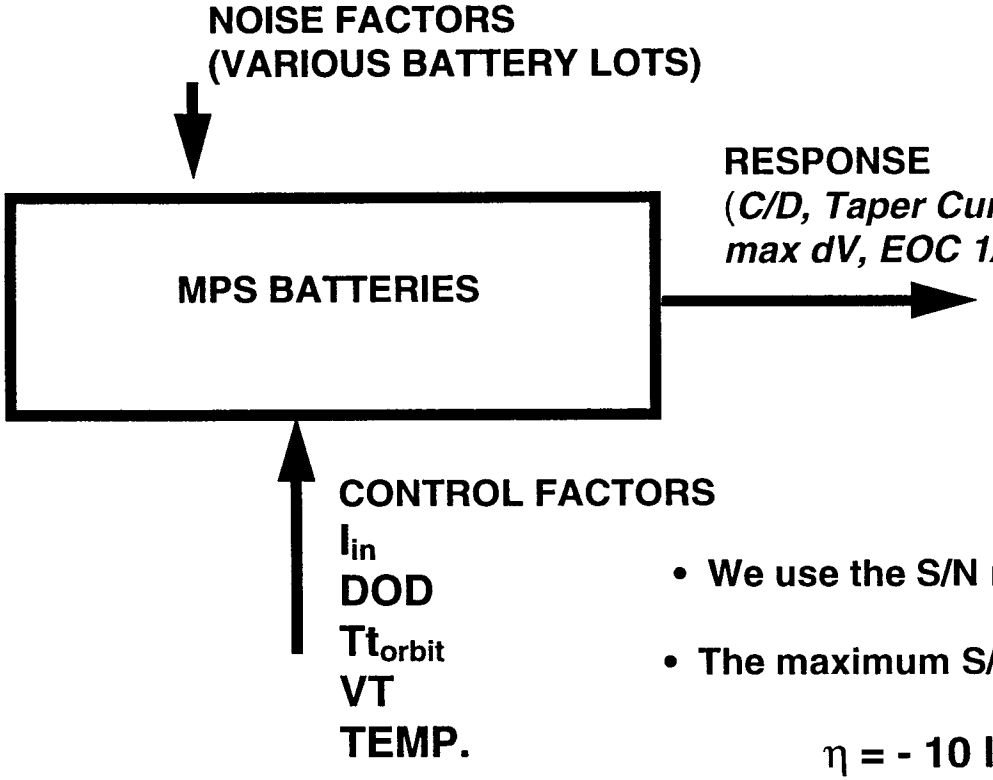

- We use the S/N ratio as the defining quality characteristic.
- The maximum S/N indicates better response (performance)

$$\eta = -10 \log_{10} (\text{mean square response})$$

NASA BATTERY TESTBED - DESIGNED EXPERIMENT
LEO OPERATIONAL PARAMETERS

Five Variables (control factors) at four levels each

I_{in} (Amp)	DOD (%)	T (°C)	t_{orbit} (min)	VT (Volt)
30	5	0	90	2
60	10	5	100	3
90	15	10	110	4
120	25	15	120	5

Battery Performance (response) Parameters - The effect of a change in variables is monitored by observing the response on the operational parameters (***C/D, Taper Current, EOC dV, max dV, EOC 1/2 batt. dV, max 1/2 batt. dV).***

FULL FACTORIAL vs. ORTHOGONAL ARRAY

- FULL FACTORIAL
  - FIVE PARAMETERS AT FOUR LEVELS REQUIRE $5^4 = 1024$ EXPERIMENTS
  - 60 SIMULATED LEO CYCLES PER EXPERIMENT
  - FOUR DAYS PER EXPERIMENT
  - REQUIRES 4096 DAYS OF EXPERIMENTATION OR 11.2 YEARS

- CHOOSING A L_{16} ORTHOGONAL ARRAY
  - REQUIRES 16 EXPERIMENTS
  - 60 SIMULATED LEO CYCLES PER EXPERIMENT
  - FOUR DAYS PER EXPERIMENT
  - REQUIRES 64 DAYS OF EXPERIMENTATION

- THE ORTHOGONAL ARRAY SAVES CONSIDERABLE TIME AND COST

TAGUCHI ORTHOGONAL ARRAY
STANDARD L_{16}

EXPT. #	CURRENT	DOD	TEMP.	ORBIT LEN.	V/T
1	10	5	0	90	2
2	10	10	5	100	3
3	10	15	10	110	4
4	10	25	15	120	5
5	20	5	5	110	5
6	20	10	0	120	4
7	20	15	15	90	3
8	20	25	10	100	2
9	30	5	10	120	3
10	30	10	15	110	2
11	30	15	0	100	5
12	30	25	5	90	4
13	40	5	15	100	4
14	40	10	10	90	5
15	40	15	5	120	2
16	40	25	0	110	3

NASA BATTERY TEST BED -- TAGUCHI ORTHOGONAL ARRAY

VARIABLE SETTINGS						AVERAGES																	
						CHARGE TO DISCHARGE AMPERE-HOUR RATIO			END OF CHARGE CURRENT (AMPERES)			END OF CHARGE RANGE OF CELL VOLTAGES (MV)			MAXIMUM RANGE OF CELL VOLTAGES (MV)			END OF CHARGE HALF-BATTERY VOLTAGE DIVERGENCE (MV)			MAXIMUM HALF-BATTERY VOLTAGE DIVERGENCE (MV)		
EXPERIMENT	TEMPERATURE (DEGREES C)	ORBIT DURATION (MINUTES)	DOD BASED ON 150AH NAMEPLATE	INRUSH CURRENT	MAXIMUM VOLTS PER CELL	A	B	C	A	B	C	A	B	C	A	B	C	A	B	C	A	B	C
11	0	100	15%	90	1.46	1.013	1.016	1.025	0.79	0.75	0.72	13.8	45.6	15.6	28.1	50.9	24.2	-4.3	4.6	-1.1	19.8	39.7	24.9
16	0	110	25%	120	1.42	1.002	1.003	1.005	2.70	2.73	1.82	2.7	5.1	17.4	21.9	28.5	18.0	-2.9	0.1	-3.8	13.0	10.5	11.1
6	0	120	10%	60	1.44	1.019	1.023	1.031	0.65	0.60	0.36	13.3	29.3	12.9	34.8	50.0	32.1	-25.9	23.4	3.0	90.9	29.0	37.1
1	0	90	5%	30	1.4	1.014	1.012	1.01	0.41	0.38	0.26	12.4	21.4	13.5	37.6	52.5	20.3	-25.0	15.5	0.2	73.7	26.1	32.9
5	5	110	5%	60	1.45	1.081	1.083	1.164	0.432	0.396	0.444	46.67	74.05	24.33	132.9	136.5	40.96	-96.1	50.48	-8	327.6	88.55	65.71
12	5	90	25%	90	1.43	1.004	1.004	1.007	5.995	5.954	3.812	4.31	9.833	23.11	30.85	27.32	23.43	31.42	31.42	31.44	21.45	15.95	12.78
15	5	120	15%	120	1.39	1.01	1.01	1.011	1.088	1.078	0.61	2.269	6.061	7.615	36.26	39.63	24.45	-2.41	4.704	3.344	15.18	13.01	19.89
2	5	100	10%	30	1.41	1.012	1.012	1.014	1.248	1.217	0.603	5.165	11.33	11.5	26.97	38.18	28.46	-9.03	9.647	3.309	15.53	11.18	38.2
8	10	100	25%	60	1.38	0.983	0.984	0.988	5.19	5.167	5.259	3.422	3.86	5.492	6.556	7.503	29.54	-5.56	-1.09	6.248	4.182	3.165	20.13
9	10	120	5%	90	1.4	1.057	1.054	1.052	0.394	0.399	0.243	4.747	5.112	14.32	38.71	40.93	33.61	11.72	1.038	-1.62	23.81	16.36	54.52
14	10	90	10%	120	1.44	1.047	1.046	1.112	1.234	1.184	0.867	29.32	50.61	22.79	56.12	67.47	34.94	-44.7	35.71	-6.97	111.7	44.4	44.97
3	10	110	15%	30	1.42	1.014	1.014	1.027	1.79	1.775	0.893	14.34	21.28	17.4	19.92	26.5	22.38	-20.4	11.97	-0.78	39.47	11.99	35.39
4	15	120	25%	30	1.425	0.986	0.986	0.99	9.051	9.13	9.782	8.011	5.771	21.24	15.02	15.75	23.89	-1.53	-2.22	1.787	4.084	4.723	18.18
7	15	90	15%	60	1.385	1.013	1.013	1.012	1.927	1.94	1.675	3.657	3.265	5.646	21.87	28.66	20.68	2.155	1.429	3.245	4.205	4.24	20.87
10	15	110	10%	90	1.365	1.013	1.012	1.014	0.699	0.691	0.473	2.567	2.445	2.864	26.93	26.6	23.08	0.122	0.664	2.163	0.248	4.582	25.21
13	15	100	5%	120	1.405	1.073	1.07	1.102	0.761	0.762	0.457	2.711	3.783	16.62	38.99	38.55	36.01	4.661	-4.49	-0.88	19.72	24.15	63.04
VER	5	120	25%	90	1.410	1.00	1.00	1.01	2.8	2.8	1.5	2.1	8.4	10.9	25.1	23.1	25.5	-4.3	4.8	0.3	-45.9	-13.9	12.7

SIGNAL TO NOISE RATIO FOR RECHARGE FRACTION

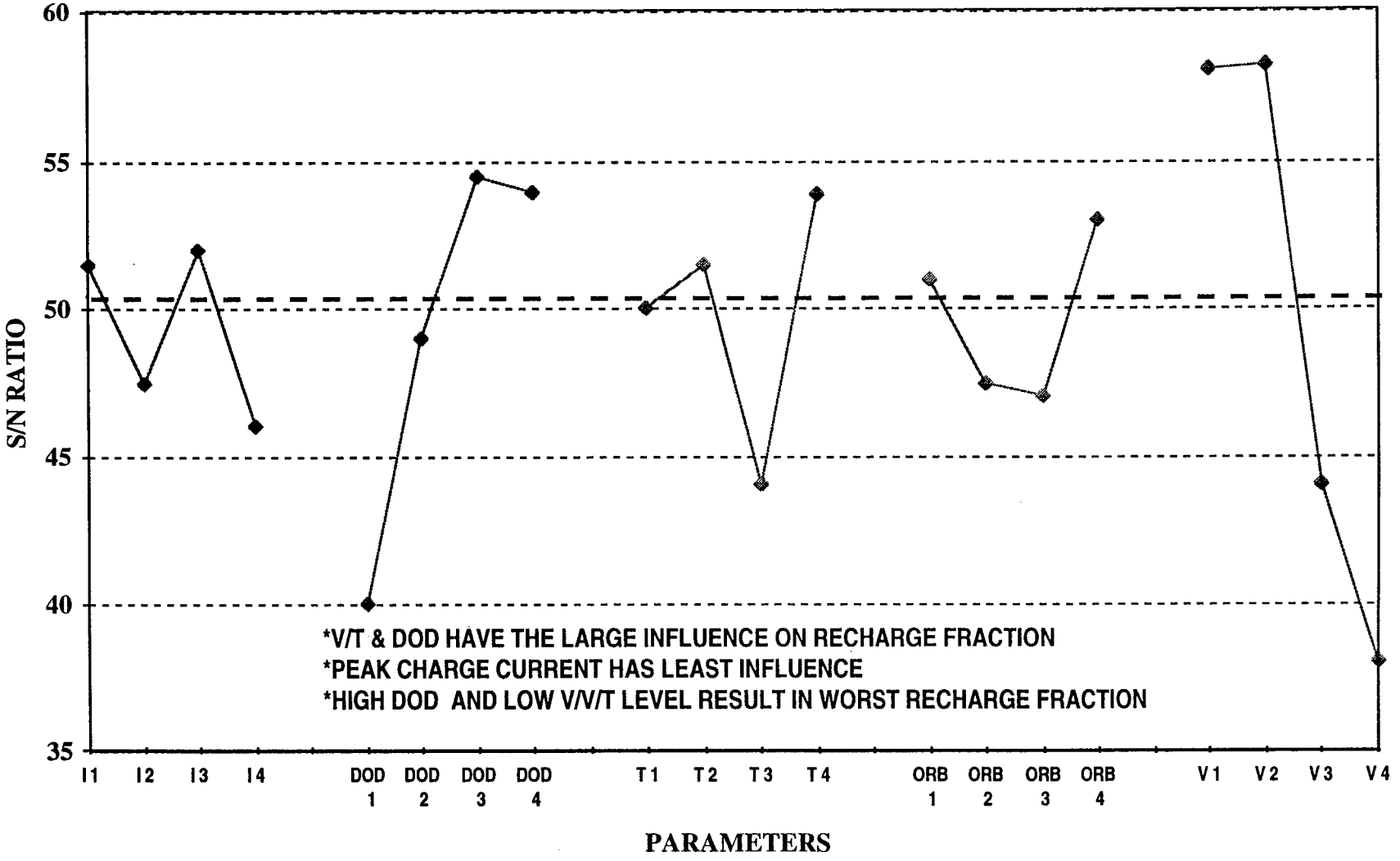

SIGNAL TO NOISE RATIO FOR END OF CHARGE DIVERGENCE

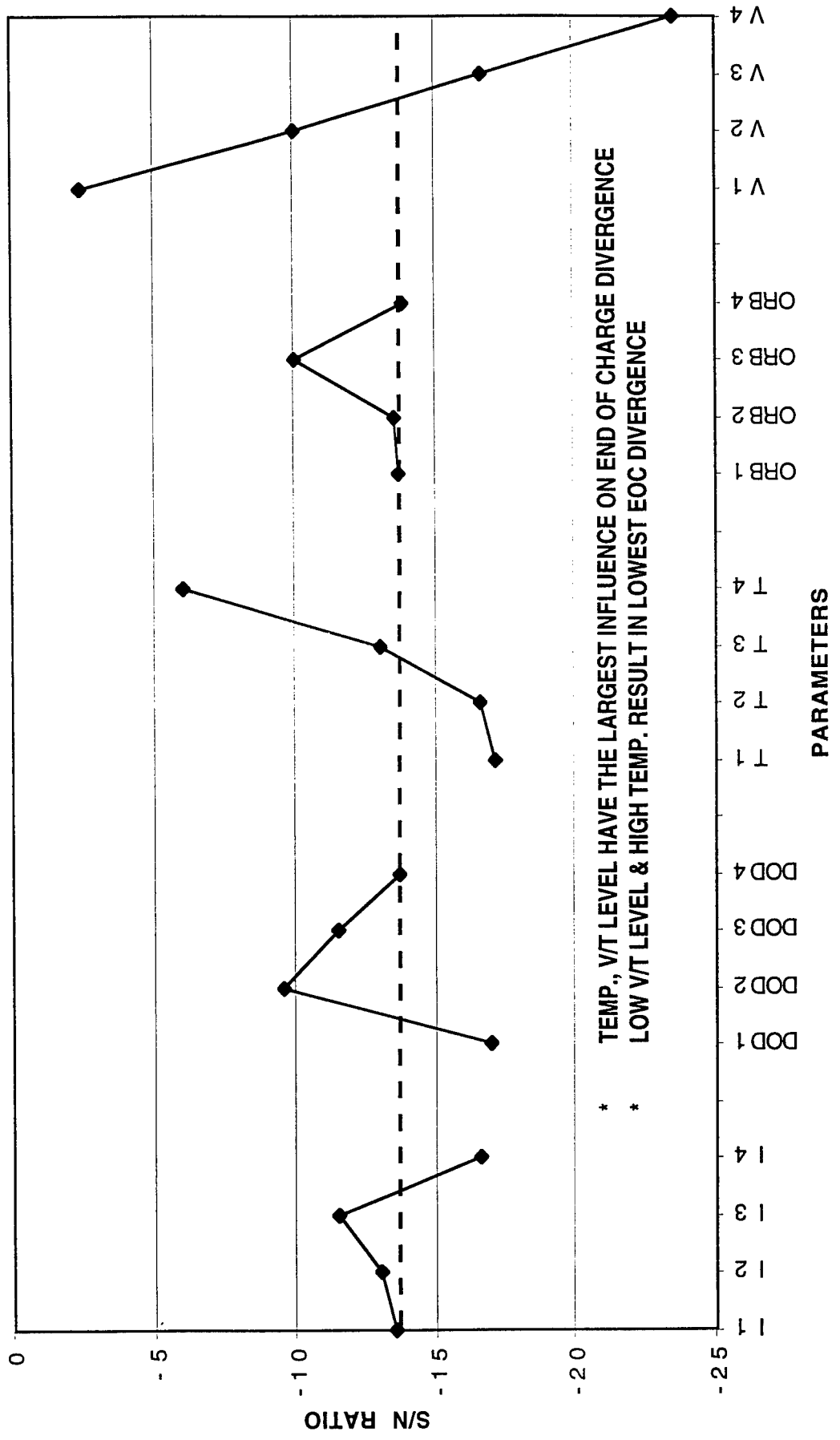

JPL

SIGNAL TO NOISE RATIO FOR MAX 1/2 BATT DIVERGENCE

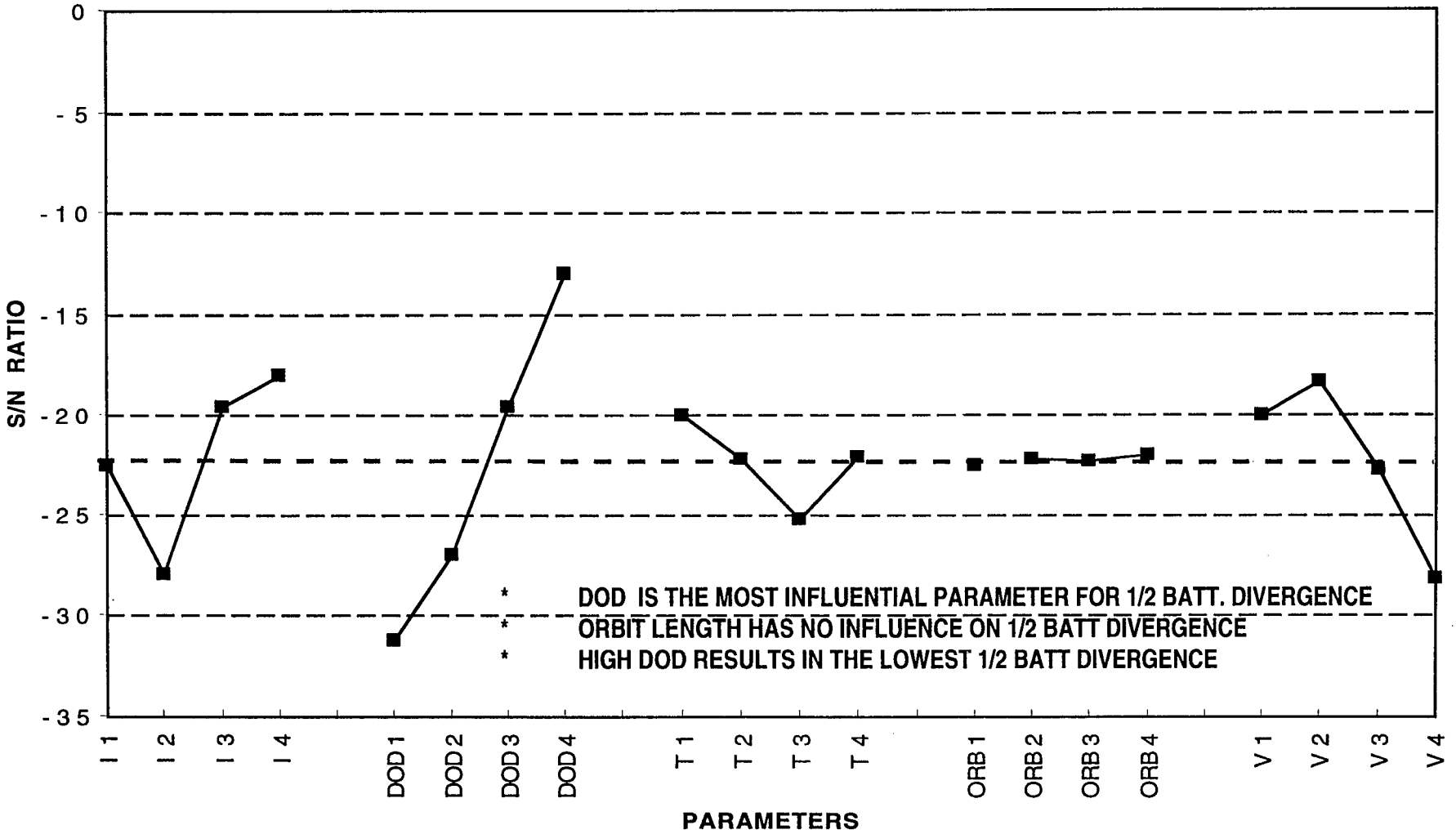

SUMMARY OF RESULTS FROM L_{16} ARRAY

	C/D RATIO	*MAX 1/2 BATT. DIV.*	*MAX CELL VOLTAGE DIV.*	*VERIF. CONDITIONS*
PEAK CHARGE (AMP)	30	40	30	30
DOD (%)	15	25	25	25
TEMP. (°C)	15	0	15	5
ORBIT DUR. (min.)	120	120	120	120
V/T LEVEL	3	3	4	3

VERIFICATION RESULTS

(25% DOD, 30 AMP PEAK, 5°C, V/T 3, 120 MIN. ORBIT)

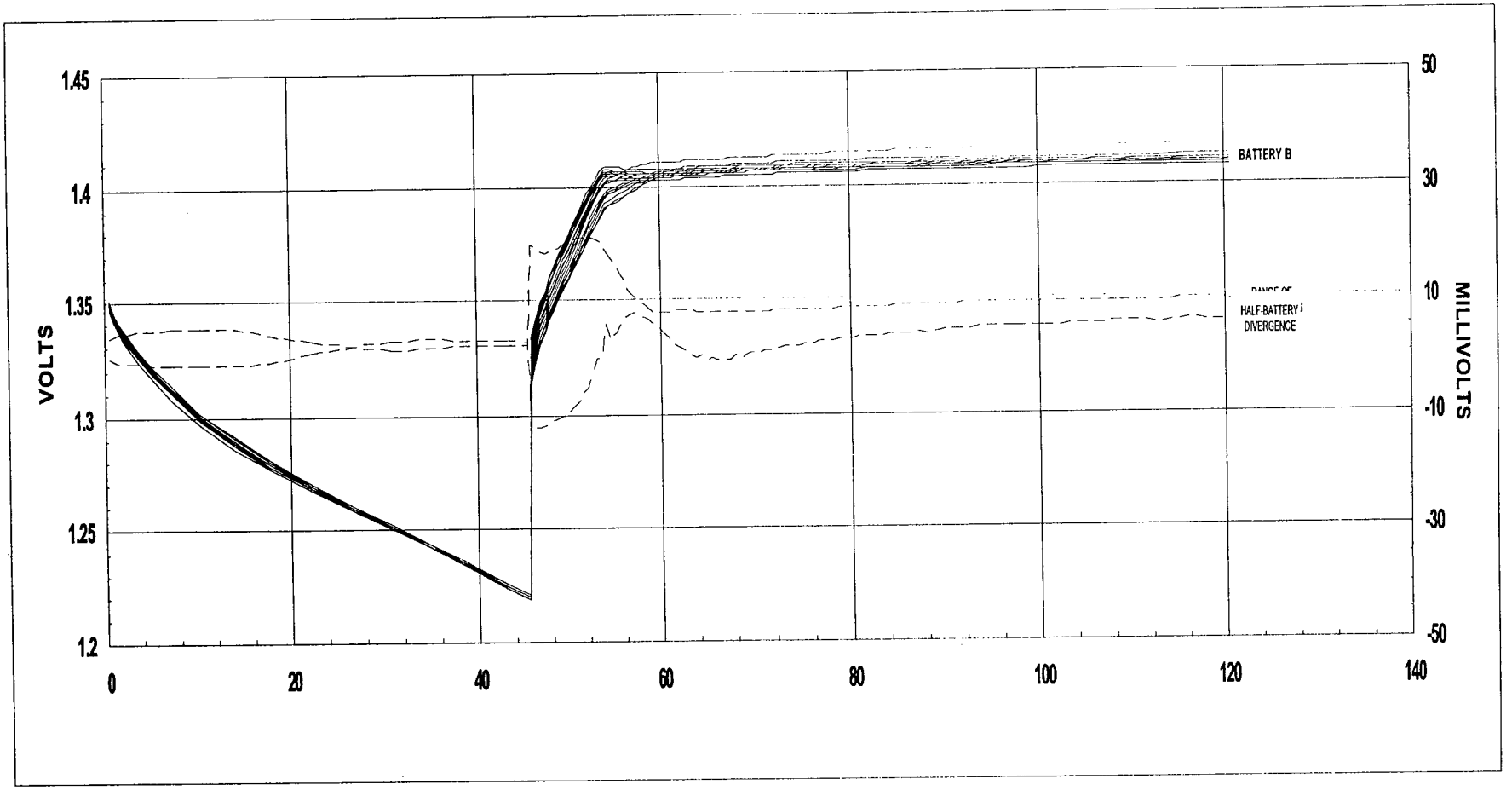

SUMMARY

- RELIABLY IMPLEMENTED SIMULATION OF SPACECRAFT BATTERY OPERATION (THREE 22-CELL, 50 AH BATTERIES IN PARALLEL)
- PERFORMED ROBUST DESIGN EXPERIMENT TO OBTAIN OPTIMUM BATTERY OPERATIONAL PARAMETERS
- PRELIMINARY DATA ANALYSIS INDICATES THAT THE THREE MOST INFLUENTIAL PARAMETERS FOR BATTERY PERFORMANCE ARE DOD, V/T AND TEMP
- SHORT TERM TESTS USING ROBUST DESIGN OF EXPERIMENTS CAN PROVIDE GUIDELINES FOR OPTIMUM BATTERY OPERATION
- ROBUST DESIGN APPROACH WILL BE USED TO PROVIDE GUIDELINES FOR BATTERY OPERATION ON CURRENT SPACECRAFT IN ORBIT AS BATTERIES AGE (GRO, UARS, EUVE, TOPEX)

ACKNOWLEDGMENT

The work described here was carried out at the Jet Propulsion Laboratory, California Institute of Technology, under contract with the National Aeronautics and Space Administration.

This work is also part of the NASA Battery Program sponsored by the Office of the NASA Chief Engineer.

Ni-Cd and Ni-H_2 BATTERY PERFORMANCE

ON ENGINEERING TEST SATELLITE-VI

1995 NASA Aerospace Battery Workshop

November 28 ~ 30,1995

S.Kuwajima & H.Kusawake

National Space Development Agency of Japan

NASDA NATIONAL SPACE DEVELOPMENT AGENCY OF JAPAN | Ni- Cd and Ni- H2 BATTERY PERFORMANCE on ETS- VI

CONTENTS

ENGINEERING TEST SATELLITE- VI

Ni- Cd BATTERY PERFORMANCE

Ni- H2 BATTERY PERFORMANCE

COMPARISON BETWEEN FLIGHT DATA and GROUND DATA

Engineering Test Satellite-VI

Major Characteristics

Shape	Rectangular body with deployable solar paddles
Weight	Approx. 2ton (Beginning of life) Payload capacity 660 kg
Attitude control	3-axis-stabilized
Life	10 years for satellite bus
Reliability	4,100 W (End of life at summer solstice)
Launch vehicle	H-II rocket
Launch site	Tanegashima Space Center, Kagoshima
Launch date	Aug.–Sept. 1993
Orbit	Geostationary orbit (154°E Logi. (tentative))

On-Board Experimental Equipment

Bus Experimental Equipment	Launch Environment Monitors Technical Data Acquisition Equipment Ni-H_2 Battery Equipment Electro-Thermal-Hydrazine Thruster Equipment On-Board Experimental Equipment for Attitude Control System
Communication Experimental Equipment	Fixed and Mobile satellite Communications Equipment S-band Inter-satellite Communications Equipment K-band Inter-Satellite Communications Equipment O-band Communications Equipment Laser Communications Equipment Feeder Link Communications Equipment

NASDA

NASDA NATIONAL SPACE DEVELOPMENT AGENCY OF JAPAN

SIMPLIFIED BLOCK DIAGRAM of THE ETS- VI EPS

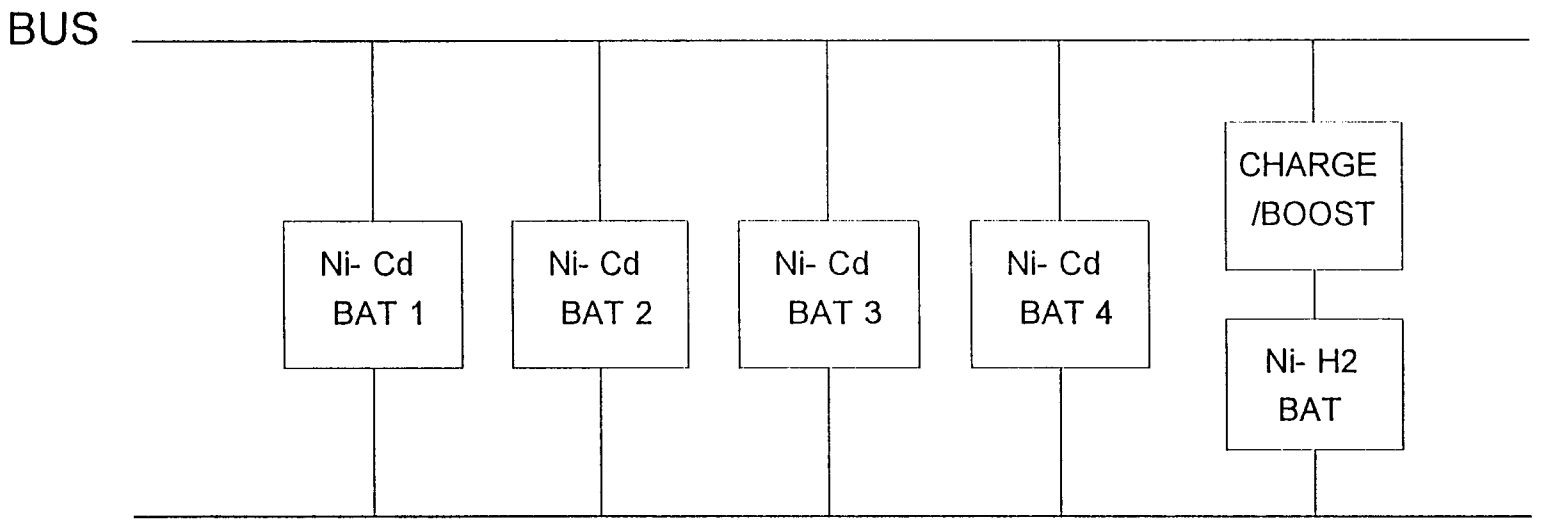

Ni-H2 and Ni-Cd batteries charge on suntime and discharge on eclipse simultaneously.

NASDA
Space Subsystems and Technology Department

Orbit of ETS-VI

ETS-VI was launched on August 28, 1994, but failed to transit from transfer orbit to geosynchronous orbit due to Apogee Engine trouble. Present orbit of the satellite and it's new orbit are as follows,

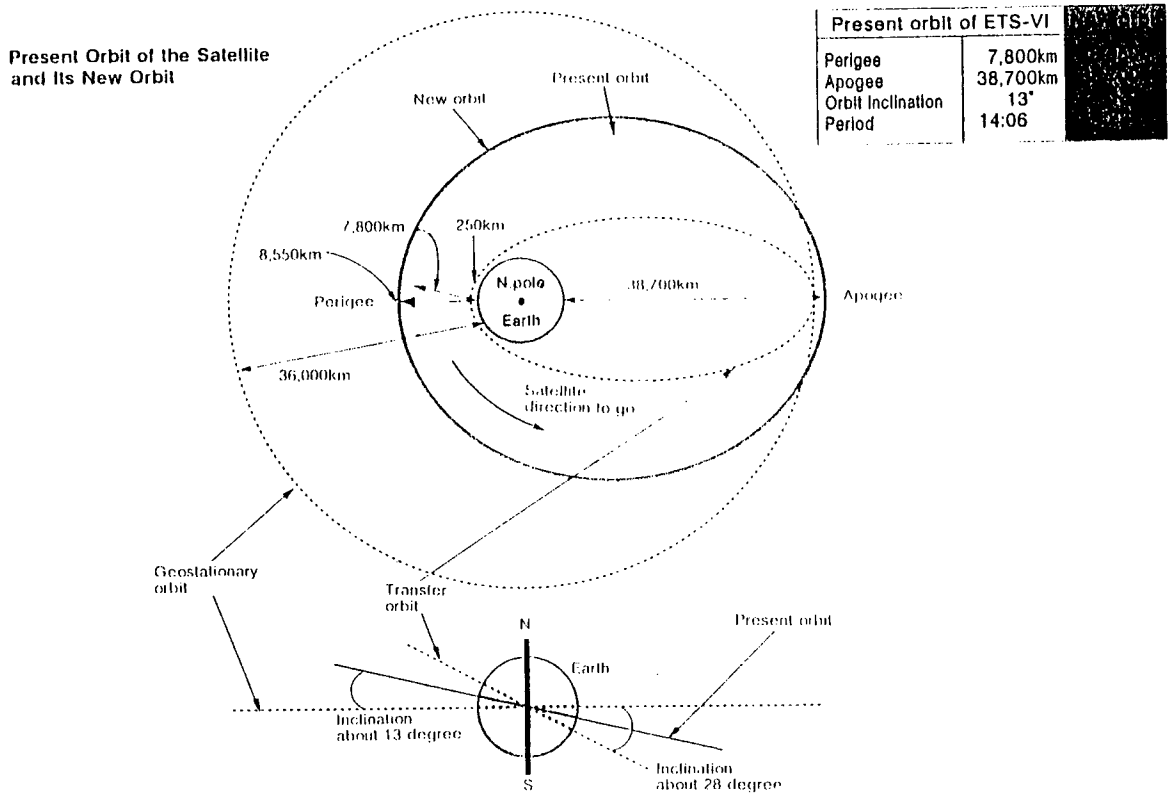

NASDA NATIONAL SPACE DEVELOPMENT AGENCY OF JAPAN

ORBITAL ECLIPSE PROFILE

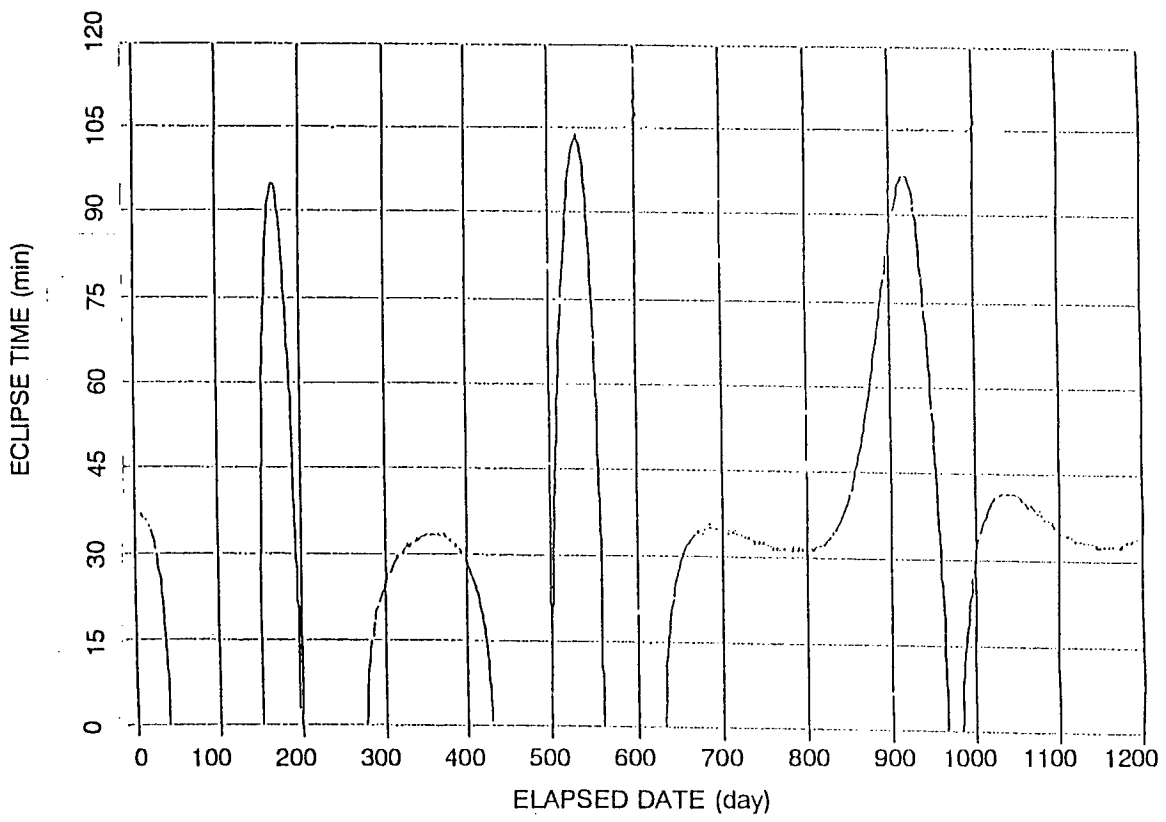

NASDA NATIONAL SPACE DEVELOPMENT AGENCY OF JAPAN

DECREASE of POWER GENERATION

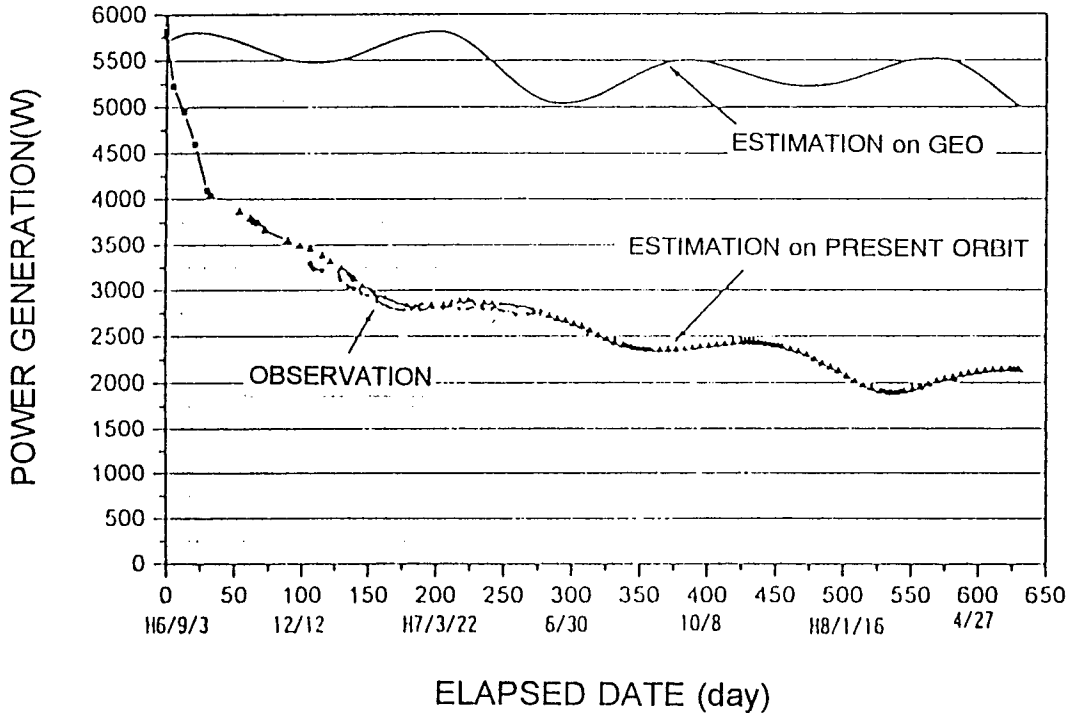

ETS-VI goes through the Van Allen(radiation) belts.
Thus power generation decreased remarkably.

NASDA
NATIONAL SPACE DEVELOPMENT AGENCY OF JAPAN

PROGRESS of OPERATION on ORBIT

	1994 8	9	10	11	12	1995 1	2	3	4	5	6	7	8	9	10	11
EVENT	▲ LAUNCH					▲ Malfunction of ACS	▲ Malfunction of ACS									
Orbital profile		1st eclipse season				1st full sun		2nd eclipse season		2nd full sun			3rd eclipse season		3rd full sun	
Operation of Ni-Cd batteries		64cyc				trickle charge *		73cyc		trickle charge *			233cyc		▲ deep discharge	
Operation of Ni-H2 battery		32cyc ▲ turn on				charge at V/T#4 ** ▲ -40 · C		73cyc ▲ deep discharge		charge at V/T#4 * *			233cyc		* ▲ 100% discharge	

*Reconditioning

NASDA NATIONAL SPACE DEVELOPMENT AGENCY OF JAPAN

35AH SPACE Ni-Cd CELL

CELL MAJOR SPECIFICATIONS

Rated Capacity		35 AH
Mission	GEO	10Years, 1,000cycles
	LEO	3Years, 20,000cycles
Weight		max. 1050g
Energy Density		40WH/kg
Mechanical Strength	Burst Pressure	35kgf/cm^2
	Pressure Cycling	50,000cycles (0~3.5 kgf/cm^{2}G)

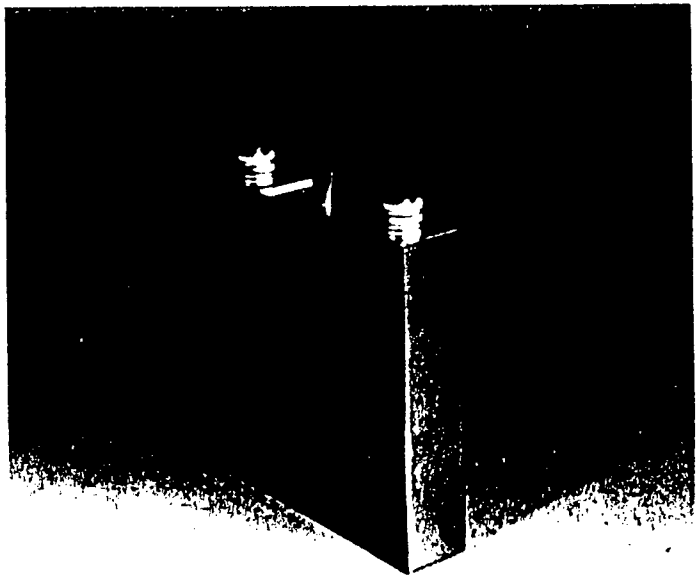

EXTERNAL VIEW OF Ni-Cd CELL

NASDA
NATIONAL SPACE DEVELOPMENT AGENCY OF JAPAN

ETS-VI Ni-Cd BATTERY

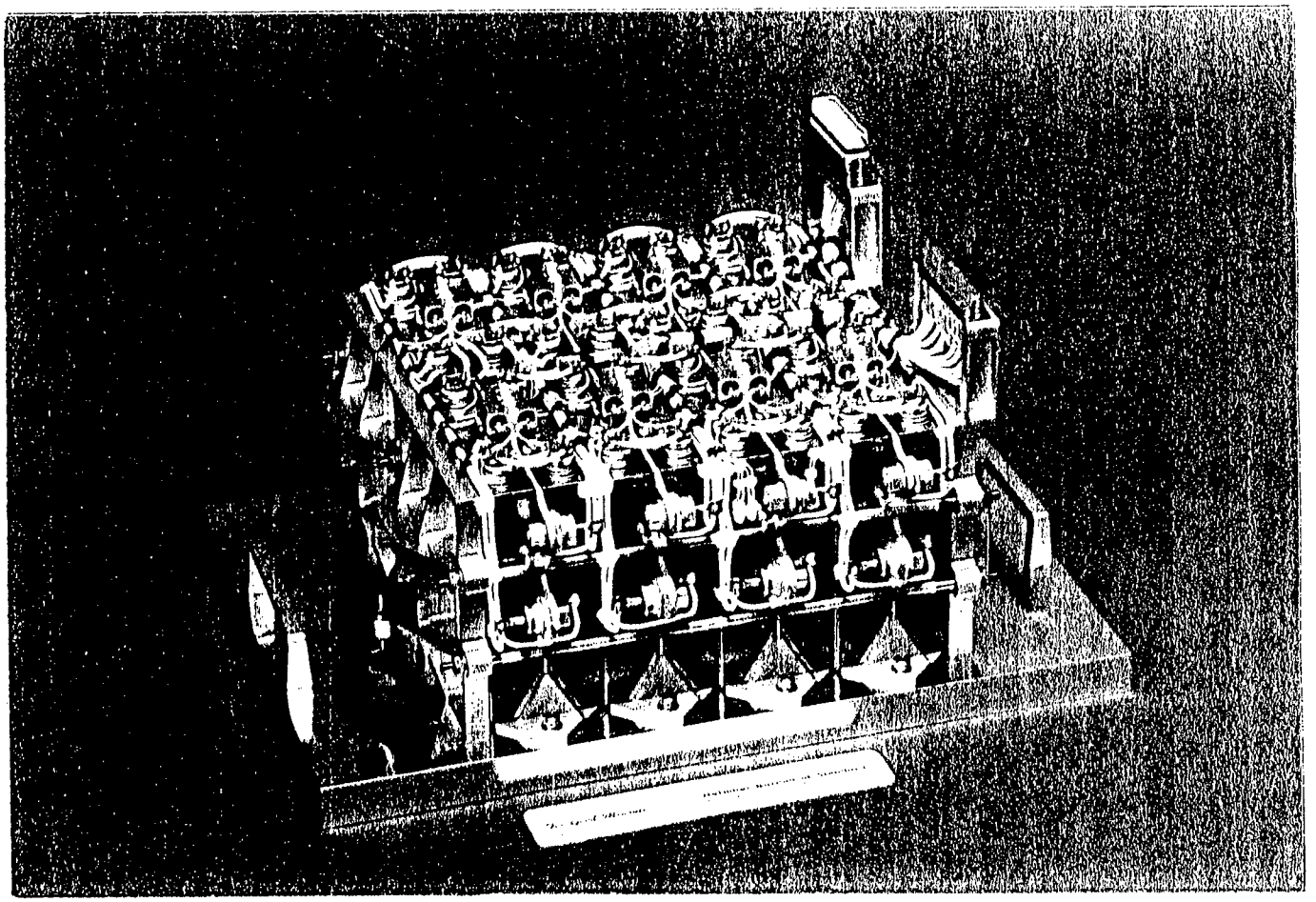

* Engineering Model

MAIN SPECIFICATION of 35Ah Ni-Cd BATTERY

Cell	Sanyo N35S/G0
Weight	19.3kg/pack(16cells)*
Volume	276(T) × 264(W) × 175(H) mm/pack
Charge Scheme	Full/Trickle (Command & Automatic by temp.)
Full Charge Rate	1.05 - 1.80A
Trickle Charge Rate	0.35 - 0.60A
Max. Discharge Rate	14.6A(normally parallel)
Max. Depth of Discharge	50%(@72min)
Mission Life	10years(@Geostationary Orbit)
Reconditioning Load	60.6 Ω
Operating Temperature	0 - 25 ° C

* ETS- Ⅵ uses 4 batteries, consists of 2packs.

NASDA NATIONAL SPACE DEVELOPMENT AGENCY OF JAPAN

TREND of 35Ah Ni-Cd BATTERIES(ECLIPSE SEASON)

BAT#1

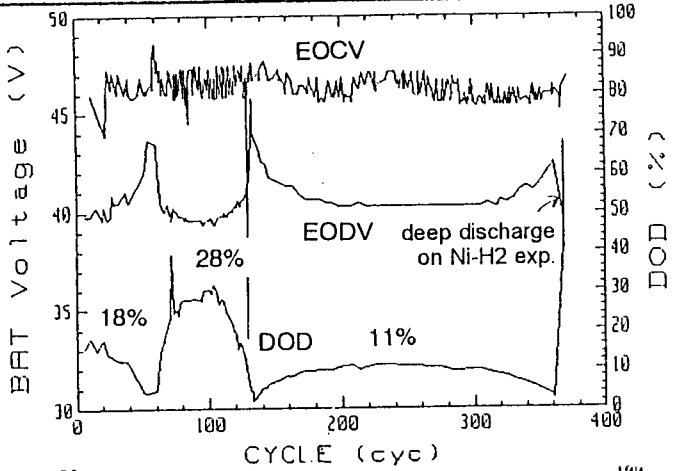

BAT#3

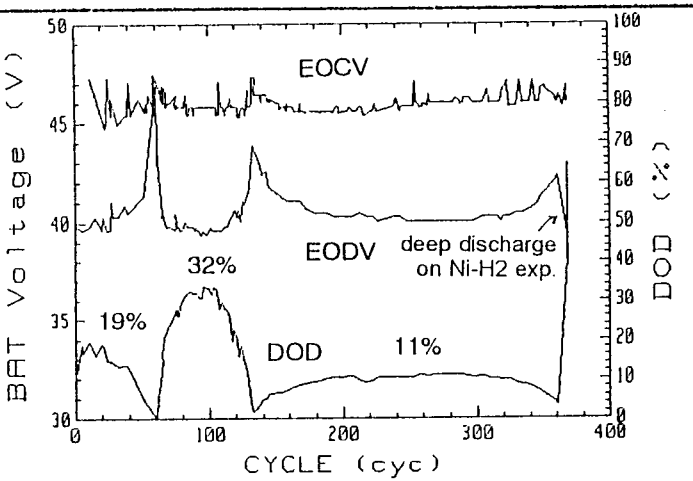

BAT#2

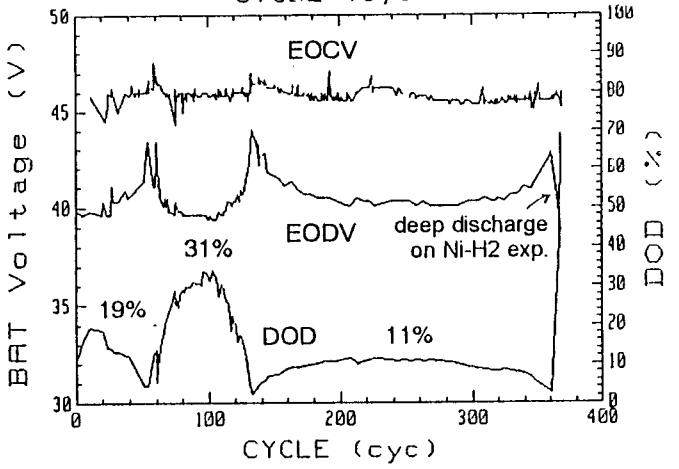

BAT#4

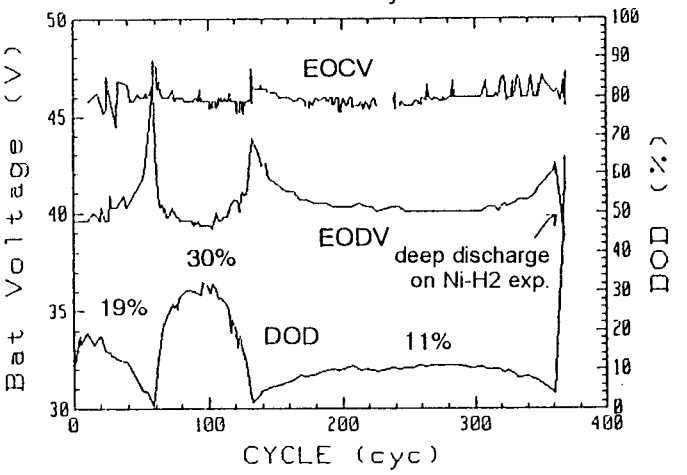

All batteries had good performance during all eclipse seasons.

NASDA NATIONAL SPACE DEVELOPMENT AGENCY OF JAPAN

EOCV and EODV of Ni-Cd CELLS(2nd ECLIPSE SEASON)

BAT#1

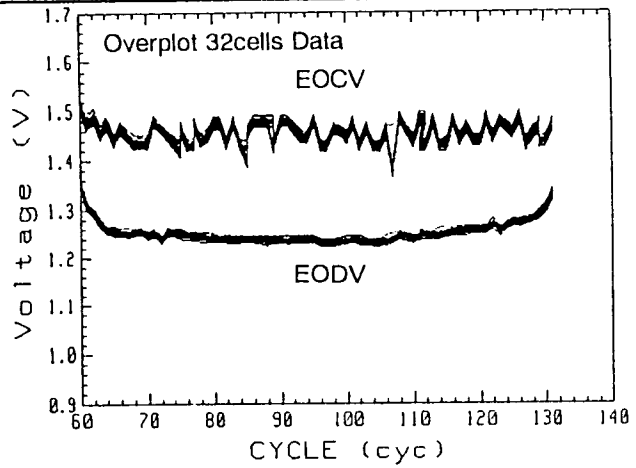

BAT#3

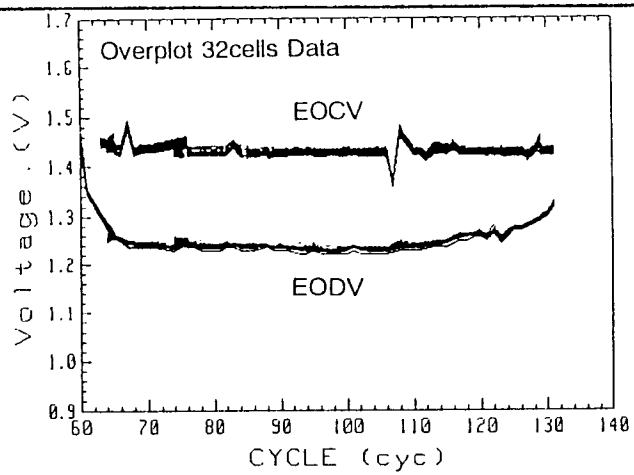

BAT#2

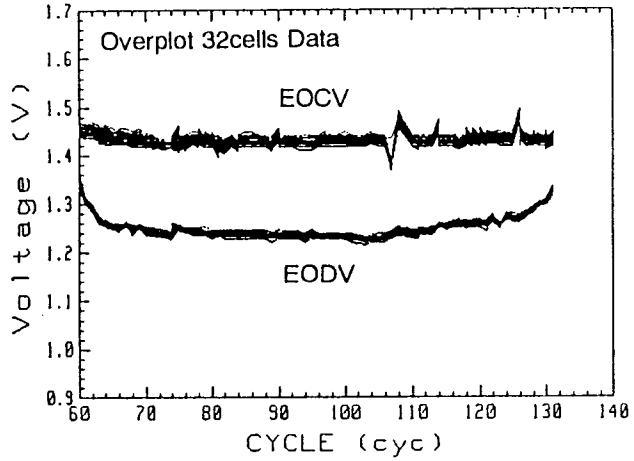

BAT#4

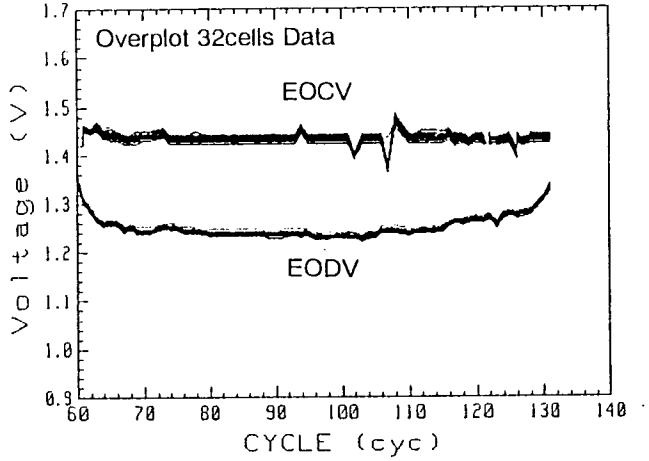

The difference between properties of cells is small.

NASDA NATIONAL SPACE DEVELOPMENT AGENCY OF JAPAN

TREND of 35Ah Ni-Cd BATTERIES(2nd FULL SUN TIME)

BAT#1

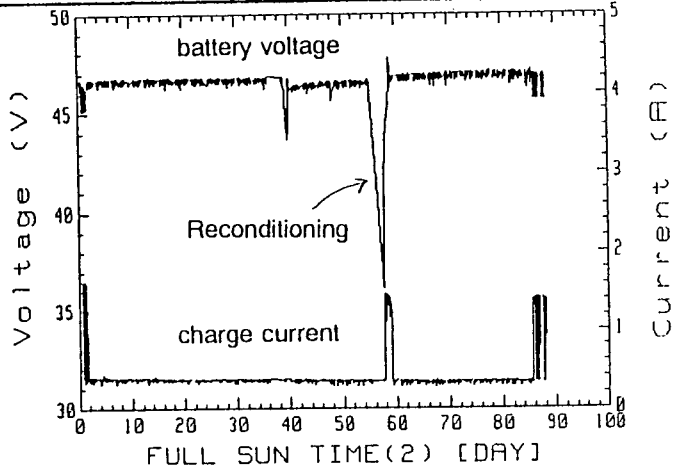

BAT#3

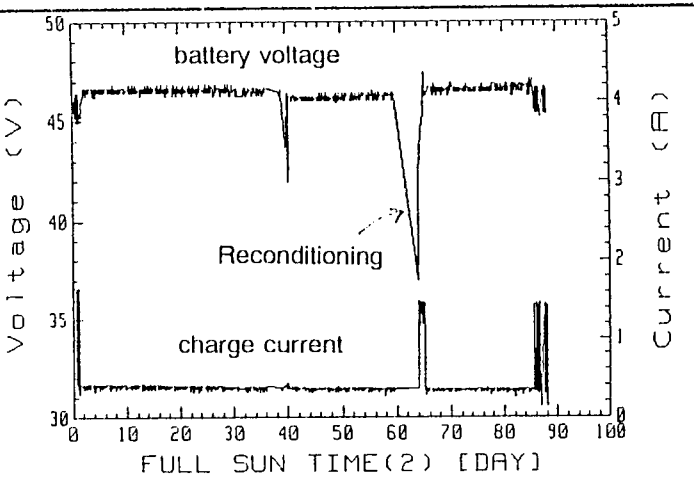

BAT#2

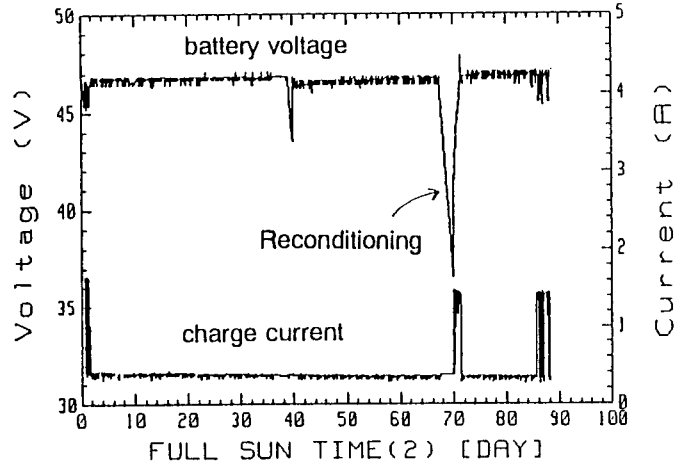

BAT#4

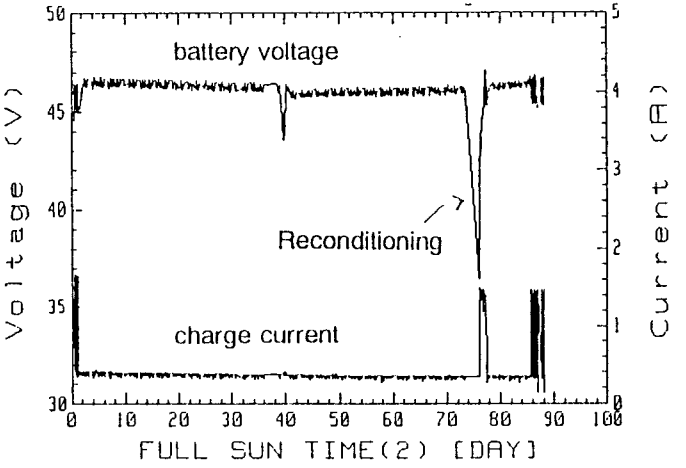

Voltage of all batteries were stable in full sun time.

NASDA NATIONAL SPACE DEVELOPMENT AGENCY OF JAPAN

RECONDITIONING of 35Ah Ni-Cd BATTERIES

BAT#1

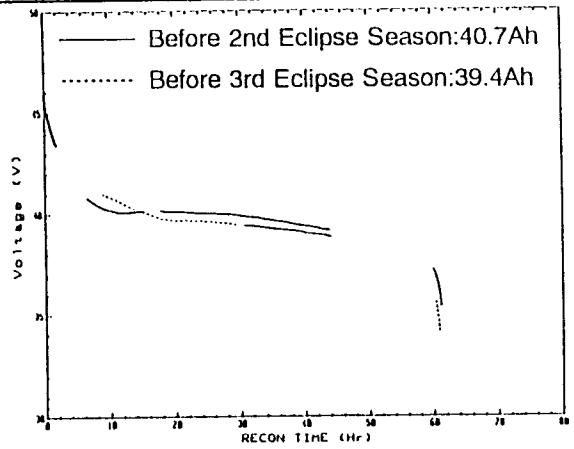

BAT#3

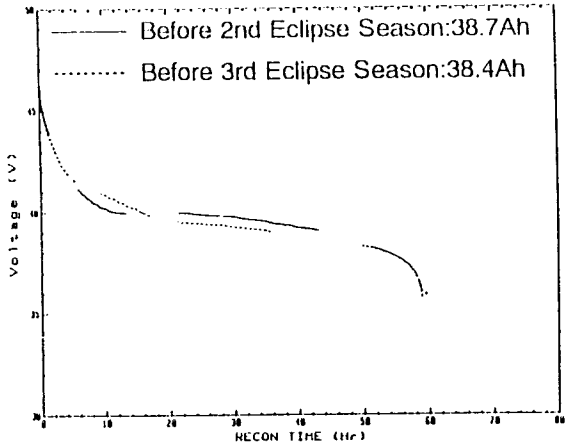

BAT#2

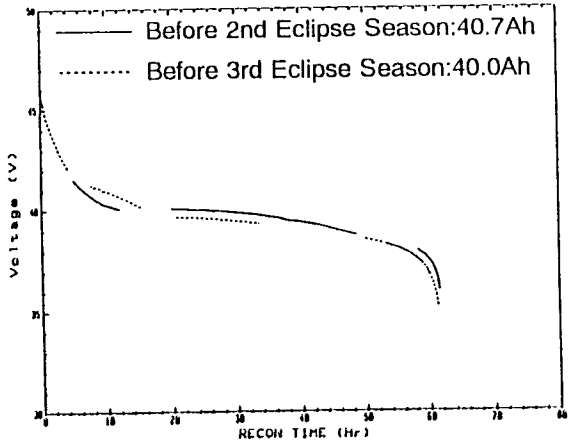

BAT#4

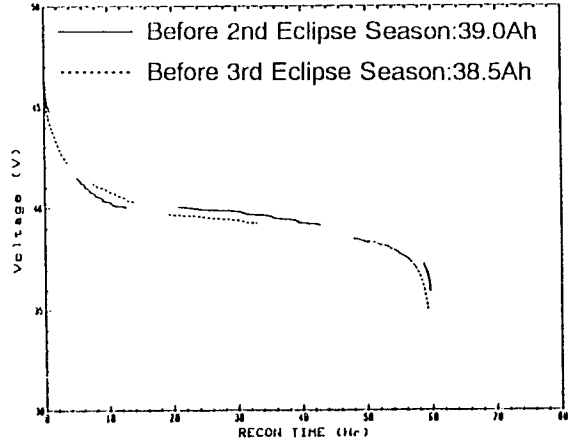

Capacities of all batteries were stable.

NASDA
NATIONAL SPACE DEVELOPMENT AGENCY OF JAPAN

DEEP DISCHARGE of 35Ah Ni-Cd BATTERIES

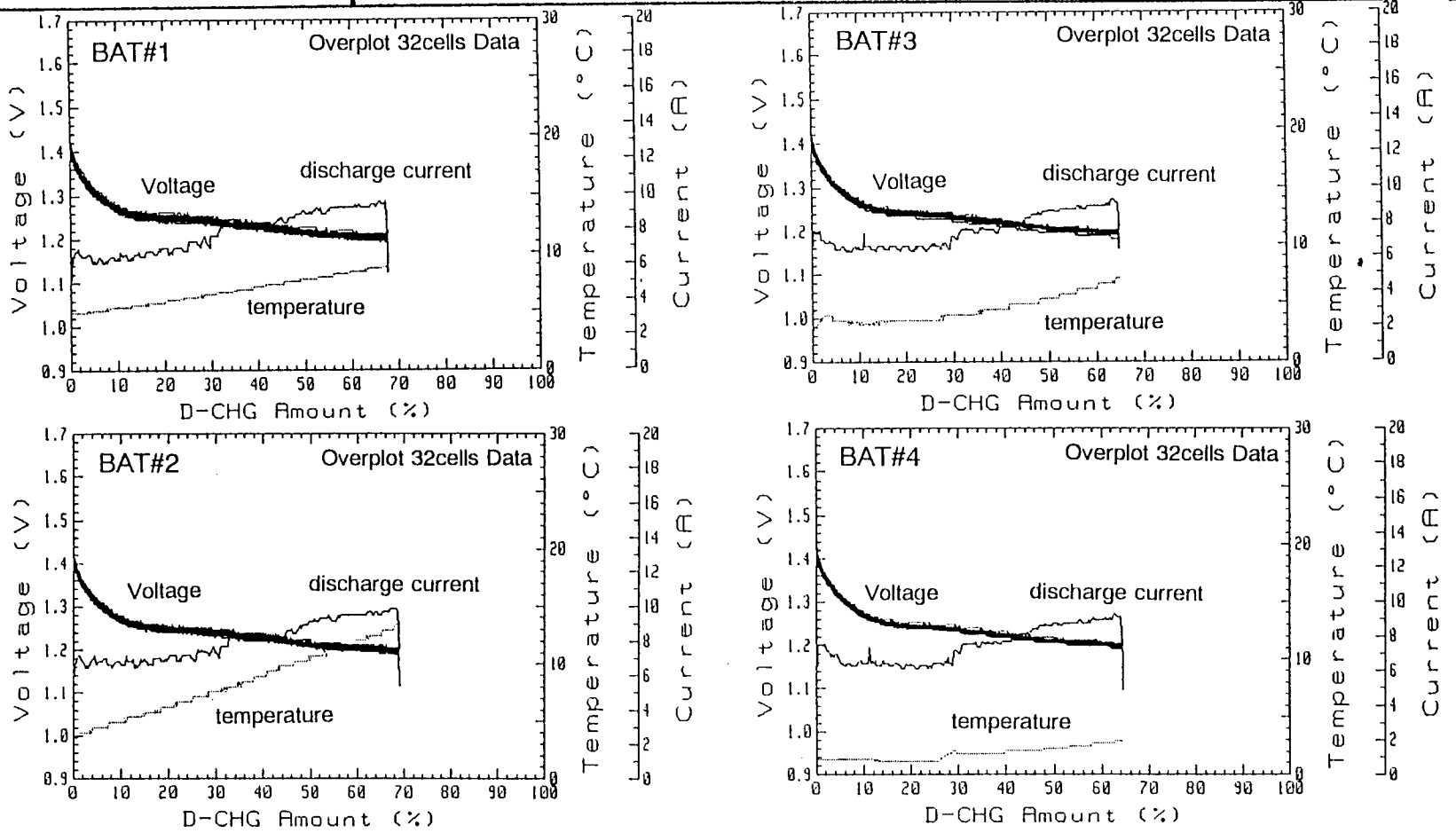

DOD was greater than 60%, but all cells had good performance.

NASDA
NATIONAL SPACE DEVELOPMENT AGENCY OF JAPAN

CHARGE CHARACTERISTICS after DEEP DISCHARGE

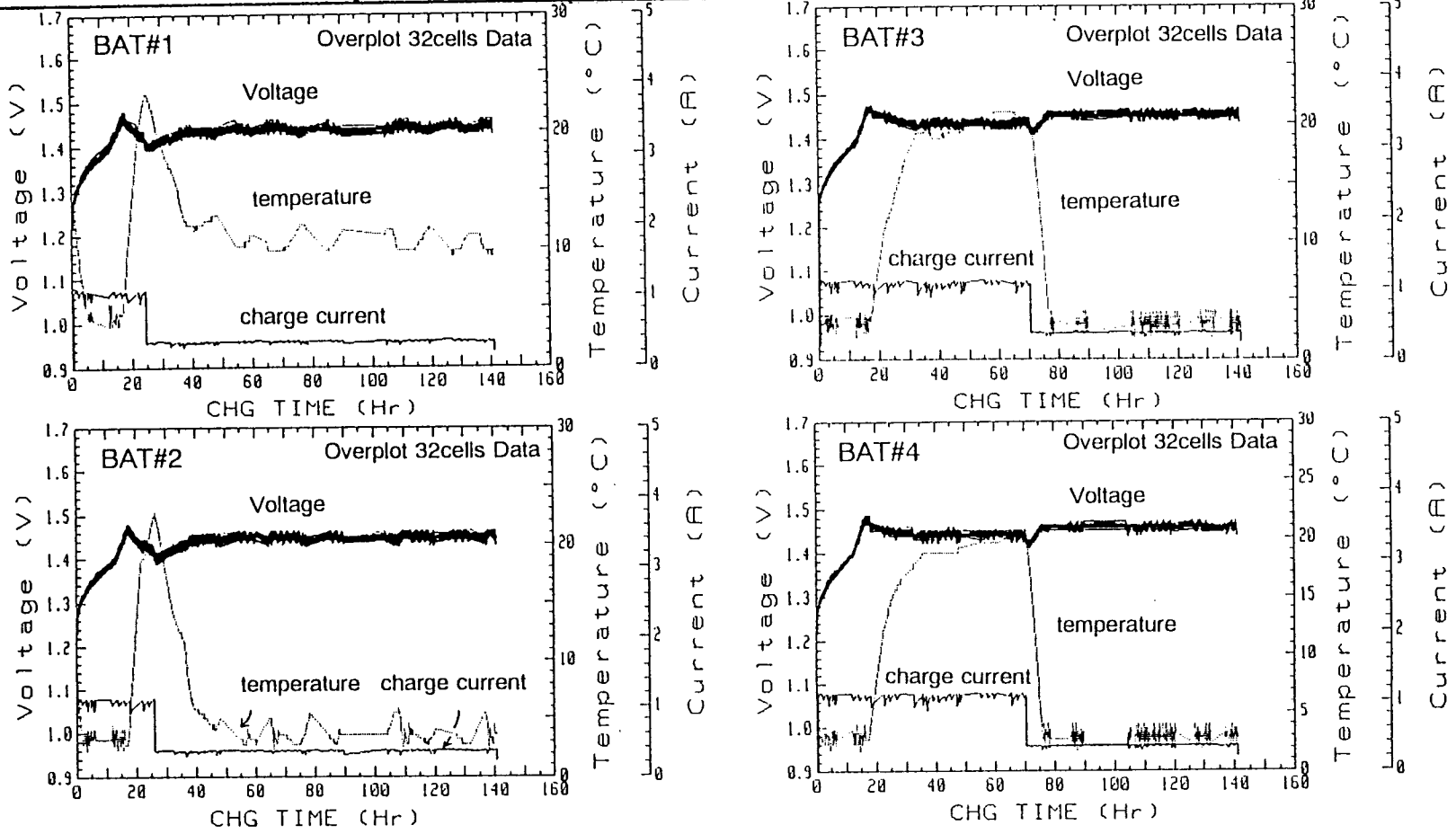

The difference between properties of cells is small in charge period.

NASDA
NATIONAL SPACE DEVELOPMENT AGENCY OF JAPAN

35AH SPACE Ni-H_2 CELL

CELL MAJOR SPECIFICATIONS

Rated Capacity		35 AH
Mission	GEO	10Years, 1,000cycles
Weight		max. 1076g
Energy Density		40 WH/kg
Mechanical Strength	Burst Pressure	min. 140 kgf/cm^2
	Pressure Cycling	5,000 cycles (14 ~70 kgf/cm^2G)
		30,000 cycles (42 ~70 kgf/cm^2G)

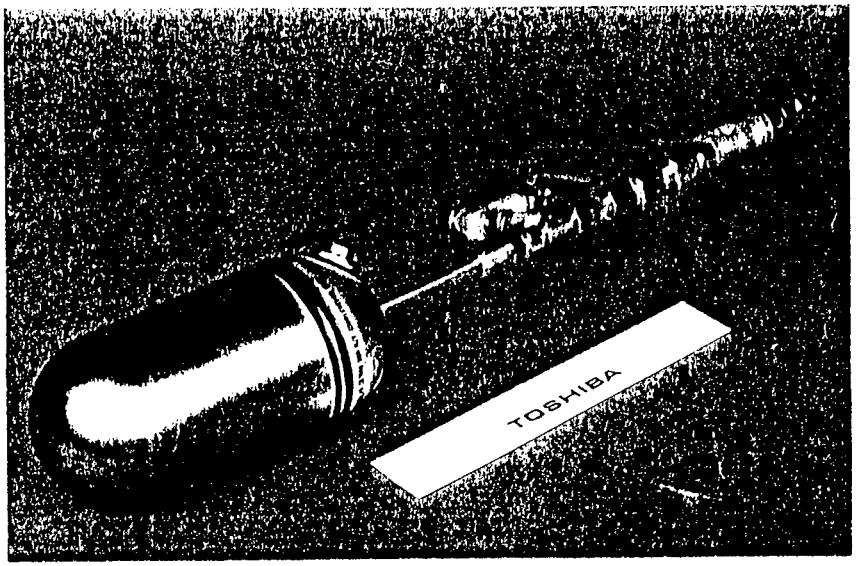

EXTERNAL VIEW OF Ni-H_2 CELL

ETS-Ⅵ 搭載実験用Ni-H_2 バッテリ (PFM)

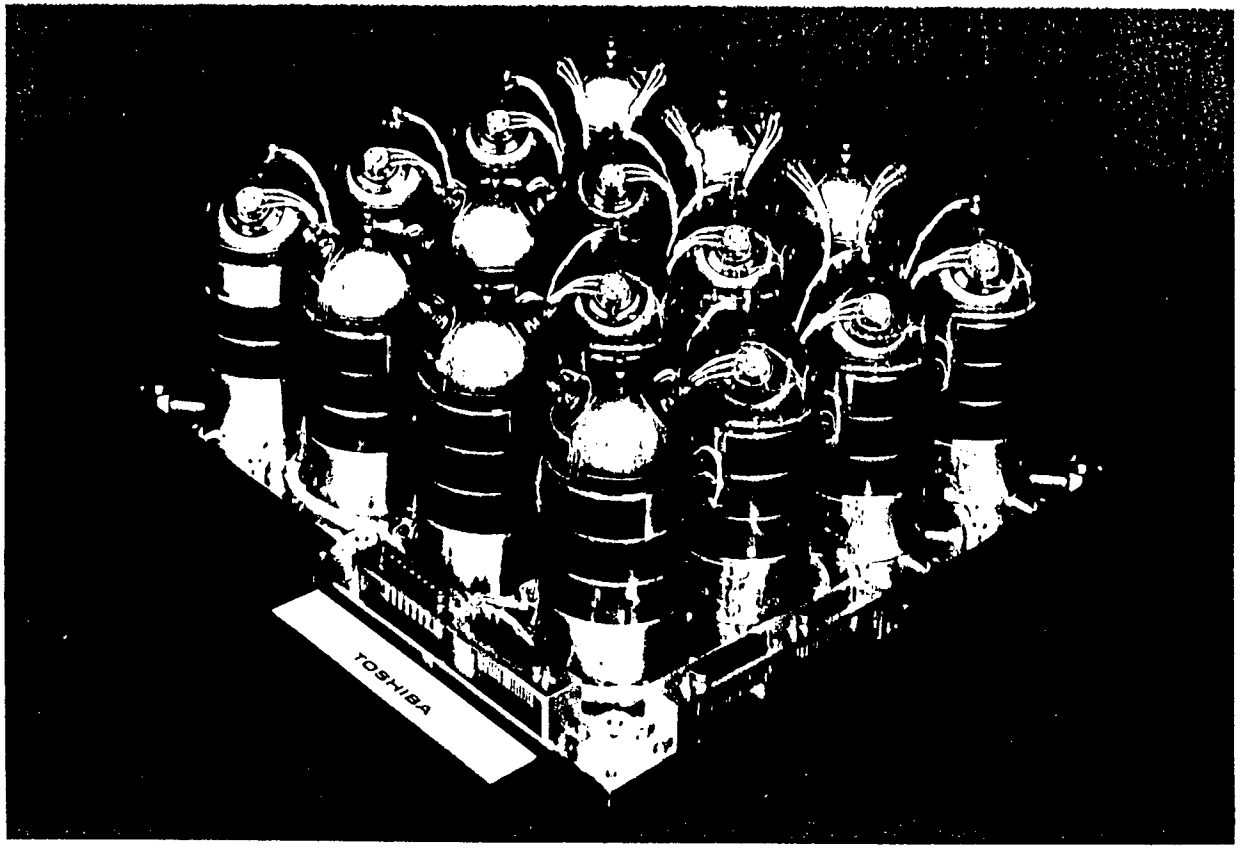

NASDA NATIONAL SPACE DEVELOPMENT AGENCY OF JAPAN

MAIN SPECIFICATION of 35Ah Ni-H_2 BATTERY

Cell	Toshiba 35Ah
Weight	24.3kg/pack 8 electrochemical impregnation(EI) & 8 chemical impregnation(CI)
Volume	461(T) * 490(W) * 241(H) mm/pack
Charge Scheme	V/T Limit (charged when bus voltage is higher than 48V)
Full Charge Rate	3.50A
Discharge Rate	17.5A or 8.8A(constant current)
Max. Depth of Discharge	60%(@72min)
Mission Life	Longer than 3years(@GEO)
Reconditioning Load	50 Ω
Operating Temperature	0 - 30° C

NASDA NATIONAL SPACE DEVELOPMENT AGENCY OF JAPAN

TREND of 35Ah Ni-H2 BATTERIES(ECLIPSE SEASON)

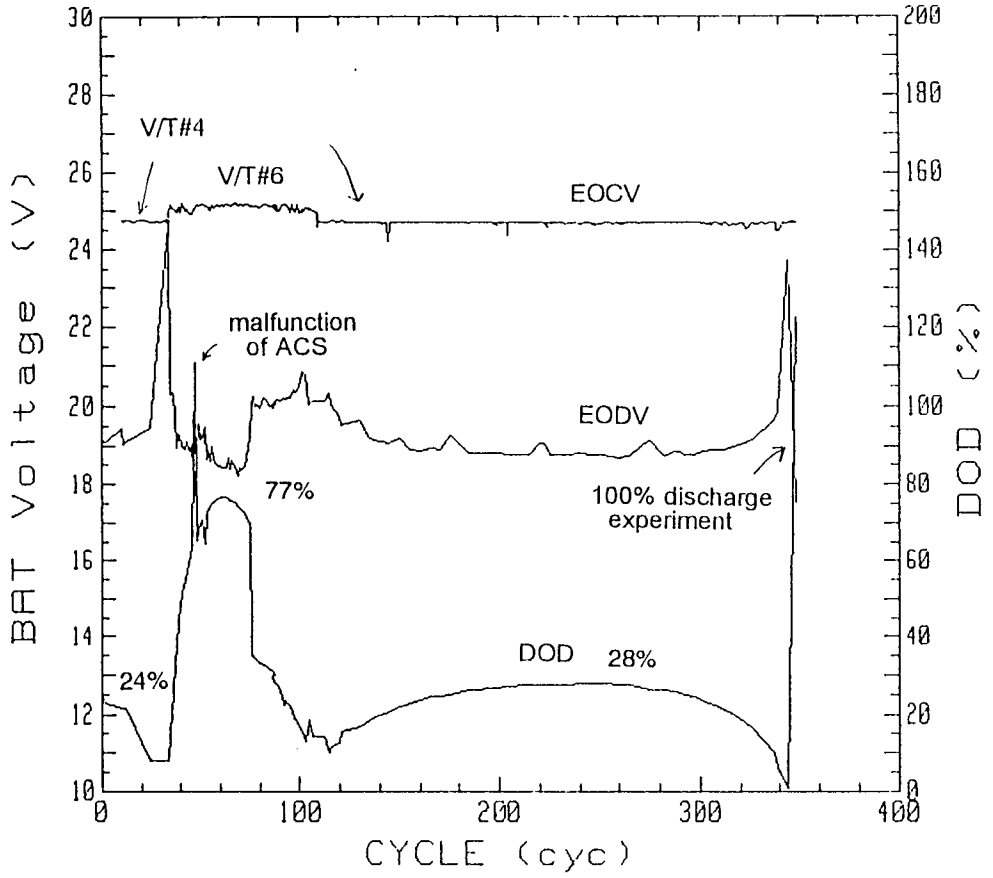

EOCV & EODV had essentially stabilized during all eclipse seasons.

NASDA NATIONAL SPACE DEVELOPMENT AGENCY OF JAPAN

EOCV and EODV of Ni-H2 CELLS(3rd ECLIPSE SEASON)

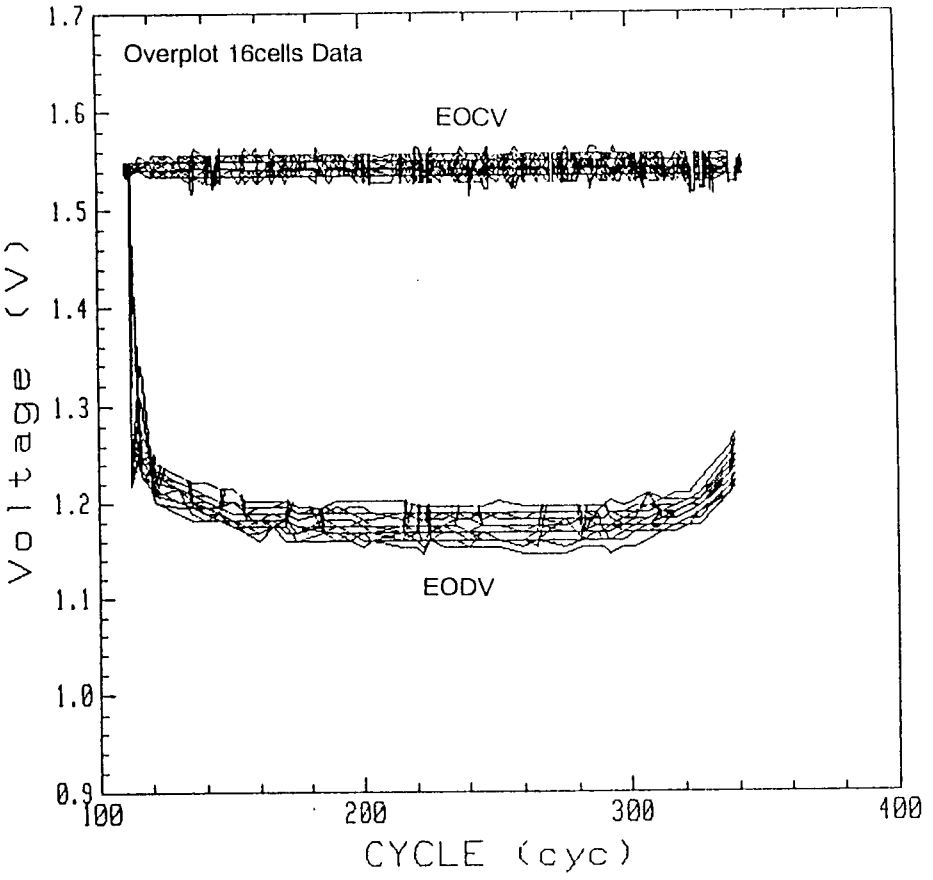

The difference between properties of cells is small.

NASDA NATIONAL SPACE DEVELOPMENT AGENCY OF JAPAN

TREND of 35Ah Ni-H2 BATTERY(1st FULL SUN TIME)

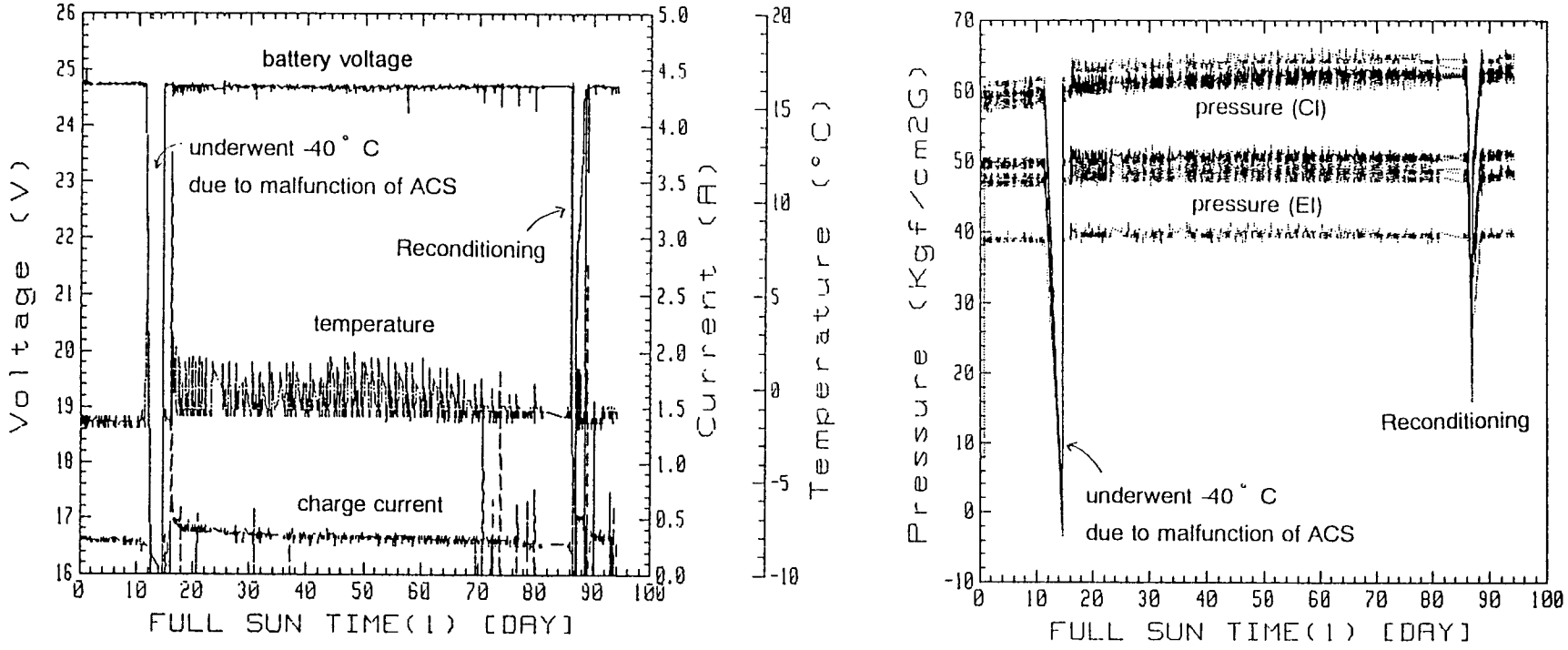

Voltage was stable in full sun time, but pressure of CI cells gradually increased.

NASDA NATIONAL SPACE DEVELOPMENT AGENCY OF JAPAN

RECONDITIONING of 35Ah Ni-H2 BATTERY

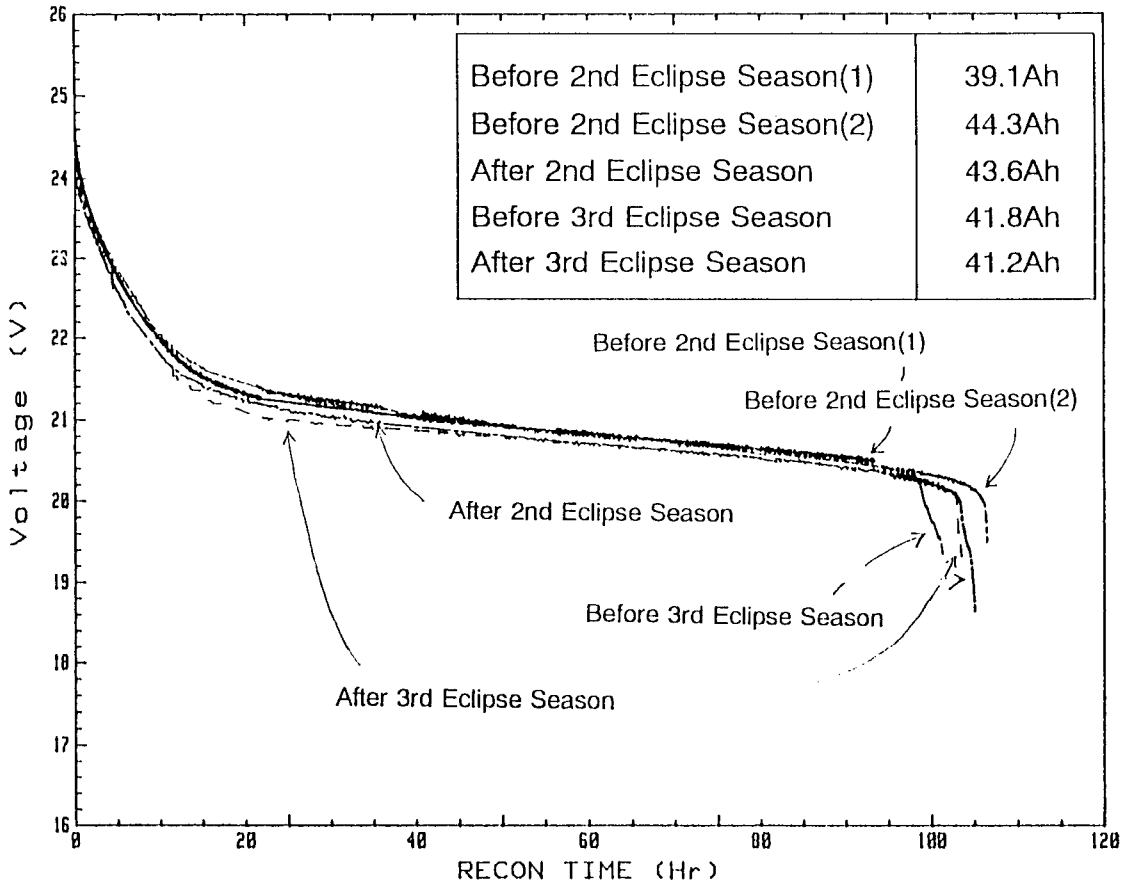

Capacity of EI cells was stable, but capacity of CI cells had decreased.

NASDA
NATIONAL SPACE DEVELOPMENT AGENCY OF JAPAN

DEEP DISCHARGE of 35Ah Ni-H2 BATTERY

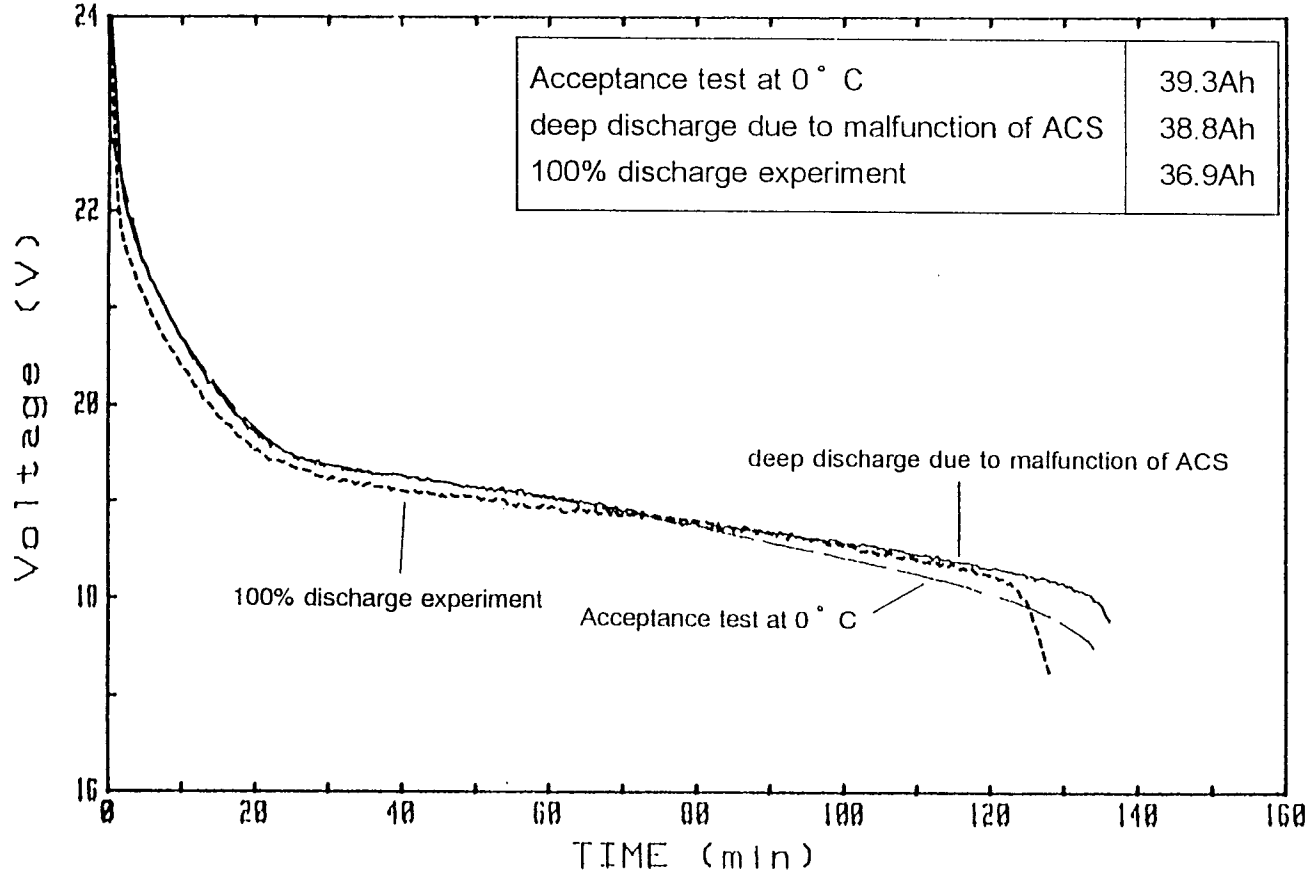

Capacity of EI cells was stable, but capacity of CI cells had decreased.

NASDA NATIONAL SPACE DEVELOPMENT AGENCY OF JAPAN

100% DISCHARGE EXPERIMENT

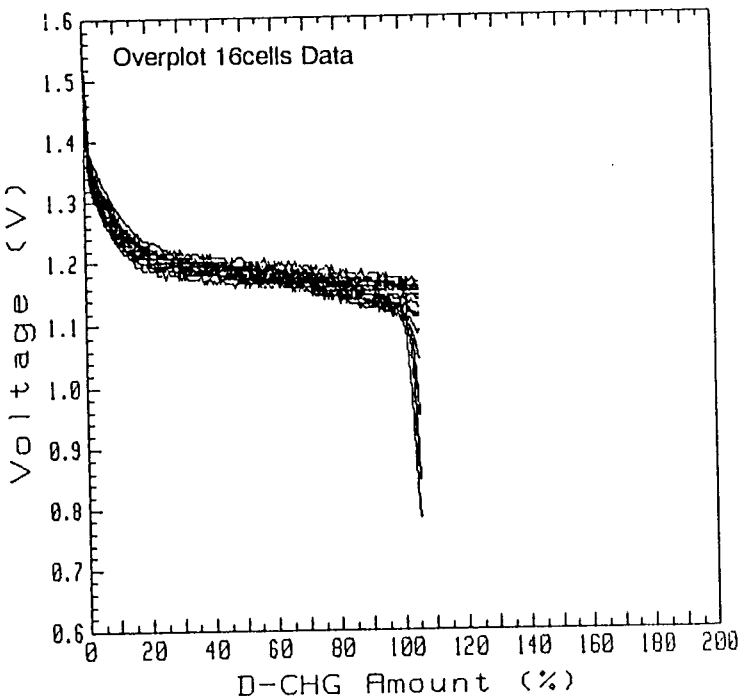

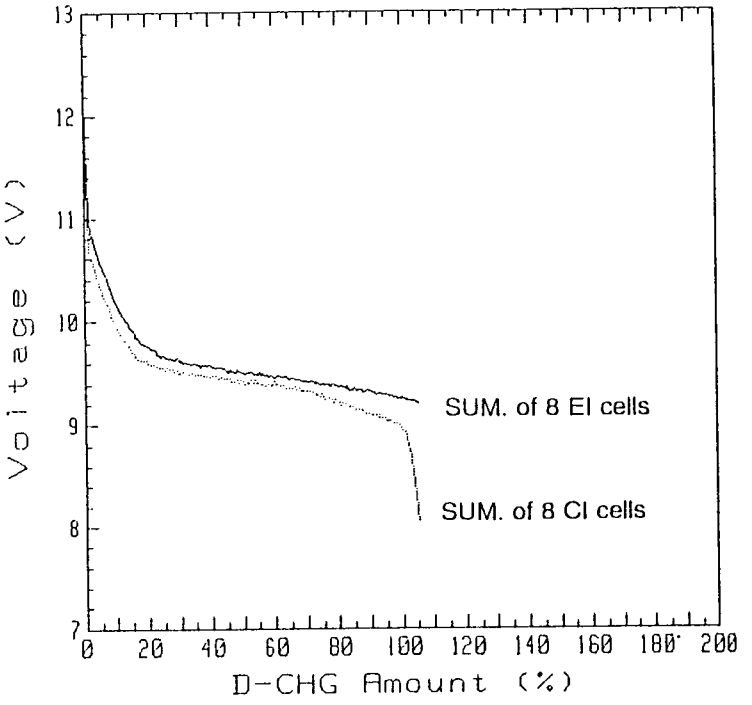

The difference between discharge voltage of cells result from the difference between CI cell and EI cell.

NASDA
NATIONAL SPACE DEVELOPMENT AGENCY OF JAPAN

CHARGE CHARACTERISTICS in ECLIPSE SEASON

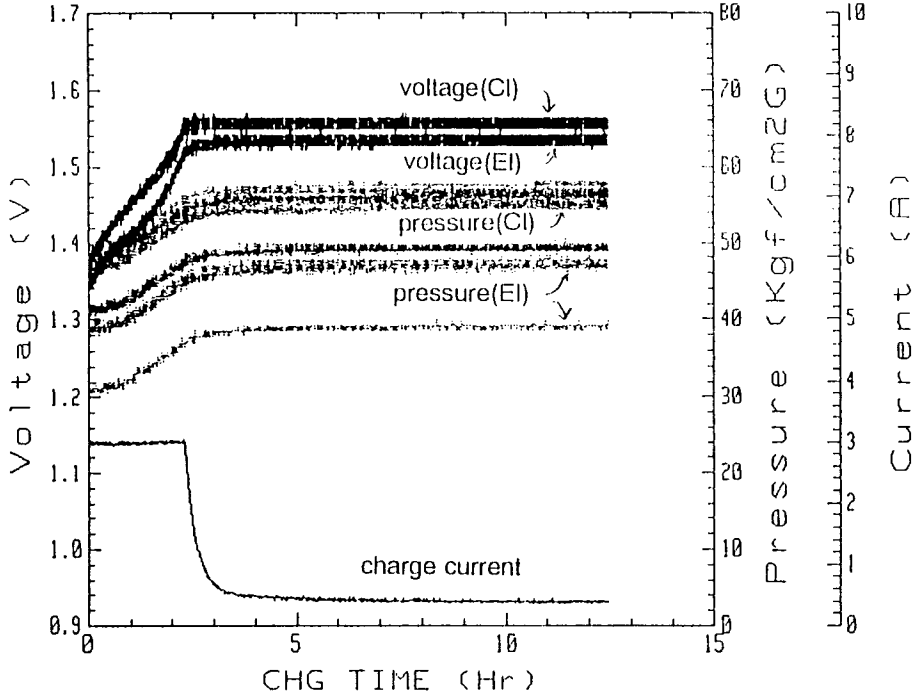

The difference between properties of CI cells and them of EI cells is remarkable.

NASDA NATIONAL SPACE DEVELOPMENT AGENCY OF JAPAN

CHARGE CHARACTERISTICS after 100% DISCHARGE

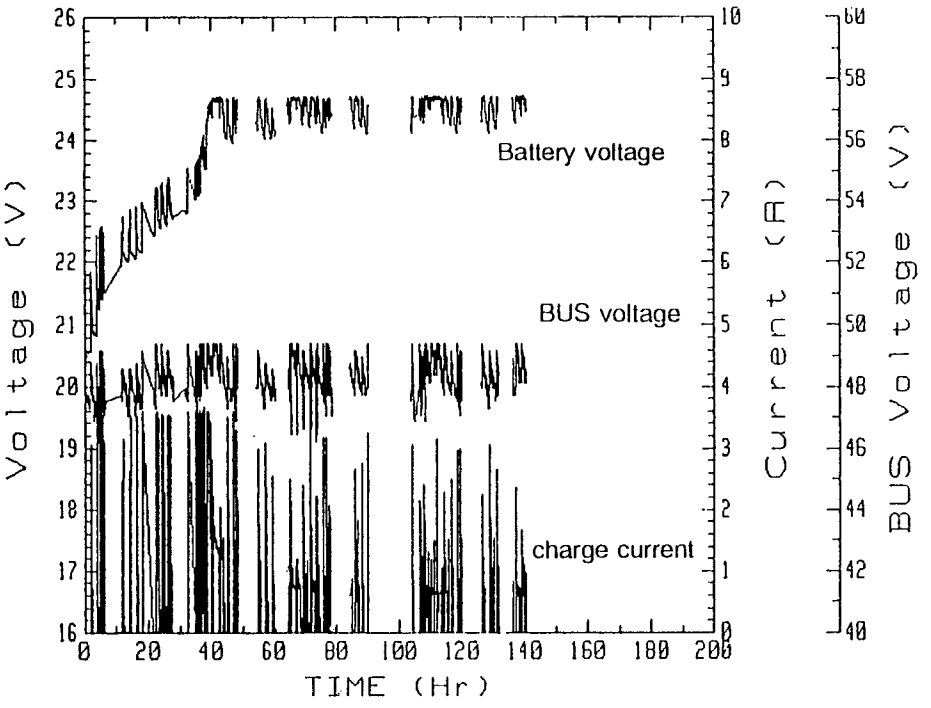

Change of bus voltage was made change of charge current.

NASDA
NATIONAL SPACE DEVELOPMENT AGENCY OF JAPAN

COMPARISON with GROUND DATA

TREND of EOCV & EODV

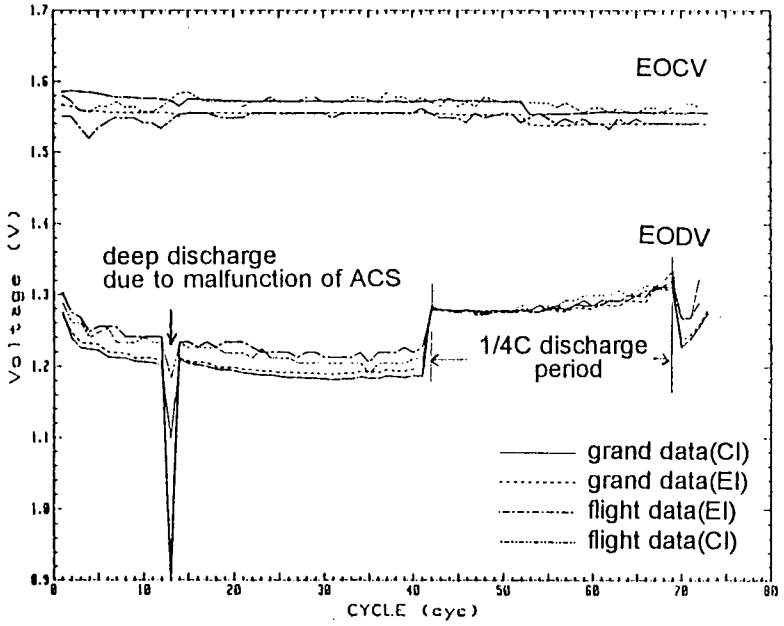

CHARGE CHARACTARISTICS

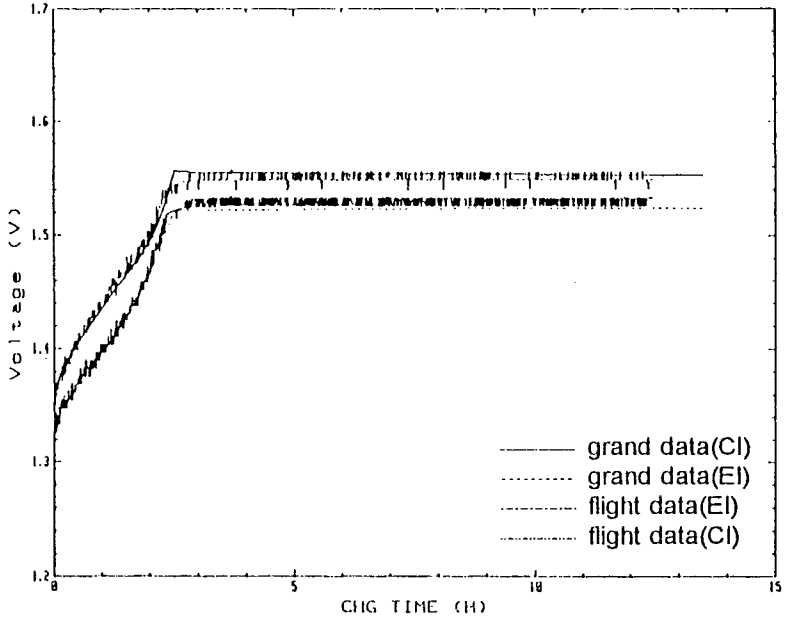

Flight data of Ni-H2 battery is similar to grand data.

NASDA NATIONAL SPACE DEVELOPMENT AGENCY OF JAPAN

GROUND TEST DATA QT Ni-Cd CELL

DOD60% GEO

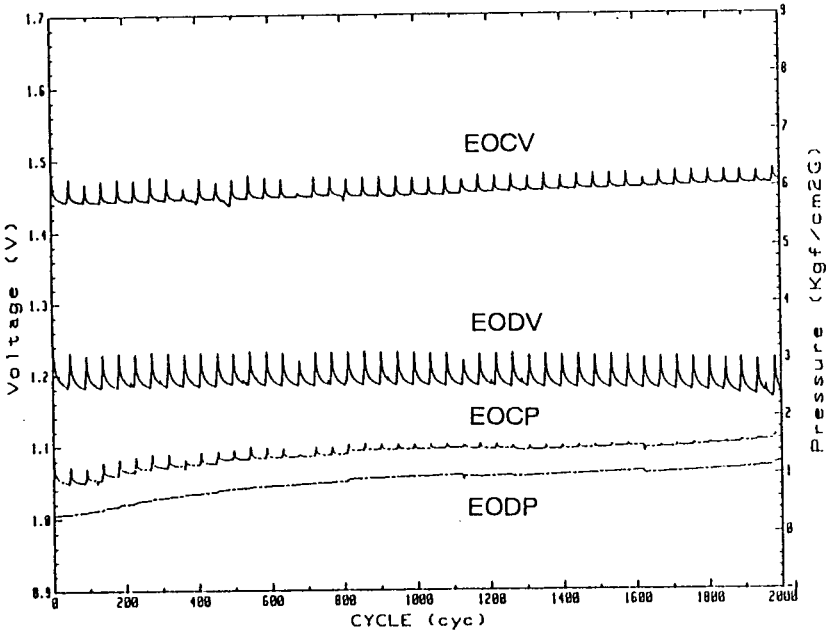

DOD40% LEO

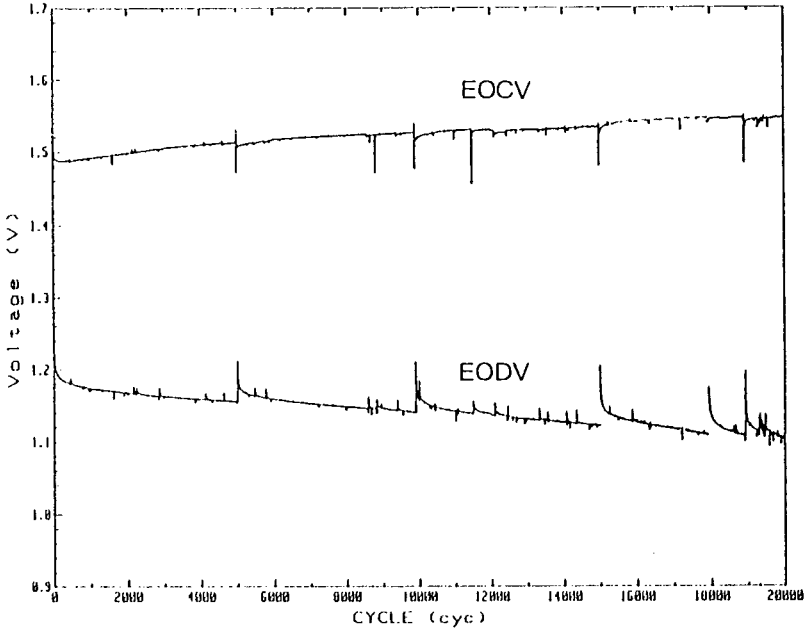

Ni-Cd cell satisfied requirements, 1000cyc on GEO & 20000cyc on LEO in ground test.

NASDA NATIONAL SPACE DEVELOPMENT AGENCY OF JAPAN

GROUND TEST DATA QT Ni-H2 CELL

DOD80% GEO

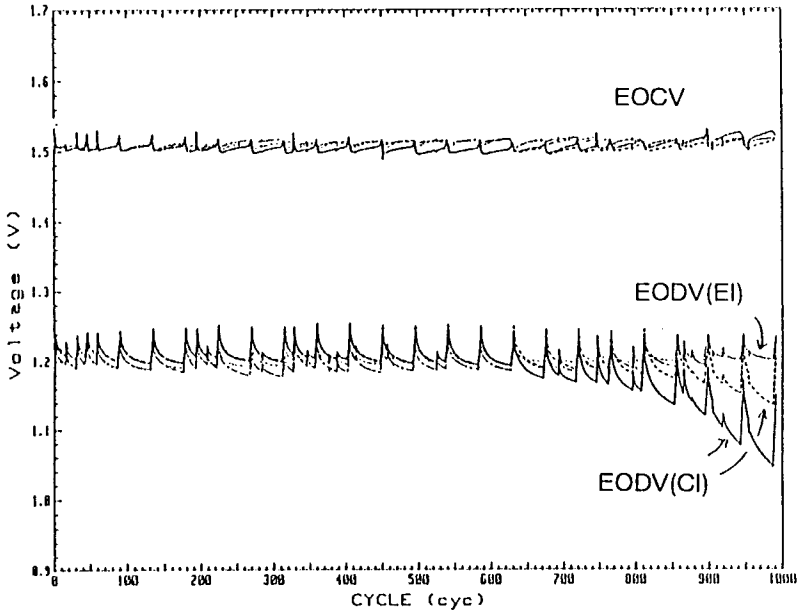

DOD40% LEO

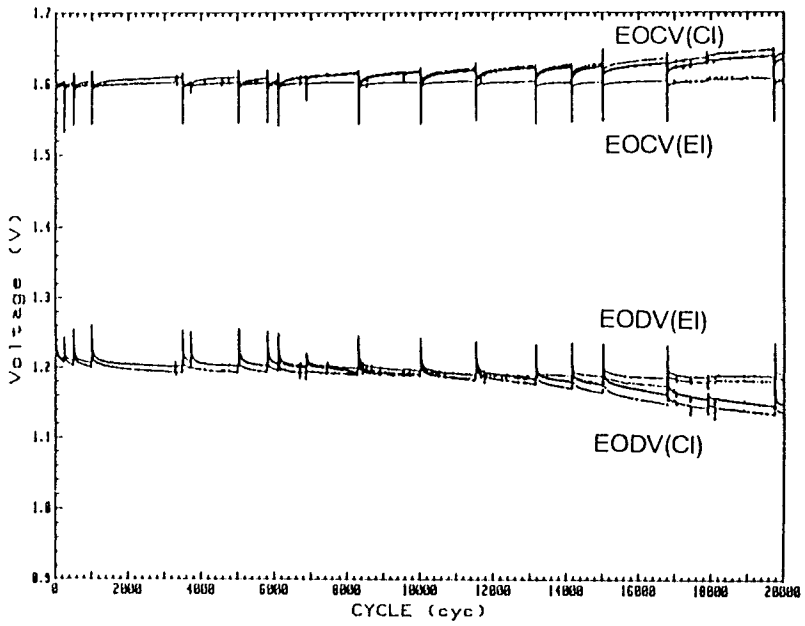

Ni-H2 cell satisfied requirements, 1000cyc on GEO & 20000cyc on LEO in ground test.

NASDA
NATIONAL SPACE DEVELOPMENT AGENCY OF JAPAN

SCHEDULE OF BATTERY DEVELOPMENT IN NASDA

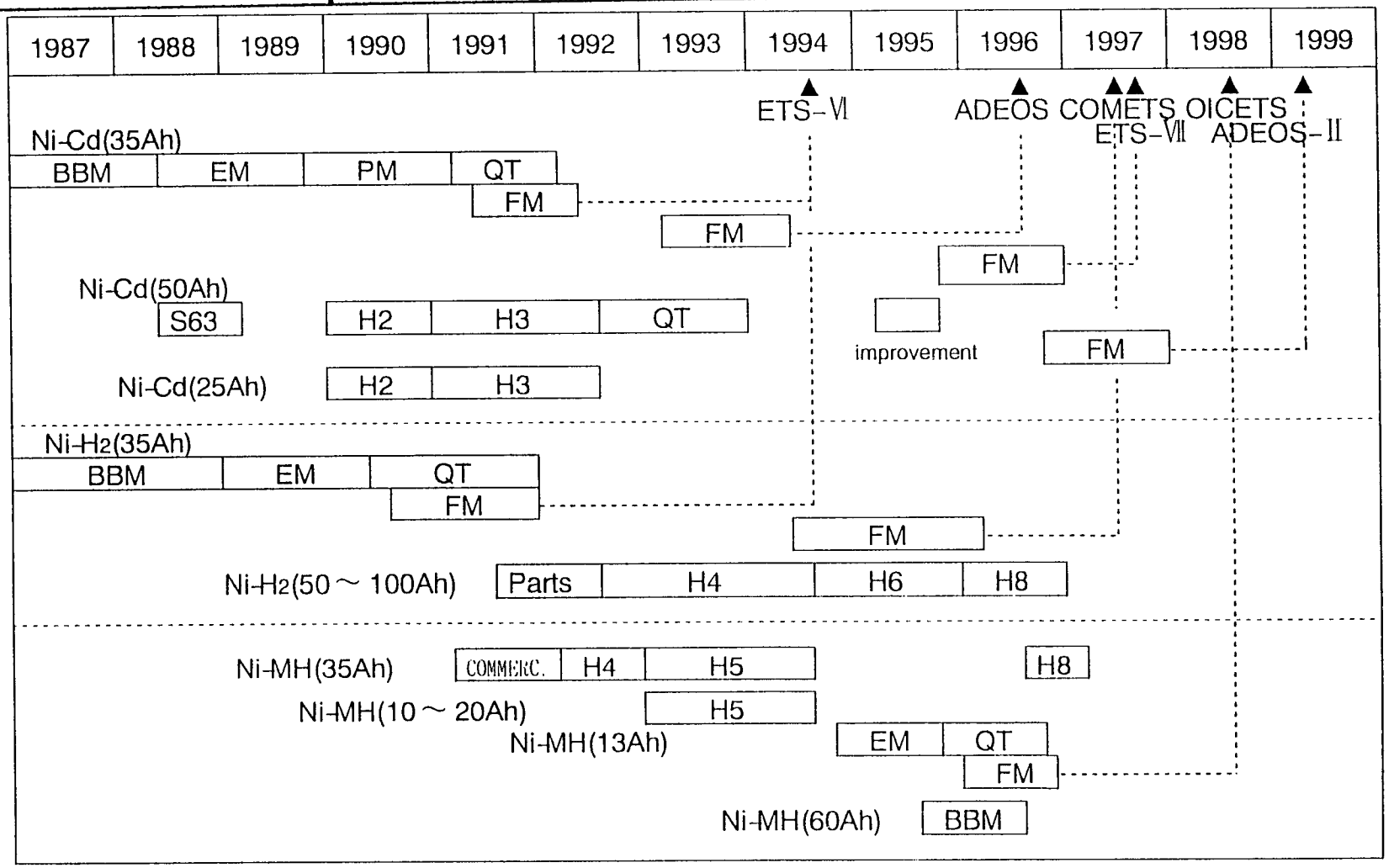

NASDA
NATIONAL SPACE DEVELOPMENT AGENCY OF JAPAN

CONCLUSION

- ETS-Ⅵ has 35Ah Ni-Cd batteries as bus equipment, and 35Ah Ni-H2 battery as experimental equipment. Both batteries are continuing to work well during over one year on high elliptical orbit.
- It is confirmed that Ni-Cd and Ni-H2 cells must satisfy requirements, base on ETS-Ⅵ flight results as well as ground test results.
- 35Ah Ni-Cd cells will be used for Advanced Earth Observation Satellite (ADEOS) to be launched in 1996, and Engineering Test Satellite-Ⅶ (ETS-Ⅶ)to be launched in 1997.
- 35Ah Ni-H2 cells(EI) will be used for Communication Engineering Test Satellite(COMETS) to be launched in 1997.

1995 NASA Aerospace Battery Workshop Attendance List

Jon D. Armantrout
Lockheed Martin
O/79-50 B/149
1111 Lockheed Way
Sunnyvale, CA 94089-3504
Ph (408) 742-5699 Fax (408) 742-7701

David A. Baer
Hughes Aircraft Company
POB 2999
Torrance, CA 90509-2999
Ph (310) 517-7604 Fax (310) 517-7676

Bob Beaman
Goddard Space Flight Center
Greenbelt, MD 20771
Ph (301) 286-2538 Fax

Bob Bechtel
Marshall Space Flight Center
MS EB71
Marshall Space Flight Center, AL 35812
Ph (205) 544-3294 Fax (205) 544-5841

Charles W. Bennett
Lockheed Martin Astro Space
MS U1219
230 E. Mall Blvd.
King of Prussia, PA 19406
Ph (610) 354-6155 Fax (610) 354-3434

Samuel Birken
The Aerospace Corporation
MS M4/986
POB 92957
Los Angeles, CA 90009-2957
Ph (310) 336-6080 Fax (310) 336-5581

Ron Bounds
Aerospace Consulting Group
423 Terhune Rd.
Princton, NJ 08540
Ph (609) 683-1963 Fax (908) 545-2180

Francis R. Boyce
Lockheed Martin (NOAA)
13300 Edinburgh Lane #23
Laurel, MD 20708
Ph (301) 457-5157 Fax (301) 457-5175

Rita Brazier
Marshall Space Flight Center
EB71
Marshall Space Flight Center, AL 35812
Ph (205) 544-3295 Fax (205) 544-5841

Jeffrey C. Brewer
Marshall Space Flight Center
MS EB74
Marshall Space Flight Center, AL 35812
Ph (205) 544-3345 Fax (205) 544-5841

Jack Brill
Eagle-Picher Industries, Inc.
C and Porter Streets
Joplin, MO 64801
Ph (417) 623-8000 X346 Fax (417) 623-8000 X441

Harry Brown
Naval Surface Warfare Center - Crane Div.
Code 6095 B2949
Commander
300 Hwy 301
Crane, IN 47522
Ph (812) 854-6149 Fax (812) 854-1212

David Burns
Marshall Space Flight Center
EB15
Marshall Space Flight Center, AL 35812
Ph (205) 544-4807 Fax

John Bush
Marshall Space Flight Center
EB73
Marshall Space Flight Center, AL 35812
Ph (205) 544-3305 Fax

1995 NASA Aerospace Battery Workshop Attendance List

Shirley Butler
Marshall Space Flight Center
EB71
Marshall Space Flight Center, AL 35812
Ph (205) 544-3298 Fax

Gerald W. Byers
Lockheed-Martin
MS B4383
POB 179
Denver, CO 80201
Ph (303) 977-6984 Fax

John E. Casey
Lockheed Martin Engineering & Sciences Co.
2400 NASA Rd. 1, C44
Houston, TX 77058-3799
Ph (713) 483-0446 Fax (713) 483-3096

Patricia L. Chilelli
Lockheed Martin Astro Space
MS 501
POB 800
Princeton, NJ 08543-0800
Ph (609) 490-6507 Fax (609) 490-4242

Fred Cohen
Rocketdyne Division / Rockwell International
MS LB-04
6633 Canoga Ave.
POB 7922
Canoga Park, CA 91309-7922
Ph (818) 586-3206 Fax (818) 586-3685

Betty Colhoun
Goddard Space Flight Center
Code 440.9
Greenbelt, MD 20771
Ph (301) 286-7691 Fax (301) 286-1726

Stephen Cox
Kennedy Space Center
CV-LOD-1
Kennedy Space Center, FL 32899
Ph (407) 853-6671 Fax (407) 853-4357

Stuart Daughtridge
Orion Satellite Corporation
2440 Research Blvd.
Rockville, MD 20850
Ph (301) 258-3219 Fax (301) 258-3319

Frank Deligiannis
Jet Propulsion Laboratory
MS 277-104
4800 Oak Grove Dr.
Pasadena, CA 91109
Ph (818) 354-0404 Fax (818) 393-6951

Robert Dan Dell
Alfred E. Mann Fdn.
12744 San Fernando Rd.
Sylmar, CA 91342
Ph (818) 362-5958 Fax

Loyd Doering
7110 Jones Valley Dr.
Huntsville, AL 35802
Ph (205) 881-6342 Fax

Michael Donnelly
Goddard Space Flight Center
Code 422
Greenbelt, MD 20771
Ph (301) 286-6316 Fax (301) 286-1653

Rajiv Doreswamy
Marshall Space Flight Center
EB73
Marshall Space Flight Center, AL 35812
Ph (205) 544-3366 Fax

John Durning
Goddard Space Flight Center
Code 422.0
Greenbelt, MD 20771
Ph (301) 286-9174 Fax (301) 286-1653

1995 NASA Aerospace Battery Workshop Attendance List

Ted Edge
Marshall Space Flight Center
EB74
Marshall Space Flight Center, AL 35812
Ph (205) 544-3381 Fax

Ted Enomoto
Sanyo Energy (USA) Corporation
2001 Sanyo Avenue
San Diego, CA 92173
Ph (619) 661-6620 Fax (619) 661-6743

Ed Fitzgerald
AZ Technology
4901 Corporate Dr., Ste. 101
Huntsville, AL 35805
Ph (205) 837-9877 X105 Fax (205) 837-1155

Chris Fox
Eagle-Picher Industries, Inc.
1215 West B Street
Joplin, MO 64801
Ph (417) 623-8000 X367 Fax (417) 623-5319

Pete George
Marshall Space Flight Center
EB74
Marshall Space Flight Center, AL 35812
Ph (205) 544-3331 Fax

Guillermo A. Gonzalez
Langley Research Center
MS 257
6 East Taylor St.
Hampton, VA 23681-0001
Ph (804) 864-7107 Fax (804) 864-8674

Sidney Gross
Northwest Engineering Consultants
7201 26 Ave. NE
Seattle, WA 98115
Ph (206) 522-2223 Fax (206) 522-2223

Blake A. Emmerich
Zircar Products, Inc.
110 N. Main St.
Florida, NY 10920
Ph (914) 651-4481 X229 Fax (914) 651-3192

Rolan C. Farmer
Eagle-Picher Industries, Inc.
Power Systems Department
3820 S. Hancock Expressway
Colorado Springs, CO 80911
Ph (719) 392-4266 Fax (719) 392-5103

Nicanor A. Flordeliza
GE American Communications Satellites, Inc.
4 Research Way
Princeton, NJ 08540
Ph (609) 987-4453 Fax (609) 987-4393

Mr. N. R. Francis
Matra Marconi Space UK Ltd.
Gunnels Wood Road
Stevenage, Hertfordshire
SG1 2AS
England
Ph 011-44-1438-313456 Fax 011-44-1438-736200

David Ginder
Eagle-Picher Industries, Inc.
1215 West B Street
Joplin, MO 64801
Ph (417) 623-8000 X345 Fax (417) 623-5319

Allora R. Goode
Goddard Space Flight Center
Code 442
Greenbelt, MD 20771
Ph (301) 286-6357 Fax (301) 286-1779

T. Guffey
Lockheed Missiles & Space Co., Inc.
8520 Cinderbed Rd.
Suite 600
Newington, VA 22122

1995 NASA Aerospace Battery Workshop Attendance List

Doug Hafen
Lockheed Martin
B/149 O/76-01
POB 3504
Sunnyvale, CA 94089-3504
Ph (408) 743-7220 Fax (408) 742-7701

David Hall
Marshall Space Flight Center
EB72
Marshall Space Flight Center, AL 35812
Ph (205) 544-4215 Fax

Gerald Halpert
Jet Propulsion Laboratory
MS 277-207
4800 Oak Grove Dr.
Pasadena, CA 91109
Ph (818) 354-5474 Fax (818) 393-6951

Rick Haynes
TRW
MS R8/2120F
One Space Park
Redondo Beach, CA 90278

Scott Hoover
Orion Satellite Corporation
2440 Research Blvd.
Suite 160
Rockville, MD 20850
Ph (301) 258-3325 Fax (301) 258-3319

Nathan Isaacs
MSA
38 Loveton Circle
Sparks, MD 21152
Ph (410) 628-5440 Fax (410) 628-0613

Doris Jallice
Goddard Space Flight Center
Code 734.5
Greenbelt, MD 20771
Ph (301) 286-4699 Fax (301) 286-1751

Dr. P. J. Johnson
Matra Marconi Space UK Ltd.
Gunnels Wood Road
Stevenage, Hertfordshire
SG1 2AS
England
Ph 011-44-1438-736031 Fax 011-44-1438-736200

Noboru Jyogo
Toshiba Corporation
1. Komukai, Toshiba-Cho
Saiwaiku, Kawasaki, 210
Japan
Ph 81-44-548-5137 Fax 81-44-541-1211

Lisa M. King
Tracor Battery Technology Center
1601 Research Boulevard
Rockville, MD 20850-3173
Ph (301) 838-6234 Fax (301) 838-6222

Donald R. Kleis
310 Plantation Dr.
Meridianville, AL 35759
Ph (205) 971-4710 Fax

Stanley J. Krol, Jr.
Lockheed Technical Operations Co.
7474 Greenway Center Drive
Suite 200
Greenbelt, MD 20770
Ph (301) 901-6101 Fax (301) 901-6076

Hiroaki Kusawake
National Space Development Agency of Japan
Tsukuba Space Center
2-1-1 Sengen, Tsukuba-Shi
Ibaraki-Ken 305 Japan

Ron Lantzy
Lockheed Martin
4041 N. 1st St.
San Jose, CA 95134
Ph (408) 752-6510 Fax

1995 NASA Aerospace Battery Workshop Attendance List

Christine Lehr
Lockheed Martin Astro Space
MS 419-3A
POB 800
Princeton, NJ 08543-0800
Ph (609) 490-3574 Fax (609) 490-2856

Danny Liu
INTELSAT
INTELSAT VIII Program Office
c/o Lockheed Martin Astro Space
POB 800 / MS 93
Princeton, NJ 08543-0800
Ph (609) 426-9225 Fax (609) 426-8968

Eric Lowery
Marshall Space Flight Center
EB74
Marshall Space Flight Center, AL 35812
Ph (205) 544-0080 Fax

Chuck Lurie
TRW
MS R4/1082
One Space Park
Redondo Beach, CA 90278
Ph (310) 813-4888 Fax (310) 812-4978

Matthew Machlis
Orbital Sciences Corp.
21700 Atlantic Blvd.
Dulles, VA 20166
Ph (703) 406-5491 Fax (703) 406-5461

Lou Magnarella
SAFT
5116 NW 75th Lane
Gainesville, FL 32653
Ph (904) 337-0925 Fax (904) 337-0415

Michael C. Maguire
SED Systems, Inc.
Canadian Space Agency
Radarsat Operations
6767 Route de l'Aeroport
Saint-Hubert, Quebec
Canada J3Y 8Y9
Ph (514) 926-5139 Fax (514) 926-5167

Dr. Tyler X. Mahy
U.S. Government
c/o OTS
Washington, DC 20505
Ph (703) 874-0739 Fax (703) 641-9830

Michelle Manzo
Lewis Research Center
MS 309-1
21000 Brookpark Rd.
Cleveland, OH 44135
Ph (216) 433-5261 Fax (216) 433-6160

Nehemiah Margalit
Tracor Battery Technology Center
4294 Mainsail Dr.
Burke, VA 22015
Ph (301) 838-6223 Fax (301) 838-6222

Jeff Martin
Marshall Space Flight Center
EB12
Marshall Space Flight Center, AL 35812

Dean W. Maurer
AT&T
Rm 2F301
101 Crawfords Corner Rd.
Holmdel, NJ 07733-3030
Ph (908) 949-6690 Fax (908) 949-8082

Kurt McCall
Marshall Space Flight Center
EB72
Marshall Space Flight Center, AL 35812
Ph (205) 961-4501 Fax

George Methlie
2120 Natahoa Ct.
Falls Church, VA 22043
Ph (202) 965-3420 Fax (703) 641-9830

1995 NASA Aerospace Battery Workshop Attendance List

Mo Mohadjer
McDonnell Douglas Aerospace
689 Discovery Dr.
Huntsville, AL 35806
Ph (205) 922-4567 Fax

Elisabeth Montagne
Oerlikon Aerospace
Canadian Space Agency
Radarsat Operations
6767 Route de l'Aeroport
Saint-Hubert, Quebec
Canada J3Y 8Y9
Ph (514) 926-5131 Fax (514) 926-5167

Dr. Dan Mulville
NASA Headquarters
Code AE
Washington, DC 20546
Ph (202) 358-1823 Fax

Phil Napala
NASA Headquarters
Code QT
300 E St. SW
Washington, DC 20546

Dave Nawrocki
Lockheed Martin
808 Loyalton
Campbell, CA 95008
Ph (408) 756-6255 Fax (408) 756-6550

Pat O'Donnell
Lewis Research Center
MS 309-1
21000 Brookpark Rd.
Cleveland, OH 44135
Ph (216) 433-5248 Fax (216) 433-6160

Rex Oswald
Hughes Space and Communications
Bldg. 231, MS 1920
Battery Operations
POB 2999
Torrance, CA 90509-2999
Ph (310) 517-7651 Fax (310) 517-7676

Paul Panneton
Johns Hopkins University / APL
Johns Hopkins Rd.
Laurel, MD 20723
Ph (301) 953-5649 Fax (301) 953-6556

Rick Parmley
Eagle Picher
POB 47
Joplin, MO 64802
Ph (417) 623-8000 Fax

David F. Pickett
Eagle-Picher Industries
Power Systems Department
3820 S. Hancock Expressway
Colorado Springs, CO 80911
Ph (719) 392-4266 Fax (719) 392-5103

Capt. Marc E. Rainbow
U.S. Air Force
PL/VTPP
Kirtland AFB, NM 87117-6008
Ph (505) 846-2637 Fax (505) 846-2885

Gopal Rao
Goddard Space Flight Center
Code 734.5
Greenbelt, MD 20771
Ph (301) 286-6654 Fax (301) 286-1751

Dr. Philip G. Russell
Yardney Technical Products
82 Mechanic St.
Pawcatuck, CT 06379
Ph (203) 599-1100 X450 Fax (203) 599-3903

Frank Scalici
INTELSAT
3400 International Dr. NW
Box 34
Washington, DC 20008

1995 NASA Aerospace Battery Workshop Attendance List

Joseph H. Schulman, PhD
Alfred E. Mann Foundation
12744 San Fernando Road
Sylmar, CA 91342
Ph (818) 362-5958 x2511 Fax (818) 364-2647

Darren Scoles
Eagle-Picher Industries, Inc.
Power Systems Department
3820 S. Hancock Expressway
Colorado Springs, CO 80911
Ph (719) 392-4266 Fax (719) 392-5103

R. Sholl
Lockheed Missiles & Space Co., Inc.
8520 Cinderbed Rd.
Suite 600
Newington, VA 22122
Ph (703) 550-3612 Fax

Luther W. Slifer, Jr.
Jackson & Tull, Chartered Engineers
NASA / Goddard Space Flight Center
Code 734.4
J & T Support
Greenbelt, MD 20771
Ph (301) 286-8433 Fax (301) 286-1751

Douglas S. Smellie
Phillips Lab / USAF
PL/VTPP
Kirtland AFB, NM 87117-5776
Ph (505) 846-0499 Fax (505) 846-2885

Christopher Smith
Orbital Sciences Corp.
7500 Greenway Center Dr.
Suite 700
Greenbelt, MD 20770
Ph (301) 220-5686 Fax (301) 474-2648

Max Solis
BST Systems, Inc.
78 Plainfield Pike Road
Plainfield, CT 06374
Ph (203) 564-4078 Fax (203) 564-1380

Andrew Somerville
The Aerospace Corporation
POB 9045
Albuquerque, NM 87119
Ph (505) 846-4952 Fax

Steve Staich
TRW
One Space Park
Redondo Beach, CA 90278
Ph (310) 813-3631 Fax

Barbara Stem-Clark
SAFT America, Inc.
107 Beaver Ct.
Cockeysville, MD 21030
Ph (410) 771-3200 Fax (410) 771-0234

Russell Stevens
Hughes Aircraft Co.
POB 64039
Sunnyvale, CA 94088
Ph (408) 744-2075 Fax (408) 747-1340

Joe Stockel
Office of Research & Development
Washington, DC 20505
Ph (703) 351-2065 Fax (703) 527-9492

Rao Surampudi
Jet Propulsion Laboratory
4800 Oak Grove Dr.
Pasadena, CA 91109
Ph (818) 354-0352 Fax (818) 393-6951

Nobuo Takeuchi
NASDA, Japanese Space Agency
Mail Code KN / NASDA
Johnson Space Center / NASA
Houston, TX 77058

1995 NASA Aerospace Battery Workshop Attendance List

Benjamin J. Tausch
Motorola GSTG SATCOM
Mail Drop G1148
2501 S. Price Road
Chandler, AZ 85248
Ph (602) 732-6164 Fax (602) 732-3868

Greg Terry
Kateli Enterprises, Inc.
295 Lakeridge Dr. S.
Lynchburg, TN 37352
Ph (205) 651-2177 Fax (615) 759-4728

Paul Timmerman
Jet Propulsion Laboratory
MS 277-215
4800 Oak Grove Drive
Pasadena, CA 91104
Ph (818) 354-5388 Fax (818) 393-6951

Robert F. Tobias
TRW
MS R4/1074
One Space Park
Redondo Beach, CA 90278
Ph (310) 813-5784 Fax

Mark R. Toft
Goddard Space Flight Center
Code 734.5
Bldg. 20, Rm. 178
Greenbelt, MD 20771
Ph (301) 286-3969 Fax (301) 286-1751

John J. Toon
Memtec America Corporation
1750 Memtec Dr.
DeLand, FL 32724-2045
Ph (904) 822-8000 X252 Fax (904) 822-8040

Walt Tracinski
Applied Power International
1236 N. Columbus Ave., #41
Glendale, CA 91202-1672
Ph (818) 243-3127 Fax (818) 243-3127

Dr. Hari Vaidyanathan
COMSAT Laboratories
22300 Comsat Dr.
Clarksburg, MD 20871
Ph (301) 428-4507 Fax (301) 428-3686

John W. Van Zee
University of South Carolina
Chemical Engineering Dept.
Columbia, SC 29208
Ph (803) 777-2285 Fax (803) 777-8265

Harry Wajsgras
Goddard Space Flight Center
Code 734.4
Greenbelt, MD 20771
Ph (301) 286-7477 Fax

Harry Wannemacher
Jackson & Tull
7375 Executive Place
Suite 200
Seabrook, MD 20706
Ph (301) 805-6090 Fax (301) 805-6099

Dr. Ralph E. White
University of South Carolina
Dept. of Chemical Engineering
Swearingen Engineering Center
Columbia, SC 29208
Ph (803) 777-3270 Fax (803) 777-8265

Tom Whitt
Marshall Space Flight Center
EB72
Marshall Space Flight Center, AL 35812
Ph (205) 544-3313 Fax

Doug Willowby
Marshall Space Flight Center
EB74
Marshall Space Flight Center, AL 35812
Ph (205) 544-3334 Fax

1995 NASA Aerospace Battery Workshop Attendance List

Cindy Winslow
Lockheed Martin
Code 442
Goddard Space Flight Center
Greenbelt, MD 20771
Ph (301) 286-0604 Fax (301) 286-1615

Mike Wong
Lockheed Martin Missiles & Space
O/31-60 B156A
1111 Lockheed Way
Sunnyvale, CA 94089-3504
Ph (408) 756-2203 Fax (408) 742-2731

Daphne Xu
INTELSAT
3400 International Dr. NW
Box 34
Washington, DC 20008-3098
Ph (202) 944-7250 Fax (202) 944-7333

Yoshiaki Yano
Sanyo Electric Co., Ltd.
222-1 Kaminaizen, Sumoto City
Hyogo, Japan
Ph 011-81-799-23-2851 Fax 011-81-799-24-4124

John Zhang
Arbin Instruments
3206 Longmire Dr.
College Station, TX 77845
Ph (409) 693-0260 Fax (409) 693-0344

Albert H. Zimmerman
The Aerospace Corporation
MS M2/275
POB 92957
Los Angeles, CA 90009-2957
Ph (310) 336-7415 Fax (310) 336-1636

☆U.S. GOVERNMENT PRINTING OFFICE—1996—717-805/82610

REPORT DOCUMENTATION PAGE

Form Approved
OMB No. 0704-0188

Public reporting burden for this collecton of information is estimated to average 1 hour per response, including the time for reviewing instructions, searching existing data sources, gathering and maintaining the data needed, and completing and reviewing the collection of information. Send comments regarding this burden estimate or any other aspect of this collection of information, including suggestions for reducing this burden, to Washington Headquarters Services, Directorate for Information Operations and Reports, 1215 Jefferson Davis Highway, Suite 1204, Arlington, Va 22202-4302, and to the Office of Management and Budget, Paperwork Reduction Project (0704-0188), Washington, DC 20503.

1. AGENCY USE ONLY (Leave Blank)	2. REPORT DATE	3. REPORT TYPE AND DATES COVERED
	February 1996	Conference Publication

4. TITLE AND SUBTITLE

The 1995 NASA Aerospace Battery Workshop

5. FUNDING NUMBERS

6. AUTHOR(S)

Jeffrey C. Brewer, Compiler

7. PERFORMING ORGANIZATION NAME(S) AND ADDRESS(ES)

George C. Marshall Space Flight Center
Marshall Space Flight Center, Alabama 35812

8. PERFORMING ORGANIZATON REPORT NUMBERS

M-802

9. SPONSORING/MONITORING AGENCY NAME(S) AND ADDRESS(ES)

National Aeronautics and Space Administration
Washington, DC 20546

10. SPONSORING/MONITORING AGENCY REPORT NUMBER

NASA CP-3325

11. SUPPLEMENTARY NOTES

Proceedings of a workshop sponsored by the NASA Aerospace Flight Battery Systems Program, hosted by the Marshall Space Flight Center, and held at the Huntsville Hilton on November 28-30, 1995.

12a. DISTRIBUTION/AVAILABILITY STATEMENT

Unclassified-Unlimited

Subject Category 44

12b. DISTRIBUTION CODE

13. ABSTRACT *(Maximum 200 words)*

This document contains the proceedings of the 28th annual NASA Aerospace Battery Workshop, hosted by the Marshall Space Flight Center on November 28-30, 1995. The workshop was attended by scientists and engineers from various agencies of the U. S. Government, aerospace contractors, and battery manufacturers, as well as international partipation in like kind from a number of countries around the world.

The subjects covered included nickel-cadmium, nickel-hydrogen, nickel-metal hydride, and lithium based technologies, as well as flight and ground test data. Nickel-hydrogen modeling was also covered.

14. SUBJECT TERMS	15. NUMBER OF PAGES
battery, nickel-cadmium, nickel-hydrogen, nickel-metal hydride, lithium, cadmium, battery tests, electrode, pressure vessel, modeling	649
	16. PRICE CODE: A99

17. SECURITY CLASSIFICATION	18. SECURITY CLASSIFICATION OF THIS PAGE	19. SECURITY CLASSIFICATION OF ABSTRACT	20. LIMITATION OF ABSTRACT
Unclassified	Unclassified	Unclassified	

National Aeronautics and
Space Administration
Code JTT
Washington, DC
20546–0001

Official Business
Penalty for Private Use, $300

Postmaster: If Undeliverable (Section 158 Postal Manual), Do Not Return